014

NO. FR-91565-430-1

437 p.

N64 11819

CODE-1

NASA CR-55060

DEVELOPMENT OF A HYDROGEN - OXYGEN INTERNAL COMBUSTION ENGINE AUXILIARY ELECTRIC POWER SUPPLY SYSTEM

Prepared for

NATIONAL AERONAUTICS AND SPACE ADMINISTRATION

by

N. E. Morgan

VICKERS INCORPORATED DIVISION

Sperry Rand Corporation

AEROSPACE DIVISION

DETROIT 32, MICHIGAN TORRANCE, CALIFORNIA

426 p.

NOTICE

This report was prepared as an account of Government sponsored work. Neither the United States, nor the National Aeronautics and Space Administration (NASA), nor any person acting on behalf of NASA:

A.) Makes any warranty or representation, expressed or implied, with respect to the accuracy, completeness, or usefulness of the information contained in this report, or that the use of any information, apparatus, method, or process disclosed in this report may not infringe privately owned rights; or

B.) Assumes any liabilities with respect to the use of, or for damages resulting from the use of any information, apparatus, method or process disclosed in this report.

As used above, "person acting on behalf of NASA" includes any employee or contractor of NASA, or employee of such contractor, to the extent that such employee or contractor of NASA, or employee of such contractor prepares, disseminates, or provides access to, any information pursuant to his employment or contract with NASA, or his employment with such contractor.

Requests for copies of this report
should be referred to:

National Aeronautics and Space Administration
Office of Scientific and Technical Information
Washington 25, D.C.
Attention: AFSS-A

(NASA CR - - - ~~NO~~; FR-91565-430-1) OTS (low)

~~PHASE REPORT~~

DEVELOPMENT OF A HYDROGEN-OXYGEN INTERNAL COMBUSTION ENGINE AUXILIARY ELECTRIC POWER SUPPLY SYSTEM

Prepared for

NATIONAL AERONAUTICS AND SPACE ADMINISTRATION

Double code

by

9172404

N. E. Morgan (Vickers, Inc.) 30 Sep. 1963 regs

September 30, 1963

(NASA Contract NAS3-2550)

Technical Management

CA - - - - - NASA - Lewis Research Center

Solar and Chemical Power Branch

Harry M. Cameron

VICKERS INCORPORATED DIVISION

Sperry Rand Corporation

Aerospace Division

Detroit 32, Mich. Torrance, Calif.

c

ABSTRACT

11819

The program described in this report consisted of two basic tasks: analytical and design studies, and component testing; leading to the preliminary design of a hydrogen-oxygen fueled space auxiliary electric power generating system. The studies included:

1. Evaluating the effect of propellant supply conditions on system configuration and performance.
2. Evaluating adaptability of the system to various space missions.
3. Preliminary design studies of an internal combustion prime mover, propellant supply components, power controls, electrical generator and voltage regulator, starting system, and other system components.
4. Materials selection.
5. Reliability studies.

Components which were designed, constructed and tested in prototype form included an internal combustion engine operating on hydrogen and oxygen (non-stoichiometric), a cryogenic hydrogen gas compressor, and a regenerative heat exchanger. The results of the analysis and design studies and the preliminary design of a flight-type auxiliary power system are presented. The component test results are presented and discussed.

AUTHOR

TABLE OF CONTENTS

Section	Title	Page
1.0	INTRODUCTION	1
1.1	Introduction	1
1.2	Summary	2
1.3	Conclusions	4
2.0	POWER SYSTEM DESCRIPTION	11
2.1	System Description	12
2.1.1	System Configuration	12
2.1.2	System Weight and Volume Estimates	12
2.2	Component Description	19
2.2.1	Engine	19
2.2.2	Hydrogen Compressor	34
2.2.3	Oxygen Compressor	35
2.2.4	Regenerator	35
2.2.5	Electrical System	36
2.2.5.1	Electrical System Requirements	36
2.2.5.2	System Components	39
2.2.5.3	Engine Starting System	50
2.2.5.4	Conclusion	55
2.3	System Operation	55
2.3.1	Operation with Supercritical Tankage	55
2.3.2	Operation with Boiloff Gases	56
2.3.3	System Cooling	56
2.3.4	Speed Control	57
3.0	PARAMETRIC STUDIES	59
3.1	Introduction	59
3.2	Description of Representative Hydrogen-Oxygen Systems	59

TABLE OF CONTENTS (Cont.)

Section	Title	Page
3.2.1	Fuel Rich Internal Combustion System	59
3.2.2	Stoichiometric Systems	60
3.2.3	Fuel Rich Internal Compression System	63
3.2.4	External Combustion System	64
3.2.5	System Considerations	65
3.3	Basic Cycle Studies	65
3.3.1	Assumptions Used in the Basic Cycle Studies	67
3.3.2	Cycle Analysis	67
3.3.3	Analysis of the Idealized Internal Combustion Engine Cycle	71
3.4	Methods of Engine Power Modulation	77
3.4.1	Variable Hydrogen Inlet Pressure with Fixed Valve Timing	82
3.4.2	Variable Hydrogen Valve Duration with Constant Hydrogen Inlet Pressure	82
3.4.3	Variable Phasing of the Hydrogen Valve with Constant Hydrogen Inlet Pressure	83
3.4.4	Hybrid System: Variable Hydrogen Inlet Pressure and Variable Hydrogen Valve Phasing	83
3.4.5	Hybrid System: Variable Hydrogen Inlet Pressure and Variable Hydrogen Valve Duration	84
3.5	Heat Rejection and Cooling Studies	85
3.5.1	Heat Rejection Analysis	85
3.5.2	Influence of Heat Rejection on Engine Performance	89
3.5.3	Engine and Power System Cooling Studies	93
3.6	Cryogenic Tankage Studies	97

TABLE OF CONTENTS (Cont.)

Section	Title	Page
3.7	Operation of Boiloff Propellants	100
3.7.1	Uncontaminated Boiloff	100
3.7.2	Helium Dilution of Boiloff Propellants	101
3.8	Compression Analysis	105
3.9	Conclusions	107
4.0	MISSION ADAPTABILITY STUDIES	109
4.1	Introduction	109
4.2	Scope of Studies and Assumptions	109
4.3	Application of H_2-O_2 SPU Concept to Space Missions	110
4.3.1	Earth to Lunar Landing	110
4.3.2	Lunar Excursion Module	112
4.3.3	Lunar Roving Vehicle	113
4.3.4	Earth Orbit Space Station	125
4.4	Application of Current 3 kw H_2-O_2 Engine Power System to Space Missions	128
4.4.1	Manned Space Station	128
4.4.2	Lunar Excursion Module	130
4.4.3	Apollo Mission	130
4.4.4	Miscellaneous Applications	132
4.5	Operational Considerations in Space Environment	132
4.5.1	Zero Gravity	133
4.5.2	High Vacuum Environment	134
4.5.3	Startup and Shutdown Procedures	136
4.5.4	Checkout	138

TABLE OF CONTENTS (Cont.)

Section	Title	Page
5.0	CONTROL STUDIES	141
5.1	Scope of Study	141
5.2	System Configuration Development	141
5.3	Engine Equations	147
5.4	Engine Representation	148
5.5	Linear Control System Studies	152
5.5.1	Introduction	152
5.5.2	Discussion of Studies Conducted	152
5.6	System Requirements	158
5.6.1	Speed Control Requirements	158
5.6.2	Actuator Design	161
5.6.3	System Requirements - Temperature Control	172
5.6.4	System Valve Requirements	176
5.6.5	Control of Propellant Source	178
5.7	Hardware and Conceptional Design	182
5.7.1	Introduction	182
5.7.2	Tachometer-Generator	182
5.7.3	Compensation and Amplification	184
5.7.4	Actuator	184
5.7.5	Exhaust Temperature Control	186
5.7.6	Overall System Control	187
5.8	Discussion of Results and Problem Areas	187
6.0	RELIABILITY STUDIES	191
6.1	Estimation of Component Failure Rates	191
6.2	Estimate of System Reliability	200
6.3	Failure Mode Analysis	203
6.4	Redundancy Requirements	204

TABLE OF CONTENTS (Cont.)

Section	Title	Page
7.0	DESCRIPTION OF PROTOTYPE COMPONENTS	219
7.1	Test Engine Description	219
7.2	Two-Stage Hydrogen Compressor	227
7.3	Regenerator	228
7.4	Materials	232
8.0	ENGINE TEST PROGRAM	235
8.1	Introduction	235
8.2	Test Facility and Instrumentation	237
8.3	Discussion of Tests and Results	242
8.3.1	Compilation of Test Results	243
8.3.2	Interpretation and Analysis of Test Results	249
8.3.3	Conclusions Regarding Combustion Phenomena	256
8.3.4	Engine Temperature Data	259
8.3.5	Engine Friction	264
8.3.6	Other Engine Data	265
8.4	Performance Corrections	265
8.5	Problem Areas	272
9.0	EXPERIMENTAL OXYGEN INJECTOR TEST PROGRAM	277
9.1	Summary	277
9.2	Test Facility and Instrumentation	278
9.3	Discussion of Tests and Performance and Design	279
9.4	Discussion of Problem Areas	286
9.4.1	Summary of Parts Failures	286
9.4.2	Cam Follower	287
9.4.3	Valve Seat Retainer	287

TABLE OF CONTENTS (Cont.)

Section	Title	Page
9.4.4	Valve Guide and Seat	288
9.4.5	Poppet Retainer Spring	288
9.4.6	Flex Pivot Bearing	289
9.4.7	Valve (Poppet), Guide, and Seat	290
10.0	EXPERIMENTAL REGENERATOR TEST PROGRAM	295
10.1	Summary	295
10.2	Test Equipment and Instrumentation	295
10.3	Discussion of Tests and Test Results	300
11.0	EXPERIMENTAL COMPRESSOR TEST PROGRAM	309
11.1	Summary	309
11.2	Test Facility and Instrumentation	310
11.3	Discussion of Tests	312
11.4	Failures	320
11.5	Discussion of Design and Redesign	321
	APPENDIX A	
	Statement of Work	323
	APPENDIX B	
	Cylinder Heat Rejection	329
	APPENDIX C	
	Electrical Component Specifications	337
	APPENDIX D	
	Regenerative Power Cycles with Heat Loss	341

TABLE OF CONTENTS (Cont.)

Section	Title	Page
	APPENDIX E	
	Engine Equations for Linear Analog and Original Computer	349
	APPENDIX F	
	System Reliability Calculations	399
	APPENDIX G	
	Prime Surface Heat Exchanger	403
	APPENDIX H	
	Summary of H_2-O_2 Internal Combustion Engine Test Results	409
	REFERENCES	413
	SYMBOLS AND ABBREVIATIONS	417

LIST OF ILLUSTRATIONS

Figure	Title	Page
1-1	Fuel Rich Regenerative System	9
1-2	Space Power Unit With Internal Combustion Engine	9
1-3	H_2-O_2 I.C. Engine Power System Dry Weight	10
1-4	H_2-O_2 I.C. Engine Power System Propellant Consumption	10
2-1	Assembly Drawing H_2-O_2 I.C. Power System	13
2-2	H_2-O_2 System Using Supercritical Tankage	15
2-3	H_2-O_2 System Using Compressors	15
2-4	Schematic - Complete H_2-O_2 System	17
2-5	Inlet Hydrogen Valve Flow	21
2-6	Hydrogen Valve Acceleration	22
2-7	Main Bearing Load - 2%	29
2-8	Main Bearing Load - 5%	29
2-9	Reciprocating Forces Vs. Crank Angle 2%	30
2-10	Reciprocating Forces Vs. Crank Angle 5%	30
2-11	Zero-G Lubrication System	32
2-12	Typical Power Profile For Space APU	37
2-13	Synchronous Alternator With Slip Rings	39
2-14	Brushless Synchronous Alternator	40
2-15	Simple Self-Excited Compound Regulated Alternator Without Voltage Reference	45
2-16	Simple Self-Excited Regulated Alternator	45
2-17	Simple Self-Excited Regulated Alternator	45
2-18	Simple Self-Excited Regulated Alternator	45
2-19	Simple Self-Excited Compound Regulated Alternator With Voltage Reference	46
2-20	Separately Excited Regulated Alternator	46

PRECEDING PAGE BLANK

LIST OF ILLUSTRATIONS (Cont.)

Figure	Title	Page
2-21	Alternator Voltage Regulator Loop	47
2-22	Alternator Voltage Regulator Loop	47
2-23	Regulator Watt Loss	48
2-24	Regulator Watt Loss	48
2-25	Regulator Watt Loss	49
2-26	Starter-Generator Functional Schematic Diagram	50
2-27	Schematic - Alternator With Inverter Starter	53
3-1	Fuel Rich Regenerative H_2-O_2 Engine System	60
3-2	Non-Regenerated Stoichiometric H_2-O_2 Engine System	62
3-3	Regenerated Stoichiometric H_2-O_2 Engine System	62
3-4	Non-Regenerated Fuel Rich H_2-O_2 Engine System	63
3-5	External Combustion Fuel Rich System With Exhaust Heat Regeneration	64
3-6	Relation Between Thermal Efficiency, BSPC, and O/F Ratio	66
3-7	BSPC Vs. O/F For Typical H_2-O_2 Engines	66
3-8	Indicator Diagram, External Combustion Engine Cycle	68
3-9	Indicator Diagram, Internal Combustion Engine Cycle	72
3-10	Combustion Temperature & Gas Constant As A Function Of Mixture Ratio	76
3-11	Typical Theoretical Indicator Cards	79
3-12	BSPC Vs. Horsepower (No Compressor Work)	81
3-13	Regenerative Power System Performance With Cylinder Heat Rejection	90
3-14	Regenerative Power System Performance With Cylinder Heat Rejection	91
3-15	Regenerative Power System Performance With Cylinder Heat Rejection	91

LIST OF ILLUSTRATIONS (Cont.)

Figure	Title	Page
3-16	Relative Propellant Consumption Vs. Cylinder Heat Rejection For Regenerated Cycles	92
3-17	Available Heat Sink From Supercritical H_2 & Engine Heat Rejection Vs. O/F Ratio	93
3-18	Heat Rejected in % Of Output Shaft Power Vs. O/F Ratio	96
3-19	Radiator Weight Vs. Radiator Temperature	97
3-20	Supercritical Tank Weight/Pound Of Propellant Vs. O/F	99
3-21	Work Required To Compress Saturated H_2 Vapor Vs. Initial Temperature	106
3-22	Work Required To Compress Saturated O_2 Vapor Vs. Initial Temperature	106
4-1	Sample Power Systems For Lunar Roving Vehicles	122
4-2	System Weight Including Propellant And Tanks At A Constant Power Output Vs. Time	126
5-1	Control Schematic - Original Concept	143
5-2	Control Schematic With Oxygen Throttle	145
5-3	Control Schematic With Propellant Mode Switching	146
5-4	Schematic - Complete H_2-O_2 System	149
5-5	Typical Theoretical Engine Cycle	148
5-6	Engine Cycle Energy	151
5-7	Root Locus Plot For Linear System	152
5-8	Linear Analysis Trace	154
5-9	Linear Analysis Trace	155
5-10	Linear Analysis Trace	156
5-11	Forward Loop Gain Change At Constant Closed Loop Gain	157
5-12	Analog Computer Block Diagram For Linear Analysis	159

LIST OF ILLUSTRATIONS (Cont.)

Figure	Title	Page
5-13	Analog Circuit Diagram For Linear Analysis	160
5-14	Block Diagram For Actuator Analysis	162
5-15	Circuit Diagram For Actuator Analysis	163
5-16	System Speed Error Vs. Actuator Maximum Rate	164
5-17	System Speed Error Vs. Actuator Maximum Rate	164
5-18	Actuator Saturation Limits On Rate Output	165
5-19	System Transient Speed Error Vs. Gain Of Load	166
5-20	Amplifier Gain Limitations	168
5-21	Breakout Force Relation To Amplifier And Clutch Or Motor Gain	169
5-22	Speed Loop Limit Cycle Characteristics	170
5-23	Transient Error Vs. Linkage Hysteresis For 0.87 KW Step Input	171
5-24	Speed Loop Response Variation In Compensation	172
5-25	Mixture Ratio Control Desired Transient Response	174
5-26	Temperature Loop Control Accuracy	175
5-27	System Valve Requirements	177
5-28	Closed Loop Compressor Control For Hydrogen Compressor	180
5-29	Typical Pressure Regulator Response Hydrogen Reservoir Pressure Regulator	181
5-30	Mechanical Thermostatic Actuator For Exhaust Temperature Control	186
6-1	Reliability Diagram For Control System	201
6-2	Reliability Diagram For Engine System (First 100 Hours)	201
6-3	Reliability Diagram For Engine System (Last 250 Hours)	202
6-4	Reliability Diagram For Electrical System	202

LIST OF ILLUSTRATIONS (Cont.)

Figure	Title	Page
6-5	Reliability Diagram For Auxiliary Power System	206
6-6	Summary Of Reciprocating Engine Failure Rate Data AAF-T.O. 00-25-128	206
7-1	H_2-O_2 Experimental Test Engine	219
7-2	H_2-O_2 Experimental Test Engine	219
7-3	Assembly Drawing, H_2-O_2 Experimental Test Engine	221
7-4	Assembly Drawing, O_2 Injector Valve	223
7-5	O_2 Injector Assembly	224
7-6	Assembly Drawing H_2 Compressor	226
7-7	Compressor Components	227
7-8	Hydrogen Compressor Gas And Inertia Forces	228
7-9	Schematic - H_2-O_2 Engine Regenerator	231
7-10	Assembly Drawing - H_2-O_2 Engine Regenerator	231
8-1	H_2-O_2 Engine Test Circuit	238
8-2	H_2-O_2 Engine Gas Control System	239
8-3	H_2-O_2 Engine On Test Stand (Insulated Head)	240
8-4	Engine Test Control Panel	240
8-5	Theoretical Combustion Temperature Rise & Gas Constant As A Function Of O/F Ratio	246
8-6	BSPC Vs. BMEP	248
8-7	BSPC·RT Vs. BMEP/P_H - No. 1	249
8-8	BSPC·RT Vs. BMEP/P_H - No. 2	250
8-9	BSPC·RT Vs. BMEP/P_{H_2} - No. 3	250
8-10	BSPC·RT Vs. BMEP/P_H - No. 4	251
8-11	BSPC·RT Vs. BMEP/P_H - No. 5	251
8-12	Photographs - Pressure Time Trace	253
8-13	Photographs - Pressure Time Trace	253

LIST OF ILLUSTRATIONS (Cont.)

Figure	Title	Page
8-14	Photographs - Pressure Time Trace	253
8-15	Photographs - Pressure Time Trace	253
8-16	Photographs - Pressure Time Trace	253
8-17	Linear Diagram - Pressure Vs. Volume	254
8-18	Log-Log Diagram - Pressure Vs. Volume	255
8-19	Energy Ratio Vs. O/F	259
8-20	Combustion Chamber Film Sequence	260
8-21	Exhaust Temperature Vs. BMEP	261
8-22	BSPC•RT BMEP/P_H (Insulated Head)	263
8-23	Motoring FMEP Vs. RPM	263
8-24	BSPC Vs. O/F	266
8-25	Heat Rejection Percentage Vs. O/F	266
9-1	O_2 Injector Test Stand	278
9-2	Schematic - O_2 Injector Test Stand	279
9-3	Arm & Poppet Lift Vs. Cam Follower Lift	280
9-4	Arm & Poppet Lift Vs. Cam Follower Lift	280
9-5	Diagram - Quill Shaft	281
9-6	Duration Vs. Pressure - O_2 Injector	284
9-7	Mean O_2 Flow Vs. Injector Inlet Pressure	284
9-8	O_2 Flow Rate Vs. O_2 Supply Temperature	285
9-9	Reused Valve (Poppet)	292
9-10	Reused Valve Guide	292
9-11	Reused Valve Seat	292
10-1	Engine Test Stand With Regenerator	296
10-2	Regenerator Test Set-Up	297
10-3	Regenerator Test Set-Up	297
10-4	Pressure Drop Vs. Flow Rate Test Schematic	298

LIST OF ILLUSTRATIONS (Cont.)

Figure	Title	Page
10-5	Temperature Rate Vs. Regenerator Length	302
10-6	Water Analysis Report	306
11-1	Schematic - Compressor Test Facility	311
11-2	Compressor Test Instrumentation	313
11-3	Compressor Test Stand	314
11-4	Koppers Piston Compression Rings	316
11-5	Cook Piston Compression Rings	316
11-6	MACE Piston Compression Rings (Teflon)	317
11-7	MACE Piston Compression Rings (Fluoroloy)	317
11-8	Failed Wire Cage Assembly	321
11-9	Floating Piston Pin Assembly	322

1.0 INTRODUCTION, SUMMARY, AND CONCLUSIONS

1.1 Introduction

This report covers the results of the work accomplished under NASA Contract NAS3-2550, from July 1, 1962, to May 31, 1963. The basic objective of the program was to conduct an engineering study culminating in the preliminary design of an electrical power generating system capable of operating on hydrogen and oxygen in a space environment, and to conduct preliminary testing on critical system components.

This program is a continuation of work which was initiated by the USAF-ASD under Contract AF-33(616)8406. Under the ASD contract, the feasibility of operating an internal combustion engine was demonstrated, and the oxygen-injection type engine was determined to have performance characteristics superior to the carburetted type. During the NASA program described herein, development testing on the oxygen-injection type engine was continued, and development testing was initiated on a cryogenic hydrogen compressor and a regenerative heat exchanger. Concurrently with the component development work, analytical and design studies were conducted to provide guide lines for the test program and to provide, in conjunction with the test program, a sound basis for the design of a space auxiliary power system. The contract Statement of Work appears in Appendix A of this report for reference purposes.

1.2 Summary

For the requirements of this program, parametric studies have shown that the best system configuration consists of a H_2-O_2 internal combustion engine driving an alternator directly at engine speed. A regenerative heat exchanger, which preheats incoming propellants with engine exhaust waste heat, contributes to the low propellant consumption of the system. Propellant is supplied to the system from either supercritical tankage or as boil-off gases from propulsion tanks. When operating on boil-off an engine driven compressor boosts the propellant pressure to that required for engine operation. Specific propellant consumption of a well developed system is predicted to be 1.02 lbs. per shaft horsepower hour or 1.52 lbs. per kwh, with a 90% alternator efficiency. The estimated dry weight of the complete electrical power generating system is 87 lbs., which includes engine, regenerator, alternator, propellant compressor, controls and plumbing. Propellant and tankage is not included in the above weight estimate. The system is estimated to occupy a volume of approximately 2 cubic feet.

Studies have shown the H_2-O_2 engine concept to be adaptable to a variety of mission requirements utilizing electrical, mechanical or hydraulic power. Attractive mission applications would include propulsion and auxiliary power for a Lunar Roving Vehicle and for a Space Station emergency power source.

The present state of development of the internal combustion engine powered space electric power system may be summarized as follows: the concept of a reciprocating internal combustion engine burning hydrogen and oxygen has been

proven to be mechanically and thermodynamically feasible. It has been shown that separate injection of the oxygen into a hydrogen filled cylinder is necessary for combustion control and that the resulting combustion is smooth, rapid, and probably complete, with spontaneous ignition. It has been shown that an oxygen injection mechanism in the form of a miniature poppet valve, hermetically sealed from its drive mechanism, gives satisfactory results and has the potential to be developed into a reliable and accurate metering device. However, evidence that the performance indicated by the results of analytical studies can be approached by an actual engine, given the proper combustion chamber environment and valve timing, needs to be established.

There is now available an experimental test engine, a two stage hydrogen compressor, and a hydrogen exhaust gas heat exchanger for use in establishing component performance data. A total of 15.7 hours test time has been accumulated on the engine, 31.2 hours on the O_2 injector, 11.6 hours on the hydrogen compressor (first-stage only), and 4.5 hours on the heat exchanger. The engine has been tested over a range of speed, power, and valve timing settings, and has demonstrated consistent performance. A complete combustion study has not been undertaken, but preliminary studies indicate that combustion stratification may have a significant effect on performance. Information is not adequate regarding the mechanism of heat loss from the cylinder and head, or the extent to which this loss can be reduced. Trouble areas on the test engine have been corrected or defined. The mechanism of engine control has been defined from test control experience and from the results of the control study.

Testing of the hydrogen compressor was limited to the first stage only. Performance capabilities were not determined due to leakage and mechanical drive problems which were not resolved before the end of the contract.

The regenerative heat exchanger was tested with the engine, but test results were meager because of time and budget limitations at that point in the program.

The one remaining question determining the future of a H_2-O_2 reciprocating engine as a prime mover for a space power system is; how readily can specific propellant consumption be reduced to acceptable levels? All other system inadequacies are apparently amenable to development. Considerably more development testing is necessary to evaluate the causes of heat loss, the heat transfer properties of the exhaust gas, and the amount of turbulence necessary to limit the deleterious effects of charge stratification without unduly raising heat transfer to combustion chamber walls.

1.3 Conclusions

While the results of the development test program have left some basic questions regarding performance and durability of the test components unanswered, much valuable operating experience has been gained which will provide a more solid foundation for future work. The analytical and design studies have provided valuable guide lines for preliminary design of the flight system and for the development testing program.

Specific conclusions resulting from the work conducted in this program are:

1. For the requirements of this program an electric power generating system consisting of a fuel-rich H_2-O_2 internal combustion engine, with exhaust heat regeneration, driving a highly efficient alternator, appears to be the best configuration.

2. An O/F ratio (oxygen/hydrogen) of 2, by weight, provides the lowest system volume if an external heat sink, e.g., a space radiator, is available for power system waste heat rejection.

   Self-cooling of the power system can be achieved at O/F between 1.2 and 1.4 at a negligible increase in BSPC, but with the penalty of increased system volume due to the larger proportion of low density hydrogen required.

3. For the power profile used as a basis for the parametric studies, in which the time-weighted average power level was approximately 50% of the peak power, the optimum BSPC can be achieved by using a combination of throttling and variable admission for power modulation control. At low power levels, the hydrogen is throttled for power control; while at higher power levels, power control is achieved by varying the opening duration of the hydrogen inlet valve at wide open throttle. Mixture ratio is maintained over the entire power range by throttling the oxygen.

4. At the present state-of-the-art of zero gravity cryogenic tankage, supercritical storage is preferred to subcritical storage. Optimum storage pressures for this system appear to be 300 psi for hydrogen and 900 psi for oxygen.

5. The system described herein is capable of dual propellant source operation, i.e., from either supercritical storage tanks or from boil-off gases derived from propulsion stage propellants. During operation on boil-off gases, engine driven compressors boost the propellant pressures to the same levels as in the supercritical storage tanks. Except for the compressor operation, system operation is the same with either propellant source. Boil-off gases must be relatively pure, i.e., uncontaminated by inert pressurization gases, for satisfactory operation of the power system.

6. The design and development of a 3 kw, 3 phase, 400 cps alternator with an overall efficiency in excess of 90% appears to be within the state-of-the-art, by making use of modern techniques of design and construction.

7. The H_2-O_2 engine lends itself readily to multiple restart applications. Electrical starting by use of a battery and starter motor appears to be the most reliable method and also offers the fringe benefit of a separate dc electrical output, if a starter-generator is used for this purpose.

8. The engine speed control can be relatively simple; essentially consisting of a tachometer-generator, an electric servo motor to actuate the engine control valves, and the associated electronics.

9. The H_2-O_2 engine lends itself to a variety of space missions and tasks, and can function as a lightweight, efficient prime mover for providing electrical, hydraulic or mechanical power output. Among the missions for which the engine appears well suited are:

Lunar roving vehicle
Orbital space station emergency power
Lunar landing vehicle
Apollo-type spacecraft
Portable power source for tools

10. The present oxygen injector is superior in design than its predecessor. Additional improvements are necessary to reduce flexibility and lost motion between the cam and the poppet valve. Additional testing is required to verify materials selection.

11. The regenerative heat exchanger tested in this program appears to be larger than necessary. This is a tentative conclusion and it must be verified by additional testing, particularly at vacuum exhaust conditions.

12. The basic design of the two-stage cryogenic hydrogen compressor is believed to be fundamentally sound except for the flexural members in the internal drive linkage. This linkage must be redesigned before it can be expected to meet the performance and durability requirements. Additional detailed development work is also necessary in the area of first stage piston ring configuration.

13. Though the H_2-O_2 engine has shown itself capable of achieving specific propellant consumption of less than 2.3 lbs. per hp/hr. at a power level of less than 3 hp, and at off-design conditions, its full potential has yet to be demonstrated. The possibility of a 40% reduction in BSPC exists by identifying and correcting certain, as yet unidentified, losses. It is believed that these unaccounted for losses consist primarily of excessive

combustion stratification, cyclic heat transfer, leakage, and excessive engine friction. Additional improvements can be expected when the engine can be operated at design conditions with exhaust heat regeneration and vacuum exhaust.

14. The salient design features and performance information for H_2-O_2 APU's are presented in illustrations as follows. Fig. 1-1 schematically illustrates the general configuration of the H_2-O_2 power unit. Fig. 1-2 is a general assembly drawing of the 3 kw APU. The estimated weight of similar H_2-O_2 APU's in the power range of 1 to 10 kw is illustrated in Fig. 1-3. Weight data are presented for APU's using both high efficiency (90%), alternators and low weight, but low efficiency (75%), alternators. The propellant consumption curve shown in Fig. 1-4 is for the high efficiency APU's.

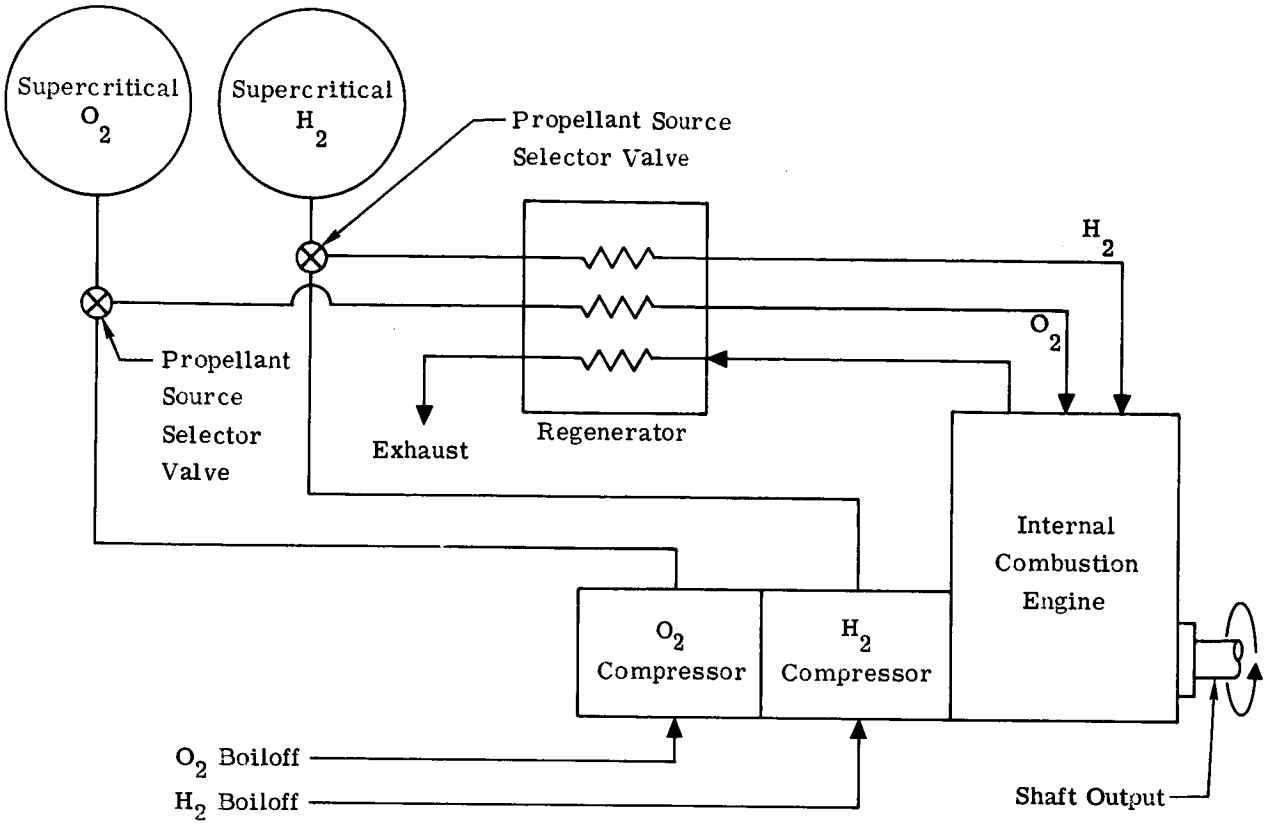

Fig. 1-1 - Fuel Rich Regenerative System

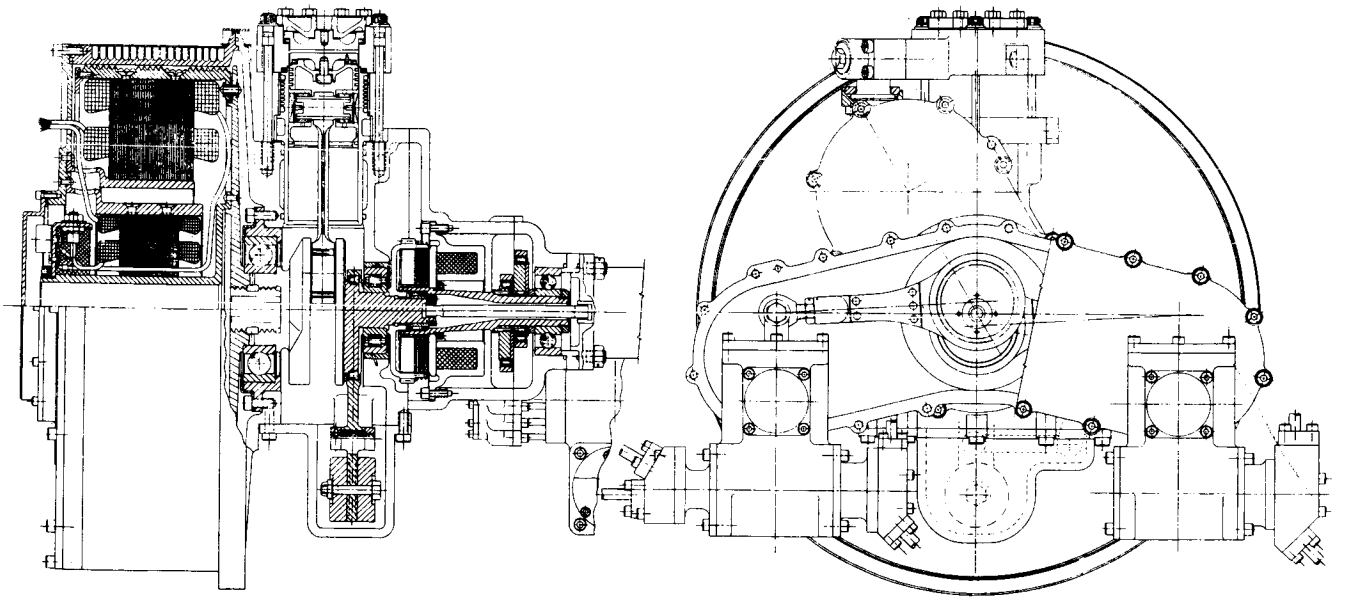

Fig. 1-2 - Space Power Unit with Internal Combustion Engine

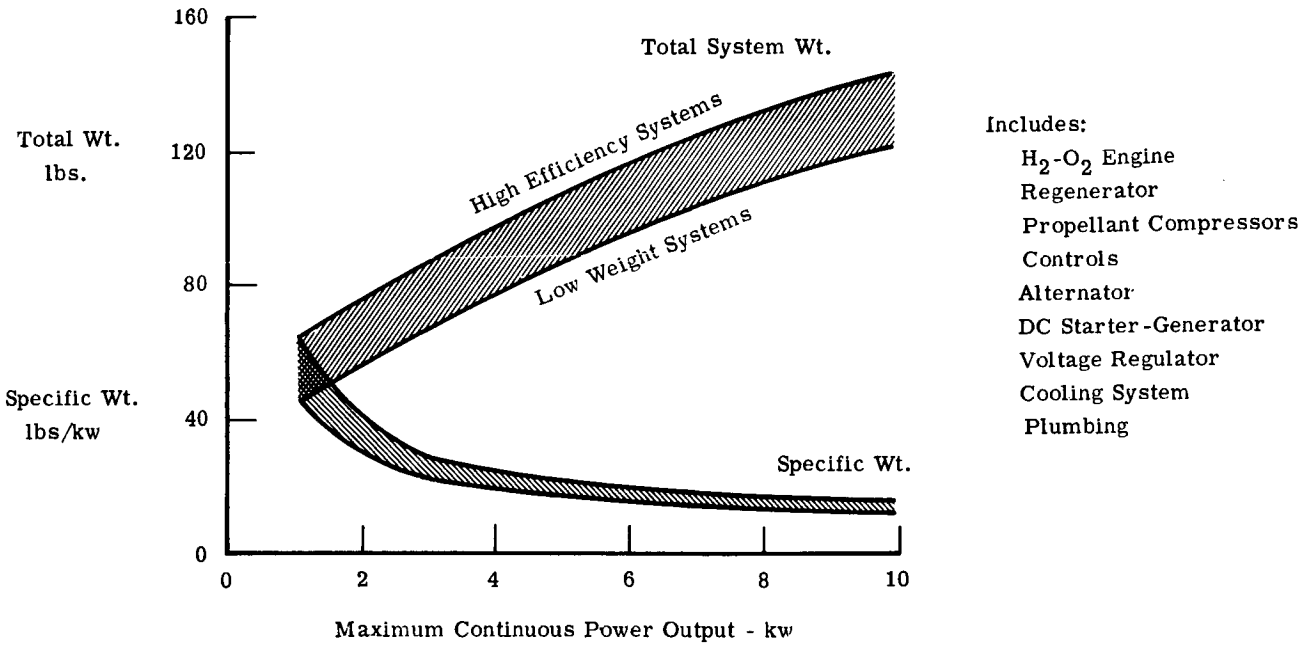

Fig. 1-3 - H_2-O_2 I.C. Engine Power System Dry Weight

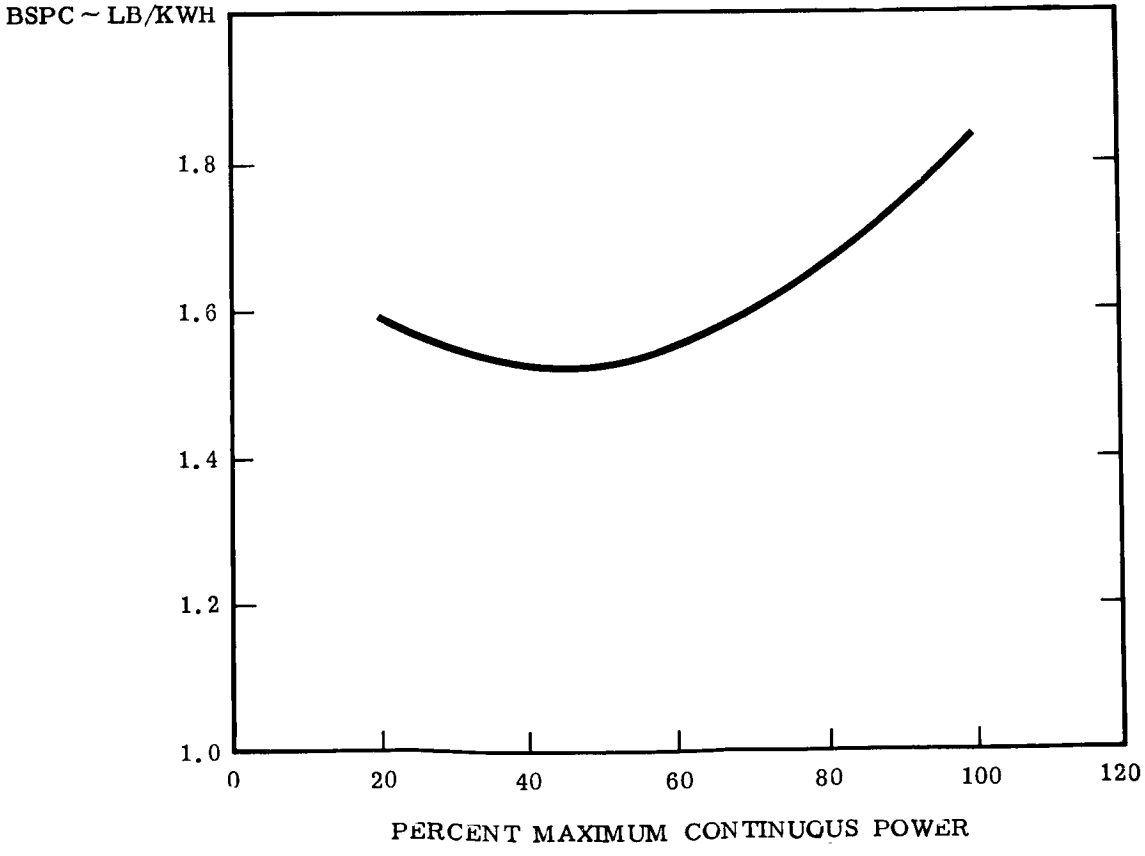

Fig. 1-4 - H_2-O_2 I.C. Engine Power System Propellent Consumption

2.0 POWER SYSTEM DESCRIPTION

The power system defined in this program consists of an internal combusion H_2-O_2 engine, utilizing oxygen injection, which drives an alternator. Propellants are supplied to the power system from supercritical storage tanks or from cryogenic boiloff gases boosted to engine inlet pressure by engine driven compressors. Hydrogen and oxygen are preheated by passing through a regenerative heat exchanger before entering the engine. Each of these components and the associated plumbing and controls are discussed in Sections 2.1 and 2.2. An assembly drawing of the system is shown in Fig. 2-1 and conceptual schematics are shown in Figs. 2-2 and 2-3.

The components of this system are now in the preliminary design stage. Their configuration is based on the results of the parametric design studies, the control studies, and the test experience accumulated to date.

The experimental test components built and evaluated in the test phase of the program were based on earlier designs. The design differences are discussed in Section 7. The major design change resulted from reducing hydrogen pressure. The hydrogen compressor is now a 20:1 compression ratio, single stage compressor discharging at 300 psi instead of the original two stage, 1200 psi compressor which had been built and tested. This change was made because analysis and preliminary test results showed more promising performance with a constant volume combustion cycle and thermal compression instead of the constant pressure combustion concept with very high inlet pressure, which was under consideration when the test compressor was designed.

2.1 System Description

2.1.1 System Configuration

While control, plumbing, and packaging details of the power system are not completely defined, all components have been designed or specified. The major mechanical and electrical components are described below while the control elements are described in Section 5.

A simplified conceptual sketch of the system using supercritical tankage is given in Fig. 2-2. This same system can use boiloff gases when compressors are employed as shown in Fig. 2-3. A detailed block diagram of the complete system showing flow paths and mechanical and electrical control paths is given in Fig. 2-4. A description of system operations is given in Section 2-3.

2.1.2 System Weight and Volume Estimates

At this point in the design of the flightweight system, it is not possible to make a precise weight and volume estimate. Additional information regarding specific application requirements would be necessary to do so. However, preliminary weight and volume estimates can now be made which will serve to put the system into proper perspective, relative to other types of space power systems.

The estimated weight breakdown is as follows*;

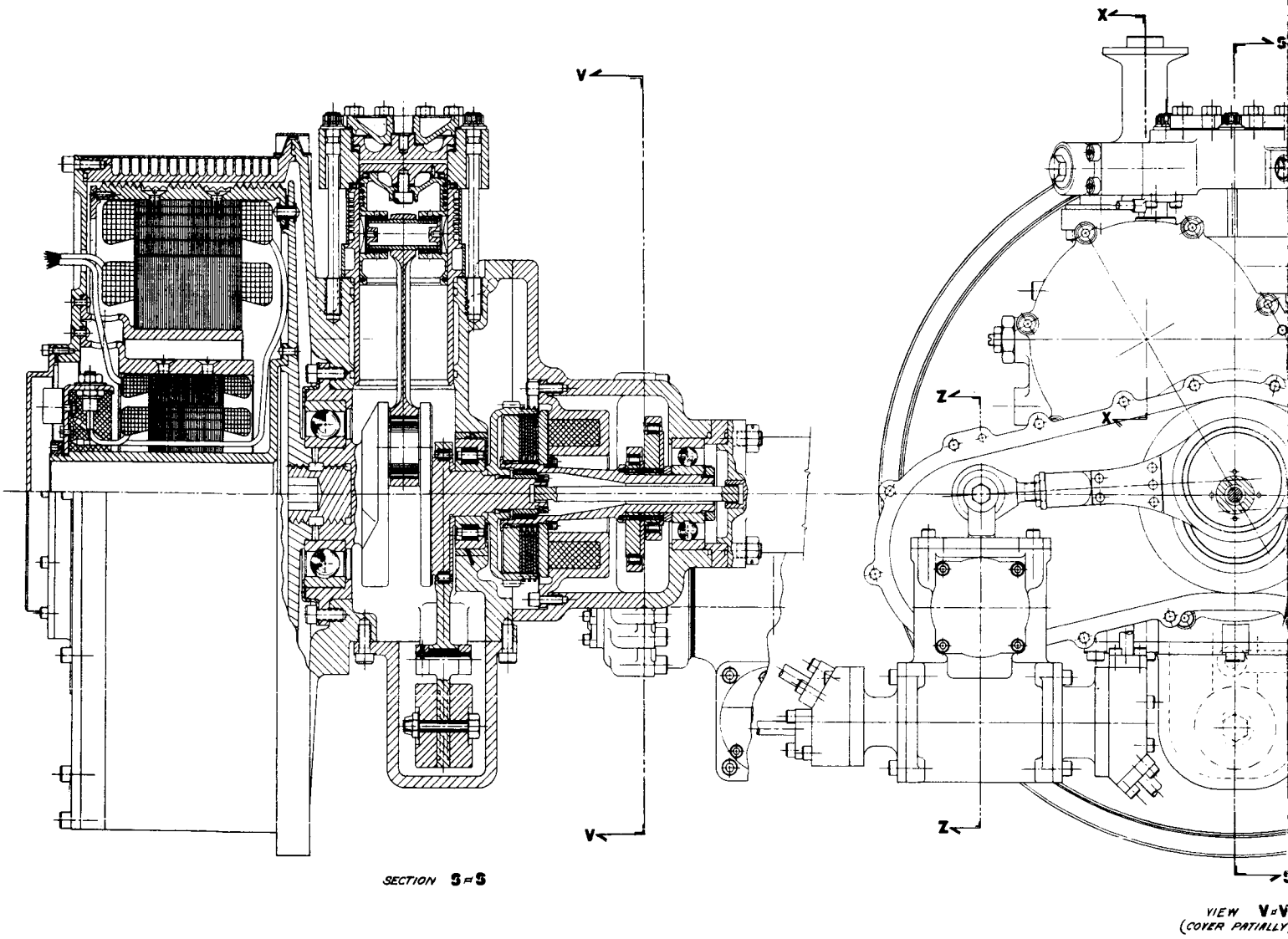

Fig. 2-1 - Assembly Drawing

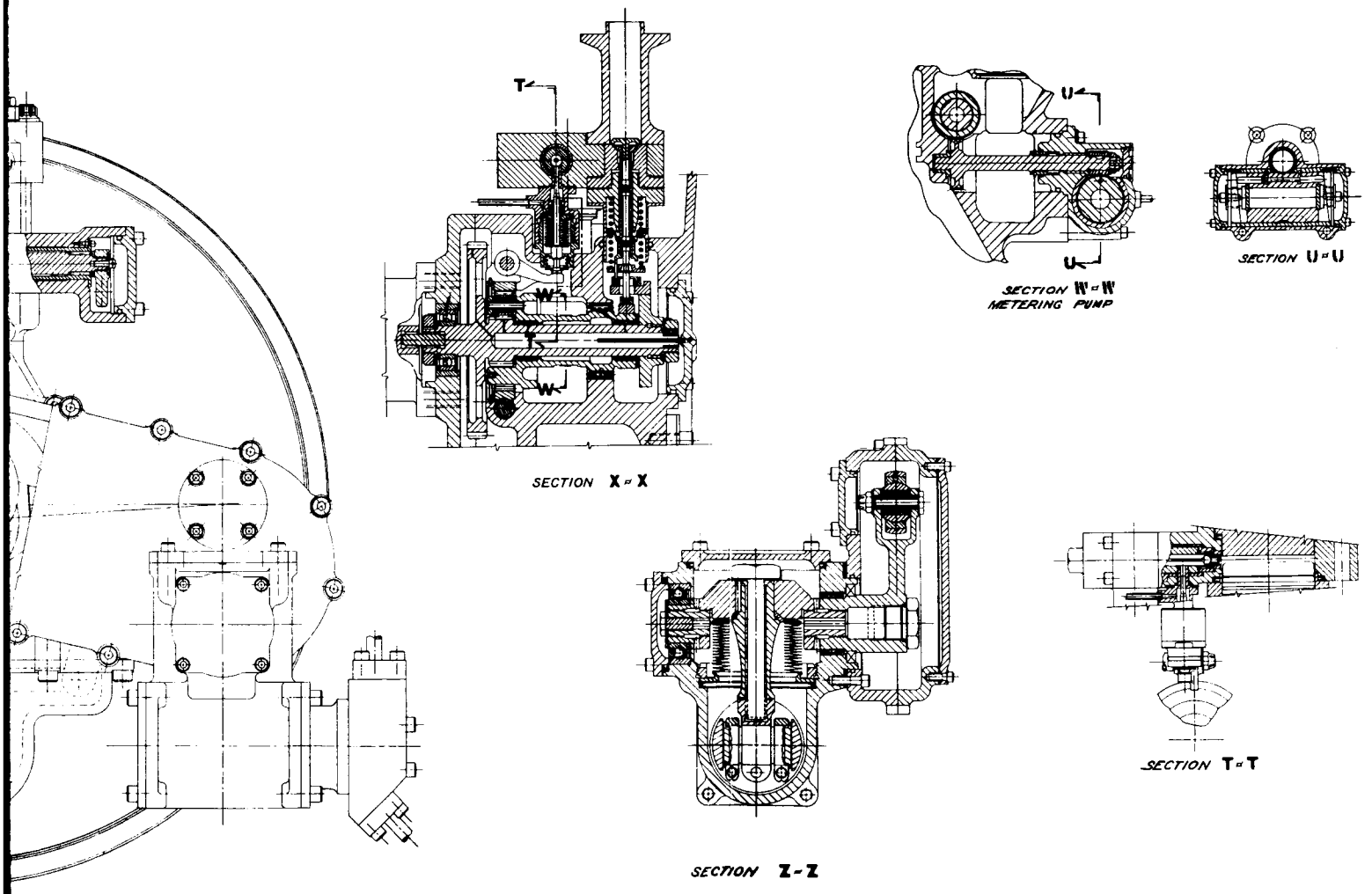

REMOVED)

H_2-O_2 I. C. Power System

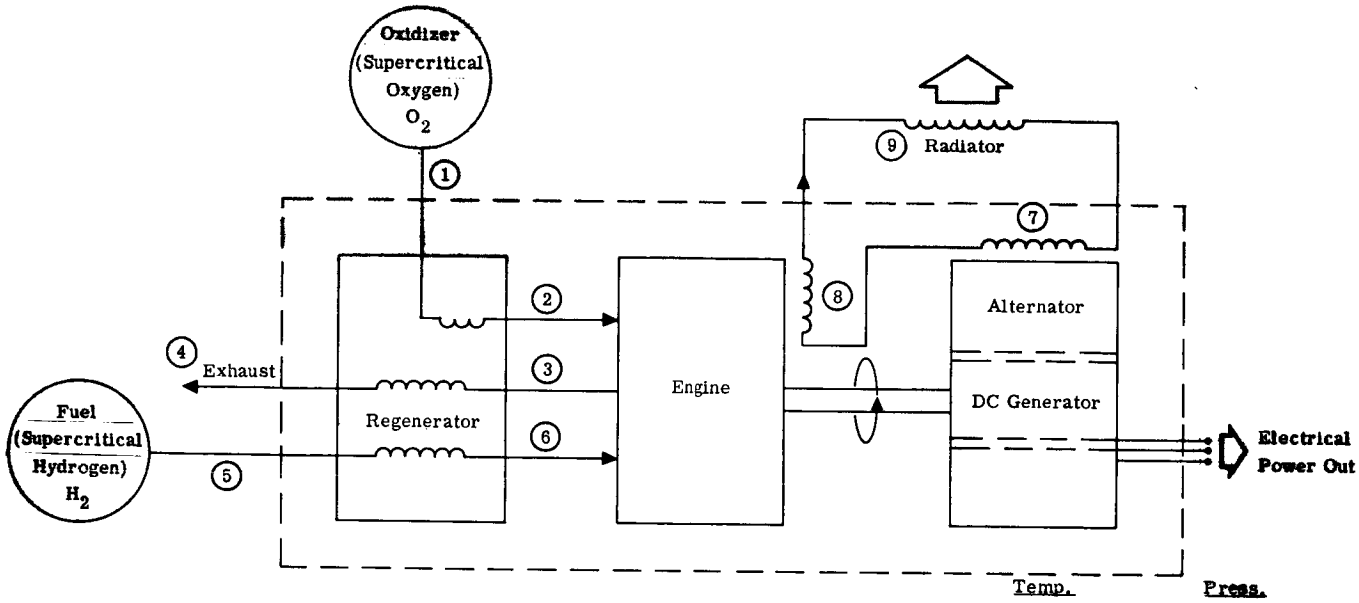

	Temp.	Press.
1. Oxygen Inlet to Regenerator (Regenerator may be bypassed)	160 - 430°R	900 psi
2. Oxygen Inlet to Engine	1440°R	900 psi
3. Hot Exhaust Entering Regenerator	1540°R	1 psia
4. Cold Exhaust Overboard	550°R	1 psia
5. Cold Hydrogen Inlet to Regenerator	45°R - 150°R	300 psia
6. Hot Hydrogen Inlet to Engine	1440°R	300 psia
7. Alternator Coolant (may not be integrated as shown)	675°R	15 psia
8. Engine Cylinder Coolant	675°R	15 psia
9. Coolant Loop Radiator	665°R	15 psia

Fig. 2-2 - H_2-O_2 System Using Supercritical Tankage

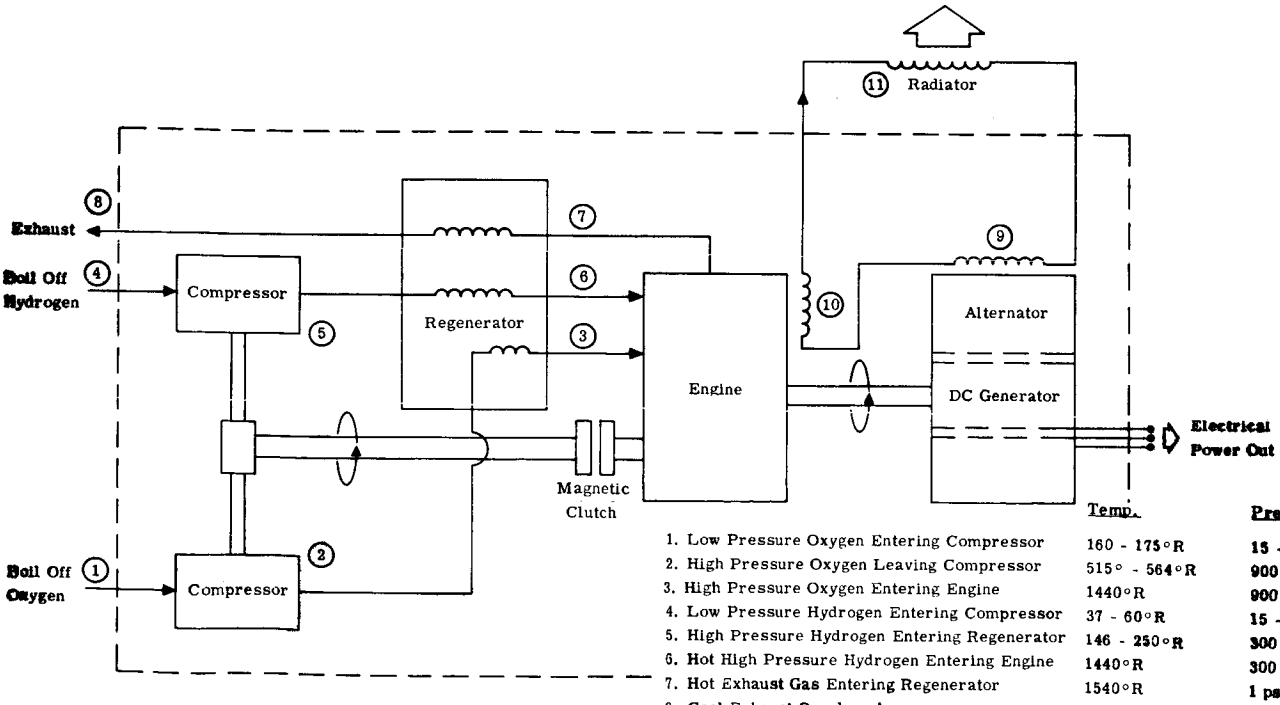

	Temp.	Press.
1. Low Pressure Oxygen Entering Compressor	160 - 175°R	15 - 175 psia
2. High Pressure Oxygen Leaving Compressor	515° - 564°R	900 psi
3. High Pressure Oxygen Entering Engine	1440°R	900 psi
4. Low Pressure Hydrogen Entering Compressor	37 - 60°R	15 - 175 psia
5. High Pressure Hydrogen Entering Regenerator	146 - 250°R	300 psi
6. Hot High Pressure Hydrogen Entering Engine	1440°R	300 psi
7. Hot Exhaust Gas Entering Regenerator	1540°R	1 psia
8. Cool Exhaust Overboard	550°R	1 psia
9. Alternator Coolant	675 °R	15 psia
10. Engine Cylinder Coolant	675 °R	15 psia
11. Cooling Loop Radiator	665 °R	15 psia

Fig. 2-3 - H_2-O_2 System Using Compressors

PRECEDING PAGE BLANK

3 kw System Dry Weight *

H_2-O_2 Engine	14 lbs.
Regenerator	12
Alternator & Exciter	35
H_2 Compressor	3 **
O_2 Compressor	2 **
Voltage Regulator	1
Inverter	9
Controls	6
Plumbing	5
Total	87 lbs.

Expendibles and Tankage Weight

Hydrogen	0.5 lbs. per kwh
Oxygen	1.0 lbs. per kwh
Lubricating Oil	0.015 lbs. per kwh
LH_2 Supercritical Tankage	0.4 lbs. per kwh
LO_2 Supercritical Tankage	0.2 lbs. per kwh
Oil Tank (bladder type)	0.0015 lbs. per kwh

* Radiator weight is not included because the power system may share heat rejection elements with other vehicle systems which must be cooled. Common radiator usage may be accomplished without significant radiator weight being charged to the power system, since the system can probably raise the average radiator rejection temperature and thus allow the additional heat to be rejected without increasing radiator area.

** Required only for operation with boiloff gases.

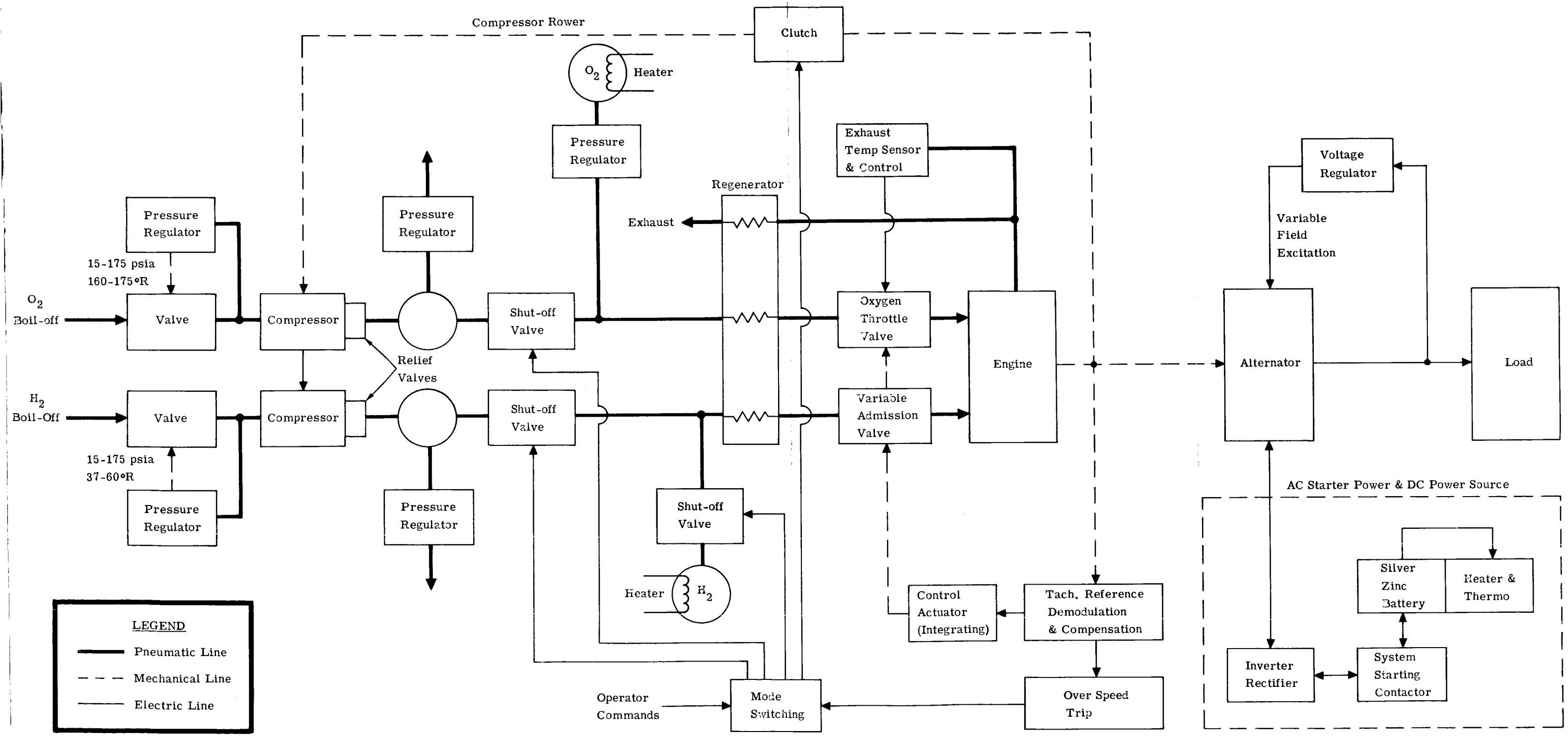

Fig. 2-4 - Schematic - Complete H_2-O_2 System

17-A

For the 350 hr, 1.6 kw average power mission which formed the basis for this program total system takeoff weight would be 1416 lbs. if boiloff gases are not available or 1068 lbs. if boiloff gases can be used for 100 hours of the mission.

2.2 Component Description

2.2.1 Engine

A single-cylinder reciprocating, internal combustion engine, operating on a uniflow two-stroke cycle is employed. Hydrogen and oxygen are supplied to the engine under pressure. The hydrogen enters the engine through a dual poppet valve with adjustable opening duration. The oxygen is injected into the cylinder shortly before hydrogen valve closing and ignites spontaneously with the hydrogen. Ignition is aided by a platinum or palladium catalyst in the combustion chamber. The exhaust gases leave the cylinder through ports uncovered by the piston 15° before the bottom of the stroke and enter the regenerator, giving up heat to the incoming hydrogen, before being exhausted overboard. Except for the induction system, the engine follows conventional design practices. The engine design is shown incorporated into the flight system in Fig. 2-1. Engine design details are discussed below.

Hydrogen Inlet Valve

The dual poppet hydrogen valve was chosen for this engine on the basis of parametric study results. The dual poppet valve concept consists of two poppet valves arranged concentrically and opening in series. The inner and outer valves are actuated by separate cams, both located on the gear-driven camshaft. The motion of the two valves is identical,

PRECEDING PAGE BLANK

but the cam for one valve can be advanced or retarded, relative to the other cam. Since hydrogen can flow into the cylinder only when both valves are open, the variable phase valve provides variable admission of gas into the cylinder. This valve design was developed by Vickers in two previous test programs and has proven to be satisfactory. The hydrogen valves are located adjacent to the cylinder head, arranged L-head fashion. Valve acceleration rates, maximum operating temperatures, and endurance requirements are all within the state-of-the-art of current internal combustion engine technology.

A high mounted camshaft was chosen, since it lowers the reciprocating mass in the valve train by permitting the use of short valve stems and low inertia rocker arms and spring retainers. The separate L-head arrangement has been used in previous designs and has the advantage of thermally isolating the hydrogen valves from the hottest part of the cylinder head and permitting cooler operating conditions at the inlet valves.

The L-head arrangement was chosen over the overhead valve configuration in this engine due to these valve dynamic and thermodynamic considerations. Some loss of freedom in combustion chamber shape and hydrogen valve and oxygen injector location is inevitable with side valves. An overhead valve configuration may afford the minimum clearance volume and the lowest pressure drop through the valve, however, there are always penalties associated with a mechanically driven overhead valve in terms of complexity, weight, bulk, and valve train dynamics. There are two unknown factors which concern hydrogen valve operation. Valve life under continuous operation at 1000°F regenerated hydrogen inlet temperature has not been determined, and although exhaust valves of conventional air-breathing engines operate at 1400-1500°F, the conditions are

not exactly comparable because of the higher heat transfer characteristics of hydrogen. Minimum valve guide lubrication requirements are also unknown as yet. Oil consumption by leakage around the hydrogen valve stem may contribute significantly to the total engine oil loss. Inlet hydrogen valve flow is shown in Fig. 2-5. A 30° valve duration following a sinusoidal lift curve, with a valve head diameter of .16 in. and a lift of .040 in. was assumed. It can be seen that this valve size is adequate for full admission.

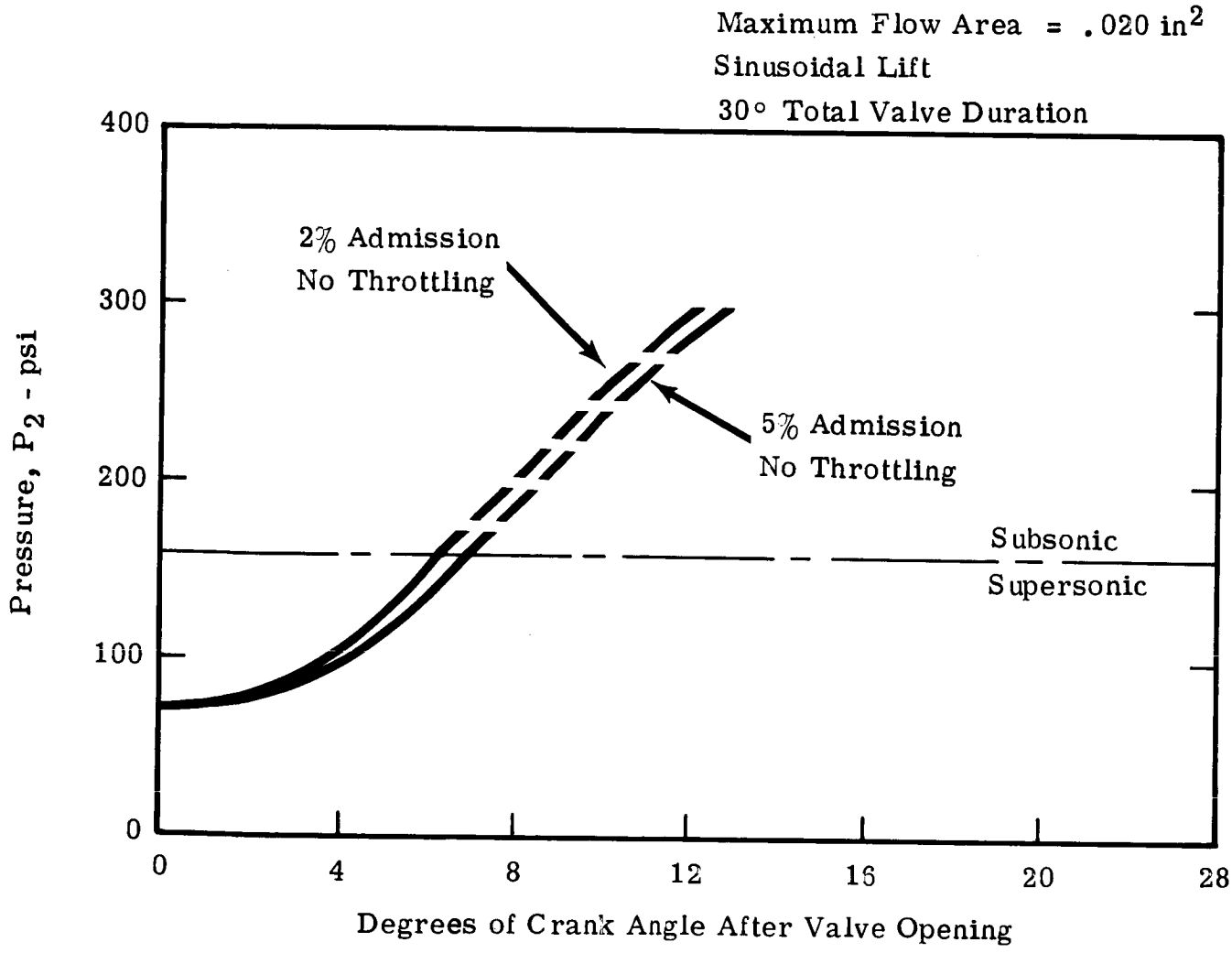

Fig. 2-5 - Inlet Hydrogen Valve Flow

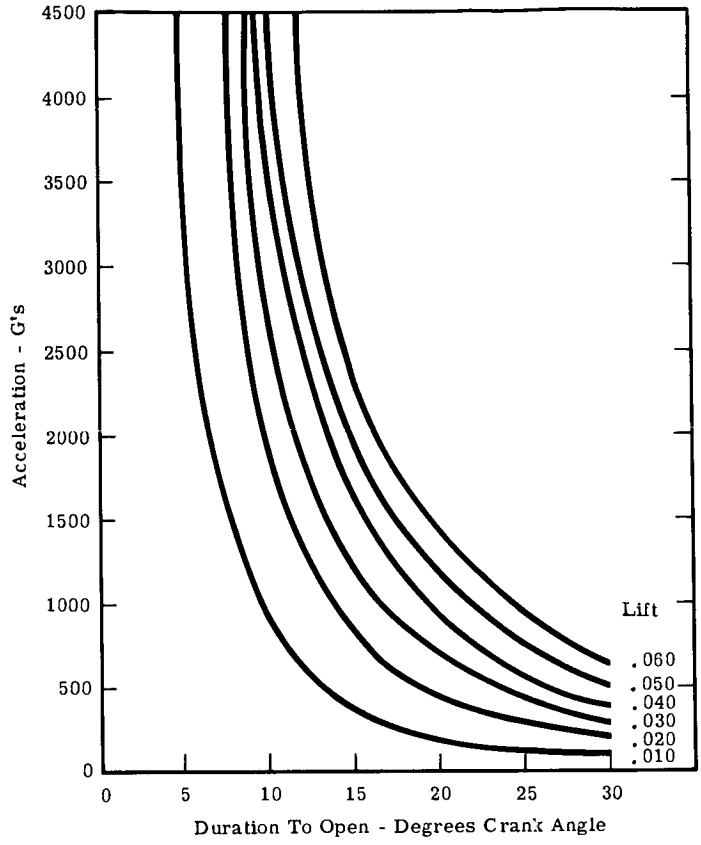

Fig. 2-6 - Hydrogen Valve Acceleration

In Fig. 2-6, maximum acceleration in g's is plotted against crank angle degrees (from opening to maximum lift) for various lifts. Sinusoidal acceleration is assumed. The current design practice for racing engines is approximately 1500 g's. Hydrogen throttling will be accomplished along with phasing by the dual concentric hydrogen valve. The valve size and lift rate will be arranged to offer considerable flow restriction at lower overlap. The effective flow area vs. overlap angle decreases drastically as overlap is decreased, so that the dual poppet valves lend themselves naturally to power control by a combination of throttling and variable admission.

Oxygen Injector Valve

The oxygen injector valve presents what is probably the most difficult design problem in the entire system. It must transmit minute quantities of oxygen at high speed with very precise timing, while isolating the oxygen from fuel, lubricants, or vulnerable bearing surfaces. At the design engine speed of 4000 rpm with an oxygen valve opening duration of 30° of crank angle, the valve must open and close in 1.3 milliseconds. For a 2:1 mixture ratio, an engine power output of 5 hp, and a

specific propellant consumption of 1.0 lb/hp-hr., the valve must pass about a .006 cubic inches of oxygen each revolution.

This injector follows the same basic design concept employed in previous oxygen injector designs (Ref. 1), in that the chamber within which the valve operates is hermetically sealed, with motion being transferred to the valve through a thin wall tube deflecting in torsion. The drive from the cam shaft to the injector valve stem is by means of rocker arms and a quill shaft.

Oxygen Throttle Valve

The purpose of the oxygen throttle valve is to regulate the oxygen supply pressure before it enters the engine through the oxygen injector poppet valve. The injector valvelift, opening duration, and phasing relative to the hydrogen cutoff valve, are all constant over the power range. Therefore, at low power operation, the inlet oxygen density must be lowered by throttling to prevent an excessively high O_2/H_2 mixture ratio and consequent overheating. This throttling has a negligible effect on system efficiency due to the low power required for compressing oxygen.

The oxygen throttle is shown in views X-X and T-T of Fig. 2-1. The oxygen throttle is a tapered needle valve of .070" maximum diameter, with a total movement of .100". The needle will be held along one side of its port to insure the same flow coefficient during valve movement. The linear movement of this valve is great enough to insure control.

The valve body is mounted between the crankcase and the injector valve housing, at right angles to the injector poppet.

The needle position is set by a 90° rocker arm resting on a cam mounted on the side of the ring gear of the phasing mechanism. A secondary temperature trim is effected by mounting the rocker arm on a eccentric shaft which is rotated by a temperature feedback mechanism.

Oxygen is contained within the valve by a double seal; a teflon packing seal around the needle, and a welded metal bellows backing up the seal. Oxygen escaping the teflon seal will be stopped by the bellows from entering the crankcase and creating a fire hazard. The chamber between the bellows and the seal is vented to the exhaust to prevent a pressure buildup and to permit the use of a small light bellows.

The active element of the temperature trim device is a capsule filled with sulfur vapor under pressure, mounted in the exhaust stream. This capsule moves a rod by expansion under a temperature rise. The rod is fastened by a rocker arm to the eccentric shaft on which the needle valve rocker arm is mounted. Such devices are now in use for furnace control and can be readily adapted for this purpose.

Valve Control Mechanism

The proposed mechanism for controlling the power setting on the flight design engine is given in view X-X of Fig. 2-1. This mechanism varies the phase relationship of the oxygen injector valve and one of the poppets of the dual poppet hydrogen valve relative to the crankshaft. It also controls the opening of the oxygen throttle valve in the oxygen line, upstream of the oxygen injector valve. By these means, hydrogen inlet pressure, hydrogen admission duration, oxygen inlet pressure, and oxygen

injection timing are continuously variable on demand over the full range of engine power.

The phasing and control mechanism consists of a planetary gearset in conjunction with two camshafts. The cam for the inner (small diameter) hydrogen valve is mounted on a shaft which is gear driven by the engine crankshaft, at engine speed.

This shaft also carries the sun gear of the planetary gearset. The camshaft for the outer (large diameter) hydrogen valve and for the oxygen injector valve is hollow, and is mounted by roller bearings around the primary shaft. This secondary camshaft is fastened to the planet carrier and turns at one-third engine speed, so that each cam has three lobes. The ring gear is the reaction member of the planetary gearset and its position is advanced or retarded to provide the variable phase relationship between the camshafts. It is phased by means of a worm drive from a dc servo motor. There is a cam formed on the side of the ring gear controlling the oxygen throttle.

The relationship between the oxygen injector valve duration and timing and the hydrogen valve cutoff point will be optimized by testing, so both valves can be phased together over the operating range. The need to vary the amount of oxygen/hydrogen flow overlap is not anticipated. Oxygen pressure is also varied over the power range by the oxygen throttle, with a secondary pressure control regulated by exhaust temperature, to prevent overheating.

Engine Balancing

For a conventional single cylinder engine operating at 4000 rpm

with a 1/2 lb. reciprocating mass, there is a primary reciprocating unbalance of approximately 85 lbs. maximum force in line with the cylinder axis, and a second order reciprocating unbalance of 43 lbs. One-half the primary reciprocating unbalance can be counterweighted, giving a primary rotational unbalance of 43 lbs. This rotating force travels at engine speed, but in the opposite sense. If an oversized counterweight is used, a reciprocating unbalance force of 43 lb. maximum, transverse to the cylinder axis, at engine speed can be achieved. This is the usual case with motorcycle engines. To completely compensate for primary and secondary unbalance would require two contra-rotating balance shafts at engine speed and two additional balance shafts running at twice engine speed, symmetrically distributed about the crankshaft. While one of the primary shafts could be used as a camshaft in the two-cycle H_2-O_2 engine, the other shafts would be useful only as additional accessory drives and would add weight, bulk, and complexity to the engine. The alternate method of achieving complete balance is the use of a dummy opposed piston which can be made to completely counterbalance all reciprocating forces. A modification of the balance piston technique has been selected for the flight engine design.

The balancing mechanism can be seen in the lower half of view S-S of Fig. 2-1. This is a dummy weight pivoting about a lever arm and driven by an eccentric on the crankshaft. Since this eccentric has a stroke of one-half the engine stroke, the balance weight must be double the total reciprocating weight. The eccentric is mounted on one crank cheek and the rotating weight is counterbalanced equally on both crank cheeks.

A balancing piston will provide complete balancing of reciprocating weight if the following conditions are met:

1. The L/R ratio (connecting rod length/radius of crank throw) of the power piston and of the balance piston are the same.

2. The total reciprocating weights operate along the same centerline.

3. The peak reciprocating forces exactly cancel each other. The dummy weight used here is off-balance in the following ways:

   a. There is a small rocking couple caused by the dummy weight and the piston operating along slightly different centerlines.

   b. The weight travels in a circular arc instead of straight line.

The unbalance forces resulting from these factors are all very small compared to the amount of unbalance found in a conventionally counterweighted single cylinder engine. Exact dynamic balancing may be obtained by the use of two dummy weights operating along centerlines at equal distances from the crank axis or by a single weight arranged on the centerline of the power piston and driven by a double linkage from a pair of eccentrics symmetrically disposed about the cylinder center. This degree of refinement is considered superfluous for the H_2-O_2 engine, since the problem of combustion induced vibration is still present.

Bearing Loads

The results of bearing load calculations are shown in Fig. 2-7

through 2-10. The methods of Reference 2 were used to calculate the main bearing loads and the connecting rod force and piston side force with combustion occurring at 2% (average power) and 5% (maximum power) of the piston stroke after TDC. The reciprocating mass is 0.5 lb. and the displacement is 2.77 cu. in (1.50" bore x 1.57" stroke). Gas inlet pressures of 300 psi and peak combustion pressure of 900 psi, without throttling, determined the gas loads. The L/R ratio is 4.0.

Cooling System

In a regenerated engine it would be desirable to transmit all waste heat to the incoming hydrogen. The use of 2/1 O/F mixture ratio, however, does not furnish enough heat capacity in the hydrogen to handle the entire rejected heat load of the system. To bring the hydrogen to the highest inlet temperature with the smallest possible heat exchanger, it is desirable to regenerate exhaust heat, and to reject the lower temperature cylinder waste heat by a separate radiator. The engine cannot be insulated so that little or no heat escapes, since this would raise the operating temperature of the metal parts far above the allowable limit. The question then arises: Since heat must be rejected, how can it be done to maximize the useful available energy and still keep engine lubricated parts to an allowable temperature?

Some answers to this question are:

1. Use high temperature materials in the critical burning region bounded by the head and piston surface, and insulate this area to protect the cylinder walls and crankcase.

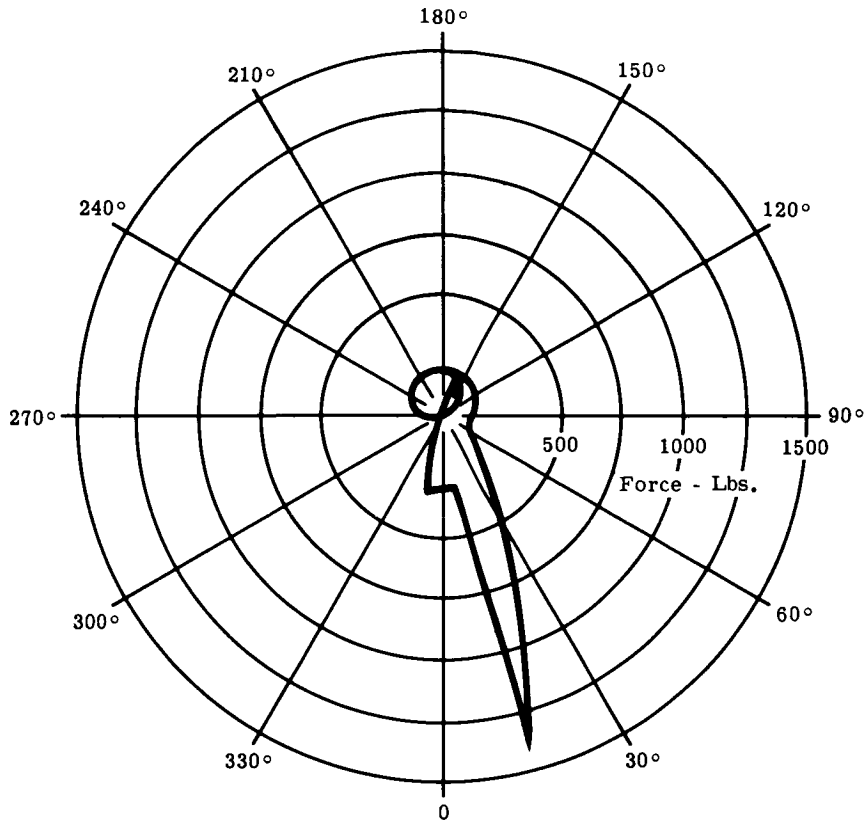

Fig. 2-7 - Main Bearing Load - 2%

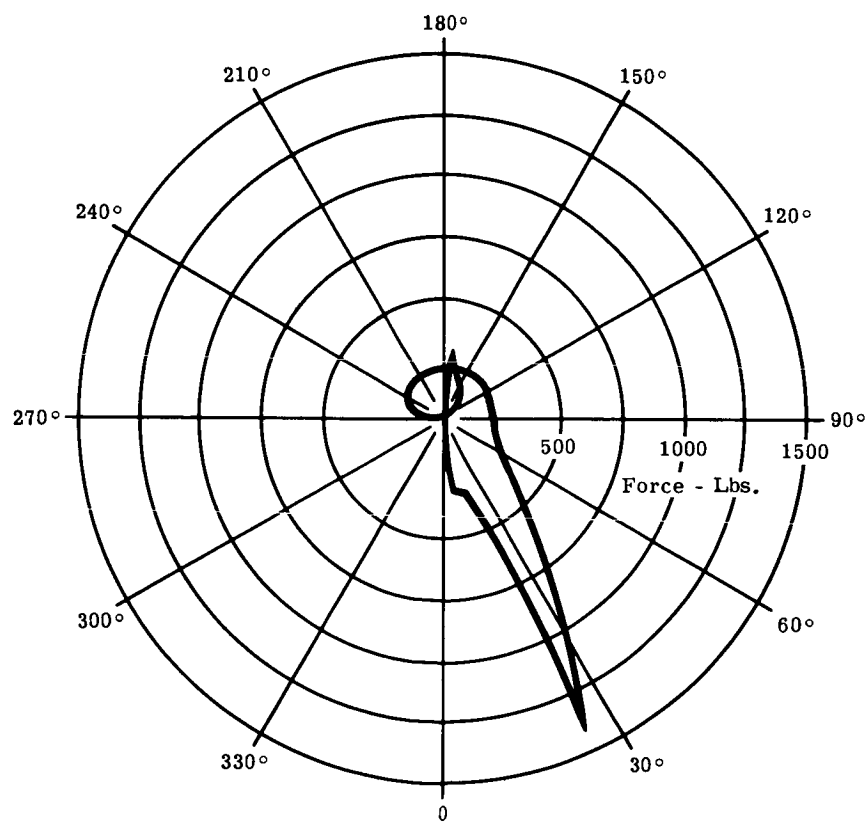

Fig. 2-8 - Main Bearing Load - 5%

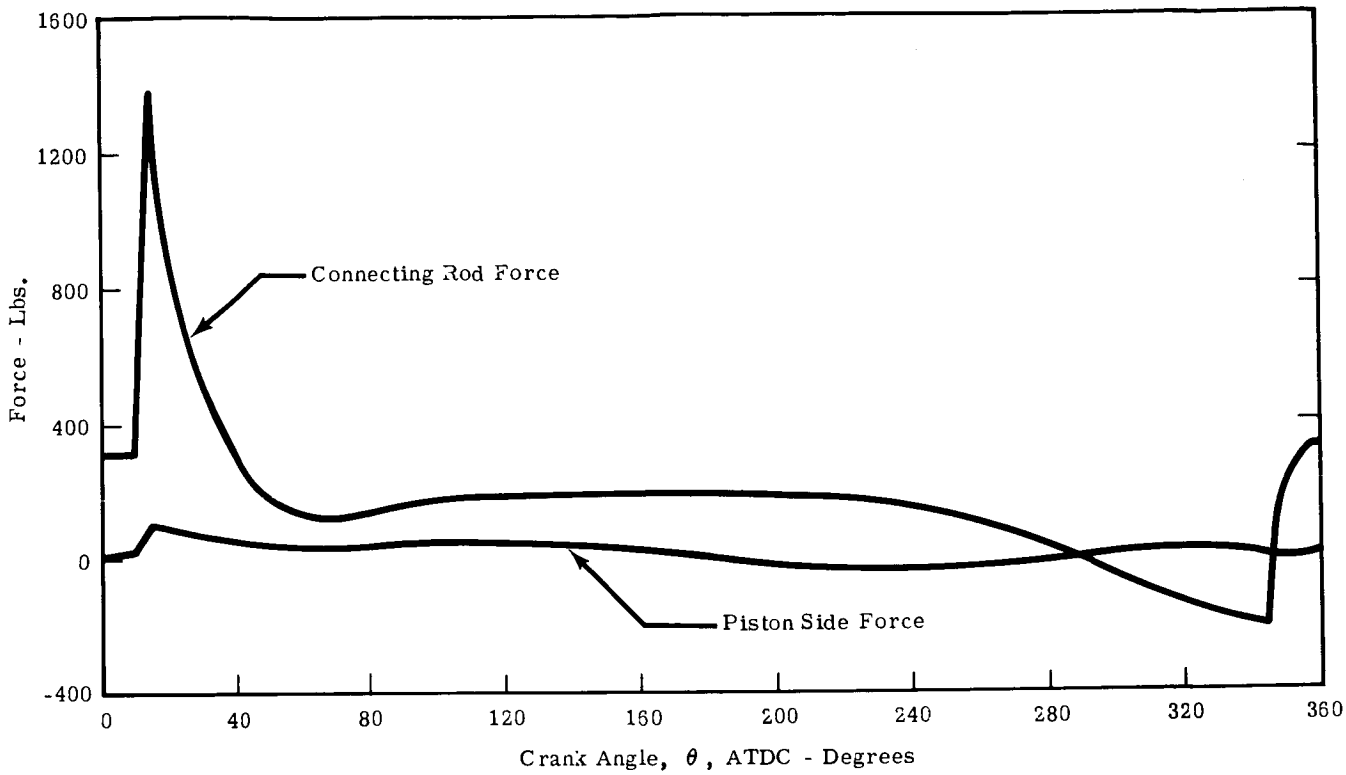

Fig. 2-9 - Reciprocating Forces vs. Crank Angle 2%

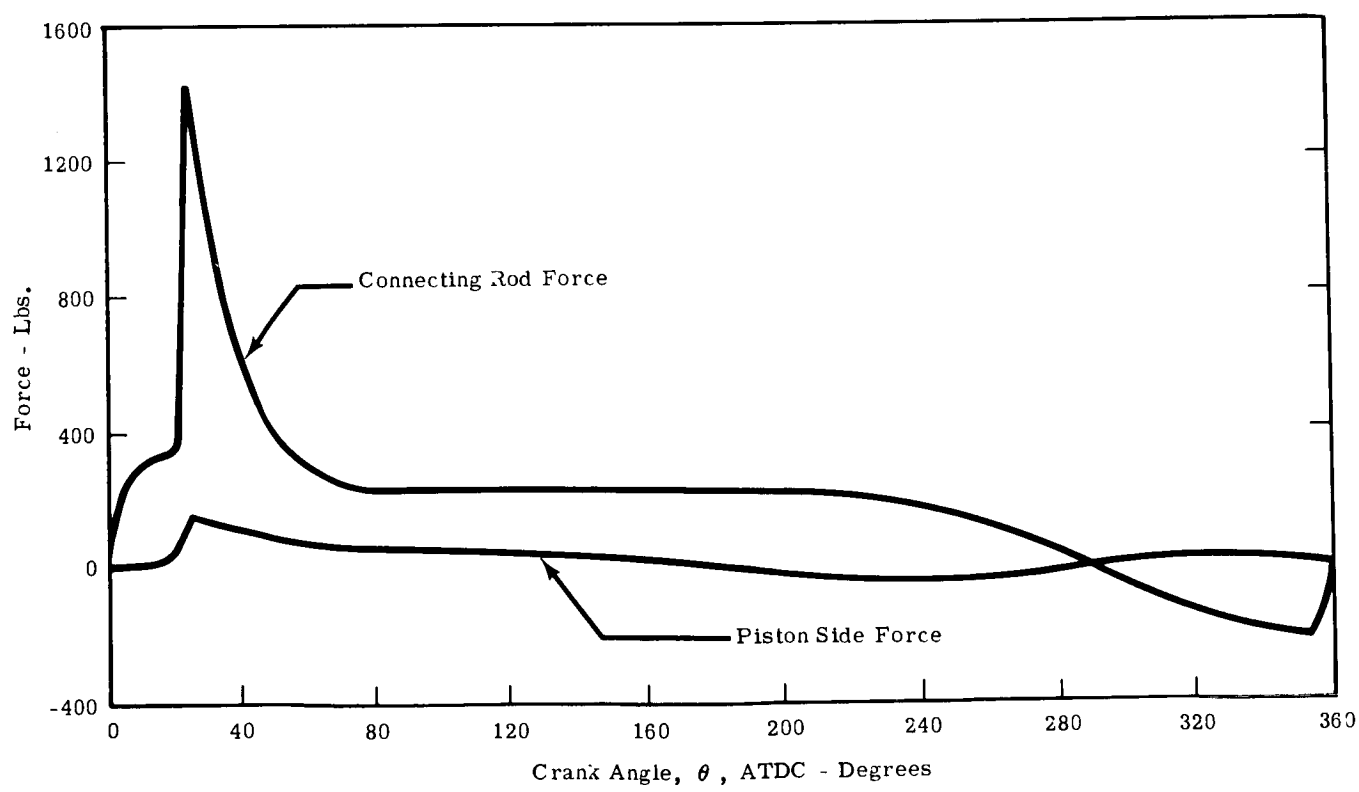

Fig. 2-10 - Reciprocating Forces vs. Crank Angle 5%

2. Keep the exhaust as hot as possible, to furnish heat for regeneration.

3. Isolate the combustion process in the combustion chamber,, so that the film coefficient between burning combustion gases and the adjacent metal surface will be as low as possible and a hotter mixture can be burned for the same peak metal temperatures.

The relative effect of heat rejection from the head or from the cylinder walls is given in Appendix B . The following two extremes are investigated in the analysis:

1. All heat rejected before the start of expansion (i.e. to the cylinder head).

2. All heat rejected to the cylinder walls during expansion.

The results show that the first assumption yields significantly lower efficiency. Therefore, from both the standpoint of efficiency and the standpoint of materials considerations, it is best to run an uncooled and/or insulated cylinder head, an insulated piston, and cooled cylinder walls.

The cylinder walls will be cooled by a liquid (such as ethylene glycol) circulating through the engine cooling jacket and rejecting heat to a space radiator. It is possible that the alternator cooling system and engine cooling systems may be integrated. However, the difference in their optimum operating temperatures makes this an area for additional study.

Zero-G Lubrication System

The lubricant metering pump is shown in View U-U of Fig. 2-1, and a sketch of the proposed lubricant flow path is shown in Fig. 2-11. A throw-away system is used which meters the correct amount of lubricant to critical areas by four independent lines. By this means the oil flow is less dependent on orifice sizes or line pressure and there is no change of one line robbing the flow from another. The four lines lead to the following critical areas:

1. Bearings (crankshaft, connecting rod, and balance weight)
2. Cylinder wall
3. Cam followers (by wick feed)
4. Hydrogen valve guides

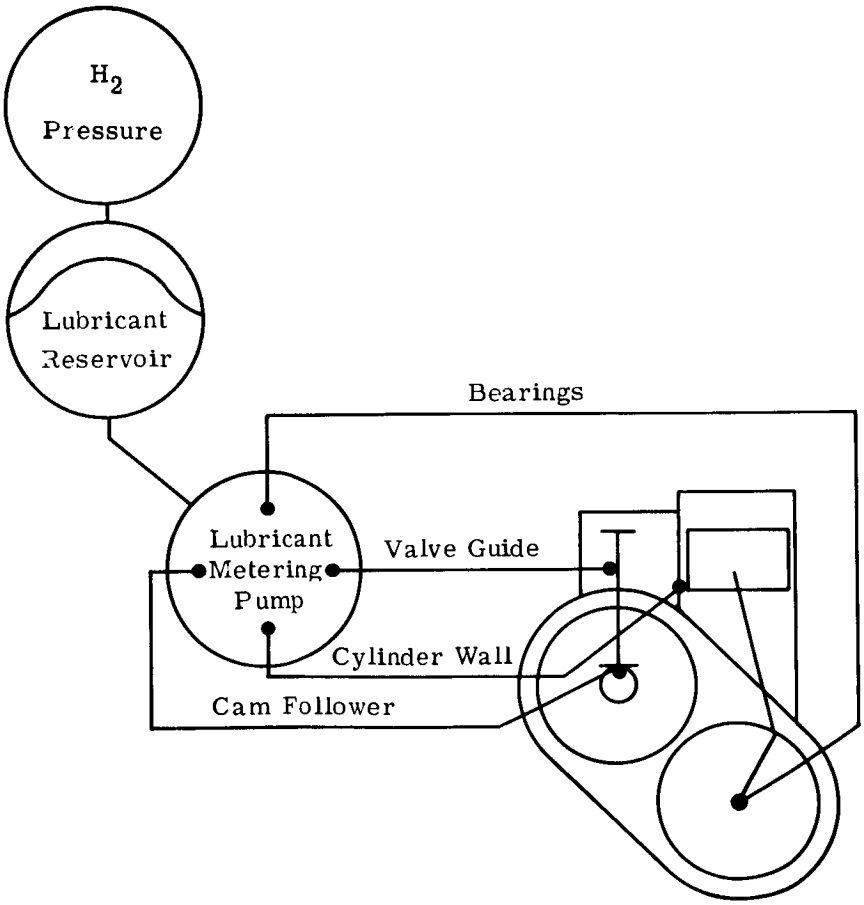

Fig. 2-11 - Zero-G Lubrication System

Flow rates will be determined by laboratory tests.

Each line is fed by a separate cylinder of the four cylinder barrel type, metering pump. A very low flow rate is possible with this pump, which uses a stroke of .062 in. imparted by the rotating barrel which contains four plungers actuated by a stationary wobble plate. Each plunger has a bore diameter of .062 in. Valving is accomplished by grooves in the cylinder as shown in View U-U of Fig. 2-1. Oil flow variation under load changes can be accomplished by providing a

variable wobble plate angle. Since the system is positive displacement and does not recirculate oil, both gravity forces and oil viscosity have no effect on system operation. Therefore, the problems of oil metering under engine warm-up or take-off operation are completely eliminated.

A throw away lubrication system is considered preferable for the following reasons.

1. The system can be tested on earth with reasonable assurance that it will work under zero-g conditions. This is not true of a recirculating system in which extensive testing under zero-g and random-g loads is necessary to ensure that oil will always return from the pockets where it might gather.

2. Less contamination problem, since oil is used once and rejected.

3. Far greater flexibility so that metering changes can be easily tested and incorporated under all stages of development without the necessity for redesign.

The reciprocating H_2-O_2 engine will consume oil:

1. By burning oil in the combustion chamber which has leaked past the piston rings or past the hydrogen valve guides.

2. By leakage of unburned oil out the exhaust ports.

3. By leakage past shaft seal, etc.

4. By accumulation in the crankcase from bearing and cam flow.

Internal combustion engine tests run with cylinder bores of varying porosity have established the fact that oil trapped and burned in pores in the cylinder wall can account for large increases in oil consumption. (See Ref. 3). Bore finish and piston ring-bore compatibility must be established by test. Careful design of the oil control rings and the exhaust ports is needed to limit oil flow into the combustion and exhaust areas and still insure adequate ring lubrication. Careful design and close tolerances can limit consumption by reducing oil leakage past the hydrogen valve guides and still assure adequate feed.

Results of tests conducted by Lycoming Inc., on their recently developed multifuel diesels show that low oil consumption is possible in a port exhaust engine. An oil consumption rate of .006 lb/hp-hr was demonstrated, (Ref. 4).

2.2.2. Hydrogen Compressor

The compressor was sized to handle incoming gas at the greatest specified volume and flow rate which would be encountered on the design mission, using the propellant consumption rates predicted by the parametric studies (Section 3). The compressor design is based on the first stage of the two-stage experimental compressor built and tested during this program. The cylinder bore diameter is .980 inches, piston stroke is .50 inch, and compression ratio is 20:1. The two stage compressor is discussed in Section 7-2.

2.2.3 Oxygen Compressor

The oxygen compressor is a two-stage design incorporating a rocking drive mechanism similar to that used in the experimental compressor built and tested in this program. The oscillating drive arm imparts a 1/2" stroke to the piston. Bore of the first stage is 0.50 inches and the bore of the second stage is 0.25 inches.

A poppet valve was selected for the first stage inlet valve. A reed type valve was considered, but it was decided that the poppet valve would be easier to manufacture successfully. The inlet and discharge valves for both stages are located in the cylinder heads to simplify the construction of the cylinders and to avoid conflicting material requirements which might be associated with attaining cylinder wear resistance and valve seat impact resistance.

2.2.4 Regenerator

The regenerator or recuperator is a compact heat exchanger which transfers engine exhaust heat energy to the incoming propellants. Although not shown in Fig. 2-1, the regenerator utilizes extended surface on the low pressure (exhaust gas) side due the lower film coefficient. At O/F ratios of 2:1 or less, practically the full thermodynamic benefit from regeneration is achieved by heating the hydrogen only. However, it is planned that the oxygen would also be heated in the regenerator to the same temperature as the hydrogen in order to simplify propellant metering.

2.2.5 Electrical System Description

This report section outlines and describes the conclusions reached as the result of analytical and design studies of electrical components carried out as part of the contract. The design philosophy is based on three major considerations: simplicity, reliability, and minimum overall weight penalty for earth take off.

The object of the studies was to specify a complete electrical generating system, associated with a hydrogen-oxygen reciprocating engine, capable of supplying the required electrical power at an overall design load efficiency of 90% for a minimum of 350 hours under conditions of zero gravity, temperature, shock, and vibration imposed by a typical manned space vehicle.

The scope of the study was limited to the analysis and description of the elements comprising an individual electrical generative system capable of ultimate paralleling with any similar system. The means, procedures, and considerations of parallel or redundant operation are subjects for further study.

2.2.5.1 Electrical System Requirements

The electrical system was designed to meet the following requirements and load profile, Fig. 2-12, as provided by NASA. Detailed electrical component design requirements are contained in Appendix C.

Operating Characteristics (Environment)

The APU will be required to operate in an environment

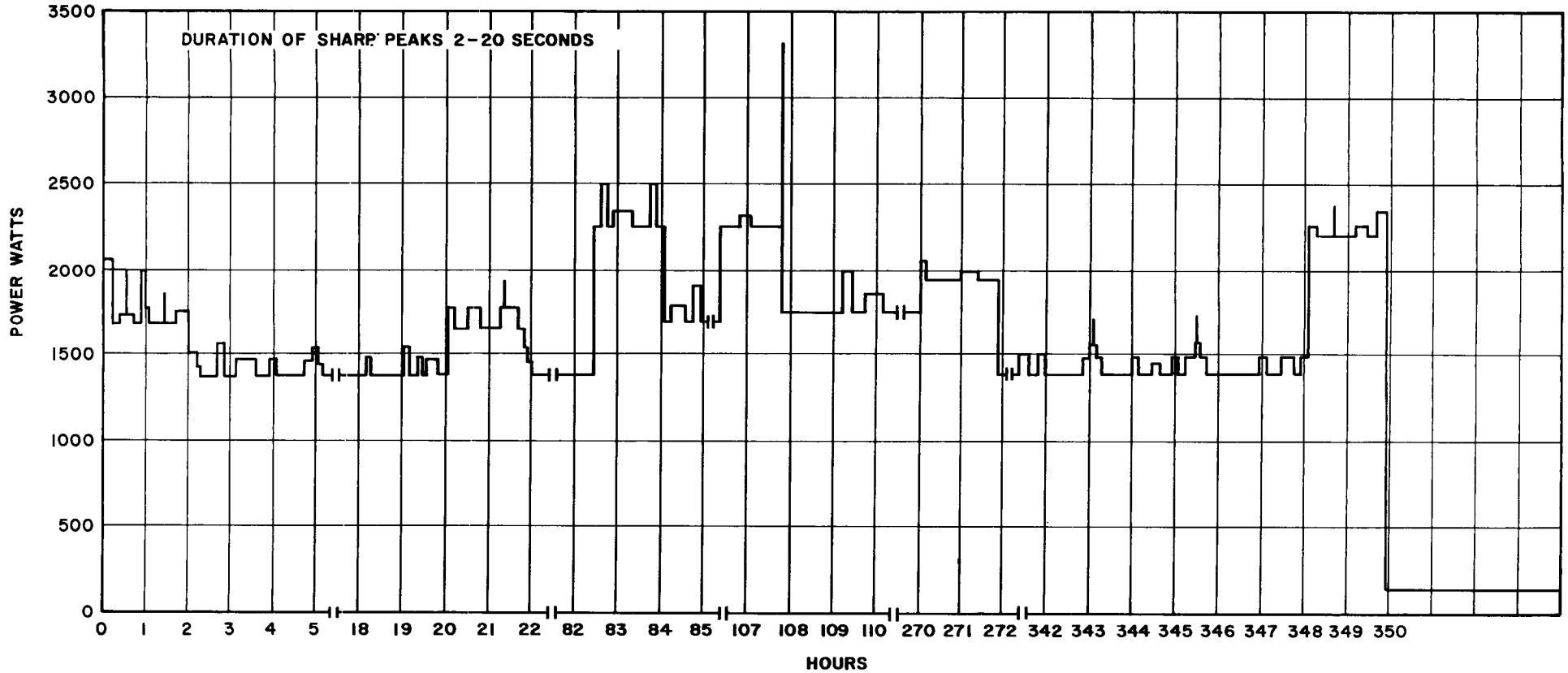

Fig. 2-12 - Typical Power Profile for Space APU

having a temperature range from +30°F to 165°F, and near absolute zero pressure.

Maximum anticipated acceleration load is 6-g.

Electrical Power Requirements

Usable average power output - 2 kw
Peak power output - 3 kw

AC Generator Requirements

400 cps ± .5%
3-phase, 4-wire, 115/200 V RMS
Tolerance: 115 V ± 2 volts. Maximum anticipated
Voltage unbalance 2% of worst phase to average
Load power factor .75
Harmonic distortion through 20 kc should not exceed 4% total
Response time: 0.7 second at output to any power level change within the operating range
AIEE and appropriate MIL standards apply in all other respects.

Control System

Control system encompassing engine speed control and generator voltage control shall be capable to accomplish above electrical requirements.

2.2.5.2 System Components

Alternator

A number of rotating machine configurations were analyzed with a primary view to obtaining a very high efficiency, i.e., better than 90%. A salient pole synchronous alternator of special design, utilizing field slip rings, was found to provide maximum efficiency on an overall excitation source-voltage regulator system basis. This type is schematically illustrated in Fig. 2-13. The maximum efficiency is attributable to the method of ingress of excitation current to the rotor, the voltage drop per brush being in the order of .3 volt with a total circuit drop of .6 volts. The analogous voltage drop of a bridge rectifier in brushless alternator designs is in the order of 1.8 to 2.0 volts. Of the "brushless" designs, the permanent

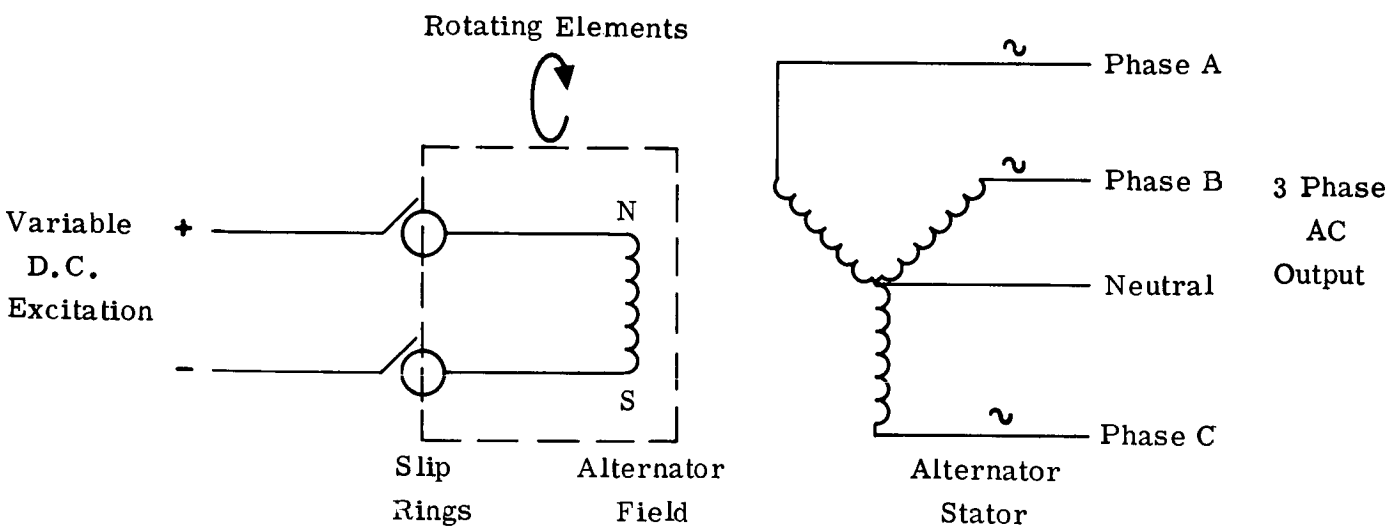

Fig. 2-13 - Synchronous Alternator with Slip Rings

magnet and the two stage wound dc field synchronous types were found capable of meeting the efficiency objective. However, the permanent magnet type was eventually abandoned for reasons of impedance and voltage regulation problems. Because of the lower voltage regulator operating power level and its reliability considerations, a "brushless" configuration alternator with one stage of exciter power gain was chosen as the preferred type. The loss in machine efficiency attributable to the exciter is partially offset by lower regulator power losses. A functional diagram of a simple two-stage "brushless" alternator of the general type is shown in Fig. 2-14. An analysis of the losses inherent in this design revealed that worthwhile improvements in efficiency may be realized by employing relatively high voltages in the rotating elements wherein the inherent voltage drop of silicon rectifiers is small in relation to the rectified output voltage applied to the field. Recent advances in insulation technology and in high

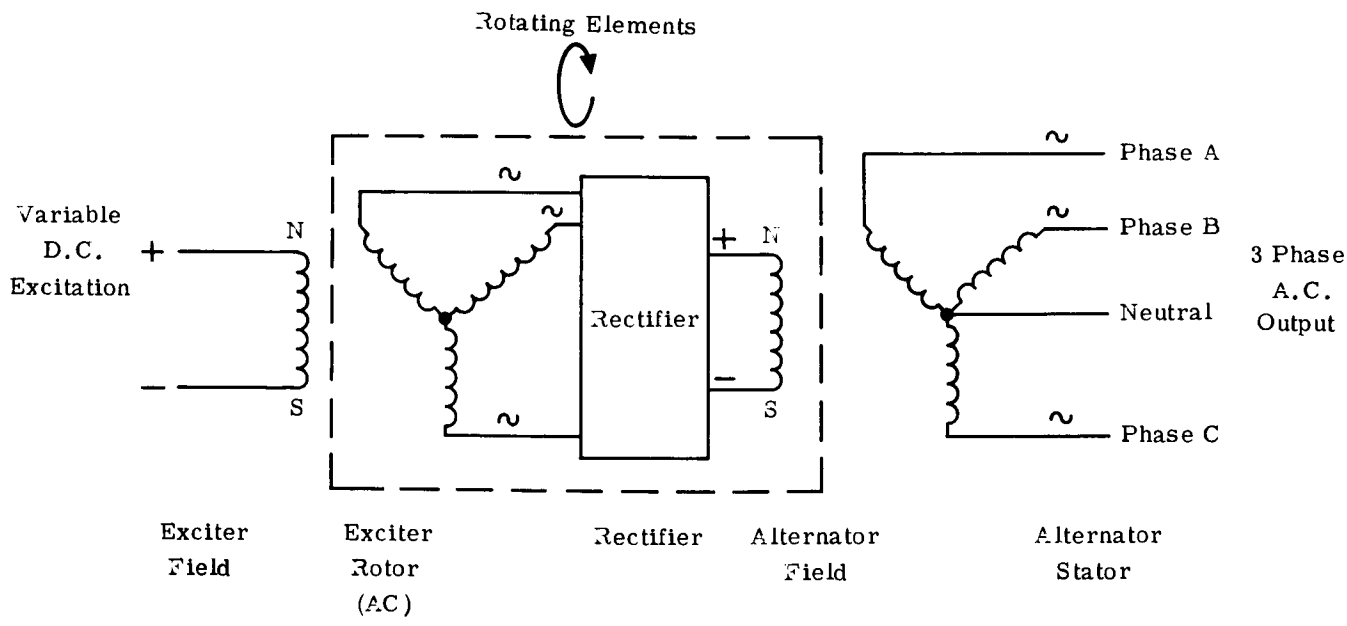

Fig. 2-14 - Brushless Synchronous Alternator

voltage, high temperature semi-conductors have solved the problems incumbent in this approach.

A novel mechanical arrangement of a two-stage "brushless" alternator was examined and is shown in Fig. 2-1. In this arrangement*, which may be termed "co-axial", the alternator field revolves on the outside of the stator, which is fixed. The exciter field is located within the alternator stator from which it is magnetically isolated. The exciter armature rotates within the fixed exciter field. It, and the alternator field are common to the shaft. The rectifier assembly is mounted on the extremity of the exciter armature from which it derives its input voltage. The rectifier output is directly connected to the alternator field.

This design lends itself to a single bearing overhung rotor as well as to a two bearing machine.

Since the rotating inertia of this design is the largest for a given machine weight, by virtue of the larger radius of the rotating mass, it is most useful for damping the velocity modulation arising from reciprocating piston engine drives. Mechanical integrity of the revolving field structure, particularly the windings, under the influence of high centrifugal forces, is superior to that of a conventional design, since centrifugal force tends to press the windings into the slots instead of the converse.

---

* Courtesy of Aeromarine Industries International, Societe' Anonyme.

Analysis of this design showed that alternator field losses and operating temperatures are materially reduced.

Correspondingly higher total flux is thus obtainable at modest excitation requirements, making it possible to reduce machine reactance sufficiently to meet unbalanced load and wave for requirements, while yet maintaining high efficiency.

Cooling

The alternator is cooled by glycol circulation through a heat exchanger located within the alternator case. An atmosphere of 1 to 2 psia comprised of hydrogen and water vapor shall be admitted to the alternator case through a partial seal from the engine crankcase at 150°F maximum. The alternator elements are cooled by conduction to the enclosed atmosphere and thence to the heat exchanger.

The circulative glycol inlet temperature is regulated within the limits of 35°F to 50°F at 1 to 2 gpm flow.

Alternator Speed vs. Efficiency and Weight

A comprehensive study of alternator losses vs. weight for 12 pole, 8 pole, and 4 pole machines, corresponding to 4000, 6000, and 12,000 rpm, was undertaken. Table 2-1 shows the tabulated results of this analysis. These data represent conventional salient pole wound rotor synchronous machines, and the efficiency figures quoted include exciter losses, regulator losses, and that portion of the starter-generator losses attributable to the excitation source, including battery.

TABLE 2-1

ALTERNATOR DESIGN PARAMETERS

Machine Parameters	Speed - rpm		
Active Materials	12,000	6000	4000
Number of Poles	4	8	12
Stator Lamination O.D., Inches	5.5	8.0	10.0
Stator Lamination I.D., Inches	3.25	5.50	7.75
Number of Stator Slots	36	36	54
Number of Stator Coils	36	36	54
Number Turns per Coil	10	6	4
Coil Connection	Parallel	Series	Series
Stator Copper Losses, Watts	24	40.8	41
Stator Iron Losses, Watts	76	49.4	56
Stator Length, Stack, Inches	3.5	1.5	1.5
Stator Weight, Lbs.	18.3	11.2	12.2
Field Rotor O.D., Inches	3.23	5.48	7.73
Pole Arc %/Inches	60/1.53	60/1.3	70/1.42
Excitation, Full Load, 1.0 p.f., at	225	257	215
Excitation, Full Load, .75 p.f., at	285	328	270
Field Rotor Length, Inches	3.75	1.625	1.75
Field Copper Losses, Watts	24	27.4	30
Field Rotor Weight, Lbs.	7.1	8.2	16.0
Total Weight, Active Materials, Lbs.	25.4	19.4	28.2
Mechanical Losses, Watts	60	60	50
Total System Losses, Watts	237	232	233
System Efficiency, Percent at 60°C	90.4	90.6	90.6
Losses in Machine plus Regulation, Watts	177	172	183

The weight shown are for active materials in the rotor, or field, and in the stator, required to meet a common system efficiency of 90.5% of overall. The weights of the exciter elements are not included, nor are the weights of the shaft, bearings, frame, and end bells. It may be reasonably estimated that weights shown are subject to a typical multiplication factor of 1.6 to obtain the total machine weight.

Voltage Regulation

Many voltage regulator and regulation system schemes were studied. Typical forms and methods are illustrated in Figs. 2-15 through 2-20.

System analysis revealed that several modes exhibit serious shortcomings during transient and fault clearing conditions. While the schematic shown in Fig. 2-15 has the highest reliability because of the nature of the components, the fastest response, and the best transient stability, it is frequency sensitive and subject to voltage drift with temperature, beyond the specification limits. It is further subject to variations with changes in alternator load power factor beyond the specification limits. A large amount of development effort would be required to perfect this scheme to meet the regulation requirements. Additional excitation circuitry is required to accomplish voltage buildup on starting. For these reasons, and for weight considerations, it was not considered further.

The modes illustrated in Figs. 2-16, 2-17, and 2-18 suffer from a common deficiency in fault clearing capability and exhibit inferior voltage recovery on large step load changes. For these reasons, they were not further considered.

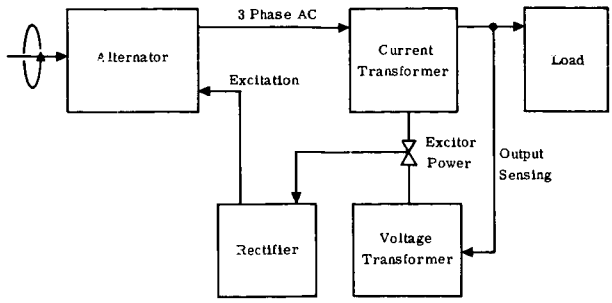

Fig. 2-15 - Simple Self-Excited Compound Regulated Alternator without Voltage Reference

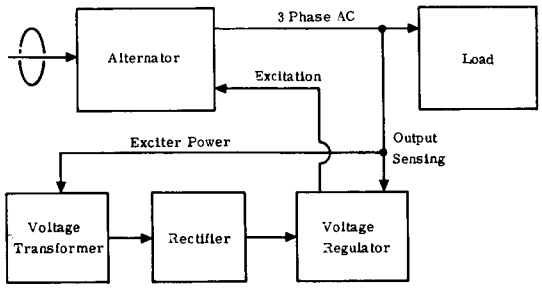

Fig. 2-16 - Simple Self-Excited Regulated Alternator

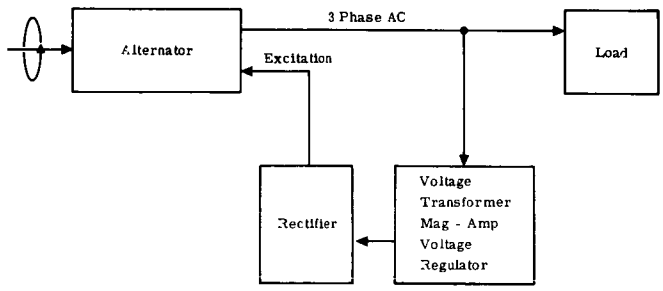

Fig. 2-17 - Simple Self-Excited Regulated Alternator

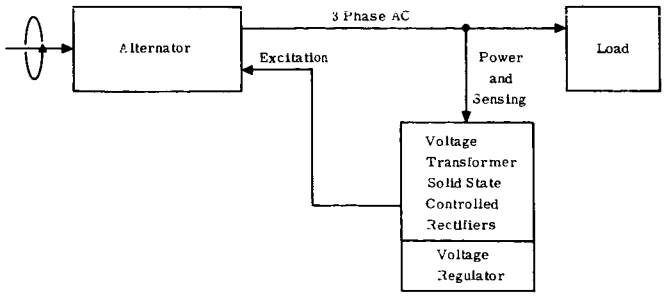

Fig. 2-18 - Simple Self-Excited Regulated Alternator

The scheme shown in Fig. 2-19 overcomes many of the deficiencies described above except that it requires an external source of dc power to accomplish voltage build-up on starting, through "field-flashing", with control circuitry. For this reason, and for reasons of incomplete reliability data on silicon controlled rectifiers used with current transformers, with consideration of complexity and weight, it was concluded that this mode should be considered with reserve.

From a system analysis, the scheme shown in Fig. 2-20 is recommended and offers the following advantages:

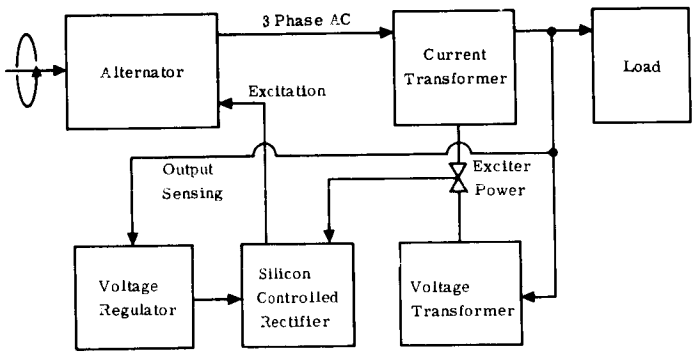

Fig. 2-19 - Simple Self-Exciter Compound Regulated Alternator with Voltage Reference

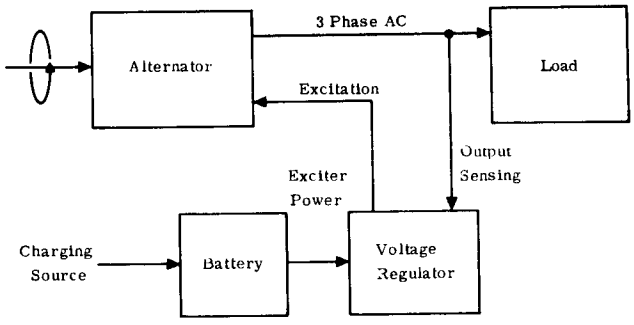

Fig. 2-20 - Separately Excited Regulated Alternator

1. Voltage build-up is inherent
2. Voltage build-up is automatic on starting
3. Fault clearing capability is inherently good
4. Paralleling characteristics are excellent
5. Fewest circuit elements are needed
6. Reliability is good
7. Weight is minimum
8. Existing engine starting battery is utilized as active element

Voltage Regulators

Several types of voltage regulators were studied to determine the most efficient method of controlling alternator excitation. The two general means are represented by Figs. 2-21 and 2-22. The means shown in Fig. 2-21, termed variable voltage source, provides the lowest regulator losses by virtue of having no

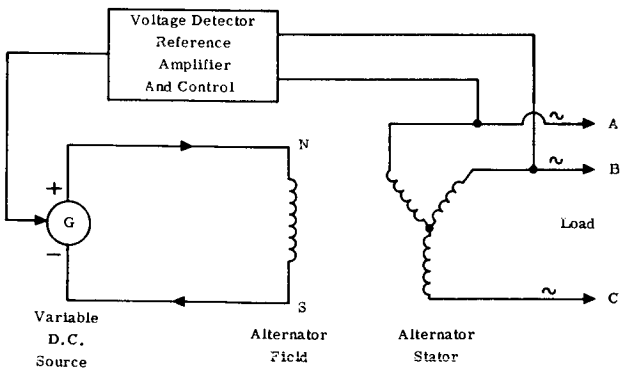

Fig. 2-21 - Alternator Voltage Regulator Loop

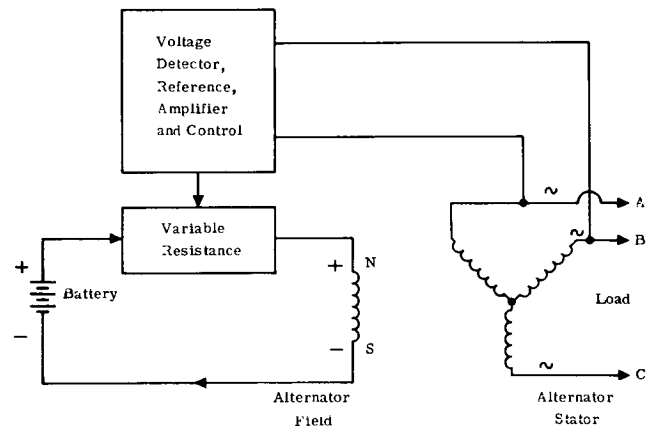

Fig. 2-22 - Alternator Voltage Regulator Loop

series resistance between the excitation source and the alternator field. The excitation source voltage must, however, be itself controlled, and some form of regulation means is required for it. The internal regulator losses involved at progressively lower energy levels become modest in this scheme in relation to the total alternator output. Typical regulator loss relationships are shown in Fig. 2-23.

The means shown in Fig. 2-22, termed fixed voltage source, variable conduction, is more common in practice. The basic form of the basic form of the means illustrated in Fig. 2-22 is shown in Fig. 2-24. The variable resistance element dissipates appreciable energy, resulting in lower overall system efficiency.

The regulator watt losses in this scheme are particularly objectionable at .5 maximum alternator output, which corresponds generally to full rated load at unity power factor. The

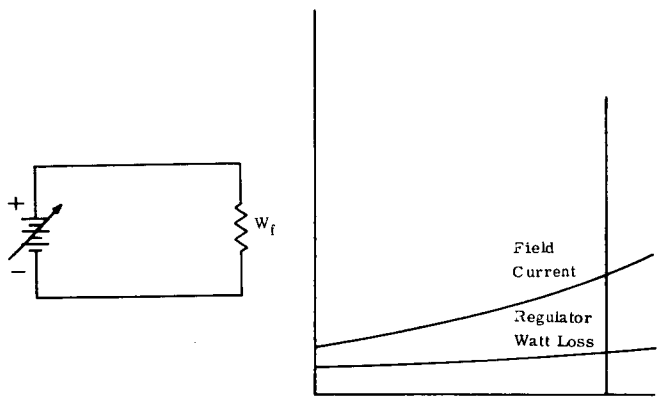

Fig. 2-23 - Regulator Watt Loss

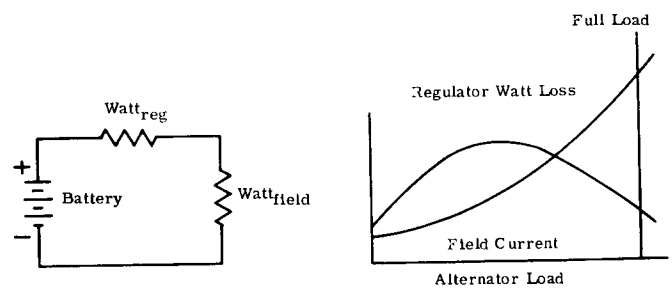

Fig. 2-24 - Regulator Watt Loss

energy so dissipated presents a hazard to other components in the regulator and reduces the intrinsic reliability of the apparatus. For these reasons, form 2-24 was not further considered.

An interesting variant of the method shown in Fig. 2-24 which overcomes this deficiency is shown in Fig. 2-25. Here, the variable resistance element is formed in effect by an opening and closing contact. The relative conductance of the circuit is determined by the ratio of closed time to open time. The energy loss of this method is theoretically zero for the reason that I (excitation current) and E (regulator voltage drop) do not exist at the same time, thus not satisfying the equation: E x I = W (loss). The on-off switch, reg., is provided in the modern concept by a solid state device with suitable forward EMF protection analogous to that of an RC spark suppression network or diode employed with contacts.

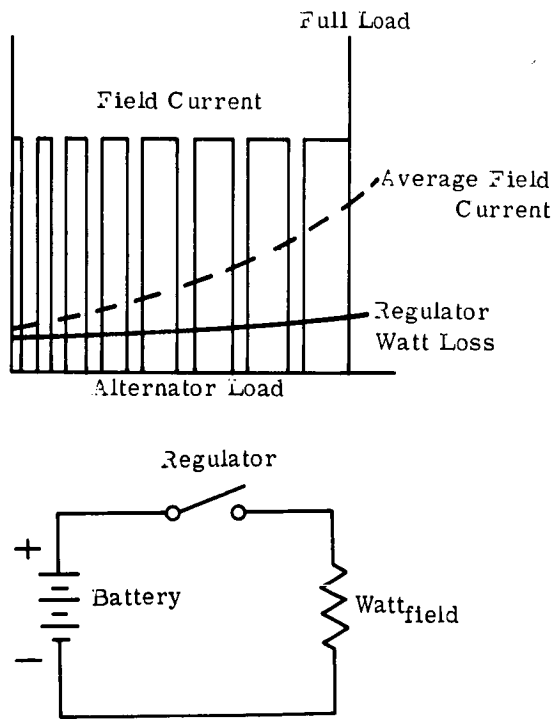

Fig. 2-25 - Regulator Watt Loss

Analysis of this scheme reveals that the lowest system weight may be obtained by reason of the elimination of current and associated voltage transformers. Examination of the reliability aspects showed that this scheme, when used in conjunction with a battery

excitation source, is capable of achieving more than adequate reliability to meet the overall system requirement. The choice of the scheme shown in Fig. 2-25 was further based on the relatively low energy levels associated with the primary excitation requirements of the "brushless" alternator configuration shown in Fig. 2-14, and similar two-stage machines.

2.2.5.3 Engine Starting System

Figs. 2-26 and 2-27 show two functional schematic diagrams representing engine starting methods.

Fig. 2-26 shows a dc starter-generator scheme with regulated voltage output and output current limiting by means of a differentially compounding series field. In the starting mode, with the engine stopped, the contactor is closed, allowing

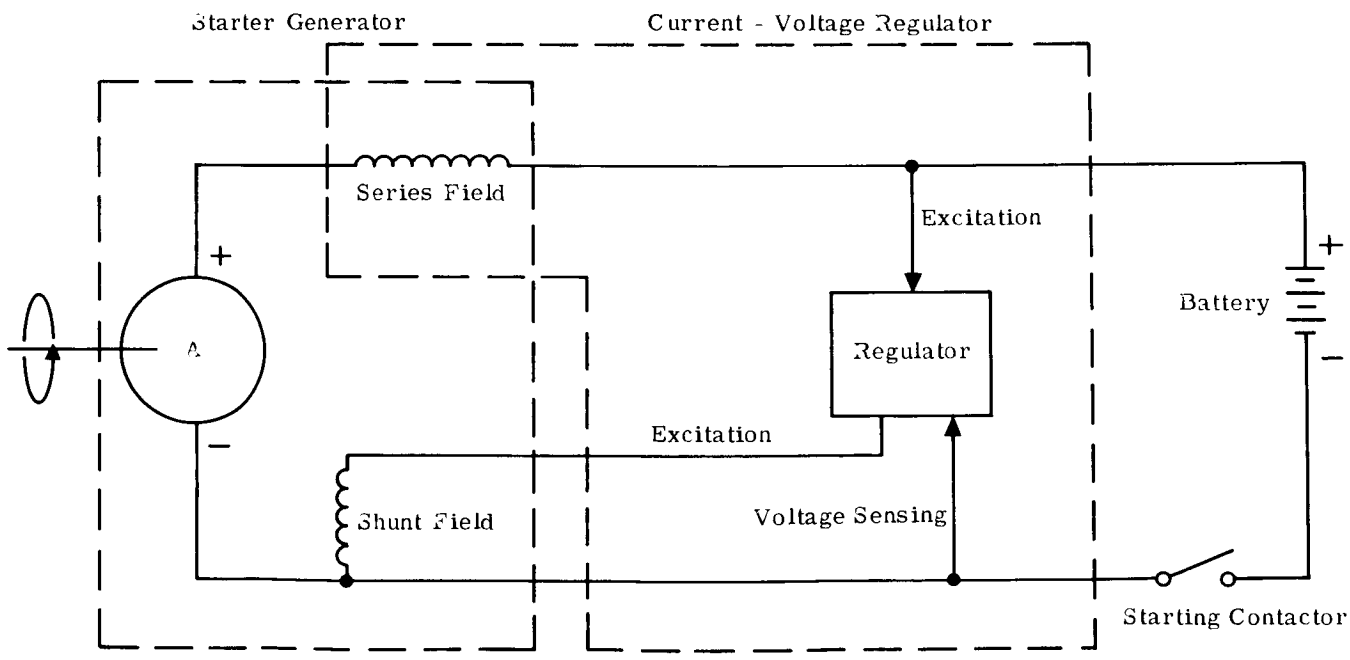

Fig. 2-26 - Starter-Generator Functional Schematic Diagram

battery current to flow through the field and armature circuit. High starting torque is inherent in this design. When the engine fuel ignites, the engine speed increases and drives the dc machine as a generator. Its output voltage is regulated by means of a shunt field to the end of charge voltage of the battery, with suitable temperature compensation. The two field constants are arranged so that the battery charging current is limited to the maximum safe operating point for the generator or the battery.

The dc starter-generator commutation requires some development for operation in low pressure hydrogen and water vapor atmospheres; however, the inherent reliability of this scheme recommends it as the preferred starting system.

The battery requirements for engine starting are based on the following parameters:

1. Minimum engine speed - 600 rpm
2. Maximum torque 30 inch-lbs.
3. Maximum cranking time-30 seconds for three consecutive cycles separated by not less than one minute
4. Minimum battery electrolyte temperature 50°F
5. Maximum battery electrolyte temperature - 160°F at end of third cycle.

From 1) and 2) the peak starter horsepower is

$$HP = \frac{600 \times 746}{630.25} = .286$$

At 70% starter efficiency, the peak input power is

$$\frac{.286 \times 746}{.70} = 304 \text{ watts}$$

At 10.8 volts input, at full load, the motor current is 31.5 amperes.

A silver cadmium battery was chosen for this application. The theoretical ampere hour capacity based on 1.5 minutes is

$$\frac{1.5}{60} \times 31.5 = 1.26 \text{ ah}$$

However, at the interrupted 1.5 minute rate, the discharge efficiency is approximately 25% at a median temperature of 95°F, hence the nominal one hour ampere hour capacity rating must be

$$\frac{1.26}{.25} = 5.04 \text{ ah}$$

For maximum reliability with a silver cadmium battery the end of charge voltage should not exceed 1.6 volts per cell. An eighteen cell battery was selected, having a total end of charge voltage of 28.8, and comprised of 5 ampere-hour cells at the one-hour rating. The terminal voltage at a discharge rate of

31.5 amperes at the end of three starting cycles will be approximately 11.0 volts.

Fig. 2-27 shows an inverter-battery charging scheme which employs silicon controlled rectifiers to convert battery voltage to low frequency alternating current in the starting mode, and which rectify a portion of the alternator output power for battery charging and maintenance in the charging mode. Operation is automatic, as in the case of the scheme shown in Fig. 2-26. During the starting mode, the inverter provides a 66 cps, 3-phase power at a voltage sufficient to motorize the alternator at 30 inch-lbs. torque as an induction motor. At 10% slip. the alternator will run at 600 rpm.

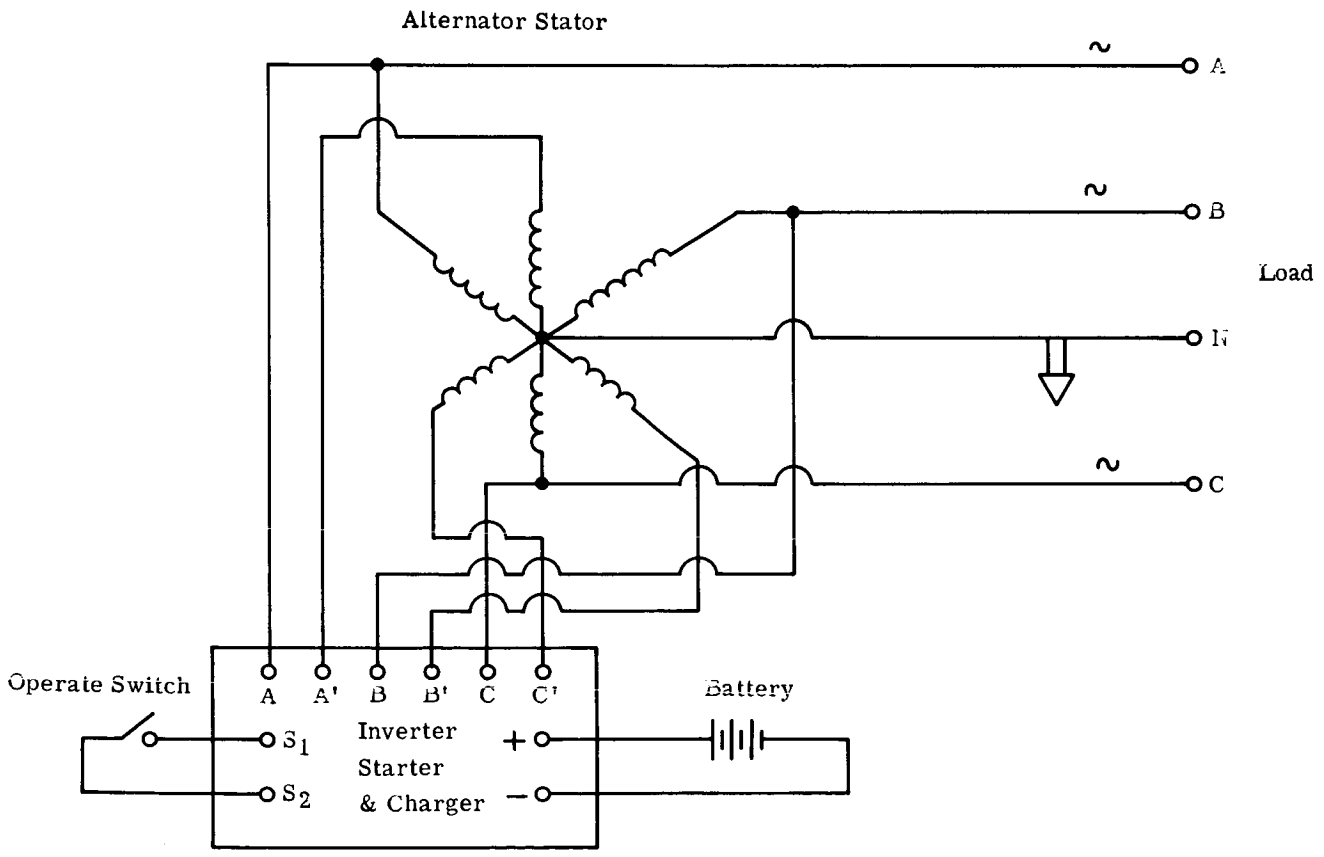

Fig. 2-27 - Schematic - Alternator with Inverter Starter

Since the efficiency of an inverter utilizing silicon semiconductors operating at 10.8 volts dc input, is in the order of 75%, slightly less battery capacity for starting is required.

Comparative weights for the two alternate starting systems are given below:

DC starter-generator, with filter - 4.3 lbs.

Silicon controlled rectifier, with filter - 8.0 lbs (estimated).

Start-Up Procedure

Regardless of which method of obtaining cranking power for use in rotating an idle engine to starting speed is employed, the tentative start-up procedure remains the same. If start-up is on supercritical tankage gas, the engine valves are timed for maximum power and hydrogen is admitted during spin-up and allowed to motor the engine. Oxygen is then admitted through an open oxygen throttle until ignition occurs. Little battery power is needed for this mode of starting since the stored hydrogen and oxygen are doing most of the work.

Start-up on boil-off gases requires enough battery power to motor the engine and compressors until there is enough propellant flow to ignite and burn in the engine. Again, the engine valves will be timed for maximum power. Minimum motoring speed must be determined by experiment, but probably need not be more than 600 rpm. Upon ignition, the engine will accelerate to 4000 rpm.

2.2.5.4 Conclusion

It is recognized that the results of this study are mainly of a system requirement nature and before system design begins, another evaluation of all the aspects of mechanization will be made. In the area of requirements, an effort to continuously update the existing requirements is necessary.

2.3 System Operation

The H_2-O_2 engine power system has been designed to operate from either of two propellant sources:

1. Cryogenic hydrogen and oxygen stored on board the spacecraft in supercritical tankage or;

2. Cryogenic hydrogen and oxygen boiloff gases which may be available as waste from propulsion stage propellant tankage. Propellant selector valves connect the power system to the proper propellant source.

2.3.1 Operation with Supercritical Tankage

Hydrogen and oxygen are maintained at supercritical pressures by heat addition to the cryogenic storage tanks using electric heating coils within the tanks. The heat addition rate is determined by the propellant withdrawal rate. The propellants are fed by tank pressure through the regenerator into the cylinder of the internal combustion engine. The hydrogen and oxygen absorb heat from the exhaust gas in the regenerator, thereby raising their temperatures and decreasing density to give lower specific fuel consumption.

Studies have shown that the optimum supercritical storage pressures for this system are 300 psia for the hydrogen and 900 psia for the oxygen.

2.3.2 Operation with Boiloff Gases

For operation with boiloff gases, the propellant selector valve is set for boiloff operation and a magnetic clutch is engaged, connecting positive displacement compressors to the engine crankshaft. These compressors raise the boiloff hydrogen to 300 psi and the oxygen to 900 psi (the same pressures as for operation with supercritical storage). The gas then enters the regenerator, following the same sequence as in pressurized tank operation. Boiloff operation is less efficient, due to the necessary compressor work performed by the engine; however, some or all of the fuel is essentially "free", since the boiloff gases would otherwise be vented to space.

2.3.3 System Cooling

The system is designed to operate at a O_2/H_2 mixture ratio of 2.0 by weight. This limitation has been fixed by maximum permissable cycle temperatures. With this mixture ratio, the heat capacity in the incoming hydrogen is insufficient to absorb the engine waste heat and the heat rejected by the alternator, so a radiator is needed. With negligible increase in SPC, but with greater propellant volume, operation at O/F = 1.25 to 1.40 would provide sufficient heat sink in the hydrogen fuel to absorb the engine and alternator waste heat, thus avoiding the need for a radiator to cool the power system. Nevertheless, a radiator would be required to reject the waste heat from the rest of the spacecraft equipment, i.e., electronics, environmental, and life support systems.

2.3.4 Speed Control

As described in detail in Section 5, the power system speed control consists of a tachometer-generator which provides an engine speed signal to an error sensing network. Deviation of this speed signal from an established reference level causes an error signal to be applied to the engine speed control activator (an electric servo motor).

The servo motor advances or retards the hydrogen and oxygen valve timing to adjust engine power output as required, to bring engine speed (and alternator frequency) back to the desired value.

3.0 PARAMETRIC STUDIES

3.1 Introduction

The parametric studies were made to rationalize an approach to the design of an optimum auxiliary power system. Hence, a number of thermodynamic cycles were analyzed and power modulation studies were made to determine the most efficient method of controlling the fuel flow requirements for various missions and off design conditions.

3.2 Description of Representative Hydrogen-Oxygen Systems

In this section various types of H_2-O_2 engines are briefly described. The contract permitted detailed study of the fuel rich regenerative internal combustion cycle only. Limited effort was devoted to study of other approaches, and they are presented for reference purposes.

3.2.1 Fuel Rich Internal Combustion System

An internal combustion, fuel rich, regenerative system is shown in Fig. 3-1. This system operates at O/F = 2.0 and and a BSPC of approximately 1.0 lb/hp-hr can be expected. This system draws cryogenic propellants, hydrogen and oxygen, from either of two propellant sources; (1) propulsion tank boil-off, (2) on-board supercritical storage tanks. It is important to note that the propellants are supplied to the system at elevated pressures, either from pressurized storage or by means of engine-driven compressors. To provide the maximum thermodynamic benefits from the recycling of thermal exhaust energy, it is important that propellant

Preceding page blank

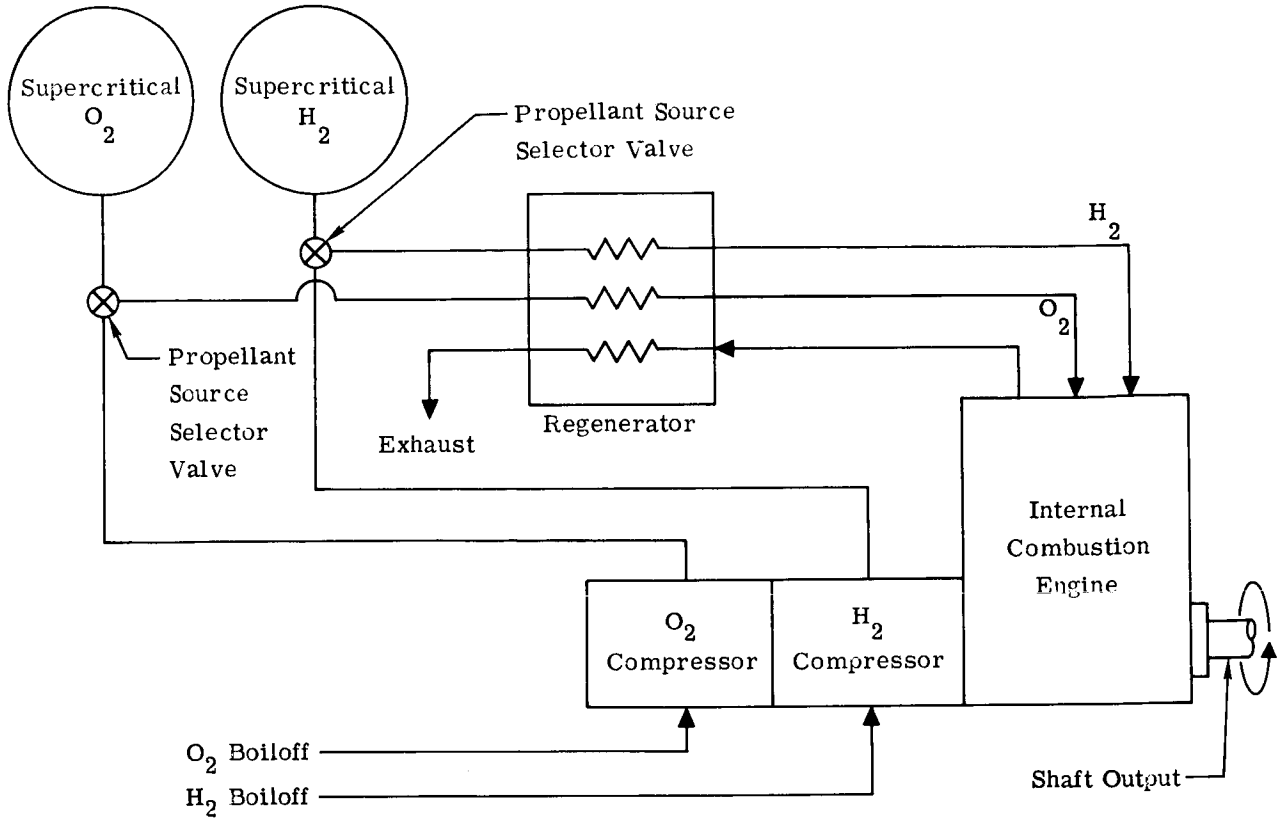

Fig. 3-1 - Fuel Rich Regenerative H_2-O_2 Engine System

pressurization occur before the heat addition and that no compression of these propellants take place after the addition of heat in the regenerative heat exchanger. The O/F ratio of 2.0 was selected because this mixture ratio results in a combustion temperature in the same order of magnitude as found in conventional air-breathing internal combustion engines. The thermal efficiency for this cycle is estimated to be in the 45% to 55% range.

3.2.2 Stoichiometric Systems

Two stoichiometric H_2-O_2 engine cycles were studied. The first system (Fig. 3-2) uses an internal compression internal combustion engine with no regeneration. This system may operate with either combustion occurring under fuel-rich conditions, with the excess hydrogen recycled to act as a diluent, or it may operate with combustion occurring at stoichiometric mixture ratio of hydrogen and oxygen, with

exhaust steam recycled as the diluent to limit the combustion temperature to acceptable values.

The second stoichiometric cycle involves the regenerated cycle illustrated in Fig. 3-3. In this cycle a portion of the engine exhaust steam is condensed and then pumped to high pressure. The propellants are also pumped to high pressure; 300 psi for the H_2 and 900 psi for the O_2. Both propellants and diluent are heated regeneratively by the exhaust prior to to their admission to the engine.

The chief advantage of the stoichiometric (O/F = 8) system is that it significantly reduces the volume of propellants required. Thermal efficiency of the non-regenerated cycle (Fig. 3-2) is estimated to be in the 35% to 40% range and for the regenerated cycle (Fig. 3-3), 40% to 55% range. The thermal efficiencies achievable are dependent upon the degree of sophistication and efficiency of the system components, i.e., heat exchangers, pumps, engines, condensers, etc. One disadvantage of the stoichiometric type of system, in any form, is that it requires a larger amount of heat to be rejected from the system than does a fuel-rich cycle. This high heat rejection results from the necessity of cooling the hot exhaust fluid down to temperatures which are acceptable for recycling a portion of the exhaust into the engine to act as a temperature limiting diluent. At the same time, the stoichiometric system has a much lower heat sink available in its cryogenic propellants than does a fuel-rich system. The net result of these effects is that the stoichiometric system will result in a higher thermal loading of the vehicle heat dissipation system than will a fuel-rich hydrogen/oxygen system.

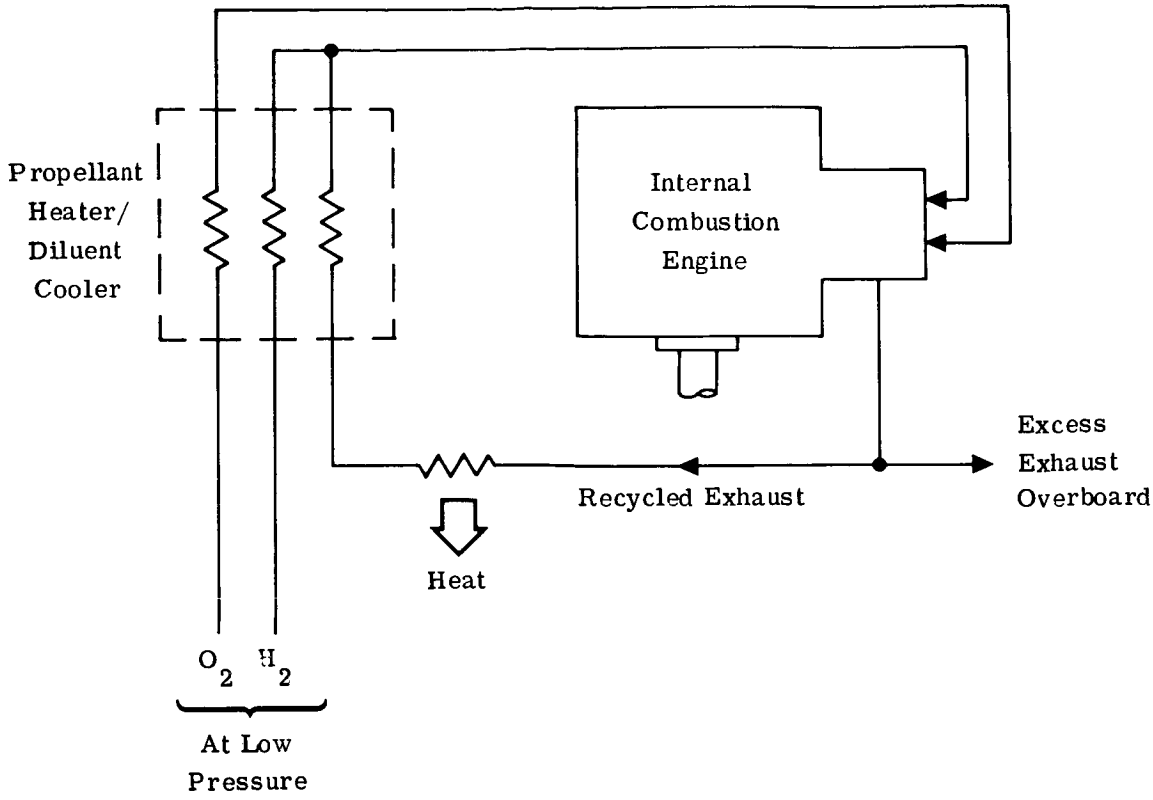

Fig. 3-2 - Non-Regenerated Stoichiometric H_2-O_2 Engine System

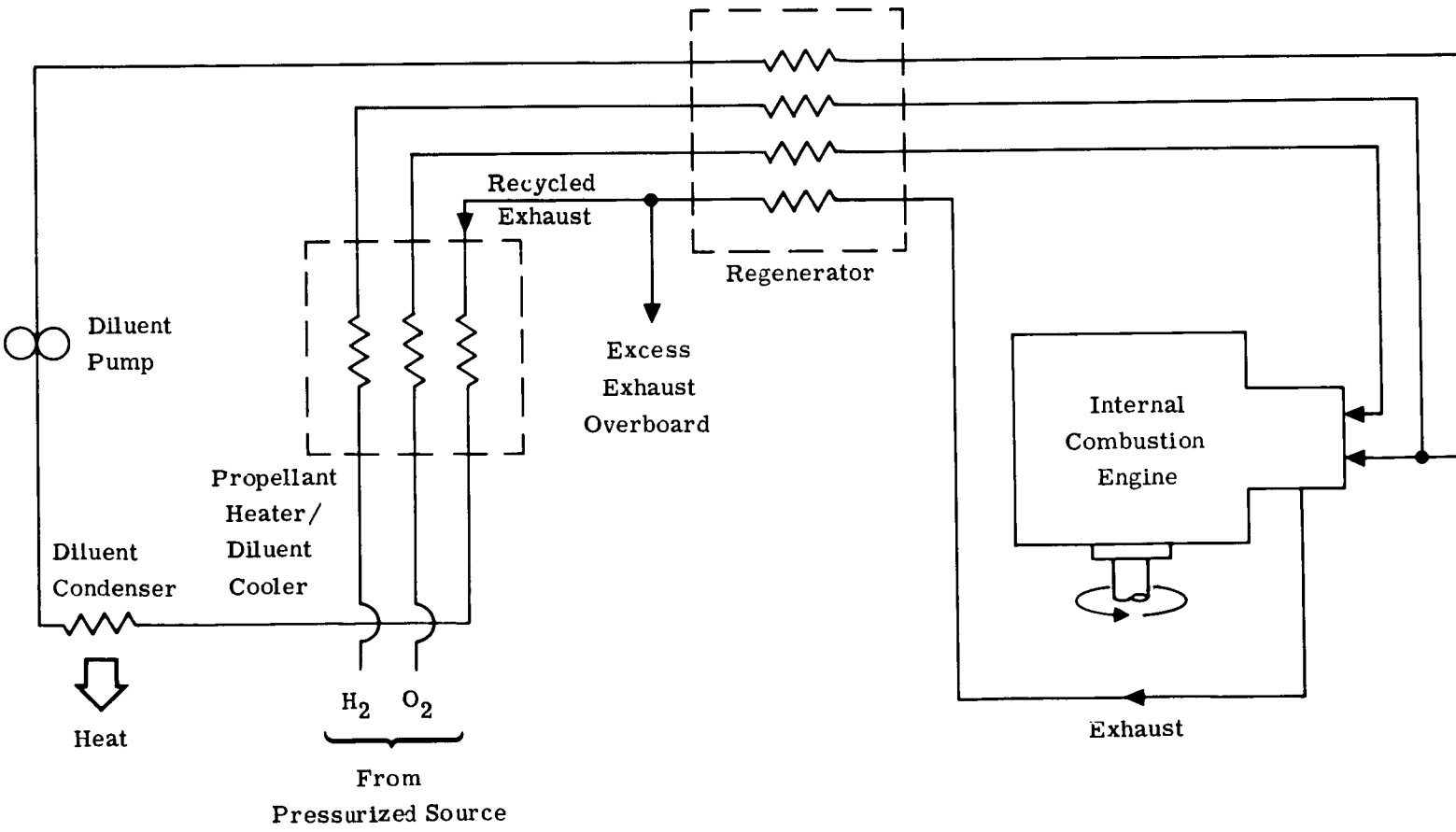

Fig. 3-3 - Regenerated Stoichiometric H_2-O_2 Engine System

3.2.3 Fuel-Rich Internal Compression System

An internal compression fuel rich cycle is illustrated in Fig. 3-4. In this system, propellants at low pressure (from boiloff, for example), are preheated by the engine exhaust to a temperature which is convenient for the propellant handling valves. They are then admitted to the engine cylinder, where compression occurs in a manner analogous to that of an air-breathing engine, followed by the other cyclic events of either the 2 stroke or 4 stroke cycle. This system may permit operation on boiloff (low pressure) propellant, but cannot enjoy the thermal benefits of regeneration since compression occurs within the engine cylinder. Thermal efficiency for this cycle is estimated to be in the 35% to 40% range.

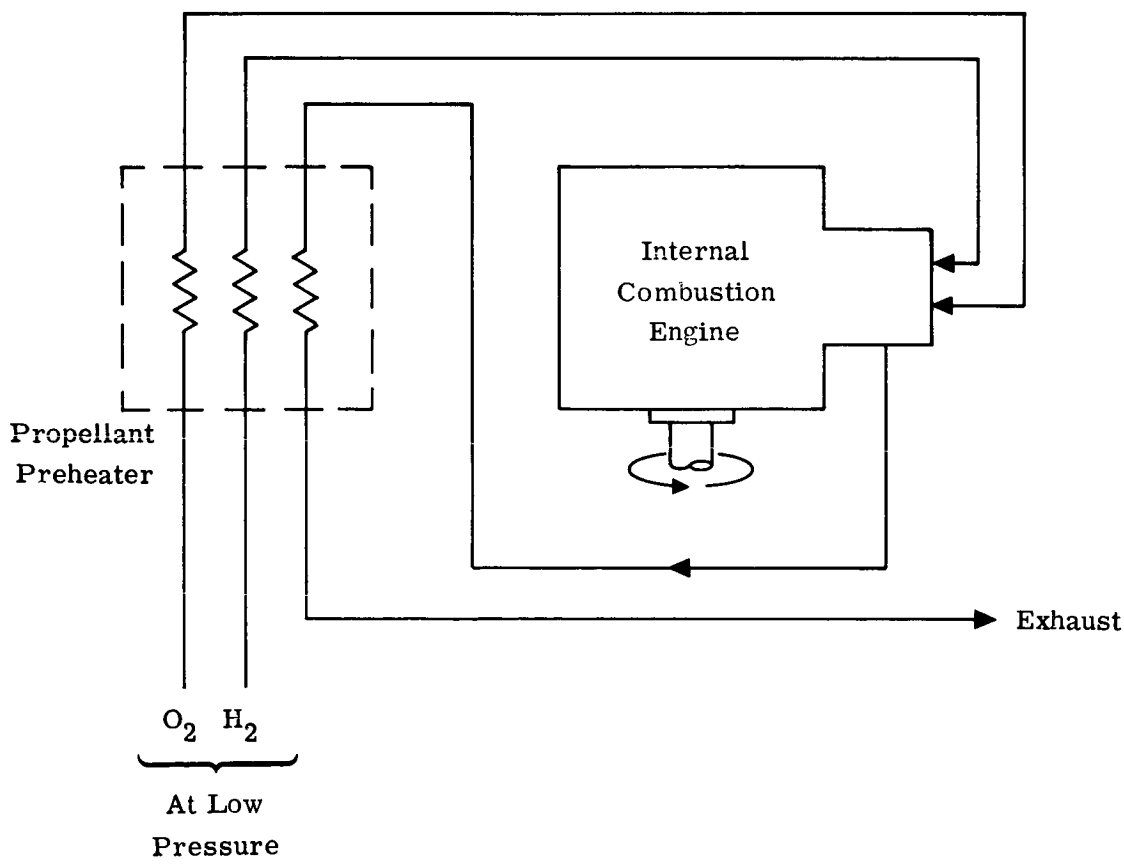

Fig. 3-4 - Non-Regenerated Fuel Rich H_2-O_2 Engine System

3.2.4 External Combustion System

An external combustion fuel rich cycle with exhaust heat regeneration is shown in Fig. 3-5. The propellants are burned in a constant pressure combustor external to the engine cylinder, after which the combustion products are admitted to and expanded in the cylinder. The H_2 is heated in the regenerator prior to combustion by the engine exhaust. The gas from the combustor is delivered to the expansion engine at 1500°F or less. This temperature limitation is necessary to prevent overheating of the engine inlet valve.

The BSPC for external combustion H_2-O_2 engines is in the range of 1.3 to 1.7 lb/hp-hr. With heat feedback from the vehicle or environmental control system, the oxidizer consumption will decrease, resulting in lower BSPC. This type of system is discussed more completely in Ref. 1.

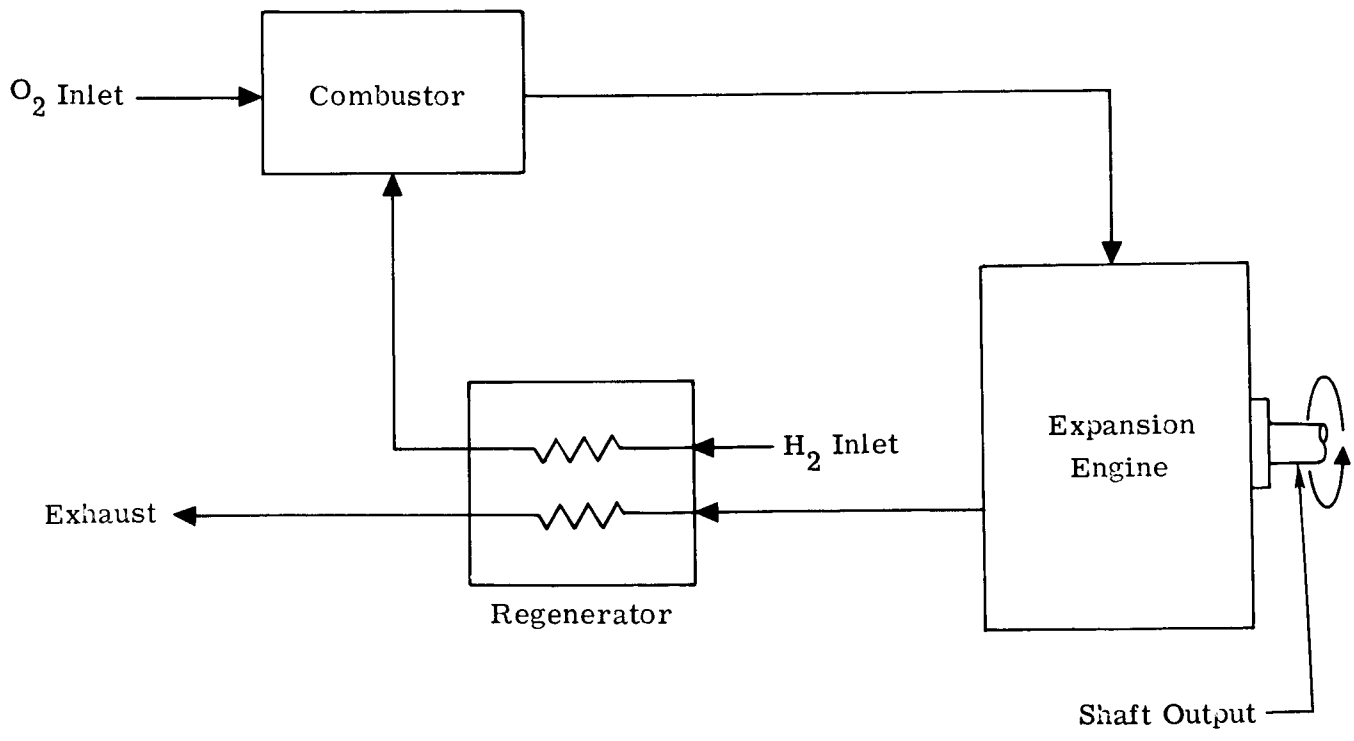

Fig. 3-5 - External Combustion Fuel Rich System with Exhaust Heat Regeneration

3.2.5 System Considerations

The interrelation of O/F ratio, thermal efficiency, and BSPC is illustrated in Fig. 3-6. This figure illustrates that performance improves as stoichiometric operation is approached, even if thermal efficiency does not decrease; however, the improvement is not dramatic after a ratio of 2:1 has been reached. In general the thermal efficiency (η_{th}) of fuel rich systems is higher than that of stoichiometric systems because of the higher heat sink capacity available in the excess hydrogen consumed by the fuel rich system.

Fig. 3-7 illustrates the theoretical BSPC for fuel rich and stoichiometric H_2-O_2 engines. Note the reduction in BSPC as O/F ratio increases. The ramifications of more nearly stoichiometric operation are:

1. Propellant weight is reduced
2. Tankage weight is reduced
3. System volume is reduced
4. Heat rejection is increased
5. Cooling weight penalty is increased

3.3 Basic Cycle Studies

After establishing that the fuel-rich internal combustion engine operating in a regenerative system, as shown in Fig. 3-1, represented the best choice for the requirements of this program, detail cycle analysis was conducted to establish the optimum operating characteristics of the engine. Trade-off studies were conducted for several methods of power modulation to indicate which approach would result in the lowest total propellant requirement for the load profile requirements used in this program.

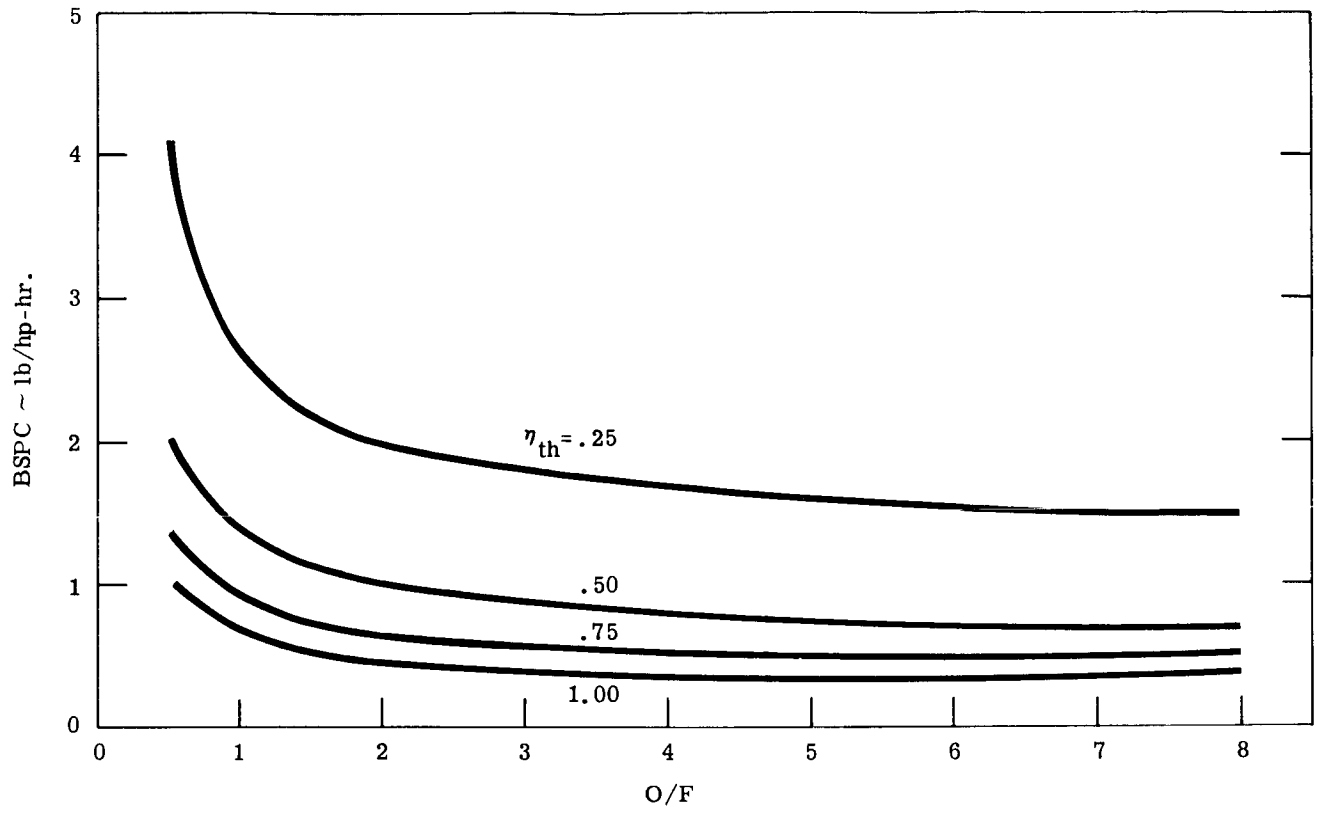

Fig. 3-6 - Relation Between Thermal Efficiency, BSPC, and O/F Ratio for Hydrogen-Oxygen Systems

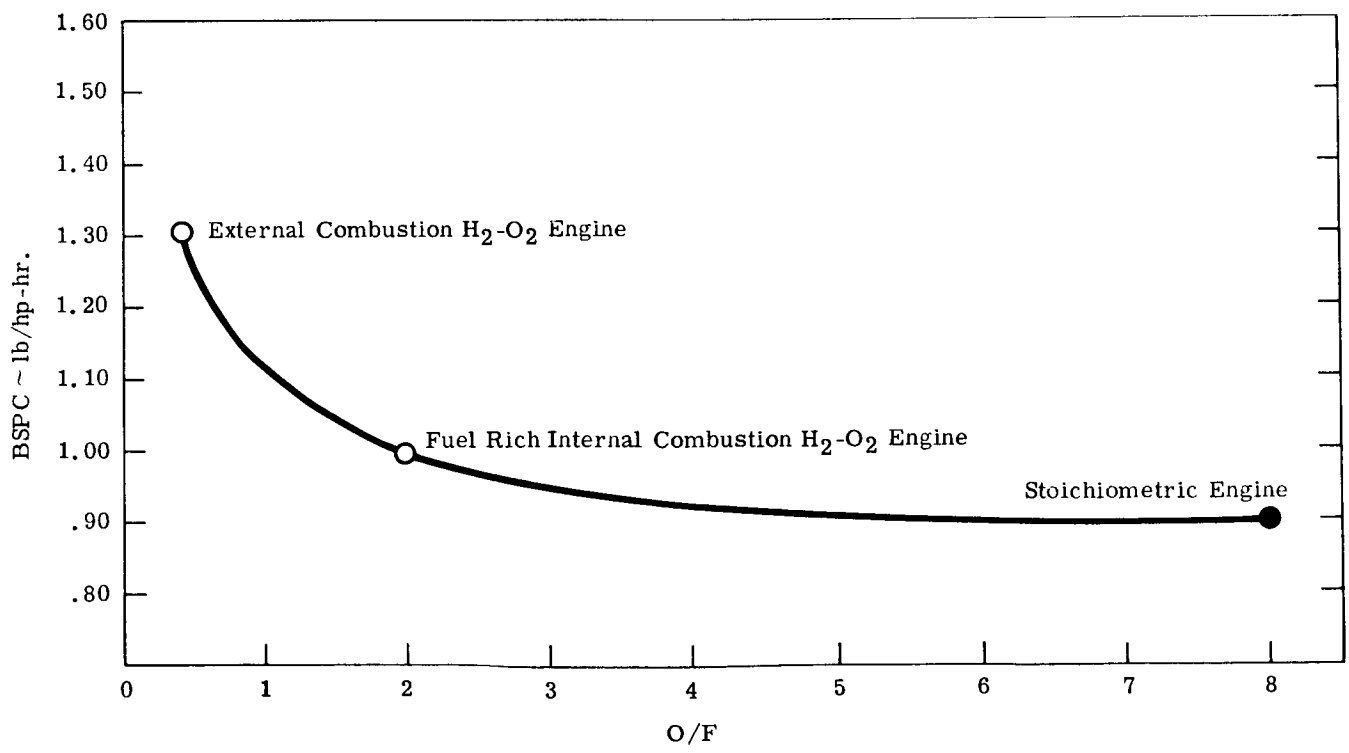

Fig. 3-7 - BSPC vs. O/F for Typical H_2-O_2 Engines

3.3.1 Assumptions Used in the Basic Cycle Studies

1. Engine speed = 4000 rpm
2. Design oxygen/hydrogen ratio = 2.0 (O/F of 0 to 8 used in cycle studies)
3. Diagram factor = 0.9
4. Maximum cylinder pressure P_1 = 2000 psi, for operation on compressed boiloff propellants, and P_1 = 900 psi for operation directly from supercritical tanks.
5. Exhaust pressure, Pe = 2 psia after blowdown in space environment and 15 psia after blowdown in sea level environment.
6. FMEP = 11 psi @ 4000 rpm
7. Alternator efficiency = 90%
8. Percent admission, a = 0 to 95%
9. Percent compression, b = 95%
10. Percent clearance volume, c = 5% for space environment (vacuum), 12.5% for sea level environment, and 5 to 50% for variable clearance vol. study.
11. Maximum exhaust temperature, Te = 2000°R

3.3.2 Cycle Analysis

The performance characteristics of hydrogen-oxygen engines are best illustrated by first studying the idealized uniflow engine cycle. External combustion H_2-O_2 engines operate on this cycle, while internal combustion H_2-O_2 engines operate on a similar cycle with modifications to account for thermal compression and cylinder filling losses.

Fig. 3-8 illustrates an indicator diagram for an idealized external combustion uniflow engine.

The work per cycle is equal to the area of the indicator card diagram 1-2-3-4-5-1 which may be expressed:

$$1)\ W = P_1(V_2 - V_1) + \frac{P_2V_2 - P_3V_3}{k-1} - \frac{P_5V_5 - P_4V_4}{k-1}$$

where k is the isentropic expansion and compression coefficient PV^k = constant.

Equation 1) may be re-written using the identities:

$V_1 = cD$ $\qquad$ $V_4 = (b + c)D = V_3$

$V_2 = (a + c)D$ $\qquad$ $V_5 = cD = V_1$

$V_3 = (b + c)D$ $\qquad$ $V_2 - V_1 = aD$

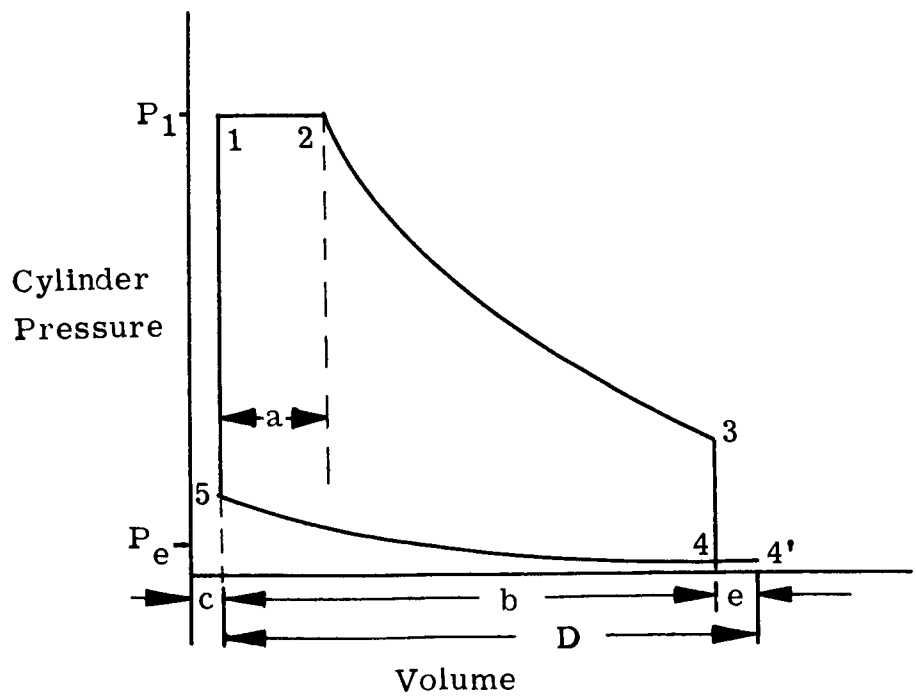

Fig. 3-8 - Indicator Diagram, External Combustion Engine Cycle

$$P_3 = P_1 \left(\frac{V_2}{V_3}\right)^k = P_1 \left(\frac{a+c}{b+c}\right)^k$$

$$P_5 = P_4 \left(\frac{V_4}{V_5}\right)^k = P_4 \left(\frac{b+c}{c}\right)^k$$

$$P_1 = P_2$$

$$P_4 = P_e$$

Thus, after simplifying and dividing by D

$$2)\ \frac{W}{D} = P_1(a) + P_1\left(\frac{a+c}{k-1}\right)\left[1-\left(\frac{a+c}{b+c}\right)^{k-1}\right] - P_e\left(\frac{b+c}{k-1}\right)\left[\left(\frac{b+c}{c}\right)^{k-1}-1\right]$$

$\frac{W}{D}$ is by definition the idealized indicated mean effective pressure

$\frac{W}{D}$ = idealized IMEP

and

$$3)\ \frac{IMEP}{P_1} = a + \left(\frac{a+c}{k-1}\right)\left[1-\left(\frac{a+c}{b+c}\right)^{k-1}\right] - \frac{P_e}{P_1}\left(\frac{b+c}{k-1}\right)\left[\left(\frac{b+c}{c}\right)^{k-1}-1\right]$$

The gas flow into the cylinder per cycle may be calculated by:

$$4)\ W_i = \frac{P_1 D}{R T_i}\left[a + \frac{c}{k}\left(1-\frac{P_s}{P_1}\right)\right]$$

where T_i = Hydrogen Inlet Temperature to the Engine

Equation 4 is derived in Reference 2.

The specific propellant consumption is by definition the propellant consumption per unit work done. Thus,

$$ISPC = \frac{W_i}{W}$$

5) $$ISPC = \frac{W_i}{D(IMEP)}$$

Substituting Equation 4) and the proper proportionality constant in Equation 5):

$$ISPC = \frac{\frac{P_1 D}{R T_i}\left[a + \frac{c}{k}\left(1 - \frac{P_5}{P_1}\right)\right]}{D(IMEP)} \times 1.98 \times 10^6 \ \frac{Lb.}{HP\ HR}$$

6) $$ISPC = 1.98 \times 10^6 \ \frac{P_1\left[a + \frac{c}{k}\left(1 - \frac{P_5}{P_1}\right)\right]}{R T_i (IMEP)}$$

The parameter (ISPC)RT is convenient for making comparisons of performance at different temperatures and/or different working fluids.

7) $$(ISPC)\, R\, T_i = 1.98 \times 10^6 \ \frac{\left[a + \frac{c}{k}\left(1 - \frac{P_5}{P_1}\right)\right]}{IMEP/P_1}$$

The performance of an actual expansion engine can be estimated from the above equations if values of diagram factor (DF) and friction mean effective pressure (FMEP) or mechanical efficiency (η_m) are known, or are estimated.

By definition, diagram factor is:

$$8)\ DF = \frac{\text{Actual IMEP}}{\text{Idealized IMEP}}$$

and mechanical efficiency is:

$$9)\ \eta_m = \frac{\text{BMEP}}{\text{Actual IMEP}} = 1 - \left(\frac{\text{FMEP}}{\text{Actual IMEP}}\right)$$

since BMEP = Actual IMEP - FMEP

Thus, brake mean effective pressure can be determined by
10a) BMEP = (DF) (Idealized IMEP) - FMEP or;
10b) BMEP = η_m (DF) (Idealized IMEP)

The brake specific propellant consumption can then be determined by substituting BSPC for ISPC in Equation 6 or 7.

$$\text{Thus, BSPC} \cdot \text{RT} = 1.98 \times 10^6 \left[\frac{a + c/k\,(1 - P_5/P_1)}{\text{BMEP}/P_1}\right.$$

3.3.3 Analysis of the Idealized Internal Combustion Engine Cycle

An analysis was made of the internal combustion cycle where unreacted propellants are admitted separately into the engine. When combustion occurs following oxygen injection, there is a rapid thermal compression (i.e. pressure rise) of the working fluid. The rate of pressure rise (dp/dt) is largely a function of the rate of oxygen injection. Rapid injection produces rapid pressure rise. Also, injection near TDC permits nearly constant volume combustion with more pressure rise, since piston velocity is nearly zero. Expansion, blowdown, and

residual compression occur as previously described in the discussion of the external combustion uniflow cycle.

Fig. 3-9 illustrates a typical indicator diagram for the internal combustion engine. Also shown in Fig. 3-9 is a superposition of an idealized uniflow external combustion expander cycle operating at the same peak pressure and admission. It is apparent that the internal combustion engine work is equal to the work of an external combustion expander minus the areas A and B on Fig. 3-9.

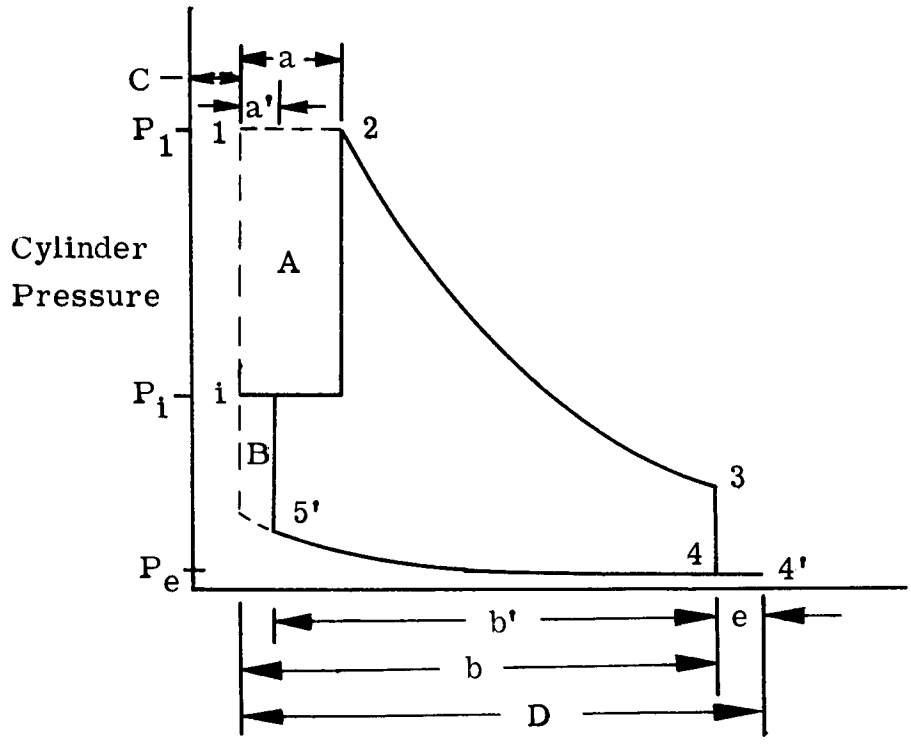

Fig. 3-9 - Indicator Diagram, Internal Combustion Engine Cycle

$$11)\ W = P_i\left(V_2 - V_5'\right) + \frac{P_1 V_2 - P_3 V_3}{k-1} - \frac{P_5 V_5' - P_4 V_4}{k-1}$$

and $\frac{W}{D}$ = idealized IMEP

Thus after simplifying and dividing by D and expressing in terms of displacement fractions

$$12)\ \frac{W}{D} = P_i(a - a') + P_1\left(\frac{a+c}{k-1}\right)\left[1 - \left(\frac{a+c}{b+c}\right)^{k-1}\right] - P_e\left(\frac{b'+c}{k-1}\right)\left[\left(\frac{b'+c}{c}\right)^{k-1} - 1\right]$$

$$13)\ \frac{IMEP}{P_1} = \frac{P_i}{P_1}(a - a') + \left(\frac{a+c}{k-1}\right)\left[1 - \left(\frac{a+c}{b+c}\right)^{k-1}\right] - \frac{P_e}{P_1}\left(\frac{b'+c}{k-1}\right)\left[\left(\frac{b'+c}{c}\right)^{k-1} - 1\right]$$

where b' = b-a'

Before Equation 13 can be used, a relationship between P_i and P_1 must be established. If constant volume combustion is assumed then

$$14)\ \frac{P_i}{P_1} = \frac{T_i}{T_1} = \frac{T_i}{T_i + \Delta T_c}$$

The ideal combustion temperature rise with constant volume combustion is

$$15)\ \Delta T_c = \frac{w_i\, Q}{(w_i + w_{5'})\, c_v}$$

where W_5' is residual gas from previous cycle.
where Q is the heat of combustion per pound of reactants.
This temperature rise would occur if no external heat leakage, no dissociation, and no piston travel occurred. Experience shows that combustion temperature rise (or pressure rise) in a constant volume combustion process seldoms exceeds approximately 80% of the theoretical value. Therefore, in this analysis, to allow for cylinder heat rejection and other deleterious effects, Equation 15 is modified to read:

$$16)\ \Delta T_c = \frac{W_i Q (.8)}{(W_i + W_5') C_v}$$

It is believed that Equation 16 presents a more realistic estimate of temperature rise ΔT_c than Equation 15.

The heat release term Q is directly proportional to the flow rate of oxidizer in stoichiometric or fuel rich engine cycles.

Stated algebraically,

$$17)\ W_i Q = W_{O_2} Q_{O_2} = 6480\ W_{O_2}\ \text{BTU}$$

where Q_{O_2} is the heat release per pound of oxygen.

Equation 16 can now be

$$18)\ \Delta T_c = \frac{6480\ W_{O_2} (.8)}{(W_i + W_5') C_v} = \frac{R T_i \times 6480\ W_{O_2} (.8)}{P_i D (a + c) C_v}$$

where W_i is related to W_{O_2} by the O/F ratio, and the residual W_5' is a function of the exhaust pressure and amount of recompression.

The relation between W_i and W_{O_2} is

$$19)\quad W_{O_2} = \left(\frac{1}{1 + 1/O/F}\right) W_i$$

By using equations 18 and 19, the combustion temperature T_1 and combustion temperature rise ΔTc can be computed for various O/F ratios. The results of the calculation are shown in Fig. 3-10 for illustrative purposes. The gas constant of the resultant combustion products is also shown in Fig. 3-10.

By using Equations 18 and 10 (the equation of state), Equation 14 can be rewritten

$$20)\quad P_i/P_1 = \frac{6480\, RT_i\, W_i\, (.8)}{P_1 D (a+c)\, C_v \left(1 + \frac{1}{O/F}\right)}$$

The gas flow into the cylinder per cycle may be calculated as follows:

$$\frac{P_1 V_1}{RT_1}\left[V_2/V_1 - 1/k\left(P_5'/P_1 - 1\right) - 1\right]$$

$$= P_1 D/RT_1 \left[a + c + \frac{a' + c}{k}\left(1 - P_5/P_1\right) - a' - c\right]$$

$$21)\quad W_i = P_1 D/RT_1 \left[a - a' + \frac{a' + c}{k}\left(1 - P_5'/P_1\right)\right]$$

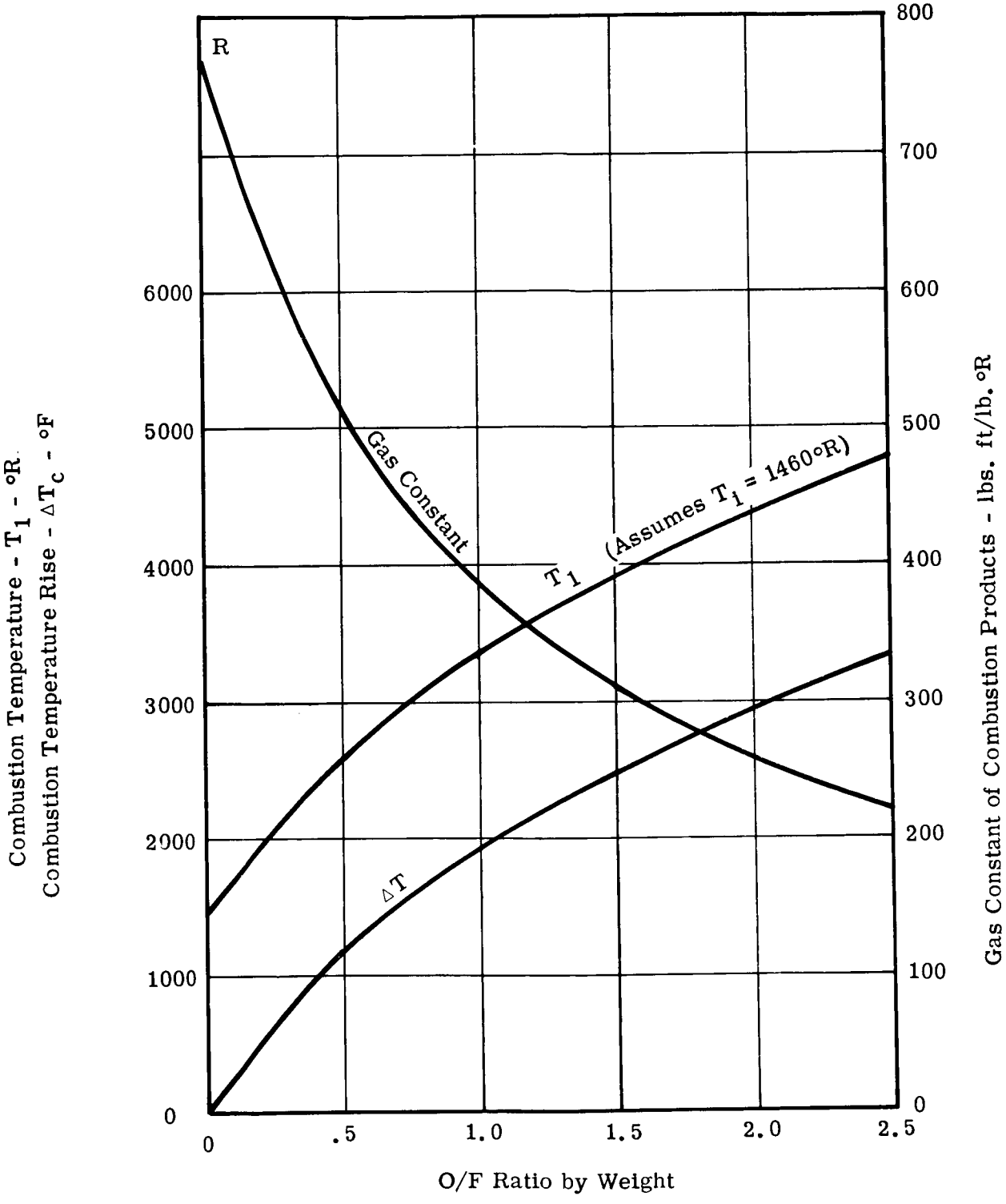

Fig. 3-10 - Combustion Temperature and Gas Constant as a Function of Mixture Ratio

The specific propellant consumption is: ISPC = W_i/W

$$22)\quad ISPC = \frac{W_i}{D\,(IMEP)}$$

Practical design consideration (exhaust temperature and heat rejection) dictates that T_1 of 4500°R or less, and T_i in the vicinity of 1460°R be selected as the design point. For this reason, operation in the O/F range of 2.0 appears near optimum. Accurate data on thermodynamic properties of H_2-O_2 products of combustion were obtained from Ref. 3.

Substituting Equation 21 and the proper proportionality constant in Equation 22.

$$23)\quad ISPC = \frac{1.98 \times 10^6\, P_1 \left[a - a' + \frac{a'+c}{k}\left(1 - \frac{P_5}{P_1}\right)\right]}{R T_1\,(IMEP)}$$

The preceding comments concerning diagram factor and mechanical efficiency are valid for both the internal and external combustion engines.

The pertinent results obtained from the parametric studies of engine performance can be seen in the following section.

3.4 Methods of Engine Power Modulation

Many different methods of engine power modulation were analysed but only five were finally considered to be practical.

1. Variable hydrogen inlet pressure with fixed valve timing

2. Variable hydrogen inlet valve duration with constant hydrogen inlet pressure.

3. Variable phasing of the hydrogen valve with constant hydrogen inlet pressure.

4. Hybrid system, combining variable hydrogen inlet pressure with variable hydrogen valve phasing.

5. Hybrid system, combining variable hydrogen inlet pressure with variable hydrogen valve duration.

These five methods were studied in additional detail based on the power profile data furnished by NASA.

The typical theoretical indicator cards at maximum and minimum power for each of the five power modulation methods are illustrated in Fig. 3-11. It should be noted that the indicator cards for the cycles using variable hydrogen valve duration and variable hydrogen valve phasing are identical except for the greater compression work at low admission in the latter method. The basic difference in these two methods of power modulation is found in the mechanical configuration. The variable phase hydrogen valve method uses a single poppet valve while the variable hydrogen valve duration method makes use of a dual poppet valve.

In all cases it was assumed that the peak combustion pressure was three times the hydrogen inlet pressure, as indicated by Equation 14 of Section 3.3, and the curve of combustion temperature rise versus O/F ratio shown in Fig. 3-10. It was also assumed that combustion occurs under constant

Typical Theoretical Indicator Cards

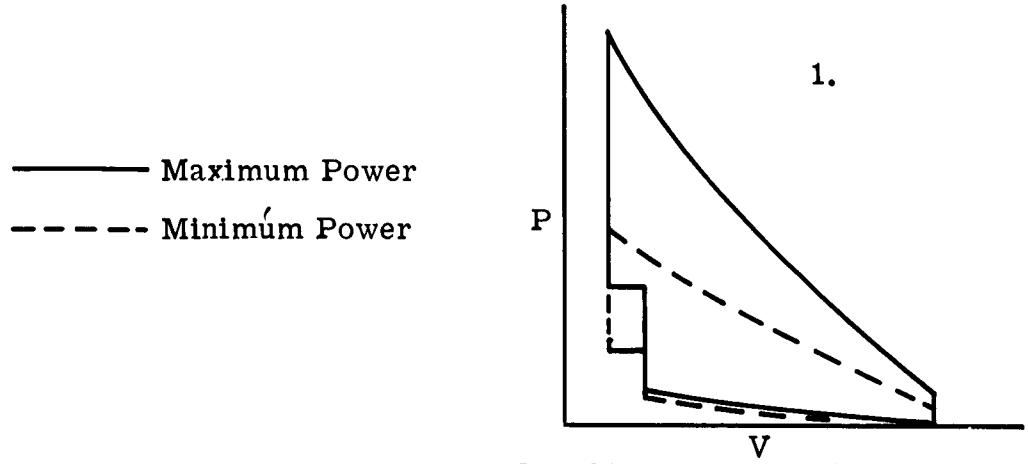

Variable Hydrogen Inlet Pressure with Fixed Valve Timing

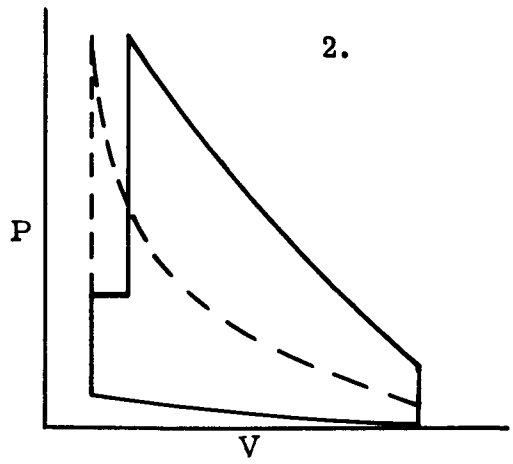

Variable Hydrogen Valve Duration with Constant Hydrogen Inlet Pressure

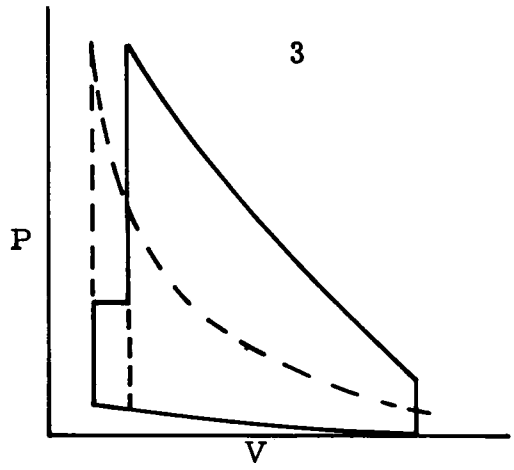

Variable Phasing of the Hydrogen Valve with Constant Hydrogen Inlet Pressure

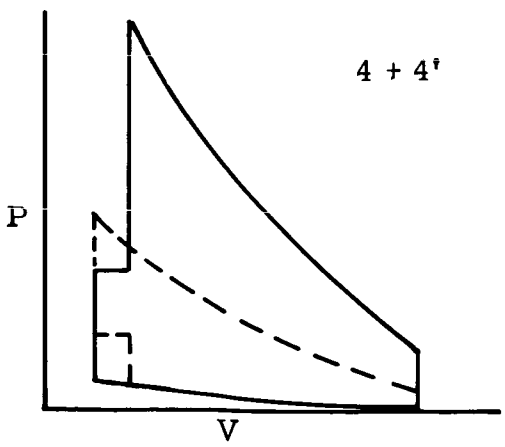

Hybrid System - Variable Hydrogen Inlet Pressure + Variable Hydrogen Valve Phase
4, P_1 = 1200 psi 4', P_1 = 900 psi

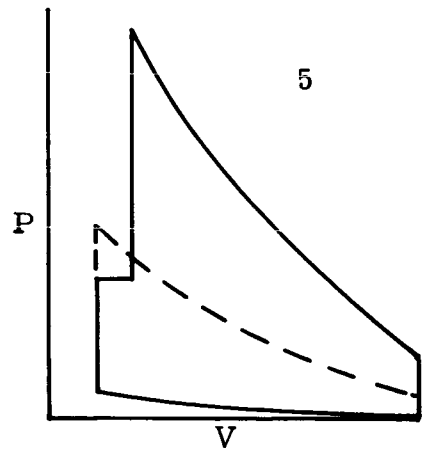

Hybrid System - Variable Hydrogen Inlet Pressure + Variable Hydrogen Valve Duration

Fig. 3-11 - Typical Theoretical Indicator Cards

volume conditions. Due to the fact that some of the power modulation techniques result in different values of BMEP, it has been necessary to vary the engine displacement from one power modulation technique to another, as indicated on curves of Fig. 3-12.

A graph of BSPC in pounds per hp-hr vs. HP is presented in Fig. 3-12. This graph is representative of an engine which will generate power between the limits of 1.25 to 5.0 hp (not including power required to drive the compressor.) Curve 4 in Fig. 3-12 shows the BSPC for the hybrid system operating directly from supercritically tanked hydrogen at 300 psi and oxygen at 1000 psi. It is clear from this curve that only a very small BSPC penalty is paid by operating directly from supercritical tanks and reducing the maximum combustion pressure to 900 psi. The BSPC penalty is approximately 4%, which is a small weight penalty to pay for a simplified system which does not require compressor operation except when utilizing boiloff propellant.

The optimum displacement may be obtained by designing to the weighted average power requirement. With a hybrid power modulation control employing variable admission and throttling techniques, an optimum but still flexible, power system can be designed.

A discussion of each of the power modulation methods analyzed is given below.

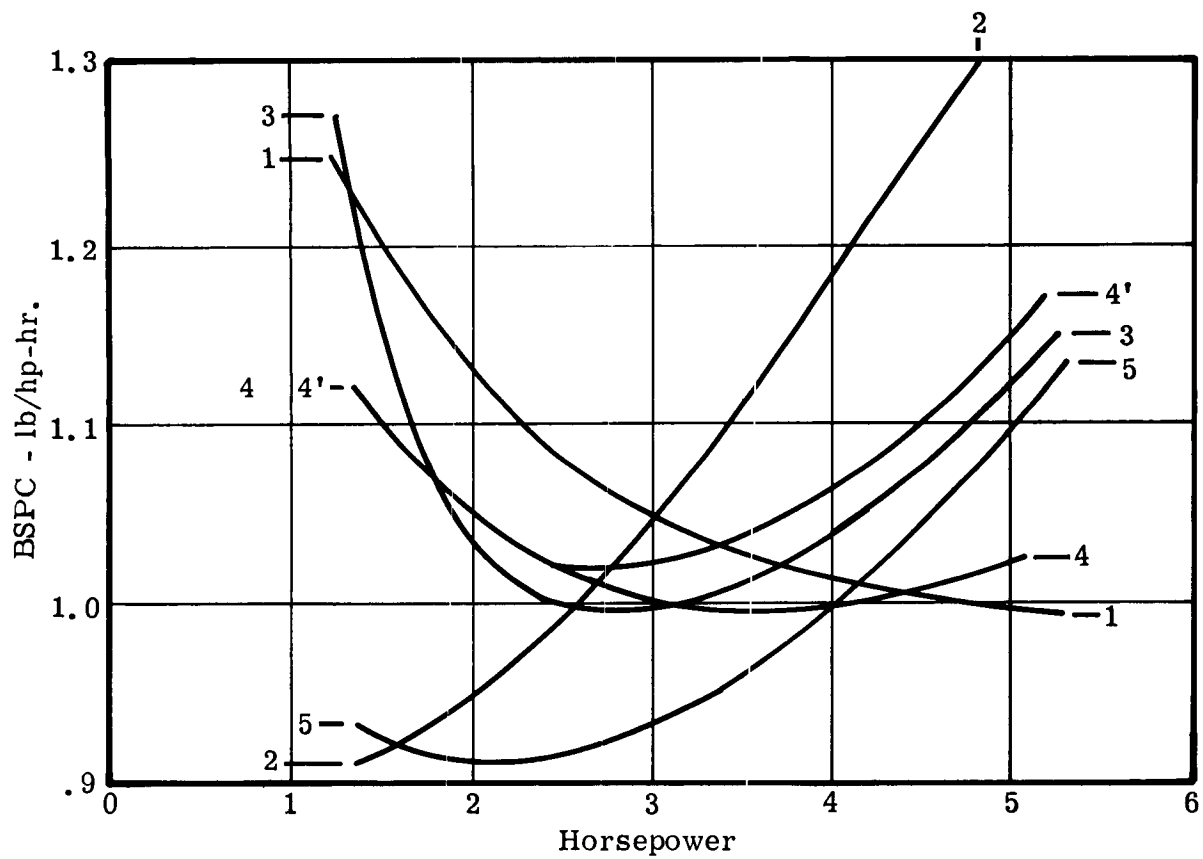

1. Variable hydrogen inlet pressure $D = 4.2\ in^3$, $a = 2\%$, $P_{in_{max}} = 1200$ psi

2. Variable hydrogen valve duration over full range of power. $D = 1.77\ in^3$, P1 max. = 900 psi

3. Variable phase hydrogen valve $D = 208\ in^3$, $P_{in_{max}} = 1200$ psi

4. Variable hydrogen inlet pressure to 3.3 hp, then variable phase hydrogen valve to full power. $D = 2.77\ in^3$, $P_{in_{max}} = 1200$ psi

4'. Variable hydrogen inlet pressure to 2.41 hp, then variable phase hydrogen valve to full power. $D = 2.77\ in^3$, P1 max = 900 psi

5. Variable hydrogen inlet pressure to 2.41 HP, then variable duration hydrogen valve to full power. $D = 2.77\ in^3$ P1 max = 900 psi

Fig. 3-12 - BSPC vs. Horsepower (No Compressor Work)

3.4.1 Variable Hydrogen Inlet Pressure with Fixed Valve Timing

This method requires a pressure regulator or throttle in the hydrogen inlet valve. If a 30° duration hydrogen valve is used, design studies show that the oxygen must be injected at 2% admission to obtain minimum BSPC. This is probably the least complicated method of power modulation. With this method the minimum BSPC is at maximum power and if the power requirement is over a large range, the BSPC becomes excessive at the low power settings (Curve 1, Fig. 3-12). The only way that more power can be derived using this power modulation system is to increase inlet pressure, which in turn increases combustion pressure to a point where the engine could be overstressed. This type of control would be best for a nearly constant power requirement near the maximum power limit.

3.4.2 Variable Hydrogen Valve Duration With Constant Hydrogen Inlet Pressure

This power modulation method has been used on the experimental test engine. The hydrogen valving consists of dual concentric poppet valves with adjustable cams so the opening point with respect to top dead center and the duration of hydrogen admission may be adjusted to any desired value. The oxygen is injected near the end of hydrogen admission. This valve mechanism which has been reliable on the test engine, is varied manually, but automatic control would be incorporated into a flight unit. This method of power modulation produces the minimum BSPC at the minimum power requirement (Curve 2, Fig. 3-12). As the power increases the percent admission is increased and BSPC also increases. An engine

with this type of control would be good for a steady, low power requirement with only short duration peak loads.

3.4.3 Variable Phasing of the Hydrogen Valve with Constant Hydrogen Inlet Pressure

This results in approximately the same engine performance as the variable duration hydrogen valve. The mechanism is simplified in that only one valve of a constant duration is used. The phase relation of the valve relative to the crankshaft is varied and the percent admission can be varied from 0 to the maximum duration of the valve. It appears that a 30° duration is about minimum due to valve dynamics limitation. The oxygen is injected just prior to the end of hydrogen admission. The performance of an engine with this type of power modulation control would be the same as an engine using the variable duration control (See Curve 3, Fig. 3-12), except that a slight BSPC penalty occurs at the minimum power requirements, due to compression work caused by early opening of the hydrogen valve, as the piston continues to travel upwards. The lost work is noted as area B in Fig. 3-9.

3.4.4 Hybrid System: Variable Hydrogen Inlet Pressure and Variable Hydrogen Valve Phasing

Combining variable hydrogen inlet pressure with the variable phasing of the hydrogen valve will result in a system which has a minimum BSPC at average power (Curves 4 and 4' on Fig. 3-12). The BSPC will increase as power is either increased or decreased. The overall propellant consumption can be minimized by designing to the average power

requirement for the whole mission. This system is flexible with respect to power requirement changes. An increase or decrease in average power, or a change in the maximum or minimum power, could be incorporated without a design change, with a BSPC penalty only while operating in the expanded region of the power profile. This type of power modulation control is slightly more complicated than a variable phase hydrogen valve, but the versatility of the system may warrant the slight increase in complexity.

3.4.5 Hybrid System: Variable Hydrogen Inlet Pressure and Variable Hydrogen Valve Duration

This system has the same advantages of flexibility and low overall BSPC over an even greater power range than the above system (See Curve 5, Fig. 3-12), and the controls would be identical. This is the most complex system with regard to the mechanism required to implement it, but is considered the best choice on the basis of overall propellant consumption.

Other power modulation techniques investigated were:

1. Variable engine displacement: This would result in an engine with minimum BSPC at all power levels. Although desirable, there is no practical means accomplishing variable displacement with high reliability.

2. Variable clearance volume: This would result in an engine with about the same characteristics as a variable phase hydrogen valve or variable hydrogen valve duration. The mechanical configuration would be more complex than that required for either of the other two systems. If a

moveable head was employed there would be sealing problems associated with the high combustion pressures and very high cyclic control forces to contend with.

3. Variable piston stroke: This would result in performance like a variable clearance volume engine but it would have a higher BSPC, since clearance volume would increase as the stroke is decreased.

4. Variable oxygen injector phasing: Phasing of only the oxygen injector for power modulation is inefficient and BSPC would be high. If the hydrogen were allowed to expand and then combusted later in the stroke, a large amount of thermal energy would not be used. The exhaust gases would be very hot and this could also cause problems with the exhaust ports or in the regenerator. The alternative is to operate at low O/F ratios and thus lower combustion temperatures. Each of the power modulation techniques in Fig. 3-11 which utilizes variation in hydrogen valve timing implies oxygen injector phasing. In each case the oxygen injector would be timed to start injection just prior to the closing of the hydrogen valve.

3.5 Heat Rejection & Cooling Studies

3.5.1 Heat Rejection Analysis

The H_2-O_2 engine has one unique characteristic which tends to increase its heat rejection, as compared to conventional air breathing engines. This is the use of a working fluid which, by volume, is primarily hydrogen gas. The small cylinder size required for the low power requirements of this program also tends to result in higher heat rejection per unit of power delivered. In recognition of this, the test engine was designed to permit high temperature operation, with heat dams on the cylinder head and piston crown, and with the intake valve isolated from

the combustion zone by stratification.

An analysis of the heat rejection characteristics of engines is presented using methods suggested in Ref. 4. . Ref. 4. presents empirical data on heat transfer coefficient which can be employed in the studies. Heat rejection is a function of the following parameters.

$$1)\ \frac{q}{HP} = \frac{hA\Delta T}{PUB^2} \quad \frac{\frac{K}{B}(PUB/\mu)^{.75} B^2 \Delta T}{PU^2 B^2} = \frac{K/B\left(\frac{PUB}{\mu}\right)^{.75} B^2 \Delta T}{PUB^2}$$

h=film coefficient, A=piston area, q=rate of heat transfer, T=temperature, B=cylinder bore, K=conductivity, μ=viscosity, U=piston speed, ρ= density, P=pressure, HP=power output.

$$2)\ \frac{\rho UD}{\mu} = \frac{PUB}{RT\mu}$$

$$3)\ \frac{q}{HP} = \frac{K\Delta T}{(RT\mu)^{.25}(PUB)^{.25}}$$

by rearranging and assuming ΔT to be constant

$$4)\ \frac{q}{HP} = \frac{1}{Pr}\left(\frac{\mu}{M.W}\right)^{.25}\left(\frac{1}{HP_s\ B^2}\right)^{.25}$$

where

M. W. is molecular wt.
HP_s is specific horsepower - hp/in^3
Pr is Prandtl number, $\frac{\mu C_p}{k}$

ΔT is temperature difference between mean expansion temperature and the cylinder wall temperature.

The heat rejection characteristics of two engines can be compared as follows:

When specific power and displacement are equal but working fluids are different:

$$5)\quad \frac{(q/HP)_{engine\ a}}{(q/HP)_{engine\ b}} = \frac{Pr_b}{Pr_a}\left(\frac{M_a}{M_b}\ \frac{M.W._a}{M.W._b}\right)^{.25}$$

When working fluids are the same but engine displacement or specific power are different:

$$6)\quad \frac{(q/HP)_{Engine\ a}}{(q/HP)_{Engine\ b}} = \left(\frac{HP_{s_b}}{HP_{s_a}}\right)^{.25}\left(\frac{B_b}{B_a}\right)^{.50}$$

A comparison between the heat rejection characteristics of the Vickers H_2-O_2 engine and a conventional air-breathing engine can be made using Equations 5 and 6. In the H_2-O_2 engine the working fluid is primarily hydrogen, and in the air breather the working fluid is mostly air.

The H_2-O_2 engine has 1.5" bore and HP_s = 2. A typical modern air-breathing engine has a 3.34" bore with an HP_s of .5 and a q/HP = .413.

Thus:

$$\left(\frac{q}{HP}\right)_{H_2-O_2} = \left(\frac{q}{HP}\right)_{air}\left(\frac{\mu_{H_2}}{\mu_{air}}\ \frac{M.W._{air}}{M.W._{H_2}}\right)^{.25}\left(\frac{HP_{s\,air}}{HP_{s\,H_2}}\right)^{.25}\left(\frac{B_{air}}{B_{H_2}}\right)^{.5}$$

$$= .413\left(\frac{.069}{.139}\times\frac{29}{2}\right)^{.25}\left(\frac{.5}{2}\right)^{.25}\left(\frac{3.34}{1.5}\right)^{.5}$$

$= .413 \times 1.64 \times .707 \times 1.495 = 0.715$

with thermal transport properties evaluated at an assumed average temperature of 3000° F

A similar analysis can be made for a H_2-O_2 engine operating on a stoichiometric ratio of hydrogen and oxygen. In this case the working fluid is steam. It can be shown that the heat rejection characteristics (q/HP) would be 40% lower than that of an engine operating on pure hydrogen, as assumed in the previous analysis. Thus, there is a convincing indication that significant reduction in heat transfer to the cylinder can be achieved in H_2-O_2 engines as more nearly stoichiometric operation is approached assuming the value of ΔT remains unchanged.

Note that the preceding discussion assumes no insulation on the H_2-O_2 engine. Effective thermal insulation should reduce heat rejection appreciably.

The above analysis is based on the heat rejection characteristics of the Willys 6-230 (as reported in SAE Paper 532A) engine which has one of the lowest heat rejection rates of any air-breathing engine reported to date. However, it should be noted that other automotive engines of similar size reject two to three times as much heat as the Willys engine, which indicates that low heat transfer characteristics can be achieved with judicious design and development.

Included as Appendix D in this report are the derivations and results of the cycle analysis with the effects of heat rejection shown.

3.5.2 Influence of Heat Rejection on Engine Performance

Regenerative Cycle

Figs. 3-13, 3-14, and 3-15 illustrate the effect of cylinder heat rejection on a regenerative power cycle. The major parameter variation in these figures is the product $y\eta_\infty$; where y represents the fraction of heat rejected after expansion is complete, and η_∞ is the expansion efficiency of the engine rated against an infinite expansion ratio.

These figures illustrate the change in cycle thermal efficiency when heat rejection is considered, assuming exhaust temperature remains constant which is dictated by material considerations. When heat rejection is increased the engine must operate at higher O/F ratios to maintain constant exhaust temperature.

O/F ratio changes cause minor variations of k and the product of RT. If these changes are small, then BSPC will vary inversely with net cycle thermal efficiency.

As expected, increasing cylinder heat rejection (x) lowers cycle thermal efficiency (η_x). In an illustrative example η_∞ is assumed to be 0.50. Automotive engine heat rejection data suggests that an emperical value of the heat rejection "weighing" factor, y = 0.6 be used, thus, $y\eta_\infty$ = 0.30. The effect of heat rejection rates (x) between 0 and 1.2 are investigated. Cycle studies indicate that cycle efficiency with η_i of about 0.5 may be achievable for H_2-O_2 engines if no cylinder heat rejection is realized. Now considering heat rejection in this example case, it can be seen from Fig. 3-13 that when x = 0, η_x = 0.50; when x = 0.40, η_x = 0.449; and when

$\chi = q/hp_x$

η_1 = Cycle Efficiency Without Heat Rejection @ $(Q_c = 0)$ $(hp_x = hp)$

q_c = Cylinder Heat Rejection

η_χ = Net Cycle Thermal Efficiency with Heat Rejection = $\dfrac{HP_\chi}{\dfrac{HP_1}{\eta_1} + Q_c + (HP_\chi - HP_1)} = \dfrac{1}{\left(\frac{1}{\eta_1}\right)\left(1 - \dfrac{\chi}{y\frac{1}{\eta_\infty} - 1}\right) + \chi + 1}$

hp_x = Net Power Output

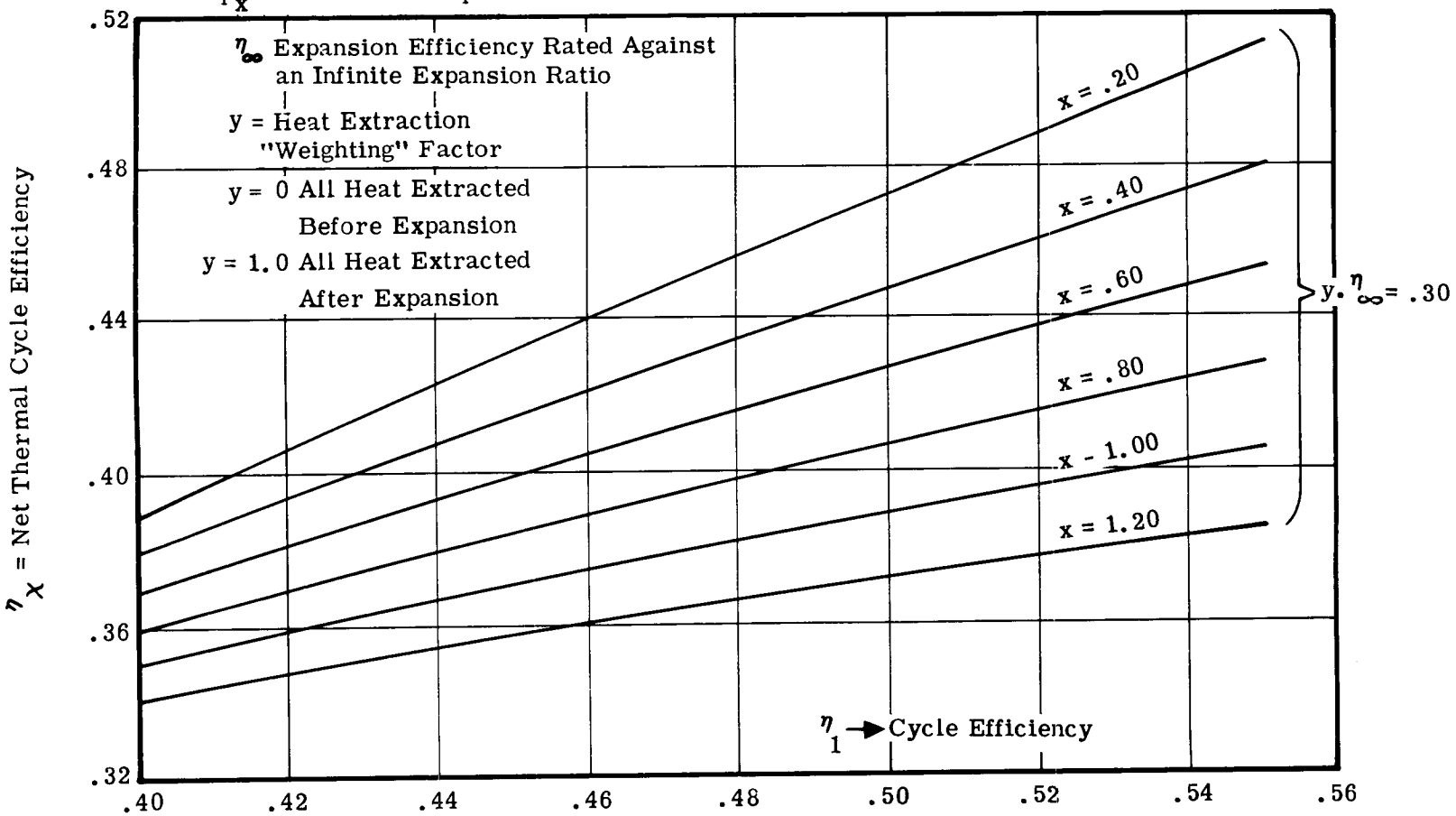

Fig. 3-13 - Regenerative Power System Performance with Cylinder Heat Rejection

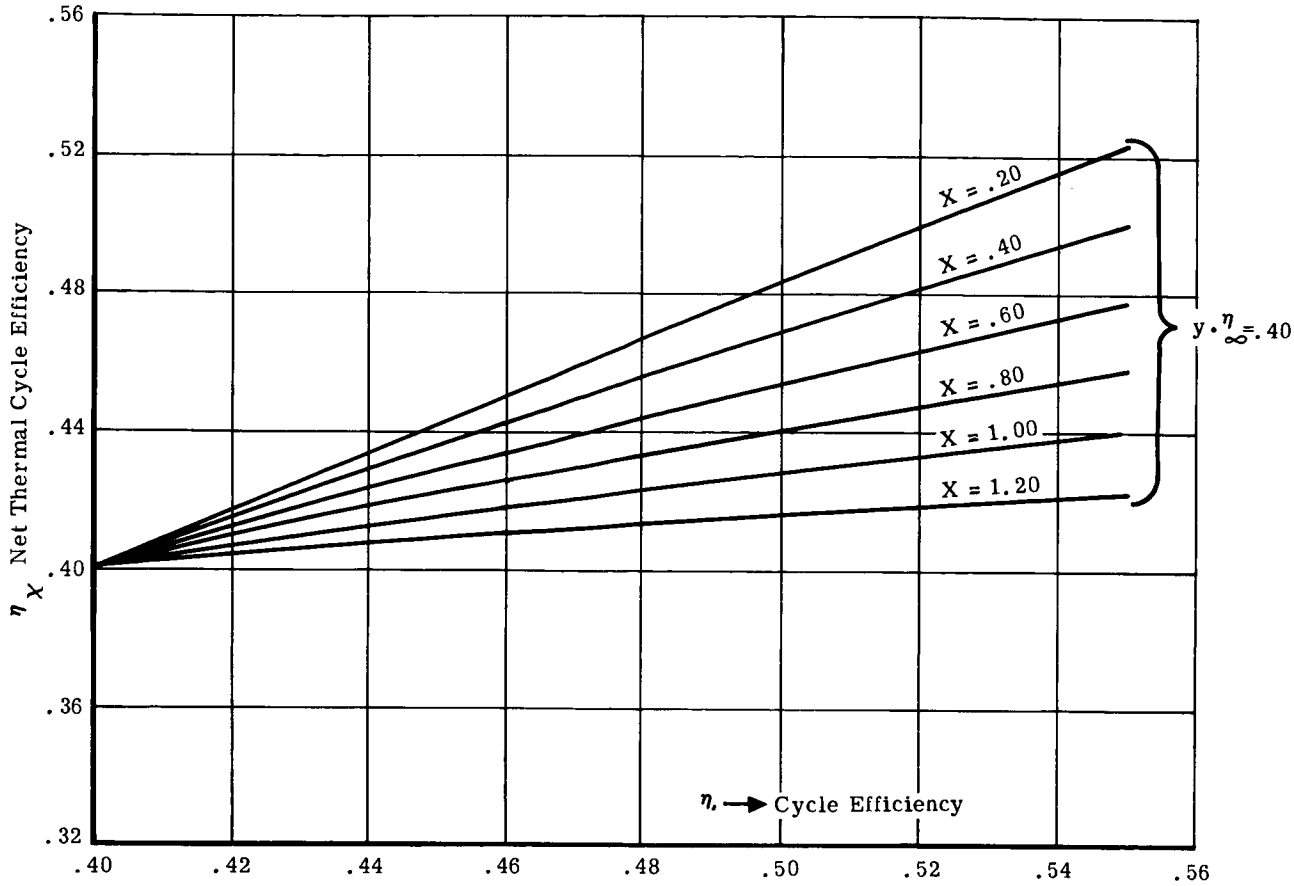

Fig. 3-14 - Regenerative Power System Performance with Cylinder Heat Rejection

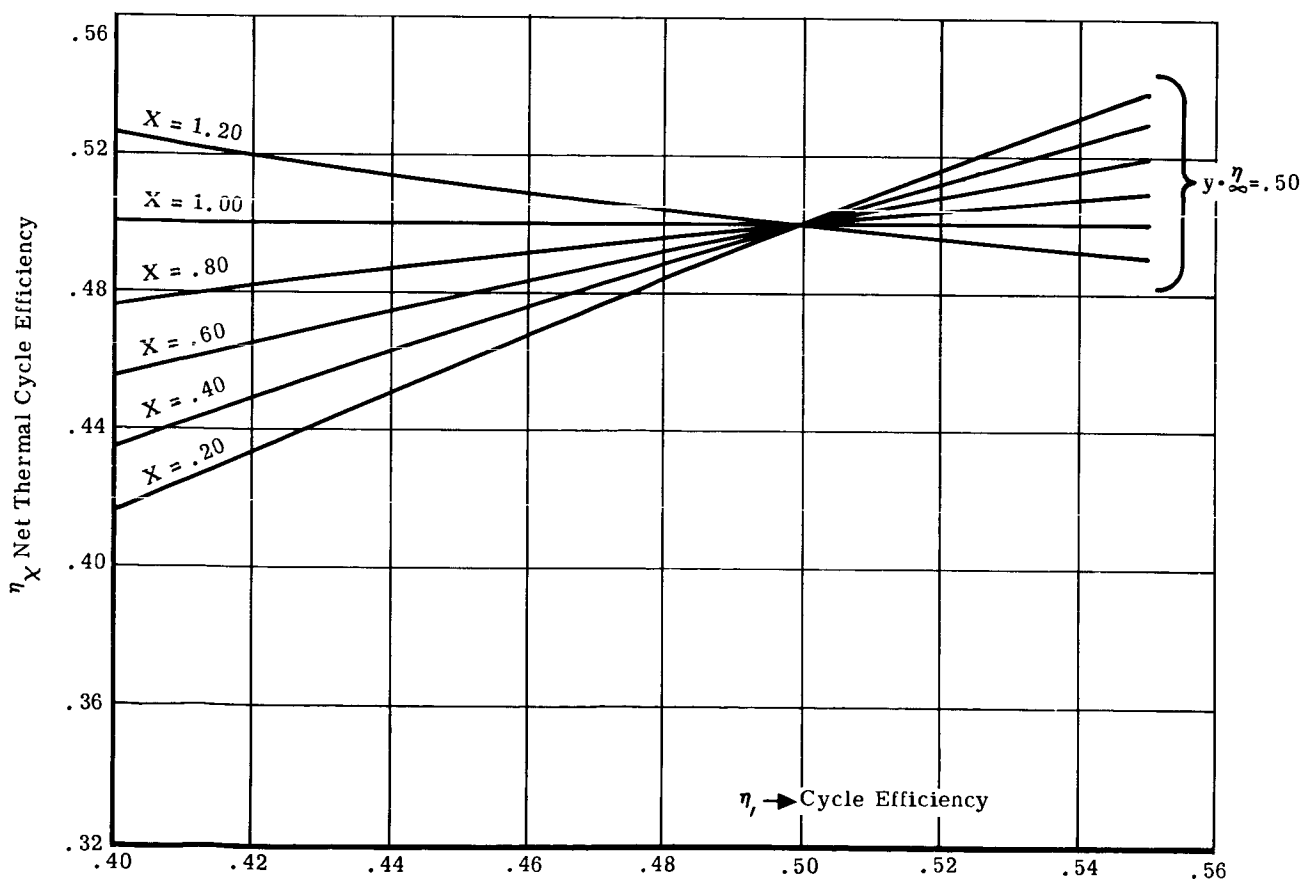

Fig. 3-15 - Regenerative Power System Performance with Cylinder Heat Rejection

$x = 1.0$, $\eta_x = 0.389$. BSPC varies approximately inversely with η_x.

To more clearly illustrate the effect of heat rejection on BSPC Fig. 3-16 is presented. This figure shows the variation of BSPC with heat transfer divided by BSPC without heat transfer vs. x for various values of y.

Non-Regenerative Cycle

Non-regenerative cycles are not affected by the heat rejection which occurs during the blowdown process, since at that point all of the cycle energy has been extracted from the working fluid. In a regenerative cycle, any heat losses which occur after blowdown will reduce the available energy which can be transferred to the incoming propellant. Although quantitative data on the non-regenerative cycles are not available at present, qualitative conclusions can be drawn.

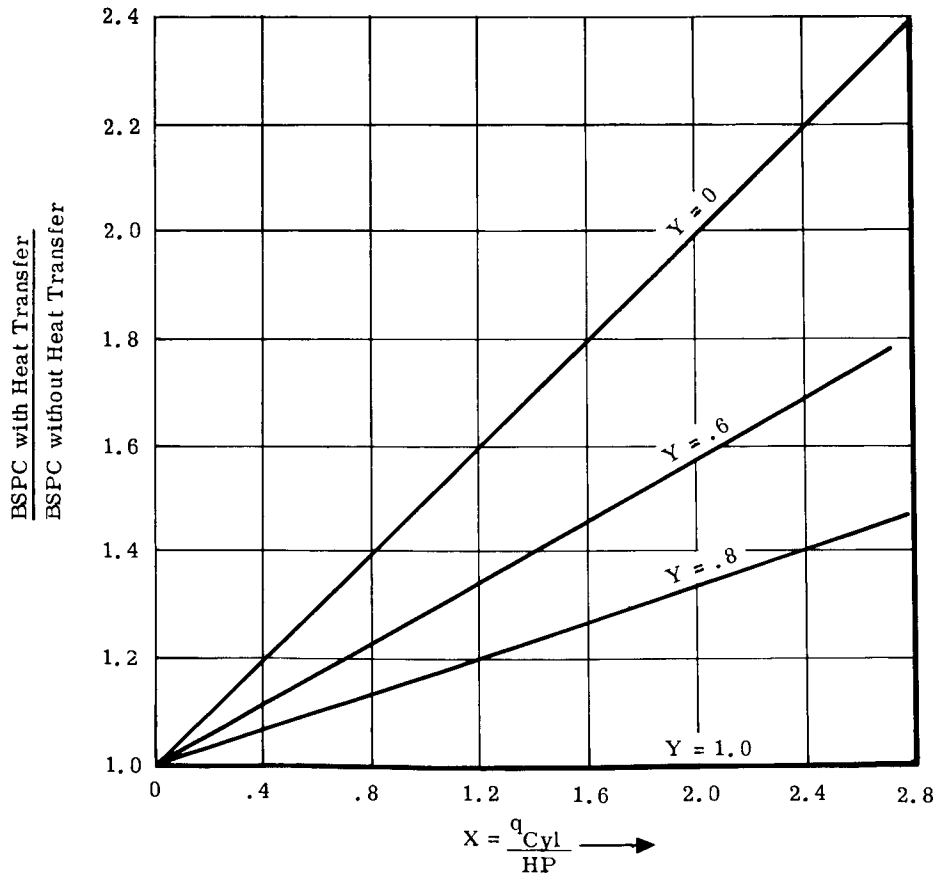

Fig. 3-16 - Relative Propellant Consumption vs. Cylinder Heat Rejection for Regenerated Cycles

A non-regenerative, stoichiometric engine cycle, will tend to reject less total heat to the cylinder because of the higher molecular weight of the working fluid. Since approximately 60% of the rejected heat is lost during the blowdown process (Ref. 3), heat rejection will have less influence on the performance of a non-regenerative cycle. It is reasonable to assume that the loss in cycle efficiency with heat rejection in a non-regenerative cycle will be less than the loss in a regenerative cycle with equal rates of heat transfer. The difference is accountable in the reduced energy transfer in the regenerator.

3.5.3 Engine and Power System Cooling Studies

Engine and power system heat rejection is illustrated in Fig. 3-17 as a function of O/F ratio. Also shown in Fig. 3-17 is the heat sink capacity of the hydrogen fuel. At O/F ratios

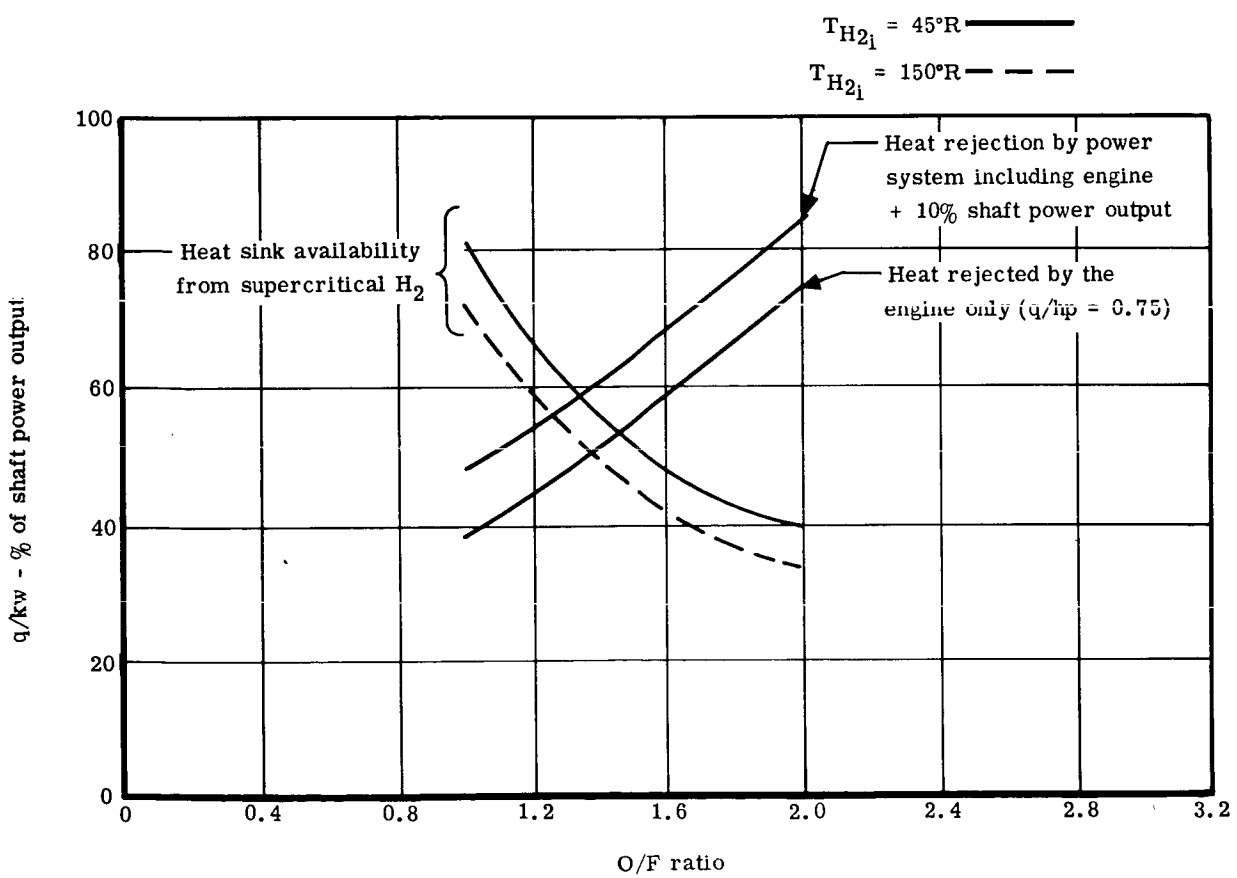

Fig. 3-17 - Available Heat Sink from Supercritical H_2 and Engine Heat Rejection

less than the 2.0 the cooling capacity of oxygen can be neglected. Clearly the intersection of the heat rejection and heat absorption curve defines an O/F region where SPU can be cooled by propellants alone. In the O/F region where heat rejection exceeds heat absorption, the net difference must be rejected by a radiator.

At the time of writing, no quantitative data on heat rejection from an optimized engine exists. For analysis purposes an assumption of q/HP = 0.75 at O/F = 2.0 is made. Heat rejection is assumed to vary with film coefficient and ΔT where:

ΔT = Tme - Tw

Tme = Arithmetic mean expansion temperature

Tw = Cylinder wall temperature assumed to be 860°R

Equation 3 is now rewritten in the form:

$$7)\quad \frac{\left(\frac{q}{HP}\right)_{O/F}}{\left(\frac{q}{HP}\right)_{O/F=2}} = \frac{\left[(K\Delta T)\left(\frac{MW}{T_{me}}\mu\right)^{.75}\right]_{O/F}}{\left[(K\Delta T)\left(\frac{MW}{T_{me}}\mu\right)^{.75}\right]_{O/F=2}}$$

By using Equation 7 the q/HP values at various O/F ratios can be calculated. Electrical losses (assumed to be q/HP = 0.10) can be added to the engine q/HP to define SPU heat rejection.

The heat absorption curves were calculated for hydrogen inlet temperatures of 45°R and 150°R. These values represent

temperatures at the beginning and termination of the design mission for supercritical storage. The hydrogen is heated to retain constant pressure. In the calculation BSPC·RT_{max} was assumed to be independent of O/F ratio.

When the hydrogen is at an inlet temperature of 150°R and the engine is generating electrical power, the hydrogen can absorb all of the rejected heat at an O/F = 1.25. Any operation at an O/F = 1.25 will not require a radiator because the hydrogen will do all the cooling. For O/F = 1.25 a radiator will be required. This points out that for a short duration mission, fuel rich operation may be advantageous, since the extra hydrogen required for cooling may weigh less than the required radiator and cooling system.

As expanded curve, (Fig. 3-18) illustrates the net heat rejection for engines and APUs with 150°R H_2 at various O/F ratios.

The weight of radiators for space applications is a function of the following:

1. Operating temperature
2. Orientation
3. Sink temperature
4. Meteoroid damage probability

Each of the above factors will be different for each mission and for this reason it is difficult (if not impossible) to generalize the weight of radiators.

In Fig. 3-19, two estimates of radiator weights are presented which indicate the approximate magnitude of weight. The upper

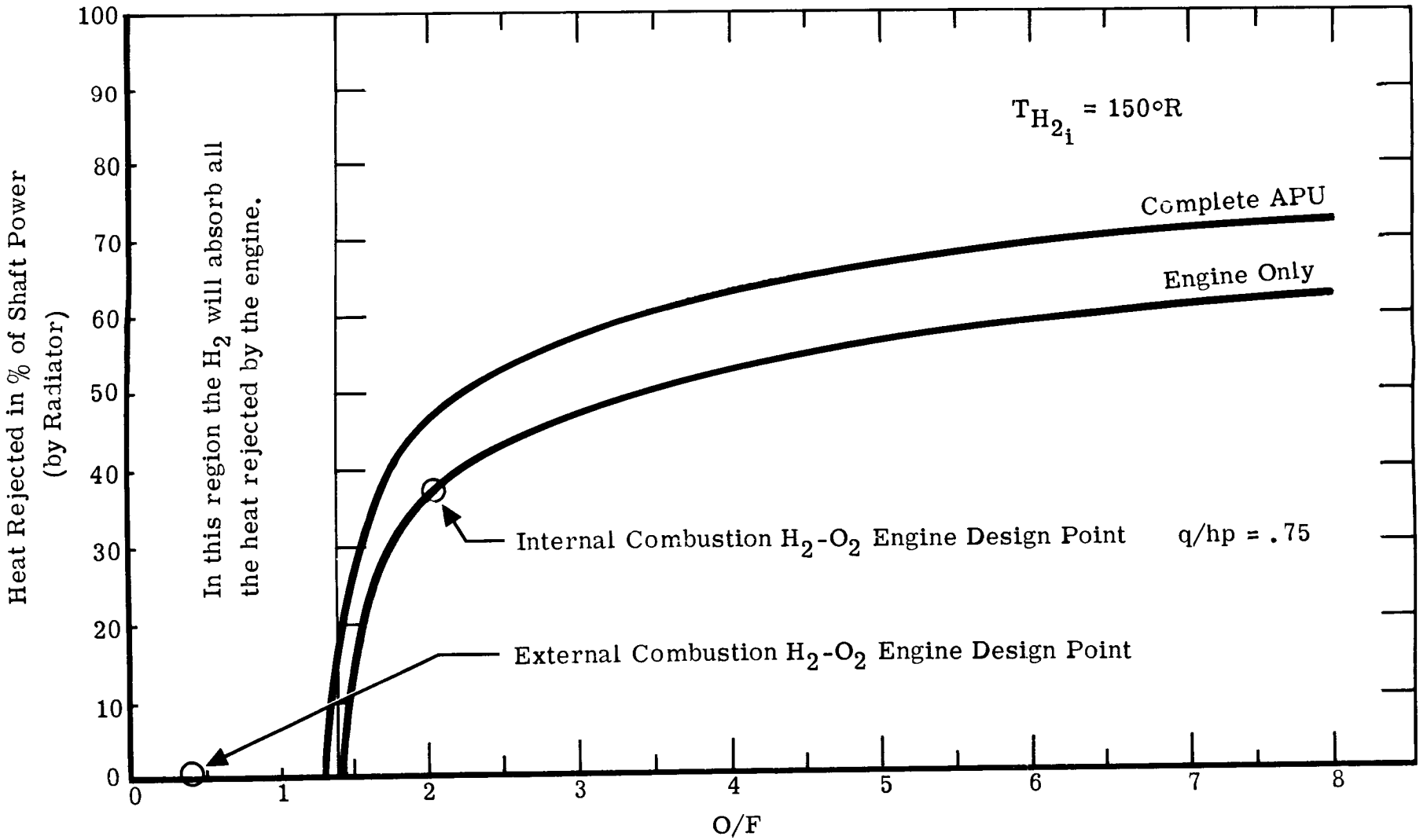

Fig. 3-18 - Heat Rejected in % of Output Shaft Power vs. O/F Ratio

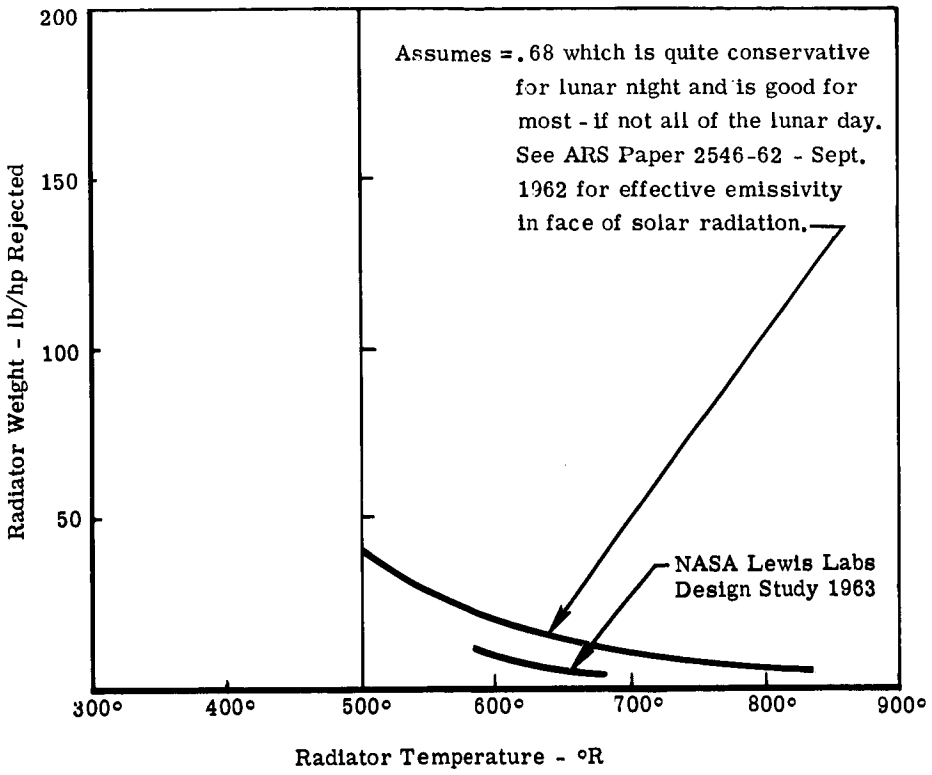

Fig. 3-19 - Radiator Weight vs. Radiator Temperature

line is based on uni-surface rejection with an effective emissivity of 0.68. The lower curve considers a radiator rejecting heat from both sides of the radiator with an effective emissivity of approximately 0.42.

The electrical components operate at greatest efficiency at low temperatures and therefore should be cooled with the cold hydrogen. The hydrogen would have to absorb some heat before it was used to cool the electrical components. The tank outlet temperatures are too cold for the electrical components.

3.6 Cryogenic Tankage Studies

The feasibility of both subcritical and supercritical tankage has been investigated. With the present day "state-of-the-art" tankage practices, only supercritical storage is feasible

for the SPU operating in a zero g, space environment.

Although subcritical storage would be lighter in weight than supercritical storage for short missions, there is at present no reliable method of expelling a single phase fluid from a subcritical storage container under zero-g conditions. This problem is being studied by tank manufacturers at this time. For longer missions, the increased weight of insulation required for subcritical tankage more than offsets the advantage of lower tank structural weight. Thus, supercritical storage would be preferred for the mission requirements of this program even if a practical subcritical tankage were available.

A supercritical tank will expel gaseous hydrogen or oxygen at the desired pressure above the critical pressure of the fluid. For the H_2-O_2 engine application, hydrogen at 300 psi and oxygen at 1000 psi were the selected design pressures. At these pressures the engine operates on propellants supplied directly from the tanks with no compression required. These selected pressures assure delivery of supercritical fluids while not imposing severe structural difficulties.

The supercritical storage tank weights are estimated to be 0.8 pound per pound of hydrogen and 0.2 pound per pound of oxygen in the propellant range required for the design mission. These tankage weight factors allow for a 100 hour storage period without venting or dumping propellant to prevent overpressurization. The effect of O/F ratio on total tankage weight is shown in Fig. 3-20, which illustrates the advantage of higher O/F ratio operation, (reduced tankage weight).

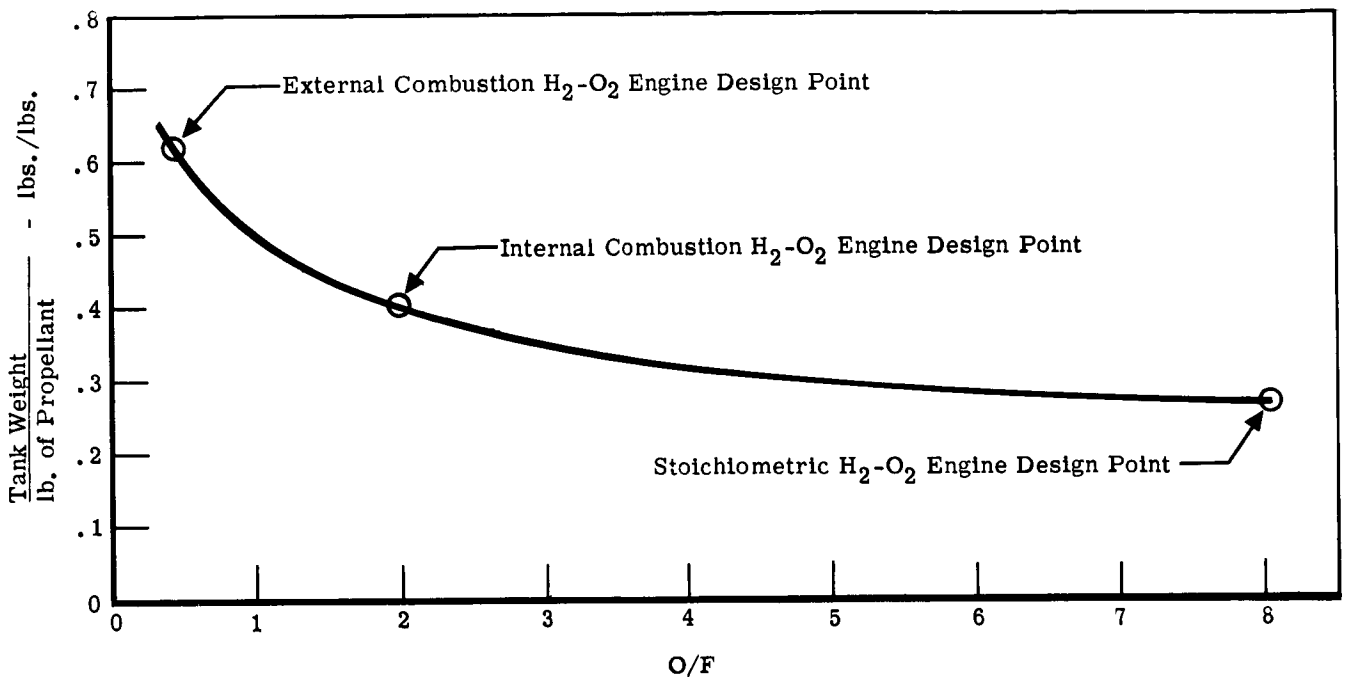

Fig. 3-20 - Supercritical Tank Weight/Pound of Propellant vs. O/F

One disadvantage of supercritical storage is that it is not practical to use more than 90% of the total stored fluid. Pressure is maintained by controlled heat input to the tank and because of this, only 90% of the total fluid is usable because of excessive heat input required to expel any significant portion of the last 10%. This necessitates carrying more propellant than is actually required for the mission. If low pressure storage was utilized, unusable residuals would be reduced, but compressors would be required and extra propellant would be needed for the engine to power the compressors. The trade-off for propellant required for compressor power vs. residual fluid trapped in the supercritical storage tanks is approximately 10 percent of the total propellant load in either case.

The reliability of supercritical storage tanks is high. The reliability for the total tankage systems design for a 350-hour mission is estimated to be: .99994 for manned vehicles and
.9993 for unmanned vehicles

The data for tankage weight factors and reliability were supplied by Beech Aircraft Corp.

3.7 Operation of Boiloff Propellants

Consideration has been given to the operation of the hydrogen/oxygen internal combustion engine system on hydrogen and oxygen boiloff which may be available from the propulsion tankage of upper stage hydrogen/oxygen fueled boosters. For the primary mission used to establish the requirements of this program, propulsion tankage boiloff may be available for the first 100 hours of the mission. During this period it was considered desirable to provide the capability of operating from either boiloff or on-board supercritical tankage. After the 100-hour point, all system operation would be on propellants derived from supercritical storage, and at this point, the hydrogen and oxygen compressors required for boiloff operation could be shut down by declutching them from the engine, as described in Section 2.

3.7.1 Uncontaminated Boiloff

Operation on boiloff propellants in a relatively pure state, that is, uncontaminated by inert pressurization gases or other impurities, appear to be completely feasible for the requirements of this program. It was assumed that boiloff hydrogen would be available to the system within the pressure range of

15 to 175 psia at temperatures between 37°R and 60°R. The oxygen would be available in the same pressure range as the hydrogen at temperatures between 160°R and 200°R. Compressor design considerations have indicated that the boiloff propellant pressure level at the compressor inlet should be reduced to 15 psia in order to simplify control of propellant flow to the compressor. The most attractive method of controlling propellant flow is to compress sufficient propellant to meet maximum engine demand and then spill or dump overboard the amount which is not required by the engine during periods of part-load operation. Although this will result in higher SPU propellant consumption, the propellant consumed during this mode of operation would be wasted anyway. Hence, this control method does not impose a weight penalty upon the boost vehicle itself. As long as relatively uncontaminated boiloff gases are available, it appears that their use as an energy source for the SPU will be simple and straightforward except for interface problems which may exist between the vehicle power system and the booster tankage system. This is an area which was beyond the scope of this program and it will require considerable attention before the use of boiloff for power generation can really be considered seriously.

3.7.2 Helium Dilution of Boiloff Propellants

One of the areas to be considered in studying the operation of the hydrogen/oxygen power system using boiloff propellants is that of the effect of helium dilution of the boiloff available from booster propulsion tankage. There is a possibility that both oxygen and hydrogen propulsion tanks may be pressurized with helium during the firing of the rocket engines for mid-course correction operations. Immediately after firing the

rocket engines the percentage of helium in the ullage space of the propulsion tankage may be as high as 65% helium in the hydrogen tank, and as high as 45% helium in the oxygen tank. The percentage dilution decreases with time, after firing of the engines, if the tank is vented, and/or if gas is withdrawn for use in the APU. This, of course, is due to additional gases being boiled off from the liquid propellant. However, it may take five to ten hours before the helium left in the tank is reduced to a negligible amount.

As many as six course-correction firings may be required in a typical mission.

Helium contamination produces two net effects: (1) propellant consumption (BSPC) is increased (2) mechanical control is severely hampered. The BSPC increases because the helium is a less effective diluent than hydrogen. When operating with contaminated propellants two events or a combination thereof could occur.

1. Hydrogen-helium mixtures: If oxidizer flow is constant (and thus power output constant), and with no He mixed therein, fuel (H_2/He) injection pressure must be increased to admit diluent to prevent excessive combustion temperature. Since the specific heat of the H_2/He mixture is lower than pure H_2 it is obvious that the weight of the H_2/He mixture will be higher than if pure H_2 were available, thereby increasing BSPC.

2. Oxygen-helium mixtures: If no He is present in the H_2 (i.e. pure H_2), but is present in the O_2, the oxidizer injection pressure must increase to a value which will

permit the same amount of O_2 to enter the engine in the O_2/He mixture as would enter with no He contamination. This is necessary to maintain constant power since power and oxidizer flow are practically directly proportioned. If the H_2 flow is not reduced, overcooling of the products of combustion will occur, which will increase the BSPC.

Of the two above events, the He/H_2 mixture presents fewer control problems. This is because the molecular weights of H_2 and He (2 VS 4) are more nearly equal than the molecular weights of O_2 and He (32 VS 4). Obviously the molecular weight of a He/O_2 mixture will be between 4 and 32 and the molecular weight of a He/H_2 mixture will be between 4 and 2. Three very apparant mechanical problems can occur.

1. Oxygen injection pressure, and thus, oxidizer compressor pressure ration, must increase inversely with the square root of mixture molecular weight to assure rapid enough injection. This may require pressures in the 3000 to 4000 psi range.

2. Besides having a variable outlet pressure, the compressor must have a throttled inlet to regulate the flow demanded by the engine. The inlet pressure must vary inversely with molecular weight while the exhaust pressure varies with the square root of the molecular weight.

3. The controls problems are certainly formidable even if a "programmed" intelligence can be built into the control system to permit it to respond to the effect of He. To date no satisfactory method of determinimg the He concentration of either H_2 or O_2 exists. The feasibility

of adequately controlling the power unit under these conditions appears doubtful unless adequate sensing can be provided. Stratification of He and O_2 or He and H_2 is a distinct possibility, which even further complicate the problems.

There are several alternative modes of operation with contaminated boiloff which may tend to reduce or eliminate some of the above problem areas. For example, during periods of relatively high helium contamination in the oxygen, it would be possible to operate from the on-board supercritical oxygen supply while continuing to operate with boiloff hydrogen, even with some helium mixed with the hydrogen. Although this would require extra oxygen to be carried on board, it might be a more attractive solution than other complex solutions which would permit the operation with contaminated oxygen. Another possibility is to include an oxygen liquification system within the boiloff propellant supply system. Boiloff hydrogen and/or hydrogen and helium mixture can be used to condense oxygen vapor present in the mixture of oxygen and helium. The liquefied oxygen and the helium still in gaseous form could be separated by means of a centrifugal separator. The liquid oxygen then could be pumped to the engine supply pressure as a liquid or it could be revaporized and compressed to the desired pressure with the oxygen compressor which is part of the SPU design evolved in this program. Oxygen liquification by this means would add considerably to the complexity of the system and require development of means of handling two-phase fluids in zero g environment. It might be justified on the basis of overall weight savings for a mission during which boiloff were available for a considerable portion of the total mission.

If pure boiloff hydrogen and oxygen are supplied to the compressors, these propellants can be used by the H_2-O_2 engine with no difficulty. Helium dilution in either the hydrogen or oxygen boiloff will cause severe control problems - particularly in the areas of matching compressor to the engine and providing adequate oxygen injection into the engine to produce power.

The desirability of making the hydrogen/oxygen SPU capable of operation from boiloff, particularly if the boiloff is unavoidably diluted with a pressurization gas such as helium, must be subject of considerable additional studies with the firm requirements of a specific application in mind. In principle, it is an attractive concept, but may involve interface problems of considerable magnitude as well as increased system complexity, particularly if the dilution of the propellants by pressurization gases or other contaminants is of significant magnitude.

3.8 Compressor Analysis

Compressor work curves for saturated vapor inlet are presented in Figs. 3-21 and 3-22.

Hydrogen compression work was calculated from a temperature-entropy diagram for hydrogen, assuming 75% compressor efficiency. Oxygen compression work was calculated from the following expression:

$$1)\quad \text{work}_{\text{actual}} = \frac{T_{in}\, C_p \left[1 - \left(P_2/P_1 \right)^{\frac{k-1}{k}} \right] (778)}{\eta_c}$$

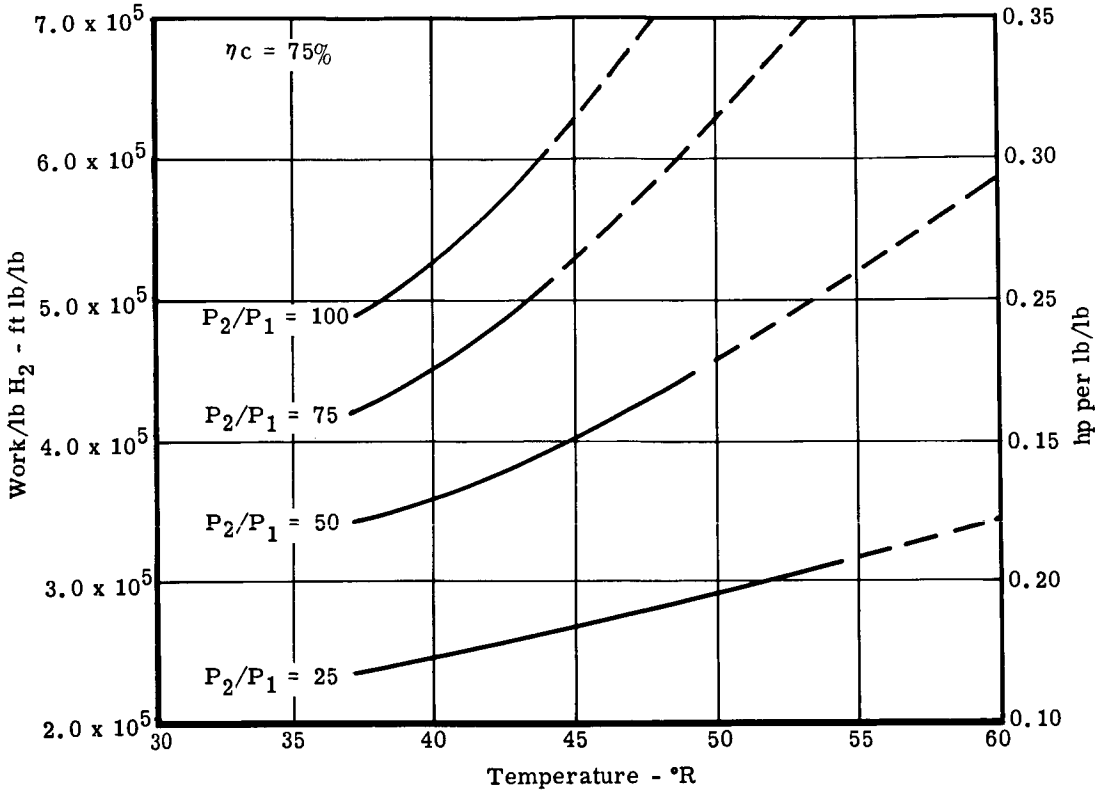

Fig. 3-21 - Work Required to Compress Saturated H_2 Vapor vs. Initial Temperature

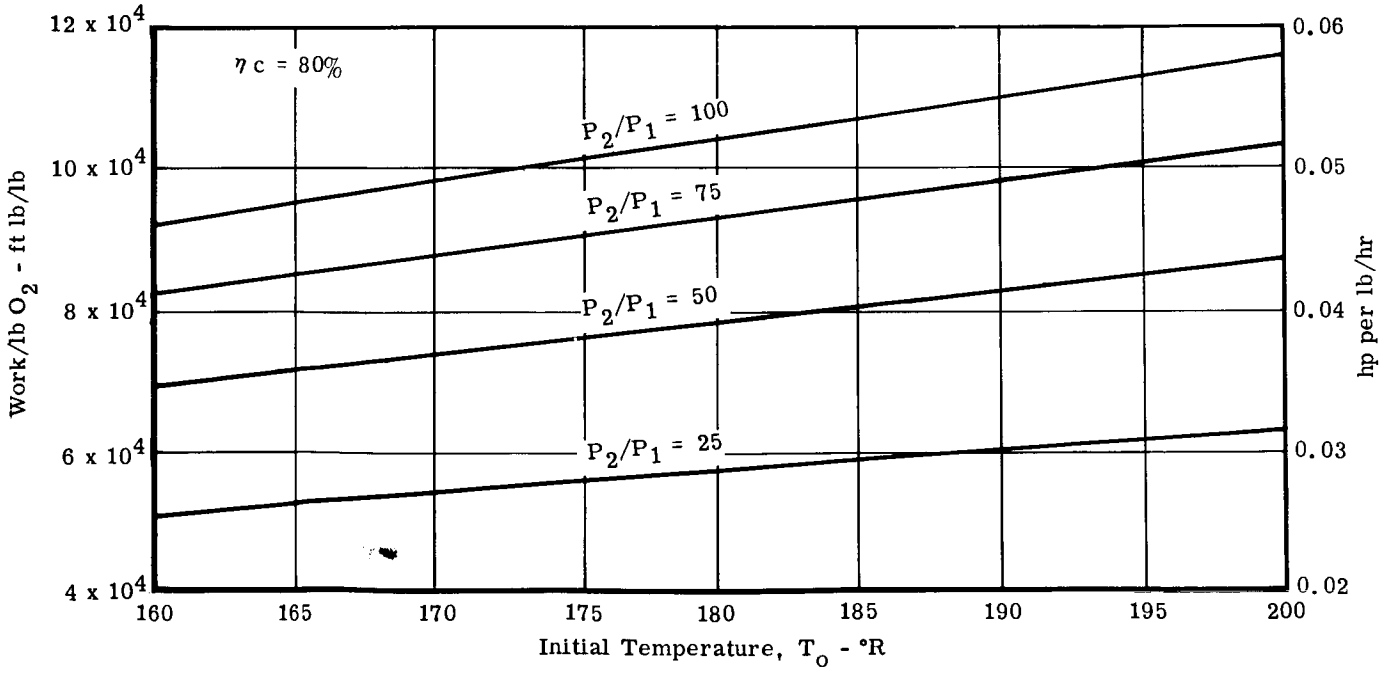

Fig. 3-22 - Work Required to Compress Saturated O_2 Vapor vs. Initial Temperature

using the following numerical values:

$$\eta_c = 0.80, \; C_p = .218 \text{ BTU}/\text{lb } ^\circ\text{F.}, \; K = 1.4$$

Because of uncertainties and lack of definite information regarding the use of helium diluted boiloff, all of the compressor analysis work was based on use of pure hydrogen and pure oxygen boiloff.

3.9 Conclusions

From the foregoing parametric studies, considering all of the influencing factors such as propellant supply conditions, thermodynamic cycle considerations, power modulation and cooling requirements, the following conclusions can be drawn.

1. The best type of power system for the mission requirements of this program is an internal combustion hydrogen/oxygen engine operating in a regenerative power cycle at an O/F ratio of 2.0.

2. Exhaust regeneration is a feasible method of increasing thermal efficiency, which results in a lower BSPC.

3. The system giving best overall performance for the sample mission uses a combination of hydrogen throttling and variable hydrogen inlet valve duration. The engine is sized so that the average power level occurs near full throttle and minimum admission, which is the most efficient operating point. This power modulation method was selected to be employed in all future development.

4. The most simple system uses a hydrogen throttle with a constant valve opening and delivers the greatest efficiency at maximum rated power. This system is not suitable for the power profile to which the present engine is designed.

5. If O/F is less than 1.25 an H_2-O_2 SPU can operate without a radiator, because the hydrogen will absorb all the rejected heat from the engine and alternator.

6. Considering 1963 technology in tankage, supercritical storage is preferred for the cryogenic propellants under zero gravity conditions.

7. If boiloff propellants are available from the booster propellant tanks in a relatively pure state, it is feasible to compress them and use them in the H_2-O_2 engine.

4.0 MISSION ADAPTABILITY STUDIES

4.1 Introduction

In order to establish areas in which the hydrogen/oxygen internal combustion engine may provide an attractive source of power, its application to a number of alternate missions in space was studied. The primary mission upon which the power system described in Section 2 of this report is based is that of a two-week, earth to lunar, landing and return mission.

The adaptability studies conducted were divided into three general areas:

1. General application of the H_2-O_2 engine APU concept to various space missions.

2. Specific application of the 3 kw H_2-O_2 APU currently being developed in this program to various space missions.

3. Discussion of operational considerations affecting H_2-O_2 APU application for spacecraft auxiliary power.

4.2 Scope of Studies and Assumptions

An H_2-O_2 power system was sized for the following four space missions, each of which have different power requirements.[1]

1. Earth to Lunar Landing

2. Lunar Excursion Module

---

[1] Load, energy, and duration requirements were supplied by NASA.

3. Lunar Roving Vehicle

4. Earth Orbit Space Station

As many parameters as possible were kept constant for the various mission studies which are listed below.

1. O/F = 2.0

2. All propellant is supplied from supercritical storage tanks

3. Hydrogen supply pressure = 300 psi

4. Oxygen supply pressure = 900 psi

5. Required propellants include 10% residual trapped in the storage tanks.

4.3 Application of H_2-O_2 SPU Concept to Space Missions*

4.3.1 Earth to Lunar Landing

This mission requires electrical power at an average load of 1.6 kw for 350 hours. The power requirements vary between 0.75 kw to 3.0 kw.

The power system designed to fulfill the above requirements would include a one cylinder H_2-O_2 engine coupled to an alternator. During the first 100 hours of operation, boiloff propellant may be available from the main propellant tanks.

Compressors are incorporated in the power system to utilize boiloff propellant if it is available. During the last 250 hours

---

* All calculations in this section are based on variable phase H_2 valve power modulation. After calculations were completed, variable duration power modulation was adopted, which results in @ 6% propellant and tankage reduction.

the propellants will be supplied from supercritical storage tanks. Total propellant requirements were determined for two possibilities (1) no boiloff available (2) boiloff available for the first 100 hours.

This mission was used as the basis of the power system design studies, therefore, the existing power system was designed to fulfill requirements of this mission.

A summary of the power system and load requirements are listed below:

	Propellants for 350 hrs	Propellants for 250 hrs (100 hrs on boiloff)
Average power	1.6 kw	1.6 kw
Maximum power	3.0 kw	3.0 kw
Total energy	558.3 kwh	558.3 kwh
H_2-O_2 engine displacement	2.77 cu. in.	2.77 cu. in.
Power system dry wt.	87.0 lbs.	87.0 lbs.
Total Duration	350 hrs.	350 hrs.
Complete system volume	88.8 cu. ft.	65.4 cu. ft.
Oil consumption	15.0 lbs.	15.0 lbs.
Propellant wt.	938.0 lbs.	690.0 lbs.
Propellant tank wt.	376.0 lbs.	276.0 lbs.
Total Weight	1416.0 lbs.	1068.0 lbs.

The mission design calls for continuous power but the power system would have startup and shutdown capabilities. For a mission of this duration a consumable oil system would be used because of minimum complexity with only a slight weight penalty.

4.3.2 Lunar Excursion Module

The LEM mission requires electrical power at an average load of 0.48 kw for 49.5 hours. The power range varies between 0.20 kw and 0.90 kw.

A power system designed to meet the above requirements would include an H_2-O_2 engine driving an electrical generator (ac or dc as required). All the propellant would be supplied from supercritical storage tanks. The propellant tank weights for this mission are slightly higher than the numbers in the cryogenic tankage section of the parametric studies would indicate because the tanks for this mission are approaching minimum weights, independent of volume.

Because of the extremely low power level requirements of the LEM, it is not the most favorable application for the H_2-O_2 internal combustion engine. For this application, the H_2-O_2 SPU appears to be slightly heavier than a hydrogen/oxygen fuel cell which would satisfy the same electrical power requirements. This is because the fixed weight of the engine does not vary linearly with power level as does the fixed weight of the fuel cell system. Engines in the small horsepower range typically weigh more per horsepower output than do higher-power, larger engines. If the power requirements for the LEM should increase from the initial levels indicated, the H_2-O_2 engine would then become increasingly attractive for this application. This is an important point to keep in mind because the final power requirements for a particular mission usually turn out to be higher than was originally estimated.

A summary of the H_2-O_2 power system specifications to meet the stated requirements of the LEM mission are:

Average power	0.48 kw
Maximum power	0.90 kw
Total energy	23.6 kwh
Duration	49.5 hrs.
Engine displacement	0.85 in^3
Complete power system volume	8.3 ft^3
Dry power system wt.	35.0 lbs.
Oil consumption	1.0 lbs.
Total propellant	84.0 lbs.
Propellant tanks	50.0 lbs.
Total Weight	170.0 lbs.

4.3.3 Lunar Roving Vehicle

Currently, there is considerable speculation as to the best means of propelling roving vehicles on the lunar surface. Undoubtedly, locomotion of lunar vehicles will be accomplished by means similar to shaft power drive systems available to today's earthbound vehicles. The basic problems of delivering power to produce torque at a wheel (or track) are quite the same whether the operation is accomplished on earth or on the moon.

Since lunar roving vehicles must be transported to the moon via a logistic carrier vehicle, every effort must be made to minimize the weight and volume of the roving vehicle and its equipment. In this respect, the selection of locomotion systems is different than on earth, where low cost and long life are the prime consideration.

In this section information is presented on various power systems. Weight and efficiency data are presented for hydrogen/oxygen fuel cell and engine power sources; and electric, hydraulic, mechanical, and pneumatic transmission systems. Various combinations of these components can be used to propel a lunar vehicle, and by using the included data, the various system parameters can be compared. To illustrate the application of the data, three (3) vehicle power systems using various combinations of the components are shown in figure 4-1.

The power system in a lunar roving vehicle must produce torque at the wheels of the vehicle as well as supply accessory requirements and, if manned, supply power for life support equipment. The methods of locomotion will probably be the same as those used on "off the road type" earth vehicles, with emphasis on light weight. The power required is estimated to be as high as 10.0 horsepower, depending on the terrain.

An internal combustion H_2-O_2 engine could be used with a mechanical drive train using either a manual or automotive type automatic transmission. Electrical and hydrostatic drives could be used, with individual motors mounted at each wheel. Another approach would be to use a central H_2-O_2 combustor with an expansion engine at each wheel. The major advantage of the latter system (at the cost of increased BSPC), is that no radiator is required for cooling the power system or vehicle. Also considered was a hydrogen/oxygen fuel cell providing power to electric motors at each wheel.

Power Plants

Both external combustion (EC) and internal combustion (IC) engine concepts were considered. The EC engine represents a

simpler configuration than the IC engine. The IC engine is more efficient than the EC engine and thus consumes less propellant. The IC engine power plant requires the following components for operation:

1. Engine
2. Regenerator
3. Controls
4. Miscellaneous accessories.

Operation at an O/F ratio of 2.0 gives the lowest BSPC but a radiator for waste heat rejection is required. Operation at O/F < 1.4 would not require a radiator for cooling but BSPC would be slightly higher and propellant volume greater.

The EC engine power plant includes the above items plus a remote combustion chamber where the propellants are burned, creating hot gases which are ducted to reciprocating expanders at the wheels and power take-offs. Operation at O/F ratio of 0.4 is recommended. No radiator is necessary with the EC engine.

Hydrogen/oxygen fuel cells being developed for scapecraft auxiliary power application could also be applied to the LRV. The fuel cell consumes less propellant than the engines previously discussed, but is penalized by a larger fixed weight than the engines. The fuel cells under consideration operate at the stoichiometric O/F ratio of 8 and weigh 100 lbs. per kw. A radiator is required with the fuel cell.

Transmission Systems

A discussion of each of the power transmissions follows.

Manual Clutch and Gearbox

A manual transmission, coupled with a differential and drives to each wheel, would be the most conventional design with the highest efficiency. A system of this type would have high reliability and the technology required to develop such a system is readily available.

Hydrodynamic Type Transmissions

A hydraulic torque converter plus automatic gearbox, as is used in modern automotive automatic transmissions, is another possibility for the lunar roving vehicle.

The torque converter may have a peak efficiency of 90%, if the efficiencies currently being achieved in larger sizes can be maintained down to the 10 hp level. However, the torque converter efficiency ranges from 0 to 90% in the usable speed range, and the overall average efficiency of the transmission would be considerably less than the peak value.

This type of transmission would have the advantage of requiring less attention from the vehicle operator so that he could devote more attention to the problems of negotiating the vehicle on unfamiliar terrain. However, this type of transmission has lower efficiency than the manual type.

Hydrostatic Transmissions

A hydrostatic transmission system requires a pump, hydraulic lines, and a fixed displacement motor at each wheel. If the vehicle requires variable speed capabilities, a variable displacement pump is needed.

The hydrostatic transmission system has two disadvantages over other types. While the system is in operation, the radiator must be used to cool the hydraulic components. Still, the hydraulic system may be the lightest in weight, even with the additional radiator area. The hydraulic component weights given in the data section have been optimized for size and minimum weight, including the radiator needed to cool them. The second disadvantage is the need to prevent the hydraulic fluid from freezing if the vehicle has a waiting period. This could be easily accomplished with a small heat source. The advantages of the hydraulic system are that the hydraulic rotating units are much lighter in weight than their electrical counterparts, and the hydraulic systems have proven reliability and should operate well in a lunar environment.

Electric Transmissions

An electrical transmission system requires electric lines and motors if a fuel cell is used as a prime mover. If an H_2-O_2 engine is the power source, a generator or alternator is also required, in addition to the motors and lines. If dc motors were used, they would have to be hermetically sealed in order to operate in a lunar environment. An alternator and an ac motor is an attractive combination because the power output and speed can be varied by changing the voltage and frequency of the electricity, which could be accomplished with the engine speed control. A disadvantage of electrical components is that they are heavier than hydraulic components. One advantage is that the electrical components can operate over a wider temperature range and are less affected by extreme low temperature than are hydraulic components.

Pneumatic Transmissions

In a pneumatic transmission, hot gas lines carry the combustion products from a central H_2-O_2 combustor to expansion engines at each wheel. These lines are sized for low pressure drop which results in high efficiencies. In a lunar environment, there would be a small radiation loss which could be minimized by gold-plating the hot gas lines. For a single shaft output, such as would be required by a tool, this type of system has the lowest total system fixed weight. The main advantage of this system is that no radiator is required.

Propellant Tankage

At the present time, supercritical storage tanks seem to be the preferable method of storing cryogenic fluids for lunar surface operation even though lunar gravity makes supercritical fluid properties unnecessary. Subcritical tanks may not be desirable because of their light structure, which may be damaged by shock-loading during landing. Also, additional insulation weight would be required if the propellants had to be stored for a long period of time before use. It may be possible to use supercritical tanks as structural members of a lunar vehicle, which would be impossible with subcritical tanks.

Cooling

Radiator weights are included in the component weights where radiation cooling is required. The radiator weight includes all coolant, pipes, fittings, etc., necessary for a complete space radiator. The weights used are based on an 840°R radiator, average temperature.

WEIGHT AND EFFICIENCY DATA

Drive Coupling

The speed reduction coupling between motor and shaft for a 50 rpm shaft weighs approximately 1 lb./hp and is 80% efficient.

Motors, Pumps and Generators

Type	Weight	Average Efficiency Over the useful speed range
Hydraulic motor*	0.8 lb./hp	88%
Hydraulic pump*	0.8 lb./hp	88%
DC Traction motors*	8.0 lb./hp	85%
DC Generator*	4.0 lb./hp	85%
AC Traction motor	6.0 lb./hp	85%
AC Generator	6.0 lb./hp	85%

Transmission Lines

Line weights include wire, tubing, or ducting, plus bracket fitting insulation, fluid, conduit, reservoir, etc., as required for each system. Note that each type of transmission line has a constant weight per foot of length up to 40 feet and up to 15 or 20 hp. This is because minimum practical sizes exist for each type of line.

Type	Length	HP	Weight	Efficiency
Hydraulic lines*	0-40'	0-15	0.45 lb./ft.	98%
Electric wire*	0-40'	0-15	0.50 lb./ft.	98%
Hot gas lines	0-40'	0-20	0.50 lb./ft.	98%

*The hydraulic and electrical components weights include the weight of the radiator necessary to reject heat from the hydraulic components. The other components do not need a space radiator, they can reject the heat themselves.

Automotive type Drive Train

Transmission Type	Weight	Average Efficiency Over useful speed range
Torque convertor and automatic gearbox	1.2 lb./hp	75%
Manual clutch and gearbox	1.0 lb./hp	95%

Final Drive Train; Shafts and Differentials**

Two Wheel Drive	1.0 lb./hp	90%
Four Wheel Drive	1.5 lb./hp	81%

**Estimates for a lunar roving vehicle application based on earth vehicle data.

H_2-O_2 Engine Weights (IC or EC)

		Min. or Fixed
Basic Engine	2.0 lb/hp from 3.5 hp	3.5 lb.
Regenerator	0.2 lb/hp add to	2.0 lb.
Control System		3.0 lb.
Lube System		5.0 lb.
Miscellaneous accessories		4.0 lb.
Radiator for IC engine	1.85 lb/hp add to	0.0 lb.
Combustor for EC engine	0.1 lb/hp add to	0.5 lb.

REPRESENTATIVE ROVING VEHICLE PROPULSION SYSTEMS

Figure 4-1 schematically illustrates three (3) representative vehicle propulsion systems. They are:

"A" External combustion (EC) expansion engine with hot gas transmission

"B" Internal combustion (IC) H_2-O_2 engine with hydraulic transmission

"C" Fuel cell with electric transmission

It must be stressed that these are only three (3) of a variety of power system configurations it would be possible to devise.

In each case illustrated, final drive to the vehicle wheel is through a harmonic drive* speed reducer, which enables a hermetic seal to be provided between the speed reducer section

*United Shoe Machinery Corp proprietary design.

Sample Power Systems for Lunar Roving Vehicles

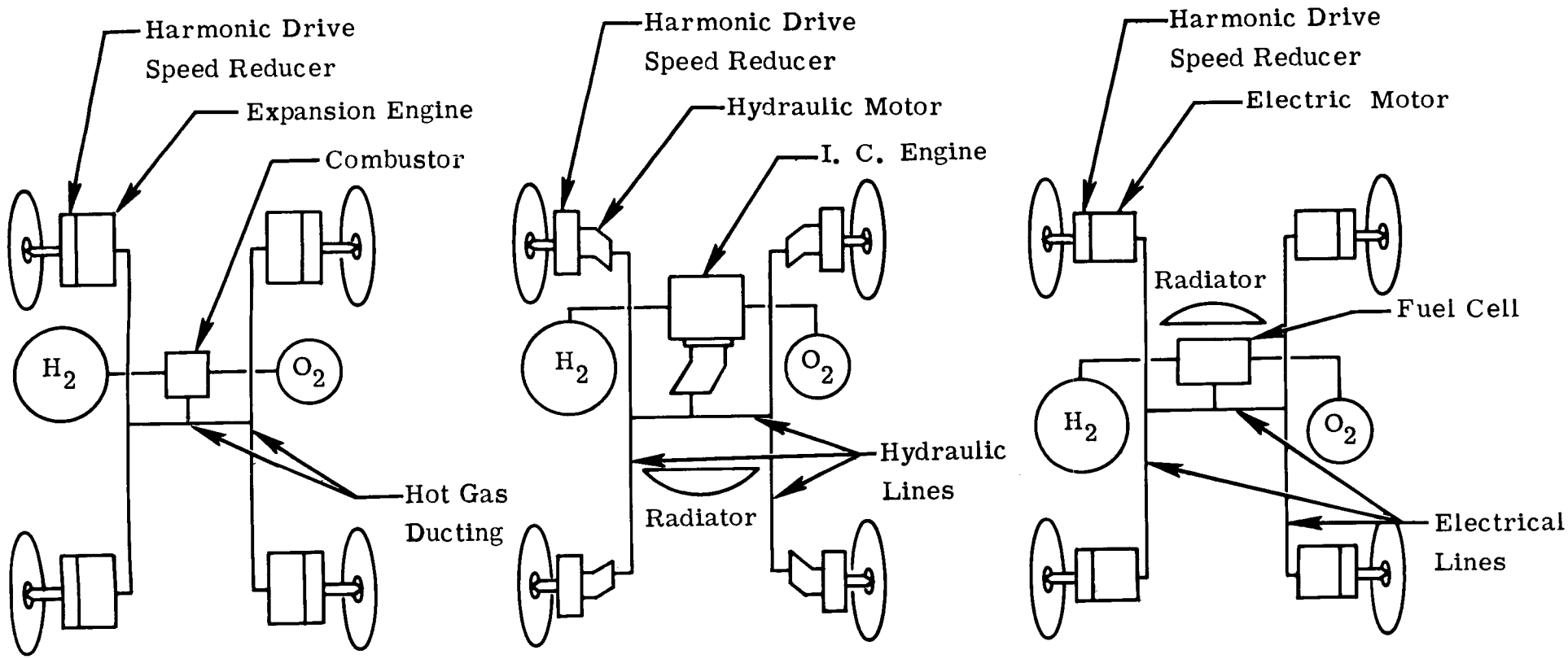

"A"
External Combustion
Engine Power System

"B"
Internal Combustion
Engine/Hydraulic
Transmission Power System

"C"
Fuel Cell/Electric
Transmission Power
System

Fig. 4-1 - Sample Power Systems for Lunar Roving Vehicles

and the wheel, thus eliminating leakage to the hard vacuum environment.

In the configuration "A" shown in figure 4-1, power is transmitted to each wheel by an expansion engine via a harmonic drive. Each engine receives the hot products of combustion of hydrogen and oxygen from the combustor through the "pneumatic" system. Each engine has individual controls to permit regulated power application to each wheel. Propellants are supplied to the combustor on demand. No cooling radiator is required for this configuration since the heat capacity of the hydrogen fuel is sufficient to absorb the entire heat load.

Configuration "B" in figure 4-1 uses a single IC H_2-O_2 engine driving a variable displacement hydraulic pump. High pressure hydraulic fluid is transferred to the fixed displacement hydraulic motors and harmonic drives at each wheel. A control system on the engine regulates the flow of hydrogen and oxygen to the engine. A radiator is required to reject the waste heat from the engine and transmission if operation is at $O/F > 1.4$.

The all electric system "C" illustrated in figure 4-1 employs a fuel cell driving traction dc electric motors at each wheel. The motors transmit power to the wheel via harmonic drives which enables each motor to be hermetically sealed. A radiator dissipates the waste heat from the fuel cell.

Mission Requirements

The power requirements for the lunar roving vehicles were given by NASA for three (3) different terrain conditions, Maria, Near Craters, and Upland.

	Maria	Near Crater	Upland
Avg. power kw	3.35	3.5	4.04
Max. power kw	6.5	6.5	6.5
Total energy kwh	200.8	215.2	242.1
Duration hrs.	60.0	60.0	60.0

The IC H_2-O_2 engine power system was sized for these power requirements for four (4) different types of power transmission. A summary of the results is presented below:

Complete sys. vol ft^3	34.1	36.7	40.4
Engine Displacement in^3	6.53	6.53	6.53
Total Propellant wt. lbs***	345.6	370.5	415.0
Propellant storage tanks wt. lbs	139.0	141.0	166.0

An estimate of total power system weights, based on a 10 hp IC engine, and transmission system efficiencies, follow:

***These performance firgures are based on an IC H_2-O_2 engine with a transmission efficiency of 64%. The propellant consumption and propellant storage tank weights will be inversely proportional to the overall transmission efficiency of the type of system used in a lunar roving vehicle.

Type of transmission	Estimated mech system wt (Less propellant and storage tanks)	Estimate overall transmission efficiency
Electrical motor on each wheel	210.6 lbs	66.7%
Hydraulic pump with a hydraulic motor on each wheel	94.2 lbs	60.5%
Mechanical (clutch, gear-box, and differentials)	69.5 lbs	77.0%
Hydrodynamic (automatic transmis sion and dif-ferentials)	71.5 lbs	73%

The H_2-O_2 engine would be capable of multiple starts and stops. The power system would be able to endure storage periods in the lunar environment without any problems.

For comparison, the weights for the three systems shown in Fig. 4-1 are presented in Fig. 4-2 at two power levels; 4 hp and 10 hp. It will be noted that the IC engine powered vehicle is the lightest (has the highest payload for same gross weight) within the range of the most probable total energy requirements.

4.3.4 Earth Orbit Space Station

Two electrical power requirements were considered for this mission. The duration of both is 1000 hours. The load profile A

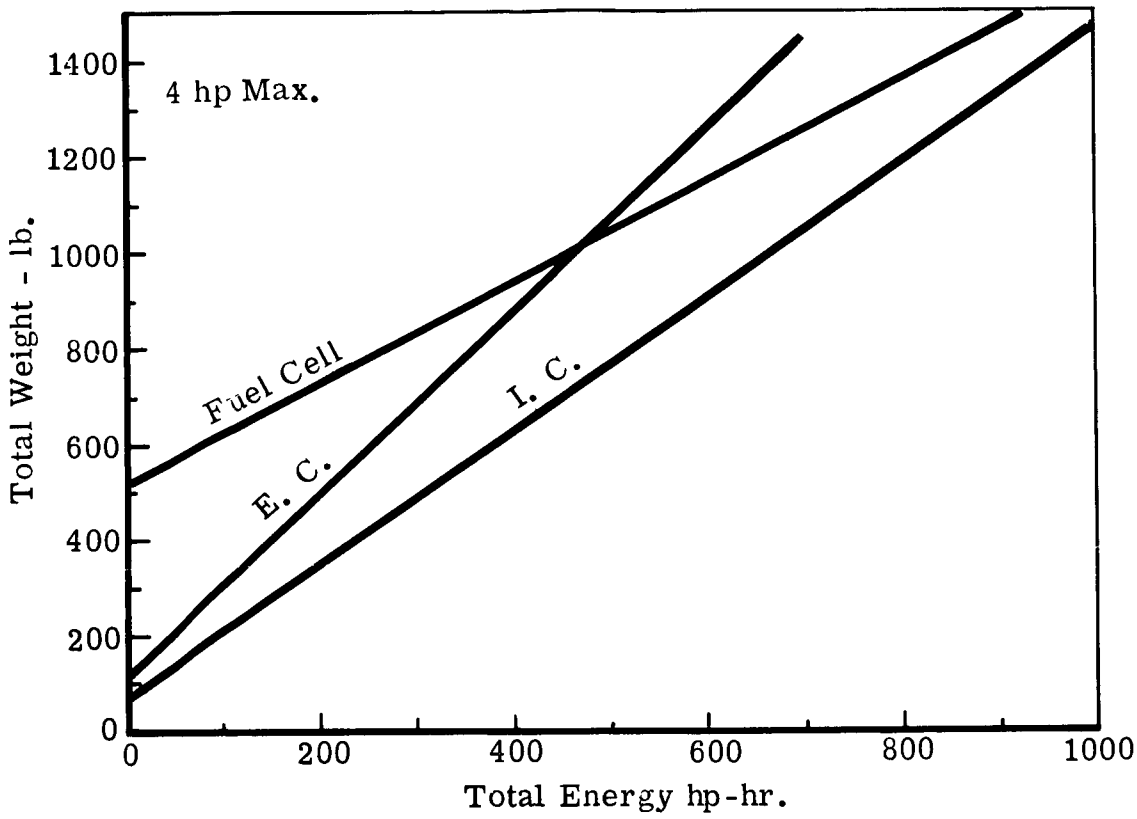

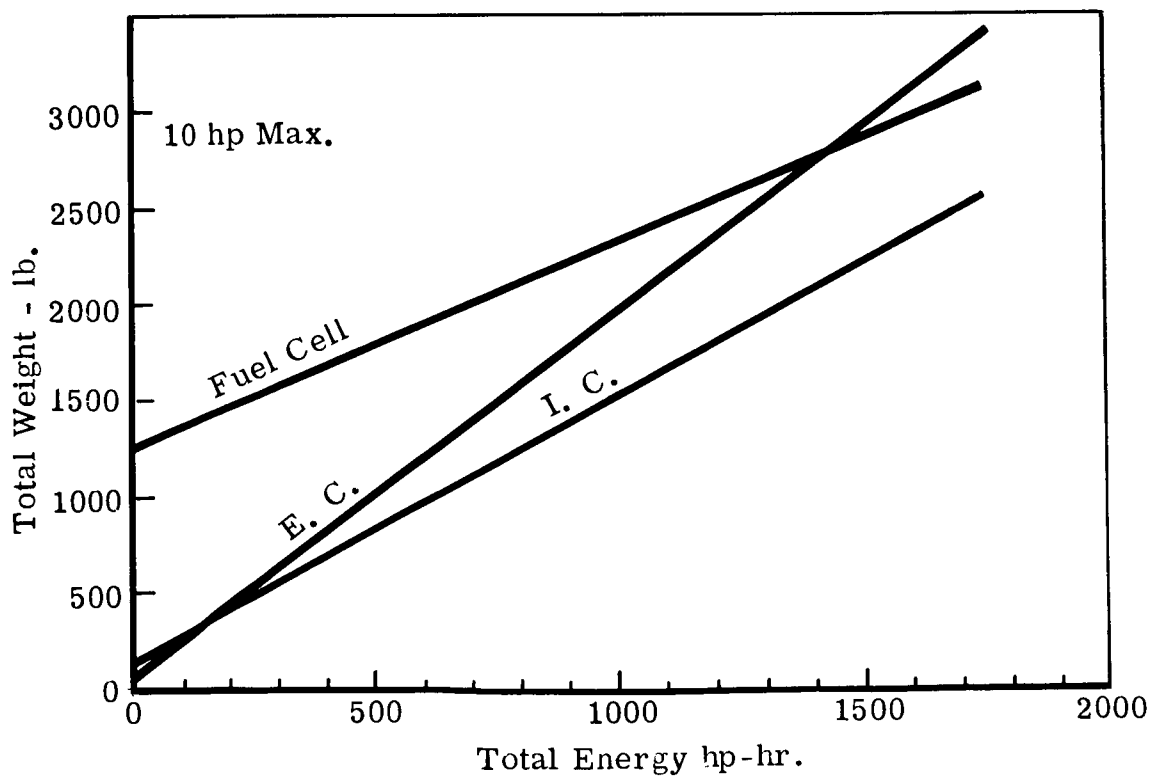

Fig. 4-2 - System Weight Including Propellant and Tanks at a Constant Power Output vs. Time

is a 7.5 kw average load with a maximum load of 12 kw, and load profile B is a constant 12 kw load.

The weights and volumes for the propellants and storage tanks shown in the performance summary were calculated on the basis that the total propellant would be available at the start of the mission. This would be unrealistic if resupply capabilities existed.

A performance summary of the specifications to meet the mission load profiles is given below:

	Load Profile A	Load Profile B
Average power kw	7.5	12.0
Maximum power kw	12.0	12.0
Total energy kwh	7500	12,000
Duration hrs.	1000	1000
H_2-O_2 engine displacement in^3	13.0	20.8
Propellant wt. lbs	12,500	20,000
Tank wt. lbs	5,000	8,000
Power unit wt. lbs	120	180
Power unit vol. ft^3	3.0	4.0
Propellant tank vol. ft^3	1164	1867
Total volume ft^3	1167	1871

The lubrication systems in this power system would preferably be the recirculating type with provision for zero g operation in order to reduce the quantity of oil required for extended periods of operations.

Due to the relatively permanent nature of an orbiting space station, neither the H_2-O_2 engine system or any other open cycle

expendable propellant power system represents an optimum selection for the main station power supply system. Undoubtedly, the first permanent space station will employ solar cell power systems for primary power. Later, solar dynamic or nuclear dynamic systems may be optimum as the state-of-the-art of these systems advances.

However, for any manned orbital space station operations, it will be necessary to have an emergency standby power system which is independent, and preferably of a different type, from the primary power system. The H_2-O_2 engine power system appears to be a very attractive choice for meeting this need. In this regard it is discussed to a greater extent in Section 4.4.1.

4.4 Application of Current 3 kw H_2-O_2 Engine Power System to Space Missions

4.4.1 Manned Space Station

The 3 kw H_2-O_2 APU being developed under this contract may serve effectively as an emergency source of electrical power for a manned space station. The power level is adequate, based on latest design information.

The selection of the primary source of electrical power will be dictated by a detailed trade-off study, considering the logistics of propellant re-supply versus use of nuclear or solar emergency power.

The use of a H_2-O_2 APU as an emergency source of electrical power is feasible for extended durations of weeks or months in view of the low boiloff rates which can be achieved with new super insulations being developed for supercritical tankage. Boiloff rates of fractional percentages per day are now

These page(s) were missing from the report when received by NTIS. Repeated efforts to obtain a replacement page have been unsuccessful.

This report is being made available in its present form with the hope it will be of sufficient value to justify its announcement and distribution.

129-130

taking place with the lunar excursion module, the power requirements of the basic Apollo vehicle still remain approximately the same. Thus, the H_2-O_2 engine powered APU still provides a possible alternate or backup system for the fuel cell power system which has been selected for the Apollo vehicle. Should the Apollo mission power requirements change and require a higher power level, particularly if the higher peak power is required only intermittently, the H_2-O_2 engine system could be installed in the vehicle to supply the peak power demands over and above the average power provided by the fuel cell system, at a much lower installed weight than additional fuel cells. Since both the fuel cells and the engine would use the same propellants, it would be necessary only to increase the tankage size slightly and the inclusion of separate tankage for the dynamic power system would be avoided. Also, the inclusion of the H_2-O_2 engine power system in the same vehicle, which also uses fuel cells to provide the basic vehicle power, could provide a degree of redundancy which is impossible to achieve by simply adding the multiple units of the identical type. With multiple identical units, a particular failure mode could possible affect all units similary within a fairly narrow time span. However, if redundancy is achieved by employing multiple systems of entirely different concept to do the same job, the chance of a single failure mode affecting all systems would be greatly reduced. Thus, for some missions where an extremely high degree of reliability is necessary, it may be possible to achieve this reliability at a much lower total weight by employing both a hydrogen/oxygen fuel cell and an H_2-O_2 engine to develop the necessary power.

4.4.4 Miscellaneous Applications

H_2-O_2 SPUs will be optimum or competitive for the following missions:

1. Recoverable liquid rocket booster

2. Manned satellite inspectors or interceptors

3. Advanced boost-glide vehicles

4. Extreme altitude (over 100,000 ft) balloons

5. Portable power for tools and other shaft power requirements in space, and lunar and planetary surface operations.

The scope of the present contract did not permit study of SPU requirements for these missions, but future effort should be directed to application studies for these missions.

4.5 Operational Considerations in Space Environment

The operation of mechanical systems in space environment, where they will be subjected to conditions of hard vacuum, radiation, and zero gravity, requires the implementation of new design concepts which are not necessary when designing for the familiar earth environment. Also, in many cases, operation of a system may be necessary in a remote or hazardous location where it cannot be conveniently reached by operating personnel. Check-out, start-up, shut-down, purging, and similar operations may be required to be remote controlled.

4.5.1 Zero Gravity

The absence of gravity will influence, primarily, the lubrication system of the H_2-O_2 engine. Other portions of the power system will be relatively unaffected by the absence of gravitational forces. As far as lubrication is concerned, the basic problem created by the absence of gravity, is how to handle the liquid lubricant within the lubricating system of the engine. Two approaches to solving this problem are: (1) Employ an open cycle lubrication system to supply lubricant to each area of the engine system in the exact amount required for that particular area. The expended lubricant is then collected and expelled overboard from the vehicle; (2) Employ a means of collecting the lubricant from the various areas of the engine and return them to an oil sump for recirculation through the lubrication system. Both of these lubrication concepts have advantages and disadvantages. The open cycle system involves less mechanical complexity, but results in a higher consumption rate of lubricant than the recirculating system. In order to minimize the lubricant consumption rate, it would be desirable to supply the minimum amount of lubricant to each area of the engine but this could be hazardous in view of the possibility of a malfunction in the lubrication system. The recirculating lubrication system would allow excess quantities of oil to be supplied to all critical areas, since the bulk of the oil would be collected and returned to the system for recirculation. The only lubricant consumed would be that which is lost to the system through leakage past seals or out the exhaust ports of the engine. This system involves more mechanical complexity than the open cycle system, and would require a means of collecting oil from the various portions of the engine and returning it to the oil sump. It may also require an oil cooler

to maintain reasonable lubricant temperatures. The collection and separation task could probably be accomplished by use of a centrifuge within the engine crankcase. Weight tradeoff studies have indicated that for missions of less than two weeks duration, the open cycle lubrication system would be preferable because of its lower degree of complexity, but only if low oil consumption rates in the order of .01 pounds per hp hour could be achieved. At higher consumption rates or for longer duration missions (beyond two weeks), the additional complexity of the recirculating oil system would probably be worthwhile in order to reduce the oil consumption rate and hence achieve a lower overall system weight.

Section 2 of this report describes in more detail the lubrication system design concepts for the power system being developed under this contract.

4.5.2 High Vacuum Environment

Operation of the H_2-O_2 power system in a high vacuum environment does not appear to involve any unique problems except when the power system is shut down or is on standby. While the system is in operation, all moving parts requiring lubrication or in rubbing contact with other parts would be shielded from the high vacuum environment by enclosing them within the engine crankcase or within the enclosure formed by other parts of the system. Thus, outgassing and cold welding problems which can be experienced in the presence of high vacuum, would be avoided. If the H_2-O_2 system is applied to a mission where its operation is required only intermittently to meet power demands, or where it is on standby for use as an emergency power system, some precaution must be taken

to prevent the moving parts of the engine from being exposed to the hard vacuum of space through the engine exhaust system. While the engine is stationary, the blowby and residual exhaust products which would normally occupy the engine crankcase along with the lubricating oil vapor would leak out past the piston and piston ring clearances to the engine exhaust ports and then, through the regenerator exhaust system and out into space. If the engine is stationary for a sufficient time for the crankcase pressure to leak down to hard vacuum levels, evaporation of the residual lubricant left in the rotating parts and outgassing of the materials within the engine crankcase and within the cylinder could occur. Under extreme conditions this could possibly result in cold welding of the piston and piston rings to the cylinder wall and cold welding of the bearings, cams, gears, and other moving parts.

There are two possible methods of preventing outgassing and cold welding during periods when the engine is inoperative. One is to operate the engine at sufficiently frequent intervals to insure that at least a minimum amount of oil film remains on the critical parts within the cylinder and crankcase at all times. A considerable amount of research and experimental testing would be necessary to determine what the minimum frequency of operation must be to prevent cold welding problems. The other solution to this problem is to provide a valve in the engine exhaust system which would be closed immediately after the engine is stopped. This valve would effectively isolate the engine crankcase and cylinder from the vacuum of space and would prevent the breakdown of crankcase pressure and, hence avoid the outgassing and cold welding problem entirely. However, the design of such a valve might be a formidable task. The valve would have to be capable of sealing tightly against the hard

vacuum of space without becoming cold welded itself because of the hard vacuum environment. High reliability would be a prime requisite for such a valve.

The problem of protecting the engine and other system components from the outgassing and cold welding problems associated with hard vacuum environment is an area which will require a considerable amount of additional detailed study and consideration; particularly, after specific mission requirements are better established.

4.5.3 Startup and Shutdown Procedures

On some missions it is conceivable that the power system would be started on the ground prior to launch and would operate continuously throughout the entire mission. In such a mission the problems of inflight startup, shutdown, and checkout would not exist. Any conceivable realistic mission requirement however, would no doubt involve the capability of inflight shutdown and startup if for no other reason than to provide for a redundant SPU (for reliability purposes) to be started up in case of failure of an operating SPU. The necessity of shutting down a deficient operating unit should also be anticipated.

Normally, the startup procedure for the flight design system being developed in this program would involve the following steps:

1. Open the hydrogen tank shutoff valve

2. Crank the engine, using the alternator as a starter motor in the starting mode described in Section 2.2.5 of this report.

3. Open the oxygen propellant tank valve

4. As oxygen reaches the engine cylinder in the presence of hydrogen and a catalyst, combustion will occur with the engine accelerating to overrun the starter motor, thus converting it back to generator operation. From this point, operation of the system would be self-sustaining.

If after starting the SPU, boiloff gas is available from the main propulsion tankage, the propellant supply system could be switched over to boiloff operation by switching the proper propellant selector valves and engaging the compressor drive clutch. Starting the system, however, would always require using the onboard propellant storage at supercritical pressures. In the starting procedure it may be necessary and desirable to preheat the cold cryogenic hydrogen during the engine cranking mode before it reaches the engine inlet valve. Since there will be no hot engine exhaust gas reaching the regenerator for this purpose, it would be relatively simple to include an electric resistance heater which would take its power from the vehicle battery, to preheat the incoming hydrogen in the hydrogen line. The battery, of course, is also required to provide the energy for cranking the engine for starting.

Shutdown of a normally operated unit would be accomplished by merely closing the oxygen tank shutoff valve and purging the oxygen line with an inert gas such as nitrogen. Combustion is the engine will cease as soon as the oxygen is used up, at which time the hydrogen tank shutoff valve would be closed. The engine should then be purged with an inert gas such as nitrogen, although hydrogen purging at this point should be safe in the absence of oxygen in the system. It may be possible to

eliminate the purging requirement, but this remains to be demonstrated conclusively. After the engine is stopped, some method of avoiding outgassing and cold welding of the moving parts must be provided, as discussed in Section 4.5.2.

It is anticipated that the H_2-O_2 power system would be applied in a redundant manner in most probable applications, with two, or even three, units aboard the vehicle, depending upon what the requirements for maintaining power output are. In case of the failure of one unit, either one or more of the redundant APUs may be stationary on standby. On the other hand, one unit may be kept idling on the line while another supplies the power requirements; or as a third possibility, two or more units may operate continuously and share the normal load requirements, each unit being capable of meeting the maximum emergency requirements by itself. These considerations require that additional attention be given to the problems of startup, shutdown, electrical paralleling, acceleration time, and other considerations which affect the power recovery characteristics of the vehicle system.

4.5.4 Checkout

In case of application to vehicles where the H_2-O_2 power system may be on standby for emergency purposes or be used intermittently to supply peak load demands, it may be necessary, and would be advisable, to periodically check out the standby unit or units. As discussed previously in Section 4.5.2, periodic checkout would provide a means of avoiding outgassing and cold welding problems which could occur with sustained exposure of the engine cylinder and crankcase to the hard vacuum of space. Furthermore, periodic checkout of a standby power

system may be accomplished by using the excess cryogenic propellant such as propellant tank boiloff gases or gas which would be vented from supercritical storage tankage to relieve excess pressures. The normal checkout procedures would simply involve starting up the engine as described in Section 4.5.3, operating it at a moderate load, or subjecting it to a typical load profile involving some operation at low load, some at moderate load, and some period of time at peak load conditions. The time involved for checkout should be between 15 and 30 minutes minimum in order to allow the system to reach a stable operating temperature. System performance during this checkout period could be monitored, checking power output, frequency control, recovery from transient loads, and monitoring the specific propellant consumption at some particular condition. Provisions could be made for accomplishing all of these tasks automatically, but this would require additional complex mechanism and monitoring equipment aboard the vehicle which might not otherwise be necessary. Under some circumstances it may be possible, even preferable, to have a crew member conduct the APU checkout procedure. In any event, the detailed checkout procedure and schedule would have to be established for a particular vehicle and mission after specific application requirements are better established.

5.0 CONTROL STUDIES

5.1 Scope of Study

The primary purpose of these studies was to define requirements for the control system of a small, high performance power plant. The object was to formulate general system requirements which could be applied to many designs. As the control hardware is designed and tested, additional requirements may be necessary to adequately insure the performance of the system.

5.2 System Configuration Development

A series of system schematics are included to show the evolution of the system configuration.

Initially, the system incorporated the following concepts:

1. Closed loop control for hydrogen compressor
2. Tankage feed through compressors to boost pressures
3. Oxygen pressure controlled at oxygen compressor inlet
4. Hydrogen flow control by a variable dwell poppet valve
5. Oxygen and hydrogen, fed (separately) through regenerator
6. O/F ratio control by sensing either cylinder head or exhaust temperature
7. Speed control using either hydraulic flyball governor or Tach generator
8. Load sensing considered as part of system

Preceding page blank

After considerable study, two possible methods of control seemed worth considering.

The primary control approach required the following changes in the system: (See Fig. 5-1).

1. Oxygen was not passed through the regenerator

2. A variably phased hydrogen valve replaced the variable duration valve. (This choice was made due to power modulation considerations observed through cycle analysis; see Section 3.5).

3. The oxygen flow control becomes a throttling valve positioned as a function of temperature and pressure. Mixture ratio control is to be effected by monitoring exhaust gas temperature.

4. The electrical tachometer appeared to be a superior method of speed control, because of the high quiescent power drain of hydraulic flyball governors.

5. Plenum chambers are inserted between the engine and the compressor. This dynamically disassociates the compressors and the engine.

6. Closed loop control for a constant compressor output and compressor exhaust valves are also added to the schematic.

An alternate approach consisted of the same system, but with oxygen pressure controlled at the compressor inlet; however, high response is required for adequate system control. Further cycle analysis indicated that a constant

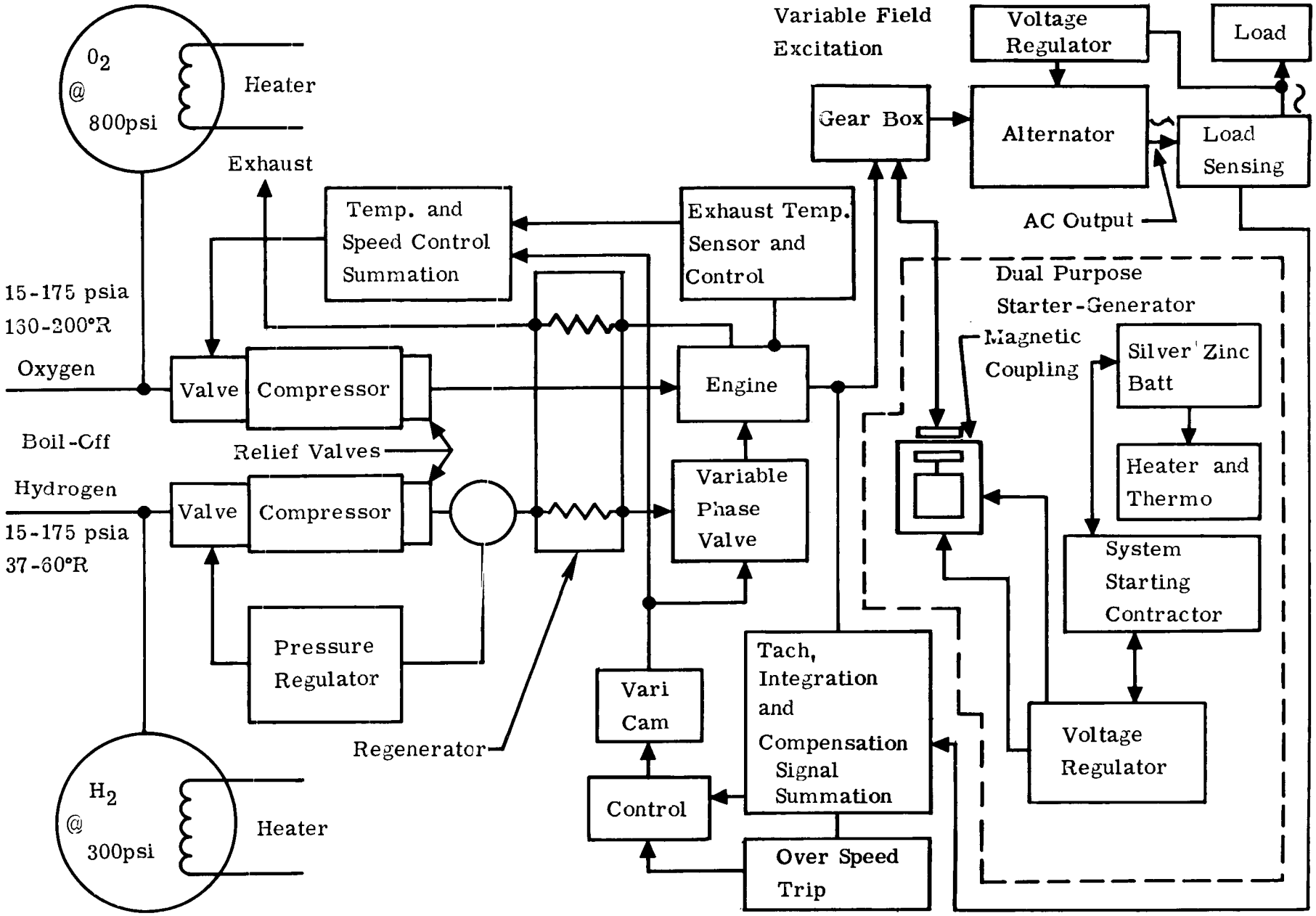

Fig. 5-1 - Control Schematic - Original Concept

volume combustion (Otto) cycle was the best choice for performance considerations, and the following conditions should be imposed:

1. Oxygen pressure to the engine should be controlled by using a throttle valve very close to the engine inlet.

2. Hydrogen should also be supplied at constant pressure to the intake valves because of the performance advantages of constant volume operation. The schematic for such a system is shown in Fig. 5-2.

As a result of continued cycle analysis, and analysis of the compressor controls and tankage systems, additional changes were made as shown in Fig. 5-3 and discussed below:

1. Studies of tankage storage pressures, and consideration of the greater complexity required for compression of high density hydrogen and oxygen, indicated that storage at directly useable pressures was advantageous. This allowed the system to be designed for compression of boil-off gases only, and allowed the addition of the tankage to the system, downstream of the reservoir.

2. The method of compressor control was changed from a closed loop type to an open loop, bypassing-type system. This allowed simplification of the system, and better operating characteristics were obtained.

3. The system of Fig. 5-3 utilized a hybrid system for engine power modulation by allowing the variable duration hydrogen valves to act as a throttle at low

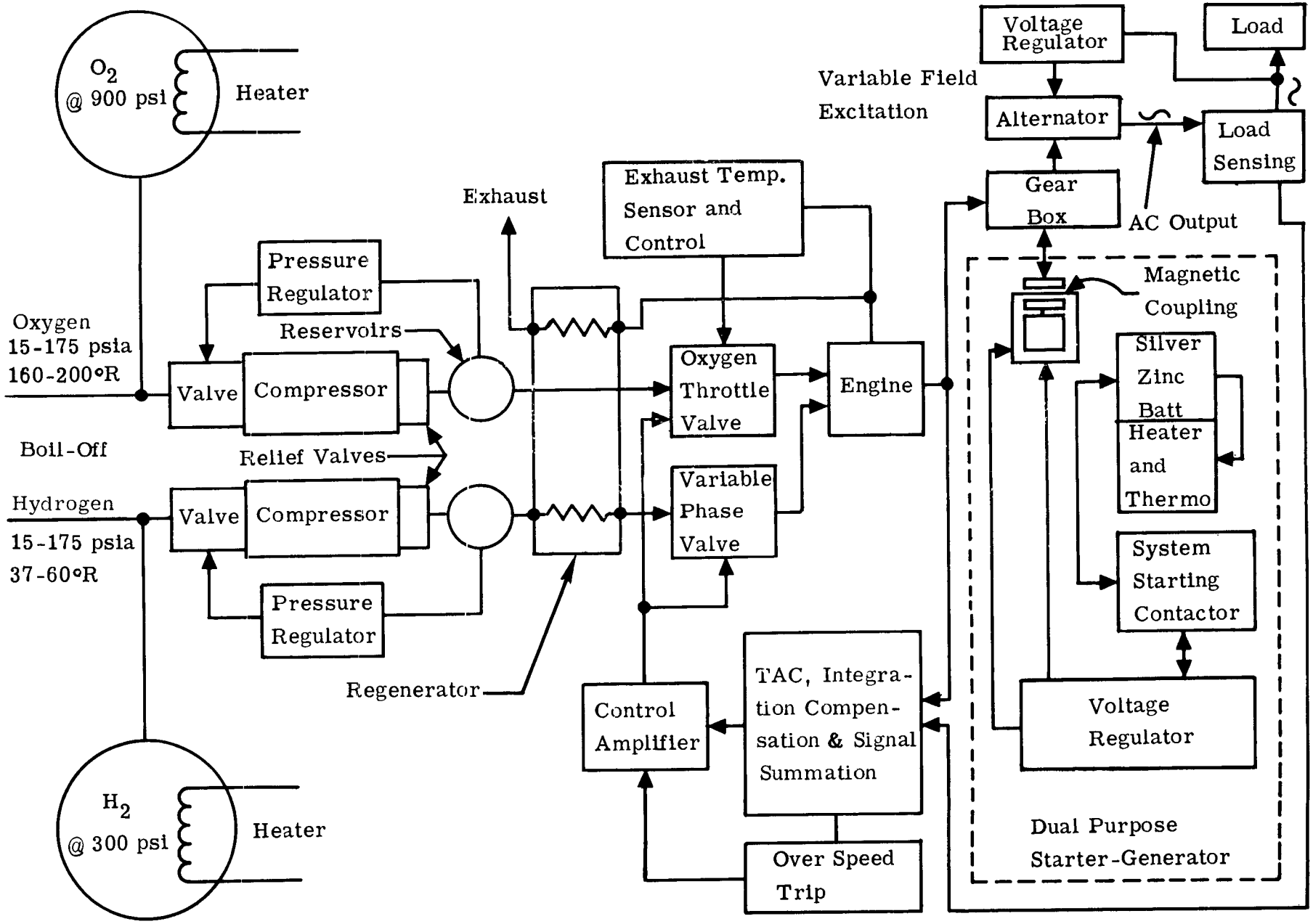

Fig. 5-2 - Control Schematic - With Oxygen Throttle

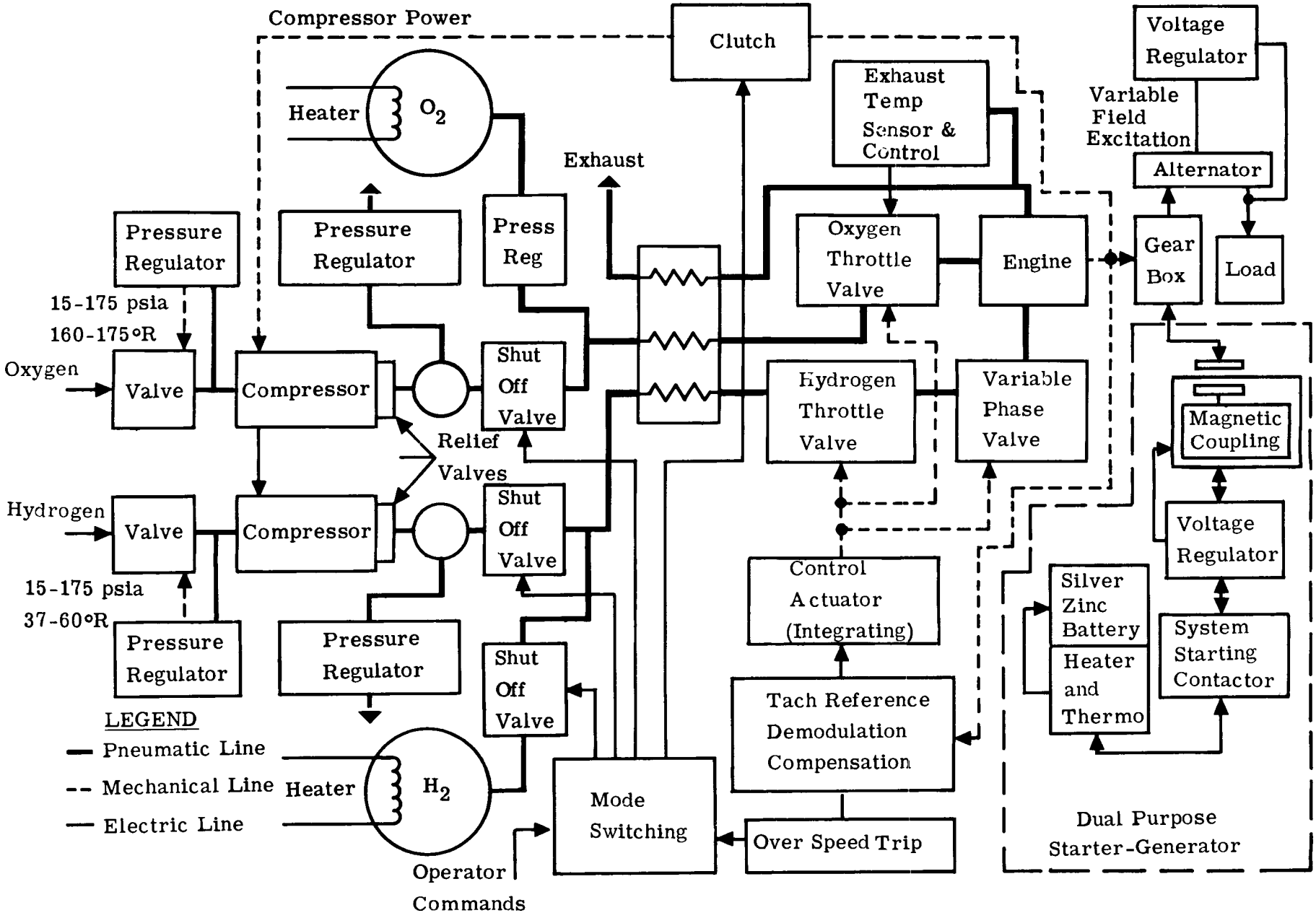

Fig. 5-3 - Control Schematic - With Propellant Mode Switching

levels, and as a variable duration valve to modulate power, at the higher power settings.

4. The control system required for operation on this system consisted of a tachometer, a demodulator, and a compensator giving a dc error signal. A control actuator to regulate all power modulating elements was provided. Integration was performed by this actuator.

5. Mode switching was provided to activate, deactivate, open, or close various components of the system. This is described in Section 5.7.6.

In the final study stages, several more changes to the system were considered. (See Fig. 5-4).

1. After considering variable lift valves for both oxygen and hydrogen inlet controls from a design standpoint, the variable admission valve proved most advantageous for hydrogen, and the throttle proved most advantageous for oxygen.

2. Fig. 5-4 reflects changes in the starting and dc power source. These are:

   a. Battery output converted to AC
   b. Alternator used as starting motor
   c. DC control voltage obtained by converting alternator output.

5.3 Engine Equations

During the course of system study, several sets of equations

were used. The engine equations used are derived from equations in Section 3 and are not rewritten in this section.

5.4 Engine Representation

Initially, an effort was made to determine the detail to which the engine dynamics would have to be considered in the control analysis. The common practice in engine cycle analysis is to integrate the cyclic power output of the engine to find the mean effective pressure generated in the cylinder, and expressing it in terms such as IMEP and FMEP. This procedure represents the cyclic process as a continuous one, and for dynamic analysis, any such process must be justified. A typical theoretical engine cycle is shown in Fig. 5-5.

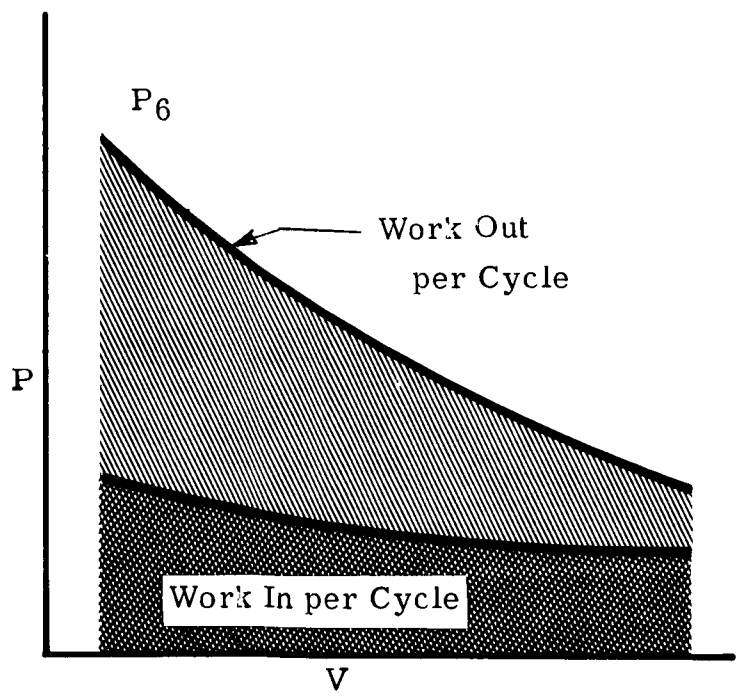

Fig. 5-5 - Typical Theoretical Engine Cycle

The energy from each cycle is stored in Kenetic form by the moving inertia of the flywheel and crankshaft. For our analysis, energy is removed from the system at a constant rate. Thus, in order to maintain constant speed, the energy in and out of the system must balance for each cycle. Energy is added as shown below in Fig. 5-6, so that the net in to the system during the expansion half of the cycle (consisting of

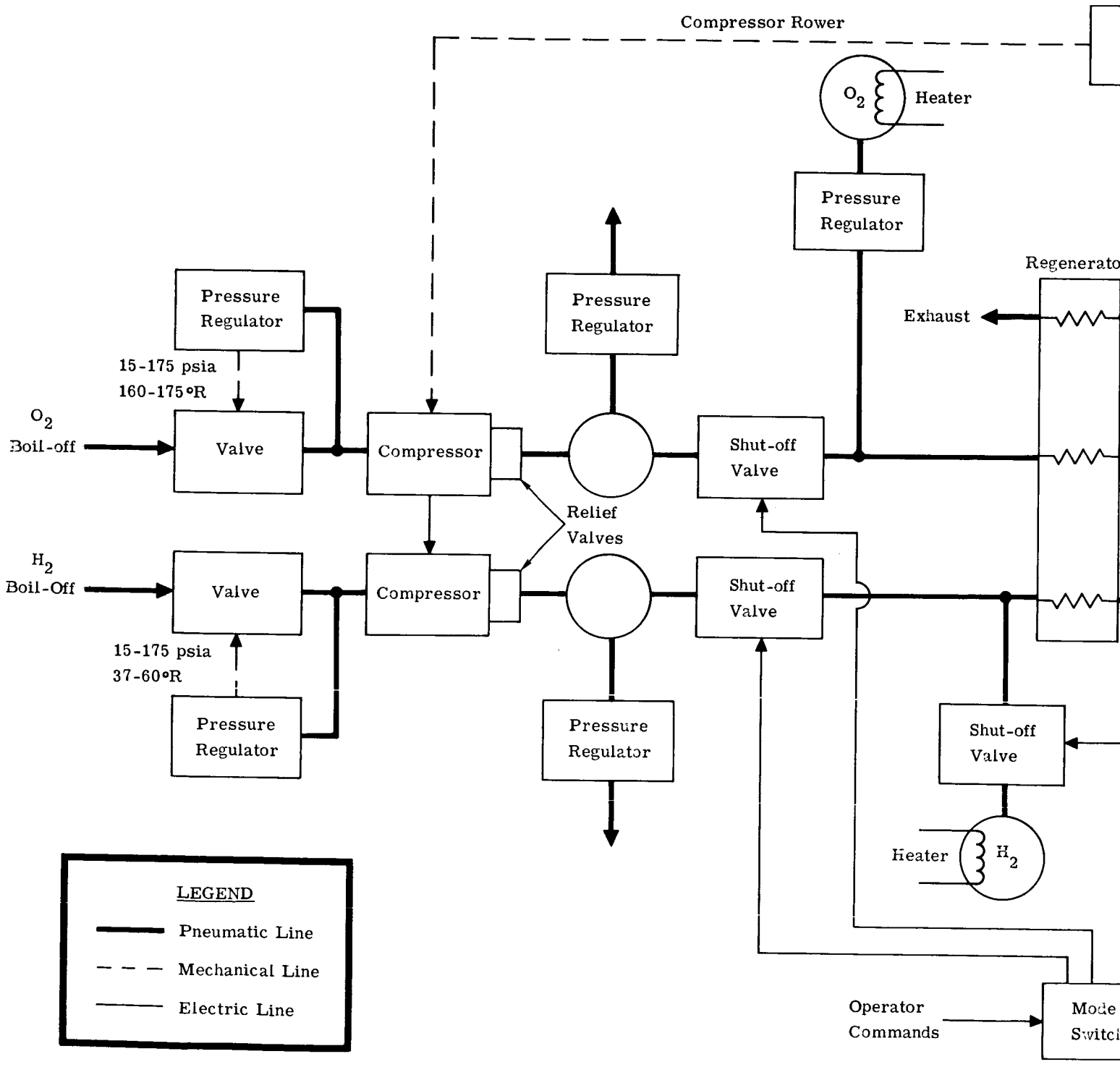

Fig. 5-4 - Schematic -

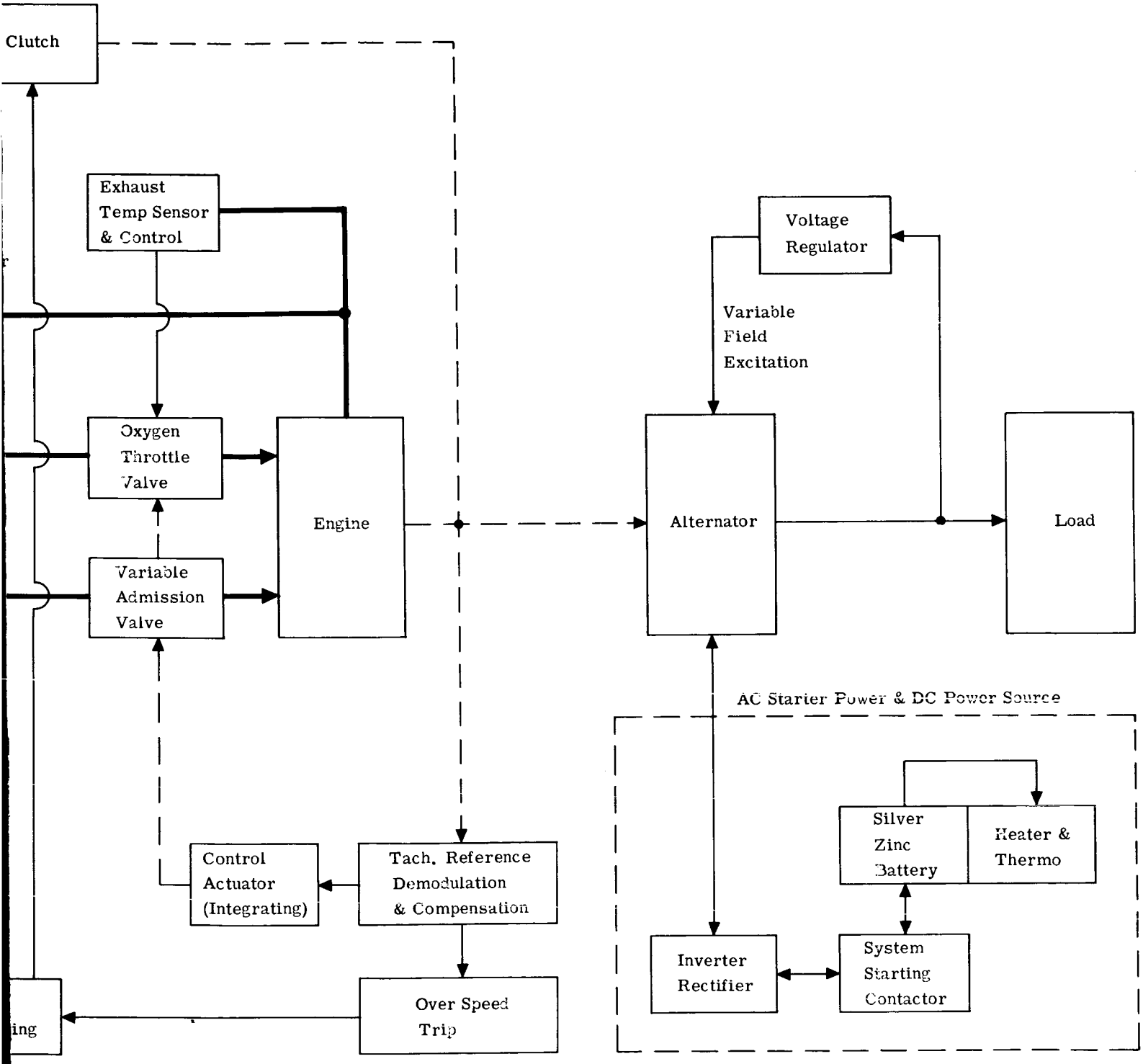

Complete H_2-O_2 System

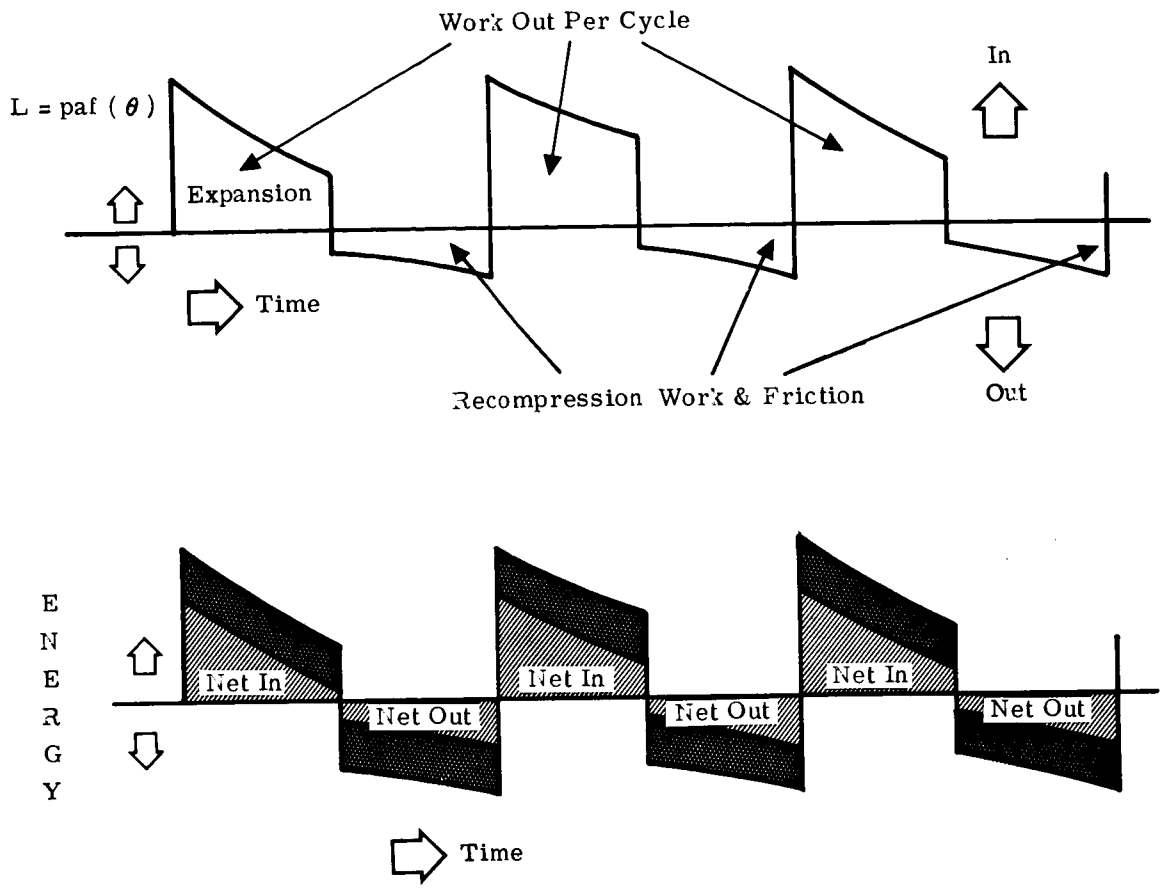

Fig. 5-6 - Engine Cycle Energy

expansion work minus energy out of the system in doing useful work) will equal net out of the system during the compression half of the cycle (recompression work and energy out of system in doing useful work during this half of cycle). Under this condition, the net energy and speed of the rotating mass remain constant. If this cycle is represented by a Fourier series, the fundamental frequency (i.e., 4000 cpm) would have the largest amplitude and this frequency, being the lowest, would have the greatest effect as a resonant frequency on the speed variation of the rotating mass. Calculations indicated that the miniumum amount of inertia which could be tolerated by the rotating system, and still restrict the amplitude of this resonant frequency to a small part of the steady state error, would be .092 in-lb-sec. The requirement that this resonant frequency be limited to a small amplitude also indicates that a continuous representation of the engine cycle would be an accurate representation for lower frequencies.

Preceding page blank

5.5 Linear Control System Studies

5.5.1 Introduction

The linear control system analysis was performed early in the program before the exact values of important system parameters were known. As a result, some calculations seem rather abstract, but help to give a better understanding of the system.

5.5.2 Discussion of Studies Conducted

Initial calculations were conducted, using Root Locus and other linear analysis techniques in order to establish an analytical picture of the system and to form a check on subsequent work done on the analog computer. Fig. 5-7 is a Root Locus plot[1] of a typical linear system under study. Agreement of stability gain was determined to be within the accuracy of the methods of solution used.

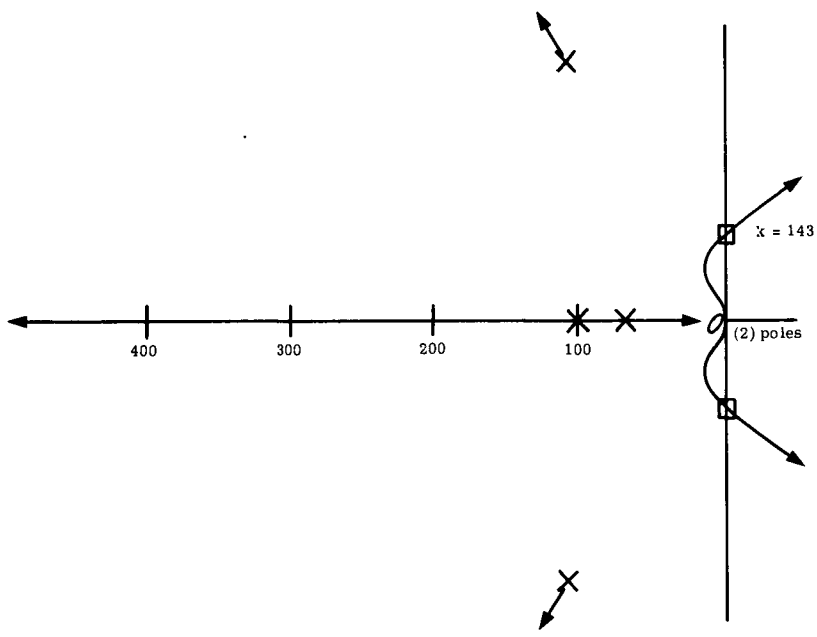

Fig. 5-7 - Root Locus Plot for Linear System Study

Determination of the transient response of the system by hand, even with some approximations made to simplify the work, proved

[1]For interpretation of Root Locus plots, see Control Engineers Handbook by Truxal.

so tedious that computer solutions were used for all calculations involving a variation of parameters. The transient response of speed to a .87 kw step input was examined in a series of tests where the compensation lead/lag ratio was varied along with speed gain loop.

A comparison of Figs. 5-8 through 5-10 indicates that as the lag time constant increases for a constant lead/lag ratio, the damping increases and the transient error increases, requiring a higher gain to maintain transient tolerances. In general, as the gain is increased, the transient error decreases but the system becomes more oscillatory.

For a constant lead term and equal gain, the system response is best understood by looking at the values of the actual lead term. If the lead/lag ratio is small, a large lag helps to generate a large lead term giving better system response. Several modes of oscillation appear over the range of parameters that are investigated.

One reason for including the analog traces is to indicate the ability to control system response, by gain and compensation selection, if this capability is required to meet specification performance.

In the case of the H_2-O_2 engine, two error envelopes are indicated on Fig. 5-11 and at the top of each column of response traces. Each represents a 100 rpm transient band but a different distribution of system loop gain. In the case of decreased inertia, K_a, (these constants are defined in Fig. 5-11), is large while K_1 is proportionally smaller, so that K_1 remains constant. For increased inertia, K_a becomes smaller, while K_1 is proportionally larger. A change of this kind does not alter

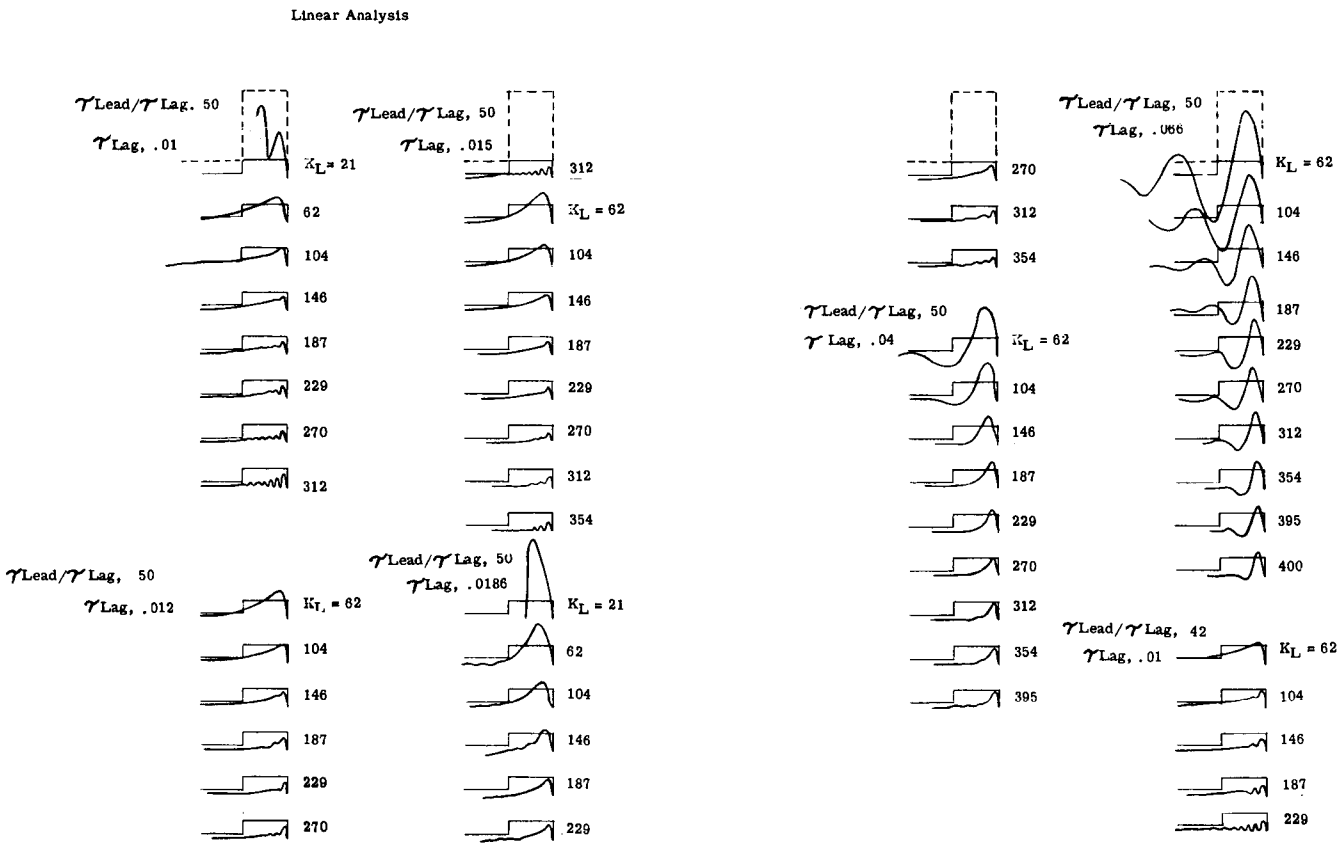

Fig. 5-8 - Linear Analysis Trace

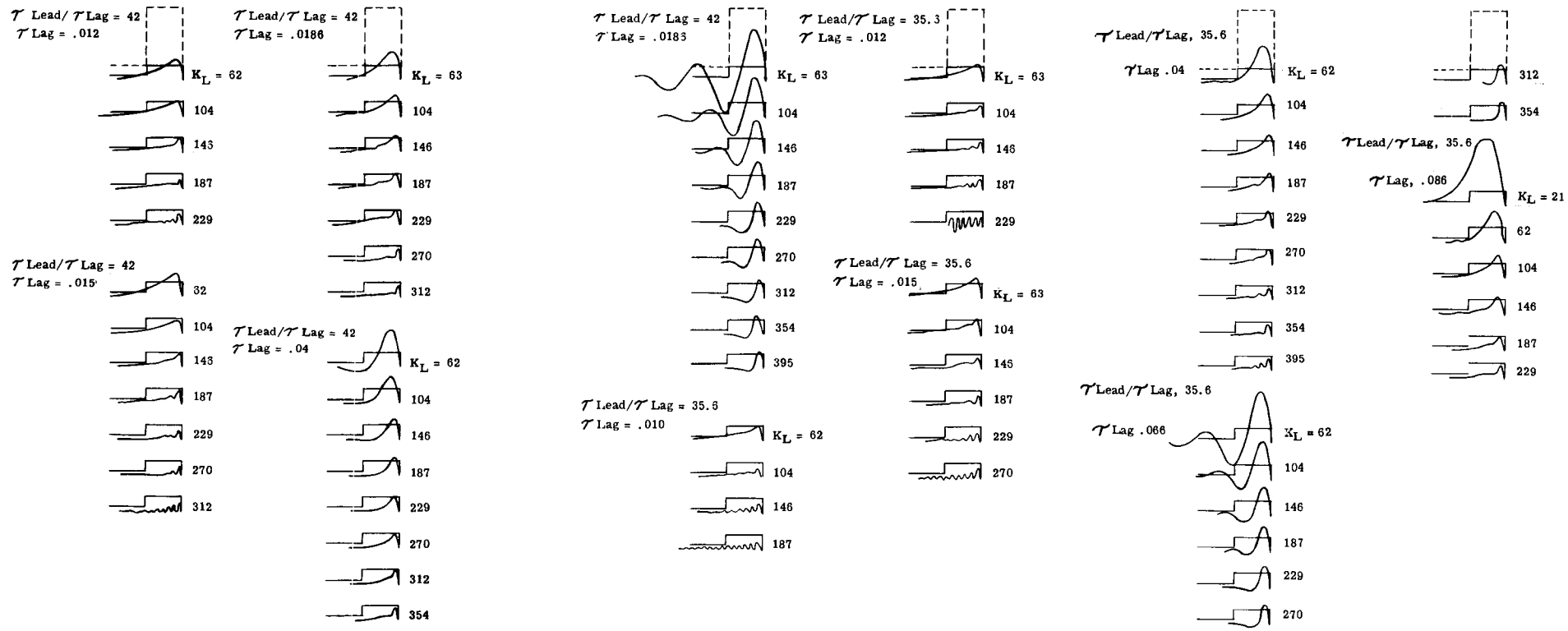

Fig. 5-9 - Linear Analysis Trace

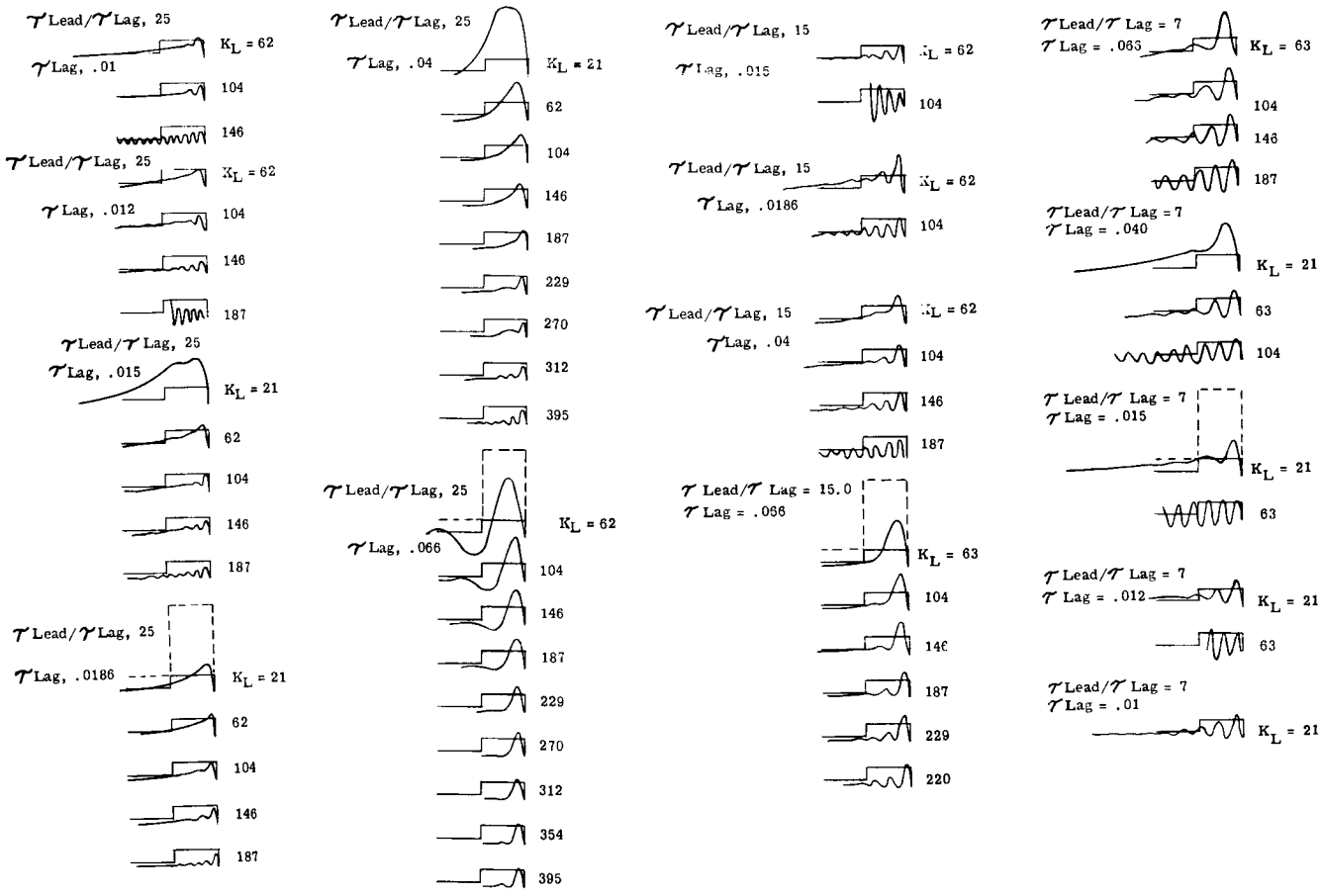

Fig. 5-10 - Linear Analysis Trace

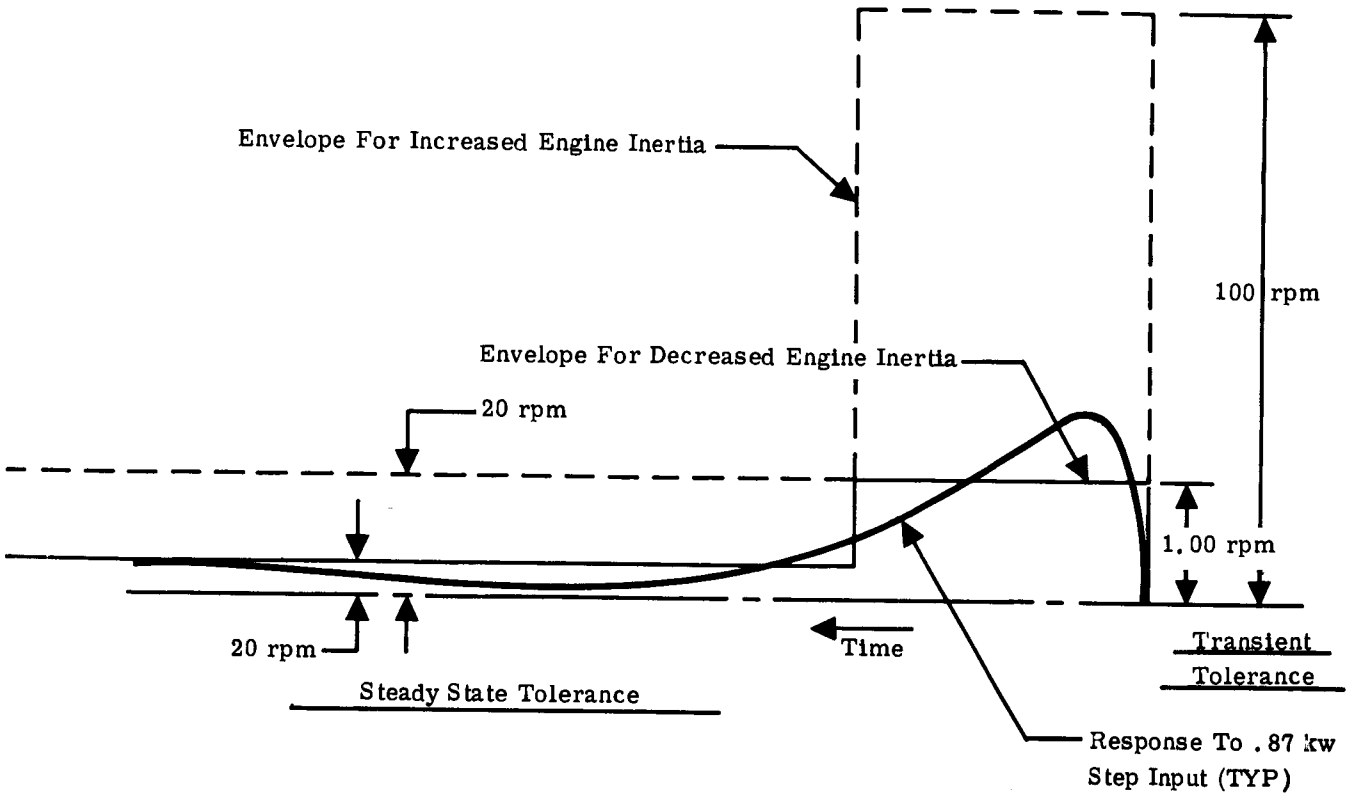

Fig. 5-11 - Forward Loop Gain Change at Constant Closed Loop Gain

the shape of the response curve, but it does change the scale or peak value directly proportionally to K_a, the forward loop gain.

Tests indicate that for decreased engine inertia, caution must be exercised in the selection of gain and compensation, if specification requirements are to be met. By increasing the rotating inertia value on the H_2-O_2 engine, undesirable resonant frequencies are avoided and nearly all test response shown will meet the specification. The control problem would be reduced by adding inertia in the form of a flywheel.

As indicated by the results of tests on the proposed system, the response is quite adequate, so that other system configurations

under consideration were not included in this series of tests. These other system configurations involve:

a. Complex compensation

b. Load anticipation

The proposed system is what is commonly referred to as a Type "1" system. A Type "O" system might also be proposed, but due to the rather stringent, steady-state-error requirements, it appears that the added complexity of the proposed Type "1" system is necessary.

The analog computer block diagram used for the linear analysis is shown in Fig. 5-12 and the analog circuit diagram is illustrated in Fig. 5-13.

5.6 System Requirements

5.6.1 Speed Control Requirements

Speed control requirements were, in general, written for a system inertia of .1159, corresponding to a system with a 6000 rpm generator. Many computer runs were also made with a system inertia of .3279, corresponding to a system with a 4000 rpm generator. The data could also apply to any system in which the rotating parts had an equivalent moment of inertia to that above, regardless of generator speed.

The system is designed to maintain the specified accuracies with a .87 kw input change in load. Tests were conducted on

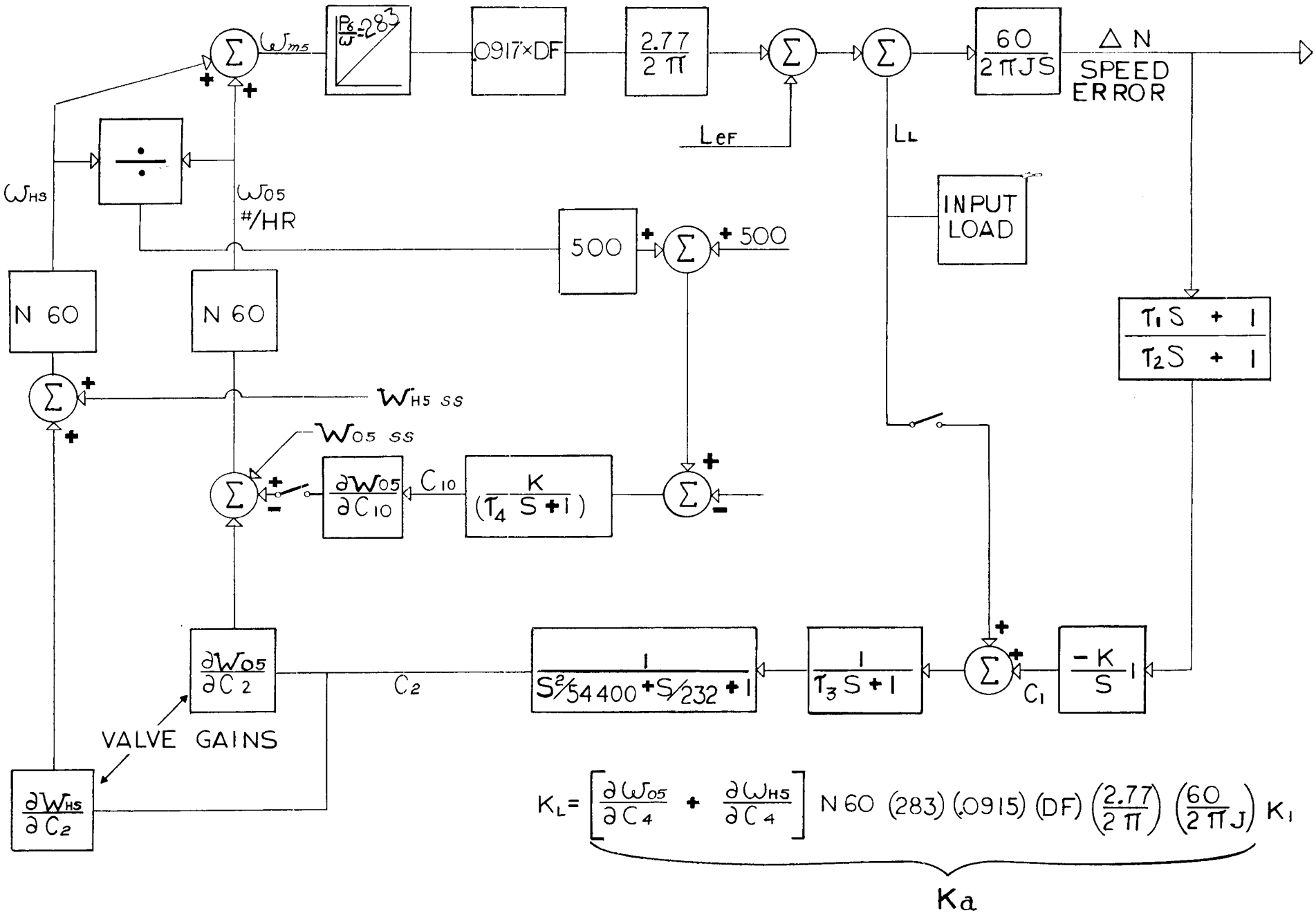

Fig. 5-12 - Analog Computer Block Diagram for Linear Analysis

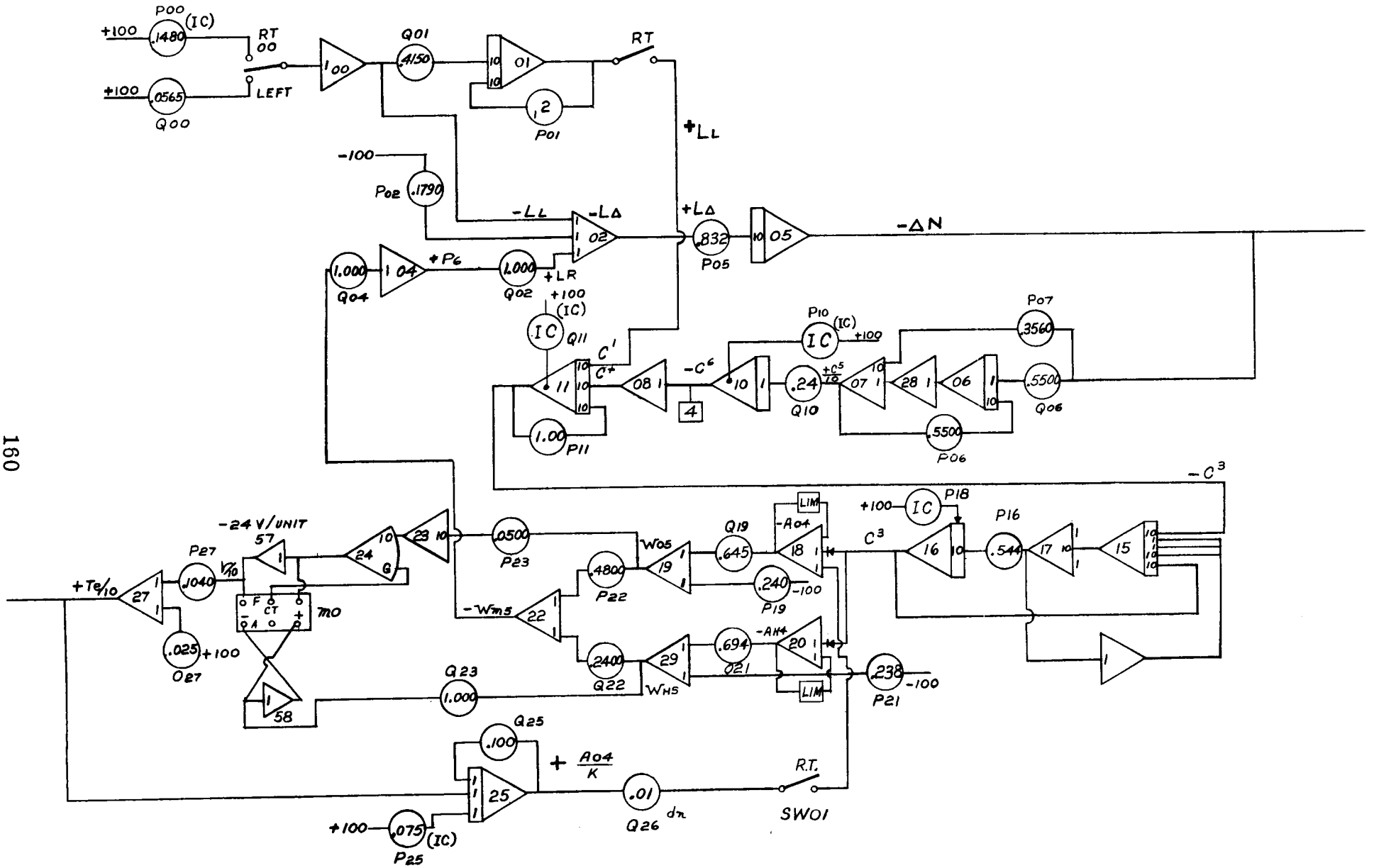

Fig. 5-13 - Analog Circuit Diagram for Linear Analysis

a system which could maintain the specified accuracies with a load change of approximately 2.5 kw. Tests indicated that actuator rate and system gains are considerably higher for this type system. In some cases the results are inconsistent due to the hysteresis and breakout friction of the system, but the analog data is sufficient to show important trends which should guide the system design.

5.6.2 Actuator Design

The actuator requirements were written specifically for an actuator utilizing magnetic particle clutches. The block diagram for this actuator is shown in Fig. 5-14, and the circuit diagram in Fig. 5-15.

Actuator Maximum Rate

The actuator maximum rates are shown in Fig. 5-16 and 5-17 for the systems under consideration.

The rates required are interpreted as follows:

Units = Actuator output displacement
Units/sec - Actuator output rate
44.5 unit = Stroke required for maximum power setting under most adverse conditions.

The stroke of the actuator is not defined, so the length of a unit is not defined at this time. In future comments, where stroke is referred to in percent of maximum stroke, 100% stroke = 44.5 units. The actuator stroke will probably be longer than 44.5 units (or 100%), to make up for changes, such as: propellant temperature, propellant pressure, or system friction.

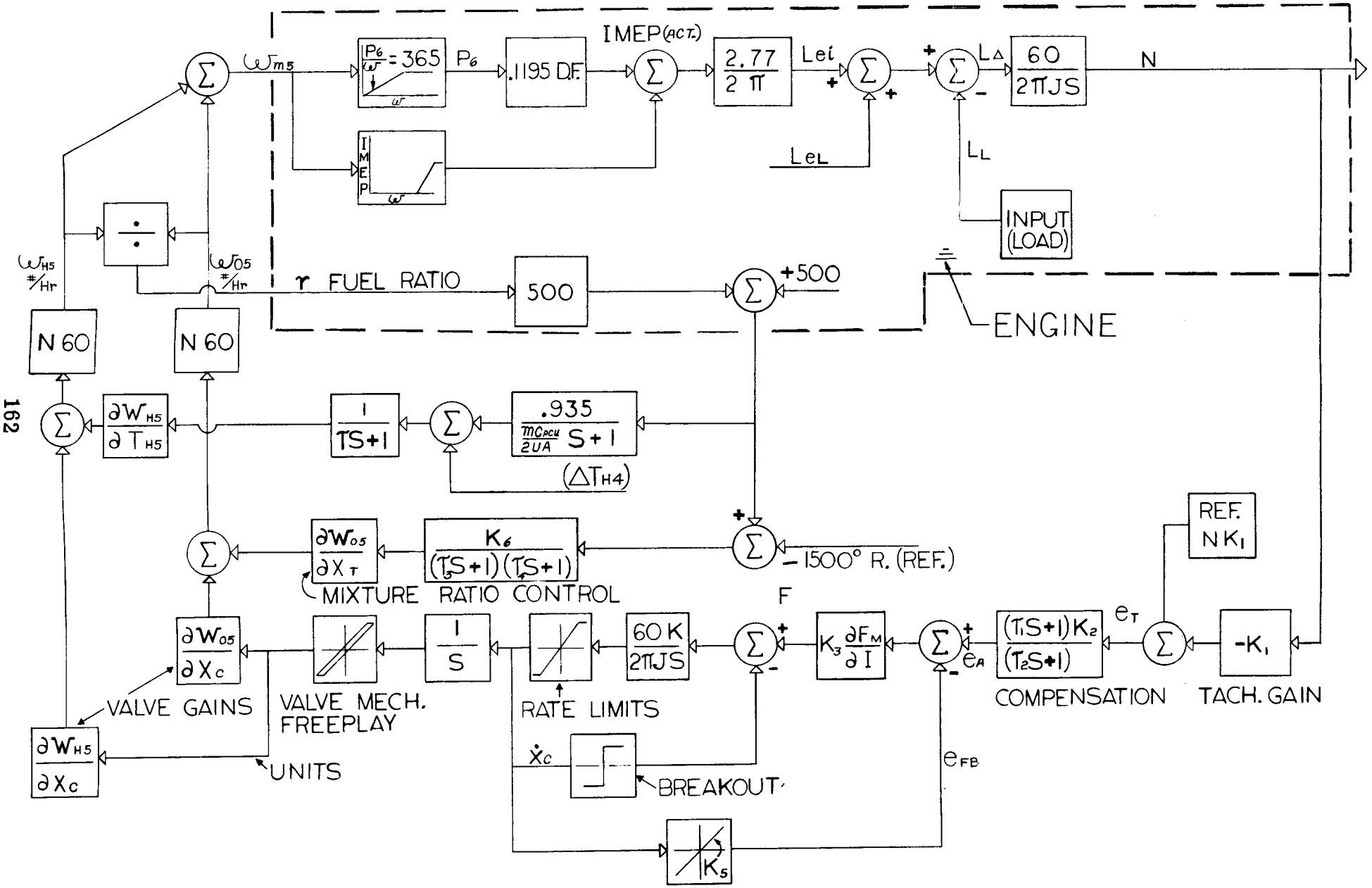

Fig. 5-14 - Block Diagram for Actuator Analysis

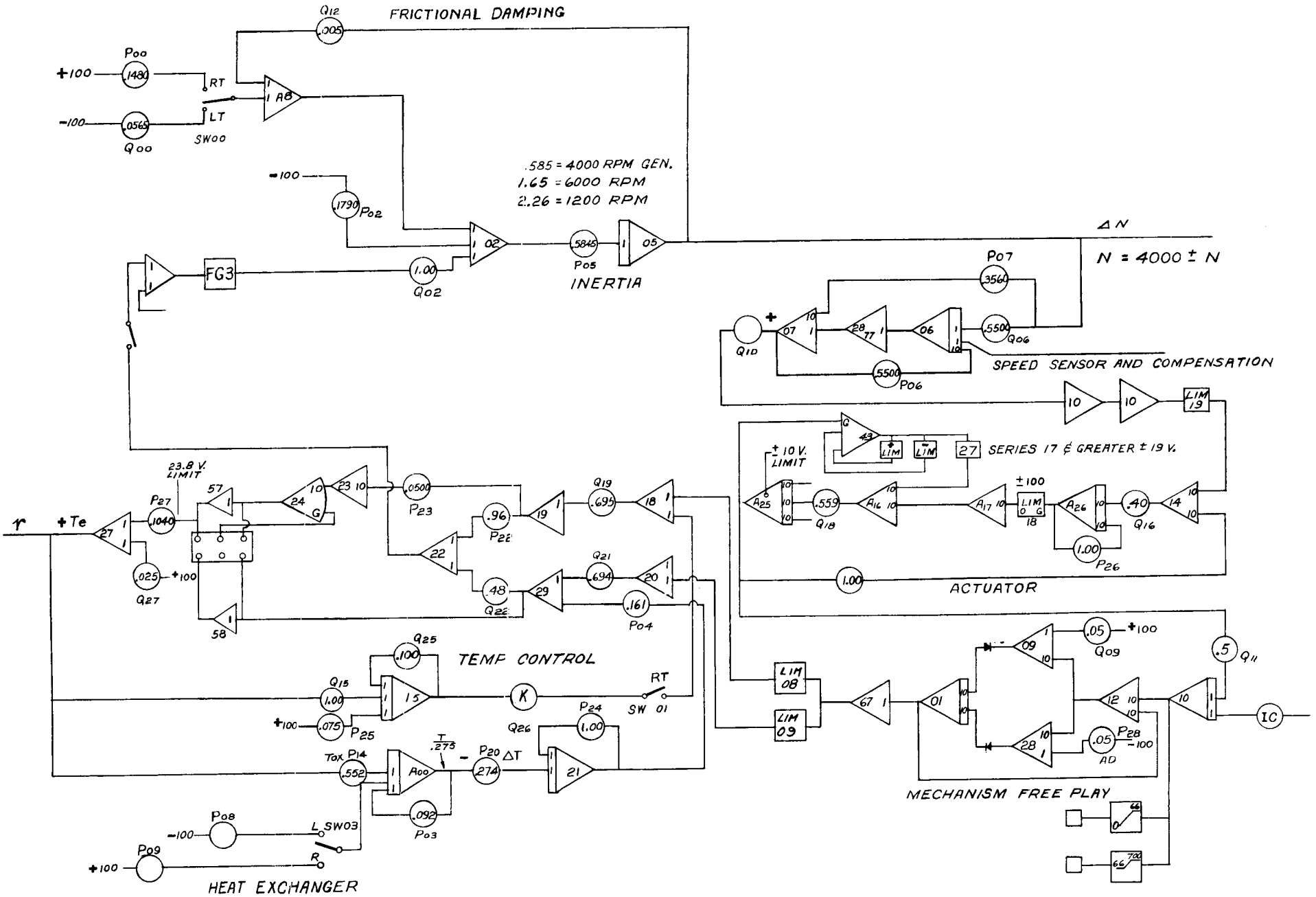

Fig. 5-15 - Circuit Diagram for Actuator Analysis

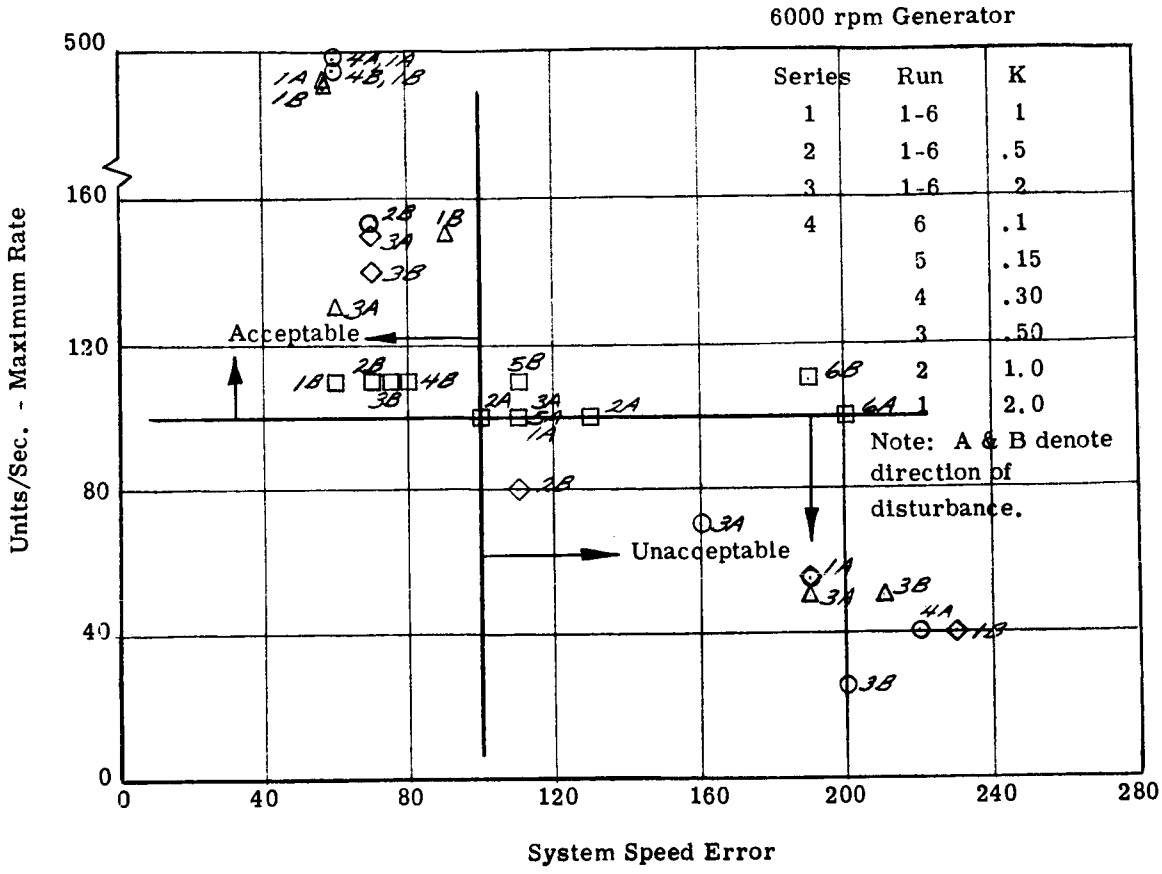

Fig. 5-16 - System Speed Error vs. Actuator Maximum Rate

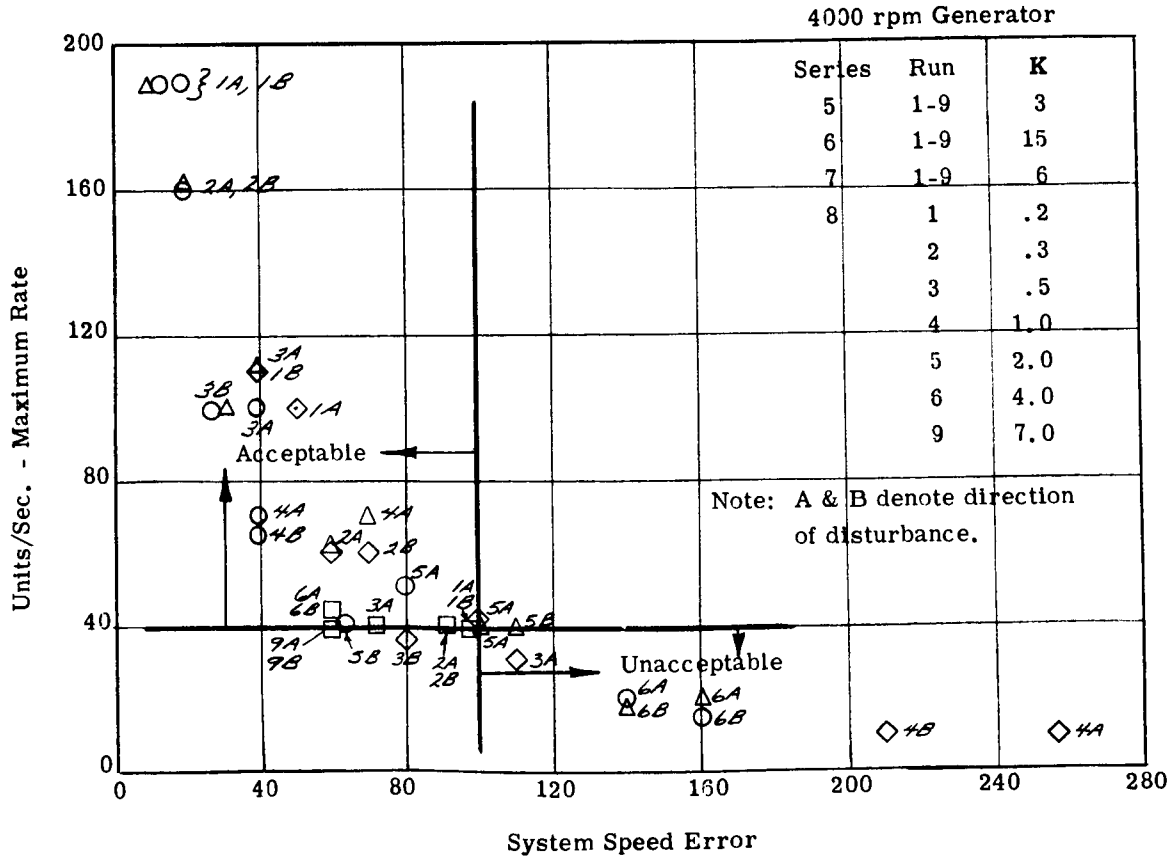

Fig. 5-17 - System Speed Error vs. Actuator Maximum Rate

The type of actuators being considered will have a rate saturation limit. If input exceeds a certain value ((a) in Fig. 5-18), the output rate will remain constant at its maximum value. For the magnetic particle clutch, the maximum speed is equal to the driving speed of the rotor, (normally about 2000 rpm).

In order to meet system speed accuracy requirements, certain restrictions must be placed upon the rate saturation limit. The minimum average[1] rates which are

[1]Average rate requires special interpretation here. The maximum rate of the actuator should be considered an average over the displacement required to correct for the system design input of .87 kw load change. Some deviation in rates over smaller displacements can be tolerated.

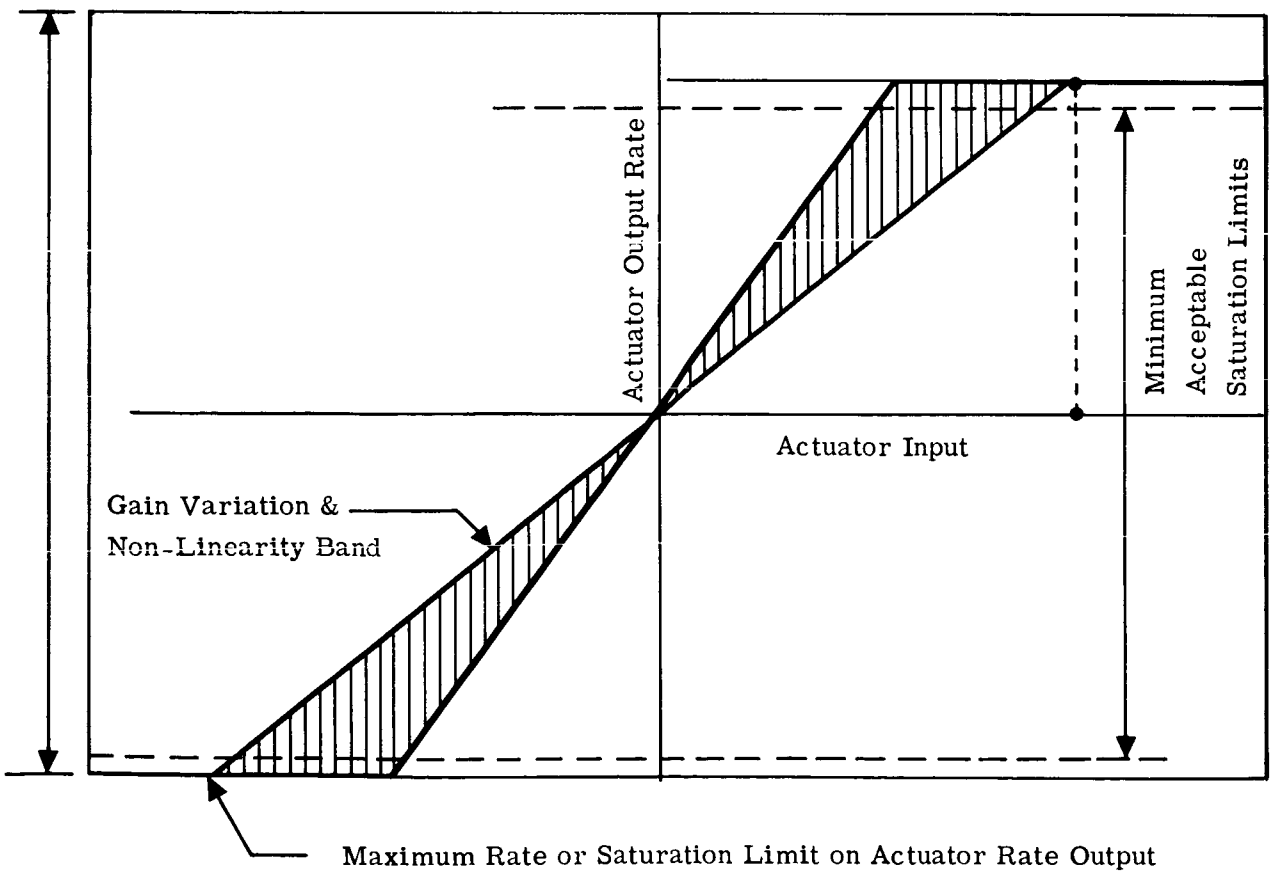

Fig. 5-18 - Actuator Saturation Limits on Rate Output

acceptable were obtained from data plotted on Fig. 5-16 and Fig. 5-17. Test results indicate that a minimum saturation limit of 100 units per second is acceptable for a 6000 rpm (inertia = .1159 in-lb-sec^2) system, and a minimum saturation limit of 40 units per second would be acceptable for a 4000 rpm system (inertia = .3279 in-lb-sec^2). Higher saturation rates are also acceptable.

The effects of gain changes on system error for various system maximum rates, obtained from analog analysis series 1 through 8, are shown in Figs. 5-16 and 5-17. Actual data may be found in Appendix E . System error vs. system gain (tachometer and compensator), is shown in Fig. 5-19.

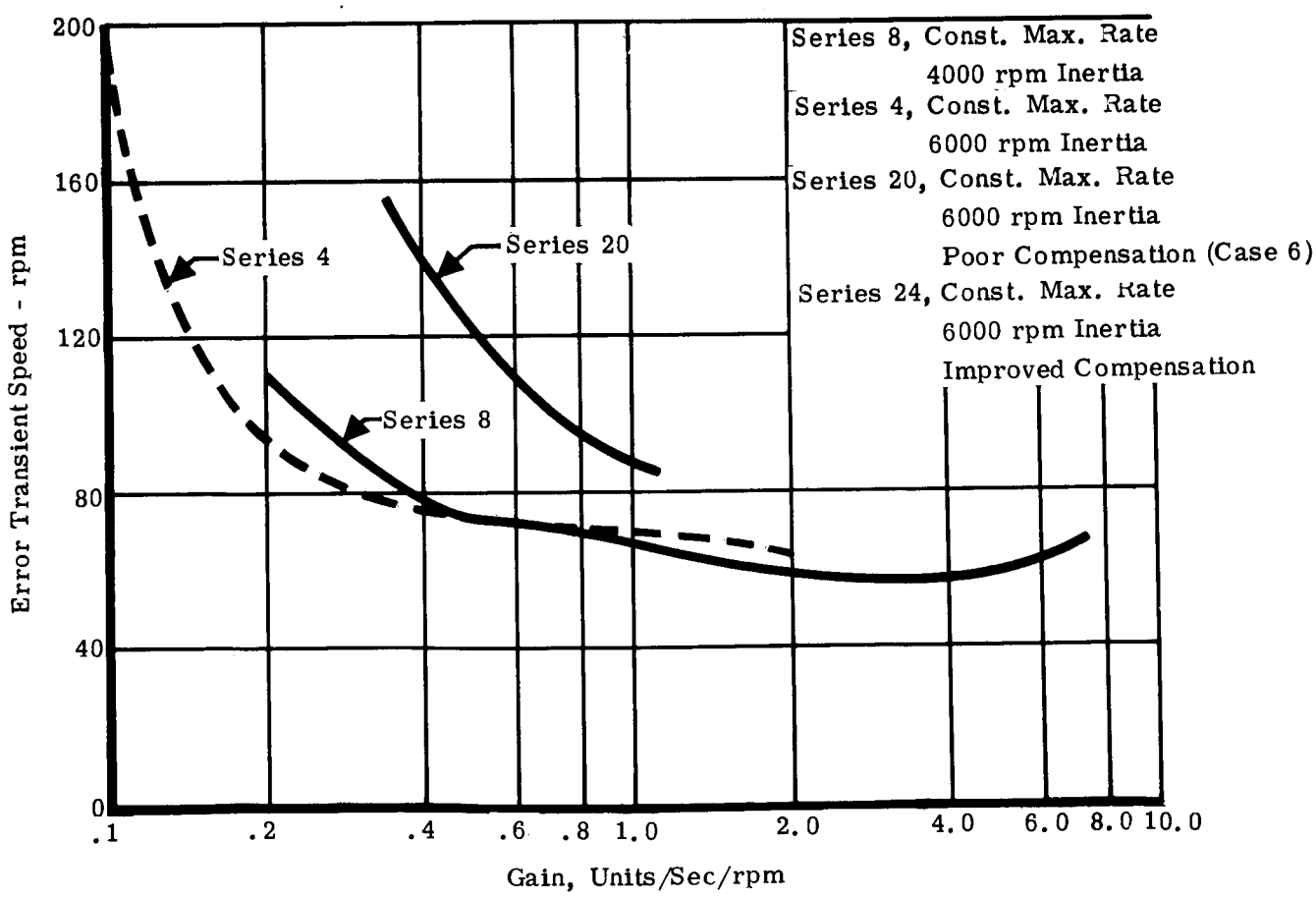

Fig. 5-19 - System Transient Speed Error vs. Gain of Load

From these data the following conclusions may be made:

1. The gains needed for the 6000 rpm system are about three (3) times lower than the gains needed for the 4000 rpm system to obtain similar results.

2. Inertia of active mass.

3. Maximum torque output of clutch or motor.

4. Amplifier gain.

The various effects are studied in terms of actuator output, without variation in rate. For example, mass is considered in terms of equivalent mass force at the output.

The difference between the breakout and maximum available torque (or force), represents the torque available to accelerate the mass of the actuator; that is, it defines actuator response. Some effects shown on analog trace series 19 through 22 (AppendixE), are not necessarily part of the actual system response, but are due to computer limitations, since the loop is basically stable.

The amount of applied force required to accelerate the active mass is determined by examining analog runs with large breakout force values. The difference between peak force and breakout force may be measured. Examination of the data indicates that an excess of about 10 lbs. for a breakout force level of 60 lbs. is satisfactory. It is believed that actual breakout force will be less than 60 lbs., so the results are conservative.

The study was conducted for an equivalent mass of enertia .0565 in-lb-sec^2 in order to adjust the excess forces. For other inertia values simply multiply the new inertia by the constant, $\frac{10}{.0565}$ to get the new excess force.

As shown in Fig. 5-20 and below, several analog runs were made to show amplifier gain limitations, using various breakout friction levels as the actuator load.

Series	Breakout	Minimum Gain $\frac{(K_3 \partial F_M)}{\partial I}$
16	±60 lb.	20
15	±40 lb.	10
14	±20 lb.	7.5
13	±10 lb.	4.0
12	±50 lb.	17.5

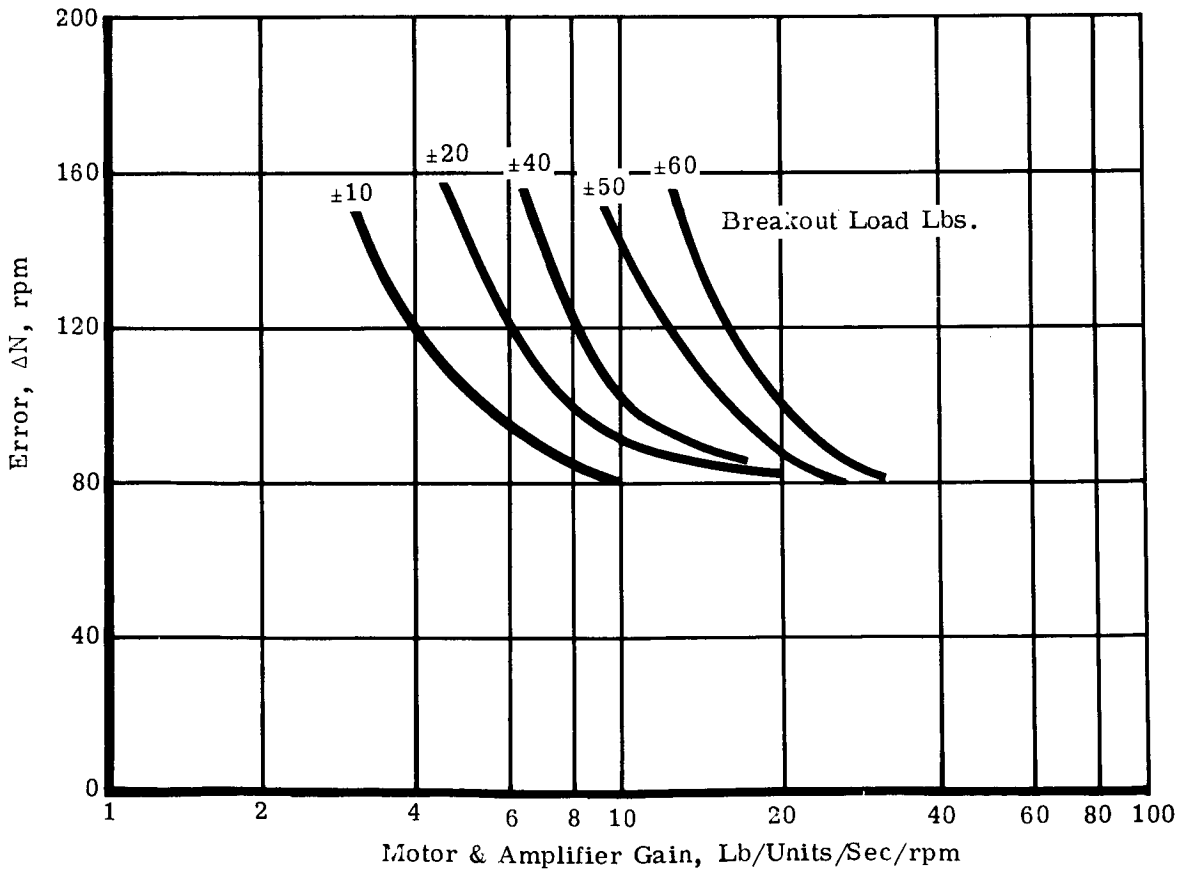

Fig. 5-20 - Amplifier Gain Limitations

Assuming that the actuator deadband due to breakout friction, must be kept to values of 11 rpm or less, the relationship of variation of gain with breakout is also explained by this analysis.

Actuator Loop Gain

This quantity varies from 1000 to 220[1] for the values of breakout examined. Although 1000 may appear very high, it should be pointed out that this high gain is used to build up a breakout force. The effective loop gain is much less than the actual loop gain without breakout forces. Similarly, if breakout forces are very low, the gain should be reduced.

The coulomb friction representation of the actuator is considered an extreme case of any forces of equal magnitude applied in other manners. Breakout force is related to actuator deadband, amplifier, and clutch-or motor gain as shown in Fig. 5-21.

[1]Actuator loop gain is a dimensionless quantity.

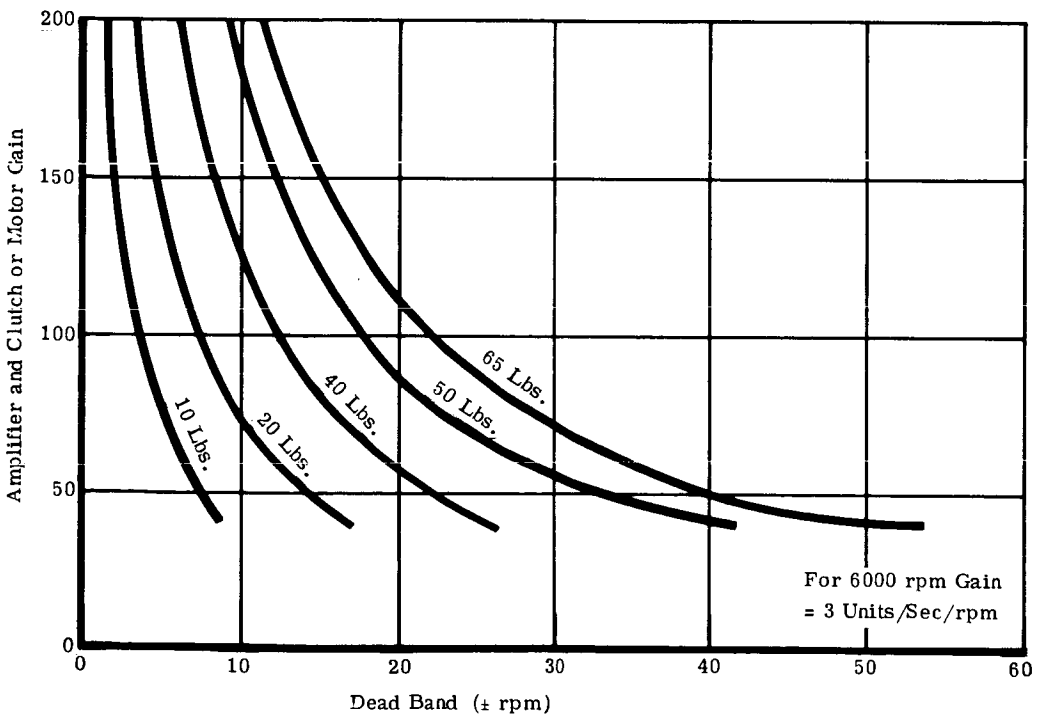

Fig. 5-21 - Breakout Force Relation to Amplifier and Clutch or Motor Gain

Valve Positioning Accuracy Requirements

Tests have been run to establish the amount of hysteresis allowable in the mechanism between the actuator and the engine power setting control valve. Test series 1 through 16 were run with values of ±2 units of hysteresis in the mechanism.

Since 44.5 units is equal to the 100% stroke, the percentage of accuracy, as previously defined, is therefore:

$$\frac{2}{44.5} \times 200 = \pm 4.5\%$$

Although it is desirable to keep this accuracy high, the ± 4.5% is acceptable and is the maximum allowable hysteresis. For a given value of gain, the limit cycle amplitude goes up with a rise in hysteresis, and frequency decreases. These qualities are dependent on loop gain, and especially on gain between engine output and actuator position. (See Fig. 5-22.)

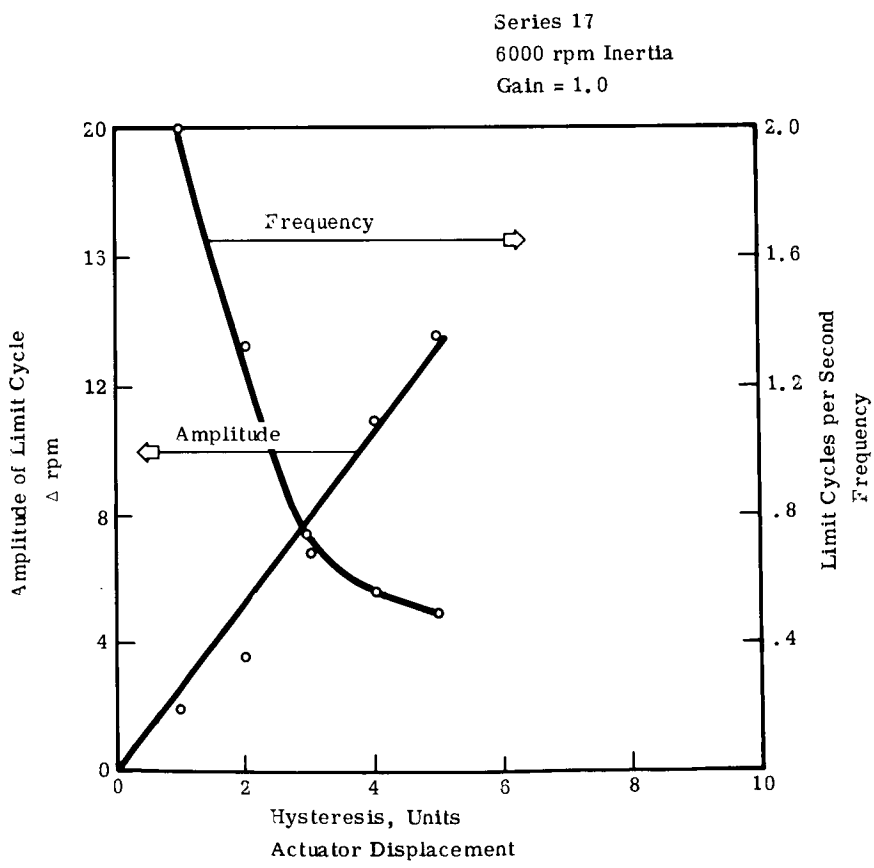

Fig. 5-22 - Speed Loop Limit Cycle Characteristics

The effect of basic hysteresis on system response is also shown in Series 17B, illustrated in Fig. 5-23. Actual analog runs are included in Appendix E . The system error obviously increases as hysteresis goes up. As stated before, values of hysteresis less than 4.5% are highly recommended. It should be pointed out that response of the system will depend upon the initial dynamic condition of the system within the limit cycle at the time the system is excited by the step input. A scattering of data results.

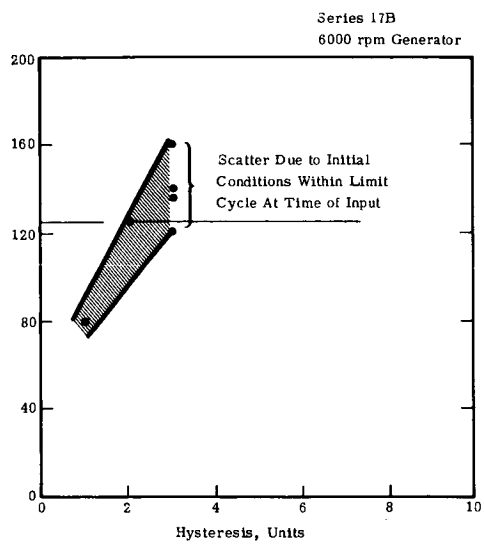

Fig. 5-23 - Transient Error vs. Linkage Hysteresis for 0.87 kw Step Input

Compensation Requirements

A series of tests (Series 18, Appendix E), were conducted to establish the effect of reducing the lead/lag ratio. All previous data were run at $\frac{.65 + 1}{.018 + 1}$. Compensation in series 18 was varied by increasing the lag term of the transfer function. Data from this study are shown in Fig. 5-24. The purpose of reducing the lead/lag ratio is to provide a more easily mechanized term. In addition, component size and noise levels will be reduced.

The results of test series 18 indicates that as the lags are increased, reducing the lead/lag ratio, the system becomes more oscillatory. The transient error, however, is not degraded a great amount.

Test series 19 and 20 (Appendix E), were conducted to investigate the transient response for various gains with a 10/1 lead/lag ratio. Some data is included in Appendix E .

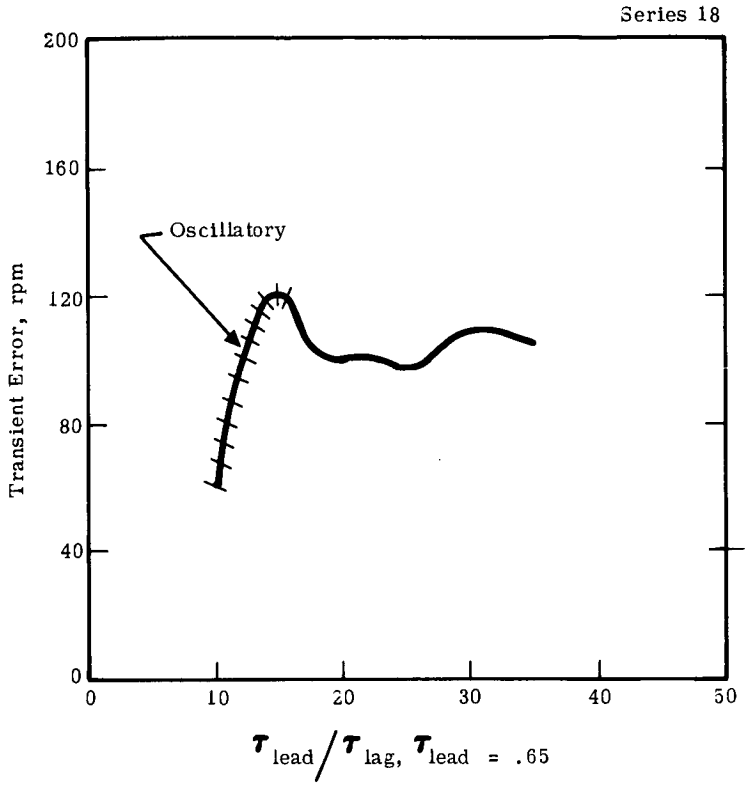

Fig. 5-24 - Speed Loop Response Variation in Compensation

In test series 21 (Appendix E), lag was set at .0258 sec., hysteresis was ± 2%, and loop gain and actuation rates were at standard values. The lead term was then varied to give various lead/lag ratios. The result of these test series indicate that for a 10/1 ratio the response was not only satisfactory, from the standpoint of error and limit cycle, but the return to steady state was accomplished much faster for 20 to 1, than 30 to 1, lead/lag ratios. The range of lead/lag ratios should be from 8 to 14, with a lag time constant of .02 or smaller. The lead time constant should be .208 sec. and may vary from .167 to .30 sec. without appreciable degradation in performance.

5.6.3 System Requirements - Temperature Control

The system requirements for mixture ratio control must be written in a very flexible manner. This is prompted by several requirements other than that normally caused by the designs not being well established. The main concern is that the error in ratio, which must be correct, is not known.

The proposed temperature controller, or mixture ratio trim controller, is a class "O" control system in which the temperature error will be proportional to the feedback gain and to the

amplitude of the uncontrolled input. The input to this system consists of the mis-scheduling error in oxygen/hydrogen ratio as a function of speed control actuator position and other system variables. In order to facilitate design of the temperature control loop, a trial set of conditions were selected and stated.

The displacement of the thermostatic activator must be such that it will be capable of maintaining the selected oxygen/hydrogen ratio when the system is subjected to a maximum error in this parameter. Constraints which should be considered are the effects of the activator position commanding an oxygen rich mixture ratio when the system is starting, and the amount of over control required to keep temperature below the maximum limit. Under temperature during transients is not expected to be a problem since the only penalty indicated is a slight degradation in BSPC. Therefore, a definite minimum stroke position is indicated.

Desired Transient Response

An example set of requirements fitting Fig. 5-25 are:

Error band, steady state	100°F.
Error band, transient	200°F.
Maximum Δr, for system design	+.5 (See Fig. 5-28)
Minimum Δr, for system design	-.5

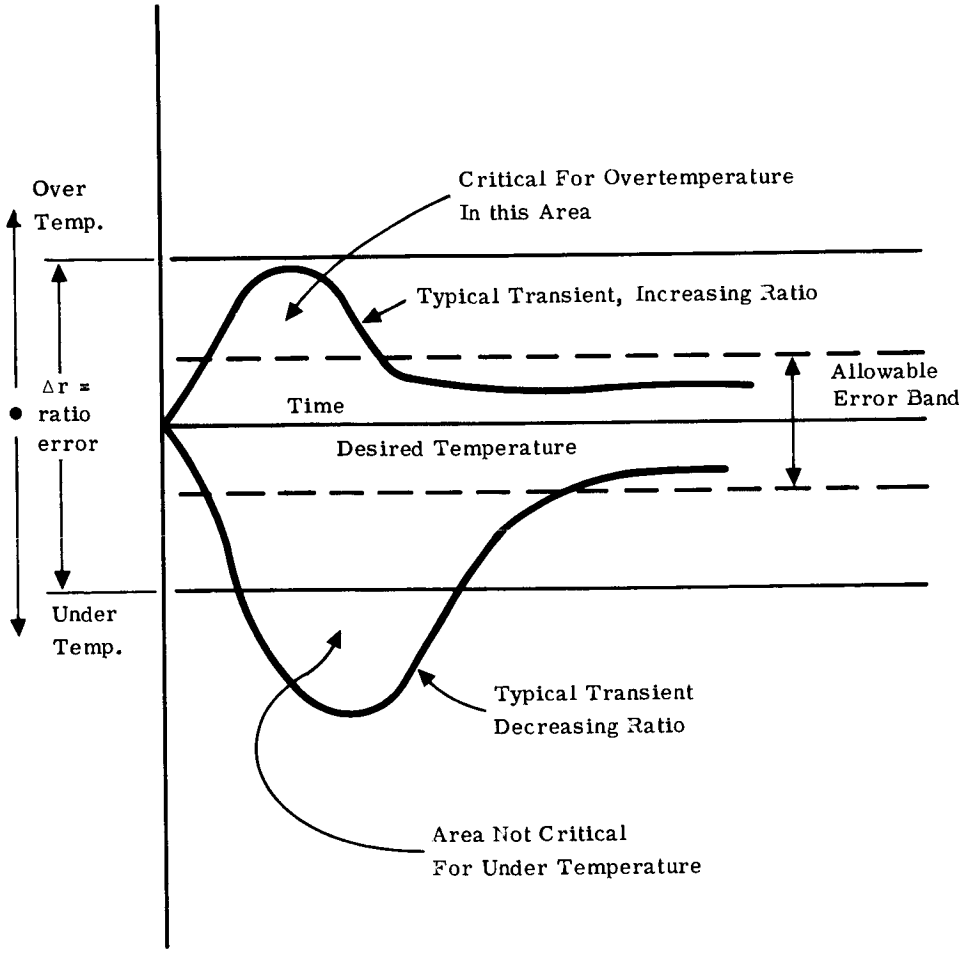

Fig. 5-25 - Mixture Ratio Control Desired Transient Response

Temperature Loop Control Requirements

Based on the set of trial requirements, the system was programmed on the analog computer and a series of runs was made varying the gain of the thermostatic actuator. The system was also examined for the effects of changes in transducer lag, and for such non-linearities as hysteresis in the temperature sensitive actuator.

Fig. 5-26 was plotted to show system transient and steady state error characteristics. Data for the test series is included in Appendix E . The system was stable for all gains examined. Reasonable variations in sensor lags and hysteresis entered into the system, but did not effect the system in a critical way. An actuator gain of .1 unit of mixture ratio per °F error is

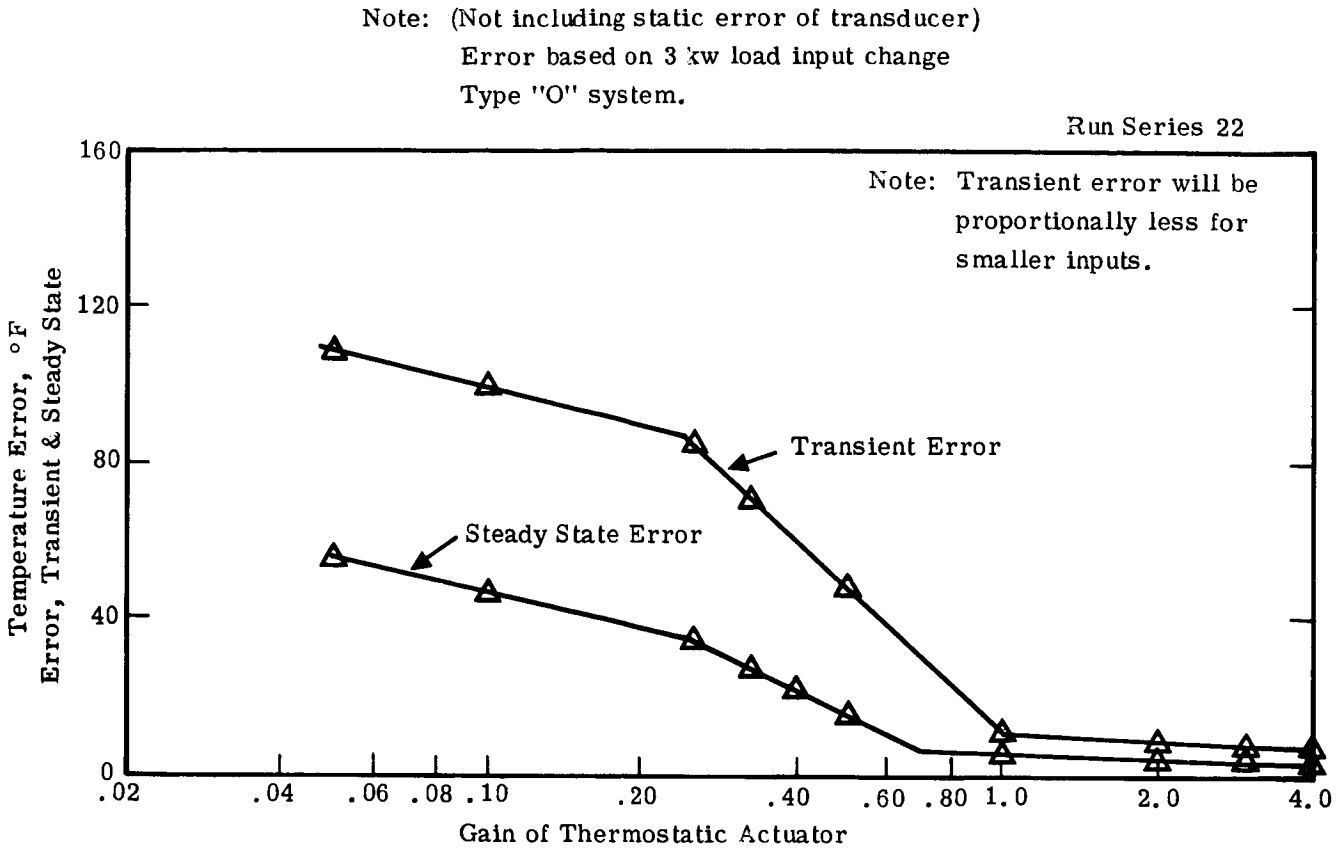

Fig. 5-26 - Temperature Loop Control Accuracy

recommended. If it can be determined with reasonable certainty that the ratio error under normally scheduled conditions would be less than the .5 assumed for this study, it is recommended that the gain of the actuator be proportionally reduced. The static actuator accuracy may be easily added to the accuracies shown in Fig. 5-26, to obtain the total system accuracy.

The gain of this loop increases inversely with power setting. If the loop is to operate at very low power settings, the gain might increase rapidly, requiring gain scheduling.

The temperature control output did not overshoot for the gain range considered, so the thermostatic actuator stroke may be adjusted to correct the error in ratio scheduling. Coupling between the two control loops did not pose a problem for the cases studied.

5.6.4 System Valve Requirements

The final system requires the valves listed in Fig. 5-27. Most of these components are associated with control of the propellant supply to the engine, and as such, do not effect the control system design except for the effects of the propellant supply as an input to the power system.

The valves required are the following:

1. Hydrogen regulator for compressor supply. This valve is required to maintain a constant pressure of 15 psi ± 1 psi to the compressor. The transient response of the regulator is not considered critical since abrupt changes in boiloff supply pressure are not expected. The ± 1 psi accuracy is determined by performance and sizing considerations of the compressor.

2. Oxygen regulator for compressor supply. The same comments apply to this regulator as for the H_2 regulator.

3. Oxygen reservoir regulating relief valve. This valve is required to dump oxygen at pressures above 900 ± 10 psi. The accuracy of this pressure regulator valve effects the power regulation of the engine valves.

4. Hydrogen reservoir regulating relief valve. The requirements for this valve are the same as those for the oxygen valve with the differences which are noted.

5. Electrically operated hydrogen tank shut-off valve. This might be combined with valve 6 to require only one 2-way, 2-position valve.

REQMT Name and Function	LEAKAGE Internal & External	TYPE	ACTUATION Source of Power	SIZE Estimate Operating Area	PRESSURE OF Supply	TEMP	WEIGHT FLOW Maximum, Minimum	PRESSURE DROP	RESPONSE	MODE OF OPERATION	RESOLUTION OR ACCURACY	COMMENTS
Oxygen Comp. Throttle Throttles O_2 Boiloff Into Comp.	.03 lb/hr External; Internal, Must Operate Under No Flow	Constant Upstream Pressure Regulator	Mech. Regulator Operated By Supply Gas	.0036 in^2 (Min-Max Area) To .000046 in^2	15 to 175 psia Temp 160-200°R	Temp. of Saturated Vapor at Supply Pressure	On 1.15 lb/hr. 2.85 lb/hr. Max. Off Leakage	Output Pressure Constant @ 15 psia	Not Expected To Be Critical Less Than .04 Sec.	Used Under Boiloff Supply Condition	1 psi, 5 psi For No Flow	
Hydrogen Comp. Throttle Throttles H_2 Boiloff Into Comp.	.03 lb/hr External; Internal, Must Operate Under No Flow	Constant Upstream Pressur Regulator	Mech. Regulator Operated By Supply Gas	.00318 in^2 (Min-Max Area) To .000021 in^2	15 to 175 psia Temp 36-60°R	Temp. of Saturated Vapor at Supply Pressure	On .57 lb/hr To 1.425 lb/hr. Max. Off Leakage	Output Pressure Constant @ 15 psia	Not Expected To Be Critical, Less Than .04 Sec.	Used Under Boiloff Supply Condition	± 1 psi, ± 5 psi For No Flow	
Hydrogen Reservoir Shutoff Valve (May be combined with hydrogen tank valve, 1,2-way valve)	.01 lb/hr Internal .01 lb/hr External	Shutoff Valve	Electrical	.005 in^2 To 0	300 psia ± 10 psi	Approx. 1050°R	1.425 lb/hr. Max.	5 psi Max.	.5 Sec. Max.	Open Under Boiloff, Closed For Tankage	On-Off	
Oxygen Reservoir Shutoff Valve	.01 lb/hr Internal .01 lb/hr External	Shutoff Valve	Electrical	.01 in^2 To 0	900 psia ± 20 psi	Approx. 1000°R	2.85 lb/hr. Max.	10 psi Max.	.5 Sec. Max.	Open Under Boiloff, Closed For Tankage	On-Off	NOTE: 1. All valves req. to be light weight for space application 2. Downstream volume Not critical on all valves.
Hydrogen Tank Valve Admits Hydrogen To System From Tank	.01 lb/hr Ext. .01 lb/hr Int.	Shutoff Valve	Electrical	.0001 in^2 To 0	300 psia Super Critical Storage	45°R To 140°R	1.425 lb/hr. Max. Off Leakage	5 psi Max.	Not Expected To Be Critical Less Than 1.0 Sec.	Used Under Tankage Supply Condition	On-Off	
Oxygen Tank Valve Admits Oxygen To System From Tank	.01 lb/hr Ext. .01 lb/hr Int.	Constant Upstream Pressure Reg. With Override To Off	Electrical Override To Off Position Mech. Relief	.0001 in^2 To 0	900 psia Super Critical Storage	190°R To 400°R	2.85 lb/hr. Max. Off Leakage	10 psi Max.	Not Expected To Be Less Than 1.0 Sec.	Used Under Tankage Supply Condition	See Pressure Drop	
Oxygen Reservoir Relief Valve Admits Oxygen To Boiloff Supply Or Overboard	External .05 lb/hr	Constant Back Pressure Regulator	Reservoir Pressure (Mech.)	.0007 in^2 To 0	900 psia ± 20 psia (Required Pressure)	Approx. 1000°R	1.42 lb/hr. Max.	800 psi Min.	Not Critical	Boiloff Supply Condition	See Pressure Drop	
Hydrogen Reservoir Relief Valve Admits Hydrogen To Boiloff Supply Or Overboard	External .05 lb/hr	Constant Back Pressure Regulator	Reservoir Pressure (Mech.)	.0003 in^2 To 0	300 psia ±10 psia (Required Pressure)	Approx. 1050°R	.75 lb/hr. Max.	225 psi Min.	Not Critical	Boiloff Supply Condition	See Pressure Drop	

Fig. 5-27 - System Valve Requirements

6. Hydrogen reservoir shut-off valve.

7. Oxygen tank relief valve with electrical override. The relief valve operates when downstream pressure is less than 1500 psi. Tolerances are incorporated which insure an adequate supply of oxygen to the engine under all conditions of boiloff. This feature may not be included in the final design, in which case, supply configuration would be the same as for hydrogen.

8. Electrically operated oxygen reservoir shut-off valve. This valve functions to shut-off oxygen tank leakage through the compressor when in a tankage mode of operation. The requirements for tankage supply pressure regulation are for a constant pressure ± 20 psi.

5.6.5 Control of Propellant Source

Careful consideration was given to the control of the compressor. A closed loop control around the compressor was proposed. Although this system is feasible, the following problems become obvious:

1. If the compressor is sized for pumping the maximum fuel rate required when the inlet pressure is 15 psia, in order to regulate flow rates down to the minimum (about 50% of maximum), the inlet pressure must be reduced to approximately 7.5 psia. For constant exhaust pressure, the pressure ratio would increase as the inlet pressure is throttled. The higher outlet temperatures which would result are undesirable.

2. If the inlet pressures are allowed to get too high, the workload on the engine would increase accordingly. This overload affects sizing of the engine. A relief valve would be required to avoid this overpressure.

3. Closing the loop around the compressor using very simple and easily mechanized techniques does not give desirable results, primarily due to the valve gain variation up-stream of the compressor. This variation in gain is due to the wide range of inlet pressures from boiloff, as well as the change in flow coefficient of an unchoked flow orifice. Runs A, B, C, D, E, F, and G in Fig. 5-28 are analog traces of the results of this type of system in terms of throttled compressor inlet pressure. If gain compensation is added to correct for this poor response, the results could be represented on the same traces, within the range of runs C to D. Adding gain compensation would add complexity to the system mechanization.

The approach proposed at present is based on the following ground rule:

<u>While operating on boiloff, a slight degradation in SPC at less than maximum power settings can be tolerated.</u>

The proposed approach is to regulate compressor inlet and exhaust pressures to constant values, retaining the feature to avoid high inlet pressures at any time. Compressor flow, work, and pressure ratio are now essentially constant. The mismatch between compressor delivery and engine demand flow rates is to be bypassed, either overboard, or to some useful purpose. The work in compressing the bypassed flow is lost.

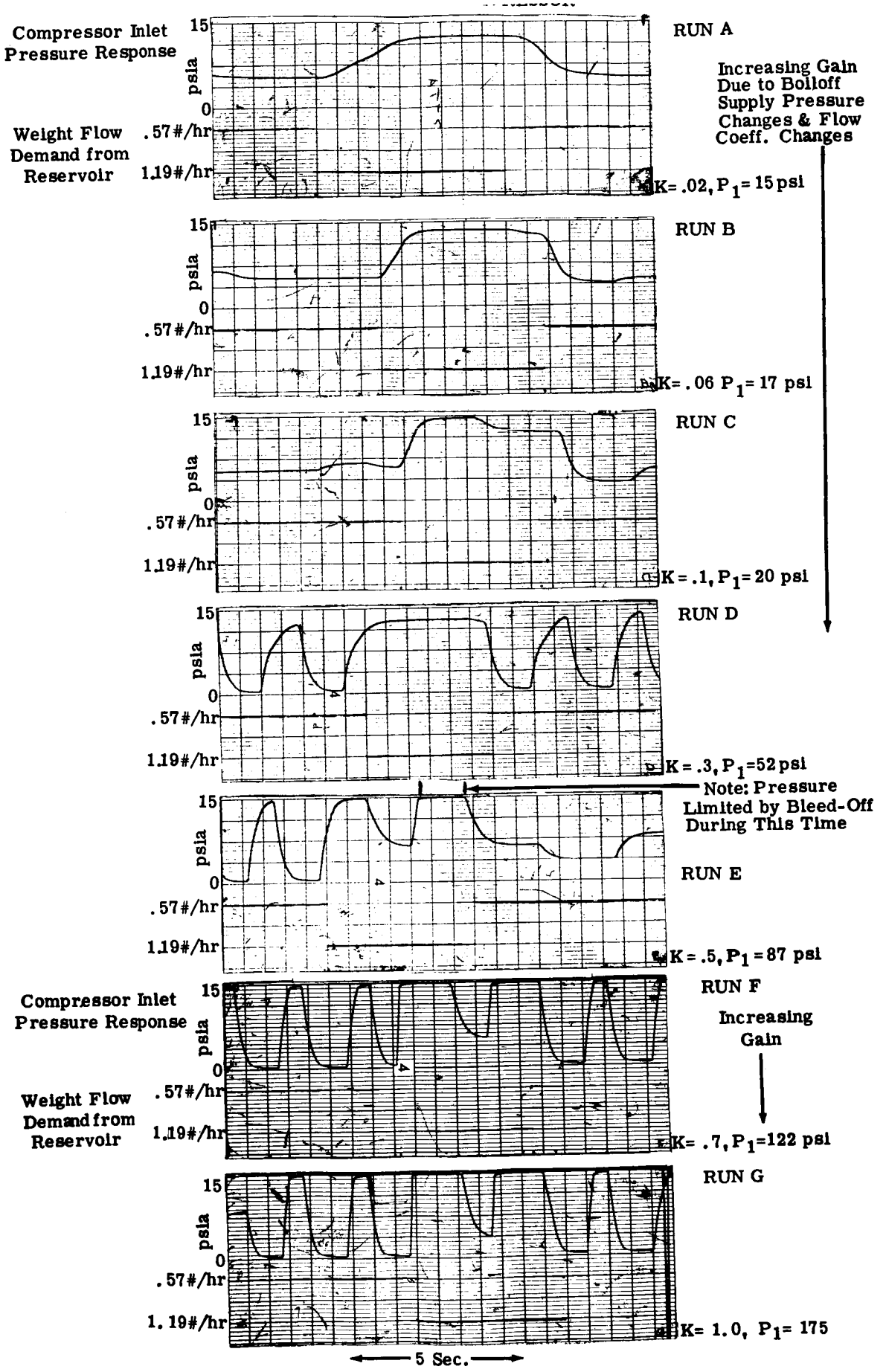

Fig. 5-28 - Closed Loop Compressor Control for Hydrogen Compressor

The only controls necessary consist of the compressor inlet pressure regulator, and the reservoir pressure regulating relief valve, which bypasses the flow necessary to maintain a constant pressure. Both of these units perform functions similar to many regulators already designed. The response of a typical regulator is shown in Fig. 5-29. Since the loop is not closed, problems associated with closing it are eliminated.

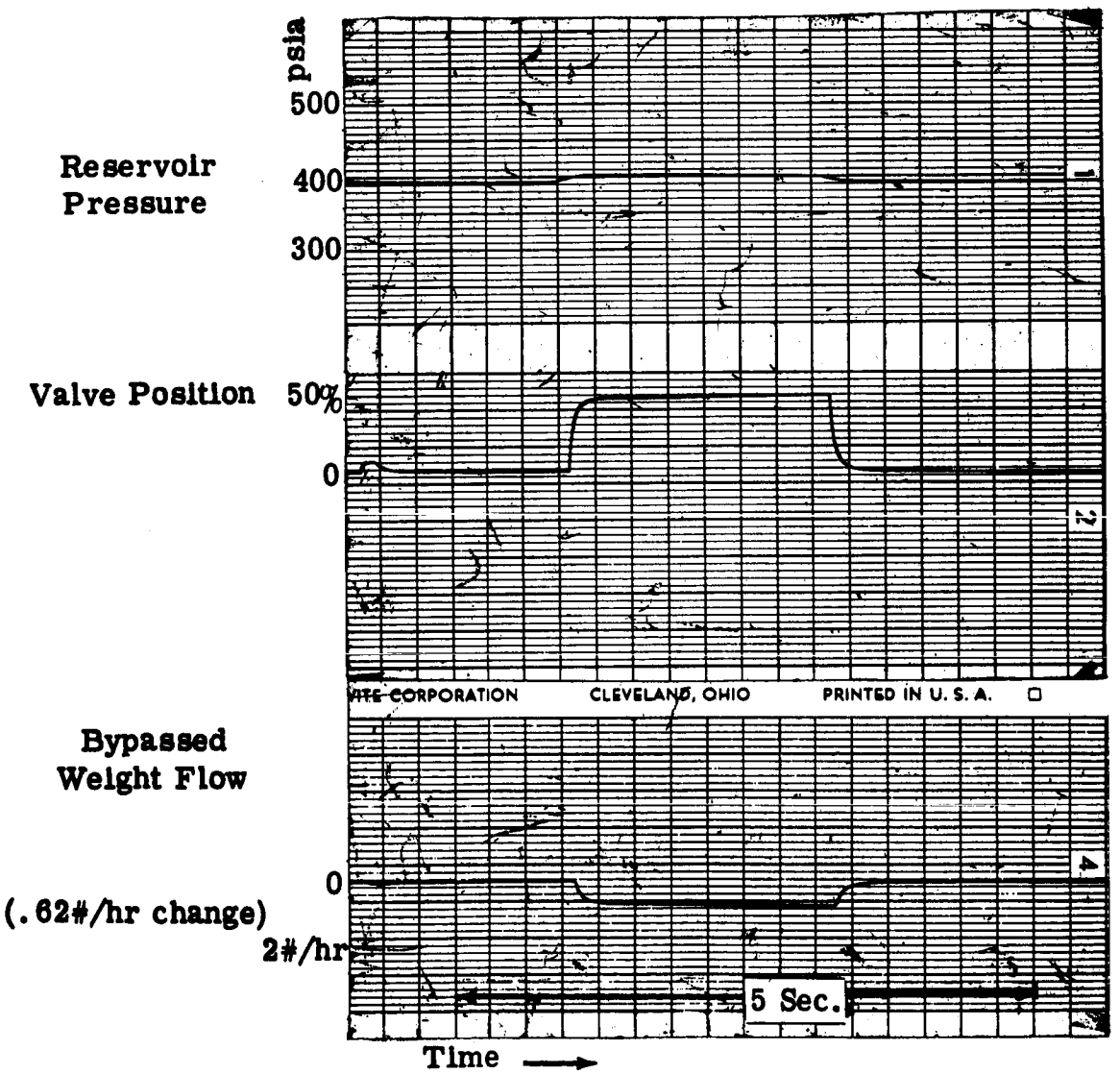

Fig. 5-29 - Typical Pressure Regulator Response, Hydrogen Reservoir Pressure Regulator

5.7 Hardware and Conceptional Design

5.7.1 Introduction

Approaches to mechanization of the control system considered, with respect to actuation power, were; electrical, hydraulic, or pneumatic. The speed sensor and compensating elements of the system were considered to use the same type of power, since conversion from electrical to hydraulic, for example, require additional elements.

Electrical power is most readily available in either ac or dc, even if the battery starter system is not used. Hydraulic power would require the addition of a pump, and limitations on size and complexity do not favor this approach. The smallest size of readily available hydraulic governors were estimated to dissipate .35 hp. This would be a considerable drain on a 5 hp system when operating at part load. Pneumatic power might be tapped from the engine or compressors. Pneumatic power would be very attractive as the actuating power if a relatively free, high pressure source could be made available.

A comparison of system characteristics is shown in Table 5-1 for fluid power and electrical systems.

5.7.2 Tachometer-Generator

A comparison of ac and dc tachometers was made. Differentiating the signal in a dc tachometer would be a problem because of brush and ripple noise. The dc tachometer does have some advantages, such as, high voltage gain, and freedom from

TABLE 5-1

COMPARISON OF SYSTEM CHARACTERISTICS

Quality	Electrical		Fluid Power	
Quiescent Power consumption	Low operating horsepower	+	High operating horsepower	-
Torque available	Low torque, requires high gear ratio	-	High torque available without gearing	+
Ease of dynamic compensation	Easy	+	Difficult	-
Ease of temperature compensation	Easy, many sensitive components	+	Difficult - governor springs in sensitive temperature changes	-
Compatible with external signals	Compatible	+	Usually requires electrical link	-
Weight	Low	+	High	-
Power source	Uses generator, which is available or battery which might be available	+	Requires pump for hydraulic, source for pneumatic power	-
Flexibility	Flexible but requires several stages of amplification	0	Inflexible, but simple, more reliable type hardware	+

wave form and phase shift. Ac tachometers, although requiring demodulation, are rugged, provide a high quality output, and operate with stability over long periods of time. The possibility of obtaining an acceleration output directly from the ac tachometer should be investigated.

5.7.3 Compensation and Amplification

The requirement for compensation is absolutely necessary and offers no obvious problems. The amplifier requirement is dependent upon the final choice of elements used to actuate the engine valve to the proper admission angle. No extension in the present state-of-the-art of electronic design and packaging is required.

5.7.4 Actuator

The actuator regulates throttling valves and cam mechanisms, which vary such parameters as oxygen inlet pressure, or hydrogen valve admission time. The load of these valves and mechanisms is a major unknown in the system design. These loads consist of friction, mass inertia, and force gradients which cannot be balanced out. Various electrical components become more applicable than others, depending on the load.

A comparison of actuation means are shown in Table 5-2.

System analysis has indicated the advantage of using the actuator as the component which provides a rate output proportional to the speed error. Although this adds another rotating device to the electrical system, it seems the best method to insure stable actuator loop operation without the

TABLE 5-2

COMPARISON OF ACTUATION MEANS

	Output Force Level	Response	Velocity F.B.
Torque Motor	Limited to short stroke 12 in. lb. torque	High	Not adaptable
Servo Motor	.45 in. lb. torque @ 2000 rpm drops off as speed increases.	Limited by inertia of active mass, especially at high speeds.	Very adaptable, unit commonly built with this feature.
Magnetic Clutch	2 in. lb. torque @ any speed up to 2000 rpm.	High - very low inertia torque constant at all speeds.	Very adaptable to speed pickup.
Fluid Actuator	Very high - high breakout forces available.	Very high	Not very adaptable, but speed control could probably be maintained through valve design.

Compared on an estimated equal system weight basis.

addition of other components such as networks required for integration, feedback pots or synchros, and stabilizing networks within the actuator loop.

The actuator output will schedule relative positions of valves, by the use of cams, to generate an O/F ratio as near as possible to 2:1. The phasing into the variable admission mode of operation will also be accomplished mechanically. This will provide a smooth and easily modified method for introducing various schedules.

5.7.5 Exhaust Temperature Control

A mechanical thermostatic actuator is suggested for introducing a temperature control input to the system. Such a device is described in Section 2 of this report, and is sketched in Fig. 5-30.

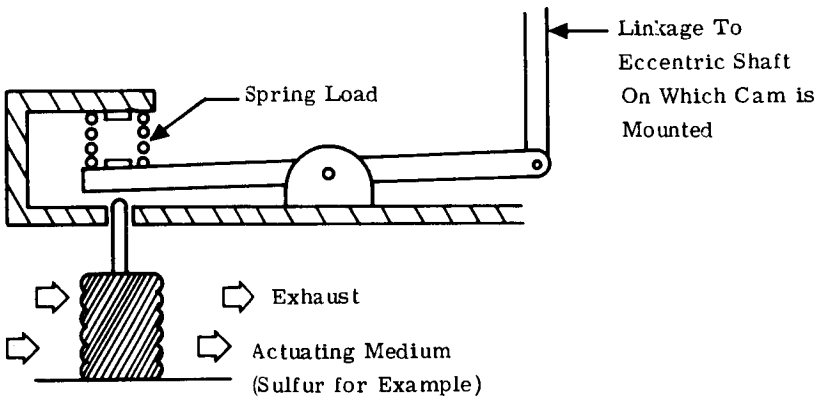

Fig. 5-30 - Mechanical Thermostatic Actuator for Exhaust Temperature Control

The actuating medium which fills the bellows is chosen to give the desired vapor pressure change in the temperature range desired. Many salts have desirable physical properties for this application. Ordinary sulphur appears to be a possibility which might work.

5.7.6 Overall System Control

It is recommended that the areas containing electrical components be provided with adequate temperature control. This will protect against damage due to high temperature, and insure that temperature dependent errors in the system will be reduced to a minimum.

It will be necessary for the system to operate remotely, following the commands of operators in space. In order to simplify and coordinate the commands to the system, mode switching must be provided to activate, deactivate, open, or close various components to allow for operation under the following modes:

a. Warm up
b. Start
c. Operate boiloff
d. Operate tankage
e. Shutdown
f. Fail - safe

The switching logic will be accomplished by using solid state switches and diodes. The pilot will command through a device compatible with vehicle requirements, such as a potentiometer or switches.

5.8 Discussion of Results and Problem Areas

In general, the results of study show a system design which is feasible and relatively easy to mechanize. Accuracies demanded of individual components are not excessively

stringent and system performance is not overly sensitive to gain variations. The linear studies show ample stability and transient accuracy. The system requirement studies indicate that adequate response and stability could be obtained by components which are reasonable to build. Control over variables such as system inertia gives a degree of flexibility to the system performance. Several problem areas might be cited such as the tachometer-generator reference accuracy, and temperature sensor gain change at low speed operation. The overall complexity problem is evident in the number of functions which must be taken care of by control loops and accessories. This complexity is also reflected in the reliability of the proposed system.

The design goal will be to simplify the system in a way which will keep reliability at a high level, with a minimum sacrifice of performance and efficiency.

Areas where the greatest development effort will be required are:

1. Small valves

2. Thermostatic actuator

3. Valve phasing mechanism, in order to establish actuator load

4. Tachometer-generator reference accuracy

5. Overall system performance.

It is recognized that the results of this report are mainly of a system requirement nature, and before system design begins, another evaluation of all the aspects of mechanization will be made. In the area of requirements, an effort to continuously update the existing requirements is necessary.

6.0 RELIABILITY STUDIES

6.1 Estimation of Component Failure Rates

General

An estimation of individual component failure rates is considered to be basic to the required reliability studies of the H_2-O_2 engine power system. A reliability estimate for each component is necessary to calculate the system reliability, to determine the redundancy requirements, and to establish areas where failure mode analysis is most necessary. If accurate estimates are not obtained for each component, little confidence will be achieved for the estimate of complete system reliability. If the estimate of system reliability is unduly low, recommendations for redundancy in certain areas may be an unnecessary addition of expense or weight. An overly optimistic reliability estimate is even more critical , for redundancy recommendations may then be insufficient to attain the needed high probability of successful accomplishment of the mission.

For this reason, a compilation of the best reliability estimates available has been made. Most of the well-known reliability manuals and failure rate documents were used (see list of references) to obtain reliability estimates of some of the more standard system components. For other components, for which no reliability information has been published, it was necessary to obtain specialized information from companies throughout the country. For components not resembling an existing item, reliability estimates were often made by a comparison with similar components of equal complexity levels. These estimates were always conservative. A more detailed explanation

of these component reliability estimates is presented below and a tabular list of all failure rates obtained is given in Table 6-1.

H_2-O_2 Engine

The engine reliability estimate cannot be based on actual H_2-O_2 engine experience since the engine extends the state-of-the-art of small reciprocating 2-cycle engines. In particular, the use of hydrogen and oxygen as fuels make the use of failure rate data from ordinary gasoline engines somewhat inapplicable. For example, common failure modes in gasoline engines, such as head deposits and spark plug fouling, are non-existent in the H_2-O_2 engine because of the clean burning qualities of hydrogen and oxygen. Since extensive failure rate data from H_2-O_2 engines is not yet available, the estimate is based on gasoline engine data and is considered to be pessimistic for a well-developed H_2-O_2 engine.

To obtain the best failure rate data available for low horsepower reciprocating engines, an extensive survey of engine manufacturers was conducted. A list of the companies contacted is presented in Table 6-2. Although a high percentage of the companies contacted submitted some useful engineering information, no applicable small engine failure rate data were received.

The failure rate estimate for the H_2-O_2 engine is based on life experience of reciprocating aircraft engines contained in USAF Technical Order T.O. 00-25-128, Procedures for Determining Aircraft Engine Failure Rates, dated 20 October 1959, Rev. 30 April 1960. These engines, for which reliability data

COMPONENT FAILURE RATES

Component	RCA	Wright-Patterson	North American	Martin	Boeing	Arinc Research	SAE
Generator	64		32.4		360	56	
(Main Alternator) Voltage Regulator	52		25.2	370	25		
Battery				1.4			
Clutch		5.7	10	6			
Regenerator				15			
Shut-off Valve				6.5			
Relief Valve				5.7			
Pressure Regulator		70	2	2.14			
Compressor							200
A.C. Tachometer	2.5						
D.C. Reference	15.7						
Summing Amplifier	20.0						
Demodulator	26.0						
D.C. Tachometer	5.3						
R.C. Circuitry	5.4						
Driving Amplifier	22.8						
Servo Motor	15.0						
(Exciter & Battery) Voltage Regulator	50						

TABLE 6-1

ORGANIZATIONS CONTACTED FOR ENGINE DATA

Company	Location
Dept. of Air Force	Washington, D.C.
Dept. of Navy	Washington, D.C.
Briggs & Stratton Corp.	Milwaukee, Wisc.
Wisconsin Motor Corp.	Milwaukee, Wisc.
Clinton Engines Corp.	Maquoketa, Iowa
McCulloch Corp.	Los Angeles, Calif.
Radioplane Div., Northrop Corp.	Van Nuys, Calif.
Continental Motors Corp.	Muskegon, Mich.
Lycoming Div., AVCO Corp.	Stratford, Conn.
U.S. Army Corps of Engineers	Ft. Belvoir, Virginia
U.S. Army Mobility Support Center	Columbus, Ohio

TABLE 6-2

is available, vary considerably in design, application, and power capabilities. For example, both opposed and radial configurations of 6 to 18 cylinders and from 200 to several thousand horsepower engines are considered. Although none of these engines were similar to the H_2-O_2 engine, by choosing a wide variety of engine configurations and thereby obtaining a vast range of reciprocating engine data, we may assume, with some confidence, that the H_2-O_2 engine failure rate will fall somewhere in this range. Engine failure rate was estimated to be 500 failures per million hours of operation. As indicated by Table 6-3, this value falls on the high side of all engine data considered. Technical Order 00-25-188 shows that failure rates of all aircraft reciprocating engines follow the standard "bathtub" distribution curve. The first 80 hours or less consists of a period of relatively high failure rate, apparently caused by "infant mortality" type failures. During the following several hundred hours, the failure rate becomes relatively constant. This is the so-called "useful life" of the component during which failures appear to be occurring at a random rate. Increased failure rate caused by wear never appears to become a problem with these reciprocating engines until 800 or more hours. This is important to note, since the duration requirement of this mission is approximately 350 hours. The failure rates estimated for the engines considered were taken from the useful life periods immediately following their "infant mortaility" period. This was done because it is assumed that the H_2-O_2 engine will be run-in sufficiently before use to eliminate a high early failure rate.

Electrical Components

Voltage Regulators: Generally speaking, estimating the reliability of devices composed of electronic elements, such

ENGINE FAILURE RATES

Engine Part No.	Failure Rate/20 Hours	F/R x 10^{-6} Hours
R-2800-103	.0005	25
R-2800-52	.0008	40
R-1830-90	.0009	45
R-2800-97	.0015	75
R-2600-29	.0016	80
O-420-13	.0020	100
R-985-AN-1, 3	.0020	100
R-2800-99	.0020	100
R-985-AN-14	.0021	105
R-3350-57, 83	.0022	110
R-3350-91	.0026	130
O-335-3, 5	.0029	145
GO-480D-1	.0030	150
R-2800-99	.0030	150
R-3350-89A	.0047	235
R-2800-75	.0048	240
R-2000-4	.0067	335
R-2800-79	.0070	350
R-3350-91	.0091	455
O-470-7	.0101	505
R-3350-89	.0136	680
R-3350-57, 83	.0151	755
R-1820-76	.0165	825

TABLE 6-3

as voltage regulators, has become a highly developed process and can be accomplished with considerable accuracy. Numerous documents have been published by the industry showing means for determining the failure rate of these devices for various environmental and operating conditions. The RCA document TR1100 (Ref. 5) is probably the best known of these, and was used as a reference. In computing the failure rate of a voltage regulator, we need only compute the individual failure rates of the transistors, diodes, capacitors, and transformers. By adding these, the expected value of reliability for the voltage regulator can be established. The failure rate for the voltage regulator used in conjunction with the main alternator is 52 failures per million hours of operation ($52/10^6$). The regulator used with the battery and exciter has an estimated rate of $50/10^6$ hours.

Generator: The estimation of reliability of small rotary electrical devices, such as generators, has become somewhat of a standard procedure. Studies by the RCA Victor Company of Montreal, Quebec, (Ref. 5) and the ARINC Research Corporation of Washington, D.C. (Ref. 7) have contributed important data for use in such estimates. Some of the important factors in determining the failure rates of generators are:

1. Stator diameter and number of windings
2. Average speed of operation
3. Number of brushes or slip rings
4. Motor shaft bearing bore diameter
5. Hot-spot temperature and type of insulation

The failure rate for the H_2-O_2 system generator is $64/10^6$ hours. This estimate includes the addition of a rotating rectifier assembly in the exciter, composed of six diodes. No consideration has been given to the possibility of increased rectifier failure rate due to g-forces.

Inverter/Rectifier: The Martin Company (Ref. 4) estimates the failure rate of inverters in general (single purpose) to be $400/10^6$ hours. It appears that the dual purpose inverter/rectifier may be a serious reliability problem because of its inherent design complexity. An estimate of 250 failures per 10^6 hours was assumed, based on a minimum number of elements contained in devices of this nature. This rate may be too low for this application and the actual failure rate could be as high as that of the H_2-O_2 engine.

Control Components

The failure rate estimates for the control components were computed similarly to those of the electrical components. That is, since each component is composed of a known number of electronic elements such as transistors, diodes, and resistors, and since the operating and environmental conditions for each can be estimated, it is possible to estimate component reliably by obtaining the sum of the element failure rates. This method was used for the demodulator, D.C. reference, summing amplifier, R.C. circuitry, and the driving amplifier. Since the ac and dc tachometers are rotary electrical devices similar to generators, their reliability estimate is computed accordingly.

Compressor

To obtain a failure rate estimate for the compressors, the Chairman of the Failure Rate Panel of the Society of Automotive Engineers was contacted. This panel of the Reliability Sub-Committee, was engaged in a study program of failure rates of various types of mechanical devices. The failure rate of $200/10^6$ hours was taken from experience with piston type air-compressors in approximately 100,000 hours of military and commercial aircraft operation.

Failure rates obtained from this panel have not yet been published, so the source documents cannot be referenced.

Supercritical Tankage

Although the tankage systems are not considered to be part of the power system, it has been determined that fuel sources of this nature are very reliable. A reliability level of .99994 for the 350-hour flight mission time has been estimated by the Beech Aircraft Corp. of Boulder, Colorado, which has a wide background of experience in cryogenic fuel systems. This value was used in computing the system reliability.

Other Components

Reliability estimates for remaining system components, such as the clutch, heat exchanger, compressor, and various types of valves, and pressure regulators, are taken as appropriate, from the failure rate documents listed in the reference. In general, the variations in failure rates listed by these documents were due to the different types of usage of these components. The attempt was made to choose the most applicable rates.

6.2 Estimate of System Reliability

From a reliability standpoint, the complete auxiliary electric power system can be thought of as being composed of three separate series connected subsystems. These are a control system composed of a tachometer, reference, demodulator and related mode switching devices: an engine system composed of a constant speed, reciprocating engine, and its fuel supply components; and an electric power system capable of generating both ac and dc power. All three are, in a sense, "series connected" because a catastrophic failure of any one of the three would lead to a complete loss of the system function.

Each of these subsystems is illustrated in detail by a Reliability Diagram in Figs. 6-1, 6-2, 6-3, and 6-4. Each block represents a component of the subsystem, and the respective failure rates per million hours of operation are shown. These individual failure rates have been combined in a manner consistent with component use to obtain an overall failure rate.

The engine system has two supplies of fuel that will be available during the first 100 hours. The primary source during this period will be "boiloff" from the main engine tanks. This will be backed by a supercritical tankage system that will be available on a standby basis. The estimated failure rates of the boiloff supply and the tankage supply are different. The reliability of this standby system, or more correctly, the reliability of the engine system for the first 100 hours can be expressed by:

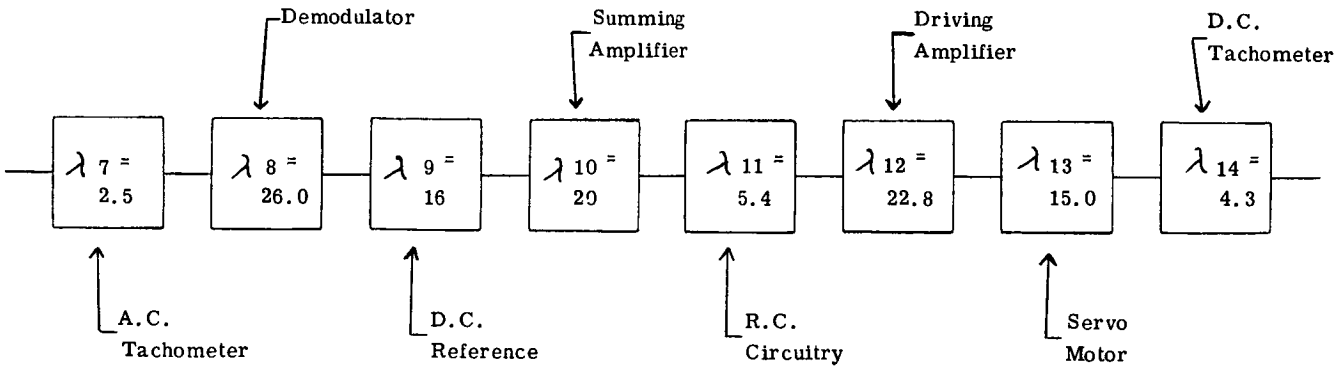

Fig. 6-1 - Reliability Diagram for Control System

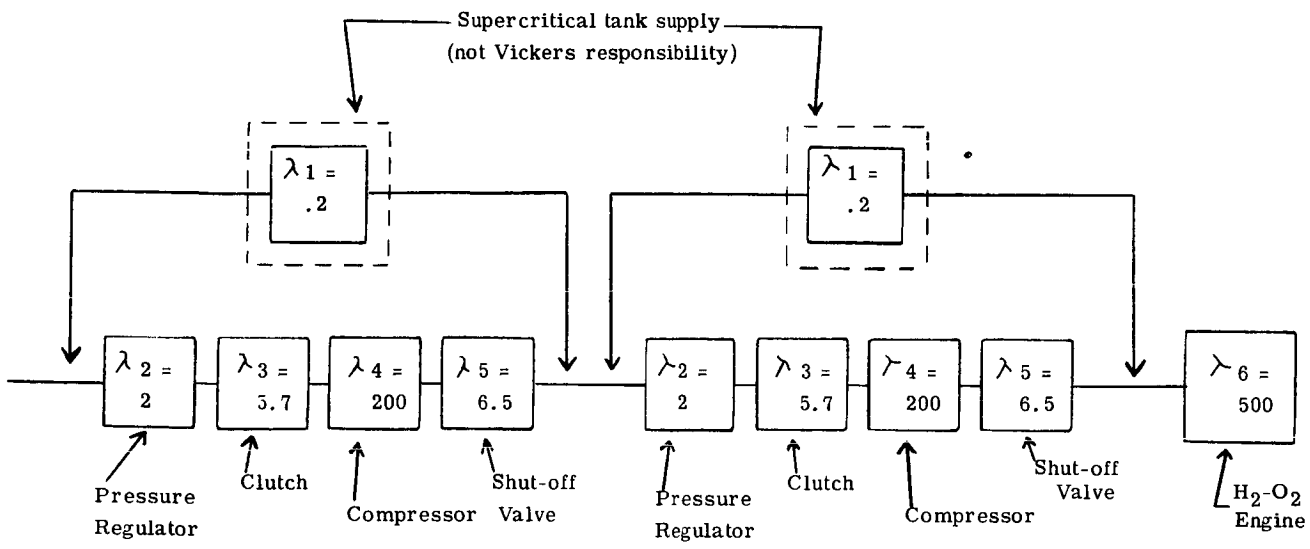

Fig. 6-2 - Reliability Diagram for Engine System (First 100 Hours)

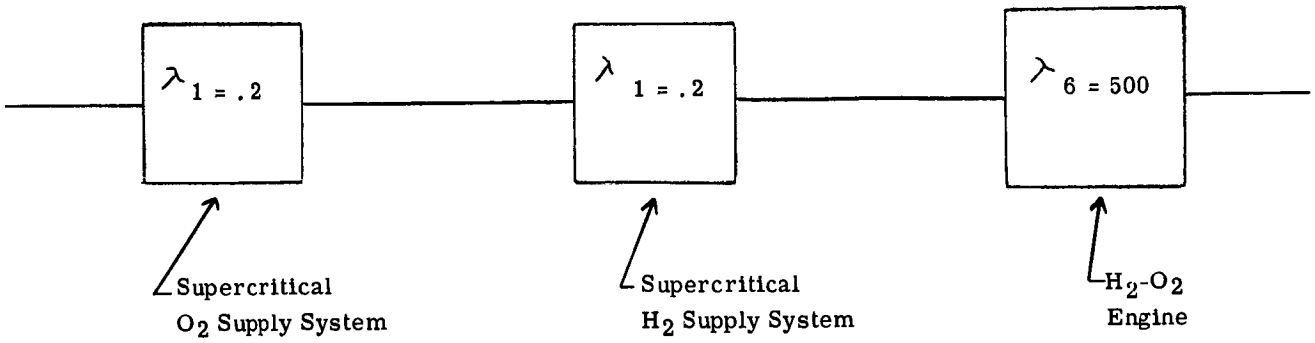

Fig. 6-3 - Reliability Diagram for Engine System (Last 250 Hours)

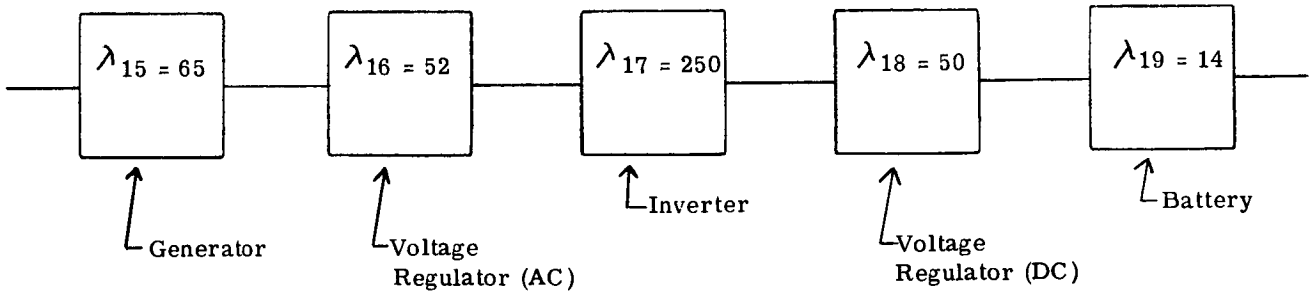

Fig. 6-4 - Reliability Diagram for Electrical System

*

Where: = failure rate of boiloff fuel supply
= failure rate of supercritical tankage system
= failure rate of H_2-O_2 engine

A summary of the complete auxiliary power system reliability calculations is presented as Fig. 6-5.

6.3 Failure Mode Analysis

A failure mode analysis for the most significant components is presented in the following tables. As indicated, this analysis consists of a list of the possible failure modes; their relative likelihood; probable effect on the complete Auxiliary Power System and the primary causes. Additional remarks are presented where appropriate.

Since at this stage of development, it is difficult to assign accurate frequency rates to failure modes, each mode was rated as "most likely", "less likely", "not very likely" and "least likely". The broad classification "most likely" should not be considered as a highly probable situation but only as the most probable of the modes presented.

The different type of failure modes have been broadly categorized as being of four different types according to their effect on the complete system. Type 1 failure modes result in "no electrical output" and are obviously the most serious.

* Bazovsky, Reliability: Theory and Practice, P. 115-6 (Ref. 1).

Any failure that would have this effect on the system must be considered "catastrophic", since the entire purpose of the APS is to generate electrical power. Most failure modes, however, are of Type 2, which have the effect of causing the system to consume fuel at an abnormal rate because of inefficiency.

Type 3 failures occur in the control system and result from an erroneous speed indication. This could result in out-of-tolerance frequency for the ac output.

Type 4 failure modes are those that would be catastrophic to the boiloff supply of fuel. Since an additional source of fuel is available, this may not be catastrophic to the complete APS.

Some failure modes of the voltage regulators would cause system voltage to rise to a destructive level if no protective relays were used. It is assumed that these protective devices would be employed and these modes would have a Type 1 effect (no electrical output).

6.4 Redundancy Requirements

First calculations with no redundancy of any type indicate the estimated system reliability for a 350-hour mission to be .69948. This means that to meet the system reliability requirement of .9977, three additional systems will be required on a standby basis.

However, this required number of APU systems can be reduced if certain component reliabilities are improved and redundancy is used effectively. For example, if within the complete Auxiliary Electric Power System two inverters are employed,

one of these in a standby redundant manner, the estimated system reliability is improved to .7633. Under these conditions only two (2) standby systems would be needed to attain a system reliability value of .9977.

The estimated failure rate of $500/10^6$ hours may be pessimistic for the H_2-O_2 engine. For example, Fig. 6-6 shows that numerous aircraft reciprocating engines have demonstrated failure rates considerably lower than 500 per million hours of operation. Specifically, of the 24 engines for which data was available, five have demonstrated failure rates lower than $100/10^6$ hours and nine between 100 and $200/10^6$ hours. A complete tabulation of the exact engine failure rates is presented in Table 6-3. If a failure rate of 225 per million hours of operation is achieved, the system reliability requirement of .9977 could be fulfilled with only one standby redundant system. It is again stressed that this may be a realistic assumption since many large and complicated aircraft reciprocating engines have demonstrated this level of reliability.

System reliability calculations verifying the above statements are submitted in Appendix F.

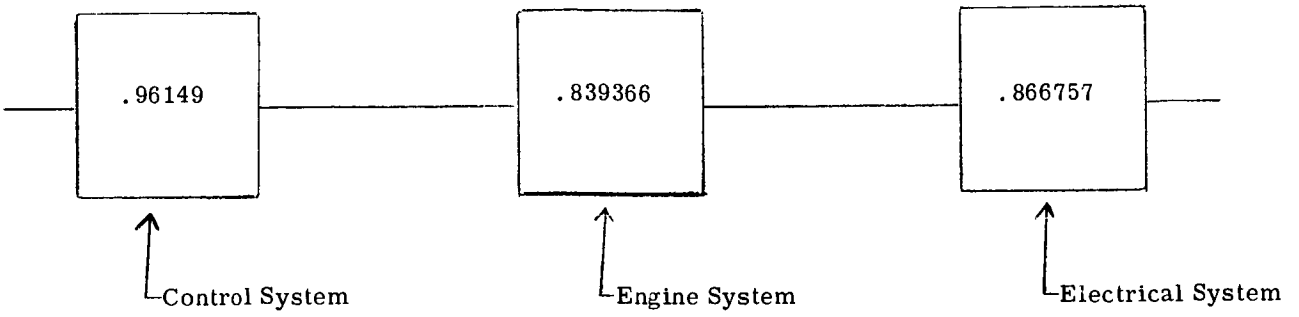

Fig. 6-5 - Reliability Diagram for Auxiliary Power System

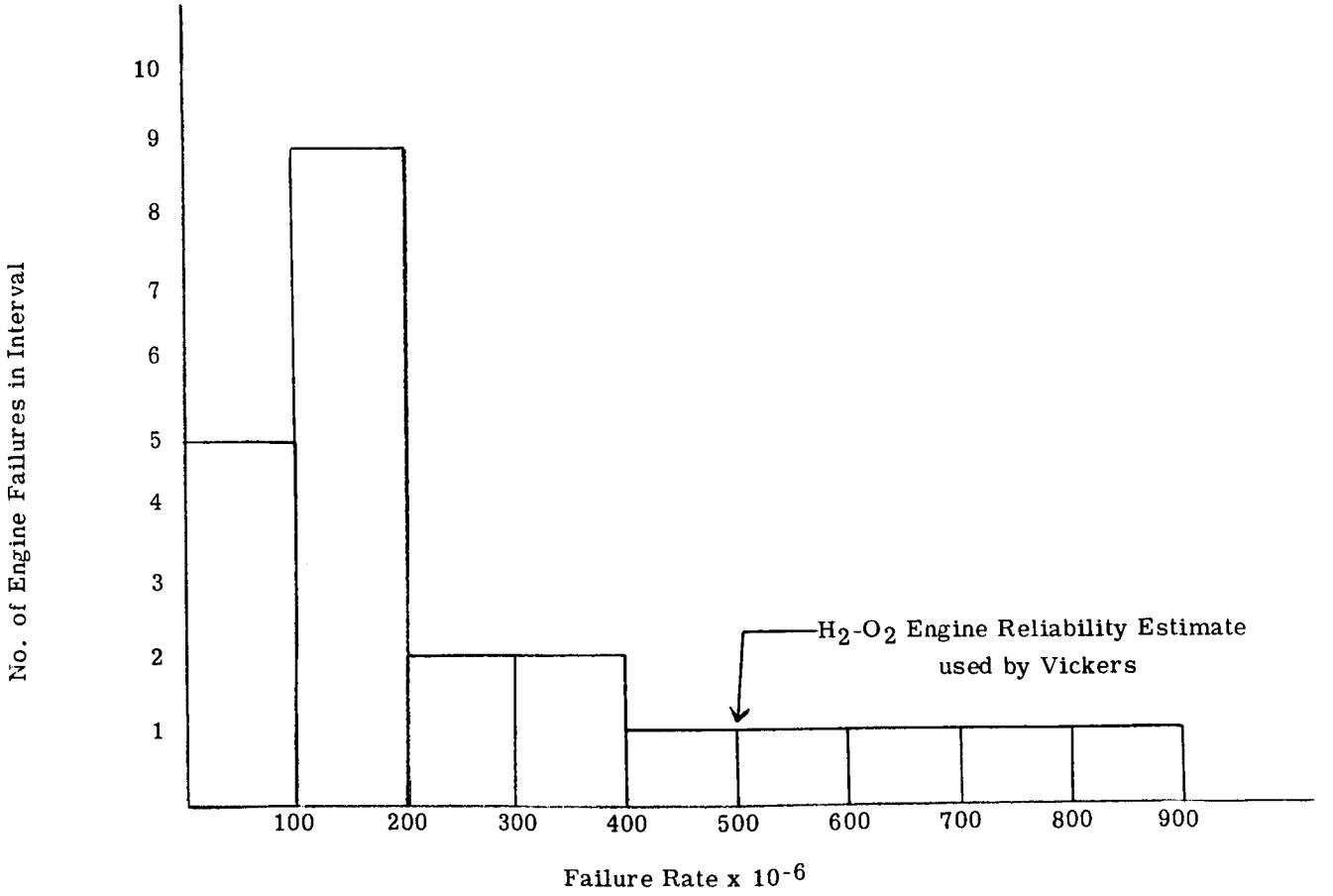

Fig. 6-6 - Summary of Reciprocating Engine Failure Rate Data AAF - T.O. 00-25-128

FAILURE MODE ANALYSIS - ENGINE

FAILURE MODE	EFFECT ON SYSTEM	*RELATIVE LIKELIHOOD	PRIMARY CAUSES	REMARKS
O_2 injector torsion tube leakage	No electrical output	3	1. Overspeed 2. Overstress 3. Fatigue	Danger of fire
O_2 injector leakage	High fuel consumption	1	1. Poppet and seal mating surface deterioration 2. Wear of valve guide	Causes increased heat rejection to cylinder walls, overloading cooling system
Sticking H_2 Valve	High fuel consumption	2	1. Contamination 2. Valve guide mis-alignment due to wear	May cause improper valve timing
Hydrogen valve leakage	High fuel consumption	2	1. Poppet and seal mating deterioration 2. Valve guide	Excessive power at low-efficiency if valve leaks at low demand levels.
Minor bearing failure	High fuel consumption	2	1. Inadequate lubrication 2. Dust 3. Bearing overload	Bearings will operate best at a high noise and friction level

* 1. Most likely
2. Less likely
3. Not very likely
4. Least likely

FAILURE MODE ANALYSIS - ENGINE

FAILURE MODE	EFFECT ON SYSTEM	RELATIVE LIKELIHOOD	PRIMARY CAUSES	REMARKS
Drastic failure of anyone of these bearings a. Main b. Rod c. Big end d. Balance weight	No electrical output	3	1. Insufficient lubrication 2. Separator misalignment 3. Raceway and ball bearing imperfections 4. Dust seal leakage	Drastic failure implies seizure induced by extreme local heating and/or mechanical collapse
Piston seizure (overheating of cylinder)	No electrical output	3	1. Leaks in cooling jacket 2. Radiator leakage 3. Coolant pump leakage 4. Temp. control failure 5. Leakage lines	
High oil consumption and combustion gas blowby	High fuel consumption	2	1. Piston ring breakage or wear 2. Scored cylinder block	
Combustion gas leakage	High fuel consumption	2	1. Seal failures in piston 2. Head gasket failures	
Broken or bent connecting rod	No electrical output	4	1. Overspeed	
Sticking O_2 injector	High fuel consumption	2	1. Contamination 2. Excessive wear causing misalignment	Could be catastrophic if stuck permanently in open position

FAILURE MODE ANALYSIS - MAGNETIC CLUTCH

FAILURE MODE	EFFECT ON SYSTEM	RELATIVE LIKELIHOOD	PRIMARY CAUSES	REMARKS
Fail closed	High fuel consumption	3	1. Failure of control system 2. Overheating of components - seize - 3. Drastic bearing failure	While operating on boil-off, this would not be determined
Fail open	Loss of "Boil-off" supply of fuel	2	1. Failure of control system 2. Insulation failures - loss of magnetic field	
Slip	High fuel consumption Lower peak power capacity	2	1. Weak magnetic field	

FAILURE MODE ANALYSIS - REGULATOR

Leakage	High fuel consumption	4	O-ring failure	
Oil contamination	High fuel consumption	1	Excessive blowby	

FAILURE MODE ANALYSIS - ALTERNATOR

FAILURE MODE	EFFECT ON SYSTEM	RELATIVE LIKELIHOOD	PRIMARY CAUSES	REMARKS
Diode failure in rotating rectifier assembly	High fuel consumption or No electrical output	1	1. Short circuited junction 2. Open circuited junction 3. Wire breakage 4. Solder failure	Short circuited junction would result in no output. Open circuited junction would result in low output voltage at full load and increased fuel consumption.
Short circuit in stator (phase to phase)	No electrical output	2	1. Insulation failures caused by temperature, vibration, etc.	Alternator burnout
Short circuit in stator (phase to ground)	High fuel consumption	3	Same as above	Not catastrophic if there is no neutral ground
Short circuit in alternator field (turn to turn)	High fuel consumption	4	Same as above	
Short circuit in alternator field (wire to ground)	None or no electrical output	3	Same as above	None if no other grounds in machine. No output if other ground in exciter
Short circuit in exciter A.C. windings (phase to phase)	No electrical output	4	Same as above	Burnout

FAILURE MODE ANALYSIS - ALTERNATOR

FAILURE MODE	EFFECT ON SYSTEM	RELATIVE LIKELIHOOD	PRIMARY CAUSES	REMARKS
Short circuit in exciter A.C. windings	None or no output	4	1. Insulation failures caused by temperature, vibration, etc.	None if no other ground in exciter. Burnout if other ground in exciter.
Short circuit in exciter field (Turn to turn)	High fuel consumption	3	Same as above	
Short circuit in exciter field (winding to winding)	High fuel consumption	4	Same as above	
Short circuit in exciter field (winding to ground)	No electrical output	3	Same as above	Not catastrophic if battery ungrounded

FAILURE MODE ANALYSIS - DEMODULATOR

Stoppage	No electrical output	3	1. Capacitor failure 2. Transformer failure 3. Resistor failure 4. Diode failure	

FAILURE MODE ANALYSIS - VOLTAGE REGULATOR

FAILURE MODE	EFFECT ON SYSTEM	RELATIVE LIKELIHOOD	PRIMARY CAUSES	REMARKS
Open power transistor	No electrical output	4	1. Vibration 2. Temperature	
Power transistor increased leakage current or collector to emitter short circuit	System voltage rises to destructive level	1	Same as above	System protection requires additional equipment
Diode opens	System voltage rises to destructive level	3	Same as above	Same as above
Change in voltage breakdown of Zenor diodes	Change in regulating voltage point	4	Same as above	
Diode failure increased current leakage	No or low output voltage	2	Same as above	
Capacitor opens	Change in % regulation under load	4	Same as above	

FAILURE MODE ANALYSIS - VOLTAGE REGULATOR

FAILURE MODE	EFFECT ON SYSTEM	RELATIVE LIKELIHOOD	PRIMARY CAUSES	REMARKS
Capacitor shorts	System voltage rises to destructive level	3	1. Vibration 2. Temperature	
Change in capacitance	Change in % voltage regulation under load	4	Temperature	
Transformer opens	Alternator voltage rises to destructive level	4	Vibration	
Transformer shorts	Alternator voltage rises to destructive level	3	Vibration	
Resistor opens	Same or no electrical output	3	Vibration	
Resistor changes	Change in voltage regulation point	2	Temperature	

FAILURE MODE ANALYSIS - COMPRESSOR

FAILURE MODE	EFFECT ON SYSTEM	RELATIVE LIKELIHOOD	PRIMARY CAUSES	REMARKS
Sticking or jamming valves	High fuel consumption	2	1. Freezing 2. Contamination 3. Spring failures	Second stage valves will not be subject to freezing
Oxygen or hydrogen leakage	High fuel consumption	2	1. Deformation of poppets or seats 2. Freezing	
Low compression and excessive blowby	High fuel consumption	1	1. Improper seating 2. Expander ring breakage 3. Ryder ring failures 4. Ring fatigue	
Bellows failures	High fuel consumption	2	1. Vibration 2. Fatigue	

FAILURE MODE ANALYSIS - DRIVING - AMPLIFIER

No signal	No electrical output	3	1. Resistor failure 2. Transistor failure 3. Transformer failure	

FAILURE MODE	EFFECT ON SYSTEM	RELATIVE LIKELIHOOD	PRIMARY CAUSES	REMARKS
Speed error	High fuel consumption & incorrect AC frequency	1	1. Drift-air gaps change 2. Magnetic property change 3. Non linearity	
No signal	No electrical output	3	1. Excitation fails 2. Mechanical failure	

FAILURE MODE ANALYSIS - D.C. REFERENCE

Speed error	High fuel consumption & incorrect A.C. frequency	1	Loss of function of any components	
Stoppage	No electrical output	3	1. Resistor failure 2. Thermistor failure 3. Diode failure	

FAILURE MODE ANALYSIS - SUMMING AMPLIFIER

FAILURE MODE	EFFECT ON SYSTEM	RELATIVE LIKELIHOOD	PRIMARY CAUSES	REMARKS
Speed error	High fuel consumption & Incorrect A.C. frequency	3	Loss of function of components	
No signal	No electrical output	2	1. Resistor failure 2. Transistor failure	

FAILURE MODE ANALYSIS - R.C. CIRCUITRY

Speed error	High fuel consumption & incorrect A.C. frequency	3	Degradation of performance of any components	
No signal	No electrical output	2	1. Resistor failure 2. Capacitor failure	

FAILURE MODE ANALYSIS - FEEDBACK TACHOMETER

FAILURE MODE	EFFECT ON SYSTEM	RELATIVE LIKELIHOOD	PRIMARY CAUSES	REMARKS
No signal	No electrical output	3	Mechanical failure	

7.0 DESCRIPTION OF PROTOTYPE COMPONENTS

7.1 Test Engine Description

The experimental engine designed and constructed for the test phase of this program is a modified version of the oxygen injection engine constructed for a previous program (USAF-ASD Contract AF33(616)8406; Ref. 1). The engine follows the operating cycle discussed in Section 3.3 and is basically a test vehicle for developing the engine combustion and timing configuration. Accordingly, the engine follows a conventional design, using commercial components when possible, except in the hydrogen and oxygen induction systems.

Photographs of the engine are shown in Figs. 7-1 and 7-2.

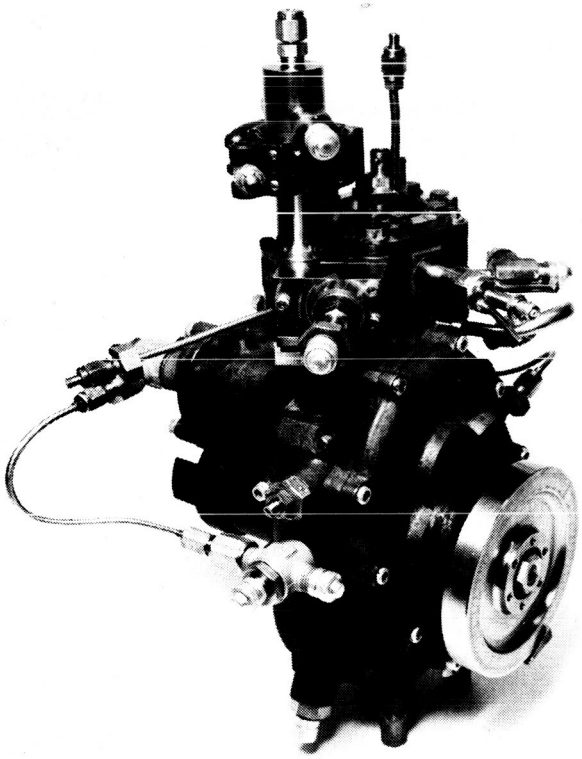

Fig. 7-1 - H_2-O_2 Experimental Test Engine

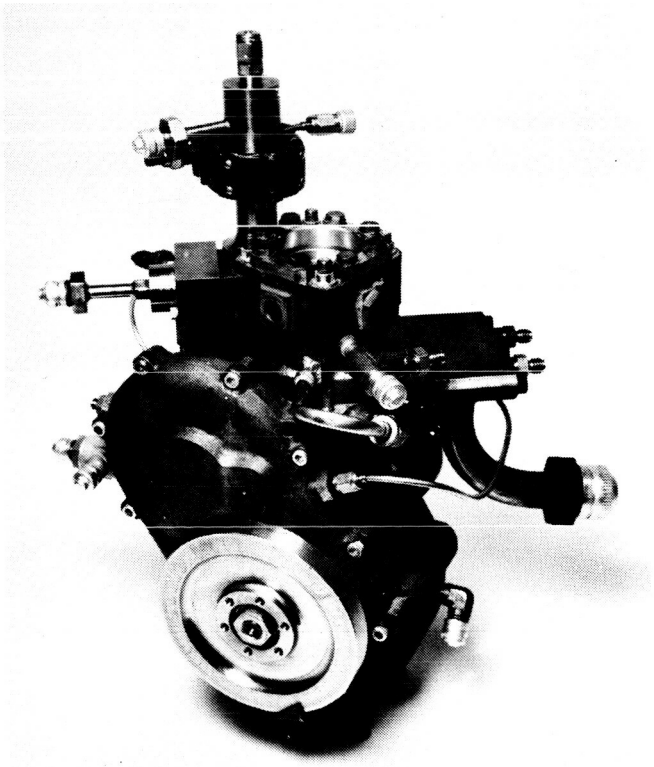

Fig. 7-2 - H_2-O_2 Experimental Test Engine

Preceding page blank

Fig. 7-3 is an assembly drawing of the engine and the oxygen injector valve is illustrated in Fig. 7-4. Areas of the engine which differ from the previous ASD test engine include the hydrogen valve spring arrangement, the methods of sealing around the hydrogen inlet, and the cylinder head and piston dome construction. The oxygen injector valve has been completely redesigned.

A design discussion of each major subassembly is given below. Some of these components were designed specifically for this program and others have evolved in concept and design from previous internal combustion and external combustion engine development work conducted by Vickers since 1958.

Oxygen Injector Valve

A new oxygen injector valve was designed for this program, to be incorporated into engine tests and for additional development as a separate component. Separate development of the oxygen injector valve was deemed necessary because of the special problems involved in the development of the injector and because of its importance in achieving satisfactory engine operation.

Fig. 7-4 is an assembly drawing of the oxygen injector valve and a photograph of an injector assembly is shown in Fig. 7-5. In order to reduce the valve seating loads on the injector poppet seat a design has been evolved which allows the inertia loads of the entire actuating system, with the exception of the poppet, to be taken on the cam. Only the inertia load of the poppet valve strikes the valve seat. The injector can be assembled as a unit on the bench and installed in the engine as a module. The cam follower shaft bearings are self-contained, the torsional

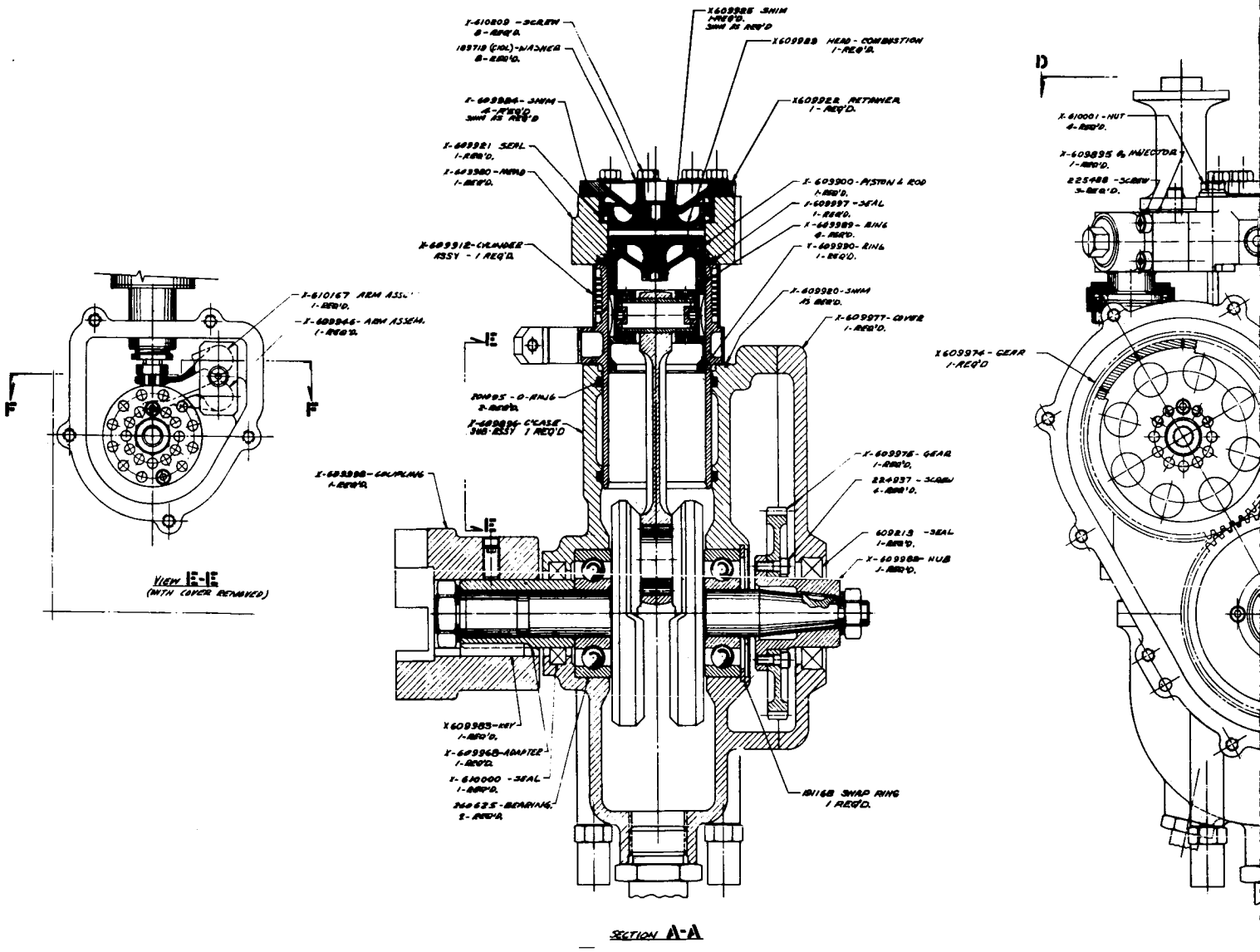

Fig. 7-3 - Assembly Drawing - H

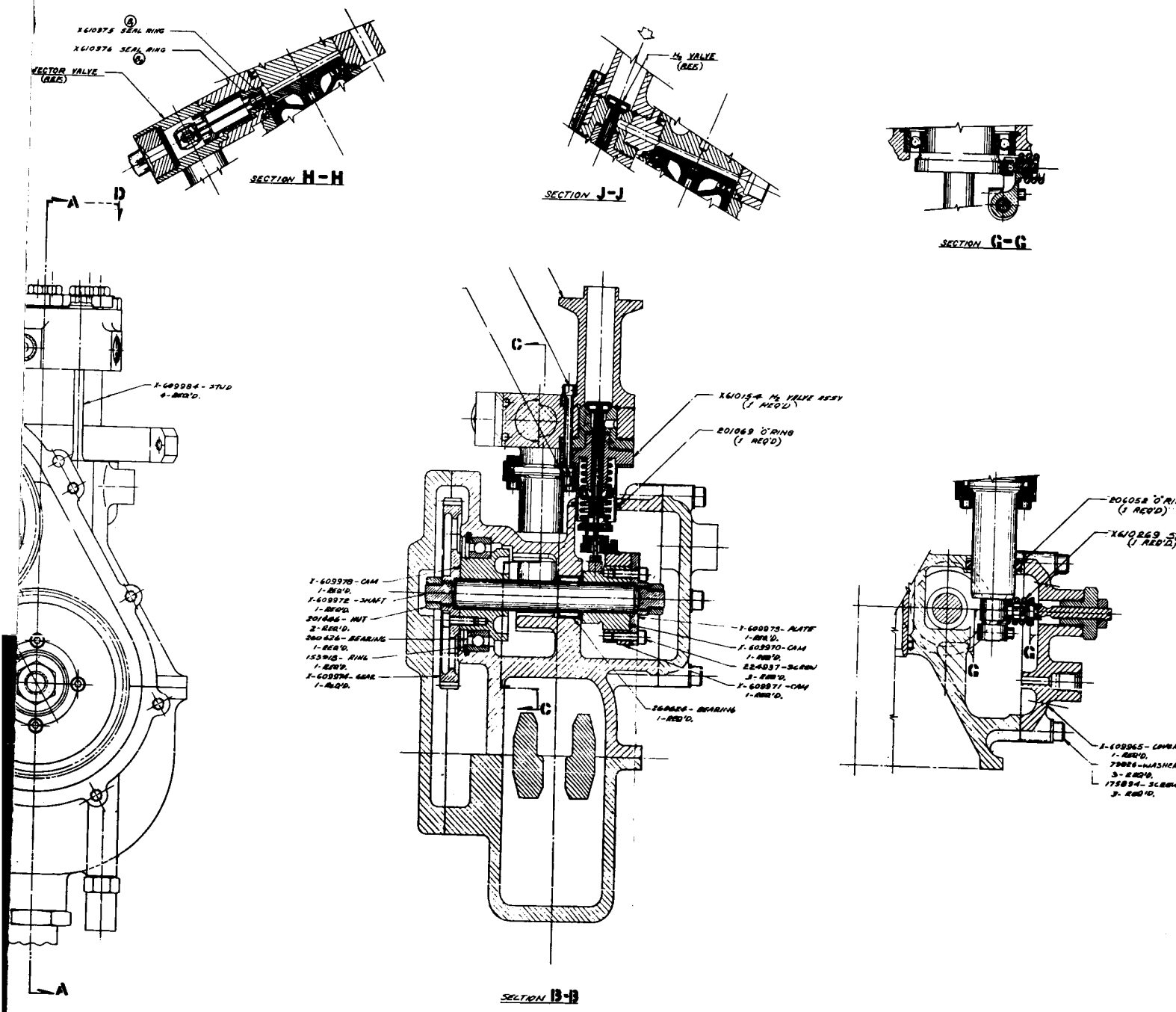

H_2-O_2 Experimental Test Engine

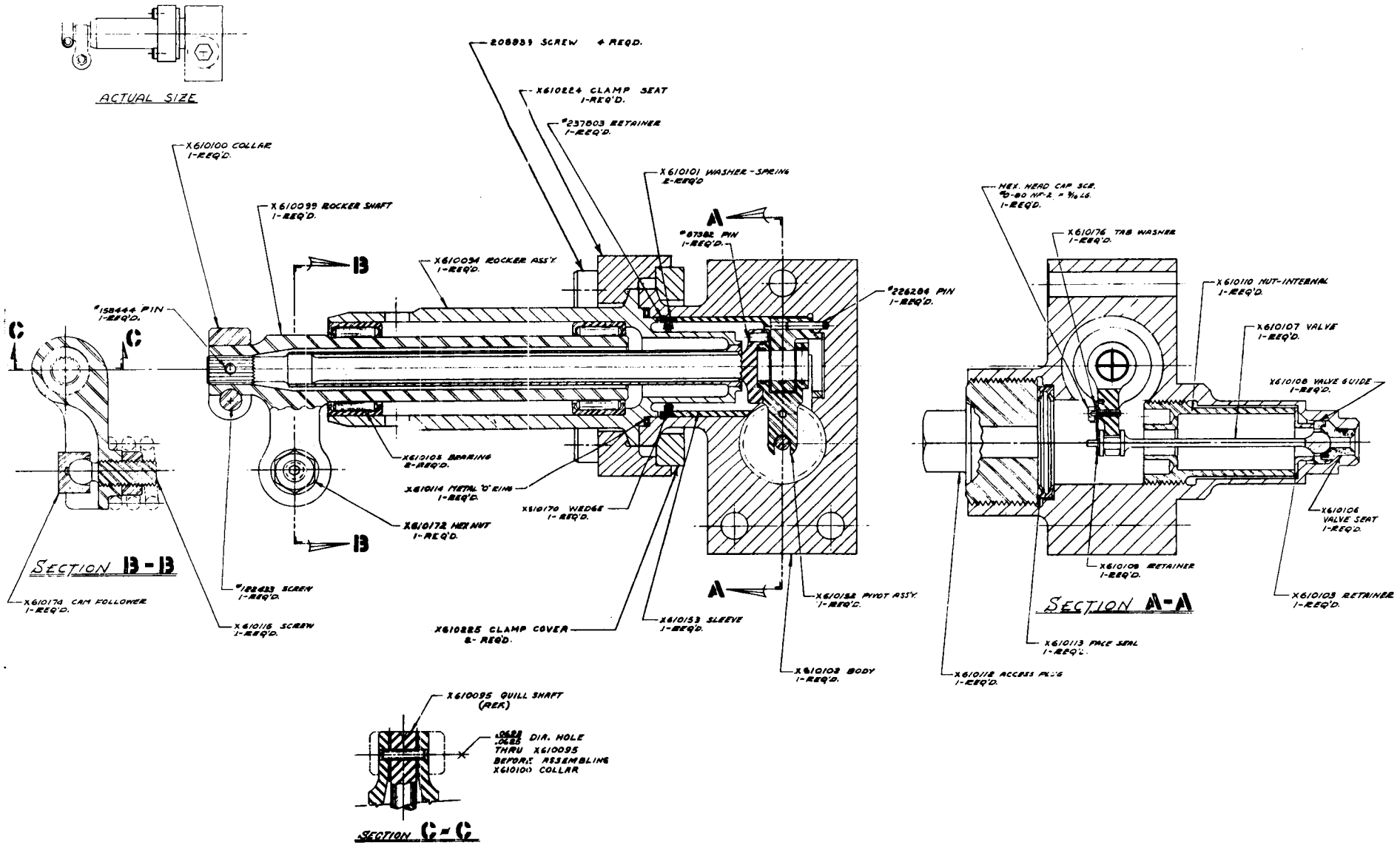

Fig. 7-4 - Assembly Drawing - Oxygen Injector Valve

PRECEDING PAGE BLANK

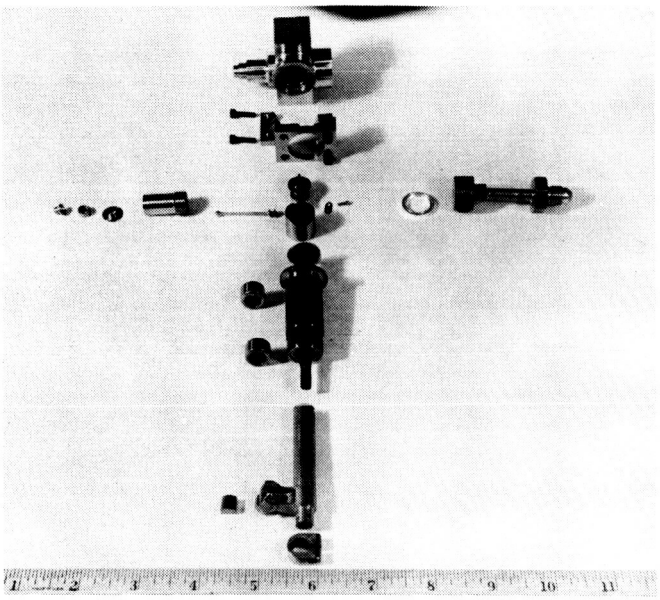

Fig. 7-5 - Oxygen Injector Assembly

seal tube has been lengthened to permit operation at lower stress levels, and the small flex pivot joint located within the sealed chamber is supported more rigidly.

Hydrogen Valves

The concentric dual poppet valve is discussed in Section 2.2. This concept has been used in Vickers experimental engines since 1958.

In this test engine the inner (large diameter stem) valve opens first and the outer (small diameter stem) valve opens second. A reverse of this procedure would possibly affect volumetric efficiency, but nothing else. The valves open outward against the gas flow, since combustion pressures high enough to blow the valves open were considered to be unlikely, and a spring strong enough to seal against supply pressures would be excessively stiff.

The hydrogen valve train on the NASA engine is much easier to assemble than on the previous ASD design. The total number of parts has been reduced, and the valves, valve guides, springs, spring keepers, and rocker arm followers may be assembled on the bench before installing the assembly in the engine. The arrangement of the hydrogen inlet adapter has been modified to reduce the possibility of leakage from the supply line. Valve timing changes are accomplished by manual adjustment during shut down in the test program.

Cylinder Head

The cylinder head is a two-piece, piston-like member, retained in the top of the cylinder bore by cap screws. It is sealed against gas leakage by static "K" type seals. Metal "O" rings were considered but it was felt that problems would occur because of differential thermal expansion between the two surfaces contacting the seal. The cylinder head has been designed to minimize the available path area for heat transfer. Lower rates of heat transfer from the combustion chamber result in higher cycle efficiencies by reducing overall engine heat rejection. See View A-A of Fig. 7-3 for a sectional view of the piston and cylinder head configuration.

Piston

A two piece insulated piston is used. The piston dome is fastened in the center by a single cap screw through a mounting flange, and is sealed around the edge by a "K" seal. The piston dome is of René 41 and the body of the piston is tool steel.

Crankshaft and Connecting Rod

The crank and connecting rod assembly are unchanged from the ASD design, i.e., an assembly from a motorcycle engine. The crankshaft is carried in ball bearings and has integral counterweights. The big end of the connecting rod uses a roller bearing. The stroke of the crankshaft is 1.53 inches, which, with a cylinder bore of 1.50 inches, gives a displacement for the test engine of 2.72 cubic inches.

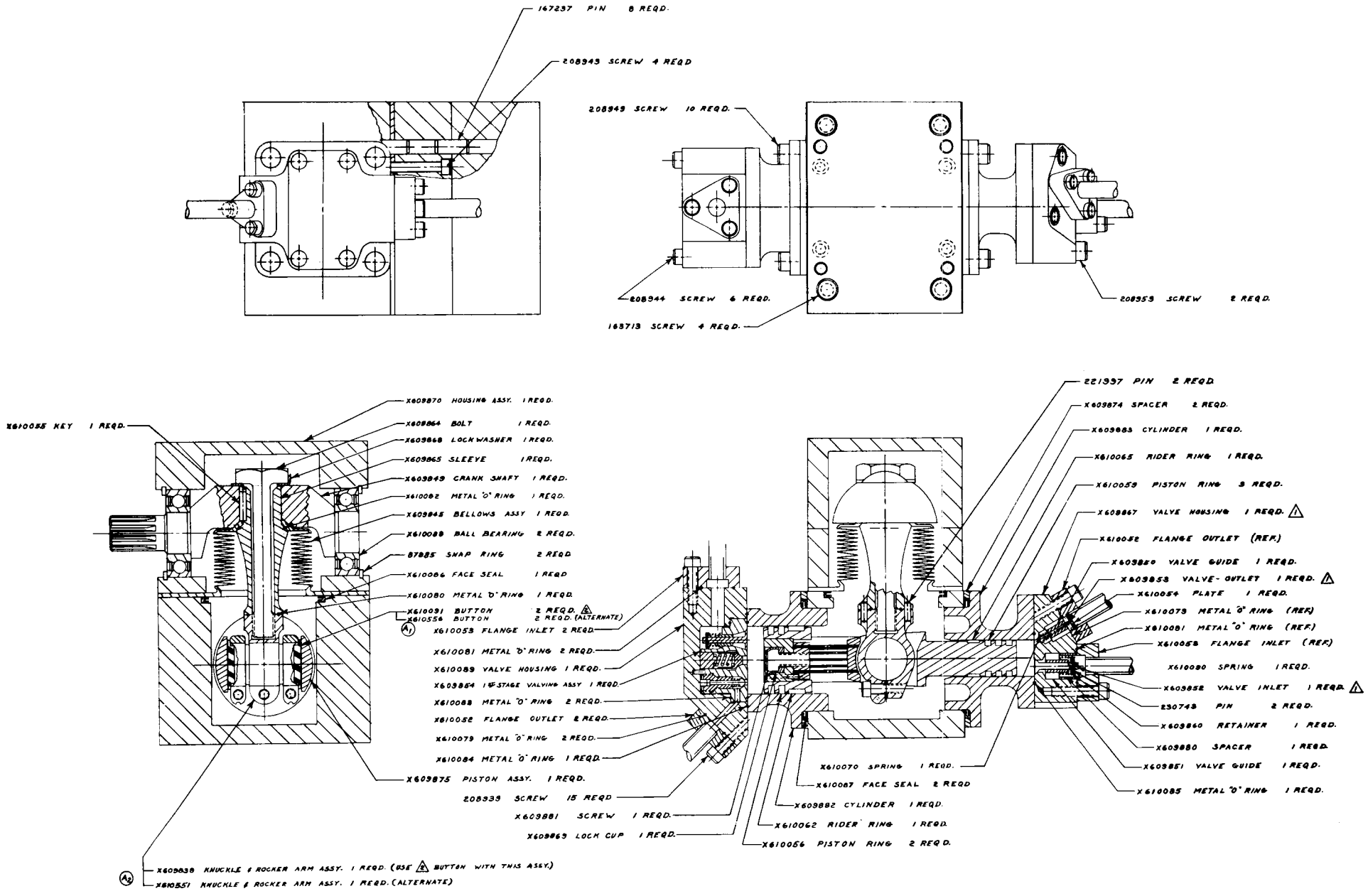

Fig. 7-6 - Assembly Drawing - Hydrogen Compressor

Crankcase and Cylinder

Nitralloy cylinder barrels are used. The cylinder barrel assembly is bolted to the crankcase to facilitate the changing of cylinders during the test program.

The cylinder barrel has an integral exhaust manifold with a ring of exhaust ports opened by the piston rings, near the bottom of the stroke. An integral cooling jacket surrounds the upper cylinder between the uncooled head area and the exhaust ports. This jacket takes the form of a helical passage, making several passes around the cylinder. The lower portion of the cylinder has been left uncooled, to reduce heat rejection. Lower cylinder cooling can be obtained if necessary by another jacket between the cylinder and the crankcase.

7.2 Two-Stage Hydrogen Compressor

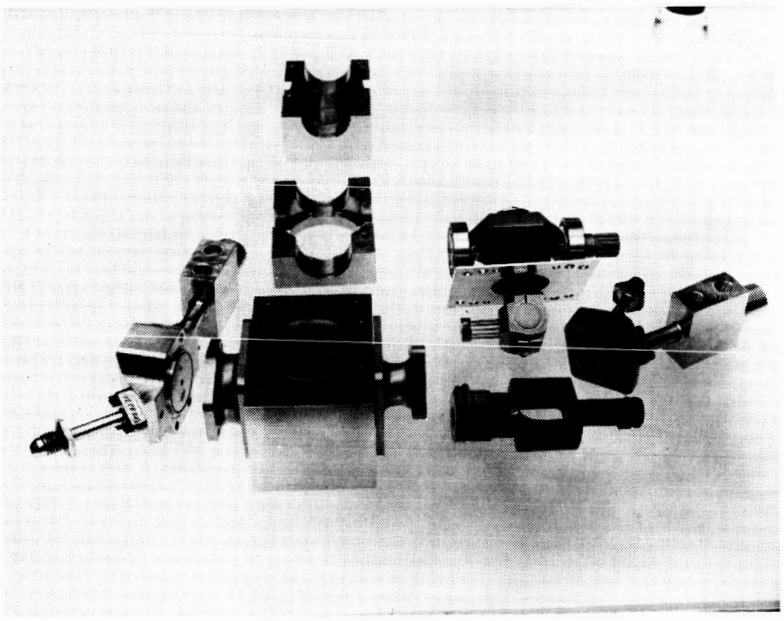

Fig. 7-7 - Compressor Components

A design drawing of the two-stage hydrogen compressor built for the test program is illustrated in Fig. 7-6 and a photograph of compressor parts is shown in Fig. 7-7. The compressor incorporates a one piece, double-ended piston and a rocking drive mechanism. Internal bearings are eliminated through the use of a Bendix flexural pivot joint. The actuating mechanism is isolated from the compressor mechanism by a bellows seal.

An extremely long fatigue life for the flex pivot joint and the sealing bellows is essential for a successful compressor design. Stresses are moderate throughout the drive mechanism. The barrel cage, made of several flexible rods, which connects the piston to the flex pivot joint, is intended to impart negligible side loads to the piston. Piston dynamic loads at 4000 rpm are considerably lower than gas loads and are opposite in direction, so that the piston unloads at higher rpm (see Fig. 7-8).

The compressor was designed as a test component for easy assembly and dimensional stability. The piston can be assembled on the bench before final assembly and is centered externally by adjusting the rocking drive mechanism. Removeable heads are used to facilitate experimentation. Due to the uncertainty of existing information regarding piston ring and bore materials, it was thought desirable to allow for easy exchange of cylinders at low cost.

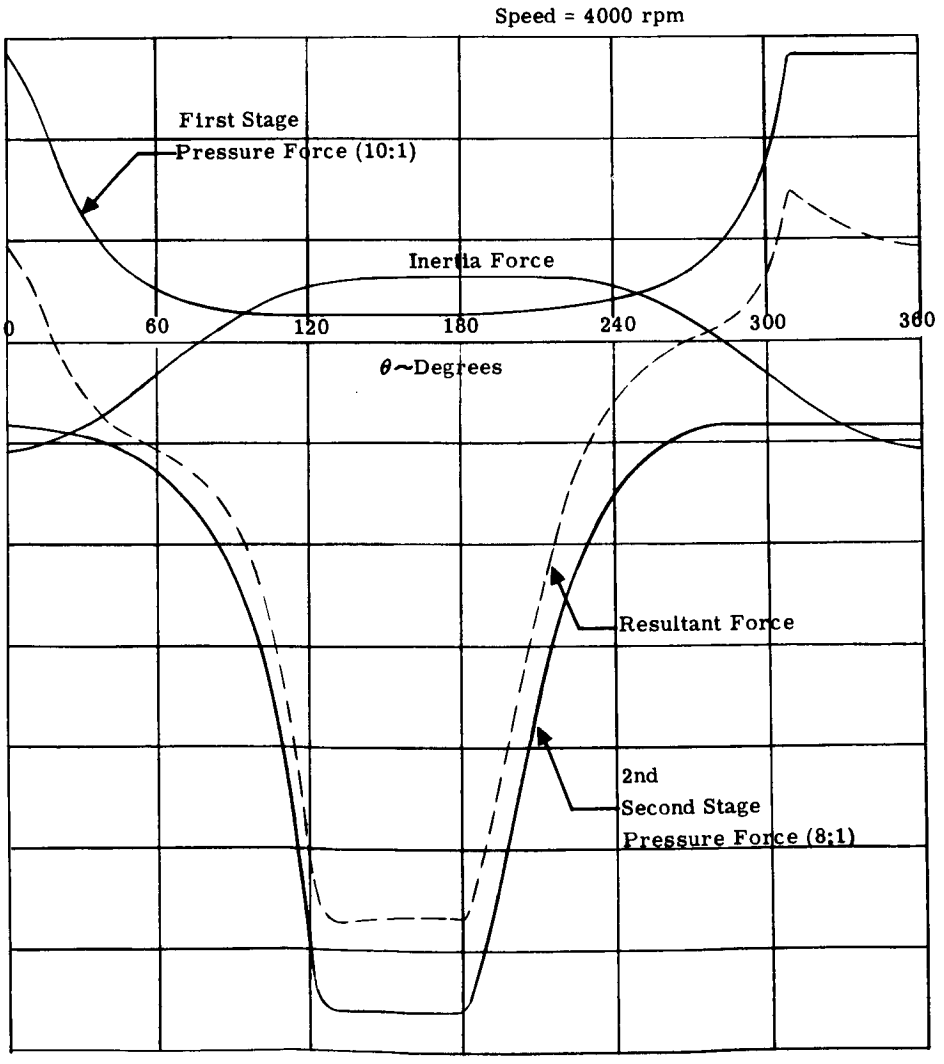

Fig. 7-8 - Hydrogen Compressor Gas and Inertia Forces

The drive arm oscillates over a 7 1/2° angle from centerline, which imparts a 1/2" stroke to the piston. The low pressure side has a bore diameter of 0.98 inches and a compression ratio of 10:1, and the high pressure side has a bore of 0.53 inches and a compression ratio of 8:1.

This work distribution gives greater gas forces on the high pressure piston, which was found desirable for optimum gas pressure loading of the flex pivot joint. Estimated piston force vs. time is given in Fig. 7-8.

The compressor was sized to handle incoming gas at the greatest volume and flow rate which would be encountered on the design mission, using the projected propellant consumption figures. With an inlet temperature range between 33° to 60°R the second stage outlet temperature is approximately 410°R (-50°F), assuming 75% efficiency with all waste heat absorbed by the hydrogen gas. Power consumption under these conditions is 0.8 horsepower at maximum load. The low operating temperature eliminates the need for a cooling system on the hydrogen compressor.

The results of parametric studies indicate the desirability of a system capable of using hydrogen at 300 psi supercritical storage pressure, therefore, a single stage compressor is now planned for the flight design system, based on the first stage of the two-stage test compressor. The two-stage configuration will be used, however, on the oxygen compressor.

7.3 Regenerator

The experimental regenerator is a cross-counterflow heat

exchanger, in which hydrogen at cryogenic temperature and high pressure is heated by the high temperature, low pressure, engine exhaust gas. A schematic of the regenerator is shown in Fig. 7-9 and an assembly drawing is shown in Fig. 7-10. This regenerator uses commercial tubing with all prime surfaces, and is designed to operate at sea level back pressure.

Designing for sea level operation avoided the requirement of a vacuum exhaust system in the test facility.

This regenerator features an all prime surface design for low cost and ease of manufacturing. The analysis upon which the prime surface design is based is in Appendix G. The prime surface regenerator consists of two concentric, cylindrical, stainless steel shells. The annular space between the shells contains five (5) concentric coils of 1/4 in. O.D., 0.016 in. wall, stainless steel hydrogen tubes. Integral with the regeneration are an exhaust gas inlet duct with connection flange, an exhaust gas outlet duct, two identical hydrogen tube manifolds, and twenty-one (21) thermocouples.

Each of the hydrogen coils has 40 turns. The concentric location of the coils is maintained by 1/16 in. diameter rods spaced 120° apart. The pitch of the coils, and the pitch relationship between the coils, is maintained by copper strips inserted into the space between the coils at an angle with the axis. The copper strips each have four holes through which the concentricity spacer rods are passed. All connections of the hydrogen tubes are heliarc welded. The outside shell has a window at the cold end for observation of ice formation. Instrumentation and test setup for the regenerator are described in Section 10.2.

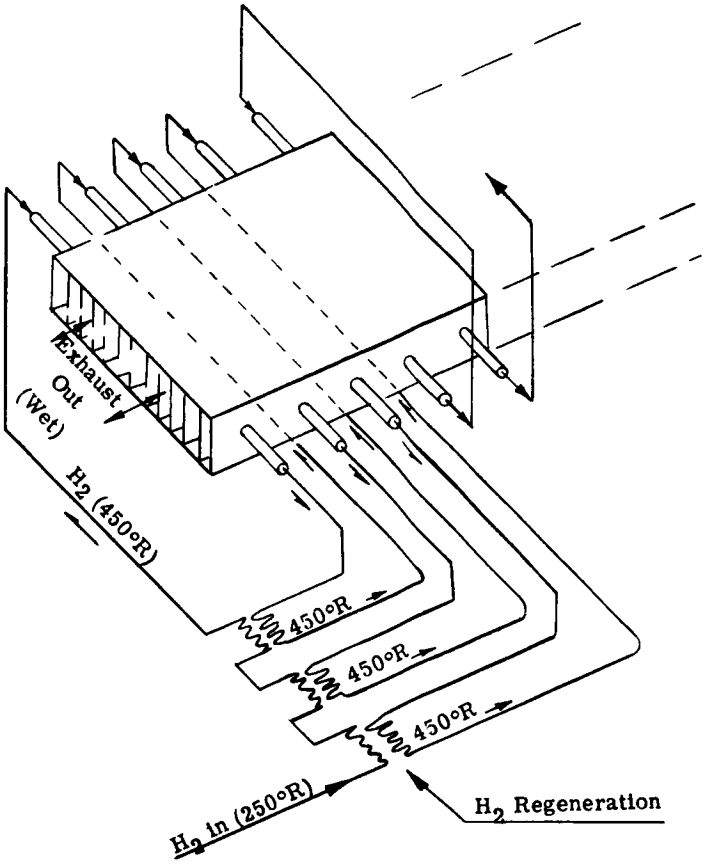

Fig. 7-9 - Schematic - H_2-O_2 Engine Regenerator

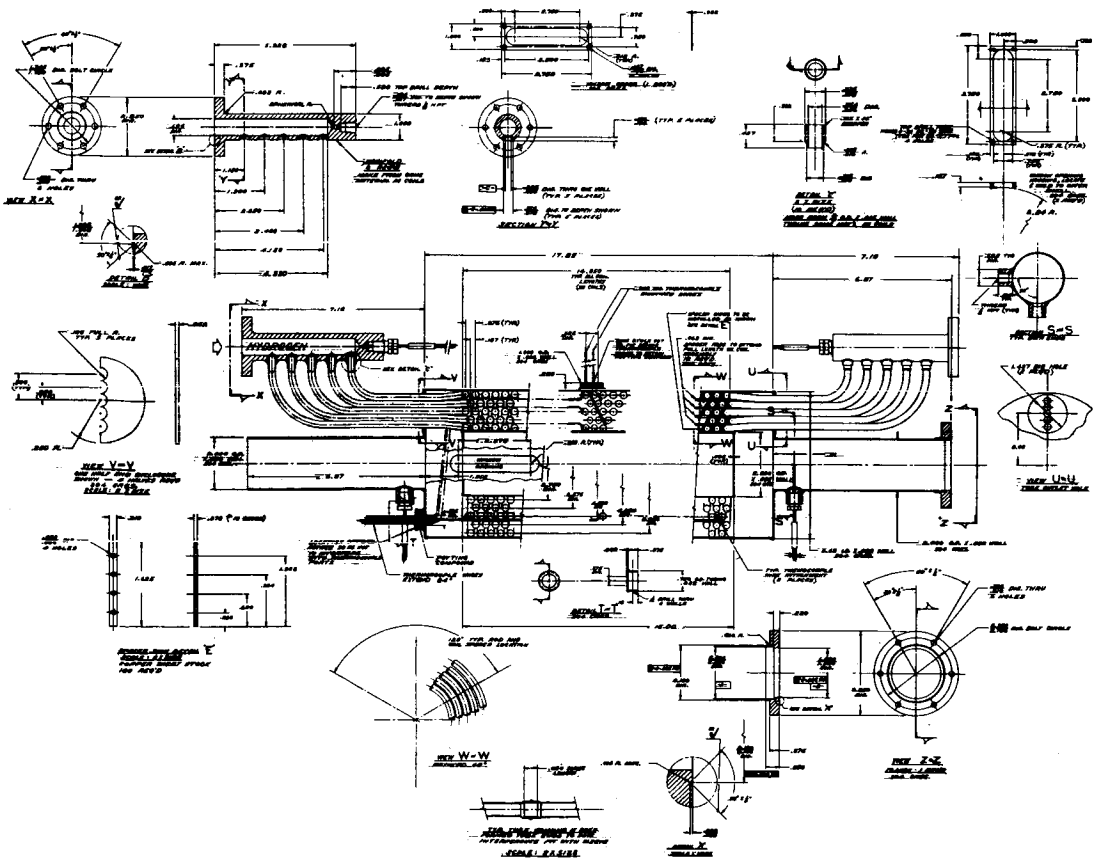

Fig. 7-10 - Assembly Drawing - H_2-O_2 Engine Regenerator

7.4 Materials

Materials selected for major parts of the test components are listed below:

Engine

Component	Material
Crankcase	Cast Iron
Welded Cylinder Assembly	Nitralloy 135 modified
Piston Head	Rene' 41
Piston Body	H-11 Tool Steel
Piston Pin	M-50 Tool Steel
Piston Rings	Chrome-plated Cast Iron
Hydrogen Inlet Manifold	347 Stainless
Hydrogen Valve Housing	H-11 Tool Steel
Hydrogen Valves	H-11 Tool Steel
Hydrogen Valve Guide	H-11 Tool Steel
Hydrogen Valve Rocker Arms	4620 Steel (case hardened)
Cylinder Head	Rene' 41
Cylinder Bolts	Inconel X
Cylinder Head Studs	Rene' 41
Gaskets	Haskell "K" Seals or Metal O-rings
Crankshaft and Connecting Rod Assembly	From Honda Motorcycle

Oxygen Injector

Component	Material
Body	Inconel 702
Rocker Assembly	Rene' 41
Flange	Rene' 41
Torque Tube	Rene' 41
Quill Shaft	Rene' 41
Rocker Shaft	4620 Steel (case hardened)
Cam Follower	52100 Bearing Steel
Sleeve	Rene' 41
Flexural Pivot	Inconel X and 420 Stainless
Valve Poppet	Haynes Stellite #25
Valve Seat	Haynes LT-1
	Haynes Stellite #25
	Haynes Stellite 6B
Valve Guide	Haynes LT-1
	Haynes Stellite #25
	Haynes Stellite 6B
Access Plug	Inconel 702
Clamp Seat	Inconel X
Clamp Cover	Inconel X

Hydrogen Compressor

Housing	304 Stainless
1st Stage Cylinder	347 Stainless - Nitrided bore
2nd Stage Cylinder	347 Stainless - Nitrided bore
Valve Housing - 1st Stage	304 Stainless
Valve Housing - 2nd Stage	AMS 5643
Springs	302 Stainless

Component	Material
Outlet Flange	304 Stainless
Inlet Flange	304 Stainless
Piston	18% N_i 300 Maraging Steel
Crankshaft	18% N_i 300 Maraging Steel
Bellows	Inconel X
Rocker Arm	300 Maraging Steel
Flexural Pivot	Inconel X
Valve Guides	Teflon Filled Bronze
Regenerator	
Shell	304 Stainless
Tubes	304 Stainless
Spacing Rods	347 Stainless Welding Rod
Spacers	Copper
Flanges	304 Stainless
Thermocouple Wires	Iron - Constantan
Insulation	Kaylon Wool

8.0 ENGINE TEST PROGRAM

8.1 Introduction

During the test program a total of 15.7 hours running time (hot) was accumulated on the test engine. The amount of running was limited primarily by the repeated teardown necessary because of deficient oxygen injector performance. Minor design and manufacturing defects which had to be corrected during assembly, and some minor engine part failures, also contributed to program delays.

Testing during this program was conducted at non-regenerated conditions (i.e. inlet gas at room temperature), with 12% clearance volume and 15 psia exhaust pressure. At these conditions, the best BSPC was an average of 2.4 lbs.per hp-hr. When this performance is corrected to design conditions of hydrogen inlet temperature (1000°F), 5% clearance volume, and 1 psia exhaust pressure, a BSPC between 1.6 and 1.7 lbs/hp-hr can be expected at an engine shaft output of 3.0 hp.

This performance compares with a calculated value of 1.05 lbs/hp-hr. The difference between the calculated and experimantally obtained performance is due to excessive heat rejection, stratification of the gases, and some presently unidentified losses. Further development work is expected to bring experimental results closer to expected values.

The conclusions drawn from the program are:

1. Design modification of the static sealing method in the area of the cylinder, head, and hydrogen valve should

be considered. This is of particular concern for development purposes where parts are repeatedly disassembled and assembled.

2. Operation at design conditions should result in greatly improved performance, but additional improvement will be required to meet design objectives. This will require considerable trial and error experimentation.

3. Peak combustion pressure was limited to values considerably below expected levels. Control over O/F ratio was also limited. Design changes are necessary to correct this condition and should result in a direct improvement in performance and the controllability of O/F ratio.

4. The mixing of combustion products and unburned hydrogen in the cylinder appears to be incomplete. Evidence of this was seen in the uneven temperature distribution in the cylinder head area by direct visual observation of the combustion process through a quartz cylinder head, by study of high speed movies of the same, and by inspection of P-V diagrams. Improved early mixing should not only increase reliability by reducing thermal stress in the cylinder head region, but should also result in a marked increase in performance, as is indicated by the empirical relationship between O/F ratio and combustion temperature. The improvement of mixing will require development effort. One approach to be taken is to induce swirl in the incoming hydrogen and to inject oxygen radially inward, toward the center of the cylinder.

5. If regeneration is to be effective, the cylinder exhaust ports must be redesigned to reduce heat loss of the

exhaust gas to the cooler portions of the cylinder.

6. As performance is improved by reducing losses, more precise instrumentation will be required to evaluate design changes.

7. Additional development is required to effectively reduce heat rejection during the expansion and exhaust blowdown phase of the cycle.

8.2 TEST SET-UP AND INSTRUMENTATION

The H_2-O_2 engine test circuit is described below and shown in Fig. 8-1. The engine power output is absorbed by a hydraulic dynomometer, which also starts the engine. A hydraulic power supply is used to supply pressure to the engine load pump during motoring and starting operations. After the engine starts, supercharge pressure (to prevent cavitation), is supplied by the hydraulic power supply, and the pump outlet pressure is regulated to control engine loading. The load pump is mounted on trunnion bearings and rotation of the pump housing is restrained by a torque arm connected to an electrical load cell which measures direct reaction torque developed by the engine. Engine lubricant is supplied from a reservoir by an electric motor driven pump. Lubrication flow and pressure are measured.

Water cooling is used on the engine cylinder and flow is measured with a glass tube flow meter. Water cooling is also used on the engine cylinder pressure transducer.

The gas pressure control system is operated from the test control panel and can control the supply of oxygen, hydrogen, and nitrogen, (for purging) at the desired pressures. Details

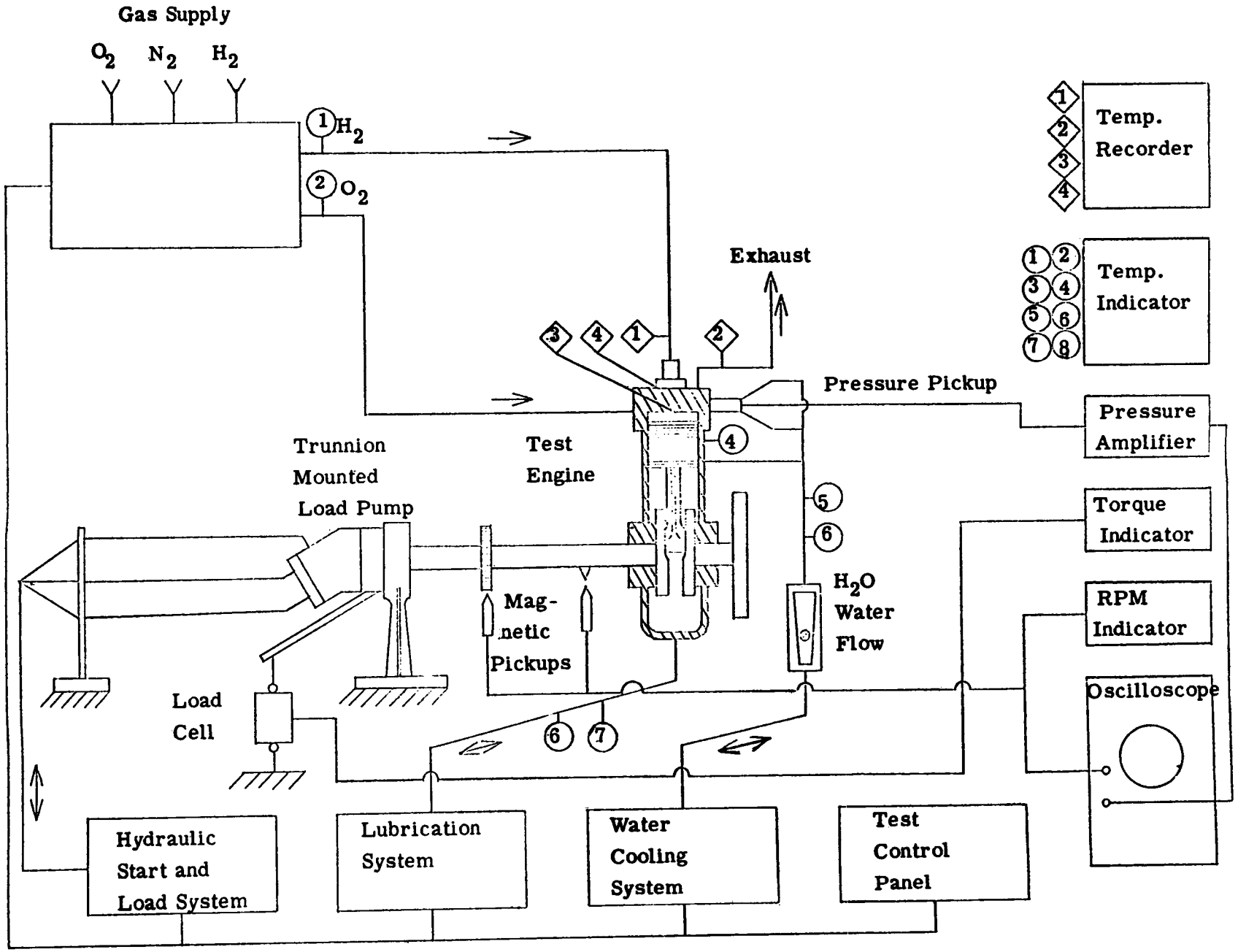

Fig. 8-1 - H_2-O_2 Engine Test Circuit

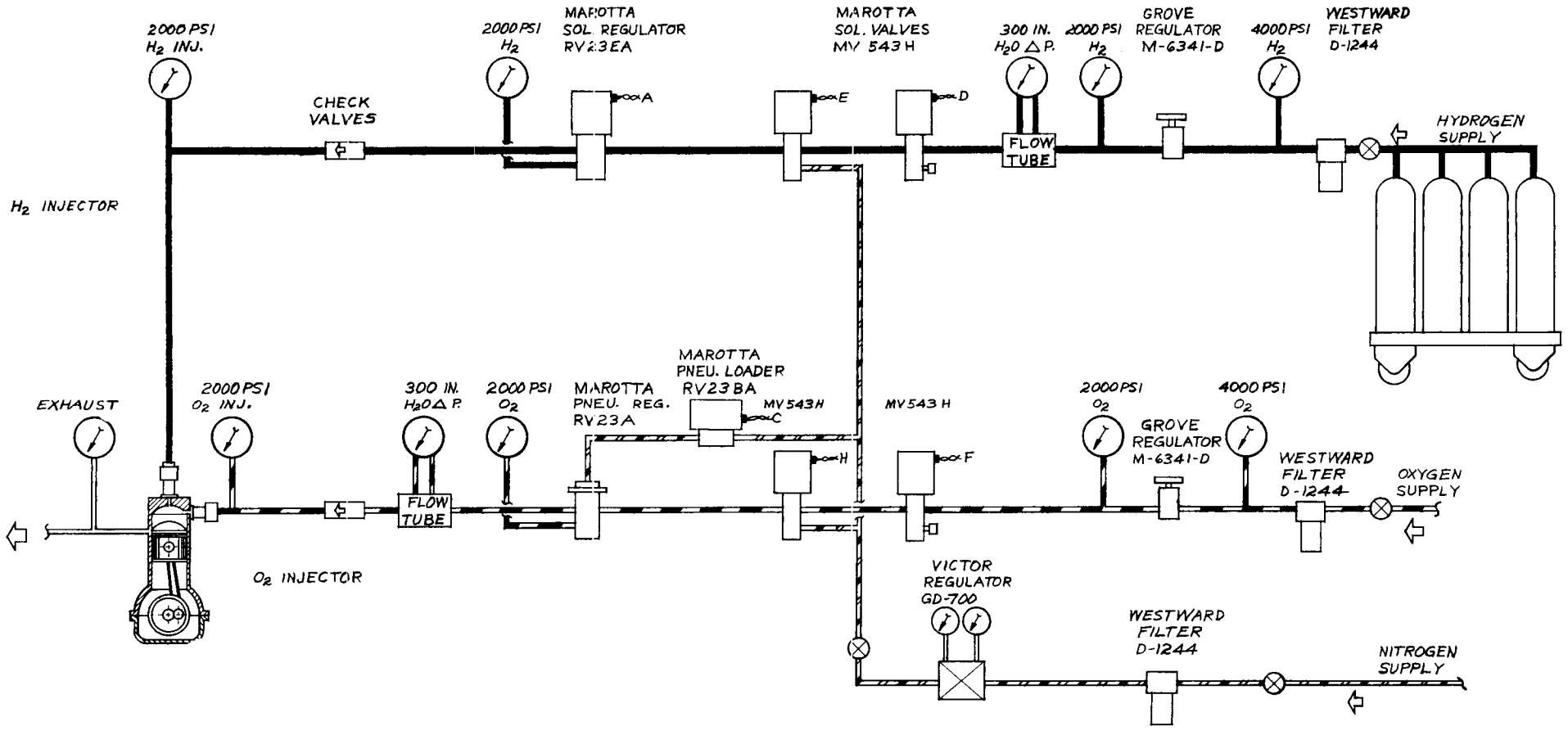

Fig. 8-2 - H_2-O_2 Engine Gas Control System

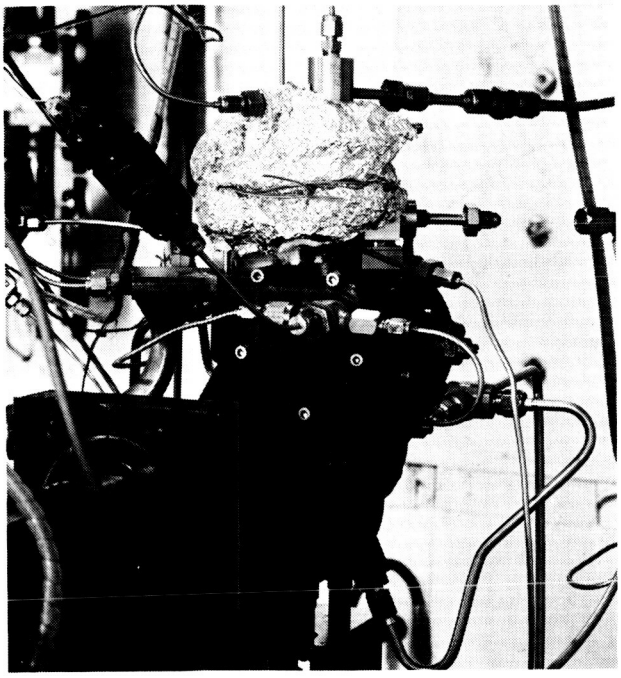

Fig. 8-3 - H_2-O_2 Engine on Test Stand (Insulated Head)

of the gas control system are shown in Fig. 8-2.

Fig. 8-3 is a photograph of the engine on the test stand (the engine cylinder head is externally insulated in this view). Fig. 8-4 is a photograph of engine control panel and instrumentation readout equipment. Some of the readout instrumentation is shared with the regenerator and oxygen injector test stand setups.

A strip chart temperature recorder and a multipoint temperature indicator are used to monitor the various temperatures throughout the test system. A Vickers direct reading torque indicator is used to monitor engine output torque. Engine rpm is read on an electronic counter from a signal developed by a magnetic pickup and a 60 tooth gear connected to the engine crankshaft. A water-cooled quartz crystal

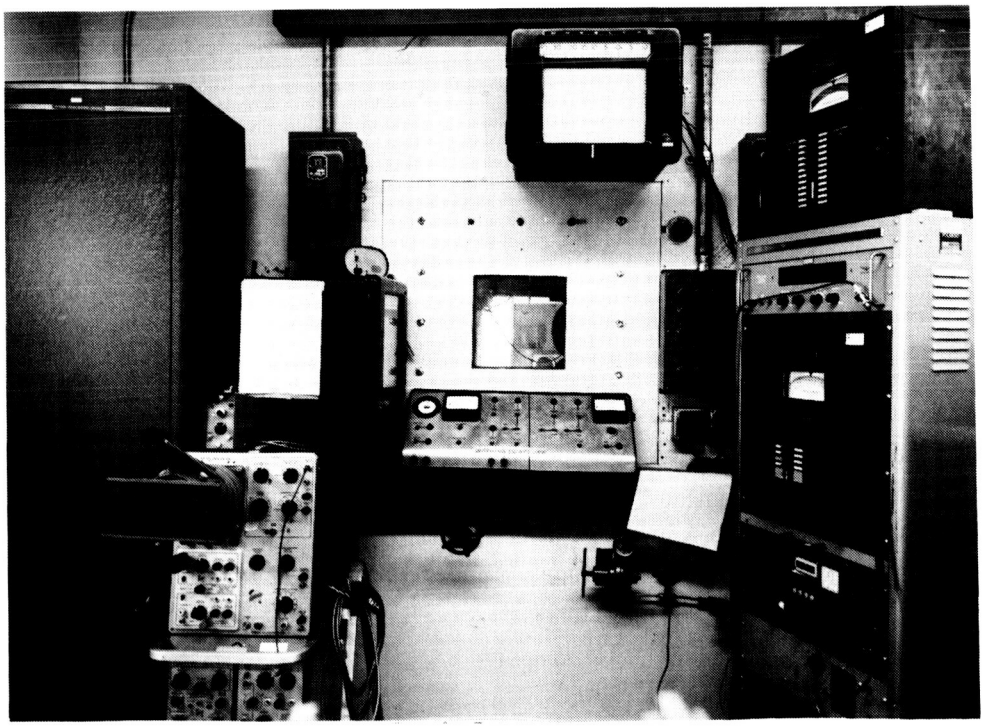

Fig. 8-4 - Engine Test Control Panel

pressure transducer is used to measure engine cylinder pressures. The transducer output is fed to a charge amplifier, which converts the signal to a dc voltage proportional to pressure. The dc signal is fed to one input of a dual trace Tektronix oscilloscope, which is calibrated directly in psi. A magnetic pickup is used to generate a single pulse when the piston is at bottom dead center, and this signal is fed to the other input of the scope to display a timing pulse for pressure versus time pictures, and also to synchronize the scope to engine speed. A Polaroid camera is used to photograph the pressure/time signals on the oscilloscope.

A table of the engine instrumentation specifications is given below:

TABLE 8-1

ENGINE TEST INSTRUMENTATION SPECIFICATIONS

Ident.	Function	Range	Accuracy	Mfr.	No.
A	Temp.	0-1600°F	±1/2%	Wheelco	3012-2500
	1. Hydrogen inlet manifold 2. Engine exhaust temp.		3. Cylinder head temp. 4. Cylinder head surface temp.		
B	Temp.	-75 to 575°F	±1°F	Honeywell	153301
	1. Hydrogen flow tube 2. Oxygen flow tube 3. Inlet water temp. 4. Cylinder wall temp.		5. Outlet water temp. 6. Inlet oil temp. 7. Outlet oil temp.		
C	Torque	0 to 99.9 in-lb	±1/4%	Vickers	54616-X

Ident.	Function	Range	Accuracy	Mfr.	No.
D	RPM	0 to 99,999 rpm	±1 rpm	Erie	720
E	Pressure	0 to 1000 psi	±1%	Kistler	568
F	Pressure Diagram	0 to 1000 psi		Tektronix	533-CA

Though the present test equipment and instrumentation has been satisfactory for the preliminary test program, more refined equipment and instrumentation will be required to evaluate the effects of development changes upon performance. Test fixtures and equipment have been fabricated and procured for a balanced pressure type transducer for cylinder pressure measurement to replace the present dynamic system. A recirculating high temperature cylinder cooling system, to replace the present straight through water system, will be required. A modified cylinder design with provisions for an accurate survey of cylinder wall temperature should be used.

8.3 Discussion of Tests and Results

The intent at the start of the test program was to obtain a map of engine performance data by varying O/F ratio and valve timing adjustments at engine speeds of 3000, 3500, and 4000 rpm and at power levels of: as low as possible, 25%, 50%, 75%, 100%, and 150% of rated shaft power. Rated shaft power is taken to be 2.92 horsepower.

This initial objective was not fully achieved because of difficulties that were encountered in (1) finding a good correlation between O/F ratio and a temperature that could

be monitored continuously, (2) an arbitrary limitation placed upon cylinder head temperature, and (3) obtaining a consistent relationship between oxygen supply pressure and oxygen flow rate. These difficulties were a result of the oxygen supply pressure levels necessary to avoid overheating and the corollary adverse effect of the low pressure drop between the oxygen injector orifice and the combustion chamber. The arbitrary limitation was placed on cylinder head temperature to avoid the possibility of developing trouble at high temperatures in order to obtain a significant amount of data without failure. The head temperature limit was gradually increased from 1000°F to 1400°F during the program.

In practice, the engine was run at a constant speed with hydrogen and oxygen valve timing set manually before the run. The desired torque setting was achieved by varying gas inlet pressure. Mixture ratio was determined by the maximum allowable cylinder head temperature. This method resulted in the highest O/F mixture ratio at lower torque levels, since less power was being generated and a higher percentage of heat was transferred to the cylinder head for the same head temperature.

8.3.1 Compilation of Test Results

Representative test results obtained during the H_2-O_2 internal combustion engine test program are shown in Table 8-2 and in Figs. 8-7 through 8-16. The significance of some of the parameters presented in Table 8-2 is given below.

The most significant index of engine performance is specific propellant consumption (SPC). This parameter is

TABLE 8-2

SELECTED PERFORMANCE DATA

Run	Date	Time	Timing	RPM	psi H_2 Press	psi O_2 Press	°F H_2 Temp	psi BMEP	$\frac{BMEP}{P_H}$	HP	O/F	$\frac{lb_m}{hp\text{-}hr}$ BSPC	$\frac{ft\text{-}lb_f}{hp\text{-}hr}$ BSPC RT	% Heat Rej.	°F Ex Temp	°F Head Temp
1	4-5-63	A	1	3036	230	250	65	21.5	.094	.45	1.06	5.06	5.37	254	325	1065
2	4-5-63	B	1	3024	270	290	65	35.4	.132	.74	.87	3.81	3.81	158	325	1030
3	4-5-63	C	1	3006	390	410	65	70.5	.181	1.45	.57	2.90	2.54	73	310	945
4	4-5-63	D	1	3026	530	550	65	106.2	.201	2.21	.53	2.66	2.25	48	300	830
5	4-5-63	E	1	3022	690	710	65	141.0	.202	2.93	.40	2.73	2.12	31	250	745
6	4-5-63	F	1	4066	600	620	65	106.2	.177	2.97	.72	2.48	2.31	67	435	1055
7	4-8-63	10:49	1	3512	475	495	65	91.0	.192	2.16	.50	2.91	2.44	50	310	880
8	4-8-63	10:57	1	3521	590	615	65	121.6	.206	2.95	.60	2.38	2.10	40	325	855
9	4-8-63	11:05	1	3526	840	865	65	179.8	.214	4.36	.52	2.50	2.11	31	340	885
10	4-8-63	11:10	1	3008	820	960	65	207.2	.253	4.48	.68	2.28	2.10	45	425	1050
11	4-8-63	11:20	1	4005	840	860	65	160.0	.191	4.44	.61	2.40	2.14	47	425	1035
12	4-24-63	8468	1	3060	580	660	200	101.8	.175	2.14	1.48	2.51	2.54	118	530	1330
13	4-24-63	8474	1	3034	585	800	230	140.0	.240	2.91	1.57	2.39	2.36	100	550	1305
14	4-24-63	8480	1	3058	585	800	230	124.0	.212	2.60	1.66	2.42	2.36	131	600	1430
15	4-24-63	8494	1	4020	670	810	300	106.5	.159	2.94	1.28	2.30	2.37	122	610	1390
16	4-30-63	8532	1	3087	610	805	300	140.0	.230	2.96	1.49	2.34	2.43	115	600	1400
17	4-30-63	8550	1	3045	610	840	300	142.0	.232	2.97	1.54	2.40	2.34	115	600	1400
18	5-1-63	8570	1	3041	605	820	295	141.0	.233	2.94	1.48	2.38	2.48	114	590	1390
19	5-7-63	1:45	2	3006	380	900	250	142.8	.375	2.94	1.04	2.51	2.81	55	475	1000
20	5-7-63	1:55	2	4007	400	900	320	106.1	.265	2.93	1.04	2.35	2.70	88	555	1355
21	5-14-63	2:07	3	4015	600	840	70	110.3	.184	3.04	1.11	2.96	3.17	106	610	1390
22	5-14-63	2:15	3	4003	670	950	70	153.0	.218	4.20	.97	2.51	2.59	62	545	1200
23	5-14-63	2:25	3	3060	450	925	70	141.3	.314	2.97	1.09	2.90	3.07	67	530	1180
24	5-20-63	1:45	4	4000	300	310	70	28.2	.094	.78	.85	4.68	4.64	155	360	1120
25	5-20-63	2:12	4	4067	300	325	70	30.5	.102	.85	1.16	4.07	4.40	214	480	1400
26	5-20-63	2:30	4	4072	400	410	70	36.3	.088	1.01	1.19	3.68	4.01	239	560	1500
27	5-29-63	2:10	5	4000	700	710	70	111.5	.159	3.06	.58	2.60			280	850
28	5-29-63	2:15	5	4000	600	640	70	84.8	.141	2.52	.35	2.73			195	670

These page(s) were missing from the report when received by NTIS. Repeated efforts to obtain a replacement page have been unsuccessful.

This report is being made available in its present form with the hope it will be of sufficient value to justify its announcement and distribution.

245-246

between individual data points.

The engine power level is a function of BMEP and rpm. BMEP is a function of inlet pressure as well as combustion energy, so it has been normalized into the dimensionless parameter $BMEP/P_H$ where P_H is hydrogen inlet pressure. This rating has the disadvantage of not taking friction MEP into account; but it is felt that the parameters BSPC·RT vs. $BMEP/P_H$ represent the most general information concerning engine performance and the investigation of these parameters as functions of engine operating variables, and affords a means of perceiving trends and relationships that would otherwise remain undetected. BSPC·RT should reach a minimum at the power level at which the engine is operating at maximum efficiency.

Data could be presented in terms of thermal efficiency, defined as the shaft output power divided by the rate of chemical energy release at the measured O_2/H_2 ratio, in terms of the higher heating value of hydrogen. This definition of efficiency cannot, however, be applied in the usual manner because it does not include the stored pressure energy available due to the pressure ratio which exists across the engine. Efficiency comparisons between two runs at different inlet pressures would need a correction to account for the difference in pressure work. For this reason the parameter BSPC·RT is used as the index of comparison.

The test data shown in this report represent a very low level of specific propellant consumption, especially when considering the low power level involved. All of the tests at design power levels resulted in SPC between 2.3 and 3.0 lbs/hp-hr.

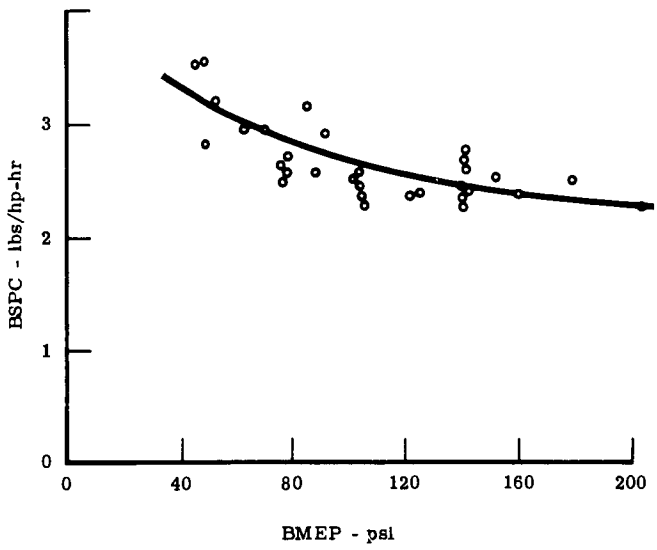

Fig. 8-6 - BSPC vs. BMEP

This exceeds the efficiency of turbines at this low power, according to the best data published.

In Fig. 8-6, all the data points at BSPC of less than 3.5 lbs/hp-hr are plotted as a function of BMEP. While a great many operating conditions are represented, a trend toward lower propellant consumption at higher BMEP is clearly evident.

In Figs. 8-7 through 8-11, the parameters BSPC·RT and BMEP/P_H are plotted for all runs in which data were taken. The band shows the range of performance of the H_2-O_2 engine as a function of these parameters.

Other parameters, shown in Table 8-2 and in the complete data compilation of Appendix H , include the hydrogen and oxygen inlet pressure, hydrogen inlet temperature, oxygen/hydrogen mixture ratio by weight, exhaust gas temperature, and maximum cylinder head temperature. This last item is measured by a thermocouple mounted in the top of the combustion chamber, which probably reaches the highest temperature of any metal section of the engine. Heat rejection, expressed as a percentage of shaft output power, is also given. This is heat rejected to the coolant water only and does not include heat lost through the cylinder head and the crankcase walls by radiation and convection.

8.3.2 Interpretation and Analysis of Test Results

An attempt was made to correlate BSPC·RT vs. BMEP/P_H with all other engine operating parameters. Valve timing was found to have the most significant effect; accordingly, test results for each valve setting on this basis are shown in Figs. 8-7 through 8-11.

Test results for timing condition No. 1 are shown in Fig. 8-7. A majority of the tests were run at this timing. It represents 2% hydrogen admission with a 7° overlap of the hydrogen and oxygen valves. A shaded band covers most of the data points. Two conclusions can be drawn from this curve:

1. Performance at 4000rpm is better than at 3500 or 3000rpm.
2. The reduction in BSPC·RT with increasing BMEP/P_H is dramatic but does not appear to reach a minimum within the range of BMEP/P_H investigated.

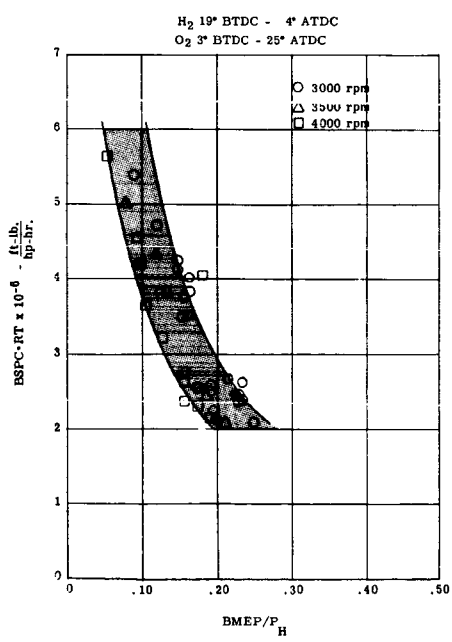

Fig. 8-7 - BSPC·RT vs. BMEP/P_H - #1

Test results for timing condition No. 2 are shown in Fig. 8-8. This engine timing represents a high value of hydrogen admission (10%) with 7° overlap.

For comparison purposes, the shaded band of Fig. 8-7 is reproduced in this and other figures through 8-11. Note that a higher level of BMEP/P_H is reached due to the higher admission level, and that performance is quite poor in most runs.

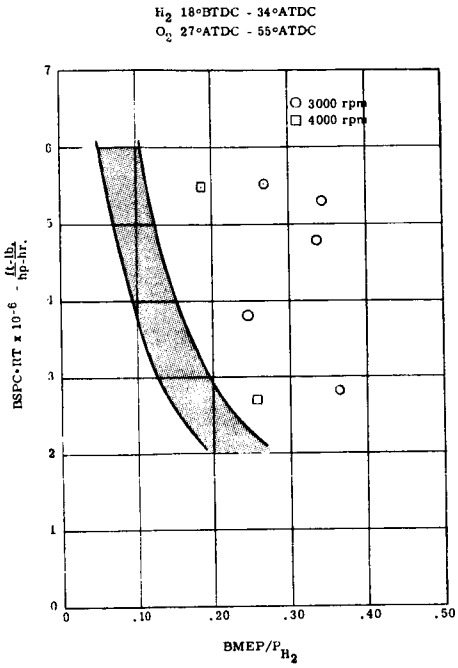

Fig. 8-8 - BSPC·RT vs. BMEP/P_H - #2

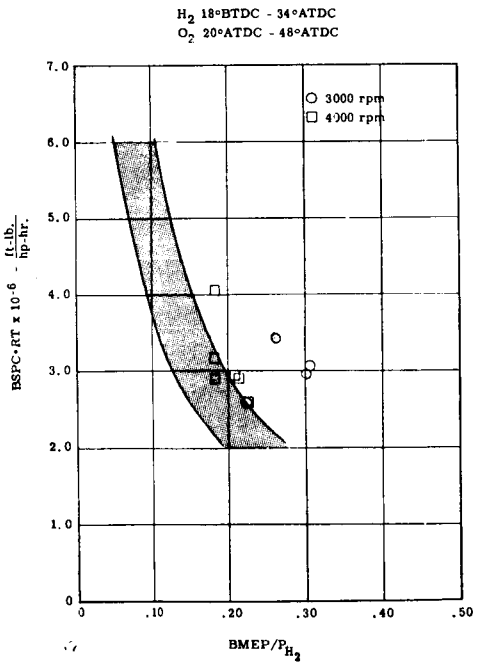

Fig. 8-9 - BSPC·RT vs. BMEP/P_H - #3

Again, BSPC·RT tends to be lower for the same BMEP/P_H at 4000 rpm than at 3000 rpm. The poor level of performance is caused mostly by the low BMEP (low absolute operating power level even though BMEP/P_H is higher). It was not possible to achieve high design mixture ratios at this timing, at high power levels, without the risk of excessive cylinder head temperature so the tests were run at low power.

BSPC·RT vs. BMEP/P_H is plotted for timing condition No. 3 in Fig. 8-9. This is the same as condition No. 2 except for the change of static valve overlap from 7° to 14°. The same trends are evident in both conditions: lower SPC @ 4000 rpm, steep slope. Performance is slightly better than for timing condition No. 2.

In Fig. 8-10 BSPC·RT vs. BMEP/P_H is plotted for timing condition No. 4. This is the same admission as No. 1 (2%) but has 10° static overlap instead of 7°.

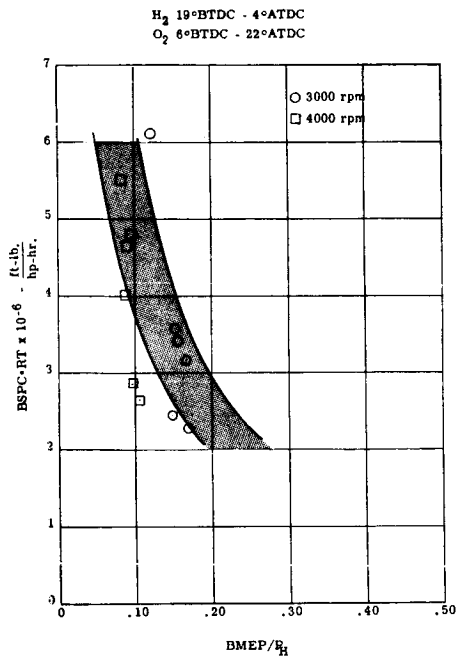

Fig. 8-10 - BSPC·RT vs. BMEP/P_H - #4

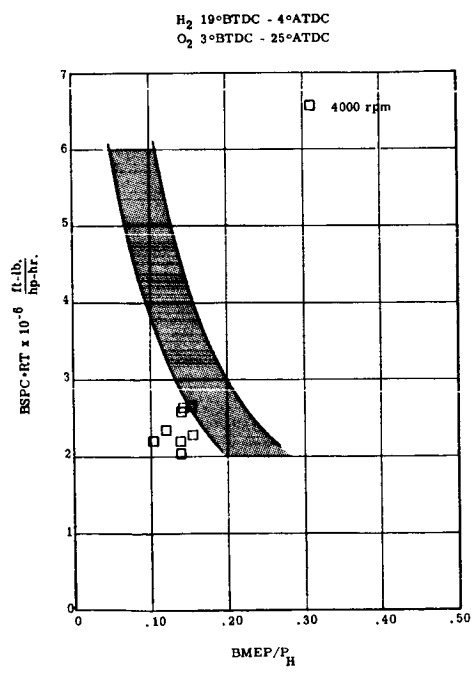

Fig. 8-11 - BSPC·RT vs. BMEP/P_H - #5

Actual performance is poor, but relative to BMEP/P_H, it falls within the band of Fig. 8-7, which verifies the expectation that BSPC·RT will be lowest at low admission ratios.

Timing condition No. 5 is shown in Fig. 8-11. This timing has the 2% hydrogen admission of condition No. 1 and No. 4 but with an overlap of 5°. Note that all points fall below the band. This is due partly to the fact that all runs were made at a high inlet pressure so that BMEP was still high enough to minimize friction effects even at low BMEP/P_H. However, the improved performance of timing condition No. 5 over timing conditions No. 1 and No. 4 is evident. The improvement is thought to be due to decreased overlap and less interference of oxygen and hydrogen flow. This improvement is not readily apparent when the data are plotted in terms of BSPC instead of BSPC·RT.

Pressure time traces were photographed on the oscilloscope at

every data point. Five typical traces, taken at various timing conditions, have been selected and are presented in Figs. 8-12 through 8-16.

Fig. 8-12 shows a pressure time trace of a run using No. 1 timing at a mixture ratio of 1.49 and SPC of 2.34. This is close to the best performance that has been achieved. There are two breaks in the rising cylinder pressure curve. The first is at hydrogen inlet, shown as point 1. Hydrogen pressure levels off and the injection of oxygen causes a further pressure rise due to combustion, causing the shoulder at point 2.

The pressure peaks at point 3 and the exhaust ports are uncovered by the top piston ring at point 4. Figs. 8-17 and 8-18 represent the same test run as Fig. 8-12 replotted on linear and log-log, pressure-volume coordinates respectively. An IMEP value of 168 psi was calculated from the measured area of the linear diagram (Fig. 8-17). As noted on the figure, a BMEP of 140 psi was measured on this run. The pressure-volume, log-log plot of an ideal adiabatic expansion or compression of the products of combustion of hydrogen and oxygen with an O/F ratio of 1.5, is a straight line with a slope of $\gamma = 1.31$. Disregarding instrumentation limitations (of the quartz crystal type pressure transducer), the curvature of the expansion and compression lines shown on the log-log diagram (Fig. 8-18), indicates the extent by which the actual processes deviate from the ideal adiabatic process. This deviation may be attributed to a combination of the following:

1. Slow mixing of steam with unburned hydrogen

2. Cyclic heat transfer

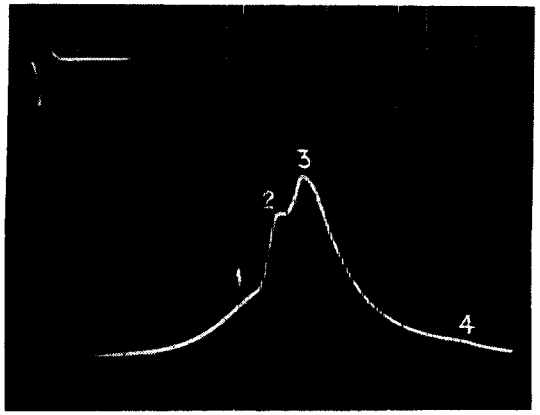

Fig. 8-12 BSPC = 2.34
O/F = 1.49
3000 rpm
BMEP = 140 psi
HP = 2.96
P_H = 610 psi P_M = 700 psi
Timing Condition #1

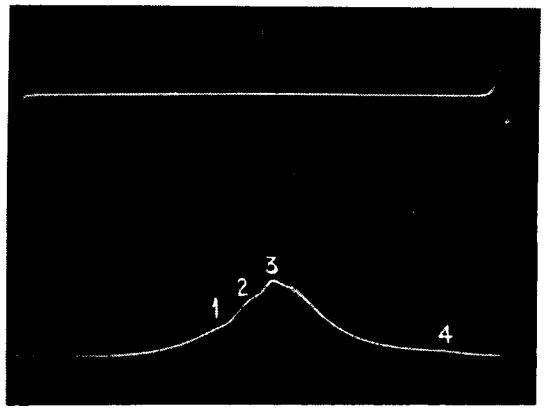

BSPC = 3.41 Fig. 8-13
O/F = 1.3
3000 rpm
BMEP = 60 psi
HP = 1.2
P_H = 365 psi P_M = 320 psi
Timing Condition #4

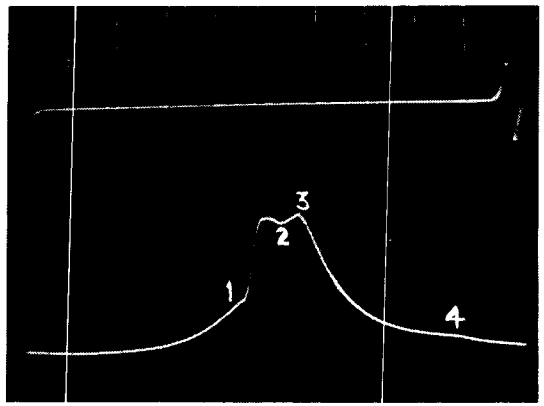

Fig. 8-14 BSPC = 2.6
O/F = .58
4000 rpm
BMEP = 112 psi
HP = 3.1
P_H = 715 psi P_M = 560 psi
Timing Condition #5

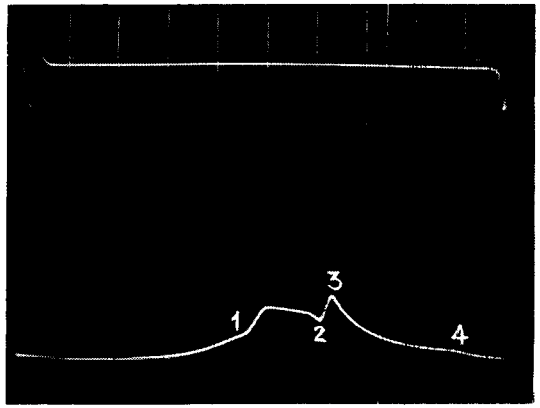

Fig. 8-15 BSPC = 4.3 O/F = 1.05
3000 rpm BMEP = 89 psi
HP = 1.2 P_H = 265 psi P_M = 260 psi
Timing Condition #2

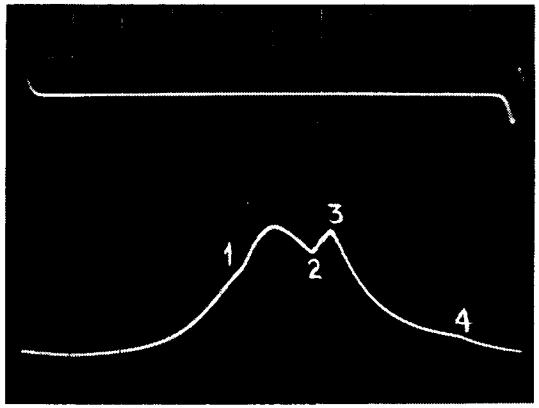

BSPC = 2.51 O/F = .97 Fig. 8-16
4000 rpm BMEP = 153 psi
HP = 4.2 P_H = 685 psi P_M = 505 psi
Timing Condition #3

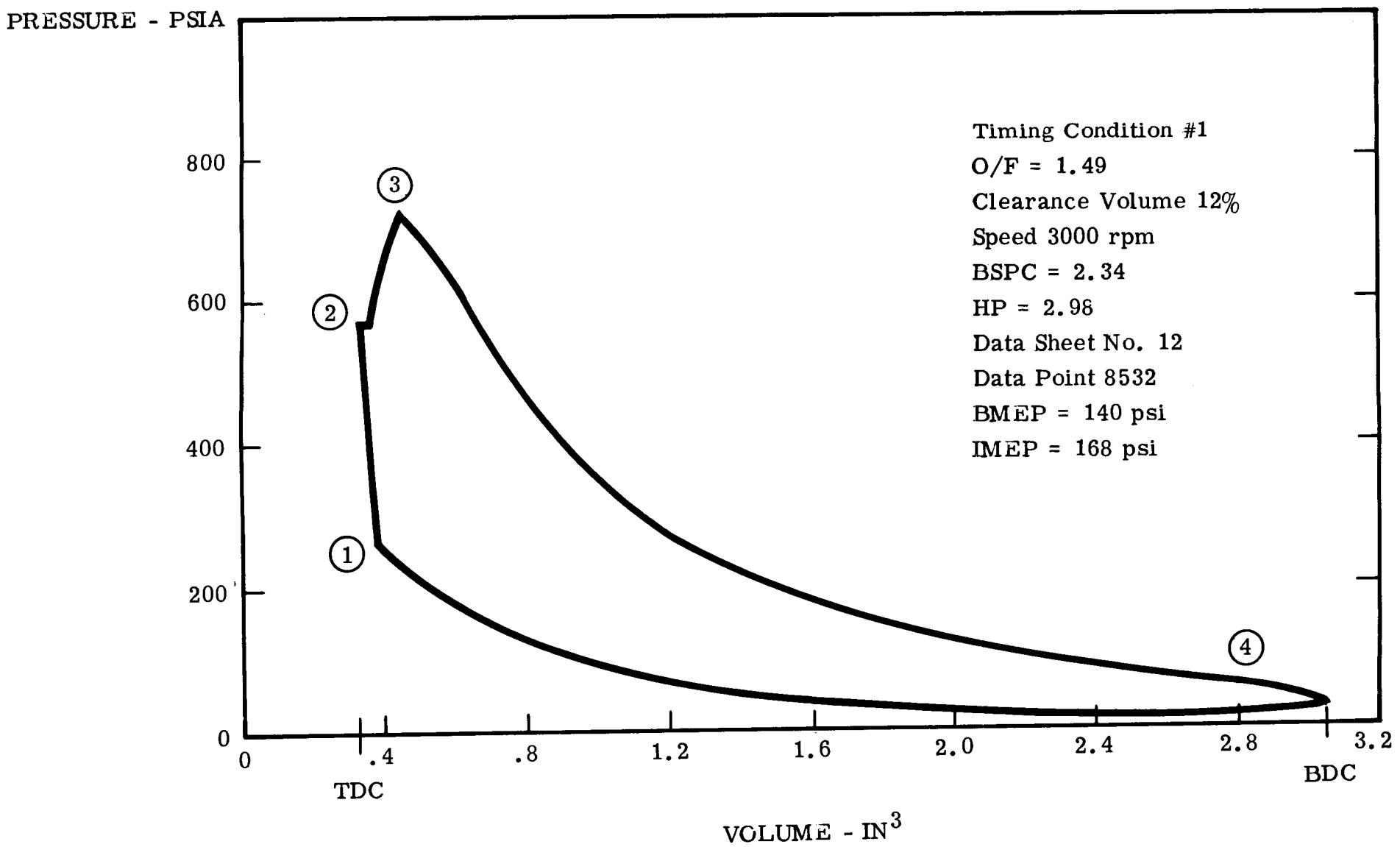

Fig. 8-17 - Linear Diagram - Pressure vs. Volume

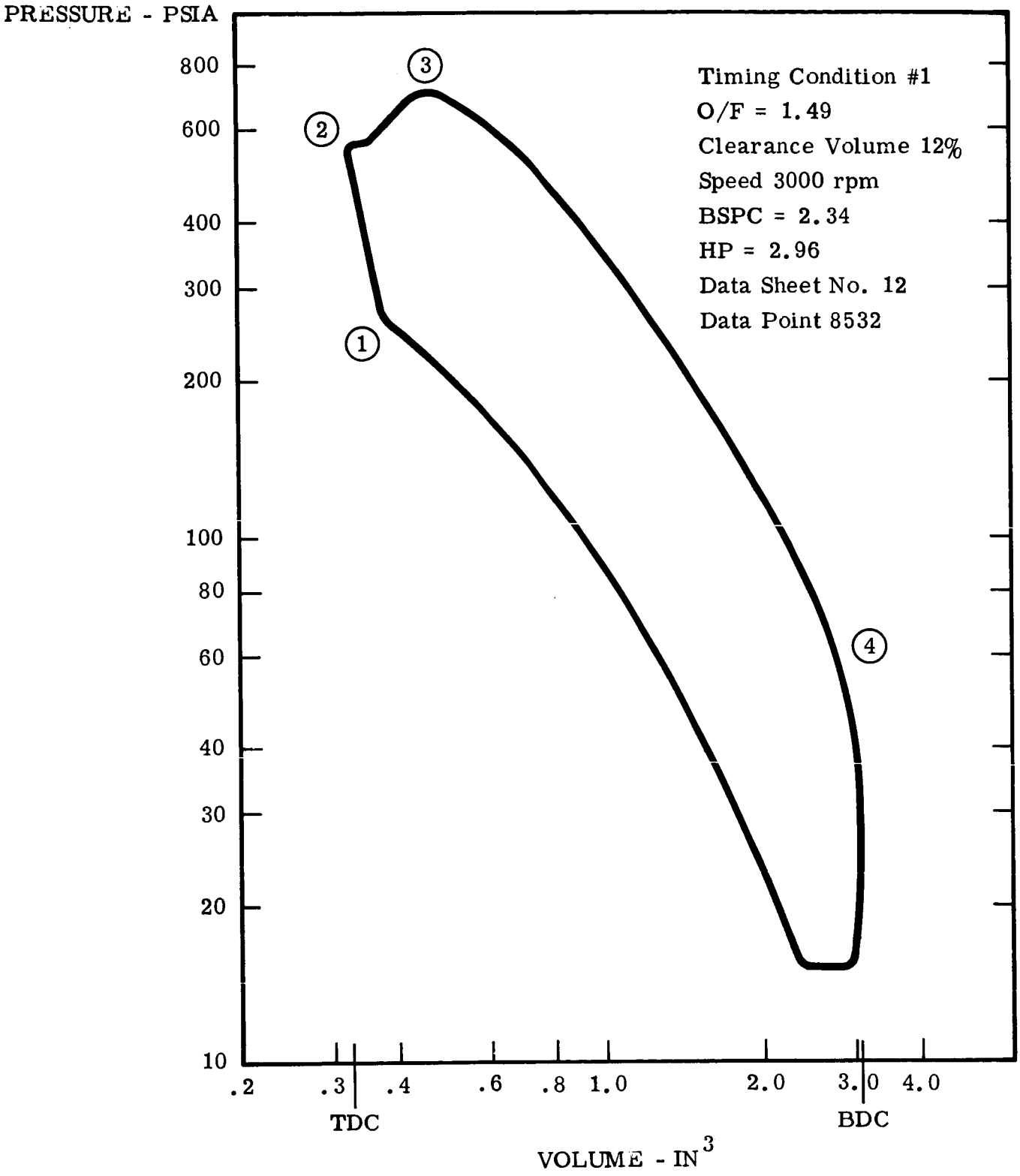

Fig. 8-18 - Log - Log Diagram - Pressure vs. Volume

3. Net heat transfer

4. Gas leakage

5. Slow combustion process

6. Incomplete combustion

In Fig. 8-13, timing condition No. 4 is shown. The four points described above are again labeled. The 'break' at point 2 is not pronounced due to oxygen-hydrogen flow overlap.

In Fig. 8-14, a trace from a test run employing timing condition No. 5 is shown. In this run very little overlap exists, so hydrogen pressure has time to drop slightly before combustion pressure rise occurs. Figs. 8-12, 8-13, and 8-14 represent engine operation at 2% hydrogen admission.

Two pressure time traces showing performance at 10% admission are illustrated in Figs. 8-15 and 8-16. The four significant points discussed above are labeled in both curves. Fig. 8-15 shows timing condition No. 2, which has 7° overlap, and Fig. 8-16 shows timing condition No. 3, with 14° overlap. The difference is not noticeably clear in these runs since burning occurs considerably downstroke. Fig. 8-16 shows a dramatic improvement in performance over Fig. 8-15. This is felt to be due primarily to the higher BMEP of the run shown in Fig. 8-16.

8.3.3 Conclusions Regarding Combustion Phenomena

The large amount of scatter present in all the more general figures is indicative of the high degree of complexity of the

physical phenomena involved. While it is inadvisable to rely on any one reading, there is enough consistency in the data to draw the following conclusions:

1. Combustion at or near top center is necessary for low propellant consumption. This is evident by comparing the performance at timing conditions 1, 4, and 5 (2% admission), with the much poorer average performance at timing conditions 2 and 3 (10% admission).

2. Propellant consumption increases with increasing overlap of the oxygen and hydrogen valves at 2% admission. This is probably due to flow limitations of this particular engine design and should not be considered a general conclusion. It is thought that overlap (and therefore combustion while the hydrogen valve is still open), perhaps interferes with hydrogen flow.

3. This engine may not be operating at its most efficient power rating. There is no data available at high levels of $BMEP/P_H$, so the minimums of Figs. 8-7 through 8-11 are not known. If friction MEP were reduced, the minimum would move toward a lower value of $BMEP/P_H$. This can be seen by viewing Fig. 8-11. On this figure, the data falls below the band of Fig. 8-7. This is due partly to timing and partly to the very high inlet pressure of all these runs (see Appendix H), which minimizes the effect of friction MEP.

   A higher level of $BMEP/P_H$ can be achieved in the following ways:

a. Raising oxygen injection rate, thereby achieving greater thermal compression.

b. Greater clearance volume, for a greater charge, at the same hydrogen admission. This unfortunately will also raise BSPC, since the expansion ratio is less.

c. Greater admission. This will also raise SPC in a manner similar to that resulting from greater clearance volume.

d. Reducing exhaust pressure, thereby decreasing recompression work.

An alternate approach would be to lower friction MEP by experimenting with ring and cylinder bore combinations, thereby lowering the point at which friction MEP cancels the benefit of low admission.

4. Combustion at higher mixture ratios appears to be less efficient in this engine configuration. This is illustrated by Fig. 8-19 which shows the ratio of accounted for energy to theoretically available energy as a function of mixture ratio.

This figure was obtained by a heat balance on runs 4-23 of Table 8-2 in which the sum of accounted for output energy, i.e., exhaust gas enthalpy rise, cylinder heat rejection, engine shaft power output, and an estimated cylinder head radiation loss was found. The result was divided by the theoretically available energy, and the

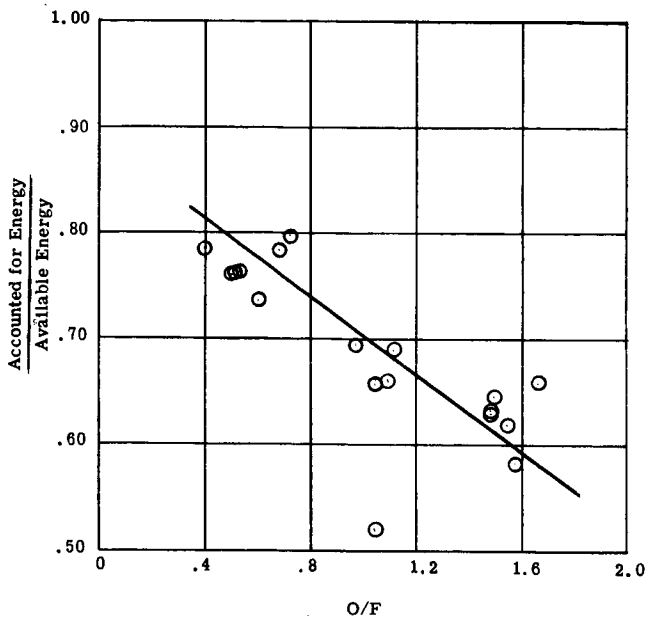

Fig. 8-19 - Energy Ratio vs. O/F

quotient is plotted vs. O/F ratio. If all lost energy were accounted for, the quotient would be one. Such items as engine friction, heat lost to the oil through the crankshaft, etc., are not included, but would not rise this much with O/F ratio. If there were an identical combustion efficiency throughout the O/F range, a straight horizontal line would result.

Combustion inefficiency could be caused by excessive heat transfer, charge stratification, or incomplete combustion. Indication that charge stratification occurs may be verified by checking Fig. 8-20, which shows a film sequence taken through a quartz cylinder head. Note that combustion begins immediately after injection of oxygen. This film was taken during the run of a similar (earlier) engine design using a previous oxygen injector design; however, combustion chamber shape and injector location and orientation are identical to the present engine configuration.

8.3.4 Engine Temperature Data

Engine Exhaust Conditions

In Fig. 8-21 the engine exhaust temperature is plotted against BMEP for various maximum cylinder head temperatures. (Head temperature was usually used as a check on the mixture ratio during a test). This curve

DATE OF RUN: 6 DECEMBER 1962

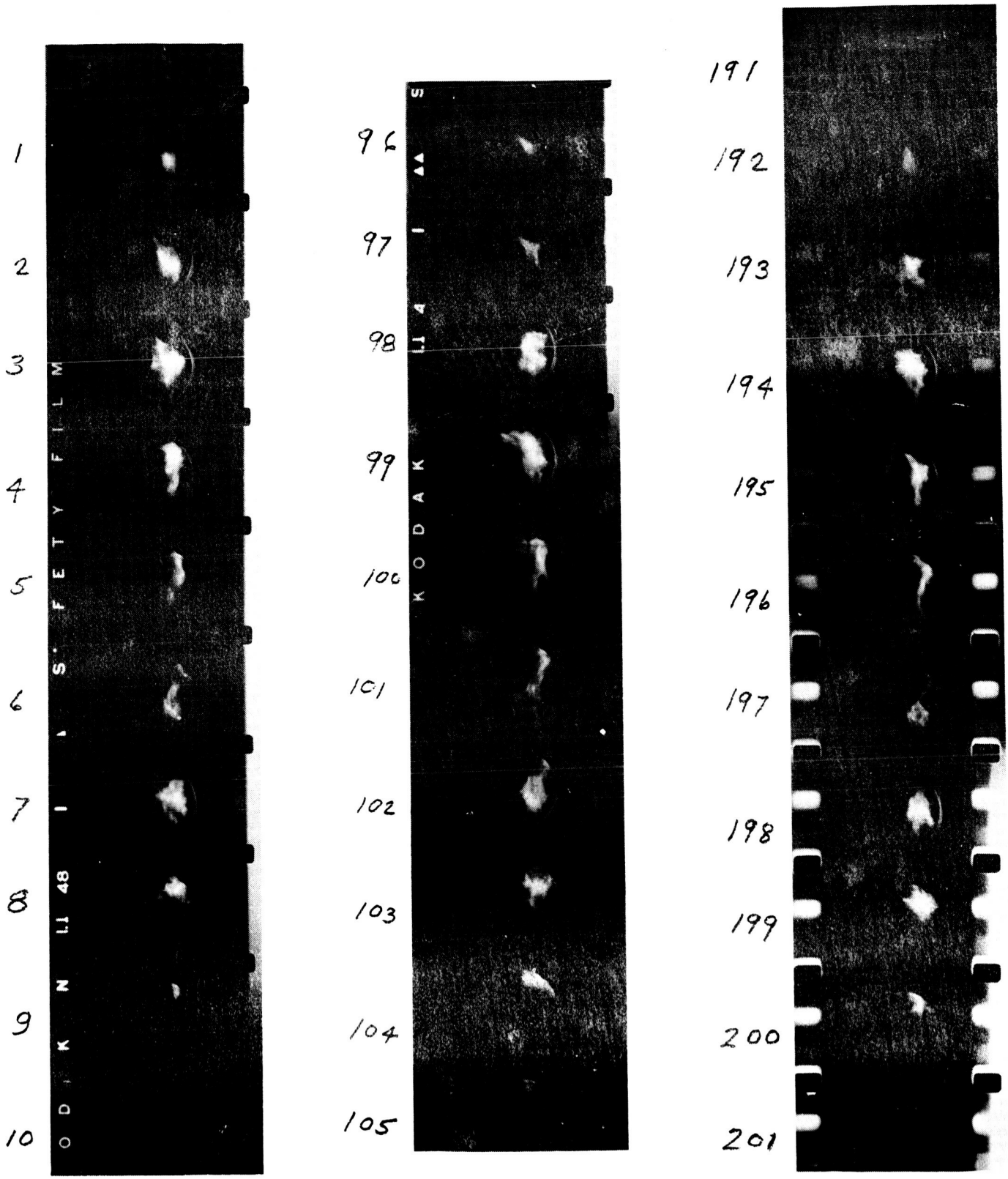

EACH FRAME EQUALS .00036 SECOND

Fig. 8-20 - Combustion Chamber Film Sequence

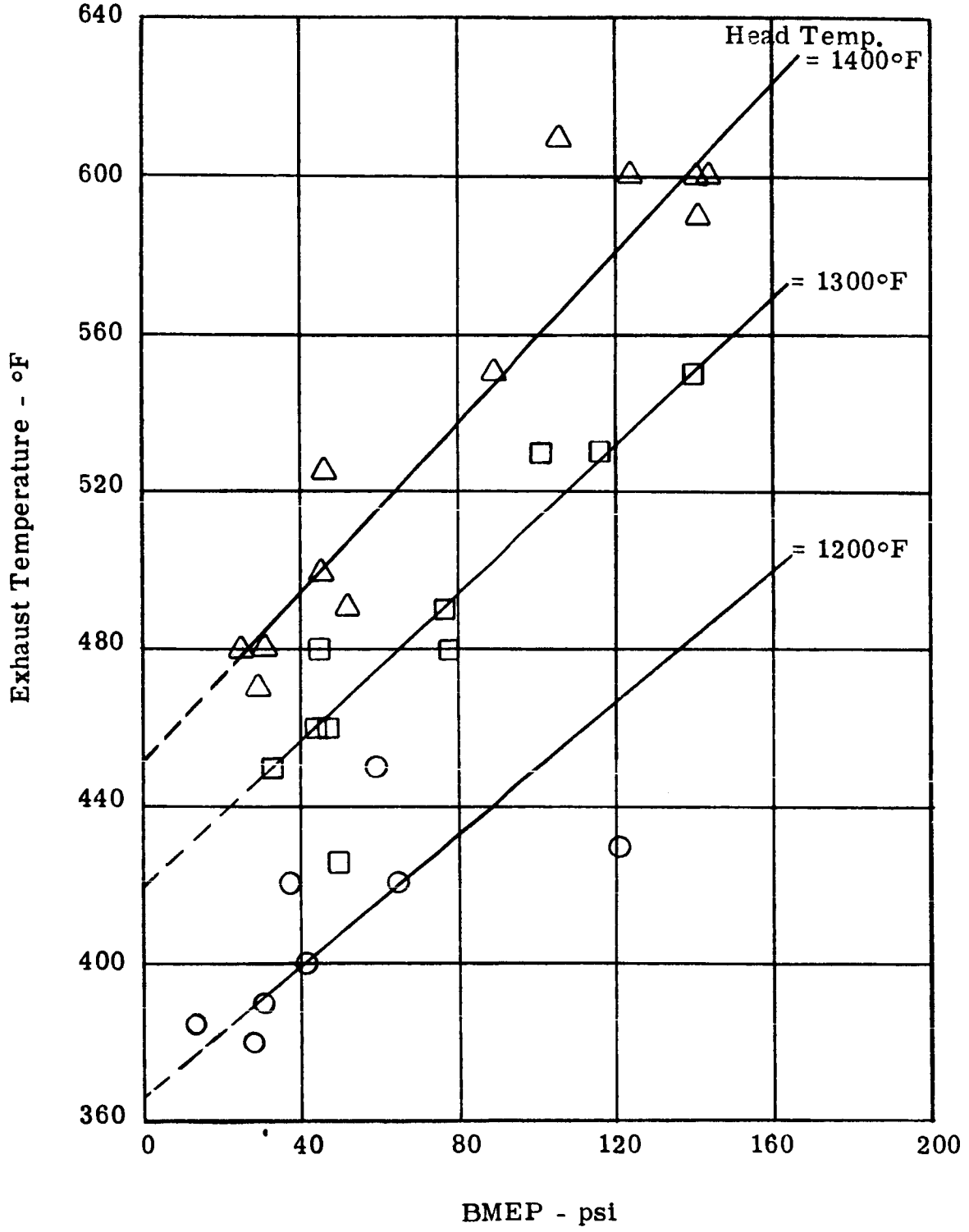

Fig. 8-21 - Exhaust Temperature vs. BMEP

indicates that the thermal loading on the engine (as represented by exhaust temperature), increases as the BMEP is raised. These data points are all for No. 1 timing. For a higher admission, an increase in exhaust temperature would be expected, since there would be less effective expansion. See, for example, entries 20 or 21 of Table 8-2.

Regenerated Performance

During engine tests using the regenerator the maximum hydrogen inlet temperature did not exceed 300°F, and thus, no startling improvement was noticeable between regenerated and unregenerated runs. Differences were usually masked by other variables such as timing, or changes in oxygen injector flow characteristics. However, a comparison of individual runs will tend to show an improvement in BSPC when running with the regenerator. For example, see entries 19 and 23 of Table 8-2. The only significant difference between these runs was the regenerated hydrogen and the lower oxygen/hydrogen overlap of run 19, both of which contributed to the much better BSPC than achieved in run 23 (2.51 lb/hp-hr. as opposed to 2.90).

Insulated Cylinder Head Performance

The runs in Fig. 8-22 were made with an insulated cylinder head. Results are inconclusive due to the poor oxygen injector performance in this run. Oxygen injector malfunctions are thought to be a result of differential thermal expansion and overheating of this area caused by the insulation.

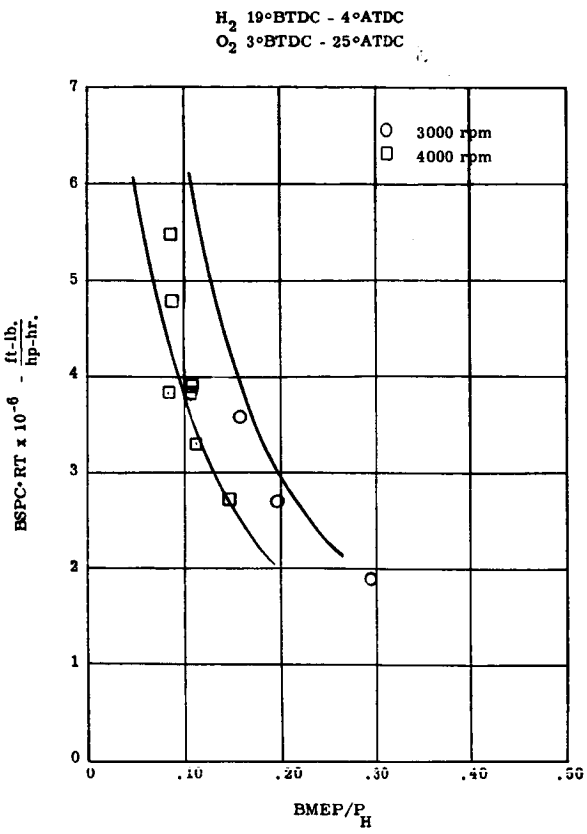

Fig. 8-22 - BSPC·RT vs. BMEP/P_H (Insulated Head)

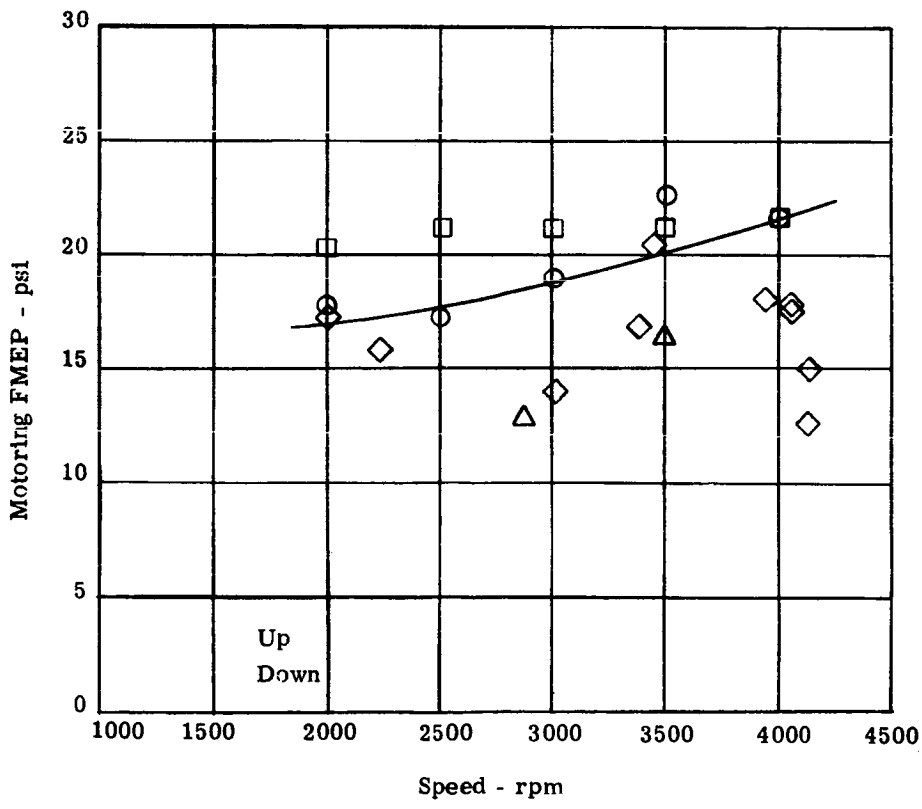

Fig. 8-23 - Motoring FMEP vs. RPM

8.3.5 Engine Friction

Motoring friction tests were run to establish the friction mean effective pressure level of the engine. The results of these tests are shown in Fig. 8-23. It will be noted that there is considerable scatter in the data. The tests were run at somewhat different conditions and cooling jacket temperature, which would effect oil viscosity, was not controlled, There is also some hysteresis evident since the FMEP with increasing speed is lower than with decreasing speed.

Motoring friction data obtained on a similar engine tested previously under Air Force contract was somewhat lower than the data shown in Fig. 8-23. The reasons for this apparent discrepancy are as yet unresolved. It was data from these prevoius engine tests that were used for establishing the FMEP level of 11 psi used for cycle analysis in the parametric studies section of this report.

It is not yet possible to correlate motoring friction data with friction MEP calculated from indicator card data obtained under firing conditions. Analysis of one typical indicator card showed an FMEP of 28 psi obtained by subtracting the measured BMEP of 140 psi from the indicator card IMEP of 168 psi measured with a planimeter. This value is not considered significant because of the limited accuracy of determining IMEP by means of the continuously indicating quartz crystal type pressure transducer. The pressure measurement errors may be of the same magnitude as the difference between IMEP and BMEP.

More accurate values of operating FMEP should be obtainable by the use of a balanced pressure pick-up. It is planned to conduct such tests in the future.

8.3.6 Other Engine Data

A great many parameters related to engine performance were examined for meaningful interrelationships.

One instructive procedure is to correlate several runs in which only one variable is changed. One example is Figs. 8-24 and 8-25, where several runs at the same speed and BMEP are plotted. Heat rejected and BSPC are shown as functions of O/F ratio. The data are quite consistent in spite of the fact that entries were taken from several different test runs.

8.4 Performance Corrections

Attempts to accurately predict design performance from the test data can be misleading because of the uncertainty as to how the relative magnitudes of the various losses will be maintained as conditions are changed. Realizing this limitation of such corrections, the steps leading to, and the results of corrective analysis based upon the original parametric design study, are presented here. The results can be used to correct test SPC to other desired conditions. The results should be considered to be preliminary.

Basis of Corrections

The test results from two runs made on different days were averaged as follows.

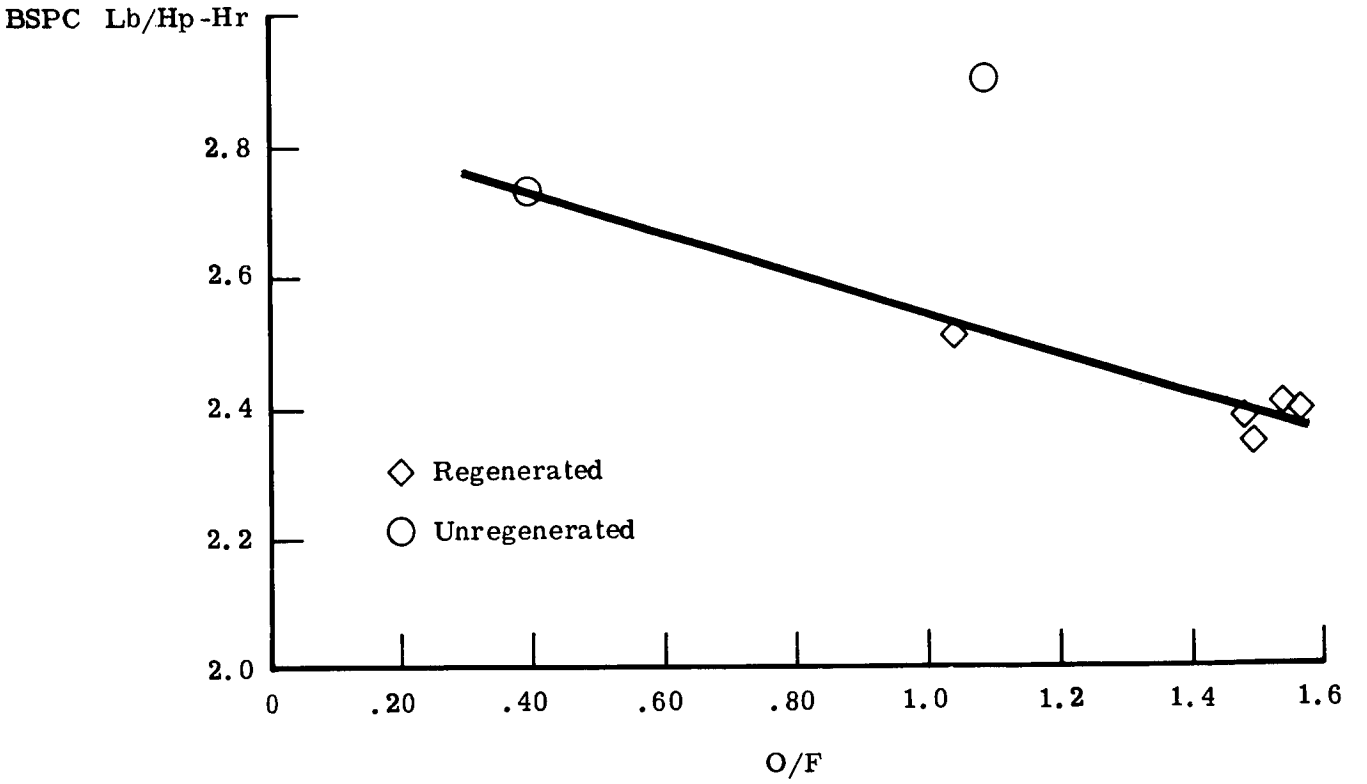

Fig. 8-24 - BSPC vs. O/F

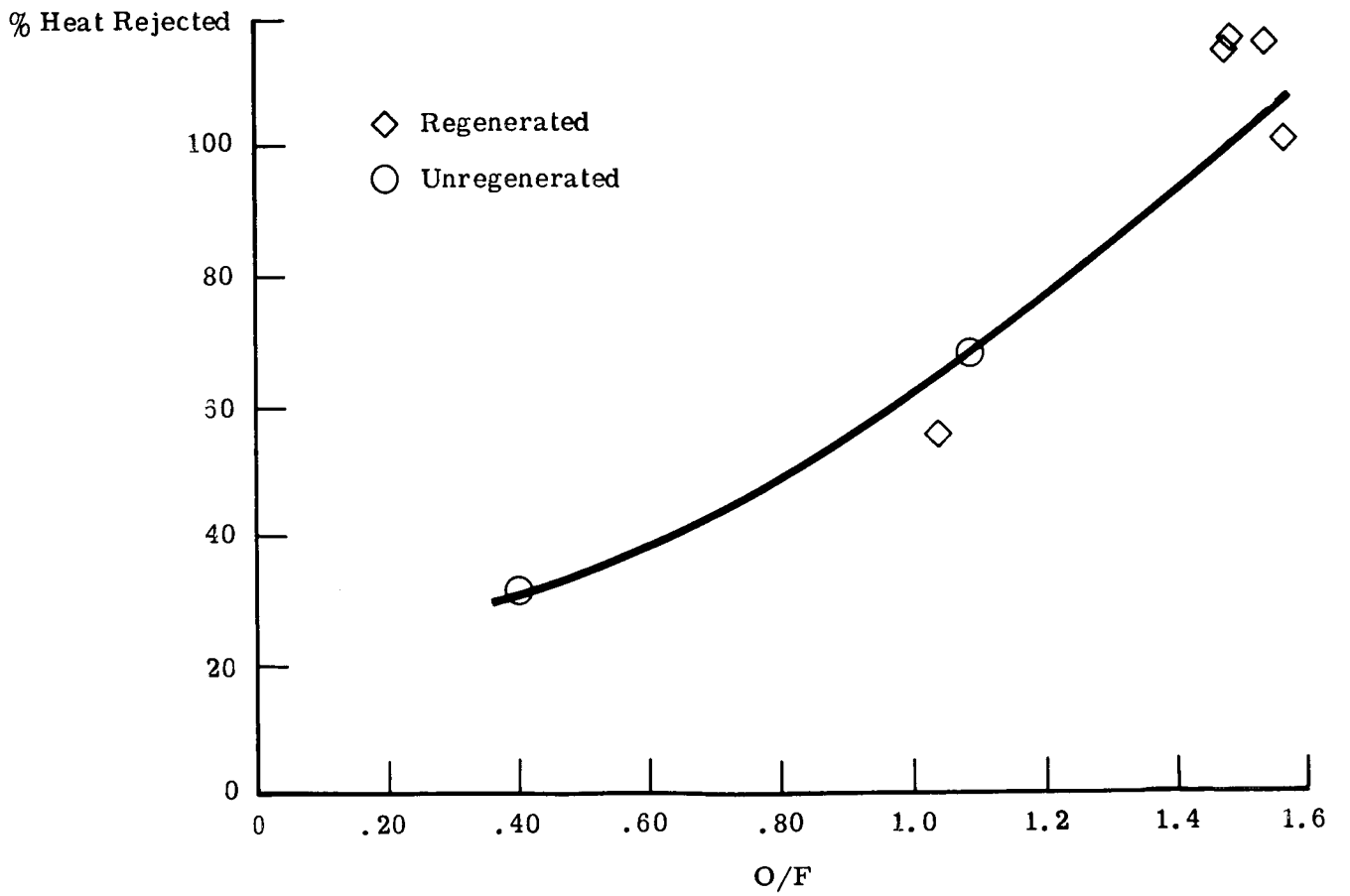

Fig. 8-25 - Heat Rejection Percentage vs. O/F

Data Sheet	Time	BSPC	O/F	Qcyl HP	BMEP	$T_{i_{H_2}}$
12	8550	2.40	1.54	1.149	142	300°F
13	8570	2.385	1.478	1.138	141	295°F
Average		2.39	1.509	1.144*	141.5	297.5°F

On the basis of performance calculations it has been predicted that the performance of the H_2-O_2 engine operating in space would be as follows:

BSPC = 1.02 lb/hp-hr.
@ BMEP = 86 psi
O/F = 2

$\frac{\text{Clearance volume}}{\text{Displacement}}$ = C = 0.05

Exhaust pressure = P_e = 2 psia
Regenerated H_2 temperature = T_i = 1000°F
Net cylinder heat rejection = Q/HP = 0.53 @ y - 0.3*

Assumed in the Calculations

No charge temperature stratification
No leakage
No cyclic heat transfer
FMEP = 11 psia
Diagram factor = 0.9
P_i = 900 psi at minimum BSPC

Calculated space performance is now corrected to sea level performance, with calculations corrected for operating conditions recorded in tests. BSPC is successively corrected for

BMEP, O/F, C, P_e, $T_{i_{H_2}}$, Q/Hp, and unaccounted losses. Each correction is treated independently. The results are tabulated below.

TABLE OF CORRECTIONS

BSPC	BMEP	O/F	C	P_e	$T_{i_{H_2}}$	Q/HP	BSPC Penalty For Unaccounted Loss
1.02	86.0	2	.05	2	1000°F	.53@y=.6*	1
1.055	141.5	2	.05	2	1000°F	.53@y=.6	1
1.045	141.5	1.5	.05	2	1000°F	.53@y=.6	1
1.12	141.5		.125	2	1000°F	.53@y=.6	1
1.16	141.5		.125	15	1000°F	.53@y=.6	1
1.375	141.5		.125	15	300°F	.53@y=.6	1
1.68	141.5		.125	15		1.34**@y=.6	1
2.39	141.5		.125	15			1.42

*The Q/HP value measured does not include cylinder head heat rejection. To account for this, the measured heat rejection was increased by a factor of 17 percent (1.144 x 1.17 = 1.34). This factor was determined by conducting an analysis of the heat radiation and natural convection from the head. Insulation of the head will reduce the net heat loss from the head.

**Explanation of weighing factor y presented in Progress Report PR91565-430-2; y = 0 when all net heat rejection occurs at TDC; y = 1 when net heat rejection occurs after expansion.

Note: The successive increases in the BSPC column are the result of cumulative effect of the difference between the design

conditions used in calculation and actual test conditions. The contributing parameter in each row has been boxed.

Comments on Corrections and Losses

In the table of corrections all readily accountable effects increase theoretical BSPC to a corrected value of 1.68 lb/hp-hr. Unaccounted losses apparently increase BSPC by an additional 42% to the measured value of 2.34 lb/hp-hr.

These unaccounted losses are no doubt composed of some or all of the following effects:

1. Cyclic heat transfer

2. Combustion charge temperature stratification

3. Leakage

4. Higher friction

5. Incomplete or late combustion

It is suspected that temperature stratification has the greatest single influence on unaccounted losses. If combustion energy were not transferred to the diluent at all, peak combustion pressure would be only about 1/2 that of an equilibrium products/diluent mixture. Thus, BSPC would be approximately twice the value calculated assuming a uniform temperature mixture. Assuming complete stratification is certainly too conservative, but considerable stratification probably does occur, with resulting BSPC penalty. High speed

photography and thermal patterns (hot spots) on piston and cylinder head indicate that increased swirl, or turbulence, in the combustion chamber should improve performance.

Cyclic heat transfer also increases BSPC. Studies on four stroke diesel engines have shown it to have an effect approximately three times more penalizing on performance than net heat transfer from the engine. Since the H_2-O_2 engine is not of the internal compression type, the effects of cyclic heat transfer should be much smaller than in an air-breathing diesel engine.

Net heat transfer results in complete removal of a portion of the heat energy from the cycle by heat rejection to the coolant, or by radiation to the environment.

Cyclic heat transfer results in removal of high-grade (high temperature) heat energy from the high temperature, high pressure portion of the cycle by transfer from the hot combustion gases to the relatively cooler cylinder walls. This heat is returned to the working fluid at a later point in the cycle when the gas is at low pressure and is cooler than the cylinder walls, but this occurs at a time when the returned heat energy can no longer be usefully extracted from the working fluid. The gross effect of cyclic heat transfer is to reduce the expansion work obtained from the cycle and to increase the work required to re-compress the residual exhaust gas trapped in the cylinder after blowdown.

Leakage may impose penalties in two ways; (1) heat transfer is stimulated and, (2) working fluid escapes. High friction will reduce mechanical efficiency. With incomplete or late

combustion, the full benefit os the potential energy release is not realized.

The data shown in the Table of Corrections should be used for comparative purposes only, and the temptation to use them in predicting performance should be firmly resisted until the effect of each factor can be demonstrated by test. It is unrealistic to expect that all of the unaccounted for losses can be isolated and recovered. It is also unrealistic to expect that the recognized losses due to off-design test conditions will be recovered in the relative magnitudes shown in the table. For example, it would not be unexpected if the net heat rejection increases when O/F is increased from 1.5 to 2.0, thus making a reduction in heat rejection even more difficult to achieve by mechanical and thermodynamic development. Conversely, the reduction of exhaust pressure from 15 psia to 2 psia could conceivably provide a greater gain in performance than indicated by the table because of a beneficial effect on cyclic heat transfer due to reduced working fluid density during the recompression process.

Although predictions of performance improvements are hazardous at best, it is felt that a realistic estimate of the perform-capability of the existing experimental engine is a BSPC of approximately 1.3 lbs per hp-hr with vacuum exhaust, regenerated inlet temperature, O/F = 2.0, 5% clearance volume, and with nominal reductions in net and cyclic heat transfer, friction, charge stratification, and unaccounted for losses. It is also felt that further improvements can be made by additional detailed refinement and development of the engine design. It must be realized that the predicted BSPC of 1.0 lbs per hp-hr for the flight type engine was based on a realistic appraisal and application of the current state-of-the-art of modern air-breathing internal combustion engines, with due

allowance being made for the differences in fluid properties. It appears reasonable to expect that a fully developed and highly refined H_2-O_2 engine should achieve a BSPC = 1.0 lb per hp-hr at design conditions, although this will not be achieved without the expenditure of considerable time and effort and the accumulation of many additional hours of diligent development testing.

8.5 PROBLEM AREAS

Mechanical Failures

The engine failures which occured during the test program are considered to be minor in nature. A summary of failures is tabulated below.

Failure Summary

Part Number	Name and Problem	Number of Occurences During 15.7 hrs of Hot & 9 hrs of cold running time
X610157	H_2 Valve guide - wear	2
X609923	Combustion chamber - crack	1
X609997	Head seal - leakage	3
X609921	Combustion chamber seal - leakage	4

Hydrogen Valve Guide Wear

The hydrogen valve guide wear problem occurred during one engine assembly, and it is attributed to misalignment of valve

parts due to unevened torquing of bolts, and uneven and incomplete crushing of static metal "O" ring seats. Reoccurrence of this problem can be prevented by modifying the hydrogen valve design to allow for a more solid assembly of parts, and by changing seal grooves from a "V" cross section to a rectangular cross section to provide for proper crush of the seals and to allow for tolerance variation in the seals.

Combustion Chamber Failure

Failure occurred in a thin (0.064 inch) annular section of the combustion chamber top during a test run where the metal temperature reached 1400°F. Failure was attributed to bending stress due to the high force applied at its center to seat the seal at the outside diameter. The design was modified so that the sealing force was applied at the outside diameter and no other failures occurred.

Combustion Chamber Seal Leakage and Head Seal Leakage

Both of these seals are silver plated Haskel "K" seals. The leakage in operation is attributed mainly to repeated loading and unloading during the test program, and to differential expansion of the head components due to poor mixing of combustion products and unburned hydrogen. One of these seals is between the head assembly and the cylinder and the other is between the combustion chamber disc and the head assembly ring.

Problems Affecting Performance and Testing Controlability

As previously mentioned, difficulty was encountered in obtaining a predictable change in oxygen flow rate for a change in

oxygen supply pressure. Since the oxygen flow is influenced by the interrelationships between oxygen supply pressure, the oxygen orifice size, the lift profile of the poppet, and the cylinder combustion pressure rise characteristic, it should be possible to correct this condition by changing the orifice size and poppet lift profile and/or increasing the oxygen supply pressure. Higher oxygen supply pressure can be used if the preload force of the hydrogen valve poppet return springs are increased to prevent the valve from blowing open from high peak combustion pressures.

Another problem concerned the opening and closing cam angles of the oxygen injector. These were found to have increased (from their cold adjustment) when the angles were checked by static test while the engine was still warm after a hot test. The change in opening angle due to heating is much more pronounced when the differential pressure across the oxygen injector is small. When attempting to run low O/F ratios with the oxygen pressure slightly above hydrogen supply pressure, hydrogen valve closing near TDC, and oxygen admission set to begin a few degrees after hydrogen valve closing, it was found that the oxygen valve opening point advanced, resulting in increased overlap with the hydrogen valve.

The shift in oxygen admission caused the inflow of hydrogen to be restricted, O/F ratio to increase, and head temperature to go up rapidly, necessitating a quick abort of the test. This overheating condition was quite evident when attempting to run with an externally insulated head. The insulation also surrounds part of the oxygen injector and accentuated the problem. It is believed that this condition occurred to a lesser extent during other tests, when higher oxygen supply pressures were used,

and that it was the cause of the occasional instability. It could also account for some of the poor performance which occurred at higher O/F ratios. When combustion occurs while both the hydrogen valve and oxygen injector are open, the combustion pressure is limited by leakage through open valves. This is particularly true when the overlap occurs before TDC.

Engine Friction

Motoring friction tests were run to establish the friction mean effective pressure level of the engine. The results of these tests are shown in Fig. 8-23. Motoring friction data obtained on a similar engine tested previously under Air Force contract was somewhat lower than the data shown in Fig. 8-23. The reasons for this discrepancy are as yet unresolved. It was data from these previous engine tests that were used for establishing the FMEP level of 11 psi used in cycle analysis studies.

It is not yet possible to correlate motoring friction data with FMEP calculated from indicator card data obtained under firing conditions. Analysis of one typical indicator card showed an FMEP of 28 psi, obtained by subtracting the measured BMEP of 140 psi from the indicator card IMEP measure with a planimeter. This value is not considered significant because of the limited accuracy of determining IMEP by means of the continuously indicating quartz crystal type pressure transducer. The pressure measurement errors may be of the same magnitude as the difference between IMEP and BMEP.

More accurate values of operating FMEP should be obtainable by the use of a balanced pressure pick-up. It is planned to conduct such tests in the future.

9.0 EXPERIMENTAL OXYGEN INJECTOR TEST PROGRAM

9.1 Summary

During the oxygen injector test program, two identical basic injector assemblies were maintained. One was evaluated by testing it as a separate component on the injector test stand and the other by running it as a part of the engine assembly. A total of 31.25 hours of running time was accumulated on the injector test stand. A total of 15.7 hours of hot running time, plus 9 hours of cold motoring test time, was accumulated on the engine. The performance of the injector was superior to the one used in the ASD engine from which it evolved. There were no failures of the critical torsion seal tube through which motion is transmitted, and it functioned properly throughout the test program. Its dynamic flow characteristics exceeded expectations. The valve did exhibit some lost motion between the cam follower and poppet. Though the flow characteristics of the injector are interrelated with, and greatly dependent upon, minor changes in engine design and adjustment, it is now felt that orifice size and lift of the injector can be reduced considerably; however, more analysis and testing will be required to prove it.

One basic problem with the present design is that performance tends to change each time the injector is reassembled, either with the same parts or with different parts. This condition is due in some degree to minor manufacturing variations of parts (spring rate and dimensions), but to a greater extent, to the inability to adjust the location of one part in a compatible arrangement with others. A number of minor design changes must be taken to correct this condition. Another

problem, was wear on the cam follower.

A number of injector failures occurred during the program which reduced the testing time of the injector, both as a component and on the engine. The most serious type of failure experienced was the gradual wear between the poppet and guide, and deformation of the poppet seating surface, which reduces the life of the unit. Reasons and corrective measures for this condition are discussed in detail, but time and funding limitations prevented the evaluation of any alternate approaches during the test program.

9.2 Test Set Up & Instrumentation

A photograph of the oxygen injector test stand is shown in Fig. 9-1 and the system schematic is shown in Fig. 9-2.

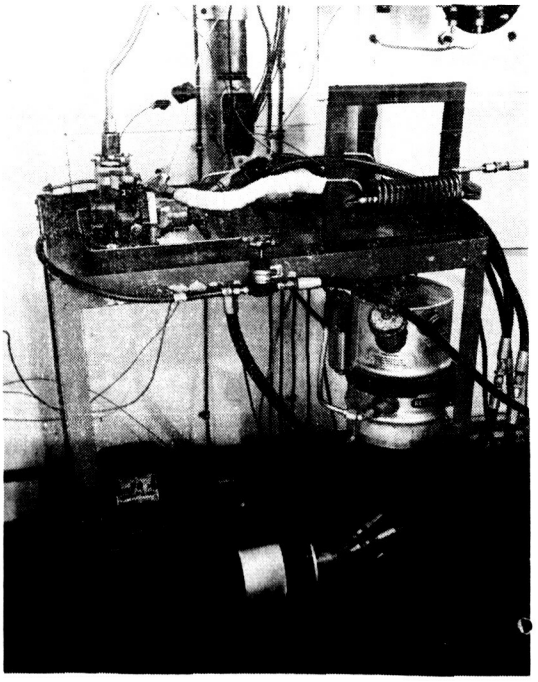

Fig. 9-1 - O_2 Injector Test Stand

A dummy engine crankcase is used to mount the oxygen injector and camshaft, which is driven by a hydraulic motor. The hydraulic power supply uses an electric motor driven pump, filter, bypass-valve for speed control, and a meter-motor to read the drive motor rpm.

Lubrication for the injector system is supplied from the engine test stand system. Nitrogen or oxygen gas is

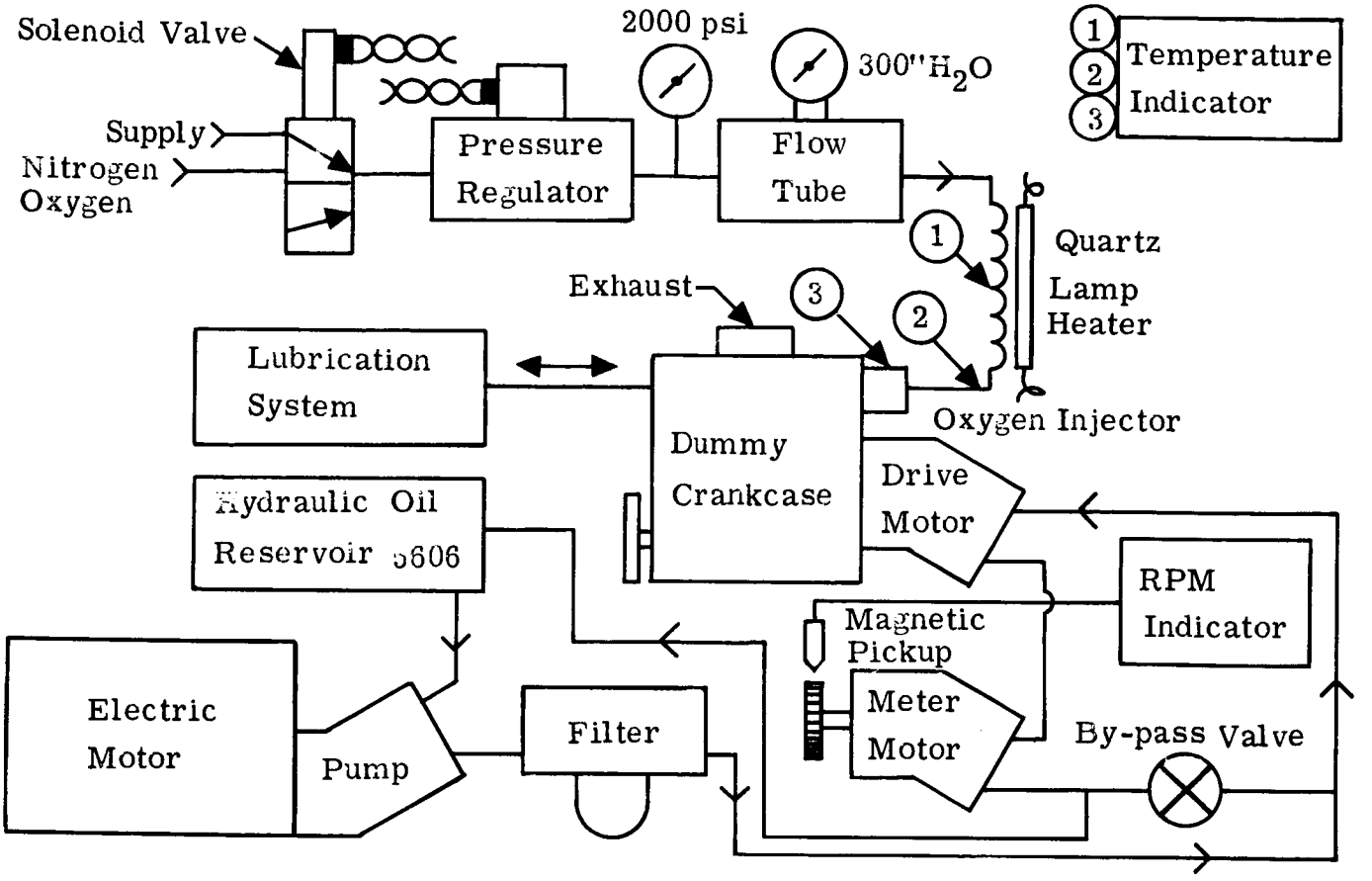

Fig. 9-2 - Schematic - O_2 Injector Test Stand

selected by a three-way solenoid valve, and pressure is controlled by a solenoid operated pressure regulator. Gas flow is determined by measuring the differential pressure across a calibrated orifice. A quartz lamp, mounted inside a coil of 1/4 inch tubing, is used to heat the incoming gas to the injector. A Variac controls the lamp temperature. Temperatures are read on a multipoint indicator with range of 0 to 1200°F. Camshaft speed is read on an electronic counter driven from the magnetic pickup on the meter motor.

9.3 Discussion of Tests and Performance and Design

Tests were run on the oxygen injector, using the component test stand to determine injector static and dynamic flow calibration, component life and to verify the materials selection.

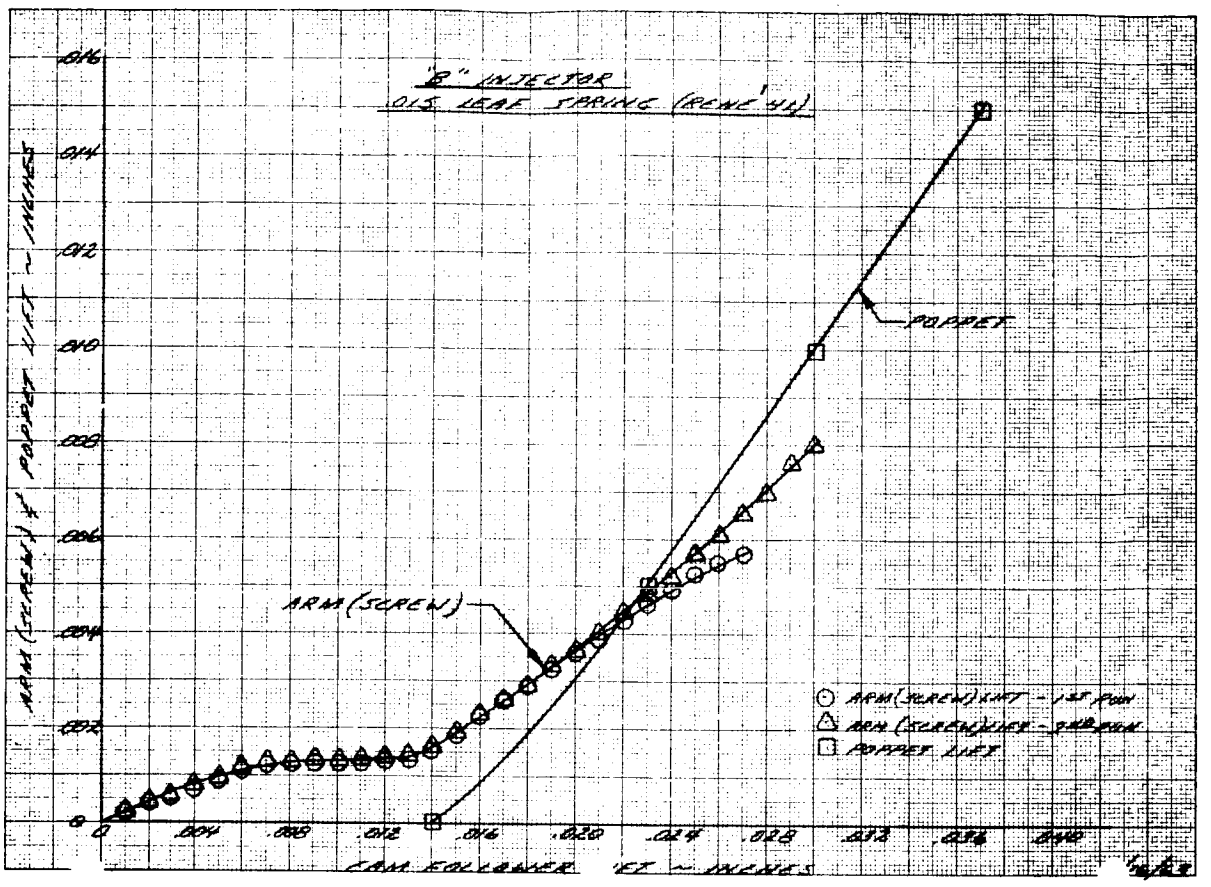

Fig. 9-3 - Arm & Poppet Lift vs. Cam Follower Lift

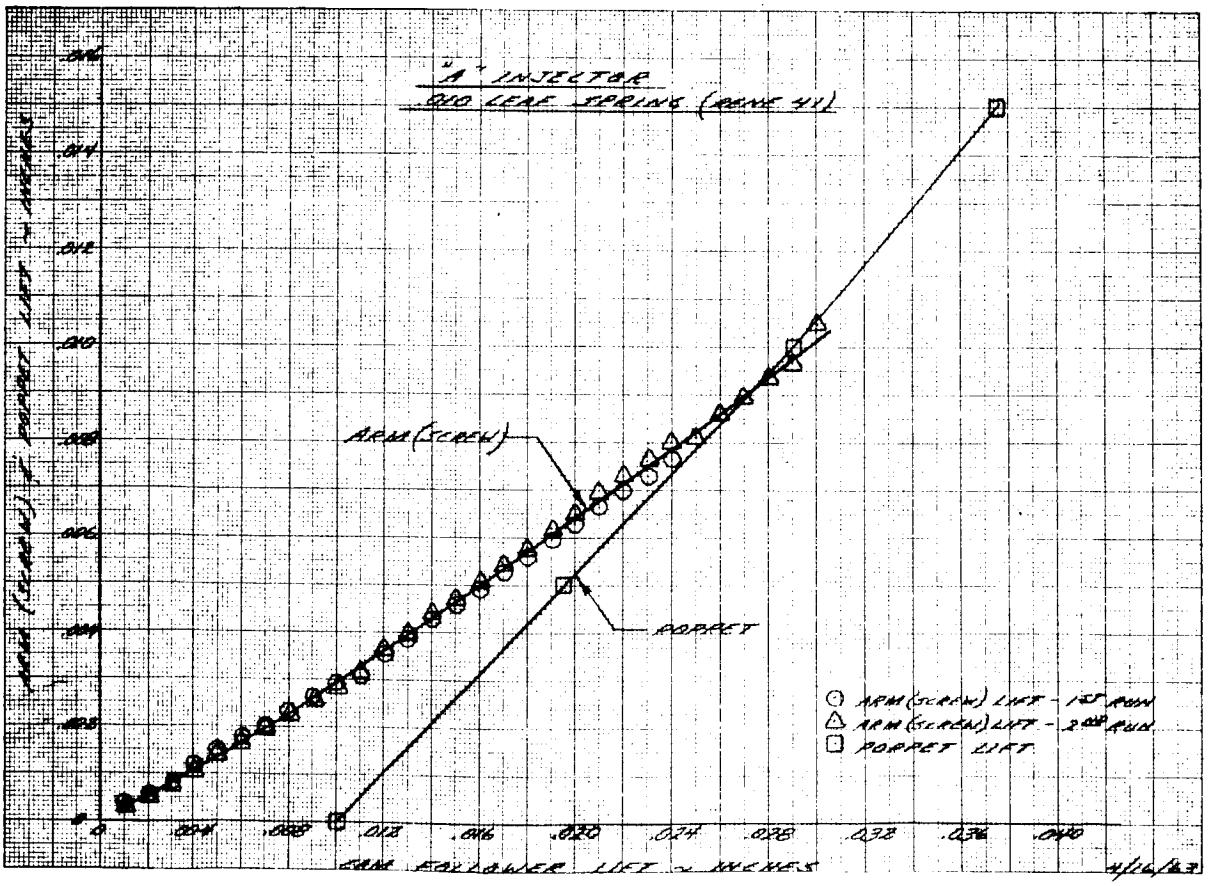

Fig. 9-4 - Arm & Poppet Lift vs. Cam Follower Lift

Static Tests

Figs. 9-3 and 9-4 are the results of static tests performed in the same manner on the same assembly build-up, except that a .015 inch thick poppet retainer spring was used for the test resulting in Fig. 9-3, and a .010 inch thick spring, was used for the test resulting in Fig. 9-4. The free body diagrams shown in Fig. 9-5 will aid in understanding of the discussion which follows. In each test the rocker arm was adjusted (without poppet retainer spring load), to just touch the bottom spool of the poppet stem when the poppet was seated. In both Figs. 9-3 and 9-4 the dial indicator reading of the poppet and rocker arm position are plotted vs. cam follower lift. Fig. 9-3 shows that relative high force imparted by the thick poppet retainer spring caused an initial windup of the quill shaft, resulting in a delay in poppet opening and a foreshortening of its lift.

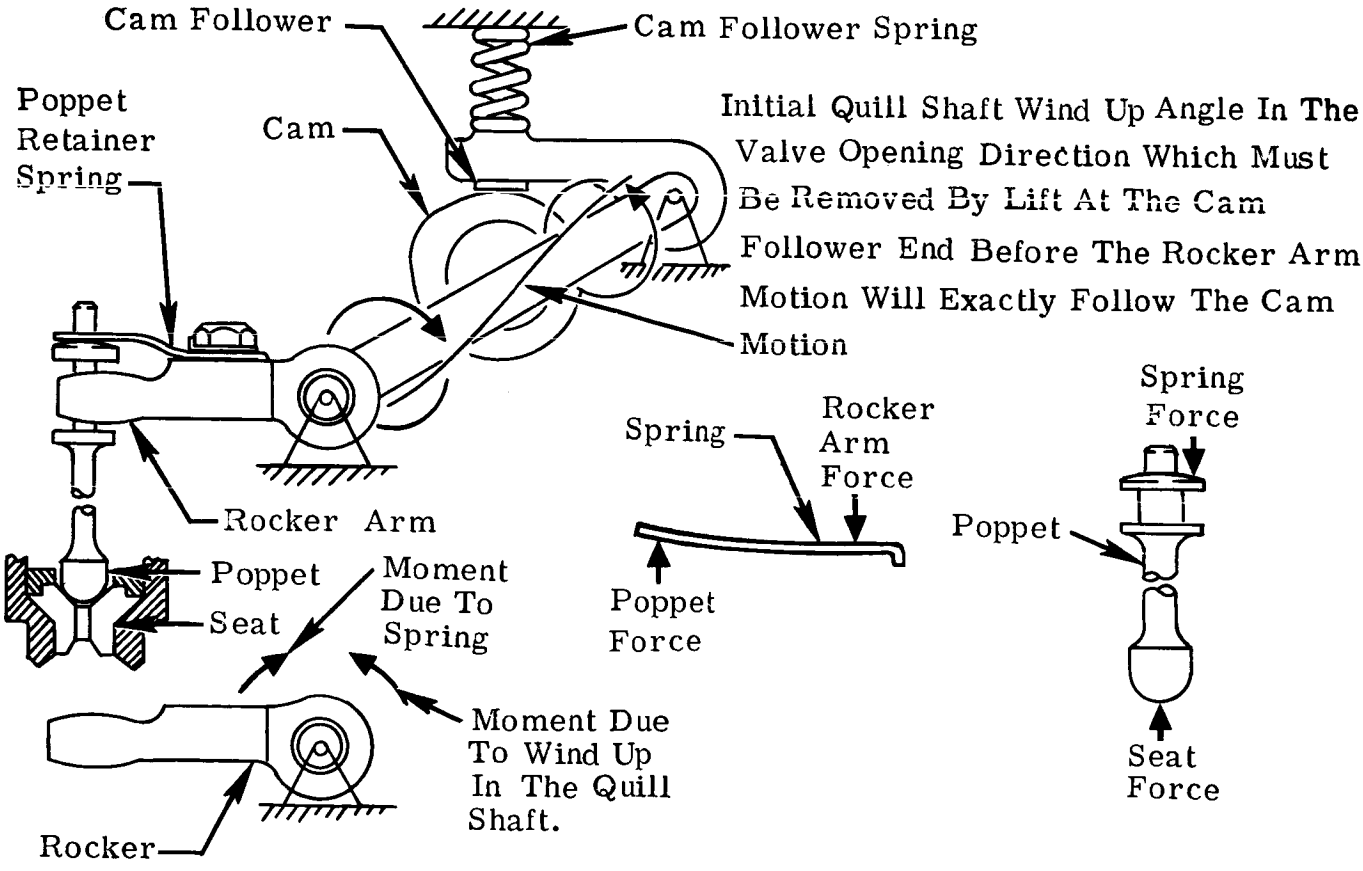

Fig. 9-5 - Diagram - Quill Shaft

Fig. 9-4 shows that the condition is somewhat alleviated by using the thin spring. The flex pivot, which supports the end of the quill shaft in the injector body, contains blade springs which are deflected when the injector is actuated and the springs apply a twisting torque to the quill shaft. Differences in the amount and direction of preload applied to the flex pivot when the injector is assembled, and variations in spring rate from one flex pivot to another, produce changes in injector performance similar to those caused by the poppet retainer spring. Considering the initial long gradual slope of the existing oxygen cam, it can be seen that small variations in the interacting effects, causing twisting of the quill shaft, can result in large variations in the crank angle of the engine at which injector poppet opens. Some steps which may be taken to reduce the quill shaft windup are as follows:

1. Replace the flex pivot with some type of low friction (possibly a flame plated journal or knife edge) bearing. If this is not successful an adjustment should be provided so that the rocker arm can be locked to the flex pivot after poppet seating adjustment is made, so that no initial preload is applied to the flex pivot.

2. Decrease clearance and reduce tolerances between the poppet and rocker arm in order to reduce the backlash, and thus reduce the travel of the poppet retainer spring. Preferably, the design should be modified so that close tolerances are not required, and adjustment is made for proper backlash.

3. Arrange the fixed end of the poppet retainer spring so that it applies minimum preload.

Fig. 9-6 shows static effect of injector differential pressure upon the engine crank angle at which the injector opens and closes. This condition can be reduced by making the poppet seating area smaller, by increasing the diameter of the quill shaft and torsion tube, and by increasing the radial rigidity of the flex pivot. The latter may not be a practical solution. Another change required to obtain better repeatability of timing and maximum opening is to tighten clearance between components and subassemblies of the injector.

Dynamic Tests

Fig. 9-7 is a plot of oxygen flow rate vs. injector differential pressure at 4000 rpm. As can be expected from the above discussion, calibrations of this type can and do vary somewhat from one injector assembly build-up to another. The curve demonstrates that the injector is capable of delivering quantities of oxygen which are adequate for the required power level of the engine. Flow does increase markedly with differential pressure, and the effect of supply pressure on timing or opening point of the poppet is not great. It should be noted, however, that the flow calibration was run on the test stand with an ambient back pressure and that during engine operation the differential pressure, and thus, the flow across the injector, is effected by the cylinder pressure as well as the supply pressure. To make flow independent of cylinder pressure, it would be necessary to maintain the supply pressure sufficiently high so that choked flow is obtained for the full injector open time, i.e., supply pressure would have to be at least twice any peak combustion pressure achieved. It would not seem practicable to attempt to maintain completely choked flow; however, it is now deemed

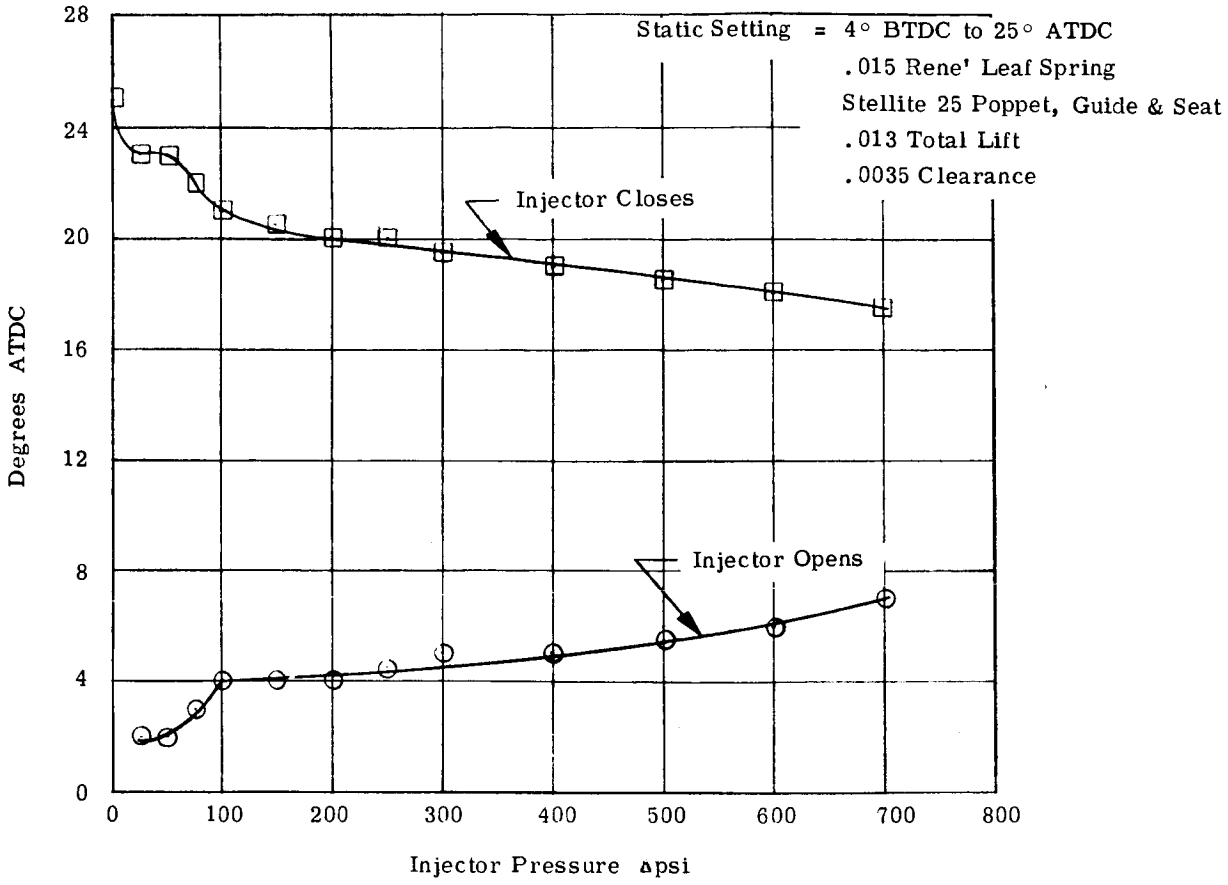

Fig. 9-6 - Duration vs. Pressure - O_2 Injector

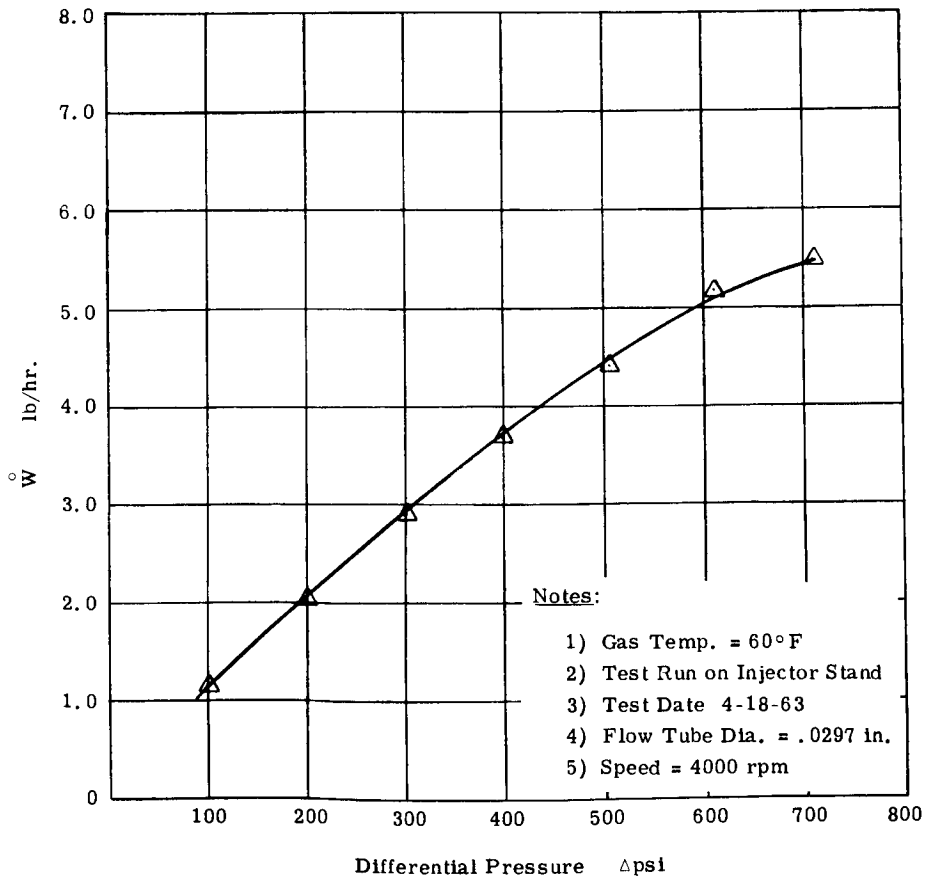

Fig. 9-7 - Mean O_2 Flow vs. Injector Inlet Pressure

advisable to try a smaller effective orifice area and higher supply pressure levels than were used during the test program.

Attempts to control the O/F ratio over a wide range during engine operation were to a great extent ineffective. For a particular valve timing arrangement, speed, and hydrogen supply, variation in oxygen supply pressure did not greatly effect O/F ratio. When the oxygen pressure was at a high level, flow would rise rapidly at first, then combustion pressure would rise rapidly and reduce the differential pressure and flow for the remainder of the injector open time. When the oxygen supply pressure was at a low level, the combustion pressure rise was less and the oxygen flow rate was more steady. In other words, the engine, within limits, had a tendency to control its O/F ratio toward a constant value.

Fig. 9-8 is a plot of oxygen flow rate vs. O_2 supply temperature. The data were obtained on the injector test stand running at 4000 rpm, and with a constant ΔP of 400 psi. The curve indicates that flow change is fairly linear with temperature, and includes the effects of both gas density and thermal expansion of the injector components.

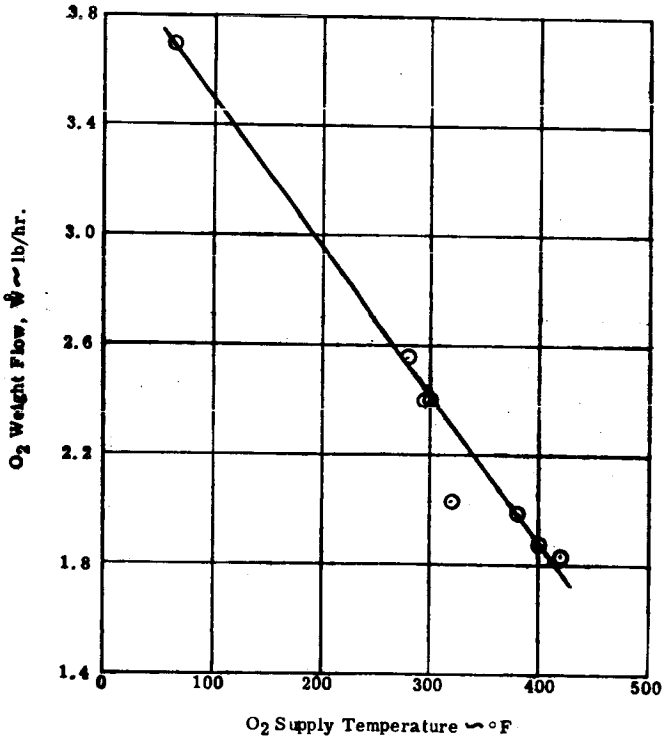

Fig. 9-8 - O_2 Flow Rate vs. O_2 Supply Temperature

9.4 Discussion of Problem Areas

9.4.1 Summary of Parts Failures

TABLE 9-1

OXYGEN INJECTOR FAILURE MODES

Failure Mode	Number of Failures	
	On Injector Test Stand	On Engine
Cam Follower Wear*	12	6
Valve Seat Retainer Failure	3	3
LT-1 Valve Guide Failure	1	1
Poppet Retainer (Leak Spring) Failure	1	2
Inconel X Flex Pivot Failure	1	1
Flame Plated Valve (Poppet) Failure		1
Valve, Guide and Seat Galling, and Poppet Leakage*	9	12
Total Running Time	31 1/4 hrs.	15.7 hrs. hot run 9 hrs. cold run

* In some cases of cam follower wear and poppet leakage, parts were reworked and reused after failure.

9.4.2 Cam Follower

During the initial engine and injector runs a serious wear problem was experienced by the cam follower. The original pivoted oxygen cam follower design had line contact with the cam, and although it appeared to follow the cam properly when the engine was turned over by hand, the cam follower had a tendency to jam into a fixed position with respect to the rocker arm. This caused point contact at the edge of the cam when side loads due to dynamic operation were applied to it. The root of the problem was ultimately traced to improper dimensioning of the drawing and unfavorable geometric proportion. The problem was eventually solved by replacing the spherical seat in the follower with a cylindrical seat so that the follower had lateral freedom to bind its natural position.

Prior to the solution of the cam follower problem, a crowned follower, which was designed to remain fixed with respect to the rocker arm, was experimentally evaluated. Wear also occurred with this design due to its inherently higher contact loading. By resorting to use of Parker Lubriting of the cam and follower surfaces, and a gear lubricant with EP additives (MIL-L-6086B), better wear characteristics were obtained during engine tests but not during injector stand tests. The crowned follower allowed considerable amount of engine testing prior to achieving a more appropriate solution of the cam follower problem, as described above.

9.4.3 Valve Seat Retainer

The valve seat retainer retains the valve guide as well as the seat. Five valve seat retainers failed during the test

program. These failures were attributed to fatigue due to repeated assembly and disassembly. The retainers were originally made of age hardened Rene' 41, which was too brittle for the flexing action that occurred during assembly and "re-setting" after disassembly. Parts later made of 17-7 PH aged at 1050°F did not fail.

9.4.4 Valve Guide and Seat

The original valve guides and seats were of a composite material, Haynes LT-1. Haynes LT-1 is a sintered composite of chromium and aluminum oxides. The brittleness of this material made it difficult to machine and handle, and proved to be unsuitable for the injector operating conditions. Two guides were probably broken during injector operation; but may have been cracked during assembly. One seat (not included in Table 9-1) was broken during assembly. After a test run with an LT-1 seat and guide, the seat was pitted and pieces of seat were present on the poppet.

For the remainder of the program, guides and seats of Haynes Stellite 25 were used and no more fracture type failures occurred. Wear type failures did continue to occur, and are described later in Section 9.4.7.

9.4.5 Poppet Retainer Spring

The retainer springs were originally made of Rene' 41 in thicknesses of .010 and .015 inches. Later, springs of .010 inch thick 17-7 PH steel were made and evaluated. One .010 Rene' 41 spring and two of the 17-7 PH springs failed during the test program. In each case the fracture

seemed to have started from a machine mark or scratch. Though it might be concluded that inspection for a smooth polished spring surface would be sufficient to prevent failure, it is felt that the spring should be subjected to further study, and possibly redesigned. The spring serves as a retainer for the outer end of the poppet and prevents rubbing contact between the poppet and rocker arm. The retainer spring should be redesigned to provide a more positive means of retention of the poppet in the rocker arm, to reduce bending stress, and to eliminate any rubbing or banging motion between the spring and the poppet.

In addition to the above, a reduction in the back lash tolerance between the poppet and the rocker arm will reduce the maximum deflection of the retainer spring and thus increase its cycle life.

9.4.6 Flex Pivot Bearing

Two Inconel X flex pivots failed after approximately 9 hours of operation. A permanent set of one of the flexible blades was noticed prior to one of the failures. Both failed pivots were examined by a representative of the supplier, and failure was attributed to excessive deflection. Because the present design does not provide an acceptable means of knowing if the pivot has an initial preload deflection when it is in the null position, and because the life of the pivot is a function of angle through which the pivot is deflected, the failures were most likely the result of an excessive initial preload. This condition should be corrected by providing an adjustment so the rocker would be locked to the pivot only after null point is found during assembly of the injector, or by

replacement of the flex pivot with another type of non-lubricated bearing.

9.4.7 Valve (Poppet), Guide, and Seat

The Stellite 25 valve, guide and seat combination is treated as one unit or assembly in order to explain the interrelated patterns of wear or galling.

As a general practice, the valve was hand lapped into the seat prior to assembly, using a rotary motion action with a levigated alumina lapping compound. This created a ball type of seat instead of a line contact. The motion of the valve in operation is not in a straight line, so a very slight rocking action of the poppet end takes place in the guide and seat. After each test run the injector was checked to see if the valve was still seating. If it was not, the injector was disassembled and the valve, guide, and seat, inspected by a microscope. It was found that valve and guide wear created extra clearance that allowed the valve to contact the valve seat off center, and cause the seat to become egg-shaped. The guide riding area of the valve would sometimes be galled or chattered, and the guide bearing surfaces would be worn and slightly galled. The seat would be galled on the elongated side of the egg-shaped seat.

Many times, the valve would be lapped into the seat again, and the same valve, guide, and seat reused for another run. This procedure would suffice for a while because the valve was seated further into the seat and allowed an unused surface of the valve to slide in the guide, and thus to some extent reduce (approximately one-half), the clearance between the guide and the poppet. It should be noted that leakage of

the valve tended to occur sooner each time parts were reused, and this became a problem toward the end of the test program, due to a shortage of useful parts. Macro photographs of a re-used poppet, guide and seat are shown in Figs. 9-9, 9-10, and 9-11, respectively.

It was suspected that part of the wear between the valve and guide was due to small concentricity misalignment resulting from the use of a separate seat and guide. By lapping the poppet to the seat after the guide was pressed onto the seat (as it is in the injector assembly), the operational life before leakage was doubled.

The seating area of one poppet was given a flame-plate coating of LW-5 (25% WC + 7% N_i + mixed W-C carbides). During test, the flame plate coating separated from the poppet after approximately 2 1/2 hours of hot, engine running time. The plated coating appeared to have come off in almost one piece. Inspection revealed that the coating had provided an excellent seating surface area and a good bearing surface for the guide. Galling did not occur. By coincidence, the failure occurred when the engine head temperature (1400° F) was equal to the maximum rated operation temperature of the LW-5 coating in an oxidizing atmosphere. The failure was attributed to a combination of thermal and impact shock in conjunction with too thick a build-up of the plating material at the end of the poppet. A coating of approximately .002 inches was desired; however, the actual thickness at the poppet end appeared to be between .010 and .020 inches.

The hardware problems described above are considered to be the most series encountered during the injector test program. The following design changes are suggested for

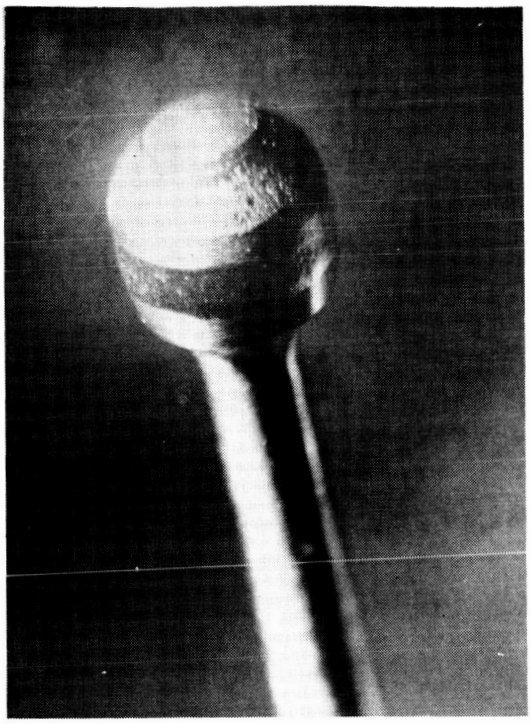

Fig. 9-9 - Reused Valve (Poppet)

Fig. 9-10 - Reused Valve Guide

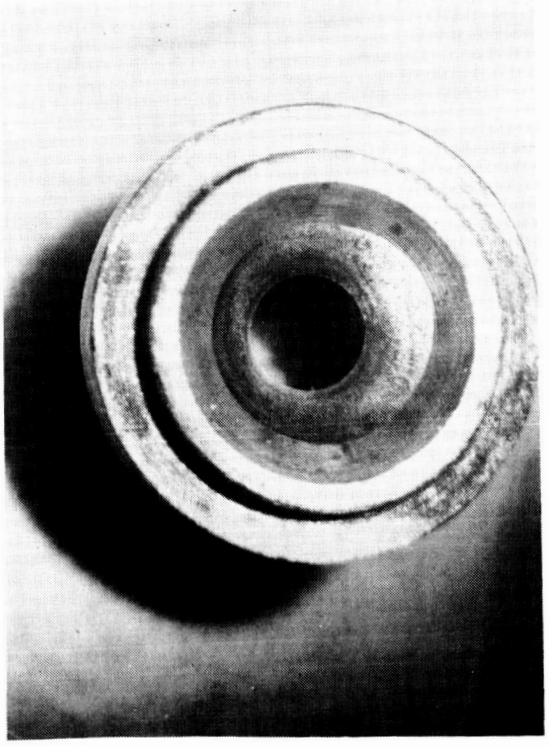

Fig. 9-11 - Reused Valve Seat

further development.

1. Provide a one-piece guide and seat (cylindrical guide and conical seat), with a poppet which has flats ground on its sides to provide gas flow area, but with sufficient cylindrical surface left for contact with the guide.

2. Evaluate several different flame plate coatings on the poppet seating and guiding surface.

3. Reduce the backlash clearance between the poppet and rocker arm.

4. If performance consideration permits, reduce poppet lift and change the cam profile to reduce the seating force on the poppet.

10.0 EXPERIMENTAL REGENERATOR TEST PROGRAM

10.1 Summary

During the regenerator test program a total of 4.48 hours of running time was accumulated. Though exhaust temperatures were below design level, and testing was hampered by large amounts of condensed steam because of high back pressure (15 psia vs. 1 psia design value), it was possible to deduce from data obtained that the design approach, based on a steady flow of 10 times maximum mean rated flow, was very conservative, and a smaller regenerator with less heat transfer surface could be used. Pressure drops across both the exhaust and hydrogen sides of the regenerator were negligible. Icing at the cold end of the regenerator presented no flow restriction problems during tests although ice did appear during warm up on one test run.

It is advisable to postpone further regenerator tests at this time until: (1) engine performance is improved so higher exhaust temperatures can be achieved (2) the engine exhaust porting is redesigned to reduce heat loss from the exhaust gas (3) a vacuum facility is available to reduce back pressure.

10.2 Test Equipment and Instrumentation

The regenerator and associated test equipment were added to the engine test stand, as shown schematically in Fig. 10-1.

The engine exhaust was connected to the regenerator with an insulated line equipped with a drain valve for sampling the exhaust condensate. Exhaust from the regenerator was

Preceding page blank

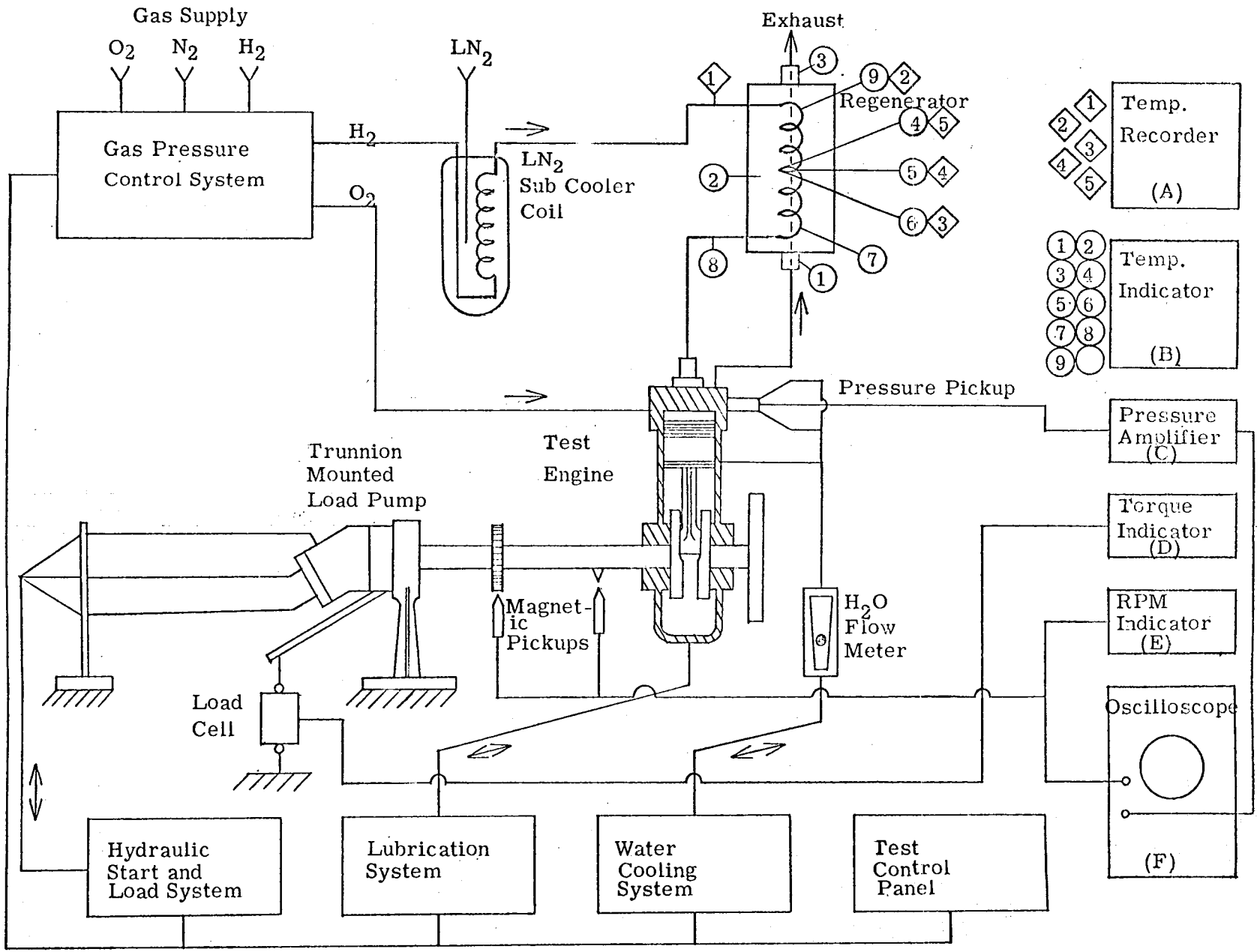

Fig. 10-1 - Engine Test Stand with Regenerator

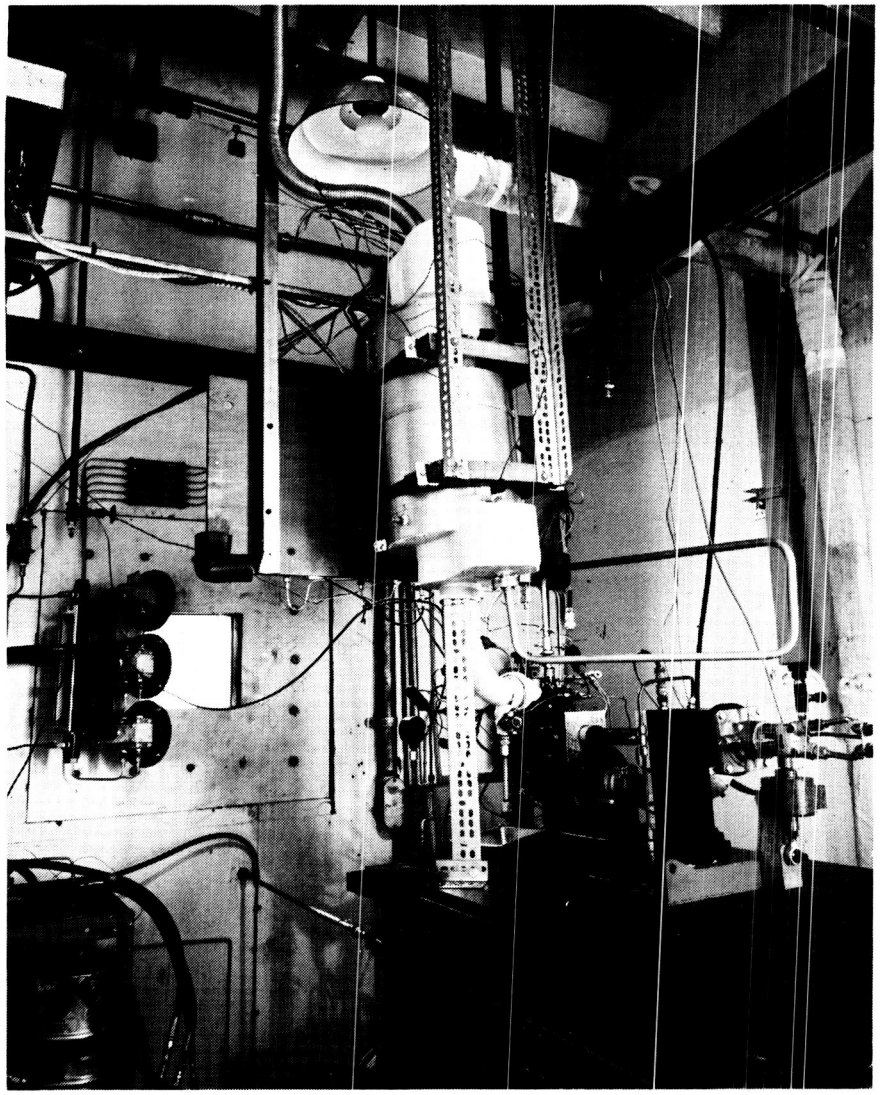

Fig. 10-2 - Regenerator Test Facility

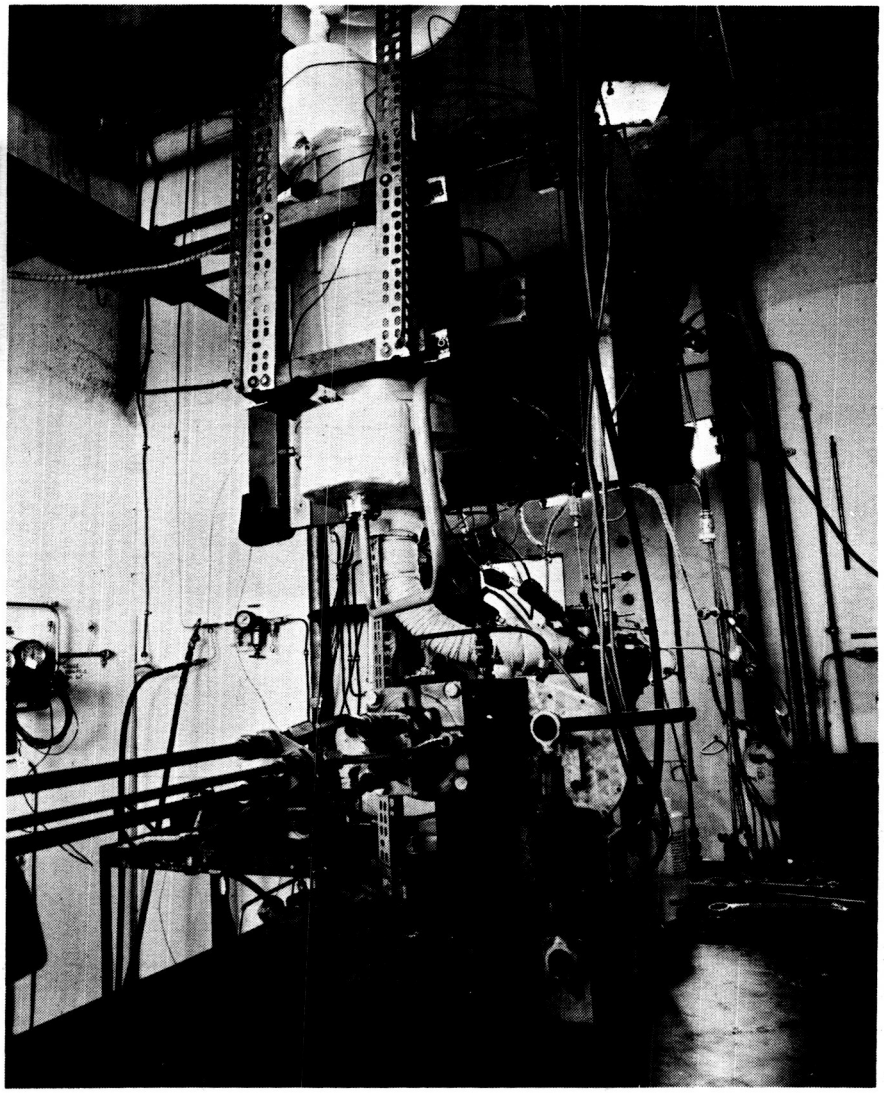

Fig. 10-3 - Regenerator Test Facility

vented to atmosphere. The hydrogen gas from the gas pressure control system was first run through a cooling coil immersed in a dewar of liquid nitrogen, then into the cold end of the regenerator tube coils, and from the regenerator into the hydrogen inlet valve of the engine.

Except for the additional temperature measurements required to determine regenerator performance the normal instrumentation and control systems used for testing the engine were also used for regenerator testing.

Photographs of the regenerator test setup are shown in Figs. 10-2 and 10-3.

Pressure drop vs. flow rate tests were run with hydrogen on both the exhaust and hydrogen side of the regenerator, as shown schematically in Fig. 10-4.

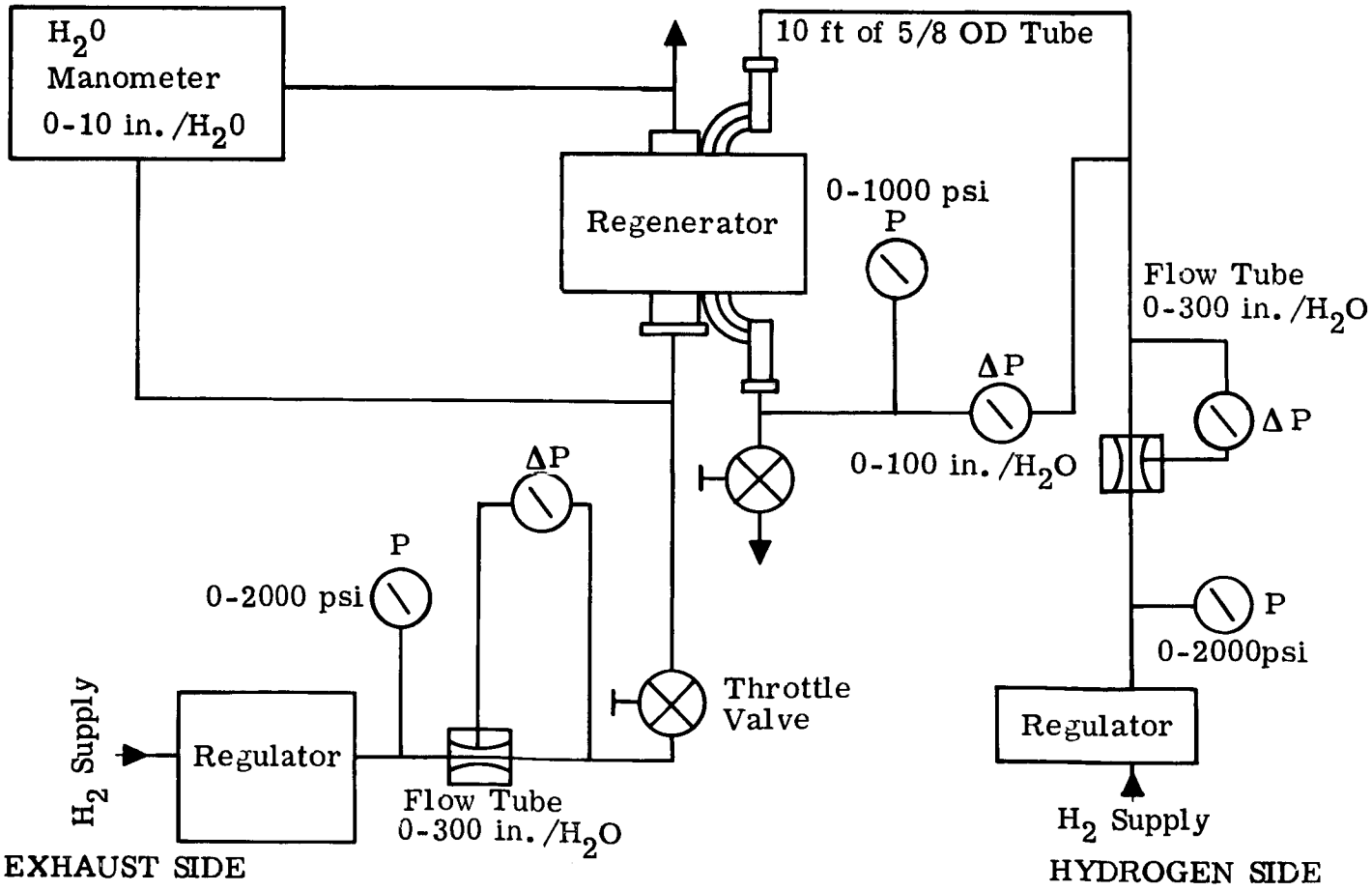

Fig. 10-4 - Schematic - Pressure Drop vs. Flow Rate Test

TABLE 10-1.

REGENERATOR TEST INSTRUMENTATION SPECIFICATIONS

Ident.	Function	Range	Accuracy	Mfr.	No.
A	Temp.	-400 to +100°F	±1%	Wheelco	8016-2500

Thermocouple Locations

1 - Hydrogen gas cold end
2 - No. 3 tube cold end
3 - No. 5 tube middle
4 - No. 3 tube middle
5 - No. 1 tube middle

B	Temp.	0-1200°F	±1/2%	Honeywell	156X63-PSI2

1 - Exhaust gas hot end
2 - Exhaust gas middle
3 - Exhaust gas cold end
4 - No. 1 tube middle
5 - No. 3 tube middle
6 - No. 5 tube middle
7 - No. 3 tube hot end
8 - Hydrogen gas hot end
9- No. 3 tube cold end

Reproduced from best available copy.

10.3 Discussion of Tests and Test Results

The test data was subject to discrepancies that preclude explicit evaluation of heat transfer coefficients. Run 1, during which inlet hydrogen was precooled with liquid nitrogen and Run 2, during which ambient hydrogen was supplied to the regenerator, indicated thet condensate was recirculating throughout the regenerator. These tests were not evaluated, but water samples were collected for evaluation during these runs. Icing occurred on the last coil during warm up of Run 1. The ice layer was very thin and did not appear to inhibit flow of the exhaust gas. During Runs 3, 4, 5, and 6, the inlet hydrogen was preheated electrically to raise the lowest temperature in the regenerator above the dew point for the partial pressure of the steam in the engine exhaust gas.

On many of the data points taken during runs 3 through 6, the exhaust gas temperature was observed to be colder than the hydrogen temperature at the cold end of the regenerator. If there is no gas leakage or secondary heat sink, a thermal balance between hydrogen and its combustion exhaust products should reflect a higher exhaust products thermal capacity rate ($\mathring{W}C_{p_{ex}} > \mathring{W}C_{p_{H_2}}$), which implies that hot end differential temperature should be less than the cold end differential temperature. For example, assume that the engine is using two (2) pounds of oxygen and one (1) pound of hydrogen per hour. The thermal capacity rate of the hydrogen side of the regenerator is 3.42 BTU per hour per °F ($\mathring{W}_{H_2}C_{p_{H_2}} = 1 \times 3.42$). The thermal capacity rate of the exhaust side of the regenerator is 3.6 BTU per hour per °F:

$$\mathring{W}_{ex}\, C_{p_{ex}} = \mathring{W}_{H_2}\, C_{p_{H_2}} + \mathring{W}_{H_2O}\, C_{p_{H_2O}} = 3/4 \times 3.42 + 2\,1/4 \times .46 \approx 3.6$$

If all the heat lost by the exhaust is transferred to the hydrogen, the temperature change of the hydrogen must be greater than the temperature change of the exhaust

$$\mathring{W}_{H_2} C_{P_{H_2}} \Delta t_{H_2} = \mathring{W}_{ex} C_{P_{ex}} \Delta t_{ex} = 3.42 \Delta t_{H_2} = 3.6 \Delta t_{ex} \therefore \Delta t_{H_2} > \Delta t_{ex}$$

Since the overall rate of temperature change with respect to regenerator length is greater for hydrogen than for the exhaust, and since at any point in the regenerator the hydrogen temperature will be lower than the exhaust temperature, the temperature difference between the two fluids must be smallest at the hot end of the regenerator (see Fig. 10-5). The fact that the data showed the cold end differential to be minimum indicates either exhaust gas leakage upstream of the regenerator, the presence of a secondary heat sink at lower temperature than the hydrogen, or both. The fact that the exhaust gas temperature was lower than the hydrogen temperature at the cold end of the regenerator definitely indicates the presence of a secondary heat sink, such as water evaporation. It was realized, that though the hydrogen had been preheated sufficiently to maintain the cold end hydrogen tube temperature above dew point, water condensed in the non-insulated duct, which was used to carry the exhaust gas from test cell, could run back into the exhaust port of the regenerator and revaporize in the location where the exhaust gas exit temperature is measured, and thus drop its temperature below that of the inlet hydrogen temperature. The fact that at some of the data points, the cold end tube temperature was equal to the hydrogen inlet temperature, and for others, was somewhat lower than inlet hydrogen temperature, indicates that the condensate recirculation condition existed somewhat down into the area of the cold end hydrogen coils. For the above reason, it was concluded that the condensate recirculation did not extend as far down as the middle of the

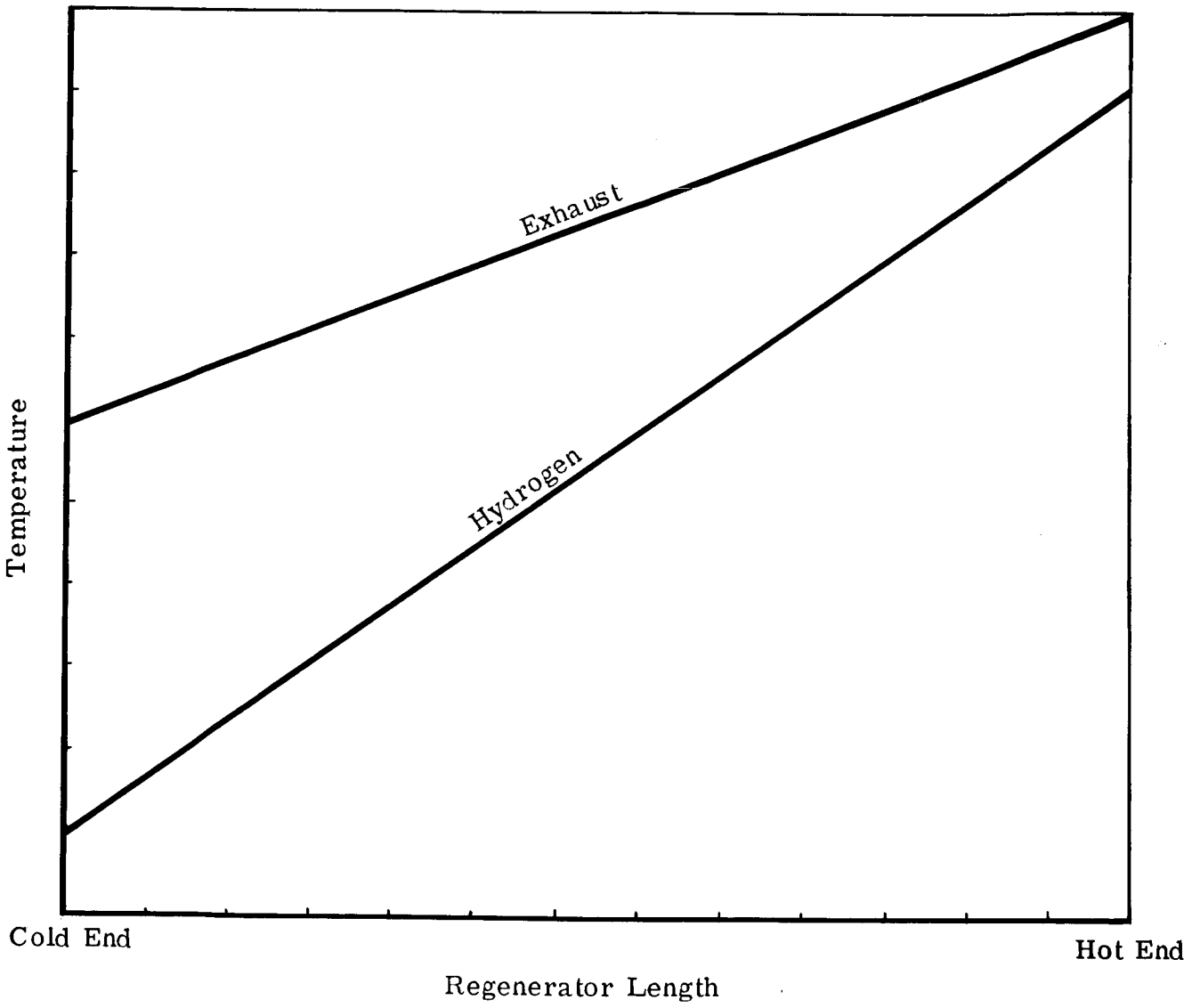

Fig. 10-5 - Temperature Rate vs. Regenerator Length

regenerator, and heat transfer coefficients were calculated for the hot half of the regenerator only.

This was done by considering actual test readings of the hot end exhaust gas temperature, the middle exhaust gas temperature, and the hot end hydrogen temperature; and assuming the heat capacity of the exhaust side equal to the hydrogen side, and calculating the middle hydrogen temperature, the log mean temperature difference, and the heat transfer coefficient. A tabulation of heat transfer coefficients calculated by this method are compiled below:

Run	Data Point	Heat Transfer Coefficient ($\frac{BTU}{hr.ft^2\text{-}°F}$)
3	8550	6.0
4	8570	5.85
6	1:45	6.12
6	8636	6.45

For comparison, a theoretical heat transfer coefficient of 8.54 BTU per hr.-ft^2-°F was calculated for the regenerator (for its present physical configuration), assuming a thermal transfer capacity of 5840 BTU per hr. with a steady hydrogen flow rate of 1.41 lb/hr., an O_2/H_2 weight ratio of 2.0, and a log mean temperature difference of 188°F. The original design was determined by a heat transfer coefficient of 29 BTU per hr.-ft^2-°F, which was calculated, assuming a square wave pulse in which 10 times the mean flow is passing only 1/10 of the time. This condition was assumed since the exhaust ports are open only during approximately 30° per revolution. A steady state flow level, which would transmit the same amount of heat per unit time, would require a

coefficient of only 2.9 BTU/hr.-ft^2-°F. (In the first case, no heat is being transferred during the 9/10 of the time that no flow occurs.)

Though realizing that test data were not at design conditions (flow rate, O_2/H_2 ratio, and temperature levels), the fact that the test values (nominally approximately equal to 6), of heat transfer coefficient are closer to the 8.54 value than to the 2.9 value, indicates that the original design approach was conservative, i.e., the regenerator has more heat transfer surface area than necessary.

Hindsight indicates that the condensate recirculation problem would have been less severe, and somewhat better results could have been obtained had the regenerator been hung with the hot end up and the cold end down. It was hung with the cold end up to obtain the shortest possible exhaust gas line from the engine, for ease of installation, to collect a water sample, and to prevent fouling from engine oil.

Though the pressure drop vs. flow rate tests were not run at flows as high as 10 times rated flow, the results indicate that the pressure drops are negligible. On the exhaust side, which can effect engine performance most, the highest flow rate was 6.06 lb/hr. of hydrogen and the pressure drop was 0.011 psi. A maximum pressure drop of 1.93 psi was obtained on the hydrogen side of the regenerator for a hydrogen flow rate of 6.89 lbs/hr. It should be noted, that to prevent the breaking of a critical joint and incurring leakage later, the ΔP of the hydrogen side was measured across the regenerator in series with a 10-foot length of line, which should have a pressure

drop of the same order of magnitude pressure drop as the regenerator itself.

Further testing of the regenerator should be postponed until; (1) the engine performance is improved to the point that higher exhaust temperatures are achieved and (2) until the engine exhaust ports are changed, to prevent the loss of heat to cooler areas of the engine before the exhaust gas is delivered to the regenerator. It was realized during the test program that actual size and weight of the heat exchanger will have a relatively minor effect upon the temperature to which the hydrogen is raised, compared to the effect resulting from the method the exhaust gas is transported from the cylinder to the regenerator; i.e., no matter how well the regenerator is designed, it cannot heat the hydrogen if the temperature of the exhaust gas is lost before it gets to the regenerator.

The water samples collected during run numbers 1 and 2 were sent to the Smith-Emery Company for analysis. The oil was extracted from the sample, the solids were allowed to settle out, and a portion of the remaining water was analyzed. The Smith-Emery report is shown as Fig. 10-6. Though it may be possible to put this type water to some use aboard a space vehicle, it should not be considered for drinking because of the borate content. The impurities found in the water can be attributed mainly to the engine lubrication oil and matter resulting from fabrication of the regenerator.

In order to obtain a clear water sample on board a space vehicle from a fluid similar to the one extracted during the test, it would be necessary to centrifuge and/or filter. In

RICHMOND 9-3411

SMITH-EMERY COMPANY

FORM C-4 1-63 LC

CHEMISTS • TESTING • INSPECTION • ENGINEERS

781 EAST WASHINGTON BOULEVARD

LOS ANGELES 21, CALIFORNIA

ALL REPORTS ARE SUBMITTED AS THE CONFIDENTIAL PROPERTY OF CLIENTS. AUTHORIZATION FOR PUBLICATION OF OUR REPORTS, CONCLUSIONS, OR EXTRACTS FROM OR REGARDING THEM IS RESERVED PENDING OUR WRITTEN APPROVAL AS A MUTUAL PROTECTION TO CLIENTS, THE PUBLIC AND OURSELVES.

FILE NO.: 2066-63
CLIENT: VICKERS INCORPORATED

ADDRESS: 3201 LOMITA BLVD.
TORRANCE, CALIFORNIA
ATTENTION: A. GARCIA

DATE RECEIVED: APRIL 18, 1963
REPORTED: MAY 22, 1963
SAMPLE: WATER
SUBMITTED BY: CLIENT
LABORATORY NO.: C-506893
MARKED: "621-816-1-MET. LAB"
SHIPPER #85913

REPORT OF WATER ANALYSIS

ANALYSIS OF DISSOLVED SOLIDS		PARTS PER MILLION	HYPOTHETICAL COMBINATIONS		PARTS PER MILLION
SILICA	(SiO_2)	16.0	SILICA	SiO_2	16.0
ALUMINUM OXIDE	(Al_2O_3)	TRACE	ALUMINUM OXIDE	Al_2O_3	TRACE
IRON OXIDE	(Fe_2O_3)	TRACE	IRON OXIDE	Fe_2O_3	TRACE
CALCIUM	(CA)	12.8	CALCIUM BICARBONATE	$CA(HCO_3)_2$	51.9
MAGNESIUM	(MG)	4.9	CALCIUM SULFATE	$CaSO_4$	NONE
SODIUM	(NA)	45.0	CALCIUM CHLORIDE	$CaCL_2$	NONE
SULFATE	(SO_4)	90.5	MAGNESIUM BICARBONATE	$Mg(HCO_3)_2$	29.3
CHLORIDE	(CL)	60.0	MAGNESIUM SULFATE	$MgSO_4$	NONE
CARBONATE	(CO_3)	NONE	MAGNESIUM CHLORIDE	$MgCL_2$	NONE
BICARBONATE	(HCO_3)	97.6	SODIUM BICARBONATE	$NaHCO_3$	NONE
NITRATE	(NO_3)	TRACE	SODIUM CARBONATE	Na_2CO_3	NONE
NITRITE	(NO_2)	N.D.	SODIUM SULFATE	Na_2SO_4	NONE
BORATE	(B_4O_7)	437.9	SODIUM CHLORIDE	NACL	NONE
POTASSIUM	K	30.0	SODIUM NITRATE	$NaNO_3$	NONE
AMMONIUM	NH_4	117.0	SODIUM NITRITE	$NaNO_2$	N.D.
			SODIUM BORATE	$Na_2B_4O_7$	327.9
			AMMONIUM COMPOUNDS (SEE BELOW)		486.6
TOTAL SOLIDS		911.7	TOTAL SOLIDS		911.7
TOTAL NON VOLATILE SOLIDS		862.1	TOTAL HARDNESS AS $CaCO_3$		52.0

DETERMINATIONS

SPECIFIC CONDUCTANCE MICROMHOS/CM	2873.6	TURBIDITY	50
HYDROGEN ION CONCENTRATION pH	6.6	COLOR	30
BORON (B) IN PPM	122.2	ODOR	CHEMICAL O
FLUORIDE (F) IN PPM	N.D.	TASTE	N.D.
LANGELIER INDEX	N.D.	SUSPENDED MATTER	N.D.

AMMONIUM BICARBONATE	NH_4HCO_3	44.3 PPM
AMMONIUM SULFATE	$(NH_4)_2SO_4$	124.2 PPM
AMMONIUM CHLORIDE	NH_4CL	90.4 PPM
AMMONIUM BORATE	$Na_2B_4O_7$	227.7 PPM
TOTAL		486.6

RESPECTFULLY SUBMITTED
SMITH-EMERY COMPANY

BY [signature]

6 VICKERS INCORPORATED
TLL

Fig. 10-6 - Water Analysis Report

any event it is felt that engine oil consumption will be reduced and the cleanliness of the system will be improved in the flight weight system.

11.0 EXPERIMENTAL COMPRESSOR TEST PROGRAM

11.1 Summary

During the compressor test program the compressor test hardware, the compressor test facility, and instrumentation were developed. A total of 11.6 hours of compressor running time was accumulated. Four different piston compression rings were evaluated in the first stage of the compressor. Performance was poor in each case, however, the "T" type rings supplied by Mace Corp. showed the most promise.

The following conclusions were drawn from the compressor test program:

1. Flexural members should not be used in the compressor drive linkage for the following reasons:

   a. Adequate fatigue life will probably require more extensive development than other design solutions.

   b. Non-lubricated, non-flexural drives can be constructed, and the bearing problems should be less severe than those of the compressor piston rings. For a single stage compressor the drive linkage can be external and lubricated.

   c. The flexural pivot originally recommended and now in use, according to the vendor's more recent test data, will not meet the required cycle life.

   d. The flexural drive members, particularly the flex pivot, deflect considerably as a function of load in the direction of piston travel. This

condition causes the clearance volume to vary with discharge pressure and speed from the value to which was adjusted statically, and thus makes performance difficult to evaluate.

2. New test fixtures and test hardware should be fabricated to facilitate use of the existing compressor hardware for development tests on piston rings and ring grooves, valving, and drive mechanism prior to performance testing of a complete compressor unit.

3. Every effort should be made to achieve the desired compression ratio in a single stage hydrogen compressor because thermodynamic efficiency advantage is not obtained by staging when the interstage temperature is below ambient.

11.2 Test Set-Up and Instrumentation

The compressor test facility is shown schematically in Fig. 11-1. The test circuit consists of the following items:

A three-way solenoid valve to select nitrogen or hydrogen gas, a pressure regulator to control upstream orifice pressure, a 10-micron filter, the inlet flow measuring orifice, a low pressure regulator to control compressor inlet pressure, a liquid nitrogen-to-gas cooling coil, a mercury manometer to measure absolute inlet pressure, valving to allow compressor case leakage to be vented through a flow meter or return it to the first stage inlet line, pressure gages to measure case pressure, interstage pressure, and outlet pressure, an acoustic filter to dampen flow pulsations on the outlet line,

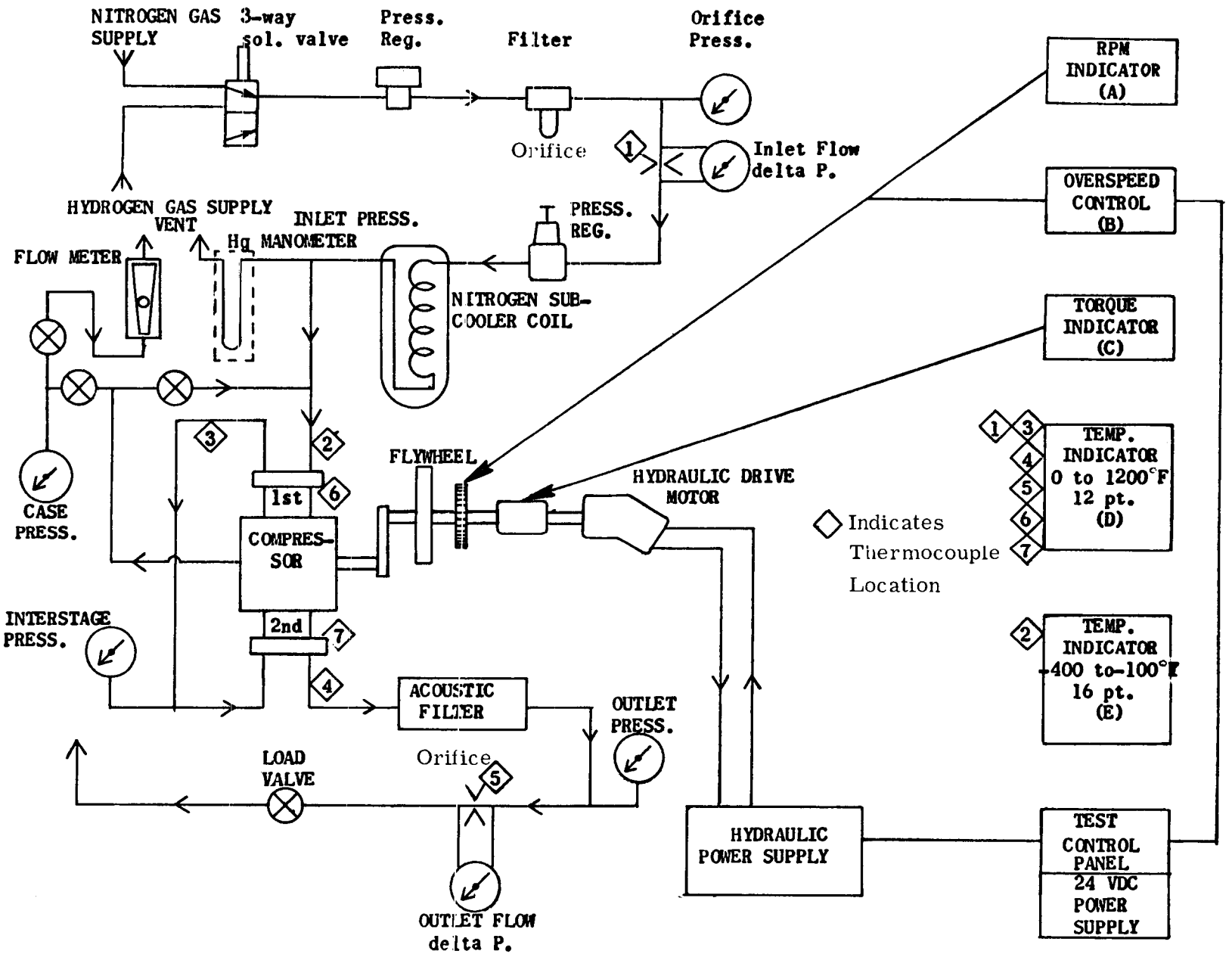

Fig. 11-1 - Schematic - Compressor Test Facility

and a load valve to control outlet flow and pressure. Drive power is supplied by a hydraulic power supply through a hydraulic motor and a 0 to 200 inch-lb. torque pick-up, incorporating a magnetic speed pickup.

Instrumentation for speed, torque, and temperatures is listed in Table 11-1 and in Fig. 11-1.

TABLE 11-1

COMPRESSOR TEST INSTRUMENTATION SPECIFICATIONS

Ident.	Function	Range	Accuracy	Mfg.	No.
A	rpm	0-100,000	± 1 rpm	Erie	720
B	Overspeed Control	100,000 rpm	± 1%	Hewlett-Packard	500B
C	Torque	0-100 lb.	± 1/4%	Vickers	54616-X
D	Temp.	0 to 1200°F	± 1/2%	Honeywell	156X63-PSI2
E	Temp.	-400° to	± 1%	Wheelco	8016-2500

Pressure gage accuracies - 1/4 of 1% of full scale

Fig. 11-2 is a photograph of the instrumentation set-up and Fig. 11-3 is a view of the compressor test stand.

11.3 Discussion of Tests

A total of 11.6 hours of compressor running time was accumulated during the test program. One quarter hour of this time

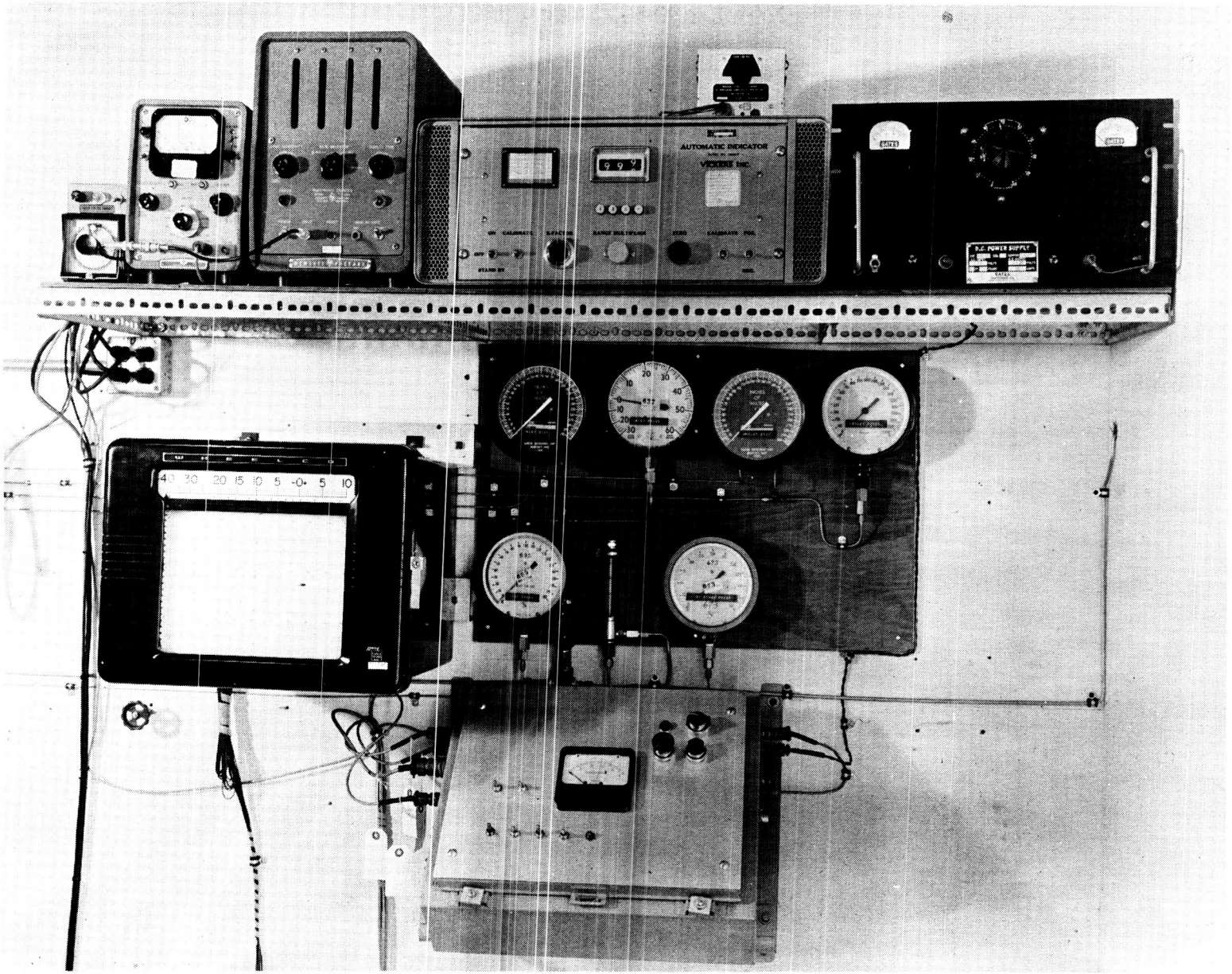

Fig. 11-2 - Compressor Test Instrumentation

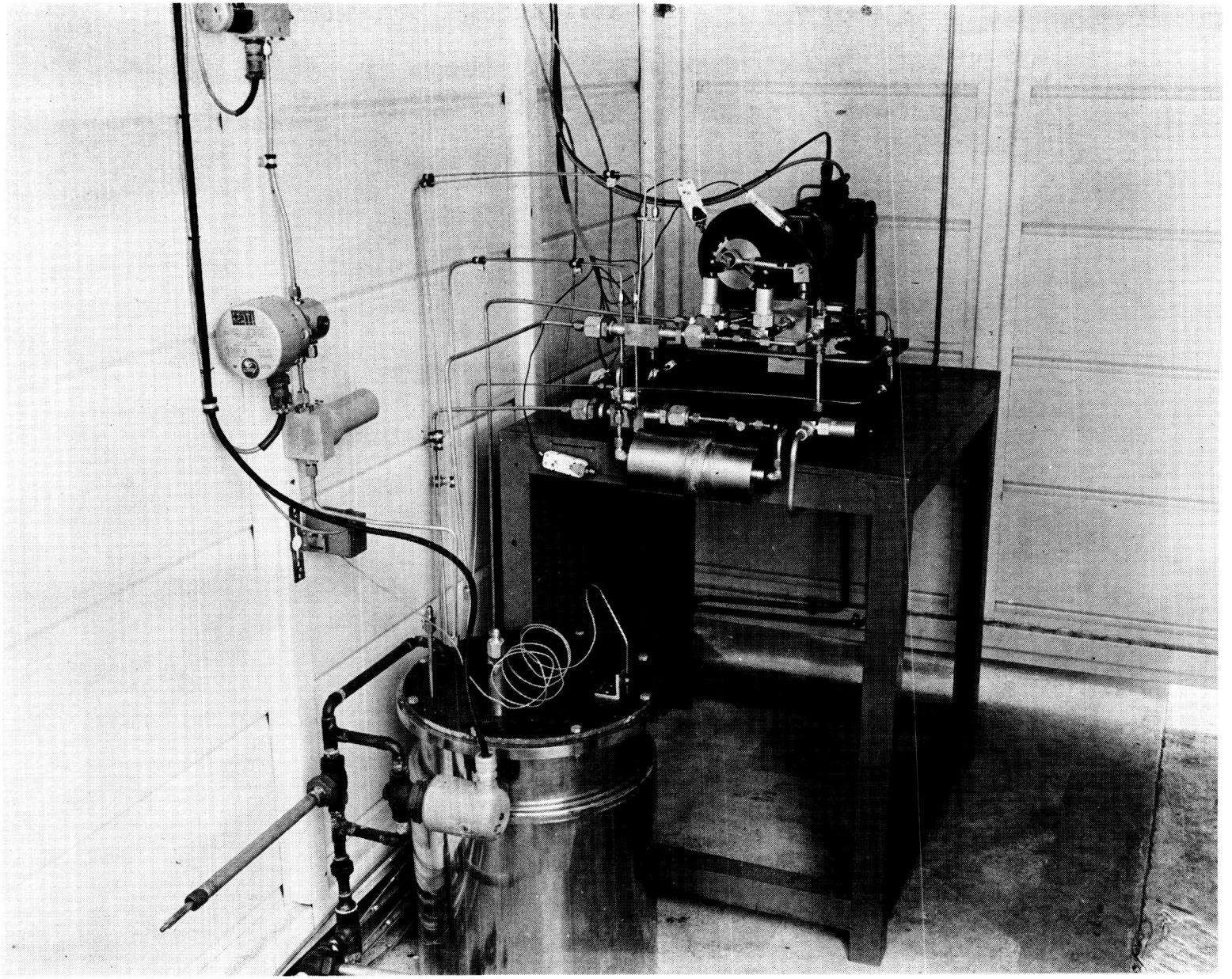

Fig. 11-3 - Compressor Test Stand

was for checkout of the test stand drive circuit. During the remainder of the time, the first stage of the compressor was evaluated with the second stage head removed. The first 1 1/2 hours of first stage operation was with nitrogen and the remainder was with hydrogen at speeds from 1000 to 4000 rpm.

Four (4) types of piston compression rings were evaluated. The rings are described in Table 11-2 and are shown in Figs. 11-4 through 11-7.

TABLE 11-2

PISTON COMPRESSION RINGS

Company	Type	Material
Koppers Company	Rectangular cross section; wide in the axial direction with a flat cross section steel expander ring.	Glass filled teflon
Cook Company	Same as Above	Same as Above
Mace Corporation	Two rectangular cross section rings, narrow in the axial direction, separated and retained by a Kel-F tee shaped expander ring.	Virgin teflon
Mace Corporation	Same as Above	"Fluoroloy" (Teflon base; mixture contains glass, iron oxide and molydisulfide).

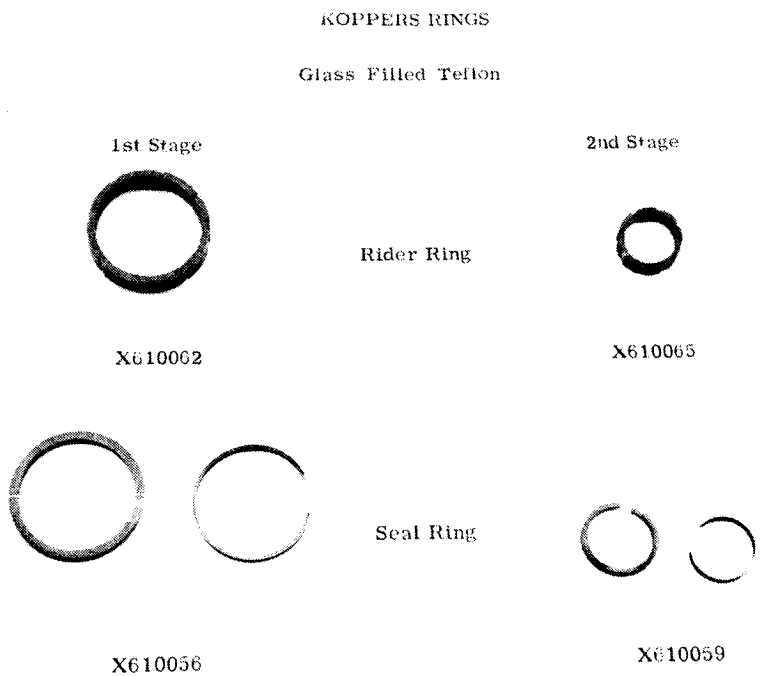

Fig. 11-4 - Koppers Piston Compression Rings

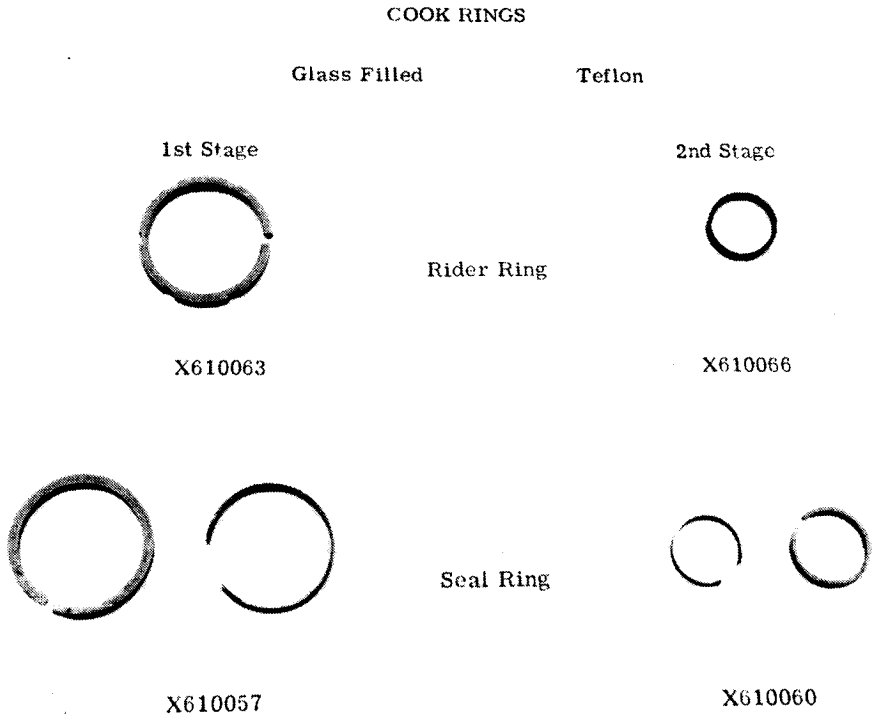

Fig. 11-5 - Cook Piston Compression Rings

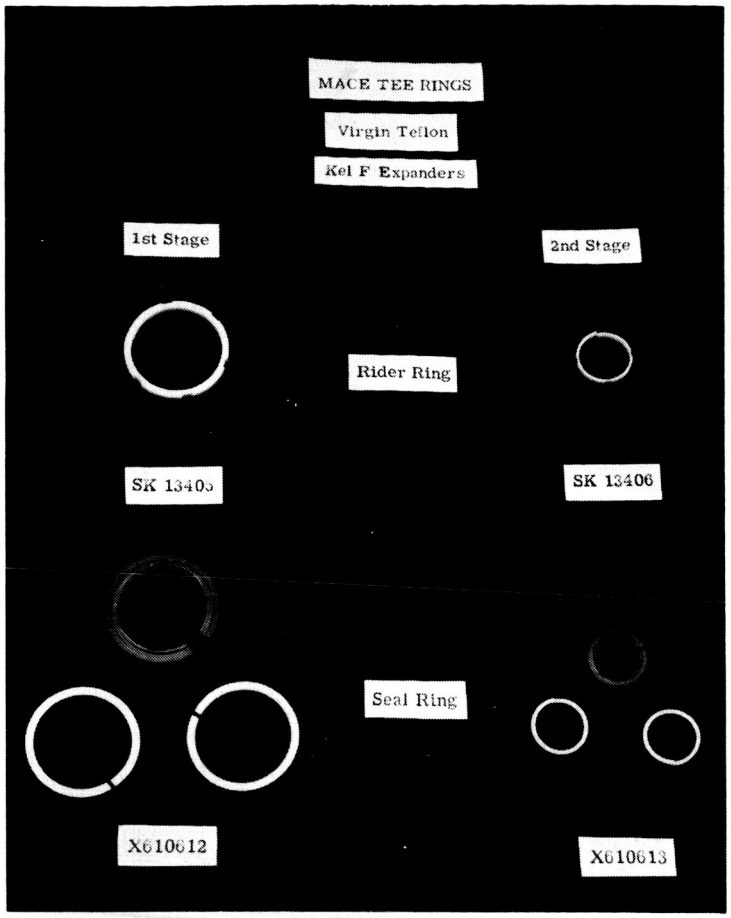

Fig. 11-6 - Mace Piston Compression Rings (Teflon)

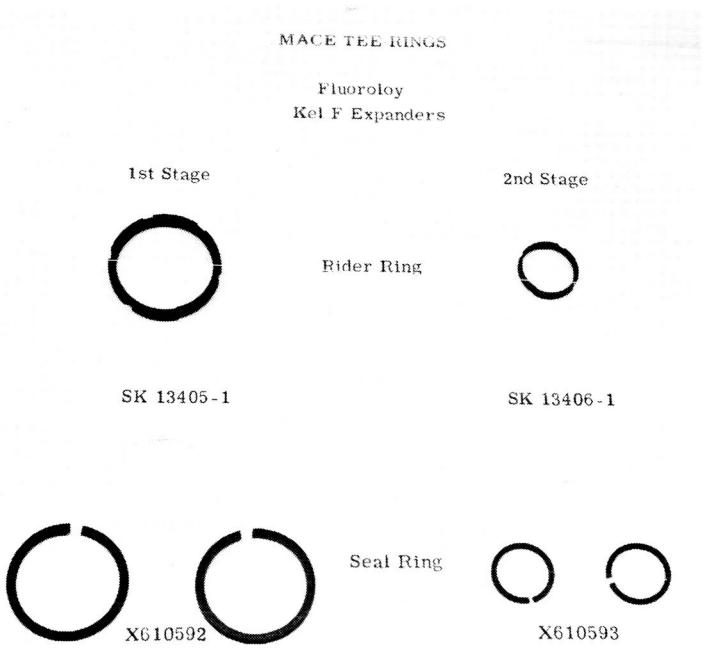

Fig. 11-7 - Mace Piston Compression Rings (Fluoroloy)

Koppers one piece piston rings of glass filled teflon with metal expander rings were used on the first compressor assembly. The first set of these rings was damaged during assembly and would not seal. A new set of Koppers rings was fitted into a cylinder bore and the fit observed against a light. This inspection revealed that from 5 to 10% of peripheral ring surface would have to be worn away before a satisfactory seal could be expected. Because of a failure (described later), which damaged the only finished piston with the proper ring groove dimensions, all work with Koppers rings was discontinued at this point. A second piston assembly was installed, using glass filled teflon Cook rings of the same configuration but different dimensions. The Cook rings gave a much better seal to the cylinder wall, but a very short duration break-in run produced a large quantity of white powder worn from the rings, packed in the space between the ring and groove. This particular grade of glass filled teflon appeared to be unsuitable for this application.

Testing with the Cook rings was discontinued and Mace Tee rings, designed to fit the same ring grooves, were tested on the same piston assembly. The Tee ring used a Kel-F, Tee shaped expander with two virgin teflon seal rings. Glass, iron oxide, and molydisulfide filled teflon (fluoroloy) seal rings were also tested on the Kel-F expander Tee ring.

Cook rider rings were used during the initial evaluation of the Mace seal rings. After a rest run the space between first stage seal rings and groove were packed with powder from the Cook rider ring. During the test, ring leakage increased rapidly with time. Part of the degradation was attributed to the relatively rough (10 to 16 micro inch RMS), surface finish of the cylinder bore (recommended for the Cook and Koppers ring). The Mace

seal rings were then tested with Fluoroloy rider rings, and with a cylinder bore finish of 2 to 4 micro inch RMS. After the tests it was found that the Kel-F Tee expander was not holding the seal ring against first stage cylinder bore. The seal ring thickness was reduced to allow pressure to build up under expander ring. This did not reduce leakage.

Although satisfactory performance was not obtained with Mace rings during first stage operation, it is believed that they can be made to seal properly by increasing the depth of seal ring grooves to allow for addition of a metallic expander beneath the Kel-F Tee ring (this is a recommended practice with Mace type rings). This was not done initially because of the time delay required to remachine the piston, and the piston could not be used with Cook rings after machining. The Mace rings were tested before the actual test run by placing the palm of the hand or a plastic film over the end of the open cylinder and moving the piston. They exhibited excellent static sealing properties during this check, while the Cook and Koppers rings demonstrated almost no compression during similar tests. The Mace second state rings were run in the compressor unloaded (with head off), while the first stage was being run for evaluation of the Mace first stage rings. After completion of the test runs, both the first and second stage rings were subjected to the static compression test. The first stage rings had lost their sealing ability, but the static compression of the second stage rings was still excellent. The fact that the second stage rings were not loaded during test may have contributed to the results of the test, but it is believed that the retension of sealing ability of the second stage ring was due to their smaller diameter and stiffer Kel-F Tee expander ring.

After approximately 11 hours of first stage running, both the first and second stages were run in series. The wire cage drive assembly failed before a complete set of data could be taken; however, pressures were observed to be approximately as follows; 15 psia inlet, 50 psig first stage outlet, and 800 psig second stage outlet. These pressures indicate that second stage performance was much superior to first stage performance.

11.4 Failures

In addition to the piston ring failures previously described, two major hardware failures occurred during the compressor test program. During Run No. 2, while the compressor first stage was being run at 4000 rpm, vibration caused loosening of the screw holding the piston to the flex drive assembly. The piston hit the cylinder head, causing failure of the test stand drive linkage, the piston, the flex pivot, and the wire cage assembly.

The failure of the wire cage drive assembly during two stage operation of the compressor is attributed to high outside fiber stress at the base of the wire columns. During the second stage compression stroke the wire cage assembly is loaded in both tension and bending. Though the wire cage assembly does not lend itself to an exact stress analysis, it was conservatively assumed that the force due to a 800 psig second stage pressure, only, was equally distributed among the nine cage assembly wires and the wires were fixed at piston junction end, and that the tension and deflection loads were applied through at pin connection at the other end. Analysis based on the above assumptions indicated that the outside fiber stress of the wires would be beyond yield. The failed wire cage assembly is shown in Fig. 11-8.

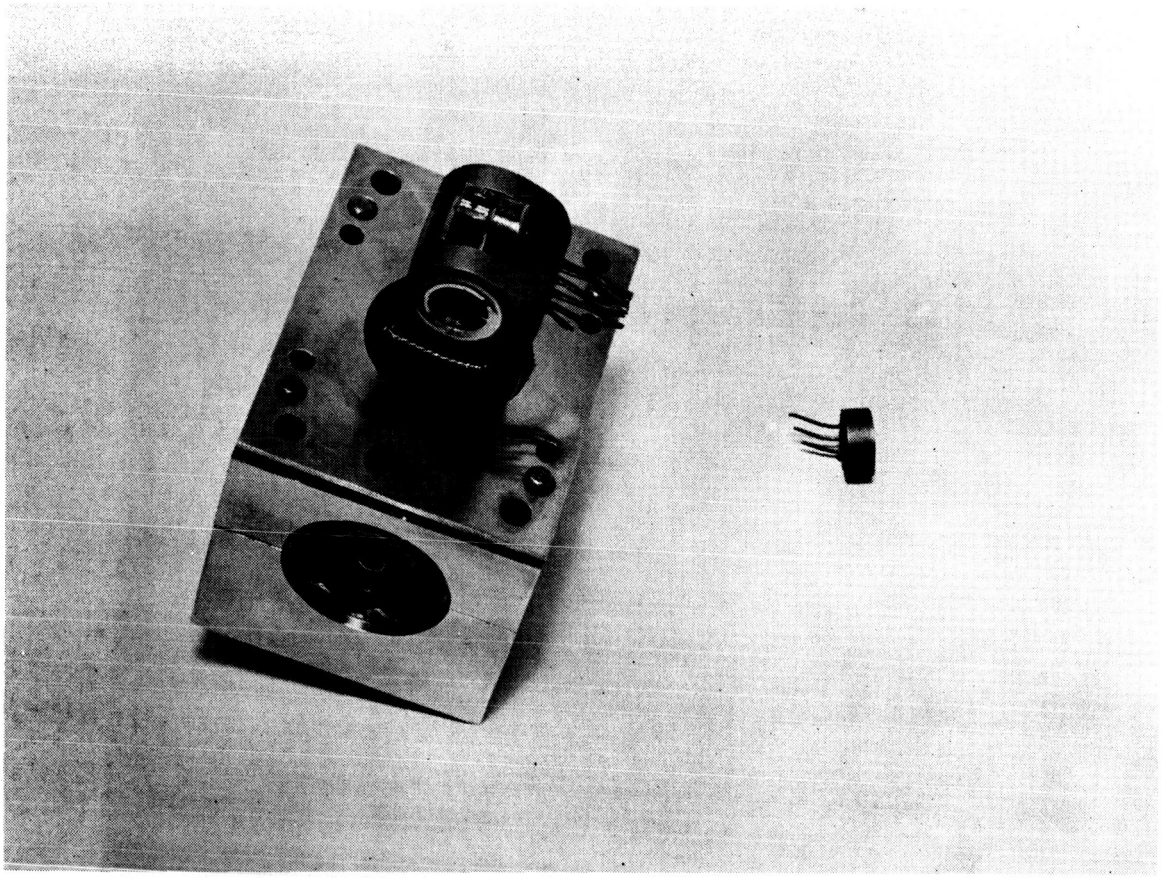

Fig. 11-8 - Failed Wire Cage Assembly

11.5 Discussion of Design and Redesign

Some minor redesign and rework was done on the first stage outlet valve to prevent poppet sticking and leakage to inlet. For future testing, the first stage cylinder head design should be changed so there is no possibility of leakage from the discharge passage to the inlet passage, and so the inlet, outlet, and relief valves can be developed as separate units.

When it was learned from the Bendix Corporation that their recent test data indicated that the life expectancy of the flex pivot would be considerably less than the original estimate, a floating piston pin assembly (shown in Fig. 11-9), consisting of a nitrited stainless steel pin and teflon filled bronze bushings, was designed and fabricated to replace it. The wire cage assembly failed before this design could be evaluated. After

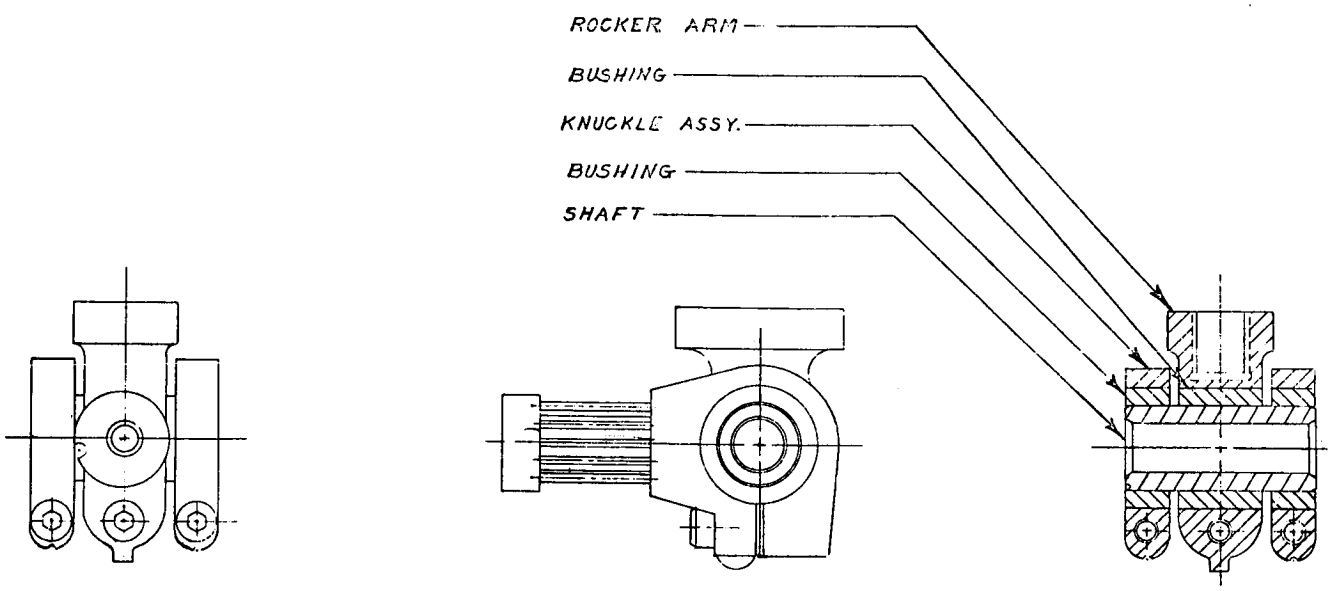

Fig. 11-9 - Floating Piston Pin Assembly

the failure of the wire cage, it was decided that all flexural members should be removed from the compressor drive mechanism. In addition to the life limitation of flexural members, the property of center deflection under load makes them undesirable. Bendix indicated that the larger pivot now recommended to meet the life requirement would have a center deflection of approximately .007 inch under first stage compression load. The deflection under load data of the pivot now being used was not available. In any event, deflection of .005 to .010 inch will greatly effect the clearance volume and discharge pressure of the compressor.

The adaptability of the present compressor components, and the addition of a few new components and test fixtures, will allow for separate development of the drive linkage, rings, and valving, as is now deemed advisable.

APPENDIX A

APPENDIX A

STATEMENT OF WORK

1. OBJECTIVE:

The purpose of this program is to conduct an engineering study culminating in a layout of an auxiliary electric power generation supply system representing an optimization of the factors derived in the study program, and to develop and test selected components.

2. REQUIREMENTS:

2.1 GENERAL REQUIREMENTS:

The Contractor shall perform engineering studies, design, fabrication, and test work on the development of an auxiliary electric power generation supply system employing a hydrogen-oxygen internal combustion engine as a prime mover, capable of reliable operation under zero g conditions for a minimum of 350 hours, and under conditions of shock and vibration imposed by a typical space vehicle; having an average power output of 2 kw, and a peak of 3 kw; being able to accept propellants either from its own primary tankage, from propulsion tank boil-off, or from propulsion tank residual gas-liquid mixture.

The basic design philosophy shall be guided by three considerations: reliability, simplicity and minimum weight penalty on the propulsion system for earth take off.

The work shall be conducted in close coordination with work currently being carried out under Air Force Contract for the development of a similar engine. Work on this Contract shall not, except as specifically requested, duplicate work on the Air Force Contract, but shall be carried out so that the latter will augment the development of the NASA engine.

In order to carry out the required engineering study, it is recognized that the need exists for certain data which cannot be derived by analytical methods. In those instances where empirical methods are required, the Contractor shall design, fabricate, assemble, and operate for testing purposes the simplest possible apparatus commensurate with the test objectives. It is not the intent of these tests to develop refined "hardware", but rather to provide the essential empirical information required to supplement the analytical studies. Areas where empirical studies may be required include:

a) demonstration of feasibility of those items which are basic to system operation
b) obtaining applicable data otherwise unobtainable, but essential to the preliminary design effect
c) obtaining operating experience

The Contractor shall conduct the study and development program essentially as outlined in Paragraph 2.2 of this EXHIBIT "A".

2.2 SPECIFIC REQUIREMENTS:

TASK I ANALYTICAL AND DESIGN STUDIES

The Contractor shall:

A. Perform Parametric Studies to determine the effect of propellant supply conditions, (temperature, pressure, quality, mixture ratio, mission duration and quantitative availability) on:

1. System configurations
2. System weight and volume
3. B.S.P.C.
4. Total changeable propellant consumption for mission
5. Total propellant consumption for mission
6. Engine types -
   a. Pressure fed - internal combustion
   b. Internal compression - internal combustion
   c. External combustion
7. Component requirements

B. Perform System Adaptability Studies for the following missions:

1. Earth-to-Lunar
2. Earth Orbital
3. Lunar Roving Vehicle

C. Perform Preliminary Design Studies, including layouts, material selection, stress analysis and drive system of:

1. Hydrogen compressor
2. Oxygen compressor
3. Oxygen injector

D. Study Power Modulation Techniques

1. Variable pressure
2. Variable opening of valves
3. Variable phasing of valves
4. Multiphase oxygen injection
5. Variable stroke
6. Variable clearance volume
7. Combinations of above
8. Other techniques

E. Design and/or select control components

1. Mixture ratio control
2. Propellant pressure regulator
3. Speed governor
4. Temperature control
5. Compressor control
6. Pilot control and overide

F. Perform Engine Configuration Studies

1. Cooling system
   a. Utilization of on-board cooling loop
   b. Hydrogen cooling
2. Injector location and orientation
3. Minimization of heat rejection
4. Lubrication system design for zero g
5. Dynamic balancing
6. Vibration isolation

G. Perform Regenerator Design Study, including thermal analysis for maximum effectiveness, materials review and stress analysis.

H. Perform Design Study of Electrical Components

1. Generator
   a. Cooling
   b. Speed
   c. Frequency
   d. Overload protection
   e. Regulation of voltage and frequency
   f. Shielding

I. Design Shielded Ignition System

J. Perform Starter Design Study

1. Start-up and shut-down

K. Perform Control System Studies

1. Synthesis of Control System
2. Analog Computer Study for:
   a. Response to load changes
   b. Stability
   c. Data generation for control components
   d. Control sensor determination

L. Perform Preliminary Reliability and Failure Studies

1. Estimate M.T.B.F. for significant components
2. Determine redundancy requirements
3. Failure analysis

   a. Failure mode and frequency estimates
   b. Identification of catastrophic failure
   c. Effect of various modes of failure

4. Recommend fail-safe techniques

M. Perform System Design

1. System Assembly drawing
2. Functional Schematic drawing showing temperatures and pressures at critical points
3. Flow Diagram
4. Control schematic
5. Electrical schematic
6. Wooden mock-up of flight weight system

TASK II MATERIAL PROBLEMS

The Contractor shall provide the services of a materials expert to select and evaluate appropriate materials and study component failures as a materials problem.

TASK III PROTOTYPE DESIGN, FABRICATION AND TESTING OF CRITICAL COMPONENTS

The Contractor shall:

A. Design, build and test compressor (leakage, friction, lubrication tests and efficiency tests)

B. Design, build and test regenerator

1. Determine effectiveness
2. Demonstrate structural integrity at design temperature distribution

C. Build new engine to Air Force Aeronautical Systems Division drawing, except that improvements based on Air Force Aeronautical Systems Division tests shall be incorporated.

D. Perform tests contingent upon results of Air Force Aeronautical Systems Division program, and such findings as are available from the results of Task I Studies. Measurements shall be made as required to produce relevant information such as:

1. Cylinder heat rejection data
2. Indicator card data
3. Operating capability at 0, 25%, 50%, 75%, 100% and 150% rated shaft power output
4. Engine friction data
5. BSPC as a function of load and mixture ratio
6. Temperature and pressure data
7. Preignition and/or Detonation data.

E. Initiate development towards:

1. Reducing friction losses
2. Reducing cylinder heat rejection
3. Increasing engine temperature
4. Reducing flow losses

F. Design, build, and test an oxygen injector configuration

G. Perform analysis of specimens of water collected from the exhaust to determine suitability for on-board use or crew consumption.

APPENDIX B

Cylinder Heat Rejection

Ref. Taylor & Taylor (1961)
Page 195

$$\frac{\dot{Q}}{A\,\Delta t} \propto \frac{k_g}{b}(R_g)^{3/4}$$

$\dot{Q}$ = heat flow rate from gas
b = bore
k_g = conductivity of gas

Assume energy output per mol of gas flowing is constant

$$R_g \propto \frac{Gb}{\mu} \propto \frac{Wb}{b^2\mu} \propto \frac{HM}{b\mu}$$

H = power output
μ = viscosity
M = molecular weight

Prandtl number $\times N_{Pr} \propto \frac{\mu C_p}{k_g} \propto \frac{\mu}{M k_g}$

Assume Δt = constant

$$\frac{\dot{Q}}{b^2} \propto \frac{k g}{b}\left(\frac{HM}{b\mu}\right)^{3/4}$$

$$\frac{\dot{Q}}{H} \propto \frac{k g \mu}{M} \cdot \left(\frac{\mu b}{HM}\right)^{1/4}$$

$$\frac{\dot{Q}}{H} \propto \frac{1}{N_{pr}} \left(\frac{\mu b}{HM}\right)^{1/4}$$

N_{pr} for air and H_2 are nearly equal.

$$\therefore \frac{\dot{Q}}{H} \propto \left(\frac{\mu b}{HM}\right)^{1/4}$$

$$\frac{(\mu/M)_{H_2}}{(\mu/M)_{air}} \approx \frac{1}{7.1} \qquad (7.1)^{1/4} = \underline{1.62}$$

$$\frac{\dot{Q}}{H} \propto \left(\frac{\mu}{M}\right)^{1/4} \left(\frac{b}{H}\right)^{1/4}$$

$$\overline{HP_s} \propto \frac{HP}{b^3}$$

$$\frac{\dot{Q}}{HP} \propto \left(\frac{u}{M}\right)^{1/4} \left(\frac{1}{\overline{HP_s}\, b^2}\right)^{\frac{1}{4}}$$

$$\propto \left(\frac{u}{M}\right)^{1/4} \frac{1}{\overline{HP_s}^{\,1/4}\, b^{1/2}}$$

If hydro engine has 1.75" bore and $\overline{HP_s} = 2$

Air breathing engine has 3.5" bore,

$HP_s = 0.5 \qquad \frac{\dot{Q}}{HP} = 0.7$

$\frac{Q}{HP}$ for hydro engine $= 0.7 \cdot \frac{\sqrt{2}}{4^{1/4}} \cdot 1.62$

$= 1.135$

Note: For equal BMEP and piston speed, $\overline{HP_s} \propto \frac{1}{b}$

then: $\frac{\dot{Q}}{HP} \propto \left(\frac{u}{M}\right)^{1/4} \left(\frac{1}{b}\right)^{1/4}$

Considering <u>steam</u> as the fluid

$\gamma \approx 1.25$ $\qquad N_{pr} \approx \frac{4}{9 - 5/\gamma}$

$$N_{pr} \approx \left(\frac{4}{9 - 5/1.25}\right) = \frac{4}{9-4} = \frac{4}{5}$$

$$= \underline{0.9} \text{ for steam}$$

$$\left(\frac{M}{\mu}\right)_{air} \approx \frac{29}{0.12} = 241$$

$$\left(\frac{M}{\mu}\right)_{steam} \approx \frac{18 \quad 2.09 \cdot 10^{-5}}{6.5 \cdot 10^{-7} \cdot 2.42}$$

$$= \frac{18}{.0752} = 239$$

N_{pr} for air ≈ 0.7

The most general convenient form is:

$$\frac{\dot{Q}}{HP} \propto \left(\frac{\mu}{M}\right)^{1/4} \frac{(\phi)^{3/4}}{N_{pr}\ \overline{HP}_s^{1/4}} \frac{(\Delta t)}{b^{1/2}}$$

Where:

$$\phi = \frac{\text{mols of working fluid}}{\text{horsepower - hour}}$$

Δt = mean gas temp. − mean coolant temp.

Note $\dot{Q}$ should be interpreted as observed heat rejection <u>minus</u> mechanical friction!

ϕ is a function of clearance volume, temperature, pressure ratio, and γ, but is primarily related to temperature.

Using Willys 6-230 engine as model (see SAE 532A) and assuming that friction heat went into oil.

at 3000 rpm, $\overline{H_s} \approx 0.5$

$$\frac{\dot{Q}}{HP} = .413 \qquad b = 3.34$$

For hydro engine $b = 1.5$

$$H_{sp} \approx \frac{5}{2.72} = 1.84$$

$$\frac{\dot{Q}}{HP} \approx 0.413 \cdot 1.62 \cdot \left(\frac{3.34}{1.5}\right)^{1/2} \left(\frac{0.5}{1.84}\right)^{1/4}$$

$$\approx 0.72$$

Allowing .15 for friction, net heat rejection of hydro engine per HP should be 0.87 for max cycle temp $\approx$ 4500°R !

APPENDIX C

APPENDIX C

ELECTRICAL COMPONENT SPECIFICATIONS

1. Alternating Current:

Voltage - 120/208 RMS 3 phase 4 wire
Frequency - 400 cps nominal ± .5% steady state
Rating - 3.0 KVA average continuous
Power Factor - .75 lagging to 1.0
Overload - 4.5 KVA at .75 power factor for 10 minutes
Short circuit capacity - 3 p.u. current on 3 phase fault
Voltage Regulation - ±2 volts phase to neutral steady state
Voltage setting - 115/200 at bus
Voltage unbalance - Balanced load ± 1%
Unbalanced load per MIL-G-6099A (ASG) Ammendment - 1 dated 15 April 1958 Paragraph 4.5.10.1 except load unbalance limited to 1/3.
Wave form - Total harmonic distortion 4% maximum to and including 7th harmonic at full rated load .75 power factor line to line and line to neutral. No harmonic shall exceed 3%.
Voltage regulation transient response - Per MIL-G-6099A (ASG) Amendment 1 dated 15 April 1958 Paragraph 4.5.7.1 except the time base seconds shall be two times the values shown in Fig. 8 of MIL-G-6099A (ASG) Amendment 1 dated 15 April 1958.
Efficiency - 90% at full load .75 power factor including excitation source and regulator losses.

Cooling - The alternator shall be cooled by glycol circulation through a heat exchanger located within the alternator case. An atmosphere of 1 to 2 psia comprised of hydrogen and water vapor shall be admitted to the alternator case through a partial seal from the engine crankcase at 150°F maximum. The alternator elements shall be cooled by conduction to the enclosed atmosphere and thence to the heat exchanger. The circulative glycol inlet temperature shall be regulated within the limits of 35°F to 50°F at 1 to 2 gpm flow. Hot spot temperatures of the alternator windings shall not exceed 130°C, NEMA Class B. No electrical insulation of a temperature class inferior to class B shall be employed.

Radio Interference - To limits of: Electro Interference Control Requirements for Minuteman (WS-133B) GM 07-59-2617A AFBSD exhibit 62-87 15 June 1962 (unclassified).

(Document GM 07-59-2617A is an electrical interference control specification to be primarily applied to the design and development of WS-133A equipment. The document not only establishes standards of performance to be met, but also contains design requirements and design guides. By omitting reference to the design requirements, this document may be used to test existing equipment for compliance with the interference limits given. This document is derived from Specification MIL-I-26600, "Interference Control Requirements, Aeronautical Equipment". The primary purpose of GM 07-59-2617A has been to add low frequency interference limits and test methods and to eliminate short duration allowance.)

Voltage taps - 3 phase 4 wire 115 volts phase to phase at 1.0 rated p. u. current per phase at two times percent voltage regulation, non-simultaneously, or any combination of loads not exceeding 1.0 rated p. u. current per phase.

2. Direct Current:

Voltage - 27.0 nominal
Rating - 8.0 amperes average continuous
Overload - 12.0 amperes for 30 minutes
Short circuit capacity - 50.0 amperes
Voltage Regulation - ±2.0 volts
Response time - 0
Efficiency - 50% or better
Cooling - Glycol circulation through heat exchanger with engine crankcase atmosphere
Radio Interference - To limits of GM 07-59-2617A
Battery - Silver Cadmium

APPENDIX D

Regenerative Power Cycles With Heat Loss

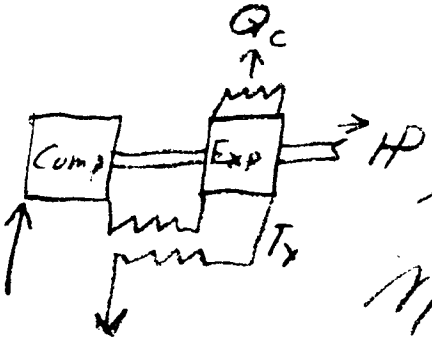

Compression function may be liquid pump.

η_∞ describes expander performance when $Q_c = 0$

T_x is held constant

η_1 is cycle performance with $Q_c =$

$$X = \frac{Q_c}{HP_x}$$

$$\eta_x = \frac{HP_x}{\frac{HP_1}{\eta_1} + Q_c + (HP_x - HP_1)} = \frac{HP_x/HP_1}{\frac{1}{\eta_1} + (X+1)\frac{HP_x}{HP_1} - 1}$$

With T_x held constant, $\frac{HP_x}{HP_1} \geq 1$ as $0 < X$. The most conservative assumption is $\frac{HP_x}{HP_1} = 1$, $\eta_x = \frac{\eta_1}{1 + X\eta_1}$

This is equivalent to assuming that all waste heat is extracted before the expansion process, and is <u>less</u> <u>conservative</u>.

$$H_x = H_1 + (Q_c + H_x - H_1) y \eta_\infty$$

$$0 < y < 1.0$$

If $y = 1$, all heat has been extracted after expansion.

$$\frac{H_x}{H_1} = \frac{1 - y \eta_\infty}{1 - (x+1) y \eta_\infty}$$

$$\eta_x = \frac{1}{\left(\frac{1}{\eta_1} - 1\right) \frac{1 - y (x+1) \eta_\infty}{1 - y \eta_\infty} + x + 1}$$

In most cycles of interest,

$.40 < \eta_\infty < .50$, and $.40 < \eta_1 < .55$

The term x is best interpreted as the heat rejection which <u>cannot be regenerated.</u>

Since η_∞ and η_1 are nearly equal, a value of $y = 1$ would imply <u>no influence</u> of x on η_x.

In evaluating y, we should remember that η_∞ includes a friction loss which is <u>part of the heat rejection</u> that behaves like exhaust heat extraction.

From automotive data, a value of $y = \underline{0.60}$ is suggested. Using $\eta_\infty = \underline{0.45}$,

$$\eta_x = \frac{1}{\left(\frac{1}{\eta_1} - 1\right)\frac{1 - .27(x+1)}{.73} + x + 1}$$

if $\eta_1 = 0.50$, $x = 1.0$,

$$\eta_x = \underline{0.38}$$

Whereas, if $\underline{y = 0}$ or $\underline{1.0}$

$$\eta_x = \underline{0.333} \text{ or } \underline{0.458}$$

The values of x and y need test evaluation!

Summary:

$$\eta_x = \frac{1}{\left(\frac{1}{\eta_1} - 1\right) \frac{H_1}{H_x} + x + 1}$$

<u>If</u> $H_x / H_1 = 1.0$,

$$\eta_x = \frac{1}{\frac{1}{\eta_1} + x}$$

$$H_x / H_1 = \frac{1}{1 - \frac{x}{\frac{1}{y \eta_\infty} - 1}}$$

$$\eta_x = \frac{1}{\left(\frac{1}{\eta_1} - 1\right)\left(1 - \frac{x}{\frac{1}{y \eta_\infty} - 1}\right) + x + 1}$$

Plot $\eta_x = f(\eta_1, x, y \eta_\infty)$

$\eta_1 < 0.55$, 0.4 $\qquad$ $x < 1.2$, $.2$

$y \eta_\infty = 0.3, 0.4, 0.5$

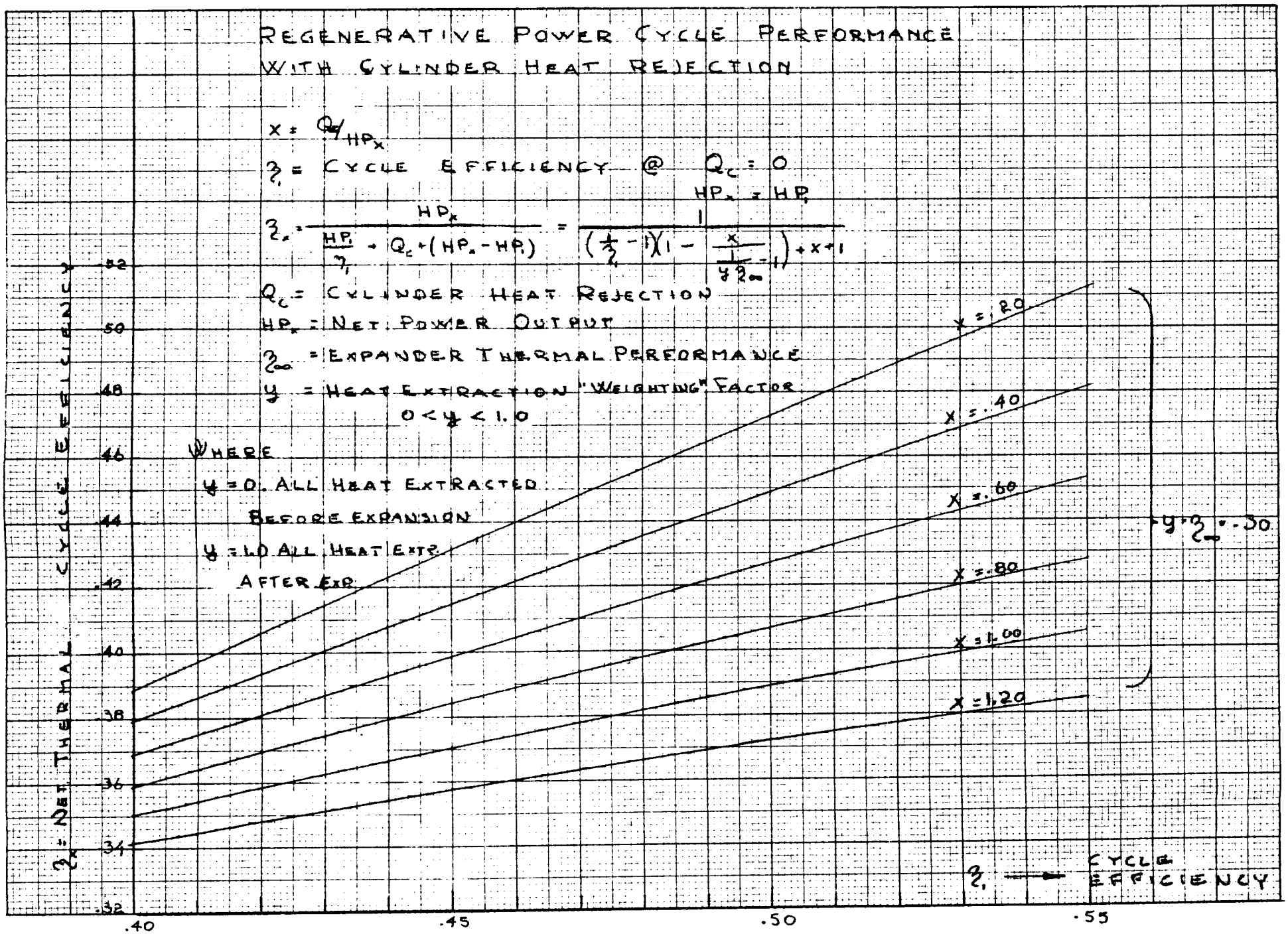
REGENERATIVE POWER CYCLE PERFORMANCE
WITH CYLINDER HEAT REJECTION
$x = Q_c / HP_x$
η_1 = CYCLE EFFICIENCY @ $Q_c = 0$
$HP_x = HP_1$
$\eta_x = \frac{HP_x}{\frac{HP_1}{\eta_1} + Q_c + (HP_x - HP_1)} = \frac{1}{\left(\frac{1}{\eta_1} - 1\right)\left(1 - \frac{x}{\frac{1}{y\eta_\infty} - 1}\right) + x + 1}$
Q_c = CYLINDER HEAT REJECTION
HP_x = NET POWER OUTPUT
η_∞ = EXPANDER THERMAL PERFORMANCE
y = HEAT EXTRACTION "WEIGHTING" FACTOR
$0 < y < 1.0$
WHERE
$y = 0$. ALL HEAT EXTRACTED BEFORE EXPANSION
$y = 1.0$ ALL HEAT EXTR. AFTER EXP.
$x = .20$
$x = .40$
$x = .60$
$x = .80$
$x = 1.00$
$x = 1.20$
$y \cdot \eta_\infty = .30$
η_x = NET THERMAL CYCLE EFFICIENCY
.52
.50
.48
.46
.44
.42
.40
.38
.36
.34
.32
.40
.45
.50
.55
η_1 → CYCLE EFFICIENCY

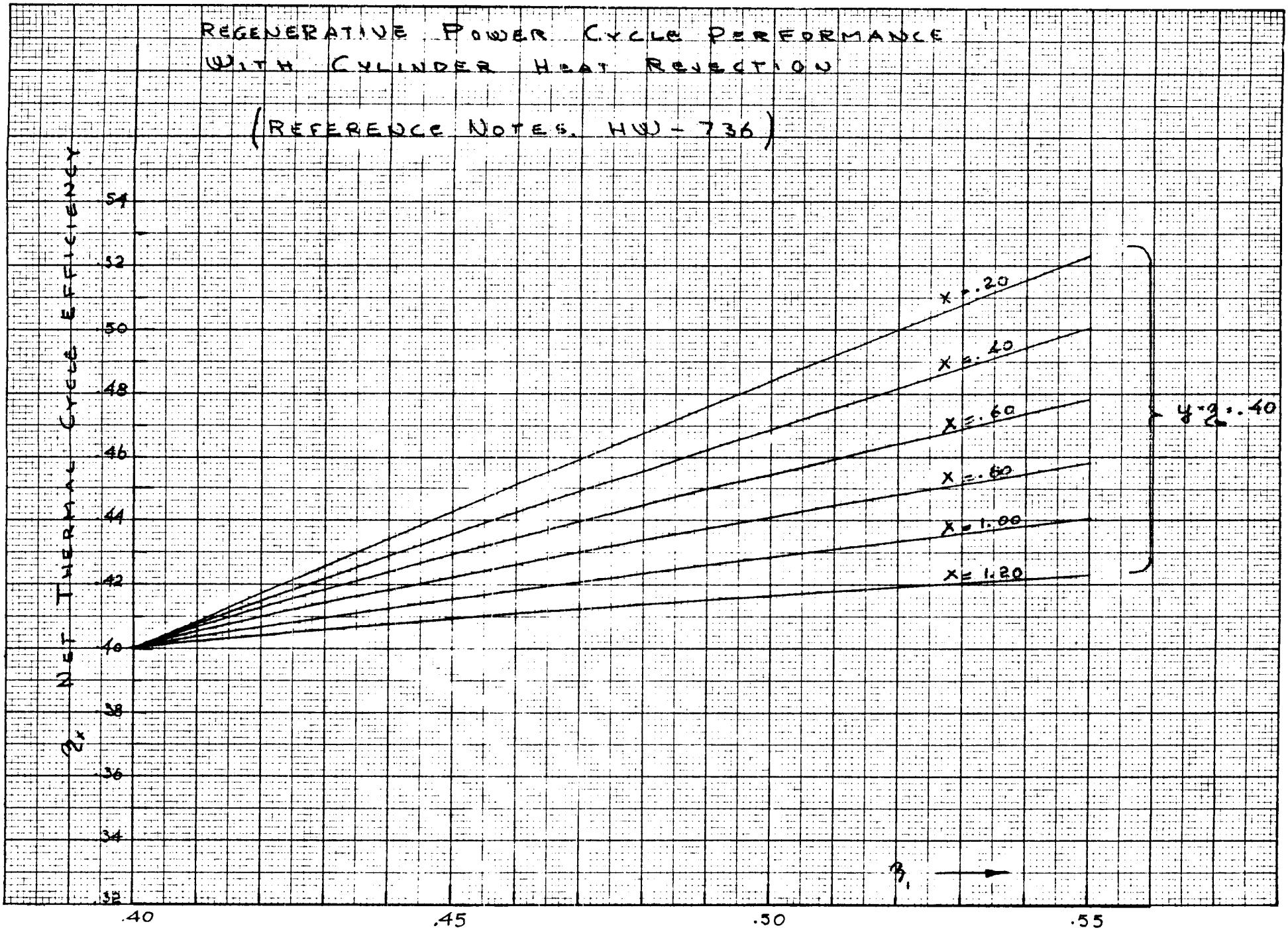
REGENERATIVE POWER CYCLE PERFORMANCE
WITH CYLINDER HEAT REJECTION
(REFERENCE NOTES, HW-736)
η_x NET THERMAL CYCLE EFFICIENCY
.54
.52
.50
.48
.46
.44
.42
.40
.38
.36
.34
.32
.40
.45
.50
.55
β_1
X = .20
X = .40
X = .60
X = .80
X = 1.00
X = 1.20
$\psi_2 = .40$

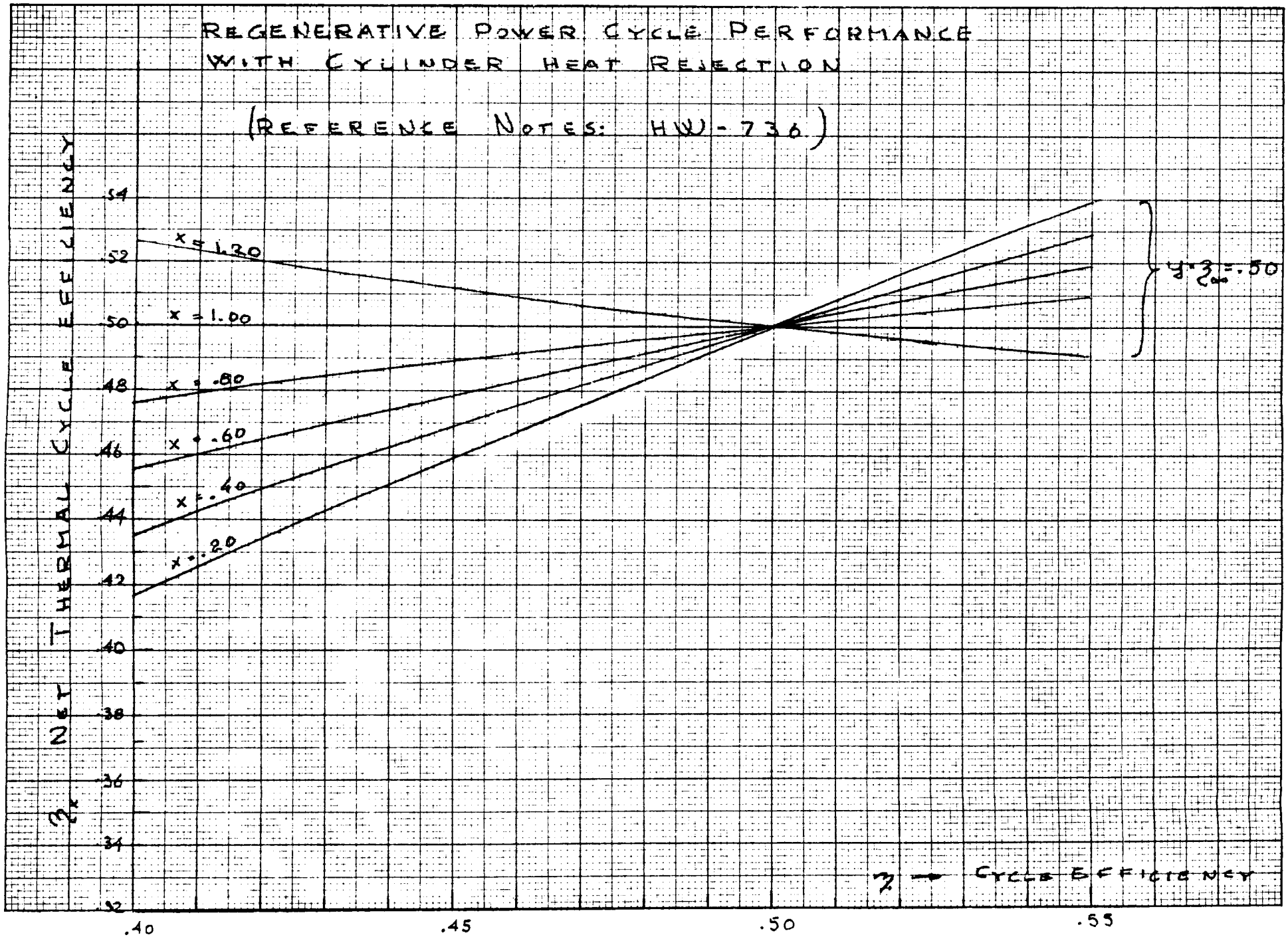
REGENERATIVE POWER CYCLE PERFORMANCE
WITH CYLINDER HEAT REJECTION
(REFERENCE NOTES: HW-736)
NET THERMAL CYCLE EFFICIENCY
η_x
.54
.52
.50
.48
.46
.44
.42
.40
.38
.36
.34
.32
x = 1.20
x = 1.00
x = .80
x = .60
x = .40
x = .20
$y \cdot \eta_\infty = .50$
η → CYCLE EFFICIENCY
.40
.45
.50
.55

APPENDIX E

V. ENGINE EQUATIONS FOR LINEAR ANALOG AND ORIGINAL COMPUTER

(Otto cycle representation)

Engine Equations

$$P_G = 283 \ W_{m5}$$

$$IMEP_{IDEAL} = P_G (.0917) \quad \text{Ref}$$

$$IMEP_{ACTUAL} = (IMEP)_{ACTUAL} \times D.F.$$

$$L_{ei} = IMEP_{ACTUAL} \left(\frac{V_L}{2\pi} \right)$$

PREPARED BY	VICKERS INCORPORATED ENGINEERING CALCULATION FORM	PAGE OF
CHECKED BY	SUBJECT	PROGRAM & PROJECT NO.
		DATE

$$L_{ef} = \frac{FMEP}{2\pi}(2.77)$$

$$L_{\Delta} = L_{ei} - L_{ef} - L_{L}$$

Mixture Ratio and Propellant Flow Equations

$$r = \frac{W_{O5}}{W_{H5}} = \frac{W_{O5}}{W_{H5}}$$

$$W_{O5} = N60\, W_{O5}$$

$$W_{H5} = N60\, W_{H5}$$

$$W_{O5} = W_{O5}^{I} + .56\,\frac{C_d P_{O4}}{\sqrt{T_{O4}}} f\left(\frac{P_{O4}}{P_{O5}}\right) A_{O4}$$

$$W_{H5} = W_{H5}^{I} + \frac{.14\, C_d P_{H4}}{\sqrt{T_{H4}}} f\left(\frac{P_{H4}}{P_{H5}}\right) A_{H5}$$

Exhaust Temperature Equations

$$T_c = 500 + 500\, r$$

$$C_{10} = \frac{T_c}{5+1}$$

$$T_{c55} = 1500^{\circ} F$$

PREPARED BY	VICKERS INCORPORATED ENGINEERING CALCULATION FORM	PAGE OF
CHECKED BY	SUBJECT	PROGRAM & PROJECT NO.
		DATE

$$K\,(C_{10} - 1500) = -\Delta A_{04}$$

Speed Equation

$$\Delta L \quad \frac{416}{S} = \Delta N$$

Control System Equations

$$C_1 = \Delta N \left(\frac{\tau_1 S + 1}{\tau_2 S + 1} \right) \frac{K_1}{S}$$

$$C_2 = C_1 \frac{1}{S^2/54400 + \frac{S}{243} + 1}$$

Valve Area Equations

$$A_{H4} = C_2$$

$$A_{04} = C_2 + \Delta A_{04}$$

PREPARED BY	VICKERS INCORPORATED ENGINEERING CALCULATION FORM	PAGE OF
CHECKED BY	SUBJECT	PROGRAM & PROJECT NO.
		DATE

ENGINE EQUATIONS REF. FIG
INCLUDING:

1. NON LINEARITIES
2. THERMAL LOOPS
3. HYBRID ENGINE CYCLE

ENGINE

OTTO CYCLE, $P_6 \leq 1170$ PSIA

$$P_6 = 365\ \omega_{m5}$$

$$IMEP_{IDEAL} = P_6\ (.1195)$$

VARIABLE ADMISSION CYCLE, $P_6 > 1170$ PSIA

$$IMEP = 129 + f(\%\theta) \qquad IMEP \geq 129$$

(REF FIG. III-2

WHERE % ADMISSION IS OBTAINED FOR COMPUTER PURPOSES AS A FUNCTION OF ω_{m5}, THERE BY ELIMINATING % ADMISSION AS A VARIABLE FROM THE MECHANIZATION.

$$Lei = \frac{2.77}{2\pi} = \frac{DISPLACEMENT}{2\pi}$$

$$Lef = \frac{FMEP}{2\pi}(2.77) = \frac{11\ (2.77)}{2\pi}$$

$$HP = \frac{L\,N}{63000}, \quad L = \frac{HP\ (63000)}{4000}$$

PREPARED BY	VICKERS INCORPORATED ENGINEERING CALCULATION FORM	PAGE 2 OF
CHECKED BY	SUBJECT	PROGRAM & PROJECT NO.
		DATE

$$HP = 1.34 \ KW$$

$$\Delta HP = 1.34 \ \Delta KW$$

$$L_L = \frac{1.34 \ (KW)(63000)}{4000}$$

AT 4000 RPM

$$L_\Delta = L_{ei} - L_{ef} - L_L$$

$$N = \frac{60}{2\pi J} L_\Delta$$

$$N = \frac{60}{2\pi JS} L_\Delta$$

$$T_{ex} = r(500) + 500 \ ^oF$$

CONTROL SYSTEM EQUATIONS

SPEED CONTROL

$NK_1 = 4000$, TACH. REF.

$-NK_1 + 4000 =$ TACH. ERROR SIGNAL $= e_t$

$$e_A = K_2 \frac{(\tau_1 S + 1)}{(\tau_2 S + 1)} e_t$$

τ_1, τ_2, & K_2 ARE VARIABLES IN THE STUDY

PREPARED BY	VICKERS INCORPORATED ENGINEERING CALCULATION FORM	PAGE OF
CHECKED BY	SUBJECT	PROGRAM & PROJECT NO.
		DATE

CONTROL ACTUATOR

$\dot{X}_c$ (SGN) + ; F_B (sgn) −

$\dot{X}_c$ (SGN) − ; F_B (sgn) +

F_B IS A VARIABLE

$$F_A \frac{K_4}{J_A S} = \dot{X}_c$$

$$\dot{X}_c \frac{1}{S} = X_c$$

$$X_c \pm h = X_c'$$

h IS A VARIABLE

$$F = [-\dot{X}_c K_5 + e_a] K_3 \frac{\partial F_M}{\partial I}$$

$$F_A = F - F_B$$

$|\dot{X}_c|$ NOT GREATER THAN $|\dot{X}_c|_{MAX}$
WHICH IS A DESIGN VARIABLE

PREPARED BY	VICKERS INCORPORATED ENGINEERING CALCULATION FORM	PAGE OF
CHECKED BY	SUBJECT	PROGRAM & PROJECT NO.
		DATE

VALVE GAINS

$$\bar{W}_{HS} = \bar{W}_{HS} + \Delta \bar{W}_{HS}$$

$$\bar{W}_{OS} = \bar{W}_{OS} + \Delta \bar{W}_{OS}$$

$$\omega_{HS} = \bar{W}_{HS} \; N60 \qquad N = 4000$$

$$\omega_{OS} = \bar{W}_{OS} \; N60 \qquad N = 4000$$

where

$$\Delta \bar{W}_{OS_{TL}} = \frac{\partial \bar{W}_{OS}}{\partial X_T} \frac{K_L}{(\tau_3 S+1)(\tau_4 S+1)} (T_{ex} - 1500)$$

$$\Delta \bar{W}_{HS_{TL}} = \frac{\partial \bar{W}_{HS}}{\partial T_{HS}} \left(\frac{1}{\tau_5 + 1}\right) \Delta T_{H4} - \left[\frac{.935 \; T_{ex}}{\frac{m C_p C_u}{2 U A} S + 1}\right]$$

$$r = \frac{\omega_{HS}}{\omega_{OS}}$$

$$\omega_{MS} = \omega_{OS} + \omega_{HS}$$

EN-230
7-60

PREPARED BY	VICKERS INCORPORATED ENGINEERING CALCULATION FORM	PAGE
CHECKED BY	SUBJECT TERMS FOR ENGINE CONTROL ANALYSIS	PROGRAM & PROJECT NO.

GENERAL TERMS:

TERM		DESCRIPTION
FMEP	LB/IN²	FRICTIONAL MEAN EFFECTIVE PRESS
γ	DL	O/H RATIO BY WT.
BMEP	LB/IN²	BRAKE MEAN EFFECTIVE PRESS
IMEP(act)	LB/IN²	INDICATED ACTUAL MEAN EFFECT-IVE PRESSURE
DF		DIAGRAM FACTOR
W	LB	WEIGHT IN SPECIFIC VOLUME
P	LB/IN²	PRESSURE AT STATION
T	°R	TEMPERATURE AT STATION
V	IN³	VOLUME
A	IN²	AREA
θ	DL	% HYDROGEN CUTOFF
η	DL	EFFICIENCY
w	LB/HR	WEIGHT FLOW
J	IN-LB-SEC²	ROTATING MOMENT OF INERTIA

EN-230
7-60

PREPARED BY	VICKERS INCORPORATED ENGINEERING CALCULATION FORM	PAGE
CHECKED BY	SUBJECT	PROGRAM & PROJECT NO.
		DATE

GENERAL TERMS, Cont,

τ	$\frac{1}{SEC}$	TIME CONSTANT
N	$\frac{1}{MIN}$	SPEED
ω	$\frac{1}{SEC^2}$	NATURAL FREQUENCY
$IHP_{(ACT)}$	$\frac{FT-LB}{HR}$	ACTUAL INDICATED HORSE POWER
BHP	$\frac{FT-LB}{HR}$	BRAKE HORSE POWER
K		CONTROL GAIN
R	$\frac{LB}{LB-{}^{\circ}R}$	GAS CONSTANT
C		CONTROL GAIN
KW		KILO-WATT
F	LBS	FORCE
X	UNITS	LINEAR DISPLACEMENT
I		CURRENT
e		VOLTAGE

SUBSCRIPTS

EXAMPLE: T_{H5}

- T ← GENERAL TERM
- 5 ← STATION
- H ← MEDIUM

SUBSCRIPT – STATIONS	DESCRIPTION
1.	BOILOFF CONDITION
2	SUPERCRITICAL TANK CONDITION
2.1	COMPRESSOR INLET
3	COMPRESSOR OUTLET; HEAT EXCHANGER PROPELLANT INLET
4	HEAT EXCHANGER PROPELLANT OUTLET; ENGINE VALVE INLET
5	ENGINE INLET
6, 7, 8, 9	VARIOUS ENGINE CYCLE STA.
e	ENGINE EXHAUST
0	AMBIENT

PREPARED BY	VICKERS INCORPORATED ENGINEERING CALCULATION FORM	PAGE
CHECKED BY	SUBJECT	PROGRAM & PROJECT NO.
		DATE

SUBSCRIPTS - CONT

SUBSCRIPT - MEDIUM	DESCRIPTION
H	HYDROGEN
O	OXYGEN
M	MIXTURE
CP	COMBUSTION PRODUCTS

EN-230
7-60

PREPARED BY	VICKERS INCORPORATED ENGINEERING CALCULATION FORM	PAGE
CHECKED BY	SUBJECT	PROGRAM & PROJECT NO.
		DATE

SUBSCRIPTS - CONT,

SUBSCRIPTS - TORQUES

e_i	ENGINE TORQUE BASED ON IMEP, N
e_f	ENGINE FRICTIONAL TORQUE INCLUDING COMP, GEARBOX, ALT, etc.
A	APPLIED ENGINE TORQUE
L	LOAD TORQUE
C	COMPRESSOR TORQUE, ACTUAL INDICATED
Δ	TORQUE UNBALANCE

TERMS & PARTIALS

V_D	VOLUME, DISPLACEMENT
ΔT_{H4}	VARIATION IN HYDROGEN INLET PRESS.
$\frac{m C_{pen}}{2 U A}$	HEAT EXCHANGER TIME CONST.
h	HYSTRESIS ($\pm$)

PREPARED BY	VICKERS INCORPORATED ENGINEERING CALCULATION FORM	PAGE OF
CHECKED BY	SUBJECT	PROGRAM & PROJECT NO.
		DATE

TERMS & PARTIALS

Te_{ss}	STEADY STATE EXHAUST TEMP
e_t	TACHOMETER VOLTAGE
e_A	ACTUATOR INPUT VOLTAGE
e_{FB}	ACTUATOR FEEDBACK "
C_{10}	TEMP CONTROL OUTPUT 1ST STUDY
C_1	SPEED CONTROL OUTPUT 1ST STUDY
C_2	ACTUATOR OUTPUT 1ST STUDY
K_1	CONTROL GAIN, 1ST STUDY
K_1	TACHOMETER GAIN
K_2	CONTROLLER GAIN, SPEED LOOP
K_3	ACTUATOR AMPLIFIER GAIN
K_4	ACTUATOR INERTIA TO OUTPUT ACCELLERATION
K_5	ACTUATOR FEEDBACK TACH GAIN
J_A	ACTUATOR INERTIA
X_c	CONTROL ACTUATOR OUTPUT

PREPARED BY	VICKERS INCORPORATED ENGINEERING CALCULATION FORM	PAGE OF
CHECKED BY	SUBJECT	PROGRAM & PROJECT NO.
		DATE

τ_1 LEAD TIME CONSTANT

τ_2 LAG TIME CONSTANT

τ_3 ACTUATOR TIME CONST. RATIO CONTROL

τ_4 TEMP. SENSOR TIME CONST.

τ_5 TIME DELAY, HYDROGEN GAS FLOW

$\frac{\partial F_M}{\partial I} = \frac{65.2}{|\dot{X}_c|_{MAX}}$ CLUTCH OR MOTOR OUTPUT FORCE, AT VALVE INPUT

$\frac{\partial W_{HS}}{\partial X_c} = 1.0 \times 10^{-7}$ lb/cycle/unit HYDROGEN VALVE GAIN SPEED CONTROL

$\frac{\partial W_{OS}}{\partial X_c} = 2.0 \times 10^{-7}$ lb/cycle/unit OXYGEN VALVE GAIN SPEED CONTROL

$\frac{\partial W_{OT}}{\partial X_T} = 2.0 \times 10^{-7}$ lb/cycle/unit OXYGEN VALVE GAIN TEMP. CONTROL

$\frac{\partial W_{HS}}{\partial T_{HS}} = 1.0 \times 10^{-8}$ HYDROGEN TEMP. EFFECT ON VALVE GAIN.

PREPARED BY	VICKERS INCORPORATED ENGINEERING CALCULATION FORM	PAGE OF
CHECKED BY	SUBJECT	PROGRAM & PROJECT NO.
		DATE

CONSTANTS:

D.F. = .9

V_D = 2.77

FMEP = 11 PSI

T_{ess} = 1500° F

τ_3 .5 sec

τ_4 .5 sec

τ_5 .02 sec

K_1 = 1

J_A = .0565 Lb-in-sec²

J = .023 Lb-in-sec² ORIGINAL ESTIMATE

J = .3279 Lb-in-sec² 4000 RPM GEN.

J = .1159 Lb-in-sec² 6000 RPM GEN

K_5 = 1

N_{ss} = 4000 RPM

K_4 = .03246

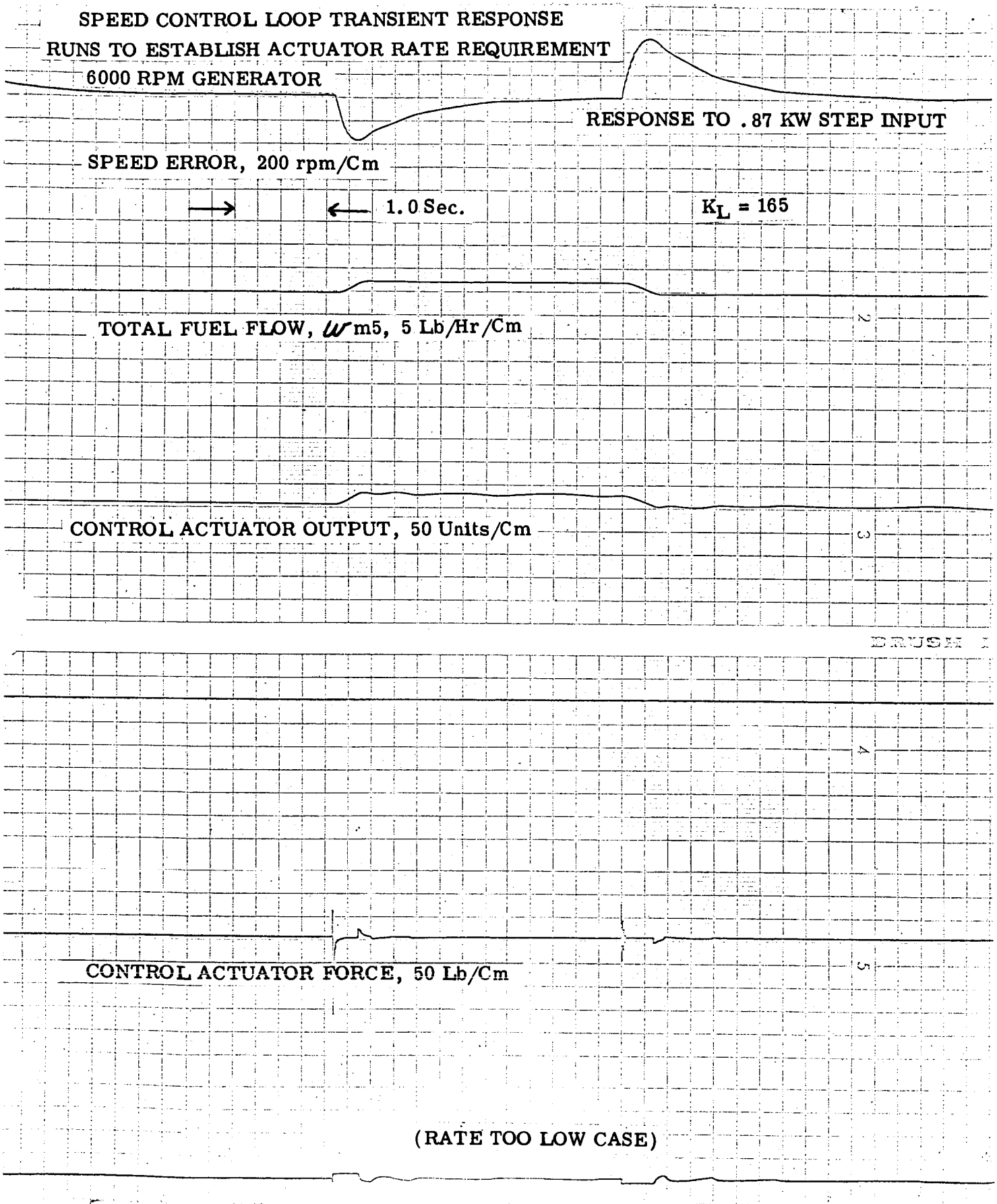

Series 1 - Run 1

SPEED CONTROL LOOP TRANSIENT RESPONSE

RUNS TO ESTABLISH ACTUATOR RATE REQUIREMENT

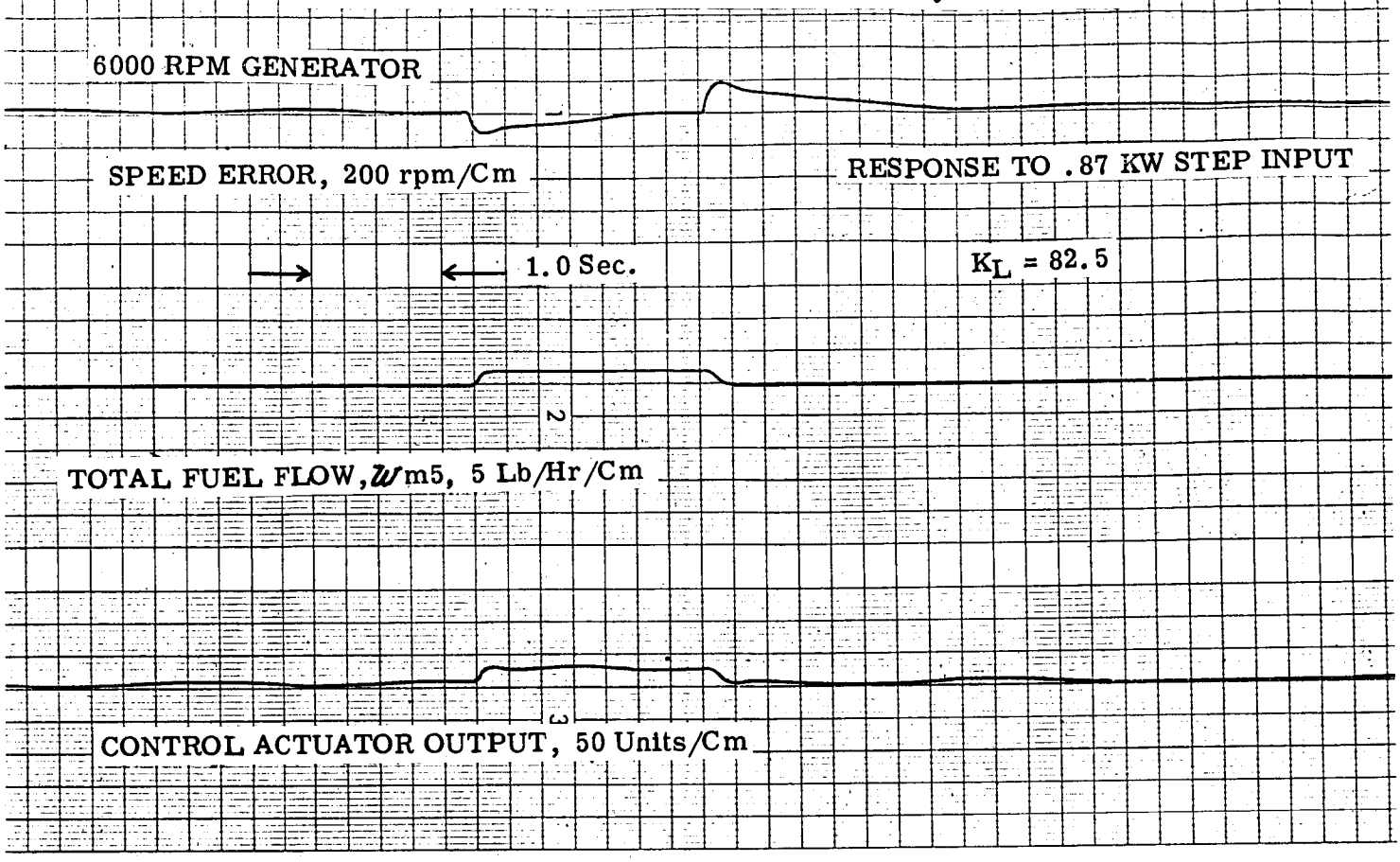

ATION CLEVELAND, OHIO PRINTED IN U. S. A.

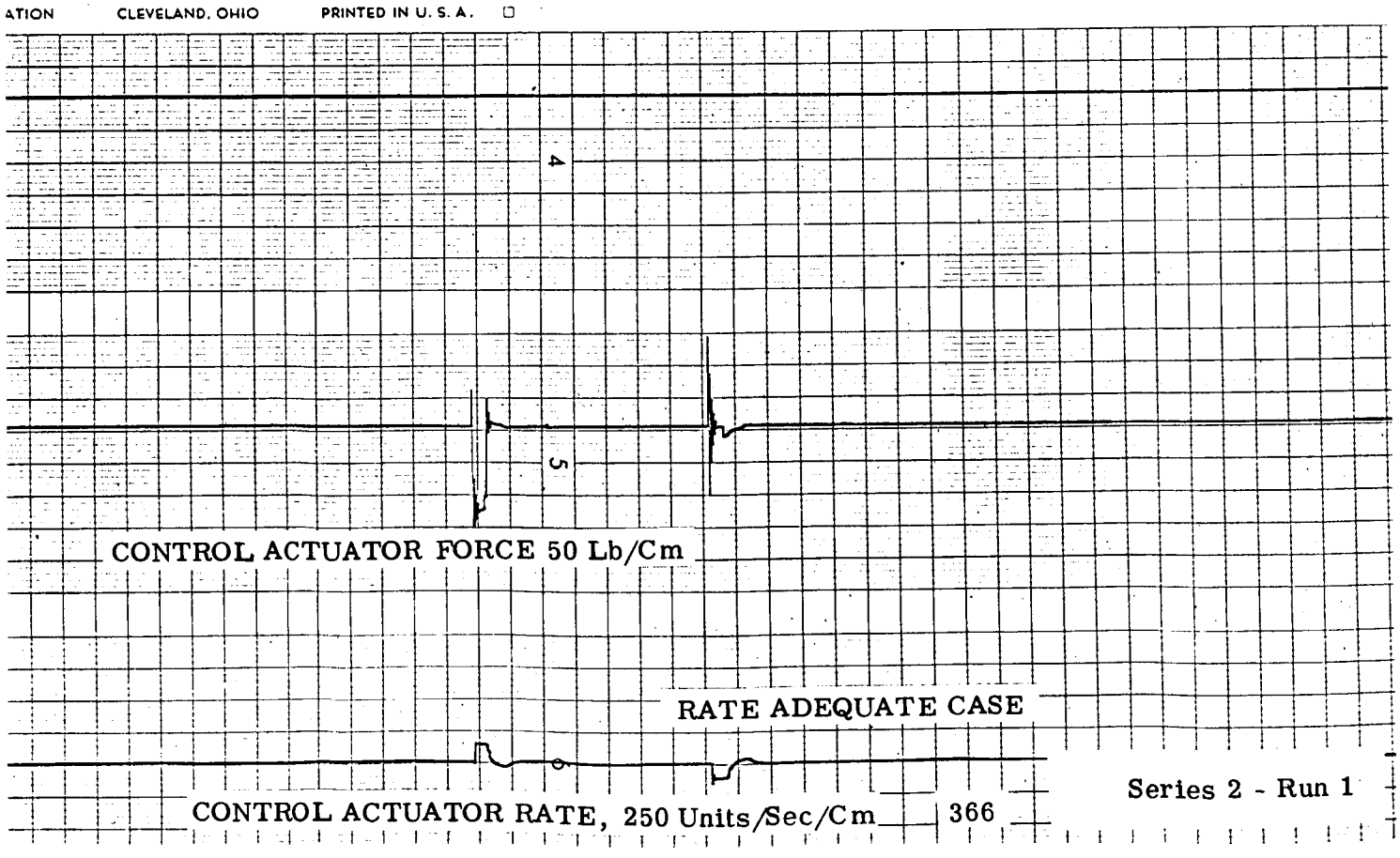

Series 2 - Run 1

SPEED CONTROL LOOP TRANSIENT RESPONSE

RUNS TO ESTABLISH ACTUATOR RATE REQUIREMENT

6000 RPM GENERATOR

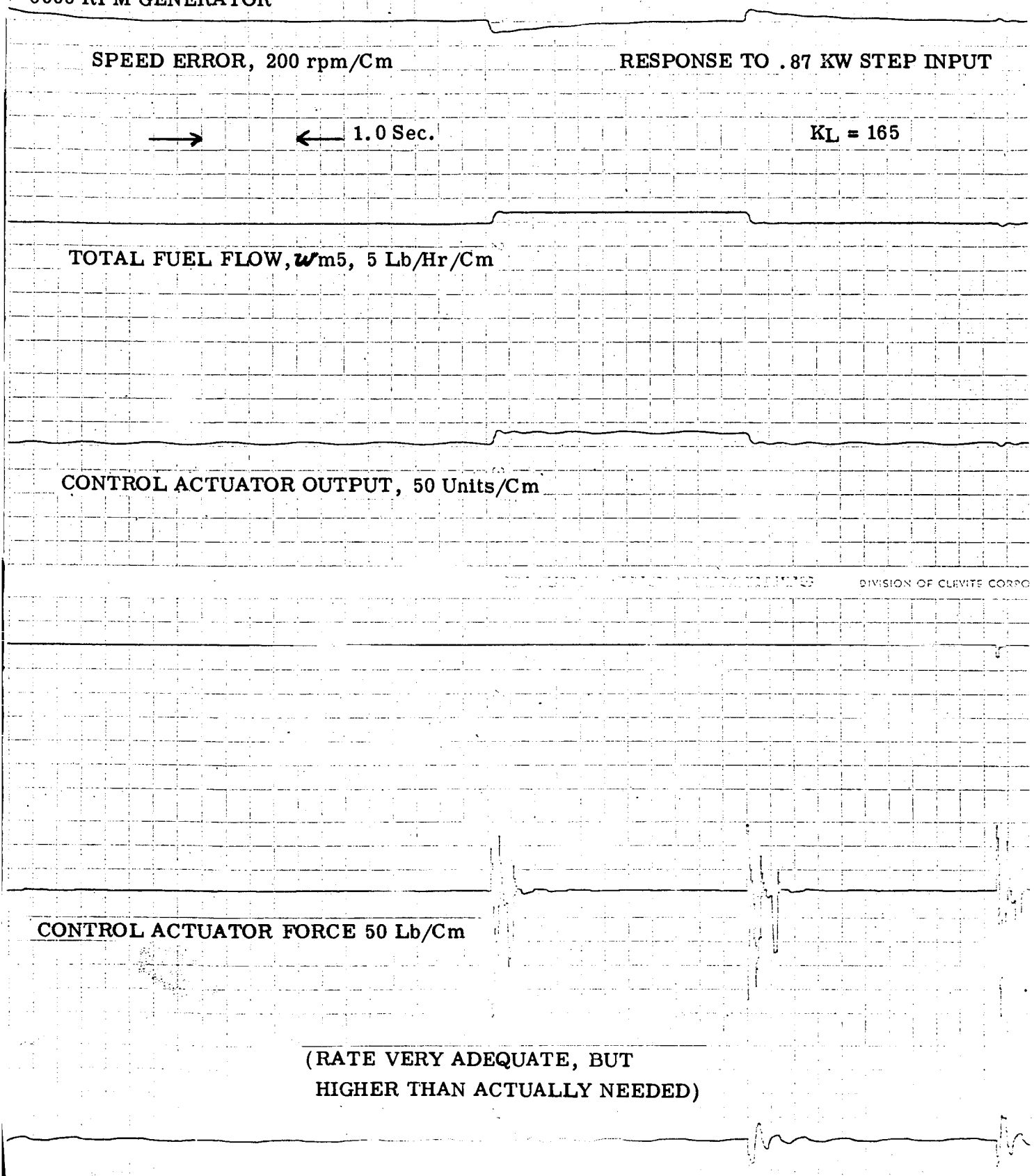

Series 3 - Run 1

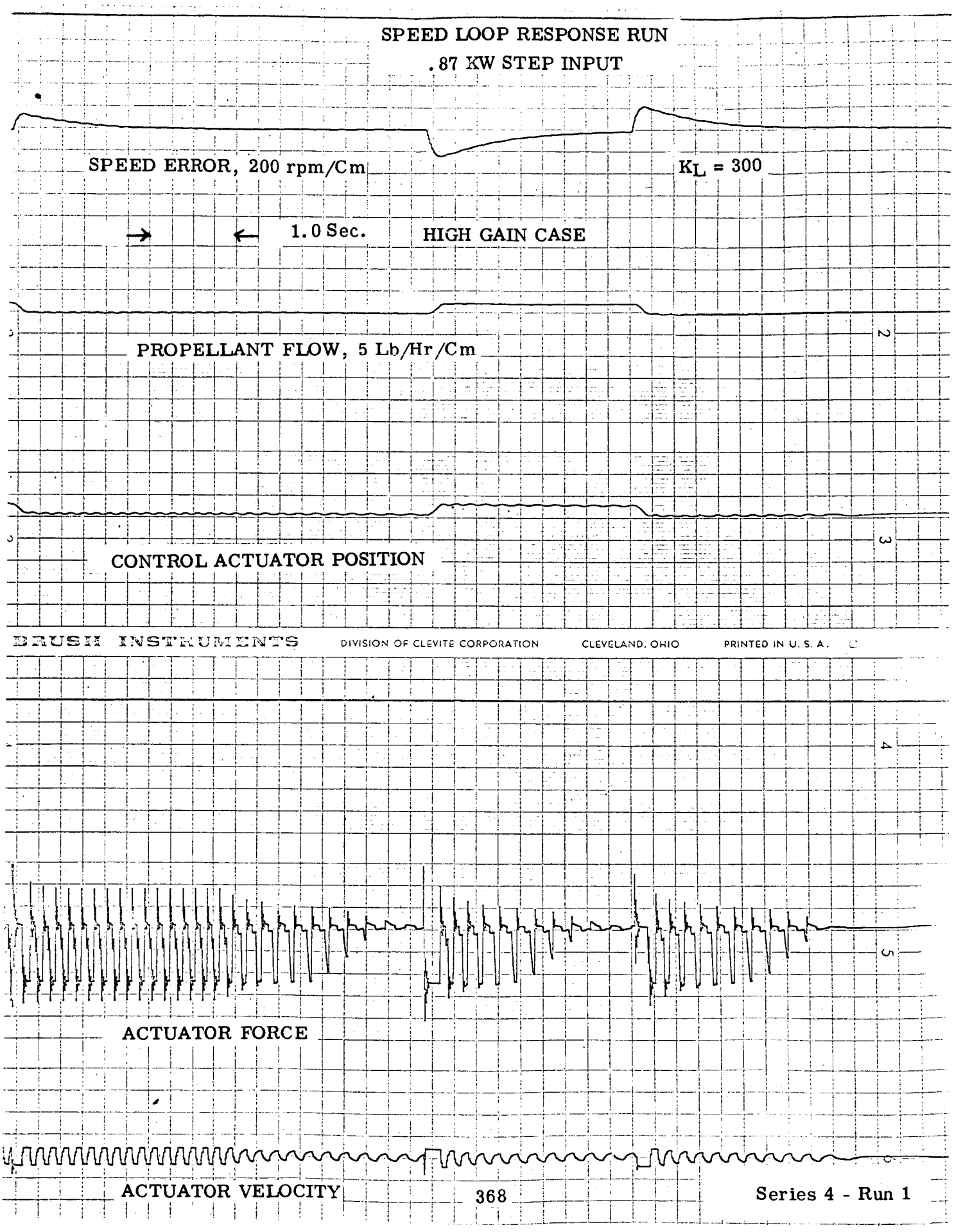

Series 4 - Run 1

4000 RPM SYSTEM
SPEED LOOP RESPONSE

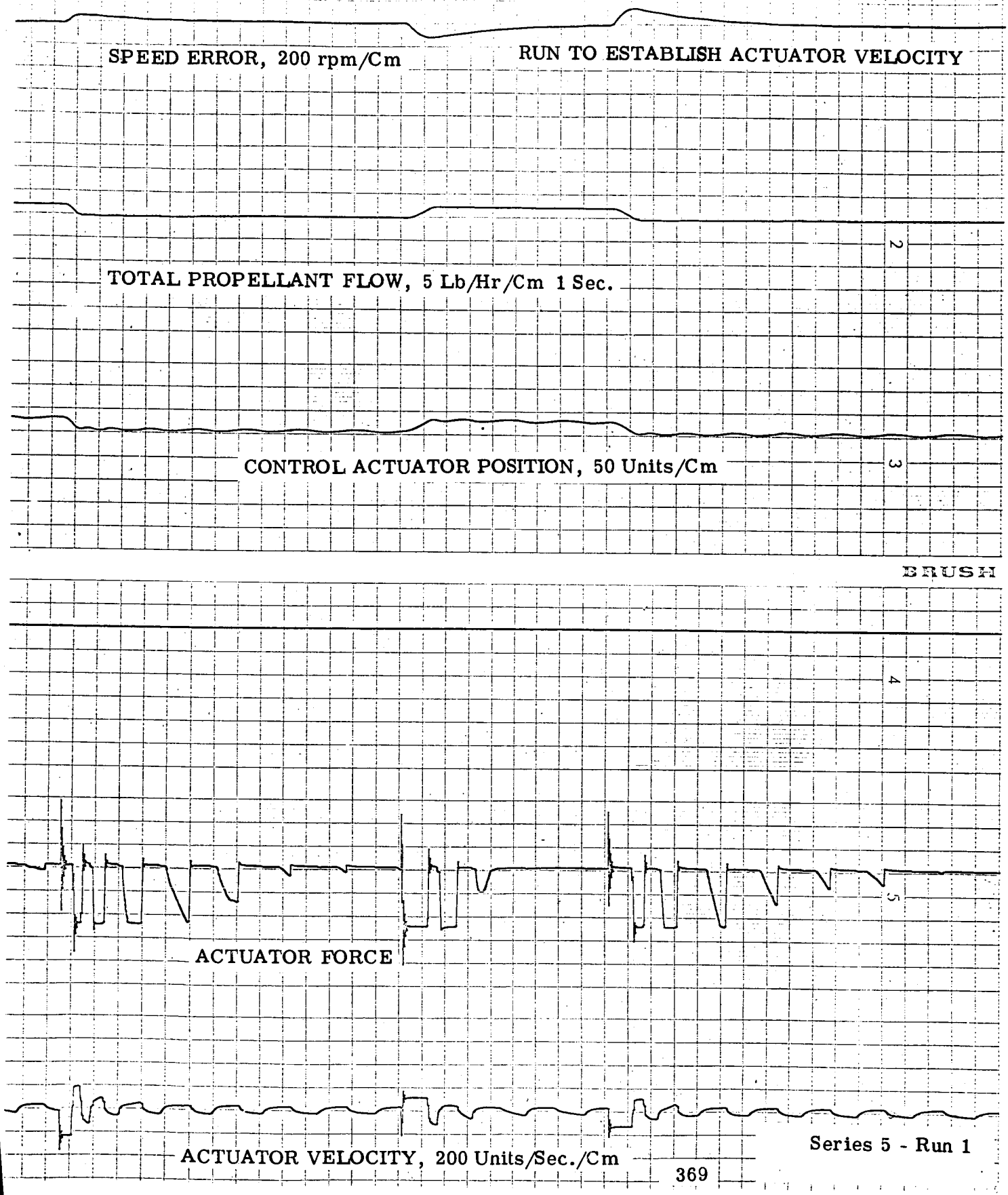

Series 5 - Run 1

SPEED LOOP RESPONSE
RATE LIMIT VARIATION RUN
4000 RPM SYSTEM

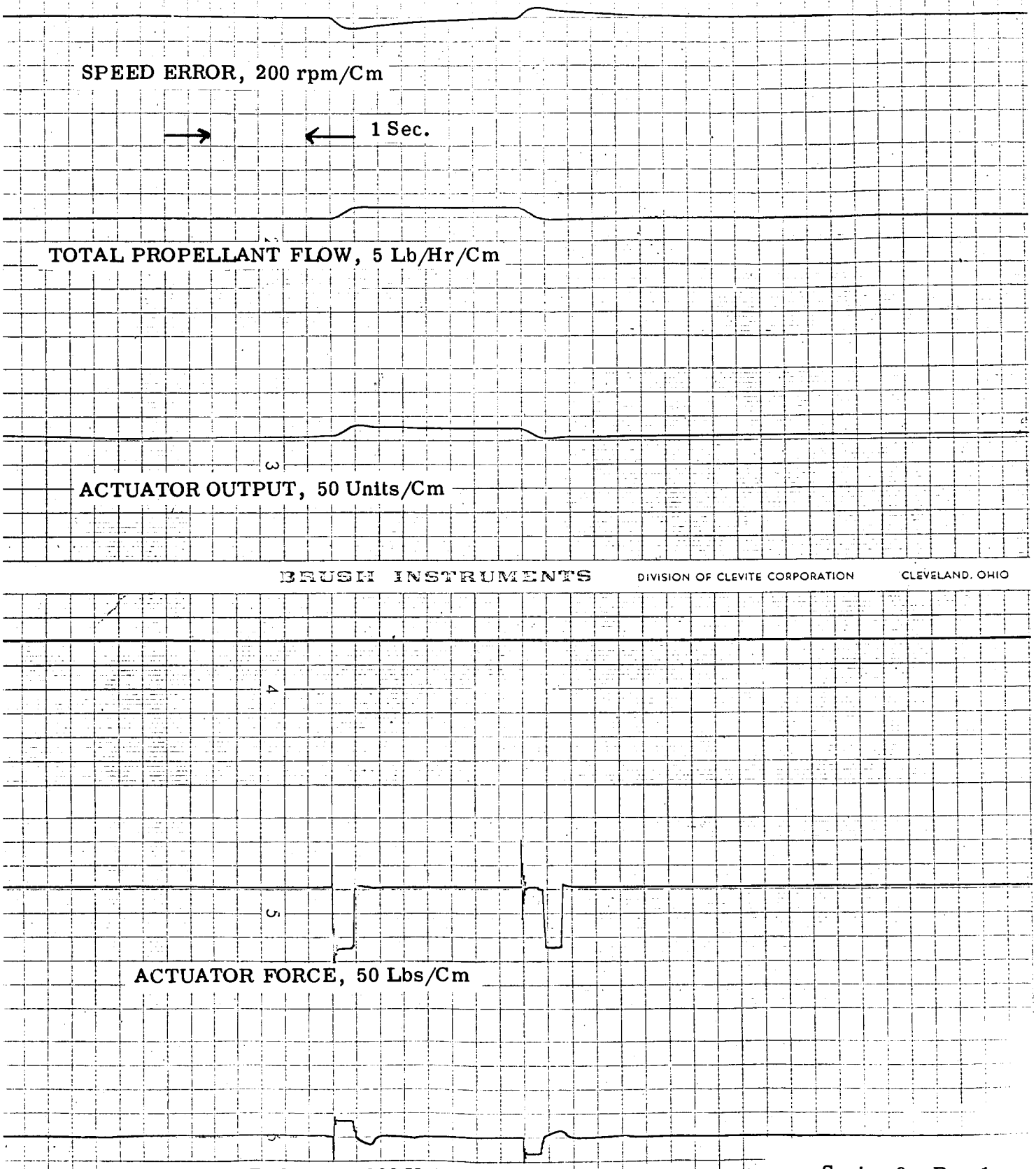

Series 6 - Run 1

SPEED LOOP RESPONSE

4000 RPM SYSTEM

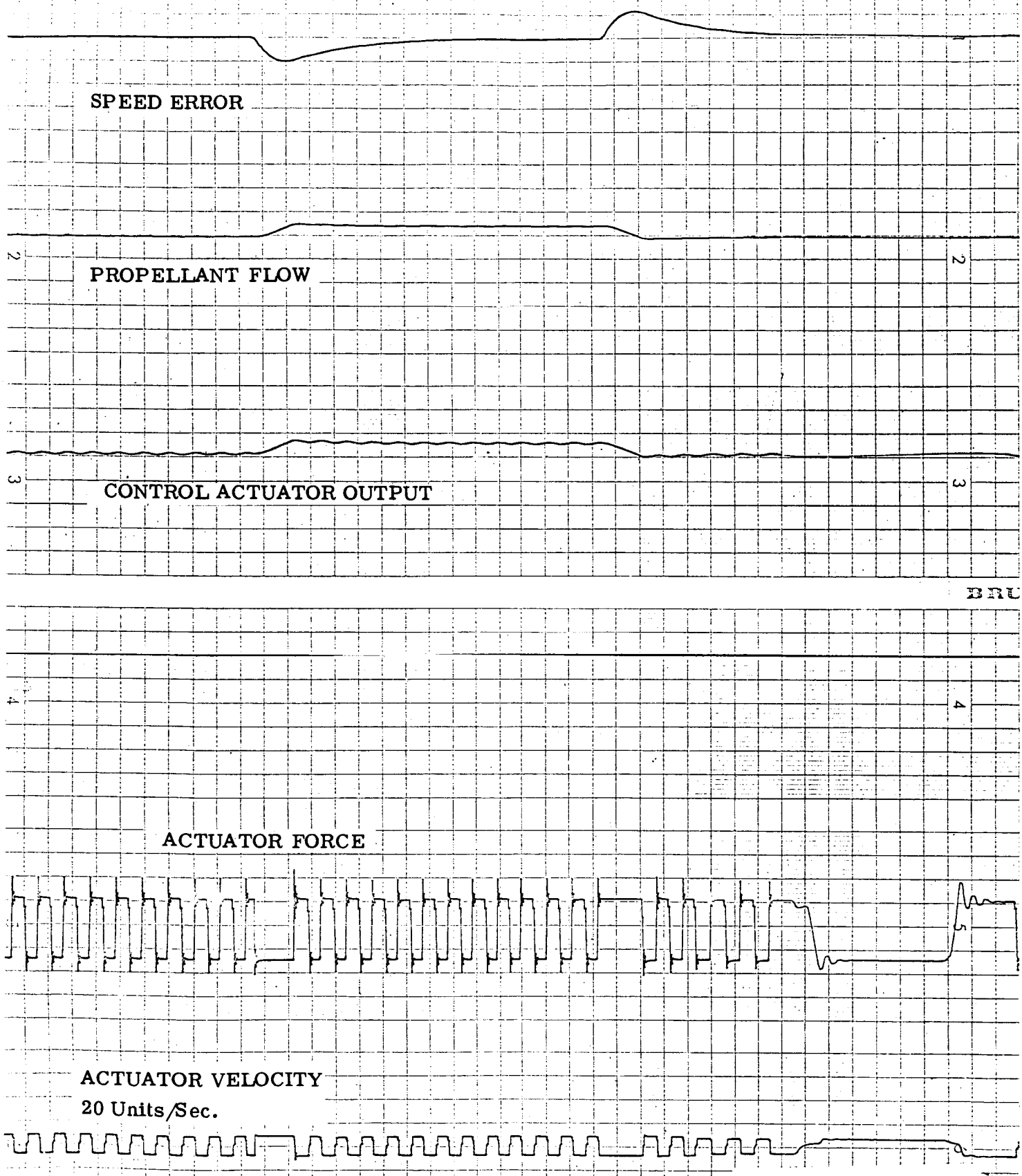

Series 7 - Run 1

SPEED LOOP TRANSIENT RESPONSE
RESPONSE TO .87 KW STEP INPUT
EXAMPLE OF HIGH ACTUATOR GAIN

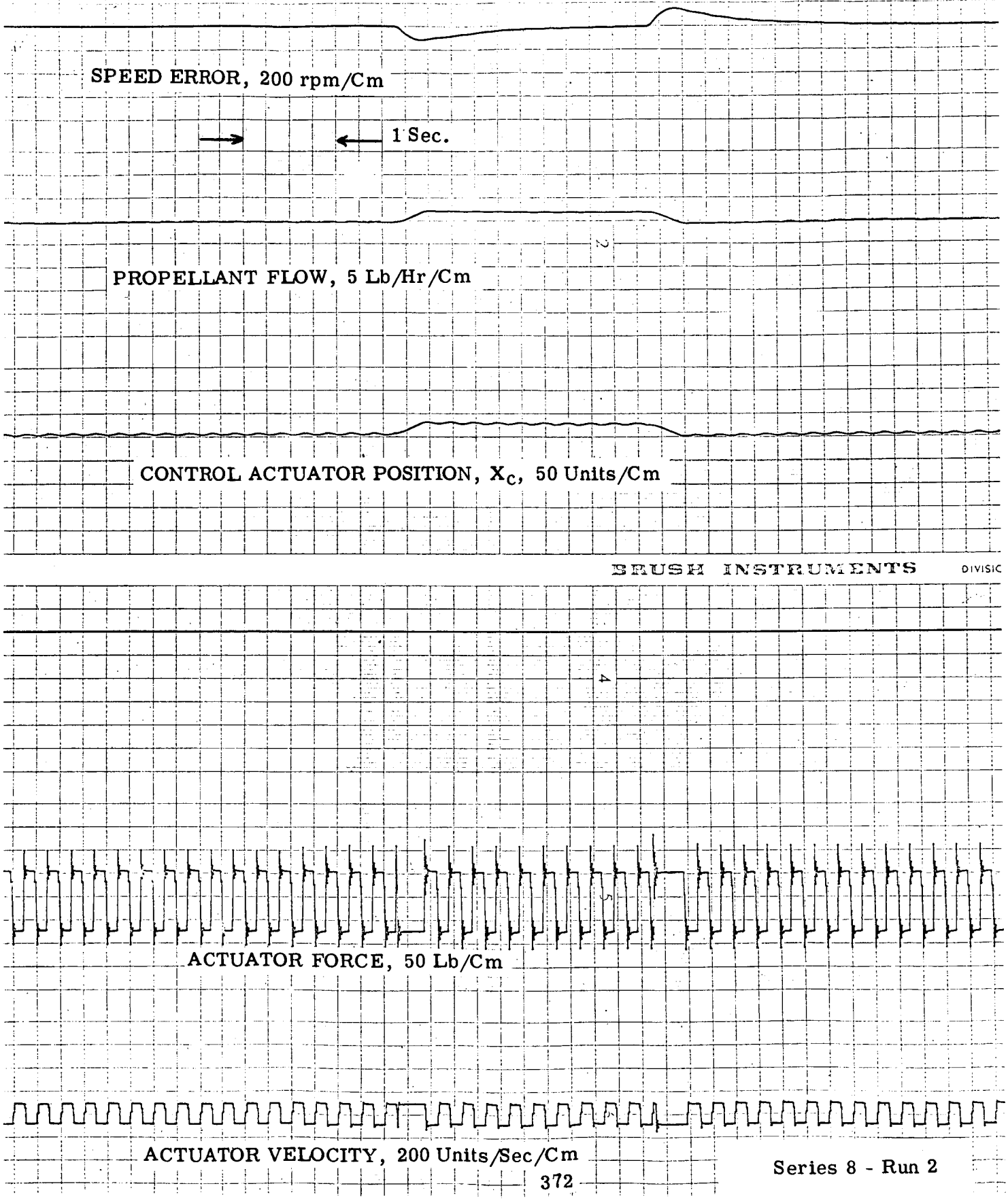

Series 8 - Run 2

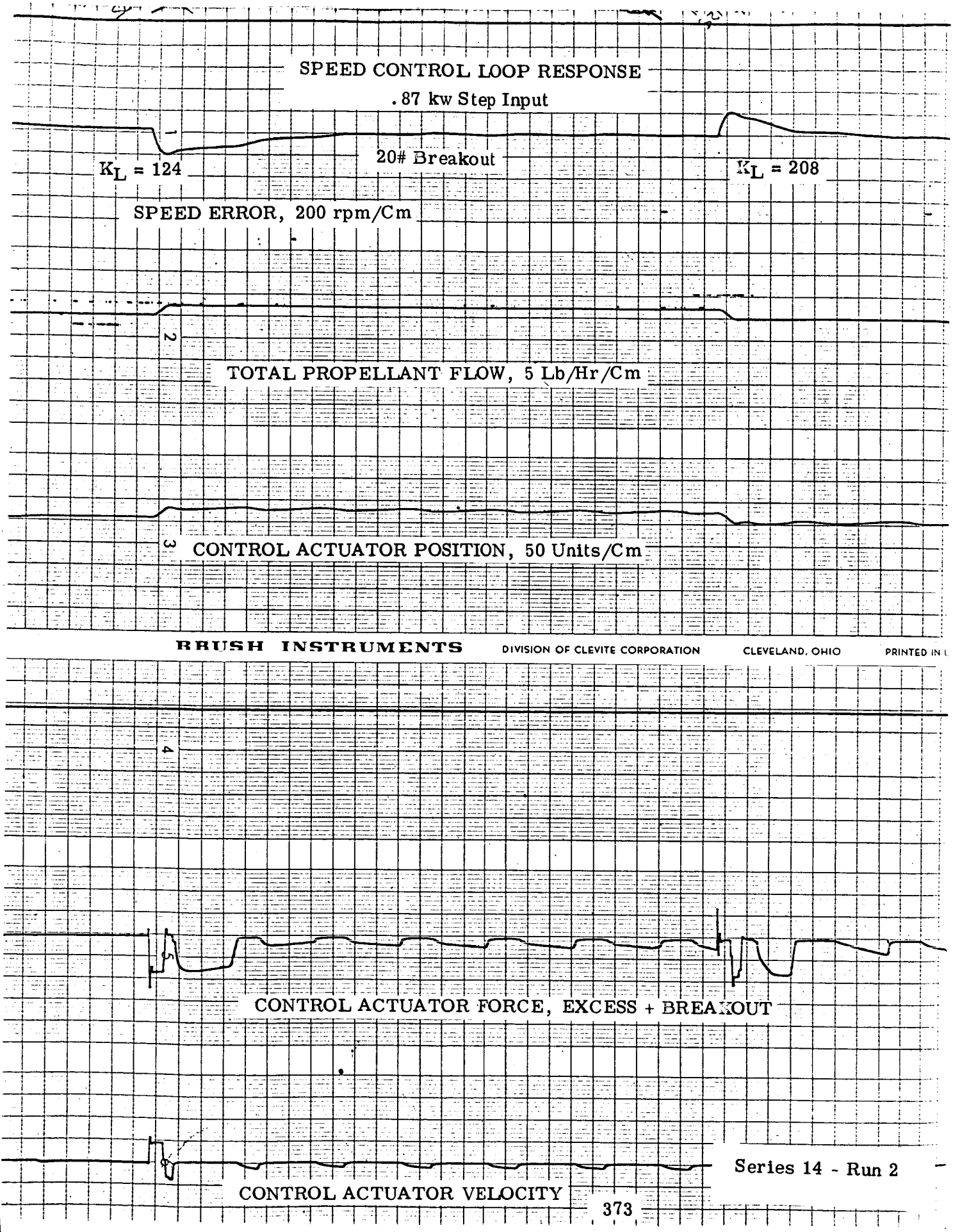

Series 14 - Run 2

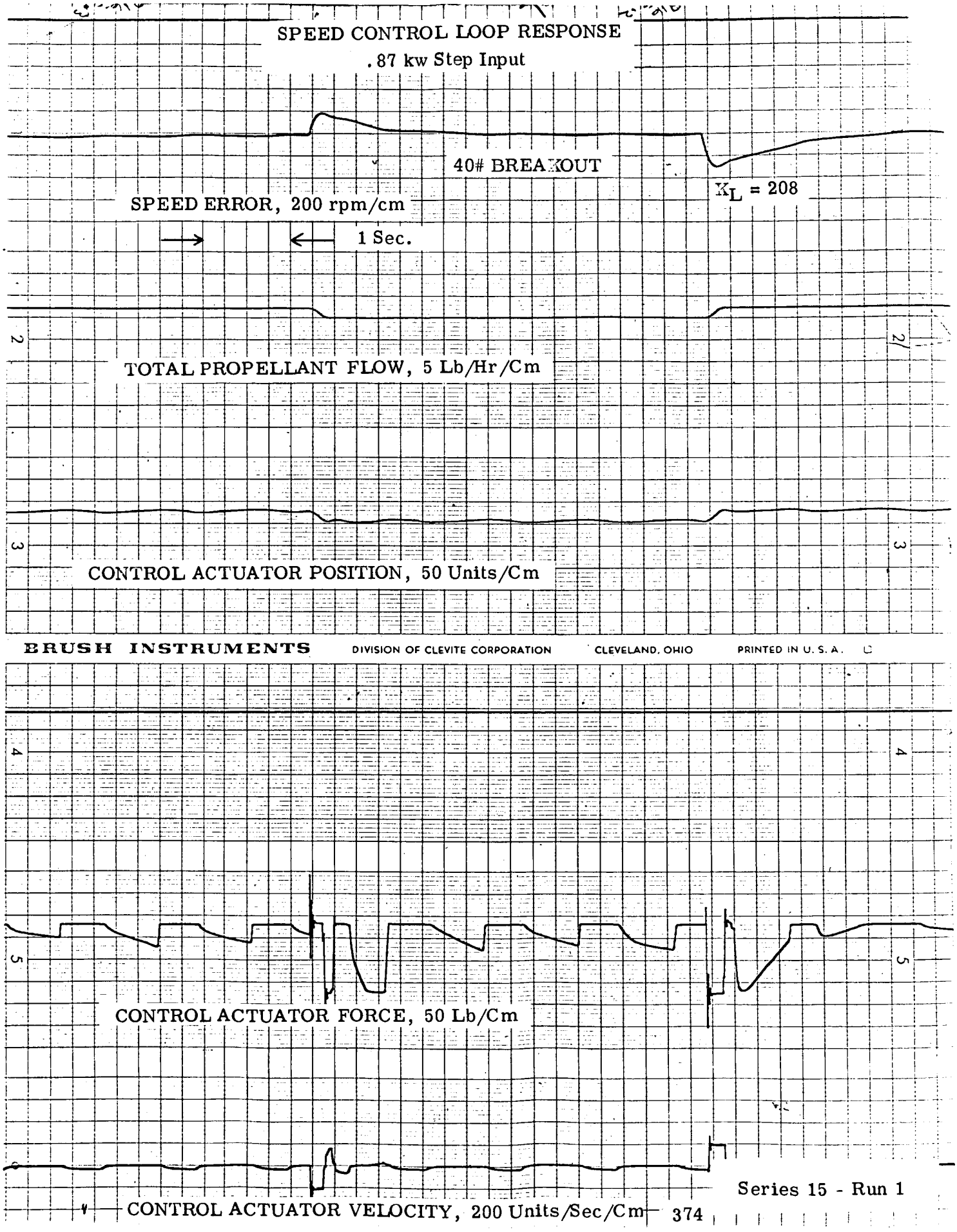
SPEED CONTROL LOOP RESPONSE
.87 kw Step Input
40# BREAKOUT
K_L = 208
SPEED ERROR, 200 rpm/cm
1 Sec.
TOTAL PROPELLANT FLOW, 5 Lb/Hr/Cm
CONTROL ACTUATOR POSITION, 50 Units/Cm
BRUSH INSTRUMENTS
DIVISION OF CLEVITE CORPORATION
CLEVELAND, OHIO
PRINTED IN U. S. A.
CONTROL ACTUATOR FORCE, 50 Lb/Cm
CONTROL ACTUATOR VELOCITY, 200 Units/Sec/Cm
Series 15 - Run 1

ENGINE SPEED LOOP RESPONSE
(Run to Establish Excess)

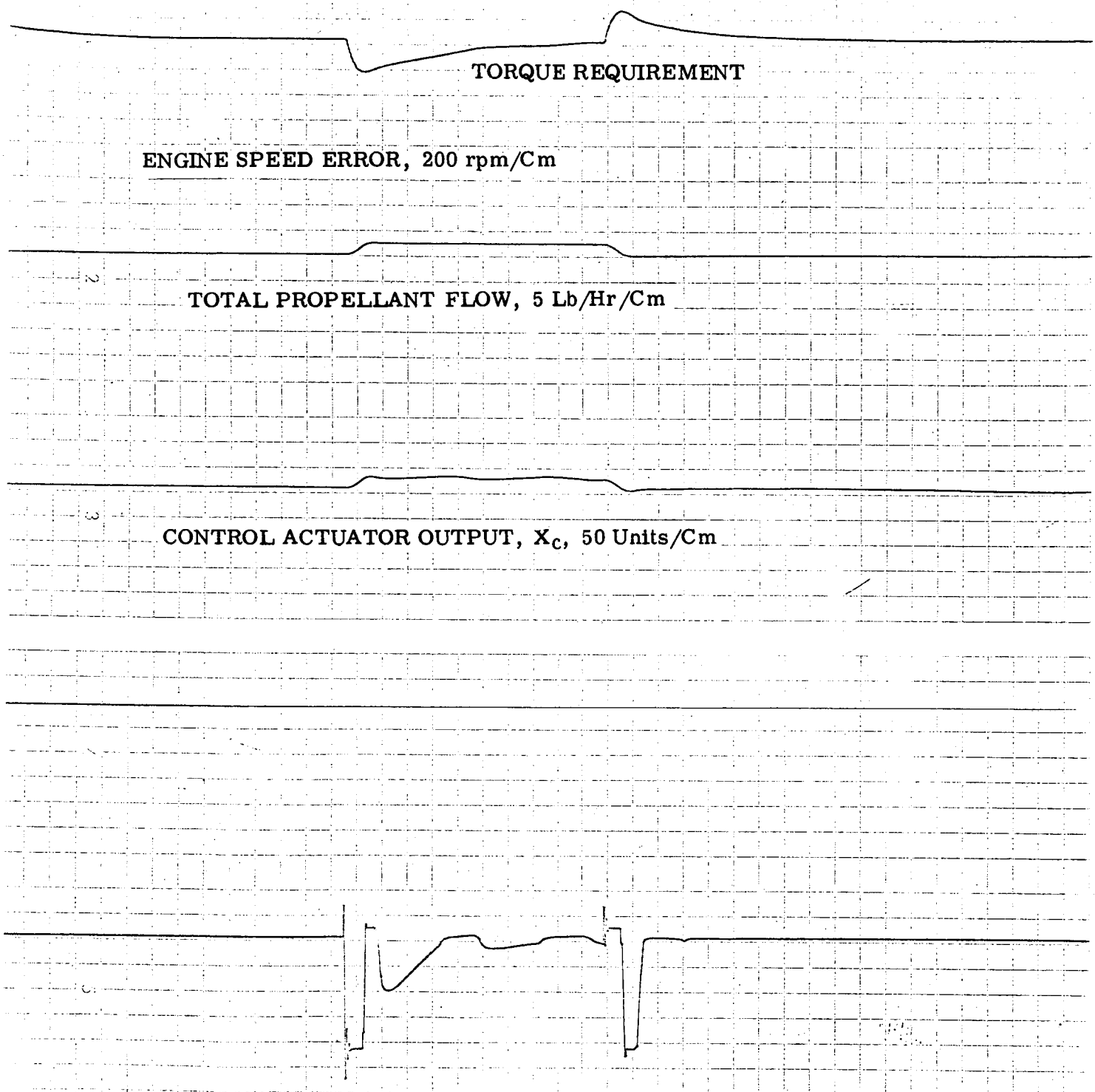

Series 16 - Run 1

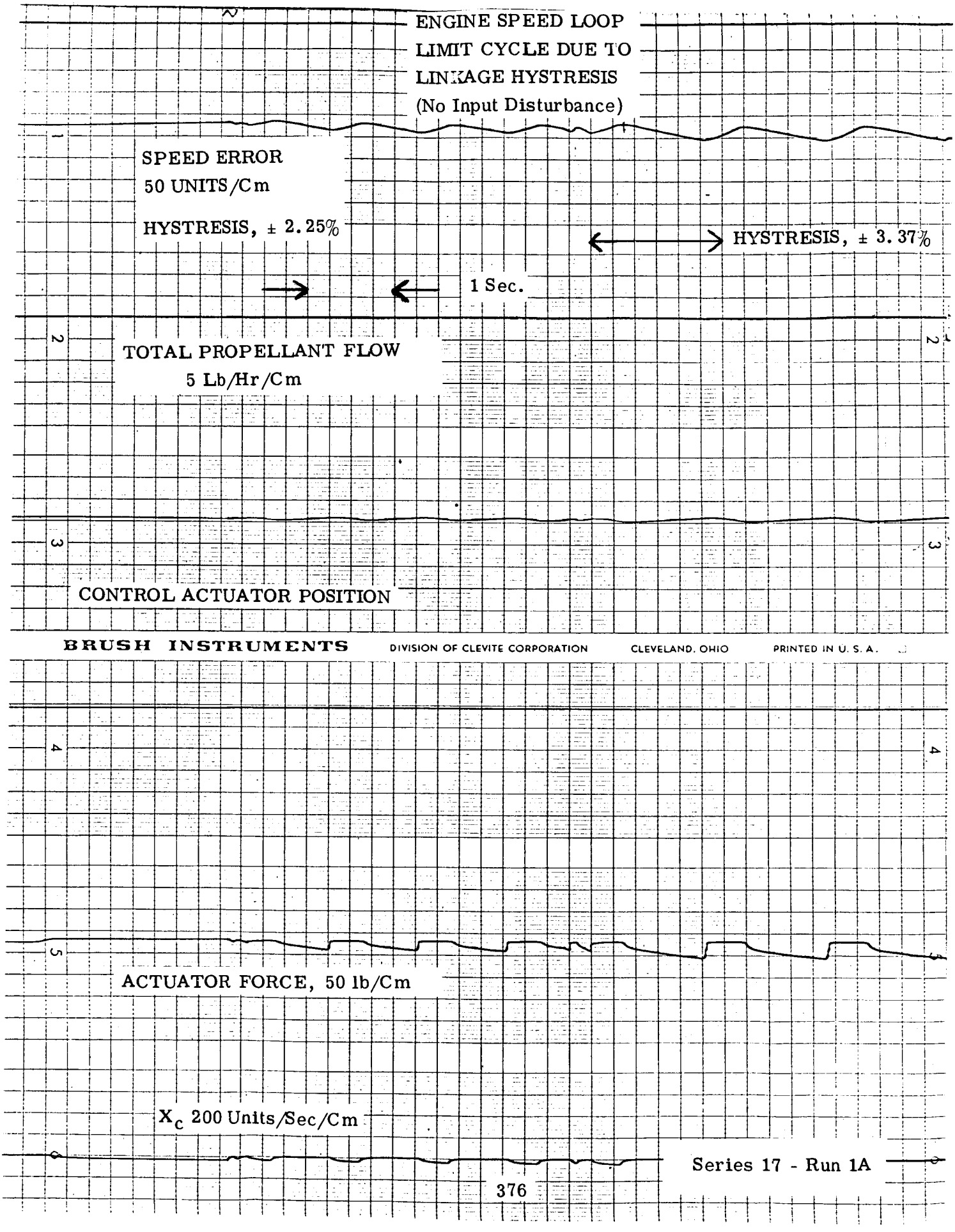
ENGINE SPEED LOOP
LIMIT CYCLE DUE TO
LINKAGE HYSTRESIS
(No Input Disturbance)
SPEED ERROR
50 UNITS/Cm
HYSTRESIS, ± 2.25%
HYSTRESIS, ± 3.37%
1 Sec.
TOTAL PROPELLANT FLOW
5 Lb/Hr/Cm
CONTROL ACTUATOR POSITION
BRUSH INSTRUMENTS
DIVISION OF CLEVITE CORPORATION
CLEVELAND, OHIO
PRINTED IN U. S. A.
ACTUATOR FORCE, 50 lb/Cm
X_c 200 Units/Sec/Cm
Series 17 - Run 1A

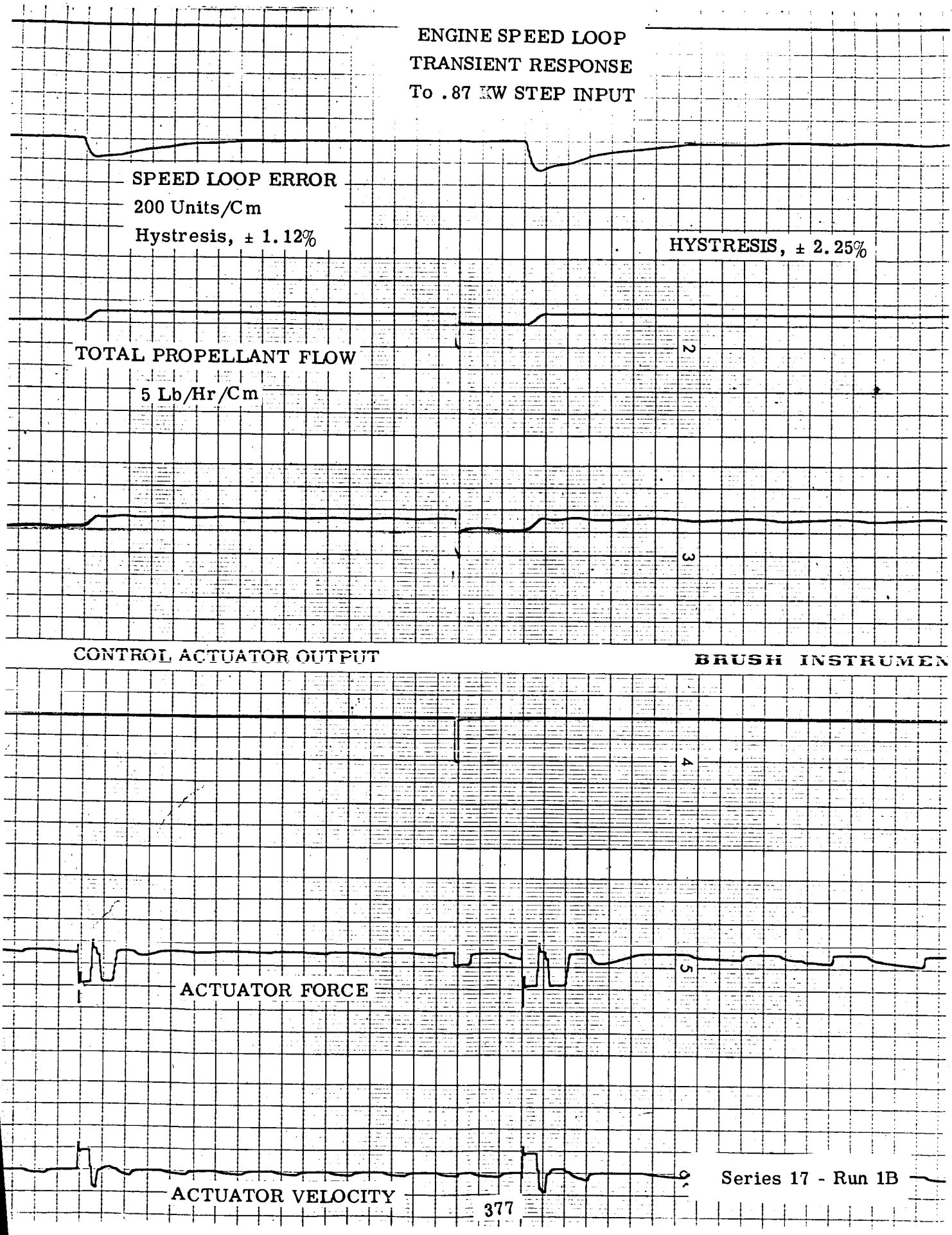
ENGINE SPEED LOOP
TRANSIENT RESPONSE
To .87 KW STEP INPUT
SPEED LOOP ERROR
200 Units/Cm
Hystresis, ± 1.12%
HYSTRESIS, ± 2.25%
TOTAL PROPELLANT FLOW
5 Lb/Hr/Cm
2
3
CONTROL ACTUATOR OUTPUT
BRUSH INSTRUMEN
4
5
ACTUATOR FORCE
ACTUATOR VELOCITY
Series 17 - Run 1B

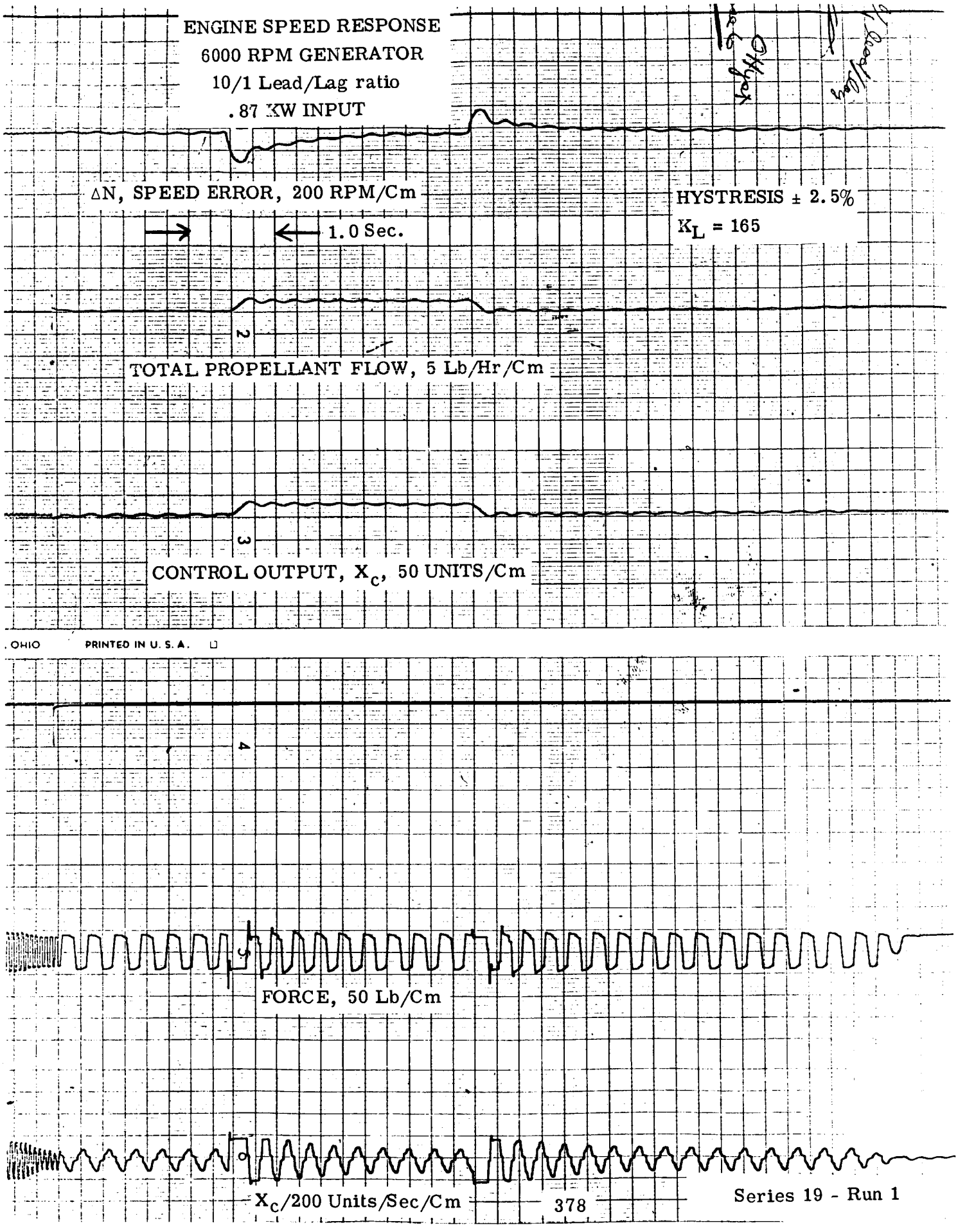

Series 19 - Run 1

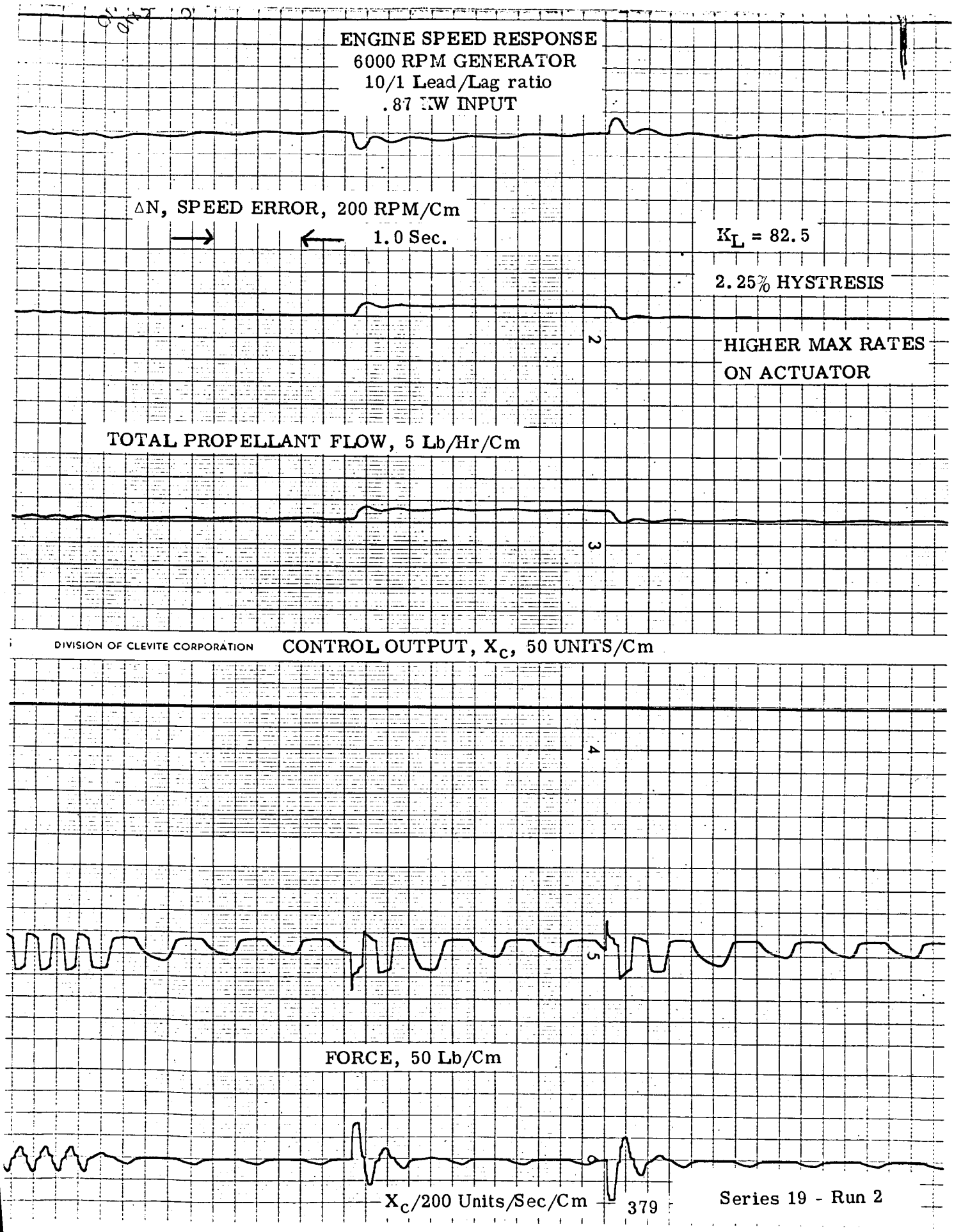
ENGINE SPEED RESPONSE
6000 RPM GENERATOR
10/1 Lead/Lag ratio
.87 KW INPUT
ΔN, SPEED ERROR, 200 RPM/Cm
1.0 Sec.
K_L = 82.5
2.25% HYSTRESIS
2
HIGHER MAX RATES
ON ACTUATOR
TOTAL PROPELLANT FLOW, 5 Lb/Hr/Cm
3
DIVISION OF CLEVITE CORPORATION
CONTROL OUTPUT, X_c, 50 UNITS/Cm
4
5
FORCE, 50 Lb/Cm
X_c/200 Units/Sec/Cm
Series 19 - Run 2

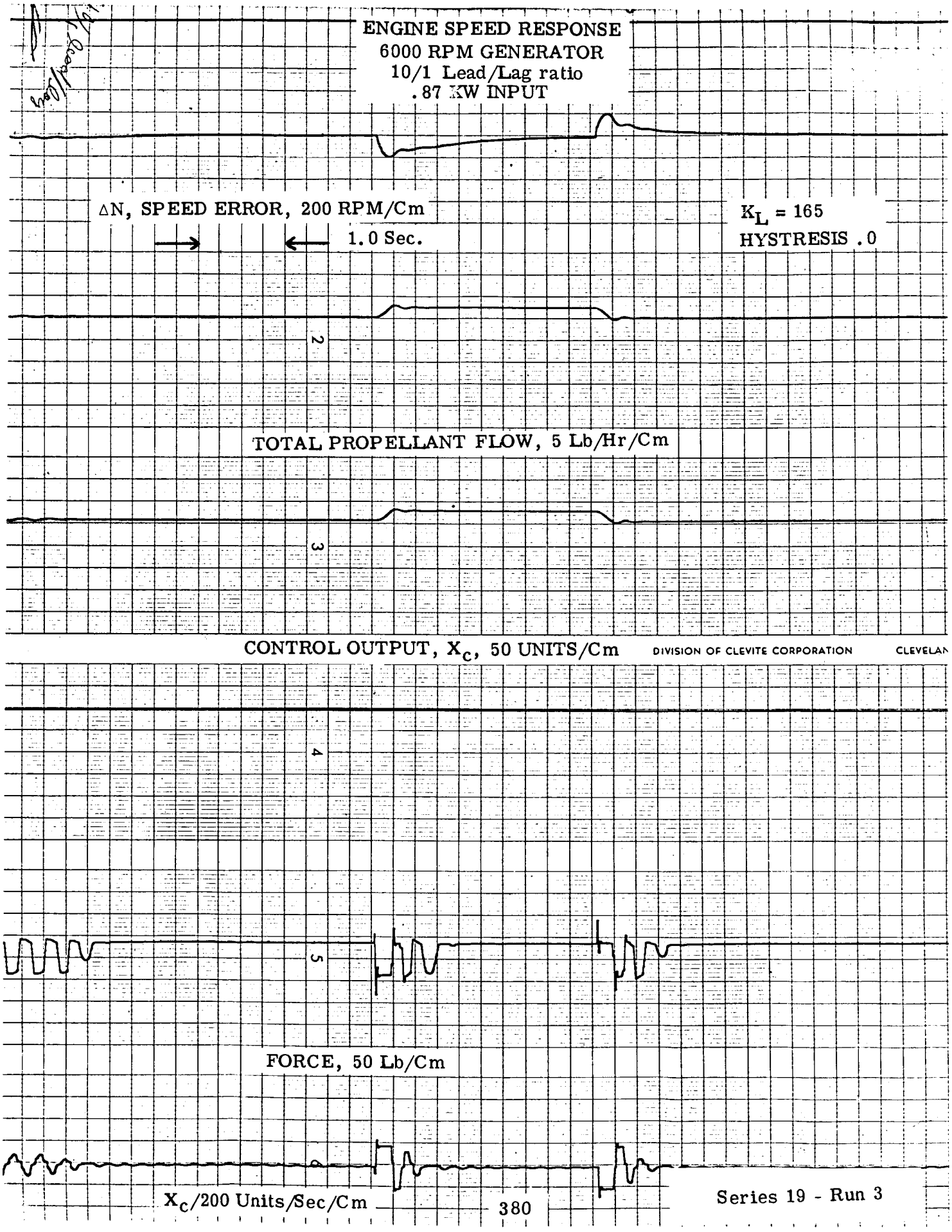
ENGINE SPEED RESPONSE
6000 RPM GENERATOR
10/1 Lead/Lag ratio
.87 KW INPUT
ΔN, SPEED ERROR, 200 RPM/Cm
1.0 Sec.
K_L = 165
HYSTRESIS .0
2
TOTAL PROPELLANT FLOW, 5 Lb/Hr/Cm
3
CONTROL OUTPUT, X_c, 50 UNITS/Cm
DIVISION OF CLEVITE CORPORATION
CLEVELAN
4
5
FORCE, 50 Lb/Cm
X_c/200 Units/Sec/Cm
Series 19 - Run 3

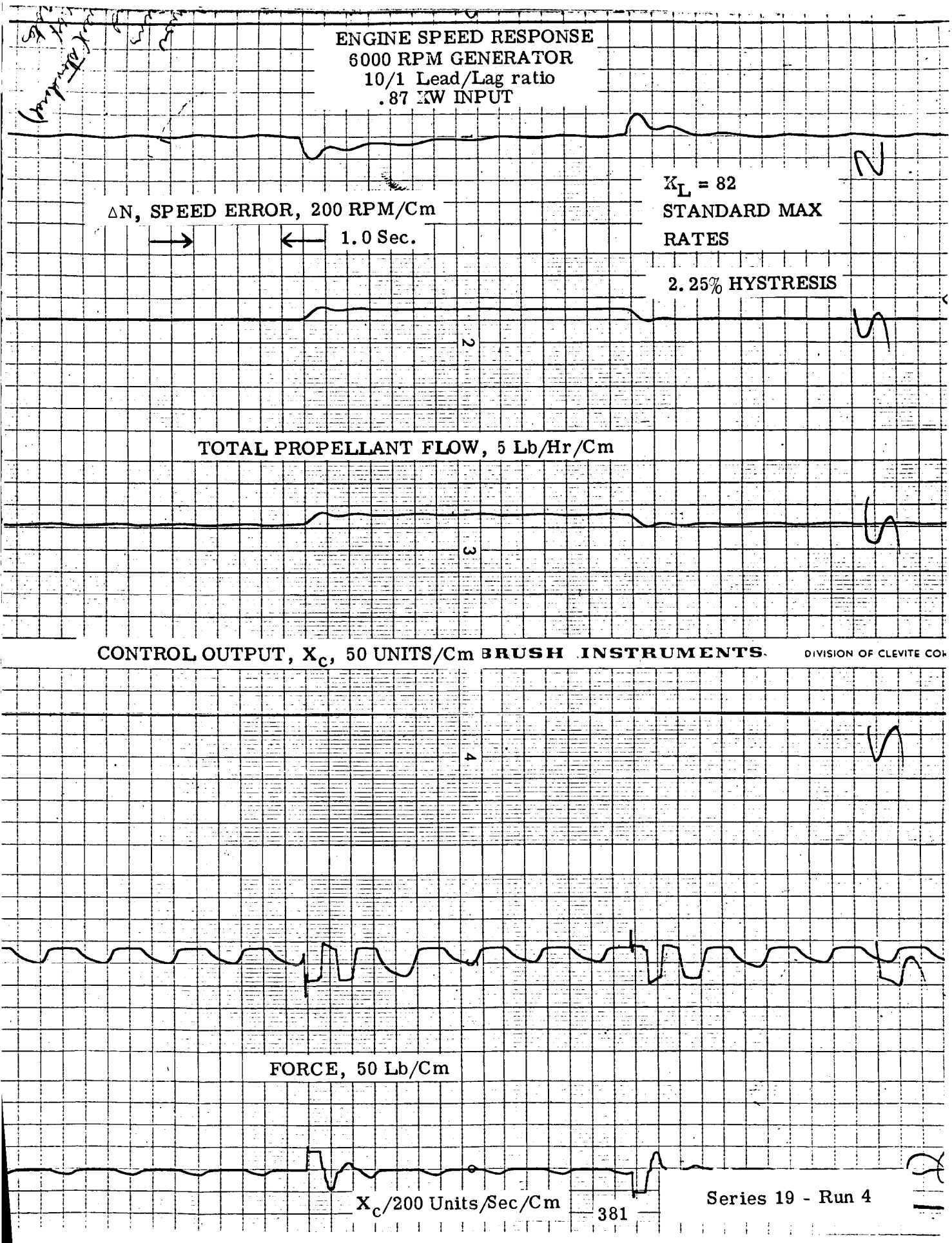
ENGINE SPEED RESPONSE
6000 RPM GENERATOR
10/1 Lead/Lag ratio
.87 KW INPUT
ΔN, SPEED ERROR, 200 RPM/Cm
1.0 Sec.
K_L = 82
STANDARD MAX
RATES
2.25% HYSTRESIS
TOTAL PROPELLANT FLOW, 5 Lb/Hr/Cm
CONTROL OUTPUT, X_c, 50 UNITS/Cm
BRUSH INSTRUMENTS
DIVISION OF CLEVITE CO
FORCE, 50 Lb/Cm
X_c/200 Units/Sec/Cm
Series 19 - Run 4

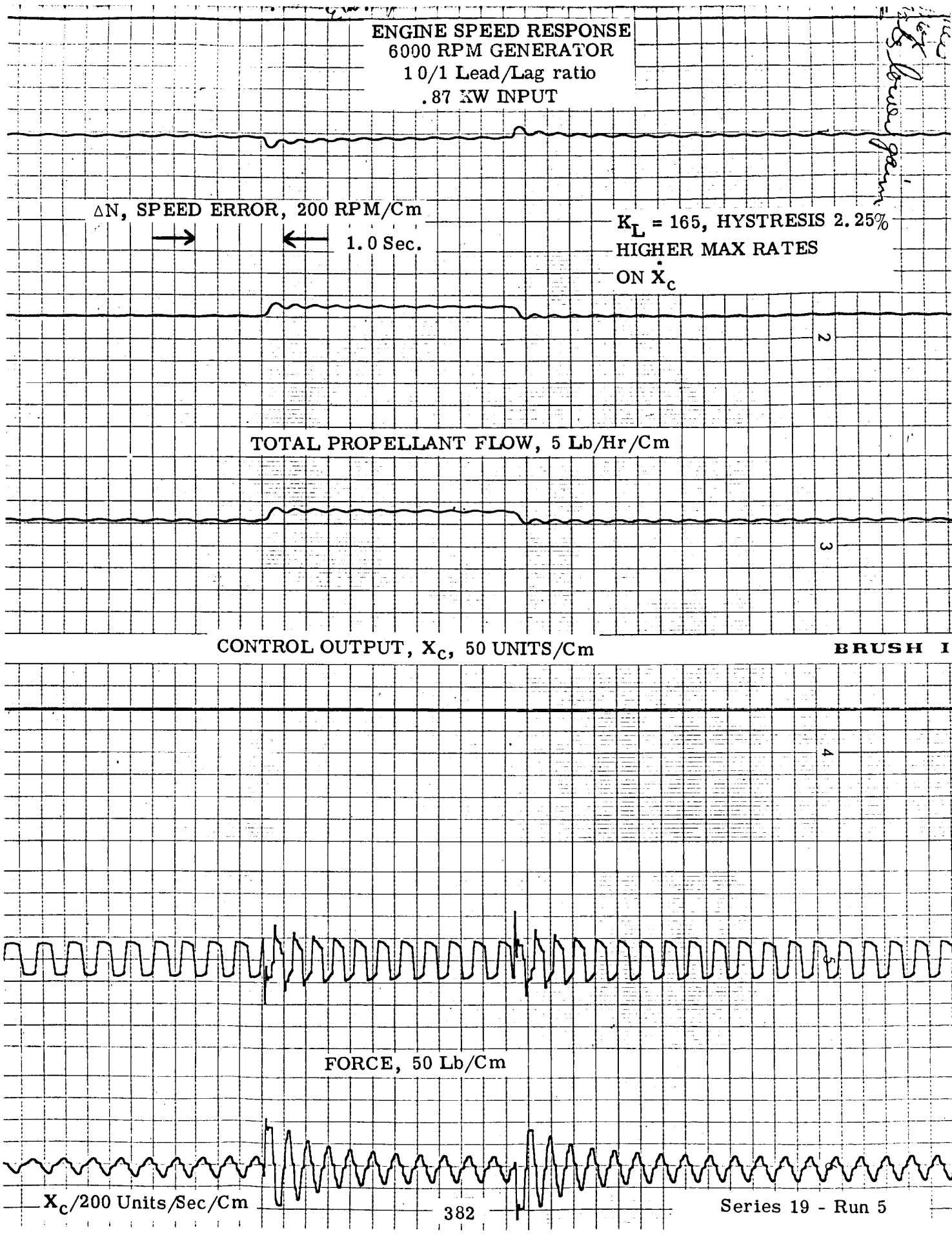

Series 19 - Run 5

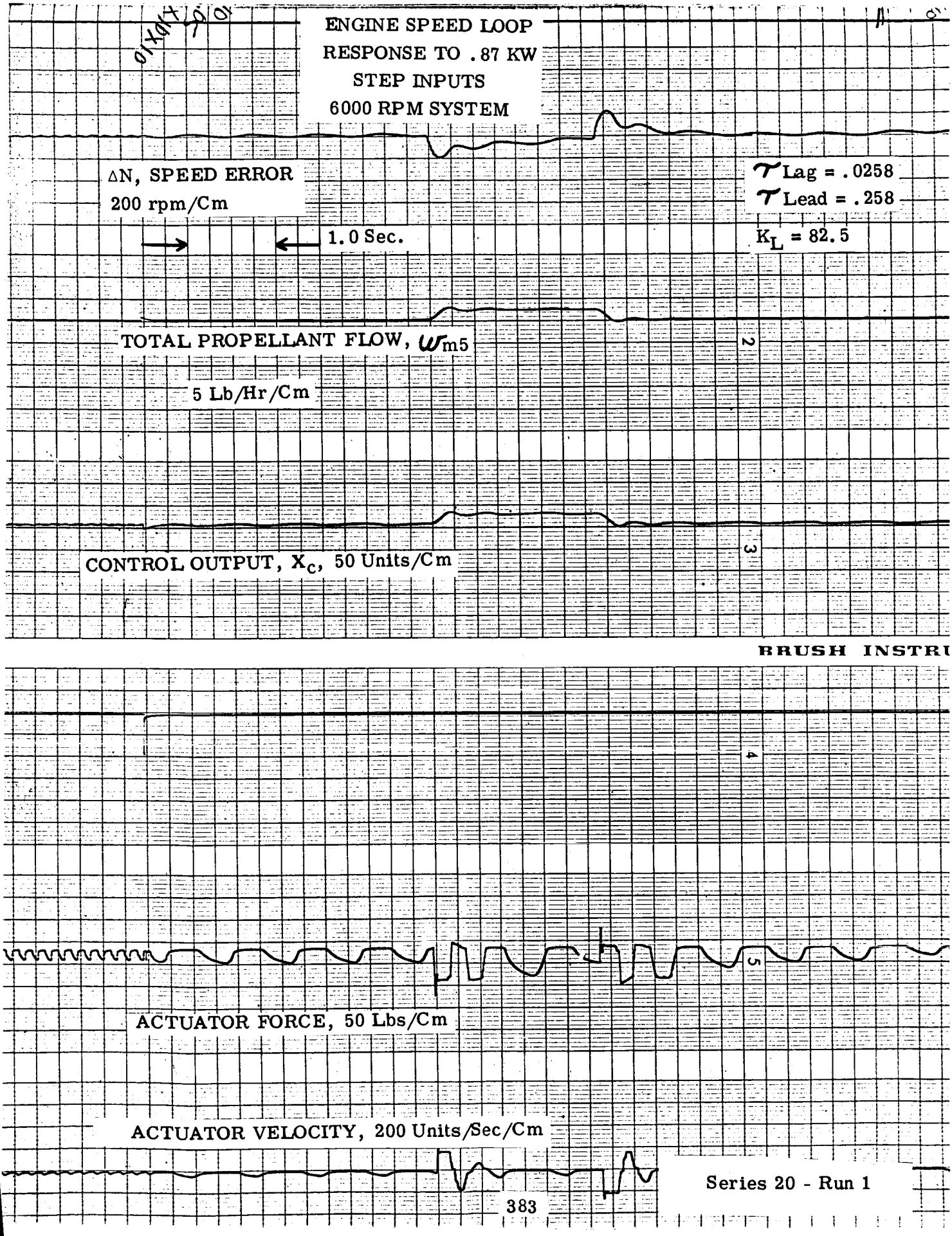
ENGINE SPEED LOOP
RESPONSE TO .87 KW
STEP INPUTS
6000 RPM SYSTEM
ΔN, SPEED ERROR
200 rpm/Cm
1.0 Sec.
τ Lag = .0258
τ Lead = .258
K_L = 82.5
TOTAL PROPELLANT FLOW, ω_m5
5 Lb/Hr/Cm
2
CONTROL OUTPUT, X_c, 50 Units/Cm
3
BRUSH INSTRU
4
5
ACTUATOR FORCE, 50 Lbs/Cm
ACTUATOR VELOCITY, 200 Units/Sec/Cm
Series 20 - Run 1

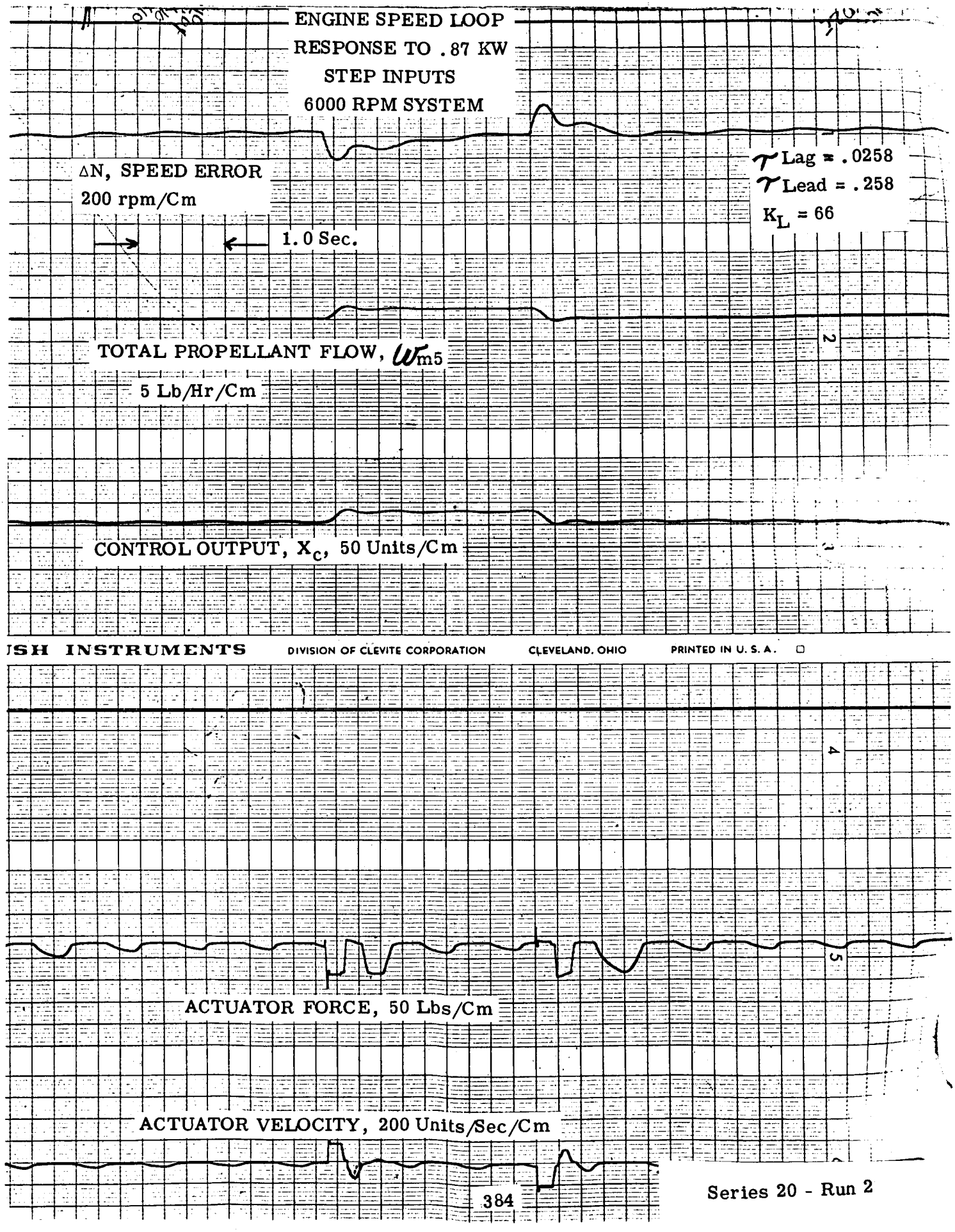

SH INSTRUMENTS DIVISION OF CLEVITE CORPORATION CLEVELAND, OHIO PRINTED IN U. S. A.

Series 20 - Run 2

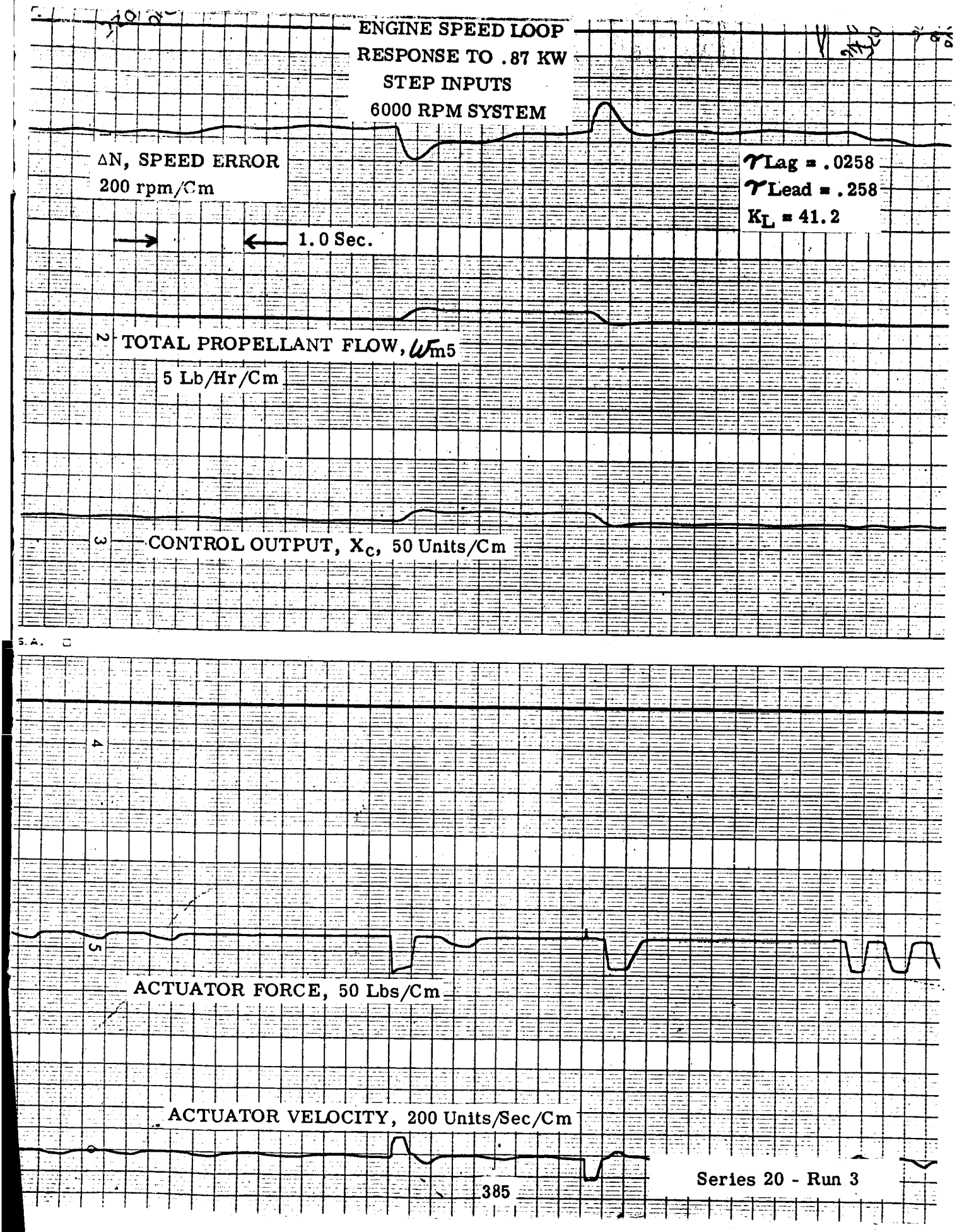
ENGINE SPEED LOOP
RESPONSE TO .87 KW
STEP INPUTS
6000 RPM SYSTEM
ΔN, SPEED ERROR
200 rpm/Cm
τLag = .0258
τLead = .258
KL = 41.2
1.0 Sec.
2
TOTAL PROPELLANT FLOW, Wm5
5 Lb/Hr/Cm
3
CONTROL OUTPUT, Xc, 50 Units/Cm
4
5
ACTUATOR FORCE, 50 Lbs/Cm
ACTUATOR VELOCITY, 200 Units/Sec/Cm
Series 20 - Run 3

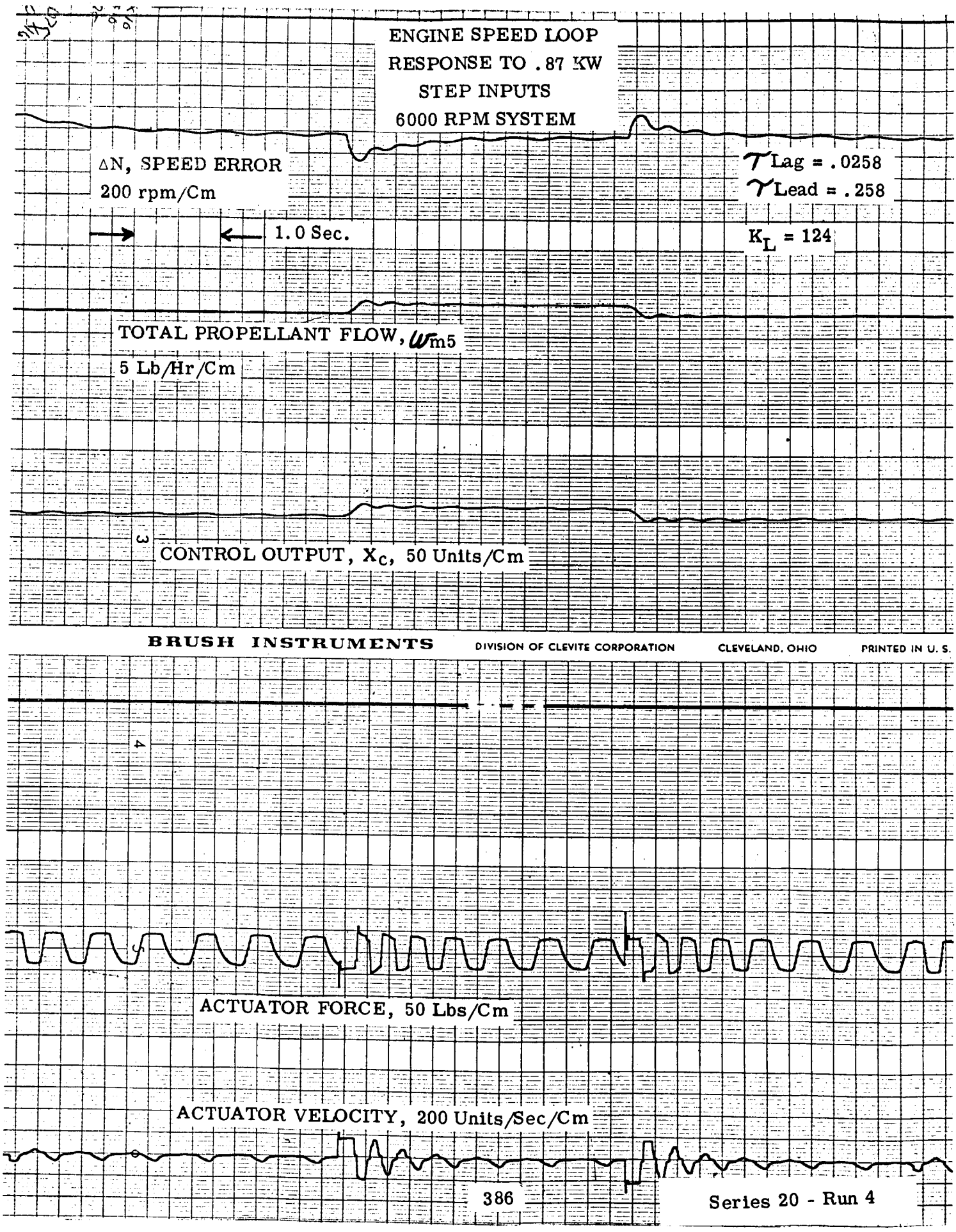
ENGINE SPEED LOOP
RESPONSE TO .87 KW
STEP INPUTS
6000 RPM SYSTEM
ΔN, SPEED ERROR
200 rpm/Cm
1.0 Sec.
τ Lag = .0258
τ Lead = .258
K_L = 124
TOTAL PROPELLANT FLOW, ωm5
5 Lb/Hr/Cm
3
CONTROL OUTPUT, X_C, 50 Units/Cm
BRUSH INSTRUMENTS
DIVISION OF CLEVITE CORPORATION
CLEVELAND, OHIO
PRINTED IN U. S.
4
ACTUATOR FORCE, 50 Lbs/Cm
ACTUATOR VELOCITY, 200 Units/Sec/Cm
386
Series 20 - Run 4

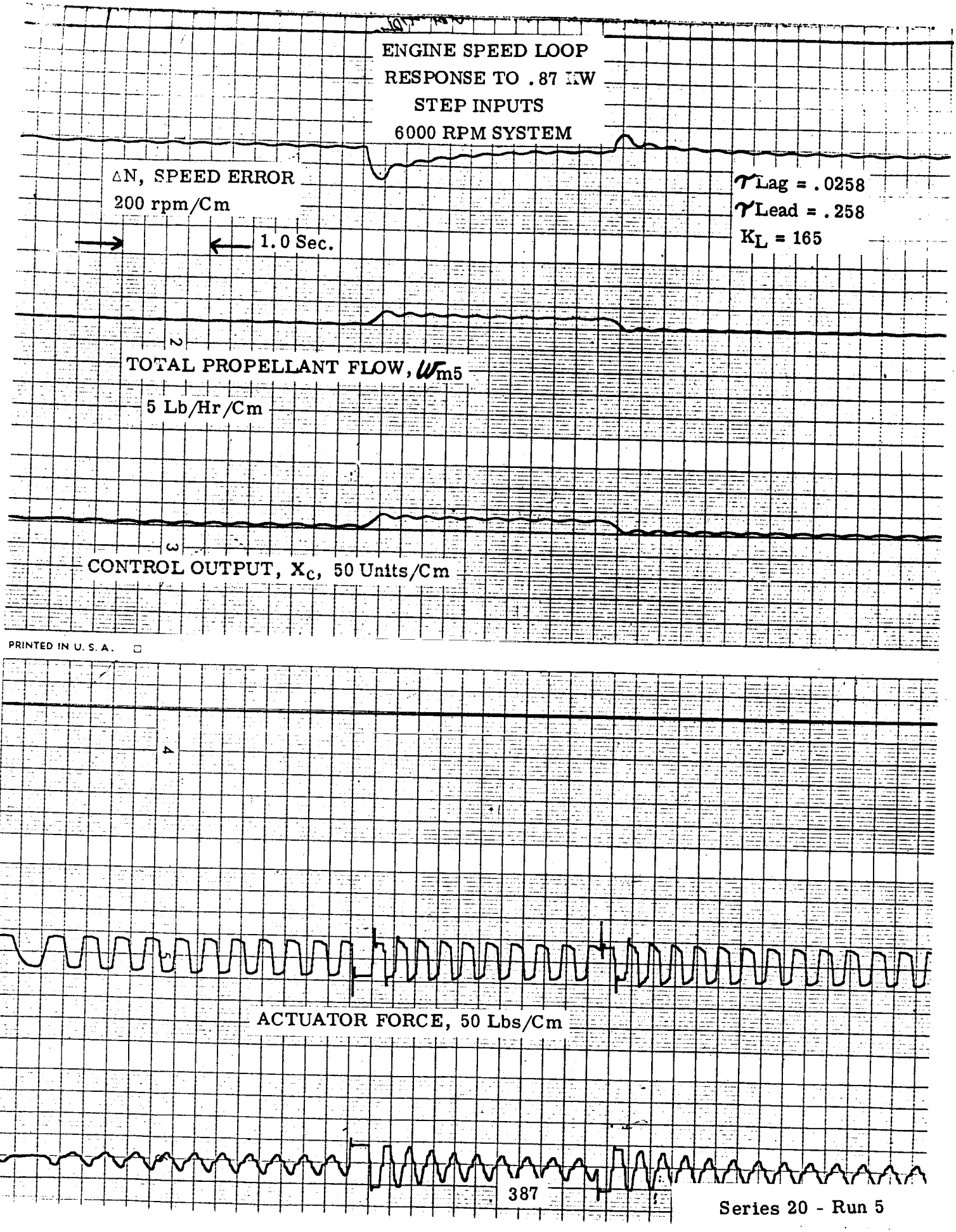

Series 20 - Run 5

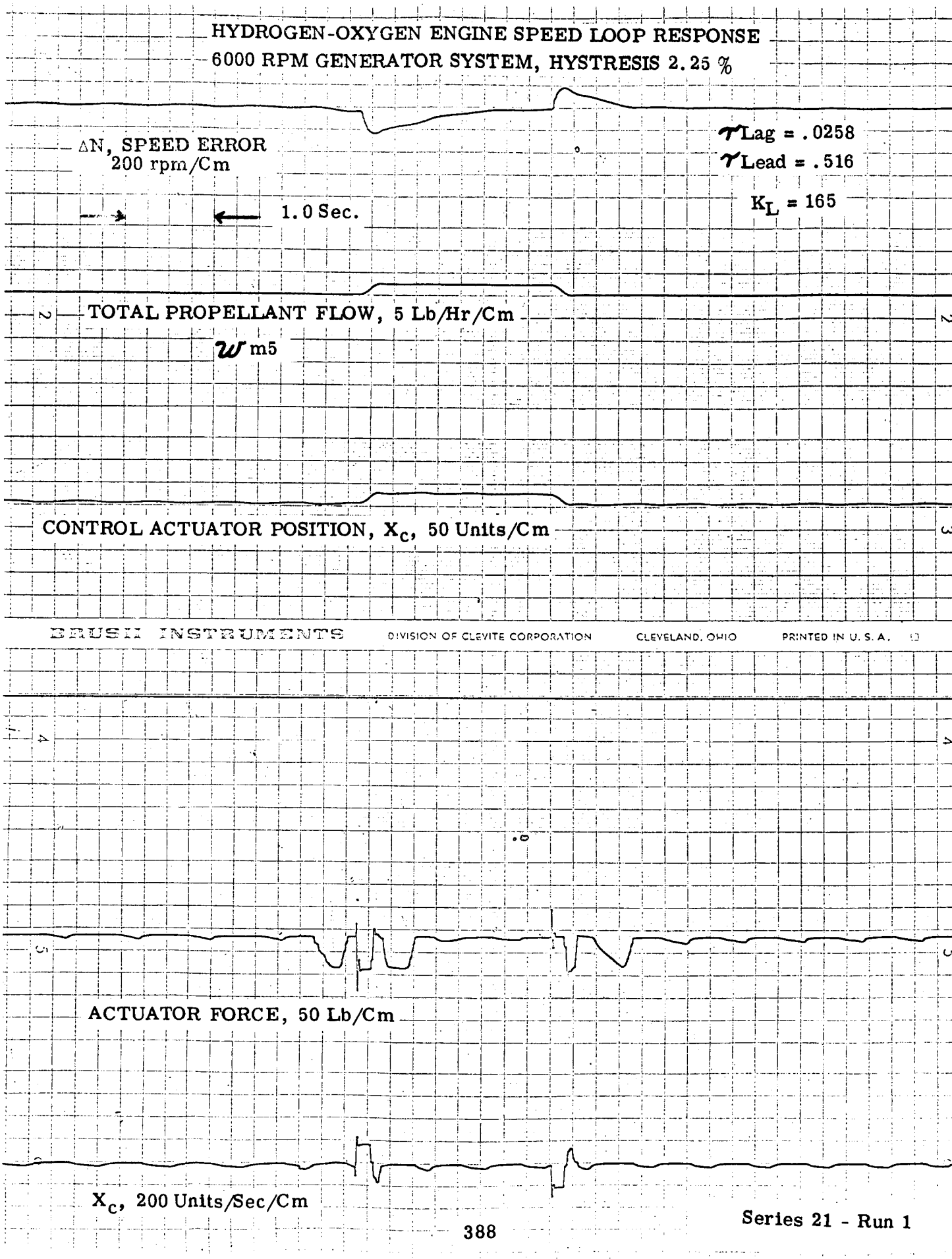

Series 21 - Run 1

HYDROGEN-OXYGEN ENGINE SPEED LOOP RESPONSE

6000 RPM GENERATOR SYSTEM, HYSTRESIS 2.25%

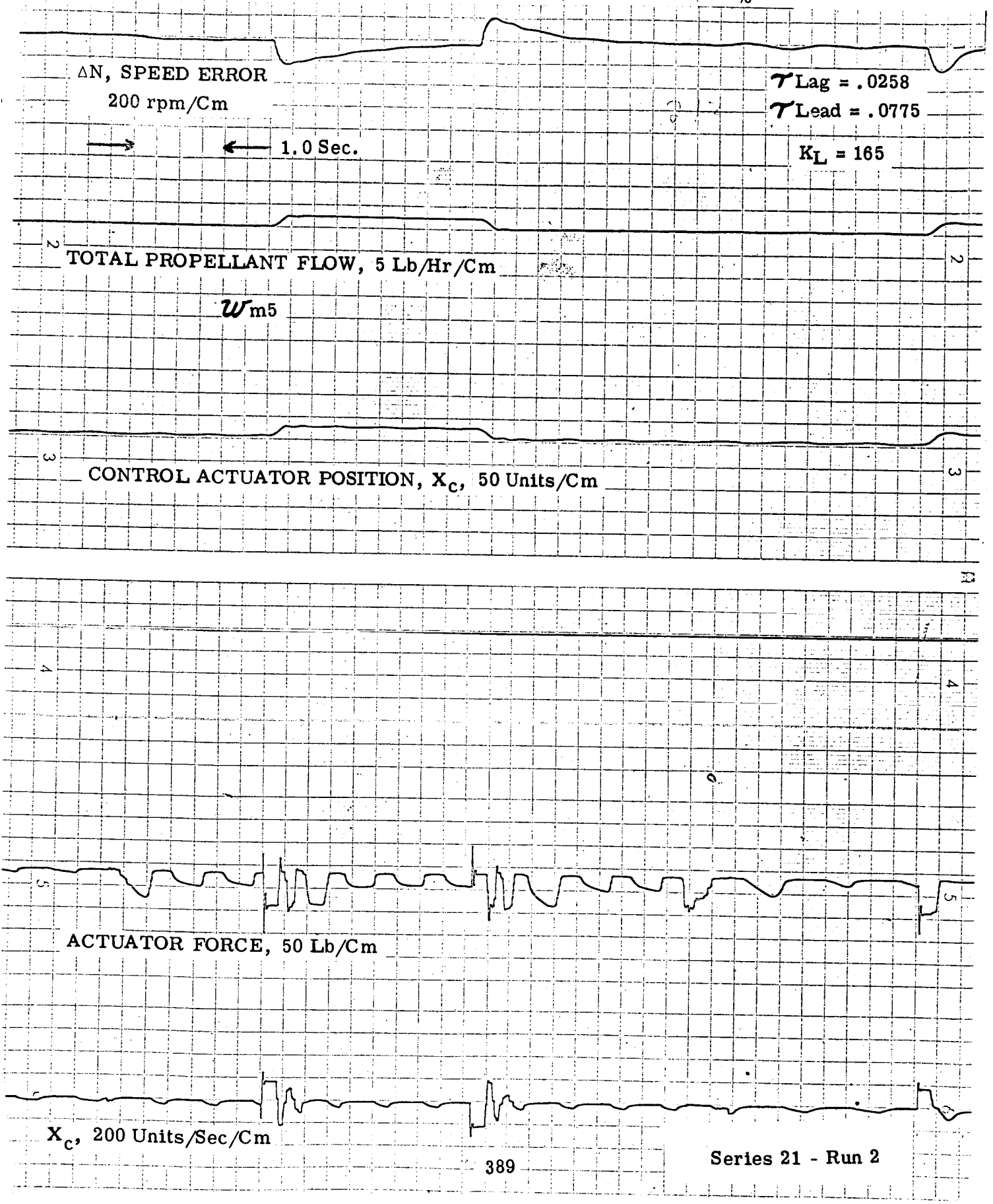

Series 21 - Run 2

HYDROGEN-OXYGEN ENGINE SPEED LOOP RESPONSE
6000 RPM GENERATOR SYSTEM, HYSTRESIS 2.25%

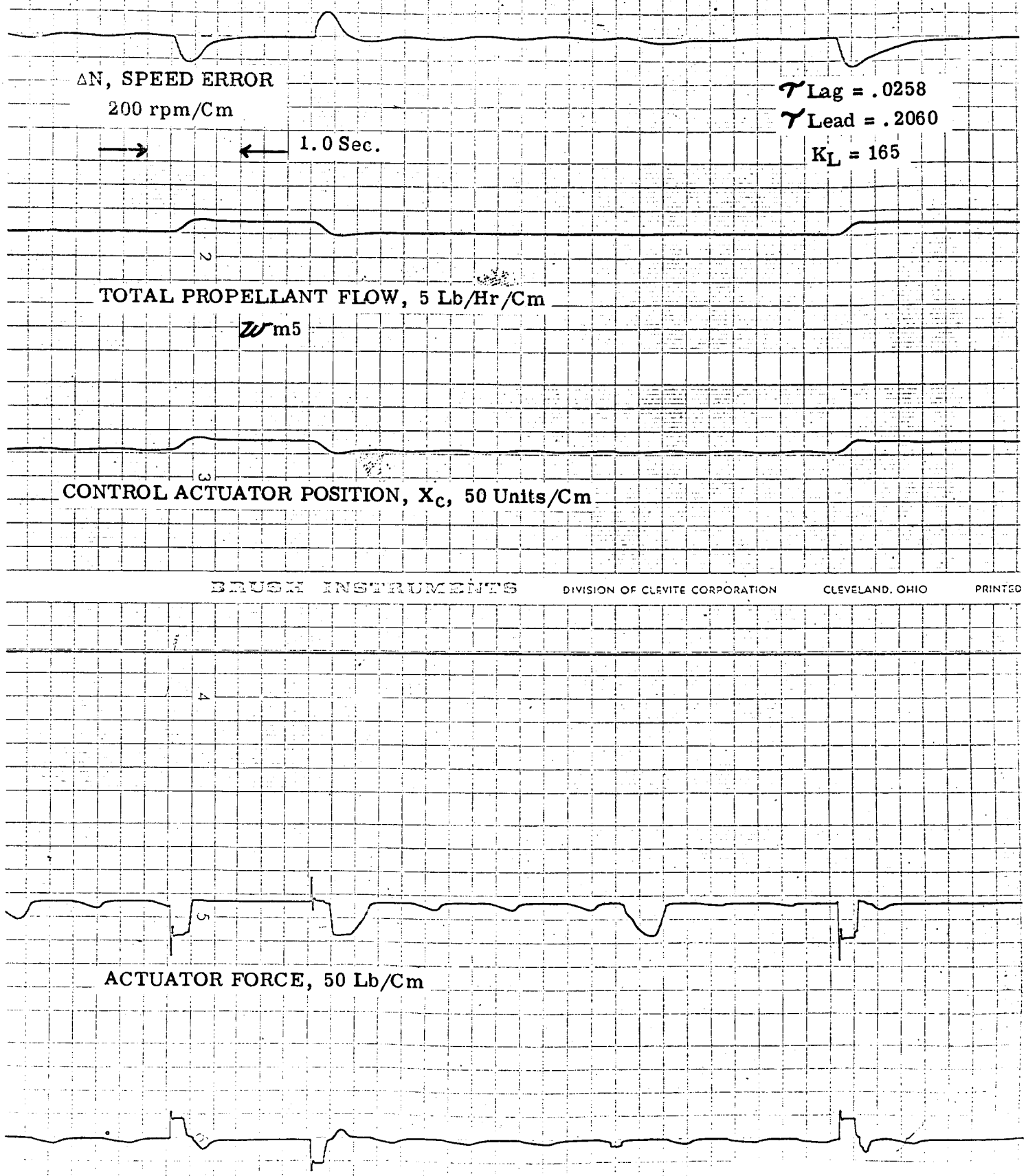

Series 21 - Run 3

HYDROGEN-OXYGEN ENGINE SPEED LOOP RESPONSE
6000 RPM GENERATOR SYSTEM, HYSTRESIS 2.25%

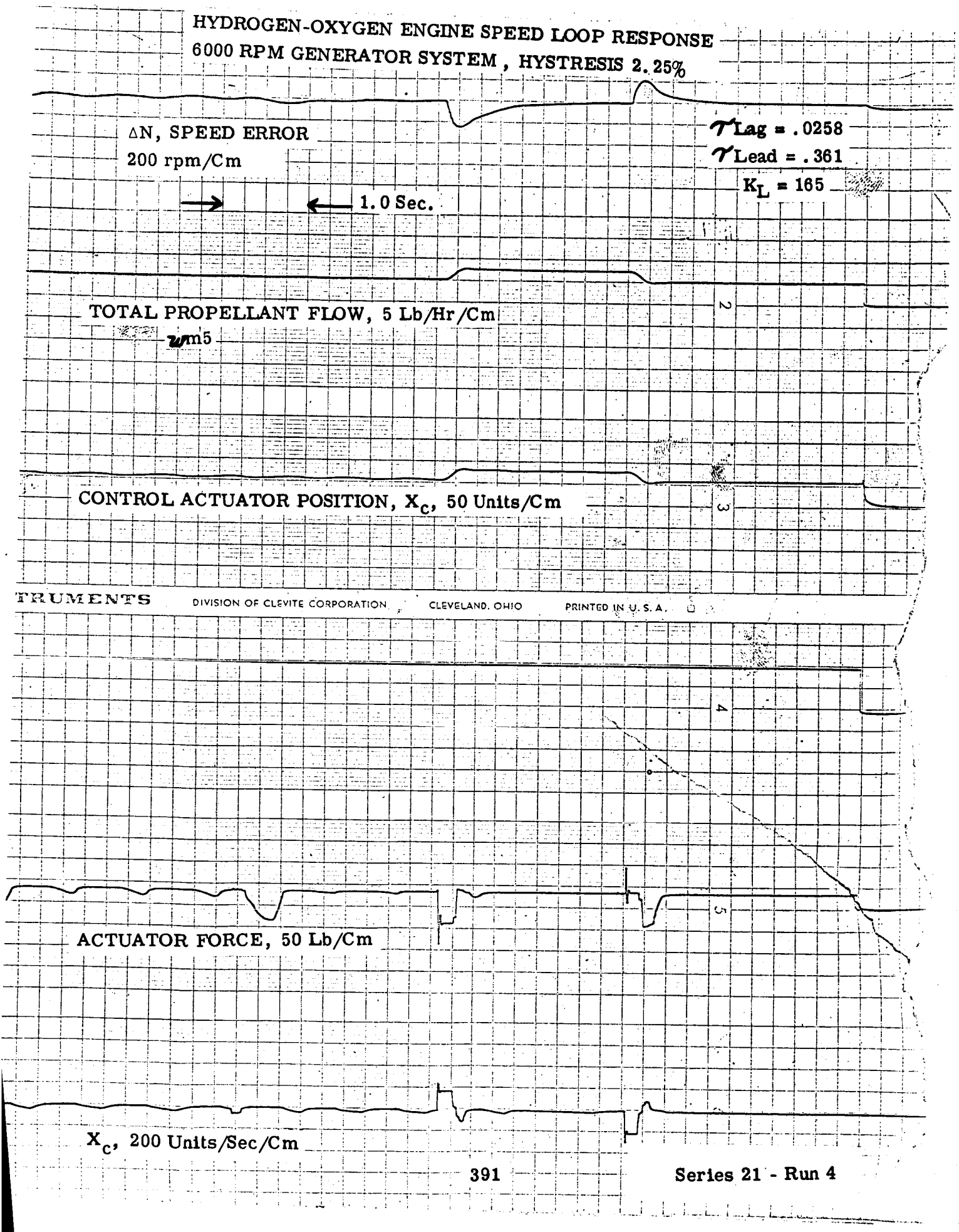

Series 21 - Run 4

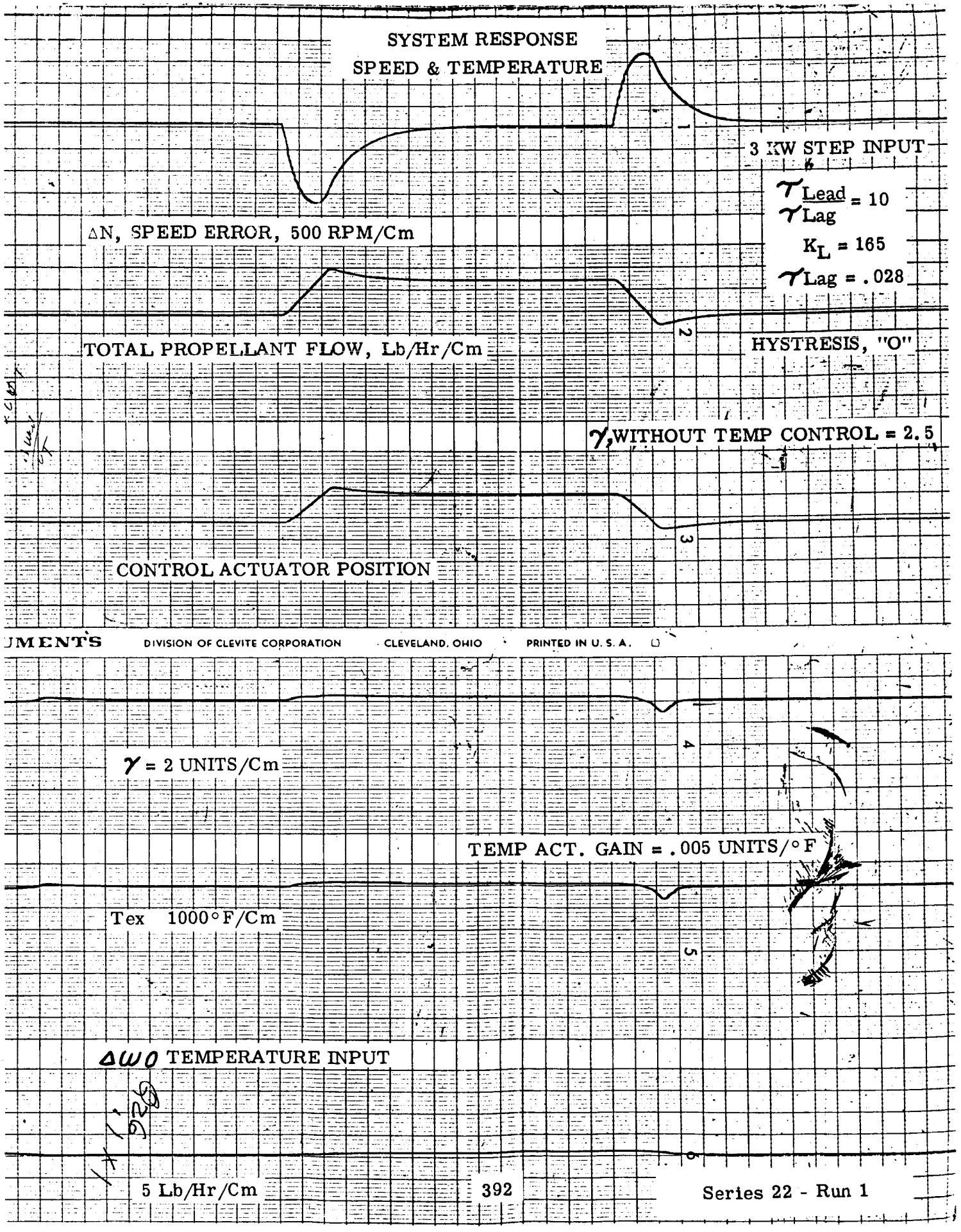
SYSTEM RESPONSE
SPEED & TEMPERATURE
3 KW STEP INPUT
τ Lead / τ Lag = 10
K_L = 165
τ Lag = .028
ΔN, SPEED ERROR, 500 RPM/Cm
TOTAL PROPELLANT FLOW, Lb/Hr/Cm
HYSTRESIS, "O"
γ, WITHOUT TEMP CONTROL = 2.5
CONTROL ACTUATOR POSITION
DIVISION OF CLEVITE CORPORATION
CLEVELAND, OHIO
PRINTED IN U. S. A.
γ = 2 UNITS/Cm
TEMP ACT. GAIN = .005 UNITS/°F
Tex 1000°F/Cm
ΔWO TEMPERATURE INPUT
5 Lb/Hr/Cm
392
Series 22 - Run 1

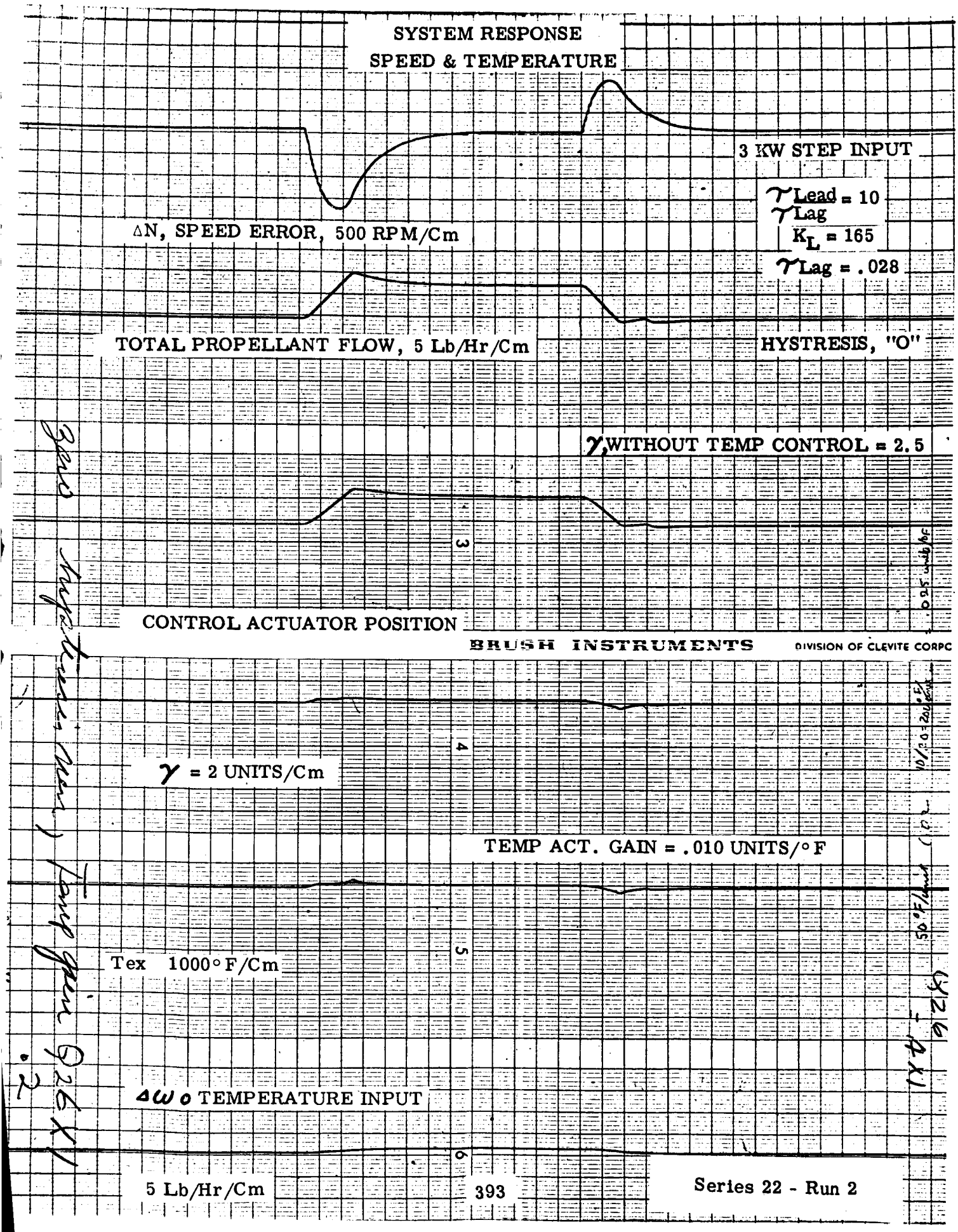
SYSTEM RESPONSE
SPEED & TEMPERATURE
3 KW STEP INPUT
τLead = 10
τLag
KL = 165
τLag = .028
ΔN, SPEED ERROR, 500 RPM/Cm
TOTAL PROPELLANT FLOW, 5 Lb/Hr/Cm
HYSTRESIS, "O"
γ, WITHOUT TEMP CONTROL = 2.5
CONTROL ACTUATOR POSITION
BRUSH INSTRUMENTS
DIVISION OF CLEVITE CORPO
γ = 2 UNITS/Cm
TEMP ACT. GAIN = .010 UNITS/°F
Tex 1000°F/Cm
ΔωO TEMPERATURE INPUT
5 Lb/Hr/Cm
393
Series 22 - Run 2

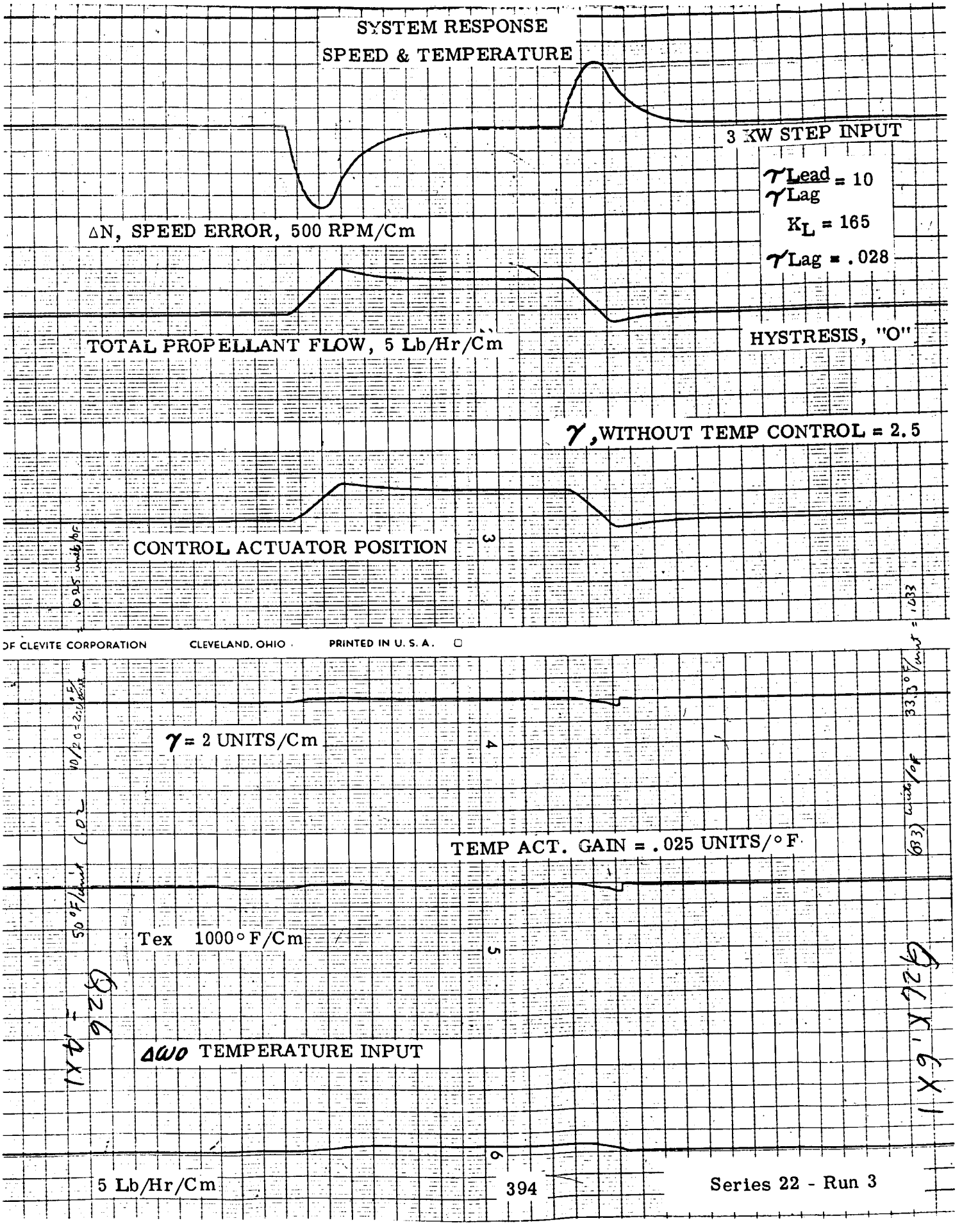

Series 22 - Run 3

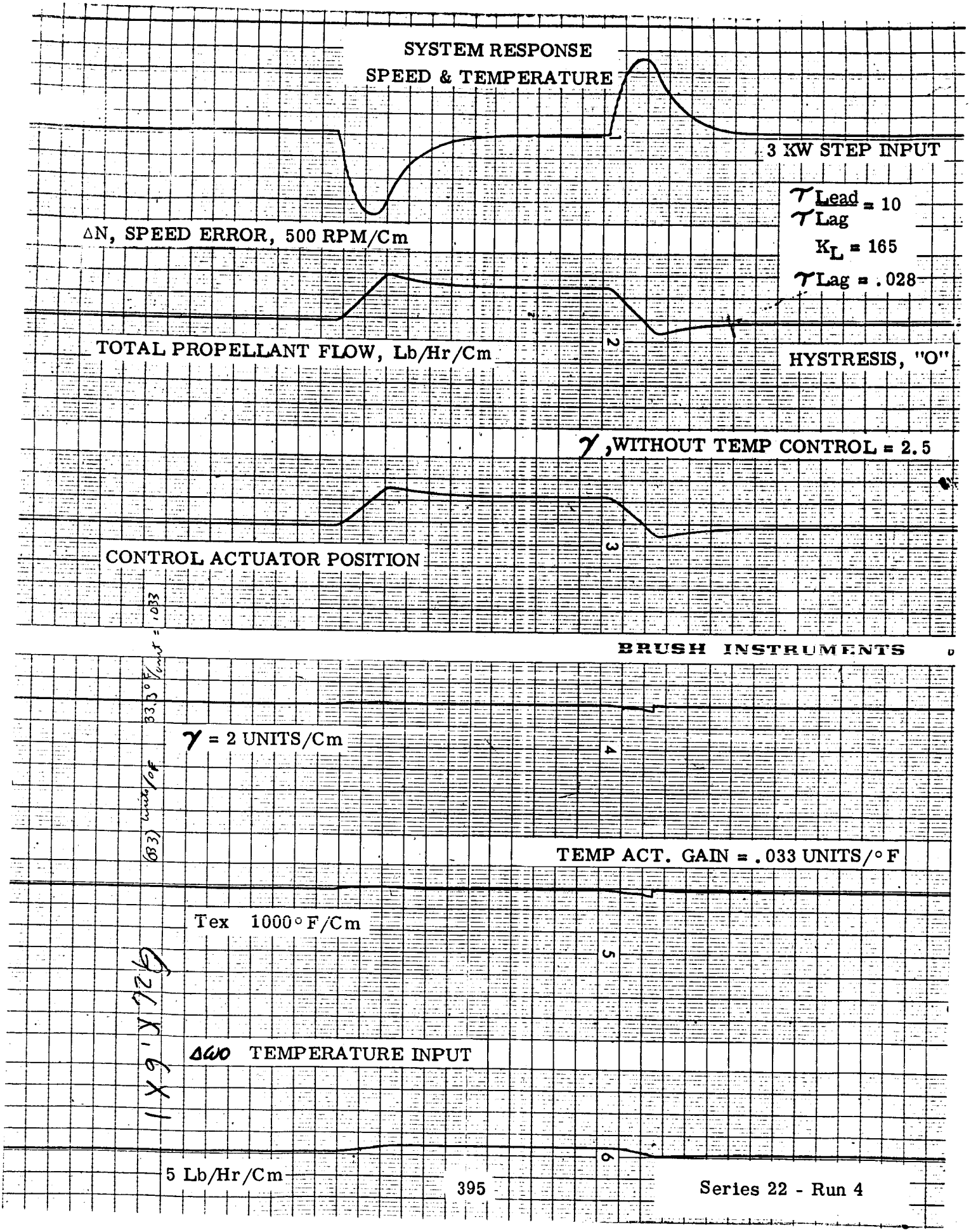

Series 22 - Run 4

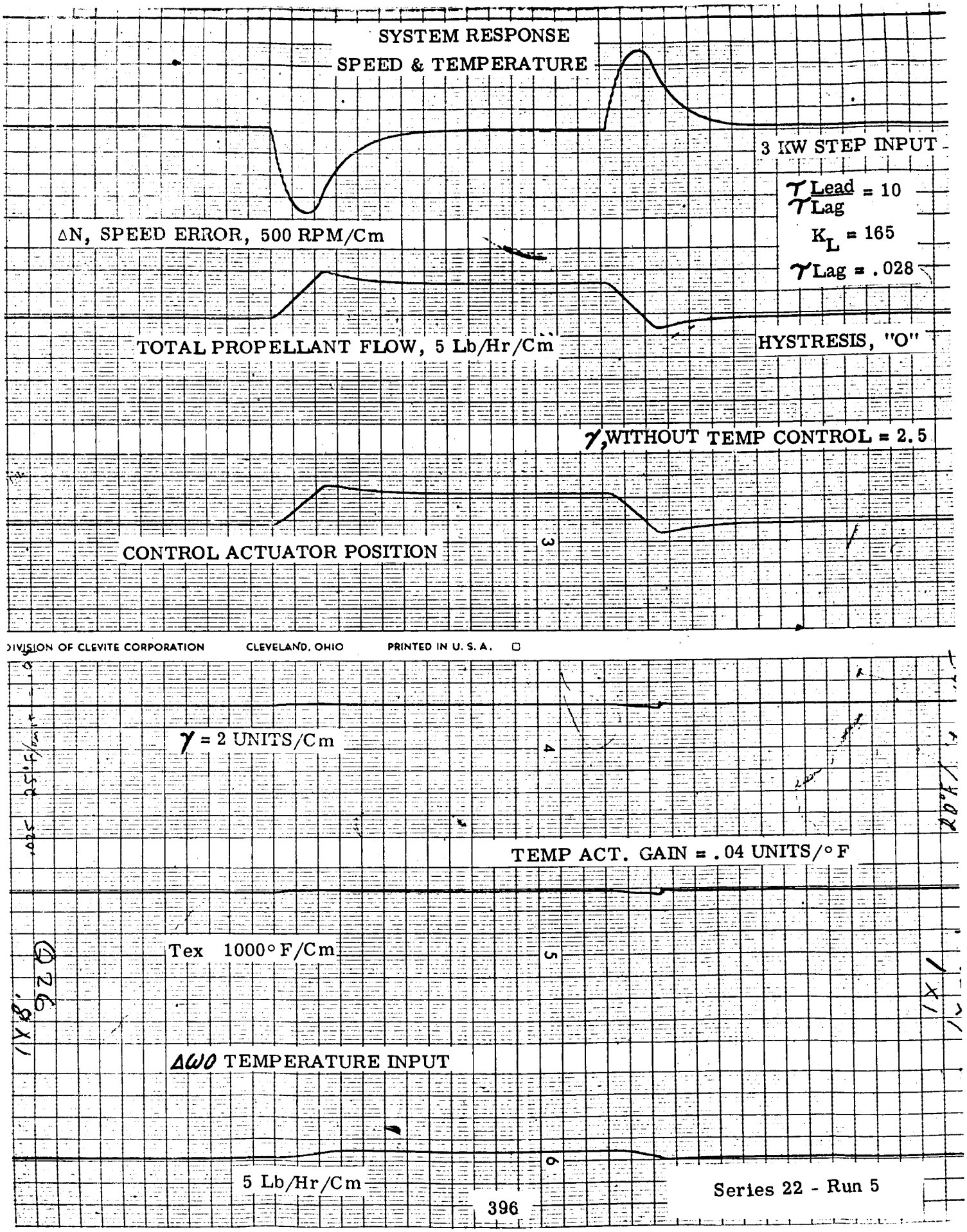
SYSTEM RESPONSE
SPEED & TEMPERATURE
3 KW STEP INPUT
τ Lead / τ Lag = 10
K_L = 165
τ Lag = .028
ΔN, SPEED ERROR, 500 RPM/Cm
TOTAL PROPELLANT FLOW, 5 Lb/Hr/Cm
HYSTRESIS, "O"
γ, WITHOUT TEMP CONTROL = 2.5
CONTROL ACTUATOR POSITION
3
DIVISION OF CLEVITE CORPORATION
CLEVELAND, OHIO
PRINTED IN U. S. A.
γ = 2 UNITS/Cm
4
TEMP ACT. GAIN = .04 UNITS/° F
Tex 1000° F/Cm
5
ΔWO TEMPERATURE INPUT
6
5 Lb/Hr/Cm
Series 22 - Run 5

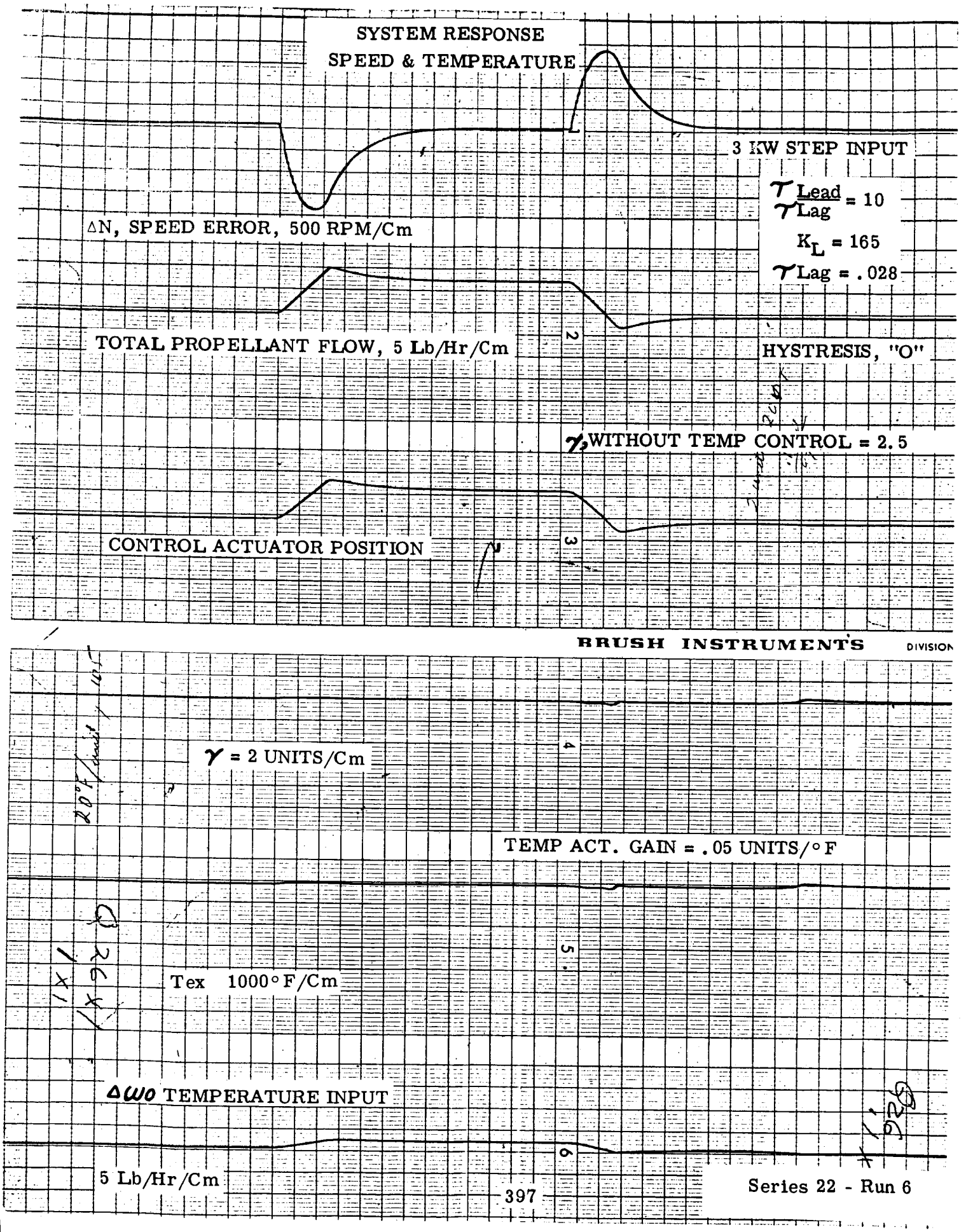
SYSTEM RESPONSE
SPEED & TEMPERATURE
3 KW STEP INPUT
τ Lead / τ Lag = 10
K_L = 165
τ Lag = .028
ΔN, SPEED ERROR, 500 RPM/Cm
TOTAL PROPELLANT FLOW, 5 Lb/Hr/Cm
2
HYSTRESIS, "O"
γ, WITHOUT TEMP CONTROL = 2.5
CONTROL ACTUATOR POSITION
3
BRUSH INSTRUMENTS DIVISION
γ = 2 UNITS/Cm
4
TEMP ACT. GAIN = .05 UNITS/°F
5
Tex 1000°F/Cm
ΔWO TEMPERATURE INPUT
6
5 Lb/Hr/Cm
Series 22 - Run 6

APPENDIX F

Preceding page blank

System Reliability Calculations

1. Control system reliability (R_c)

$$R_c(t) = e^{-\sum_{i=1}^{14} \lambda_i t}$$

$$R_c(100) = e^{-112\times10^{-6}(100)} = .98879$$

$$R_c(250) = e^{-112\times10^{-6}(250)} = .97239$$

2. Engine system reliability

(a) First 100 hours (R_{E_1})

$$R_{E_1}(t) = e^{-\lambda_6 t}\left[e^{-\lambda_E t} + \frac{\lambda_E}{\lambda_1 - \lambda_E}\left(e^{-\lambda_E t} - e^{-\lambda_1 t}\right)\right]^2$$

$$\lambda_E = \sum_{i=2}^{5} \lambda_i$$

$$R_{E_1}(100) = e^{-(500\times10^{-6})(100)}\left[e^{-(214.2\times10^{-6})(100)} + \frac{214.2\times10^{-6}}{.2\times10^{-6} - 214.2\times10^{-6}}\left(e^{-214.2\times10^{-6}} - e^{-.2\times}\right.\right.$$

$$= .95122$$

(b) Last 250 hours (R_{E_2})

$$R_{E_2}(t) = \left[e^{-\lambda_1 t}\right]^2 e^{-\lambda_6 t}$$

$$R_{E_2}(250) = \left[e^{-.2\times10^{-6}(250)}\right]^2 e^{-500\times10^{-6}(250)} = .88241$$

3) Electrical System Reliability (R_e)

$$R_e(t) = e^{-\sum_{i=5}^{19} \lambda_i t}$$

$$R_e(100) = e^{-420.4 \times 10^{-6}(100)}$$

$$R_e(100) = .96270$$

$$R_e(250) = e^{-420.4 \times 10^{-6}(250)} = .90034$$

4) Complete System Reliability

(a) First 100 hours (R_{100})

$$R_{100} = R_c(100) \times R_{E_1}(100) \times R_e(100)$$

$$= (.98879)(.95122)(.96270)$$

$$= .90547$$

(b) last 250 hours (R_{250})

$$R_{250} = R_c(250) \times R_{E_2}(250) \times R_e(250)$$

$$= (.97239)(.88241)(.90034)$$

$$= .77253$$

5) Estimated Reliability for 350 hour mission (R_M)

$$R_M = R_{100} \times R_{250}$$

$$= .69950$$

(6) Reliability with three systems in standby, each system having .69950 reliability.

$$R = e^{-\lambda t}\left(1+\lambda t+\frac{\lambda^2 t^2}{2!}+\frac{\lambda^3 t^3}{3!}\right)$$

$$= (.69950)(1+.359+.06372+.00758)$$

$$= .9990$$

APPENDIX G

VICKERS INCORPORATED
ENGINEERING CALCULATION FORM

PAGE

SUBJECT: PRIME SURFACE HEAT EXCHANGER

DATE

ASSUMED CONFIGURATION:

HYDROGEN TUBE 1/4" O.D. – .016" WALL
NUMBER OF COIL SETS – 5
TRANSVERSE PITCH = 1.25 (TUBE OD)
AXIAL PITCH = 1.50 (TUBE O.D.)
MEAN COIL DIAMETER OF MIDDLE COIL = 4" = .333' = D_M

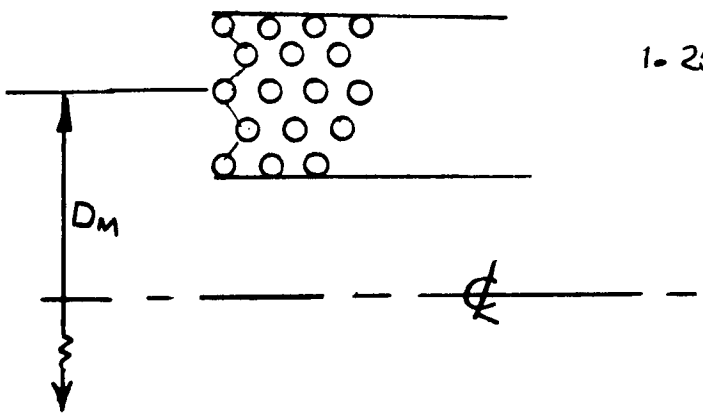

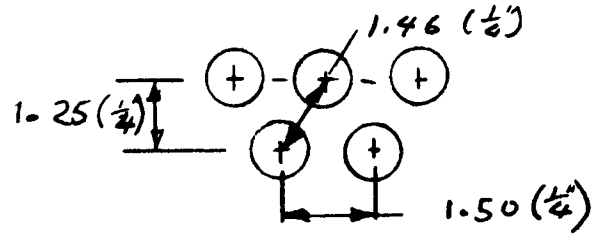

EXHAUST GAS SIDE:

EXHAUST FLOW AREA = $(4)\pi(.333)\frac{.46}{4(12)} = 0.0401\ ft^2$

TRANSFER SURFACE (4 COILS) = $4\left[\frac{\pi}{4\times12}\right]\frac{ft^2}{ft} \times .333\ \frac{\pi\ ft}{coil} \times \frac{48\ coil}{1.5\ ft} \times L\ ft$

WHERE L = EXCHANGER LENGTH

$= .833\pi^2 L\ ft^2$

$W = 42.3\ \#/HR$ (REQD)

$G = \frac{42.3}{.0401} = 905.\ \frac{\#/HR}{ft^2}$

PREPARED BY	VICKERS INCORPORATED ENGINEERING CALCULATION FORM	PAGE
CHECKED BY	SUBJECT PRIME SURFACE HEAT EXCHANGER	
		DATE

$$r_h = \frac{A_{flow}}{A_{SURFACE}/L} = \frac{.0401}{.833\pi^2} = .00488 \quad *$$

$$D_h = 4 r_h = .0195'$$

$$N_{Re} = \frac{D_h G}{\mu} = \frac{.0195(905)}{.0286} = 617$$

Let $\frac{h_f}{G C_p} N_{Pr}^{2/3} = .026$ **

$$h_f = \frac{905(1.22)(.026)}{0.79} = 36.4 \ \frac{B}{HR\,Ft^2\,{}^oF}$$

DESIGNING FOR 58,400 B/HR & $\theta_{FILM} = 150\,{}^oF$

$$A_s = .833\pi^2 L = \frac{58,400}{36.4(150)} = 10.7\ ft^2$$

$$L = \frac{10.7}{.833\pi^2} = 1.3'$$

$$n = \frac{1.3 \times 12}{.375} \simeq 40 \text{ turns/coil set}$$

MEAN TUBE LENGTH = $40\pi D_m = 42$ ft

** fig 12 pg 50 COMPACT HEAT EXCH.
* Pg 3 COMPACT HEAT EXCHANGER BY KAYS & LONDON

PREPARED BY	VICKERS INCORPORATED ENGINEERING CALCULATION FORM	PAGE
CHECKED BY	SUBJECT PRIME SURFACE HEAT EXCHANGER	DATE

HYDROGEN SIDE

$$\frac{W}{N} = \frac{14.1 \ \#/HR. \ (REQ'D)}{5 \ TUBES} = 2.82 \ \frac{\#/HR}{TUBE}$$

TUBE I.D = .0182

$$G = \frac{2.82}{\frac{\pi}{4}(.0182)^2} = 10,900$$

$$N_{Re} = \frac{(.0182)(10,900)}{.0306} = 6,500$$

$$\text{SURFACE AREA} = 5 \ \text{TUBES} \times 42 \ \frac{ft}{COIL} \times (.0182)\pi$$

$$= 12 \ ft^2$$

$$\Theta \cong \frac{58,400}{12 \ h_f}$$

$k_{H_2} = 0.15$ $\qquad N_{PR} = \mu C_p / k$

$\mu_{H_2} = .03$

$D = .0182$

$$h_f = .0225 \frac{k}{D} \left(\frac{DG}{\mu}\right)^{.8} (N_{PR})^{.08}$$

$$= .0225 \left(\frac{.15}{.0182}\right)(6,500)^{.8}(.75)$$

$$= 156 \ B/HR. \ ft^2 \ {}^oF$$

$$\Theta_{FILM} = \frac{58,400}{12(156)} = 31 \ {}^oR$$

Log_e MEAN $\Delta T \cong 150 + 31 \cong \underline{181 \ {}^oR}$ + WALL ΔT

PREPARED BY	VICKERS INCORPORATED ENGINEERING CALCULATION FORM	PAGE
CHECKED BY	SUBJECT PRIME SURFACE HEAT EXCHANGER	PROGRAM & PROJECT NO.
		DATE

PRESSURE DROP

EXHAUST GAS SIDE

$$\Delta P \cong \left(\frac{G}{3600}\right)^2 \frac{f L F_s}{2g F_2 \rho_m}$$

{EQ 15 Pg 7 ANALYTICAL METHOD FOR COMPACT REGEN, REPORT NO. HWR-130 BY H. WOOD}

WHERE:

$$F_s = \frac{A_{surface}}{Vol\ Exchanger} = \frac{A_{surface}}{L \times A_{FRONTAL\ TOT.}}$$

$$F_2 = \frac{A_{FLOW}}{A_{FRONTAL\ TOT.}}$$

$$\therefore \frac{L F_s}{F_2} = \frac{A_{SURFACE}}{A_{FLOW}}$$

$$\therefore \Delta P \cong \left(\frac{G}{3600}\right)^2 \cdot \frac{f}{2g\rho_m} \frac{A_{surface}}{A_{flow}}$$

FOR $N_{Re} = 617$, $f = .125$ {Pg 50 COMPACT HEAT EXCH.}

$$\rho_m = \frac{P}{RT_m} = \frac{144 \times 2\ PSIA}{257 \times 1000°R} = .0011\ LB/FT^3$$

$$\Delta P = \left(\frac{905}{3600}\right)^2 \times \frac{.125 \times 10.7}{2(32.2)(.0011)(.041)} = 30\ LB/ft^2$$

$$\Delta P = \frac{30}{144} = .208\ PSI$$

PREPARED BY	VICKERS INCORPORATED ENGINEERING CALCULATION FORM	PAGE
CHECKED BY	SUBJECT PRIME SURFACE HEAT EXCHANGER	PROGRAM & PROJECT NO.
		DATE

PRESSURE DROP

HYDROGEN SIDE:

$$\Delta P = \frac{G^2(v_2 - v_1)}{\alpha g_c} + \frac{f_m G^2 v_m l}{2g\, r_h} \quad *$$

MODIFY TO

$$\Delta P \cong \frac{G^2(v_2 - v_1)}{g_c} + \frac{C_F f_m G^2 v_m l}{2g\, D/4}, \quad (l = \text{tube length})$$

FRICTION FACTOR, $f_m = .009$ FOR $N_{Re} = 6{,}500$ **

CURVATURE FACTOR $C_F = 2.8$ FOR $N_{Re}\sqrt{\frac{D}{D_H}} = 6500\sqrt{\frac{.0182}{.333}} = 500$ ***

LETING $v_2 = \frac{767 \times 1440}{1200 \times 144} = 6.4$

$v_1 = \frac{767 \times 250}{1200 \times 144} = 1.1$

$\Delta v = 5.3$

ASSUMING $v_m = 7.5/2 = 3.75$

$$\Delta P \cong \left(\frac{10{,}900}{3600}\right)^2 \frac{(5.3)}{(32.2)} \frac{1}{144} + \frac{2.8 \times .009}{144}\left(\frac{10{,}900}{3600}\right)^2 \frac{(3.75)}{64.4}\left(\frac{42}{\frac{.0182}{4}}\right)$$

$$= \underline{\underline{.88}} \text{ PSI}$$

*** fig 6-6 Pg 151 "
** fig 6-11 Pg 156 "
* EQ 6-9b Pg 158 McAdams

APPENDIX H

APPENDIX H

SUMMARY OF H_2-O_2 INTERNAL COMBUSTION ENGINE TEST RESULTS

Valve Phase Conditions:

1. H_2 = 19° BTDC, 4° ATDC O_2 = 3° BTDC, 25° ATDC
2.
3.
4.
5.
6.
7.
8.
9.

Run No. & Date	Time	RPM	Shaft HP	BSPC	O/F	Cyl. HP Loss	% Cyl/Shaft	Valve Phase Cond No.	EX TEMP °R	HEAD TEMP °R	BMEP PSI
Sheet 1 3-13-63	1	3000	1.95	3.36	.533			1	885	1860	94.6
"	2	3500	2.06	3.19	.53			1	860	1740	83.5
Sheet 2 3-18-63	1	3227	1.23					1			55.5
"	2	4000	1.27	3.52	.83			1	750	1760	46.2
Sheet 3 3-28-63	1	3060	.92			.92	100.0	1	810	1740	43.9
Sheet 4 4-2-63	1	3020	1.005	4.012	.627	1.225	122.0	1	835	1560	48.5
Sheet 5 4-5-63	A	3074	1.02	3.56	.8125	1.42	139.0	1	835	1535	48.5
"	B	3520	1.005	3.7	.985	1.72	172.0	1	860	1660	41.6
"	C	3994	.885	3.85	1.255	1.98	224.0	1	910	1780	32.4
"	D	4030	.832	4.09	.955	1.28	154.0	1	850	1660	30.0
Sheet 6 4-5-63	A	4020	.796	4.36	1.02	1.51	190.0	1	830	1510	28.9
"	B	4031	.352	5.17	1.19	1.54	435.0	1	845	1670	12.7
"	C	4057	1.48	3.23	.855	1.54	102.0	1	885	1640	53.2
"	D	4026	2.175	2.7	.803	1.84	84.6	1	910	1630	79.7
"	E	3514	1.53	2.93	.71	1.23	81.7	1	795	1475	63.5
"	F	3569	.765	3.94	1.23	1.51	197.5	1	845	1590	31.2
"	G	3550	.45	5.43	1.29	1.32	293.0	1	815	1590	18.5
Sheet 7 4-5-63	A	3036	.448	5.06	1.06	1.13	254.0	1	785	1525	21.5
"	B	3024	.735	3.81	.872	1.16	158.0	1	785	1490	35.4
"	C	3000	1.45	2.9	.57	1.06	73.0	1	770	1405	70.5
"	D	3026	2.21	2.66	.53	1.06	48.0	1	700	1290	106.4
"	E	3022	2.93	2.73	.396	.924	31.5	1	710	1205	141.0
"	F	4066	2.97	2.48	.717	2.0	67.4	1	835	1515	106.4
Sheet 8 4-8-63	10:49	3512	2.16	2.91	.495	1.085	50.1	1	770	1340	91.0
"	10:57	3521	2.95	2.38	.596	1.175	39.8	1	785	1315	121.5
"	11:05	3526	4.36	2.505	.516	1.335	30.6	1	800	1345	179.5
"	11:10	3008	4.48	2.28	.680	2.005	44.8	1	885	1510	207.5
"	11:20	4005	4.44	2.395	.610	2.075	46.7	1	885	1495	160.0
Sheet 9 4-8-63	2:35	2996	2.93	2.67	.783	2.3	78.5	1	970	1770	142.0
"	2:45	3029	2.96	2.76	.795	2.44	82.5	1	950	1770	142.0
Sheet 10 4-17-63	2:48	3005	1.03	2.87	1.87	1.74	169.0	1	885	1760	49.7
"	3:07	3027	1.58	2.58	1.41	1.94	2.16	1	920	1720	76.2
"	8391.1	3099	1.64	2.55	1.48	2.16	131.7	1	940	1750	77.2
"	8399	3041	1.59	2.69	1.4	2.08	130.8	1	930	1760	76.0
"	4103	3099	3.04	2.38	1.04	2.47	81.2	1	960	1720	141.0
Sheet [illegible]	[illegible]	3066	2.14	2.51	1.485	2.52	118.0	1	990	1790	101.8
	[illegible]	3034	2.91	2.39	1.57	2.90	99.6	1	1010	1765	140.0
	[illegible]	3038	* 2.6	2.42	1.66	3.40	130.7	1	1060	1890	124.0
	[illegible]	[illegible]	2.933	2.295	1.28	3.57	121.6	1	1070	1830	106.5
[illegible]	8532	3087	2.96	2.34	1.49	3.41	115.0	1	1060	1860	140.0
"	8550	3043	2.97	2.40	1.54	3.41	114.9	1	1060	1860	142.0

* Computed from hydraulic horse power.

SUMMARY OF H_2-O_2 INTERNAL
COMBUSTION ENGINE TEST RESULTS

Valve Phase Conditions:

1. H_2 = 19° BTDC, 4° ATDC O_2 = 3° BTDC, 25° ATDC
2. H_2 = 18° BTDC, 34° ATDC O_2 = 27° ATDC, 55° ATDC
3. H_2 = 18° BTDC, 34° ATDC O_2 = 20° ATDC, 48° ATDC
4. H_2 = 19° BTDC, 4° ATDC O_2 = 6° BTDC, 22° ATDC
5.
6.
7.
8.
9.

Run No & Date	Time	RPM	Shaft HP	BSPC	O/F	Cyl. HP Loss	% Cyl. Shaft	Valve Phase Cond No.	EX TEMP °R	HEAD TEMP °R	BMEP PSI
Sheet 13 5-1-63	8570	3041	2.94	2.385	1.478	3.34	113.8	1.	1050	1850	141.0
Sheet 14 5-2-63	8604	2995	1.172	4.72	1.13	1.72	146.5	2.	860	1360	90.5
"	8612	3008	1.16	4.33	1.052	.324	27.9	2.	875	1360	89.0
"	8623	3060	.765	5.39	1.41	.669	87.4	2.	910	1495	57.7
Sheet 15 5-3-63	8624	3027	.935	3.84	2.875	1.73	183.0	2.	910	1680	45.0
"	1:45	3006	2.94	2.51	1.035	1.62	55.1	2.	935	1460	142.8
"	1:55	4007	2.925	2.35	1.042	2.56	87.5	2.	1020	1625	106.1
"	8636	4000	1.043	5.43	1.51	3.04	291.0	2.	1085	1850	60.3
Sheet 16 5-9-63	8653	3010	1.397	4.08	1.4	2.27	163.0	3.	1015	1815	67.7
Sheet 17 5-13-63	4:28	4036	1.48	3.08	1.42	2.66	179.6	3.	1010	1835	53.6
"	4:36	4027	2.34	2.73	1.16	2.48	106.0	3.	1085	1795	84.8
Sheet 18 5-14-63	8681	4020	1.61	3.35	1.18	2.27	141.0	3.	1010	1810	58.2
"	8693	4044	2.38	2.74	1.12	2.422	102.0	3.	1010	1780	86.0
"	2:07	4015	3.035	2.96	1.11	3.22	106.0	3.	1070	1750	110.3
"	2:15	4003	4.2	2.51	.97	2.75	61.5	3.	1005	1660	153.0
"	2:25	3060	2.97	2.9	1.085	2.0	67.3	3.	990	1640	141.3
"	2:30	3004	2.29	3.13	1.312	1.89	93.5	3.	1030	1700	111.0
"	2:35	3027	1.6	3.68	1.64	2.3	143.8	3.	1000	1760	76.2
Sheet 19 5-17-63	10:37	3987	.804	3.99	1.31	1.59	198.2	4.	930	1880	29.3
Sheet 20 5-20-63	1:45	4000	.715	4.68	.85	1.2	155.0	4.	820	1580	28.2
"	1:55	4040	.717	5.12	1.132	1.645	229.5	4.	910	1770	25.85
"	2:02	4000	.824	4.29	1.308	1.727	210.0	4.	925	1815	30.0
"	2:12	4067	.852	4.07	1.157	1.821	214.0	4.	940	1860	30.5
"	2:30	4072	.012	3.685	1.19	2.43	239.5	4.	1020	2160	36.25
"	2:35	3006	1.022	3.415	.87	1.231	120.0	4.	830	1570	49.5
"	2:40	3040	.78	5.81	1.04	1.37	175.5	4.	880	1670	37.4
Sheet 21 5-20-63	2:45	3036	.971	3.68	1.32	1.485	153.0	4.	920	1780	46.7
"	2:50	3000	1.06	3.415	1.62	1.72	162.0	4.	950	1880	51.5
"	3:00	2970	1.185	3.385	1.052	1.325	116.0	4.	910	1710	58.2
"	3:05	3000	1.22	3.41	1.3	1.65	135.0	4.	940	1820	59.4
"	3:10	2970	1.303	3.455	1.19	1.72	131.7	4.	950	1810	64.0
"	3:15	3000	1.252	3.76	1.368	1.86	148.2	4.	1170	1890	60.8
"	3:30	3060	.906	4.33	1.185	1.515	167.0	4.	920	1760	43.2
Sheet 22 5-24-63	10:25	4007	.745	4.77	.881	1.4	188.0	1.	840	1630	27.0
"	10:35	4000	.73	5.35	.952	1.74	238.0	1.	890	1810	26.6
"	10:45	4010	.682	4.44	1.93	2.02	296.0	1.	940	1910	24.7
Sheet 23 5-24-63	10:55	4000	1.22	3.72	.965	1.667	136.5	1.	940	1770	44.4
"	11:05	3950	1.21	3.62	1.127	1.932	159.8	1.	960	1870	44.6
"	11:13	4017	1.268	3.345	1.25	2.65	209.0	1.	985	1900	46.0
"	11:20	4025	2.47	2.6	1.009	2.18	88.3	1.	1010	1840	89.5

?

SUMMARY OF H_2-O_2 INTERNAL
COMBUSTION ENGINE TEST RESULTS

Valve Phase Conditions:

1. H_2 = 19° BTDC , 4° ATDC O_2 : 3° BTDC , 25° ATDC
2.
3.
4.
5. H_2 = 19° BTDC , 4° ATDC O_2 - 1° BTDC , 25° ATDC
6.
7.
8.
9.

Run No & Date	Time	RPM	Shaft HP	BSPC	O/F	Cyl. HP Loss	% Cyl/Shaft	Valve Phase Cond No.	EX TEMP °R	HEAD TEMP °R	BMEP PSI
Sheet 24 5-24-63	11:25	3000	2.485	2.75	.832	1.445	58.2	1.	890	1640	120.05
"	11:35	3035	2.41	2.875	.943	2.1	87.0	1.	990	1790	116.0
"	11:40	2985	1.334	3.65	.83	1.445	108.2	1.	880	1690	65.2
Sheet 25 5-28-63	2:00	4000	.818	4.16	.982	1.177	144.0	1.	850	1640	29.8
"	2:05	4000	.932	3.71	1.078	1.328	142.5	1.	880	1700	34.0
Sheet 26 5-29-63	2:05	4000	2.71	2.865	.371			5.	615	1070	98.6
"	2:10	4000	3.06	2.6	.576			5.	740	1310	121.5
"	2:15	4000	2.515	2.73	.352			5.	655	1130	84.8
"	2:17	4000	2.36	2.94	.578			5.	760	1400	86.0
Sheet 27 5-29-63	2:45	4020	2.995	2.795	.712			5.	860	1360	102.8
"	2:50	4000	2.96	2.745	.872			5.	930	1760	108.0
Sheet 28 5-29-63	3:40	4000	2.01	3.25	.2613			5.	560	860	73.2
"	3:45	4000	2.01	3.29	.2953			5.	590	970	73.2

REFERENCES

REFERENCES

SECTION 2 - REFERENCES

1. Final Report No. FR-91565-318-1A, "Hydrogen-Oxygen Internal Combustion Engine," Vickers Incorporated.

2. Lichty, L. C., "Internal Combustion Engines," 6th Edition. McGraw-Hill (1951) p. 484.

3. "Factors Affecting Piston Ring Life and Performance in Small Two and Four Cycle Engines", SAE Report #601A.

4. "Lycoming S & H Light Weight Multifuel Engines," Automotive Industries, April 1, 1963.

SECTION 3 - REFERENCES

1. ASME Paper 62AV39, "Piston Engines Are Reborn For Space Power," Deacon, W.K. & Morgan, N.E.

2. Report 1060-039, "Analytical Study of a Hot Gas Motor for Torpedo Propulsion," Vickers Incorporated, 1959.

3. NASA Memo 5-20-59, "The Performance of Liquid H_2 with Liquid O_2 as a Rocket Propellant."

4. Taylor, C.F., and Taylor, E.S., "The Internal Combustion Engine," 2nd Edition

SECTION 6 - REFERENCES

1. Bazorsky, I., "Reliability: Theory and Practice," N.J. 1961.

2. "Reliability Design Manual," Report No. NA59-582, 27 July 1959, North American Aviation, Inc.

3. "Reliability Guide for Vendors," Document No. D6-5762, June, 1961, The Boeing Company.

4. "Reliability Application and Analysis Guide," July, 1961, The Martin Company.

5. "Reliability Stress Analysis for Electronic Equipment," Report TR1100, November 28, 1956, RCA.

6. "Flight Vehicle Power Systems Reliability Criteria," Report No. ASD-TR-61736, March, 1962, American Power Jet Company.

7. "Failure Rates and Failure Modes of Small Rotary Electrical Devices," Publication No. 160-2-269R, ARINC Research Corp.

8. "Procedures for Determining Aircraft Engine Failure Rates," T.O. 00-25-128, USAF.

SECTION 7 - REFERENCES

1. "Hydrogen-Oxygen Internal Combustion Engine," ASD-TDR-62-961.

SYMBOLS AND ABBREVIATIONS

Preceding page blank

LIST OF SYMBOLS

Symbol	Description	Units
A	Piston Area	in^2
a	Piston Admission	Percent of Dspl.
B	Cylinder Bore	in.
b	Percent Compression	Percent of Dspl.
BSPC	Brake Specific Propellant Consumption	lb/hp-hr
BMEP	Brake Mean Effective Pressure	psi
c	Clearance Volume	Percent of Dspl.
C_p	Specific Heat for Constant Pressure Process	BTU/lb °F
C_v	Specific Heat for Constant Volume Process	BTU/lb °F
D	Displacement in Cubic Inches	in^3
DF	Diagram Factor	
FMEP	Friction Mean Effective Pressure	psi
h	Film Coefficient	BTU/hr °F ft^2
He	Helium	
hp or HP	Horsepower	HP
HP_s	Specific Horsepower	HP/in^3
H_2	Hydrogen	
IMEP	Idealized Mean Effective Pressure	psi
ISPC	Ideal Specific Propellant Consumption	lb/hp-hr
K	Thermal Conductivity	BTU ft/hr °F ft^2
k	Ratio of Specific Heat	
MW	Molecular Weight	lb/mole
O/F	Oxidizer - Fuel Ratio (Oxygen/Hydrogen)	lb/lb
O_2	Oxygen	
P_e	Exhaust Pressure	psi
P_i	Hydrogen Inlet Pressure	psi

LIST OF SYMBOLS

Symbol	Description	Unit
P_r	Prandtl Number	
P_1	Theoretical Combustion Pressure	psi
Q	Heat of Combustion per Pound of Reactants	BTU/lb
q	Rate of Heat Transfer	BTU/hr
qc	Cylinder Heat Rejection	BTU/hr
Q_{O_2}	Heat Release per Pound of Oxygen	BTU/lb
R	Gas Constant	ft/°R
SPC	Specific Propellant Consumption	lb/kwh
TDC	Top Dead Center	
T_e	Maximum Exhaust Temperature	°R
TH_{2_i}	Hydrogen Inlet Temperature from Storage Rank	°R
T_i	Hydrogen Inlet Temperature to Engine	°R
Tm_e	Mean Expansion Temperature	°R
T_W	Cylinder Wall Temperature	°R
T_1	Maximum Temperature	°R
U	Piston Speed	ft/min
V	Cylinder Volume	in^3
W	Work per Cycle	ft/lbs
W_i	Propellant Weight per Cycle	lbs/cycle
X	Cylinder Heat Rejection	
y	Heat Extraction "Weighting" Factor	
ΔT	$Tm_e - T_W$	°R
ΔT_c	Change in Temperature Due to Combustion	°R
η_c	Compression Efficiency	
η_m	Mechanical Efficiency	
η_{th}	Thermal Efficiency	
η_x	Cycle Thermal Efficiency	
η_1	Cycle Efficiency at qc = 0	
η_∞	Expander Efficiency Related to an Infinite Expansion Ratio	
μ	Viscosity	$lb\text{-}sec/ft^2$
ρ	Density	lb/ft^3